PROCEEDINGS OF OLIVEBIOTEQ 2018 – OLIVE MANAGEMENT, BIOTECHNOLOGY AND AUTHENTICITY OF OLIVE PRODUCTS

EDITED BY: José Enrique Fernández, Antonio Diaz Espejo,
José Manuel Martínez-Rivas and Wenceslao Moreda

PUBLISHED IN: Frontiers in Plant Science,
Frontiers in Bioengineering and Biotechnology,
Frontiers in Nutrition and Frontiers in Sustainable Food Systems

frontiers Research Topics

frontiers

ISSN 1664-8714
ISBN 978-2-88963-950-2
DOI 10.3389/978-2-88963-950-2

About Frontiers

Frontiers is more than just an open-access publisher of scholarly articles: it is a pioneering approach to the world of academia, radically improving the way scholarly research is managed. The grand vision of Frontiers is a world where all people have an equal opportunity to seek, share and generate knowledge. Frontiers provides immediate and permanent online open access to all its publications, but this alone is not enough to realize our grand goals.

Frontiers Journal Series

The Frontiers Journal Series is a multi-tier and interdisciplinary set of open-access, online journals, promising a paradigm shift from the current review, selection and dissemination processes in academic publishing. All Frontiers journals are driven by researchers for researchers; therefore, they constitute a service to the scholarly community. At the same time, the Frontiers Journal Series operates on a revolutionary invention, the tiered publishing system, initially addressing specific communities of scholars, and gradually climbing up to broader public understanding, thus serving the interests of the lay society, too.

Dedication to Quality

Each Frontiers article is a landmark of the highest quality, thanks to genuinely collaborative interactions between authors and review editors, who include some of the world's best academicians. Research must be certified by peers before entering a stream of knowledge that may eventually reach the public - and shape society; therefore, Frontiers only applies the most rigorous and unbiased reviews.
Frontiers revolutionizes research publishing by freely delivering the most outstanding research, evaluated with no bias from both the academic and social point of view. By applying the most advanced information technologies, Frontiers is catapulting scholarly publishing into a new generation.

What are Frontiers Research Topics?

Frontiers Research Topics are very popular trademarks of the Frontiers Journals Series: they are collections of at least ten articles, all centered on a particular subject. With their unique mix of varied contributions from Original Research to Review Articles, Frontiers Research Topics unify the most influential researchers, the latest key findings and historical advances in a hot research area! Find out more on how to host your own Frontiers Research Topic or contribute to one as an author by contacting the Frontiers Editorial Office: researchtopics@frontiersin.org

PROCEEDINGS OF OLIVEBIOTEQ 2018 – OLIVE MANAGEMENT, BIOTECHNOLOGY AND AUTHENTICITY OF OLIVE PRODUCTS

Topic Editors:
José Enrique Fernández, Institute of Natural Resources and Agrobiology of Seville (CSIC), Spain
Antonio Diaz Espejo, Institute of Natural Resources and Agrobiology of Seville (CSIC), Spain
José Manuel Martínez-Rivas, Instituto de la Grasa (IG), Spain
Wenceslao Moreda, Consejo Superior de Investigaciones Científicas (CSIC), Spain

Citation: Fernández, J. E., Espejo, A. D., Martínez-Rivas, J. M., Moreda, W., eds. (2020). Proceedings of Olivebioteq 2018 – Olive Management, Biotechnology and Authenticity of Olive Products. Lausanne: Frontiers Media SA.
doi: 10.3389/978-2-88963-950-2

Table of Contents

frontiers in Plant Science

EDITORIAL
published: 02 July 2020
doi: 10.3389/fpls.2020.00860

Editorial: Proceedings of Olivebioteq 2018 – Olive Management, Biotechnology and Authenticity of Olive Products

José Enrique Fernández[1]*, *Antonio Díaz-Espejo*[1], *José Manuel Martínez-Rivas*[2] and *Wenceslao Moreda*[2]

[1] Institute of Natural Resources and Agrobiology of Seville (CSIC), Seville, Spain, [2] Instituto de la Grasa (CSIC), Seville, Spain

Keywords: biotechnology, abiotic stress, crop management, oil quality, table olive

Editorial on the Research Topic

Proceedings of Olivebioteq 2018 – Olive Management, Biotechnology and Authenticity of Olive Products

OLIVEBIOTEQ'18 was the 6th International Conference on the Olive Tree and Olive Products. Held in Seville, Spain, in October 2018, it gathered 218 registered participants from 16 countries with the objective of bringing together the latest advances and knowledge in the areas of breeding and propagation; reproductive and molecular biology, genomics, and biotechnology; crop response to biotic and abiotic stresses and crop management; economics of the olive crop and olive products; table olive and olive oil quality, authenticity, technology, and by-products; and nutrition and health. For all these areas, we considered research, technological, industrial, and commercial aspects.

The publication of this special issue was one of the activities organized within the frame of OLIVEBIOTEQ'18. We contacted 252 potential contributors and received 50 abstracts. Eventually, 31 manuscripts were submitted and 21 accepted for publication. Seventeen are published in Frontiers in Plant Science, within the Crop and Product Physiology section; two in Frontiers in Nutrition, Food Chemistry section; one in Frontiers in Sustainable Food Systems, Crop Biology and Sustainability section; and one in Frontiers in Bioengineering and Biotechnology, Industrial Biotechnology section.

Three of the accepted manuscripts are related to breeding and propagation. The work by Miazzi et al. addresses the recovery and conservation of ancient and rare olive germplasm from the Apulian region (Southeast Italy). A total of 177 genotypes were recovered, analyzed, propagated and transferred to an *ex-situ* field. The identification of genotypes useful for breeding programs was key among the outputs of this work. French genotypes were studied by Khadari et al., who used molecular characterization to both elucidate their origin and facilitate cultivar management. They found high genetic diversity in the 113 studied olive accessions, suggesting that French olive germplasm resulted from the diffusion of material from Spain and Italy. With an interest in selecting cultivars with an improved ability to better adapt to new management systems, de Castro et al. developed a UAV-based high-throughput system for the improvement of olive breeding programs. The system includes a new, high-performance object-based image analysis algorithm, suitable for the quantification of tree architectural traits, especially tree height and crown area. These three approaches illustrate the key role that molecular biology and remote imagery techniques play in the identification of genotypes for breeding programs and in the identification of links between genotype and phenotype.

OPEN ACCESS

Edited and reviewed by:
Eddo Rugini,
University of Tuscia, Italy

***Correspondence:**
José Enrique Fernández
jefer@irnase.csic.es

Specialty section:
This article was submitted to Crop and Product Physiology, a section of the journal Frontiers in Plant Science

Received: *27 April 2020*
Accepted: *27 May 2020*
Published: *02 July 2020*

Citation:
Fernández JE, Díaz-Espejo A, Martínez-Rivas JM and Moreda W (2020) Editorial: Proceedings of Olivebioteq 2018 – Olive Management, Biotechnology and Authenticity of Olive Products. Front. Plant Sci. 11:860. doi: 10.3389/fpls.2020.00860

The role of genomics and biotechnology in plant protection is outlined in the work by Narváez, Martín et al., wherein they analyse the response of transgenic olive plants to *Verticillium dahliae* and *Rosellinia necatrix*. These plants constitutively expressed the *NPR1* gene from *Arabidopsis thaliana* as a response to the infection by both species of fungi. An embryogenic line from a seed of cv. Picual was used to obtain several transgenic plants showing different responses to a variety of pathophyte species. In another work, Narváez, Prieto et al. perform a pioneering analysis of the regeneration capacity, via somatic embryogenesis, of four wild olive genotypes with different responses to defoliation caused by *V. dahliae*. Another example of genomics, this time applied to the fatty acid composition of olive oil, is given by Salimonti et al. This group worked with the oleate desaturase enzyme encoding-gene (*FAD2-2*), which is the main gene responsible for the linoleic acid content in the olive oil. More precisely, they performed an *in silico* and structural analysis of the 5′UTR intron of the *FAD2-2* gene to explore the natural sequence variability and its role in the regulation of gene expression. Their findings reveal new structural variants within the *FAD2*-2 gene in olive, putatively involved in the regulation mechanism of gene expression associated with oleic and linoleic acid content variation. These lines of research highlight the utility of molecular approaches for the improvement of olive biotic stress resistance and oil quality.

In the field of reproductive biology, the work by Jimenez-Quesada et al. addresses the production of Reactive Oxygen Species (ROS) in the olive reproductive tissues as a response to intense metabolism. After localizing the Rboh-type gene (*OeRbohH*) through pollen ontogeny and pollen tune elongation analysis, they found that a balanced activity of tip-located *OeRbohH* during pollen tube growth is important for normal pollen physiology. With respect to fruit development, Diarte et al. studied fruit skin properties in the fruits of nine olive cultivars. They isolated cuticular membranes to analyse the composition of cuticular waxes and cutin monomers, and performed microscopy observations of fruit pericarp sections. Skin surface topography was also analyzed by means of fringe projection and significant differences among cultivars were found and discussed.

Furthermore, Muzzalupo et al. discuss an innovative plant protection approach. They investigated the *in vitro* antifungal activity of two olive extracts against a *Fusarium proliferatum* strain that causes diseases to many economically important plants. Olive extracts are known to exert anti-inflammatory, antioxidant and antimicrobial activities. Among other important findings, the authors show enhanced antifungal effects obtained with the encapsulation of leaf extracts in chitosantripolyphosphate nanoparticles before application. This result suggests that new application techniques can be developed to reduce the dosage of fungicides, which are potentially harmful to human health. Herrera et al. focused on the potential of *Dittrichia viscosa*—a plant common in olive growing areas—for the development of pest management systems in olive orchards. They studied the arthropofauna associated with *D. viscosa* and found that the plant's phenology influences the populations of a variety of arthropods, and that plants of *D. viscosa*, grown along the borders of and inside olive groves, serve as natural reservoirs of predators and *Hymenoptera* parasitoids, protecting olive trees from attacks by any *D. viscosa*-related phytophages. The work by Campos et al. describes a new quantitative PCR analysis based method for the detection of several viruses in olive trees. This innovative detection system was tested in trees of different cultivars, resulting in sensitive and reliable estimation of virus accumulation in infested trees. The system, therefore, can be an effective tool for sanitary certification of olive propagative material.

With the goal of elucidating the effect of abiotic stress on olive growing, Conde-Innamorato et al. investigated the performance of six Mediterranean olive cultivars for the temperate humid climate conditions of Uruguay. Main aspects of phenology, growth, production and oil quality were addressed. This extended study in which 10 growing seasons were considered, revealed that, although the performance of some of the tested cultivars was promising, the alternate bearing is a limiting factor. Their findings reveal a need for further research on cultivar × environment × management interactions. In an assessment of the growing conditions in the neighboring country of Argentina, Miserere et al. evaluated the response of olive trees to sap flow, stomatal conductance, and xylem anatomy to elevated temperature, as well as the effect of crop load on that response. The authors were concerned about the possible effects of climate change in that part of the world, where temperatures are already above those considered as optimal for olive growing. Once again, findings from this work outline the importance of considering the interactive effects of multiple factors when assessing olive performance. The problem of salinity is addressed by Regni et al. They induced saline stress in potted plants of four olive cultivars and studied the effect of salt stress on plant growth and the main physiological and biochemical variables. Photosynthesis, chlorophyll content in the leaves, and plant growth were negatively affected by increasing salinity, while the GSH and CAT enzymatic activities increased. In addition, proline content in leaf tissues decreased, which, in turn, altered osmotic regulation. The greater activity of the two antioxidant enzymes was effective in counteracting the effects of saline stress. The effect of water stress and its influence on the hydraulic performance of olive plants was addressed by Hernandez-Santana et al. More specifically, they evaluated whether hydraulic traits contributed to differences among water treatments in the leaf gas exchange and plant growth of four wild olive genotypes. They found that both the leaf area:sapwood area and the leaf area:root area ratios decreased with water stress, with differences among genotypes. Their findings show that hydraulic allometry adjustments at the plant level were coordinated with the physiological response in leaves, and the authors go on to outline the relevance of plant hydraulic traits, i.e., the efficiency of water transport throughout the plant's hydraulic system, as useful to both anticipate the impact of climate change and improve crop water productivity.

On irrigation, Romero-Trigueros et al. evaluated the impact of using reclaimed saline water and deficit strategies on the ripening indexes, olive yield, and oil quality of "Arbosana" trees. The combined effect of the salt and water stresses did not decrease fruit yield, but did reduce oil yield because the oil

content per fruit dry weight was affected as compared to control trees. Full irrigation with reclaimed saline water decreased oil quality, but with deficit irrigation, the total polyphenols increased. These findings will be of interest to many because the use of low quality water for irrigating olive orchards is expected to increase. On fertilization, Fernández-Escobar offers a review on the question of whether the olive tolerance or resistance to biotic or abiotic stresses can be affected by the nutritional status. It seems that an adequate nutritional status improves the plant's behavior under stress conditions, and the role that certain nutrients have on a number of physiological mechanisms has already been clarified, e.g., the role of potassium on stomatal control. In this work the author explores several of these cases and focuses on the formation of a physical barrier by silicon deposition in the epidermal cells of the leaves, and on the benefits of such barrier to control pest and diseases in olive.

The work by Dias et al. focuses on the effect of pruning on both olive yield and the performance of the Side-Row Continuous Canopy Shaking Harvester. The test was performed in a high density "Picual" orchard, under different pruning treatments. Neither the average yield per tree, for the 4-year testing period, nor the average olive removal efficiency, were affected by the pruning treatment. Goldental-Cohen et al. addressed the mechanical harvesting of table olives. They evaluated the sensitivity of 106 olive cultivars to browning caused by mechanical injury, and identified 14 resistant genotypes that could serve as table olive cultivars. Their findings suggest that cuticle thickness can be an indicator to identify table olive cultivars suitable for mechanical harvesting.

In relation to olive oil quality, 11 olive cultivars were evaluated by El Riachy et al. Their findings show that local and foreign varieties growing in Lebanon produce good quality olive oil. They identified the time course of principal quality variables including ripening, and concluded that further investigations for the characterization and authentication of Lebanese olive oil are required. Concerning olive oil technology, Veneziani et al. studied the impact of the pulsed electric field on the efficiency of the oil extraction process. For three Italian cultivars, they evaluated the diffusion of oil and microconstituents determined by the disruption effects on olive cell tissues carried out by the non-thermal method. Their results show not only an increase in the percentage of oil extracted but also in the concentration of hydrophilic phenols.

All these contributions to OLIVEBIOTEQ'18 demonstrate the scientific community's synergism and cooperation with the industrial olive sector. Our interest is to provide knowledge and technology to study and solve the problems that the industry faces in the cultivation of olive trees, and in the production of high quality olive oil with the objective of increasing efficiency through the use of natural resources while ensuring the profitability for orchardists and producers. The increase in global population taken together with climate change pose new challenges to achieve that target, but this special issue confirms, once again, that science and technology are powerful tools to overcome new problems. The thanks of the committee behind the OLIVEBIOTEQ meetings go out to our colleagues for their continuous efforts to support olive growing and production.

AUTHOR'S NOTE

The authors were conveners of Olivebioteq'18, the 6th International Conference on Olive Tree and Olive Products, held at Seville in October 15-19, 2018.

AUTHOR CONTRIBUTIONS

All authors listed have made a substantial, direct and intellectual contribution to the work, and approved it for publication.

ACKNOWLEDGMENTS

We thank the Consejería de Agricultura, Pesca y Desarrollo Rural of the Junta de Andalucía for its financial support, and all the companies that have collaborated in the development of Olivebioteq'18.

Conflict of Interest: The authors declare that the research was conducted in the absence of any commercial or financial relationships that could be construed as a potential conflict of interest.

frontiers in Plant Science

ORIGINAL RESEARCH
published: 13 March 2019
doi: 10.3389/fpls.2019.00291

Hydraulic Traits Emerge as Relevant Determinants of Growth Patterns in Wild Olive Genotypes Under Water Stress

Virginia Hernandez-Santana[1], Pablo Diaz-Rueda[1], Antonio Diaz-Espejo[1], María D. Raya-Sereno[1,2], Saray Gutiérrez-Gordillo[1,3], Antonio Montero[1], Alfonso Perez-Martin[1], Jose M. Colmenero-Flores[1] and Celia M. Rodriguez-Dominguez[1,4]*

[1] Irrigation and Crop Ecophysiology Group, Instituto de Recursos Naturales y Agrobiología de Sevilla, Consejo Superior de Investigaciones Científicas, Seville, Spain, [2] School of Agricultural Engineering, CEIGRAM, Universidad Politécnica de Madrid, Madrid, Spain, [3] Centro "Las Torres-Tomejil", Instituto Andaluz de Investigación y Formación Agraria y Pesquera, Seville, Spain, [4] School of Biological Sciences, University of Tasmania, Hobart, TAS, Australia

OPEN ACCESS

Edited by:
Johannes Kromdijk, University of Cambridge, United Kingdom

Reviewed by:
Meisha Holloway-Phillips, Australian National University, Australia
Brunella Morandi, University of Bologna, Italy

***Correspondence:**
Virginia Hernandez-Santana
virginiahsa@gmail.com

Specialty section:
This article was submitted to Crop and Product Physiology, a section of the journal Frontiers in Plant Science

Received: *15 November 2018*
Accepted: *22 February 2019*
Published: *13 March 2019*

Citation:
Hernandez-Santana V, Diaz-Rueda P, Diaz-Espejo A, Raya-Sereno MD, Gutiérrez-Gordillo S, Montero A, Perez-Martin A, Colmenero-Flores JM and Rodriguez-Dominguez CM (2019) Hydraulic Traits Emerge as Relevant Determinants of Growth Patterns in Wild Olive Genotypes Under Water Stress. Front. Plant Sci. 10:291. doi: 10.3389/fpls.2019.00291

The hydraulic traits of plants, or the efficiency of water transport throughout the plant hydraulic system, could help to anticipate the impact of climate change and improve crop productivity. However, the mechanisms explaining the role of hydraulic traits on plant photosynthesis and thus, plant growth and yield, are just beginning to emerge. We conducted an experiment to identify differences in growth patterns at leaf, root and whole plant level among four wild olive genotypes and to determine whether hydraulic traits may help to explain such differences through their effect on photosynthesis. We estimated the relative growth rate (RGR), and its components, leaf gas exchange and hydraulic traits both at the leaf and whole-plant level in the olive genotypes over a full year. Photosynthetic capacity parameters were also measured. We observed different responses to water stress in the RGRs of the genotypes studied being best explained by changes in the net CO_2 assimilation rate (NAR). Further, net photosynthesis, closely related to NAR, was mainly determined by hydraulic traits, both at leaf and whole-plant levels. This was mediated through the effects of hydraulic traits on stomatal conductance. We observed a decrease in leaf area: sapwood area and leaf area: root area ratios in water-stressed plants, which was more evident in the olive genotype *Olea europaea* subsp. *guanchica* (GUA8), whose RGR was less affected by water deficit than the other olive genotypes. In addition, at the leaf level, GUA8 water-stressed plants presented a better photosynthetic capacity due to a higher mesophyll conductance to CO_2 and a higher foliar N. We conclude that hydraulic allometry adjustments of whole plant and leaf physiological response were well coordinated, buffering the water stress experienced by GUA8 plants. In turn, this explained their higher relative growth rates compared to the rest of the genotypes under water-stress conditions.

Keywords: hydraulic allometry, leaf hydraulic conductance, leaf:sapwood area ratio, leaf:root area ratio, net photosynthesis rate, stomatal conductance

INTRODUCTION

One of the main challenges facing the world today is to achieve food security, a problem that is aggravated by climate change, natural resource depletion and adverse impacts of environmental degradation (desertification, drought, freshwater scarcity, etc.) (United Nations, 2015). Promising approaches for ensuring the stability of food production under limited water availability involve breeding practices that take advantage of the genetic variability of wild related species and different cultivars that have better adapted to environmental constraints (Nevo et al., 2012; Burnett et al., 2016), such as water-deficit conditions (Ruane et al., 2008; Reddy et al., 2017; Trentacoste et al., 2018). Crop breeders seek to identify and select traits or mechanisms that enable high biological or reproductive yields to be achieved under water-limited conditions (Turner, 2017). As demonstrated in recent studies, some morphological leaf traits (López-Sampson et al., 2017) or processes such as osmotic adjustment (Blum, 2017) explain a large proportion of a tree species' growth, which indicates the potential value of focusing on certain traits to help in the selection of the most productive species or varieties.

Specific knowledge of how hydraulic traits of plants (i.e., the efficiency of water transport throughout the plant) limit plant performance could help to anticipate the impact of climate change (Anderegg et al., 2016) and to improve the security and sustainability of our food supply. Nevertheless, the mechanisms explaining the role of hydraulic traits on growth are complex and only just beginning to be elucidated (Sack et al., 2016). Stomatal control of transpiration is directly or indirectly regulated by changes in plant water status, produced by changes in the soil-to-leaf water transport properties (Buckley, 2005). Under water deficit conditions, stomata close to avoid leaf desiccation but in doing so, carbon dioxide uptake is restricted, and in turn, assimilation rate. Thus, growth can be limited by both carbon supply and turgor pressure. Above-ground hydraulic resistances to water flow mainly lie in leaves (Nardini and Salleo, 2000; Nardini et al., 2001, Brodribb and Holbrook, 2003; Sack et al., 2003), creating a positive link between leaf hydraulics and leaf gas exchange (Brodribb and Holbrook, 2004, 2006; Brodribb et al., 2005, 2007; Brodribb and Jordan, 2008; Scoffoni et al., 2016; Reddy et al., 2017; Xiong et al., 2018). In that sense, leaf hydraulics have been suggested to be important to both water and carbon (C) fluxes (Reich, 2014).

These studies highlight the coordination of maximum values of leaf gas exchange and leaf hydraulic conductance, i.e., under steady-state, non-stress conditions. The potential relevance of this coordination to plant performance under water-deficit conditions has also been investigated (Brodribb and Holbrook, 2004; Lo Gullo et al., 2005; Gortan et al., 2009; Chen et al., 2010; Hernandez-Santana et al., 2016). Besides these short-term mechanisms of stomatal control through leaf hydraulics, plants also respond to water stress through processes influencing equilibria and steady-state behaviors across the entire plant system, adjusting their root/shoot functional balance accordingly (Mencuccini, 2014), i.e., changing the hydraulic allometry of the plant. Nevertheless, in response to water stress, more research is needed to quantify responses in relation to plant anatomy, allocation, architecture and physiology (Addington et al., 2006; Martínez-Vilalta et al., 2009; Zhou et al., 2016; Martin-StPaul et al., 2017) to better understand how development is coordinated in different environments based on the underlying mechanisms (Sterck and Zweifel, 2016).

In relation to olive genotypes, very little is known about how hydraulic traits and photosynthetic assimilation rates in response to water stress influence growth. We know that olive species rely on a range of physiological traits and mechanisms to cope with water deficit (Fernández, 2014; Diaz-Espejo et al., 2018). However, to progress breeding efforts, knowledge of genotypic variation for water-use traits and how they influence plant performance under water stress is required. As such, we conducted an experiment that employed both well-irrigated and water-stress conditions to identify differences in growth patterns among different wild olive genotypes, and to determine whether hydraulic traits may help to explain such differences through their effect on stomatal conductance and photosynthesis rate.

Our objectives were: (i) to evaluate whether different relative growth rate (RGR) patterns representing different physiological strategies arise in wild olive genotypes at leaf, root and plant level and to determine the effects of water availability on these growth patterns and (ii) to determine the role of hydraulic traits (mediated by their effect on leaf gas exchange) at the leaf and whole-plant levels to explain differences in RGR patterns at plant scale in two contrasting olive genotypes.

MATERIALS AND METHODS

Experimental Overview

We conducted our experiment using four genotypes (AMK6, ACZ9, GUA6, and GUA8) selected from a first screening of 39 wild genotypes representing three different subspecies of *Olea europaea* (*europaea* var. *sylvestris*, *guanchica* and *cuspidata*). We assessed the effect of long-term deficit irrigation on growth patterns of these four genotypes, and afterward, we focused on two of them that presented the most contrasting trends in growth (GUA6 and GUA8) to explore the physiological and morphological traits that explained these differences in growth performance. The specific measurements performed during each period of the experiment are provided in **Table 1**.

Screening of 39 Wild Olive Genotypes Before Harvest 1

The seeds for this first screening were obtained from trees located in the World Olive Germplasm Collection of Córdoba (Spain) and Grahamstown (South Africa). The plants were propagated and rooted *in vitro* from zygotic embryos obtained from the prospected seeds during 2014. Seeds were obtained by breaking olive pits with a tube cutter and surface sterilized with hypochlorite. Sterile embryos were obtained from the seeds and placed in test tubes with hormone-free olive medium (Rugini, 1984). After *in vitro* germination, the genotypes were multiplied through propagation of nodal segments in Rugini medium supplemented with 1 mg L^{-1} zeatin (Rugini, 1984).

TABLE 1 | Period, frequency, and number of replicates per genotype and irrigation treatment for the variables measured along the experiment and the genotypes where they were measured.

Measurement period	Dates	Genotypes	Variables	Measurement frequency	Replicates
Harvest 1–Harvest 2	From 06-04-2016 to 05-04-2017	ACZ9 AMK6 GUA6 GUA8	Relative growth rate (RGR, g g^{-1} day^{-1}) Leaf mass fraction (LMF, g g^{-1}) Root mass fraction (RMF, g g^{-1}) Specific leaf area (SLA, m^2 g^{-1}) Specific root length (SRL, m g^{-1}) Net assimilation rate (NAR, g m^{-2} day^{-1}) Maximum stomatal conductance ($g_{s,max}$, mol m^{-2} s^{-1}) Maximum net photosynthesis rate ($A_{N,max}$, μmol m^{-2} s^{-1})	Once Once Once Once Once Once Fortnightly-Monthly Fortnightly-Monthly	Four Four Four Four Four Four Two (2016) and three (2017) Two (2016) and three (2017)
After Harvest 2	From 06-04-2017 to 29-08-2017	GUA6 GUA8	Maximum stomatal conductance ($g_{s,max}$, mol m^{-2} s^{-1}) Maximum net photosynthesis rate ($A_{N,max}$, μmol m^{-2} s^{-1}) Maximum velocity of carboxylation (V_{cmax}, μmol m^{-2} s^{-1}) Mesophyll conductance (g_m, mol m^{-2} s^{-1}) Leaf water potential (Ψ_{leaf}, MPa) Foliar N (gN m^{-2}) Osmotic pressure at full turgor (Π_0, MPa) Turgor loss point (TLP, MPa) Vulnerability curve of leaf hydraulic conductance (K_{leaf}, mmol m^{-2} s^{-1} MPa^{-1}) Leaf:sapwood area (cm^2 mm^{-2}) Leaf:root area (m^2 m^{-2})	Twice Twice Once Once Twice Once Once Once Once Once	Four Four Four Four Four Four – Four Four

The explants were kept in an *in vitro* culture chamber at 25°C and subjected to a photoperiod of 16 h light/8 h darkness, using LED illumination 70% red plus 30% blue (70/30) with 34 μmol m^{-2} s^{-1} of photosynthetic photon flux. Plants were rooted in 1/2x Rugini medium supplemented with 0.8 mg/L Naphthaleneacetic acid for 3 weeks. After *ex vitro* acclimatization, plants were grown under greenhouse conditions for 9 months in 1 L pots. Healthy and homogenous plants were selected and transplanted into 10 L pots containing vermiculite:peat:perlite substrate (40:40:20) and acclimatized for a further 2 months. The 39 genotypes were evaluated during 2015 to assess their water use and fresh weight below and above-ground components as well as the whole plant. For each of these 39 genotypes, six well-irrigated plants (100% field capacity) and six water-stressed plants (60% field capacity) were maintained. Every 2–3 days water loss was quantified and plants were re-watered up to their corresponding water status. Plants were harvested at the end of the trial, and the fresh and dry weights of shoots (leaves and stems) and roots were recorded.

Experimental Management During the Measurements Performed in AMK6, ACZ9, GUA6, and GUA8 From Harvest 1 to Harvest 2

We selected these four genotypes because they presented contrasting behaviors to water deficit in terms of water use and plant, shoot and root fresh weight (**Supplementary Figure S1**). Plants from these four genotypes were grown outdoors in 25 L pots in La Hampa CSIC experimental orchard, near Seville (Spain) (37°17′N, 6°3′W, altitude 30 m), filled with soil (sandy loam) from this orchard. The size of the pot was not limiting for plant growth. This was based on the observation that roots did not grow enough to fill the entire volume of the pots and some parts of the soil were not explored by them at the end of the experiment. The pots were distributed randomly in rows of 20 plants at 1 × 1.5 m, alternating well-watered (WW) rows and water-stressed rows (WS). This distribution was sufficient to avoid shading by neighboring plants (based on *in situ* observations). Initial sizes of the plants are shown in **Table 2** and although sizes were different among the groups,

TABLE 2 | Average and standard error of the leaf area, basal diameter and maximum height of the plants used in the beginning of the experiment (H1).

		Leaf area (cm^2)	Basal diameter (mm)	Maximum height (cm)
WW	ACZ9	370.45 ± 27.87	6.16 ± 0.35	92.92 ± 2.47
	AMK6	89.81 ± 15.45	4.74 ± 0.39	51.82 ± 7.07
	GUA6	178.49 ± 18.58	4.51 ± 0.29	72.27 ± 9.49
	GUA8	59.09 ± 15.92	3.47 ± 0.14	20.84 ± 6.08
WS	ACZ9	518.15 ± 28.42	6.37 ± 0.23	99.92 ± 10.33
	AMK6	99.59 ± 10.78	4.59 ± 0.22	53.72 ± 4.11
	GUA6	257.13 ± 13.95	5.68 ± 0.20	83.02 ± 5.64
	GUA8	47.75 ± 12.11	2.99 ± 0.23	17.70 ± 3.26

we calculated growth using RGR, which uses initial and final sizes, to minimize size dependent effects (Hunt et al., 2002). The experiments lasted for 19 months (from February 2016 to August 2017) including the measurements specifically performed only in GUA6 and GUA8 (see next section). The plants of all genotypes were the same age (16 months) when the experiment started. Plants were well-irrigated from February 18 to April 26, 2016. After this date they were irrigated differently until the end of the experiment: WW plants, in which plants were irrigated daily to non-limiting soil water conditions to achieve the highest possible stomatal conductance ($g_{s,max}$); and WS, in which plants were irrigated to a level representing 40% of the $g_{s,max}$ measured in WW plants throughout the experiment to achieve a moderate water-stress status. To achieve these values of $g_{s,max}$, we conducted regular gas exchange measurements and modified the irrigation schedule accordingly (**Figure 1**), i.e., reducing or increasing the frequency and time of irrigation to change the total amount of water depending on WS $g_{s,max}$ values compared to WW $g_{s,smax}$. Reference evapotranspiration (ET_o) was collected from a nearby standard weather station (37°13′N, 6°8′W) belonging to the Agroclimatic Information Network of the local government (Junta de Andalucía, Spain). Two harvests were conducted: on April 6, 2016 after a period when all the plants were well irrigated (harvest 1, H1) and on the April 5, 2017, to assess the effect of the long-term deficit irrigation treatment on the olive plants (harvest 2, H2).

Experimental Management During the Measurements Performed in GUA6 and GUA8 After Harvest 2

After H2, 20 pots of GUA6 and GUA8 were kept under the described irrigation treatments (WS and WW) at the same field experimental site prior to conducting leaf hydraulic conductance measurements, pressure–volume curves and photosynthetic response curves, together with additional gas exchange, plant water status and morphological measurements (**Table 1**).

Growth Parameters (AMK6, ACZ9, GUA6, GUA8, From Harvest 1 to Harvest 2)

Plant growth was determined by harvesting four plants per genotype and irrigation treatment (n = 4) at H1 and H2. Before harvesting, basal stem diameter was measured to estimate sapwood area (m^2). After harvesting, total plant leaf area (m^2) was determined using a Li-Cor 3000-A area meter (equipped with a LI-3050C Transparent Belt Conveyor; Li-Cor, Lincoln, NE, United States). To calculate the biomass (g) of roots, stems and leaves, each component was separated and oven-dried at 60°C for at least 2 days. The following plant traits were calculated for each harvest based on the material obtained: leaf mass fraction (LMF, g g^{-1}), root mass fraction (RMF, g g^{-1}), specific leaf area (SLA, m^2 g^{-1}) and specific root length (SRL, m g^{-1}). The data from each genotype and irrigation treatment for the two consecutive harvests were used to compute the net assimilation rate (NAR; g m^{-2} day^{-1}) and the RGR (g g^{-1} day^{-1}) for the plant (RGR_{plant}), roots (RGR_{root}) and leaves (RGR_{leaf}) according to Hunt et al. (2002):

$$RGR = NAR \times SLA \times LMF \quad (1)$$

Each component was calculated as follows:

$$(1/W)\,(dW/dt) = (1/L_A)\,(dW/dt) \times L_A/L_W \times L_W/W \quad (2)$$

where t is time between harvest 1 and 2, W is total dry weight per plant, L_A is total leaf area per plant and L_W is total leaf dry weight per plant.

Root Length and Area (AMK6, ACZ9, GUA6, GUA8, From Harvest 1 to Harvest 2)

The root samples were separated into two groups: fine roots or roots thinner than 2 mm and roots thicker than 2 mm. From the first group of roots (thinner than 2 mm), roots were randomly subsampled, scanning 10% of total biomass using the WinRHIZO system (Regent Instruments, Québec, Canada). The roots thicker than 2 mm were not considered in this analysis as fine roots constitute the primary exchange surface between plants and soil (Jackson et al., 1997). The scanning enabled us to directly obtain the root length (cm) and root area (cm^2) through the WinRHIZO software.

Field Gas Exchange Measurements (AMK6, ACZ9, GUA6, GUA8, From Harvest 1 to Harvest 2)

To verify our irrigation treatments, maximum stomatal conductance ($g_{s,max}$ mol m^{-2} s^{-1}) and net photosynthesis rate ($A_{N,max}$, μmol m^{-2} s^{-1}) were measured at ∼10.30–11.30 GMT from May 2016 to April 2017 (H2) with a portable gas analyzer (Li-6400; Li-Cor, Lincoln, NE, United States) using a 2 × 3 cm standard clear-top chamber under ambient light, vapor pressure deficit and CO_2 conditions in healthy, sunny leaves. Preliminary measurements demonstrated that $g_{s,max}$ occurred at this time of the day. During this period, gas exchange was measured fortnightly during the summer months, and once every month during the rest of the year. In 2016 we measured gas exchange in one leaf from each of two plants of every genotype and for the two irrigation treatments (n = 2). From January 2017 to April 2017 we increased the number of sampled plants to three (n = 3).

Field Gas Exchange and Leaf Water Potential Measurements (GUA6, GUA8, After Harvest 2)

In addition to monitoring $g_{s,max}$, gas exchange was measured once in June and July 2017 together with leaf water potential measurements to have concurrent measurements of both variables for the GUA6 and GUA8 genotypes (four plants per irrigation treatment and genotype).

Leaf water potential (Ψ_{leaf}) was undertaken immediately after gas exchange measurements with a Scholander-type pressure chamber (Soilmoisture Equipment Corp., Santa Barbara, CA, United States) in one fully expanded leaf per plant.

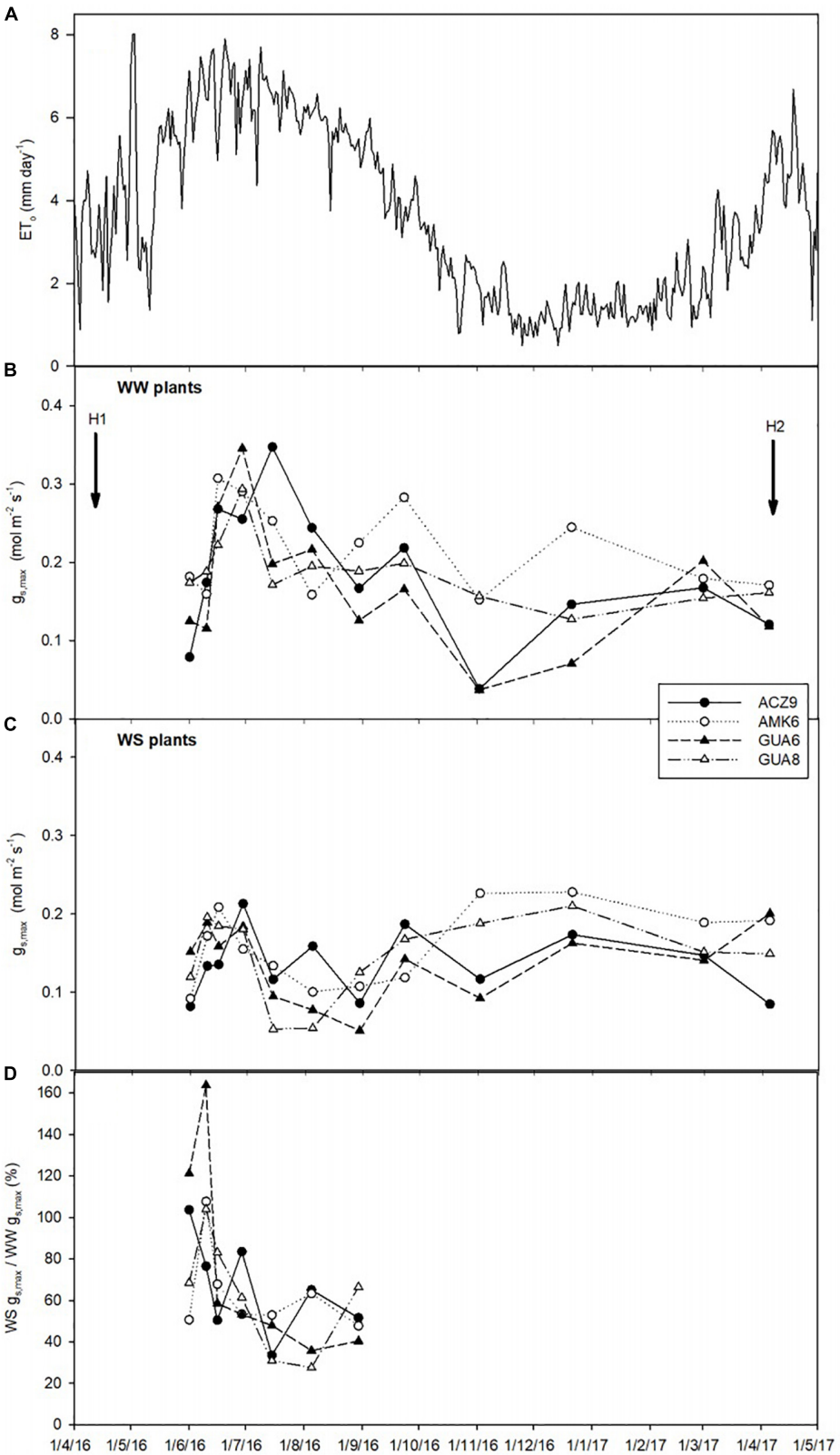

FIGURE 1 | Temporal dynamics of reference evapotranspiration, ET_o **(A)**, maximum stomatal conductance ($g_{s,max}$) for the different genotypes for well-watered plants (WW) **(B)**, water-stressed plants (WS) **(C)**, and percent of WS compared to WW $g_{s,max}$ **(D)** (only June–August data shown for clarity purposes). Each data-point in 2016 represents the average of two plants, while from January to April 2017 the average of three plants is used. H1 and H2 indicate when harvests 1 and 2 took place.

Leaf Hydraulic Vulnerability Curves (GUA6, GUA8, After Harvest 2)

Leaf hydraulic conductance (K_{leaf}, mmol m^{-2} s^{-1} MPa^{-1}) was measured after H2 (June of 2017) in fully developed, current year and sun-exposed leaves of WW plants of the GUA8 and GUA6 genotypes to obtain leaf hydraulic vulnerability curves ($\Psi_{leaf} - K_{leaf}$). To measure K_{leaf}, we used the Evaporative Flux Method (EFM, Scoffoni et al., 2012), with the results obtained by this method being similar to K_{leaf} measurements in olive achieved by the Dynamic Rehydration Method (DRKM, Blackman and Brodribb, 2011) as demonstrated by Hernandez-Santana et al. (2016). Briefly, the method consists of measuring the flow rate of water through the leaf (mmol m^{-2} s^{-1}) and the corresponding Ψ_{leaf}. To achieve this, we sealed the pots containing the plants at the field in dark plastic bags containing wet paper towels inside to create a low-demand atmosphere. The plants were left to equilibrate at the laboratory for at least 30 min and then, to measure the leaf water flow, leaves were cut from the bagged plants under purified water and rapidly connected to a flowmeter consisting of silicon tubing containing purified, degassed water. The tubing was connected to a pressure transducer (PX26-005GV, Omega Engineering Ltd., Manchester, United Kingdom), which, in turn, was connected to a Campbell data logger CR1000 (Campbell Scientific Ltd., Shepshed, United Kingdom) which recorded water flow readings every 1 s. Reference tubing of different resistances was used to minimize measurement errors (Sack et al., 2011; Melcher et al., 2012). Once connected, the leaves were allowed to transpire inside a Li-Cor 6400-22 Opaque Conifer Chamber for at least 30 min with the photosynthetically active radiation (PAR) level set to 1,200 μmol m^2 s^{-1} using the Li-Cor 6400-18A RGB Light Source (both instruments were from Li-Cor, Lincoln, NE, United States) until the water flow was stable (coefficient of variation < 5% for the last 5 min). We chose EFM because using the Li-6400 gas analyzer also allowed us to measure the water vapor flux simultaneously with the liquid water flow. When both gas and liquid flows reached a steady state, leaves were removed from the tubing and stored for equilibration in dark and halted transpiration conditions for at least 30 min. Then, Ψ_{leaf} was measured with a Scholander-type pressure chamber (PMS Instrument Company, Albany, OR, United States). The plants were left to gradually dehydrate in the field so that a wide range of hydraulic conductance and Ψ_{leaf} values were obtained.

Pressure–Volume Curves: Turgor Loss Point and Osmotic Pressure at Full Turgor (GUA6, GUA8, After Harvest 2)

We used one leaf from four plants for each irrigation treatment (WW, WS) and genotype (GUA6 and GUA8) to calculate pressure–volume curves (n = 4). Leaves were sampled in the morning of August 29, 2017 and were rehydrated for 24 h, then left to desiccate. Leaf weight and Ψ_{leaf} were measured many times during that desiccation period until the leaves reached minimum Ψ_{leaf} values of ca. −5 MPa. The turgor loss point (TLP, MPa) and osmotic pressure at full turgor (Π_0, MPa) were calculated according to Sack and Pasquet-Kok (2017).

Photosynthetic Response Curves (GUA6, GUA8, After Harvest 2)

Four A_N–C_i response curves (the response of net CO_2 assimilation to varying intercellular CO_2 concentration) were measured between 09:00 and 13:00 GMT on different days in July 2017 for the GUA6 and GUA8 genotypes and for each irrigation treatment (WW and WS) (four repetitions, 16 curves per genotype). Measurements were made using two LI-6400 portable photosynthesis systems (LI-COR, Lincoln, NE, United States) at 28°C (close to ambient temperature), saturating photosynthetic photon flux density (1,600 μmol m^{-2} s^{-1}) and an ambient CO_2 concentration (C_a) of between 50 and 1,150 μmol mol^{-1}. After steady-state photosynthesis had been achieved (usually after 20–40 min exposure to saturating PPFD), the response of A_N to varying C_i was measured by lowering C_a stepwise from 400 to 50 μmol mol^{-1}, returning to 400 μmol mol^{-1} and then increasing C_a stepwise from 400 to 1,150 μmol mol^{-1}. Each A–C_i curve comprised 16 measurements. The maximum carboxylation rate (V_{cmax}, μmol m^{-2} s^{-1}), maximum rate of electron transport (J_{max}, μmol m^{-2} s^{-1}) and mesophyll conductance to CO_2 (g_m, mol m^{-2} s^{-1}) were estimated by the curve-fitting method proposed by Ethier and Livingston (2004). Prior to curve analysis, CO_2 leaks in the chamber were corrected by following the procedure described in Flexas et al. (2007). Rubisco kinetic parameters were taken from Bernacchi et al. (2002). Values of V_{cmax}, J_{max} and g_m obtained from the A–C_i curve analysis were recalculated at 25°C using the temperature dependence parameters specific for olive reported in Diaz-Espejo et al. (2006, 2007).

Foliar N (GUA6, GUA8, After Harvest 2)

Leaf samples were taken for N analysis from the H2 samples of all the genotypes and irrigation treatments. Enough current-year leaves were sampled to have at least 0.4 g of dry weight to analyze leaf N. Samples were washed in distilled water, dried at 70°C until constant weight, ground and passed through a 500 mm stainless-steel sieve. N concentration was determined by Kjeldahl method.

Data Processing and Statistical Analysis (AMK6, ACZ9, GUA6, GUA8)

Statistical analyses were performed to assess the effect of the irrigation treatment and genotype on leaf, root and the whole-plant RGR values, in addition to LMF, RMF, SLA, SRL, and NAR for H2. V_{cmax}, g_m, Π_0, TLP, foliar N, leaf area – root area ratio (LA:RA) and leaf sapwood area ratio (LA:SA) were also estimated for the GUA6 and GUA8 genotypes after H2. One-way ANOVA was used in cases where more than two levels were compared, while the Student's t-test was used for comparisons between two levels. No transformations were needed to achieve normality. Differences were considered significant for values of $p < 0.05$. SigmaPlot software (version 12.0, Systat Software, Inc., San Jose, CA, United States) was used to conduct these analyses and provide best-fit curves to the dataset to determine the relationships between the different variables analyzed. In addition, two-way ANOVA was used to analyze the interaction between irrigation treatment and

genotype RGR at leaf, root and plant level. We used a mixed model in which we included genotype, irrigation treatment and the interaction between both variables. Finally, we also used analysis of covariance (ANCOVA) that included the interaction term of each component related to RGR with irrigation treatment to test its effect on the relationships established for RGR. For these analyses we considered that variables were linearly related. These analyses were conducted with R software (R Core Team, version 3.4.3, 2018) using the "lm()" function.

Path analysis (structural equation modeling with no latent variables) was used to compare four alternative conceptual models to reveal the causal relationships that link hydraulic variables with A_N through their effect on g_s. We stated *a priori* the relationships among variables with a strong mechanistic or well-established and accepted empirical basis only (Shipley, 2000). The main underlying hypotheses were: (i) A_N is determined mainly by g_s, g_m, and V_{cmax} (Niinemets et al., 2009; Flexas et al., 2014; Perez-Martin et al., 2014); (ii) g_s is influenced by leaf hydraulic conductance (Brodribb and Holbrook, 2004; Sack and Holbrook, 2006; Scoffoni et al., 2016), LA:SA and LA:RA (Magnani et al., 2002; Addington et al., 2006; Martínez-Vilalta et al., 2009); and (iii) the major determinant of V_{cmax} is foliar nitrogen (Walcroft et al., 1997; Diaz-Espejo et al., 2006, 2007; Niinemets, 2012). We compared four models that differed according to whether K_{leaf}, LA:SA and LA:RA influence g_s directly (see **Figure 4A**), LA:SA and LA:RA are covariates (see **Figure 4B**), LA:RA effects on g_s are mediated by LA:SA (see **Figure 4C**) and LA:RA and LA:SA influence g_s through their impact on K_{leaf} (see **Figure 4D**). For the path analysis we have a total of 16 data points obtained from 16 plants, for each variable: 4 replicates × 2 genotypes × 2 treatments. All variables were measured or estimated on each of the 16 plants. To perform this analysis it is not important to consider or compare treatments or genotypes, but to provide estimates of the magnitude and significance of hypothesized causal connections between sets of variables. Although our small sample size (16 points for each variable) limits the complexity of the models and the strength of our conclusions, the results on how the hydraulic variables are related to each other and to g_s complement the simple regression analyses and comparisons conducted. All regression, covariance and variance relationships were determined and are shown in path diagrams. Gas exchange data used for the analysis were those measured in the A–C_i curves: average g_s and A_N obtained at 400 ppm CO_2 and vapor pressure deficit between 1.5 and 2 kPa. Leaf hydraulic conductance was estimated using the vulnerability curves and Ψ_{leaf} measured for those same plants around the time the data for the curves were obtained. The remaining variables were measured or calculated with the data from each plant. All variables were Ln-transformed before analysis to obtain linear relationships because structural equation modeling assumes linearity between variables and (approximate) multivariate normality (Shipley, 2000). Each path model was fitted and compared with the observed results using maximum likelihood. We conducted a Confirmatory Factor Analysis to test whether the Fit Indices of the model were acceptable in terms of similarity between observed and predicted matrix [P-value (chi-square) > 0.05], discrepancy adjusted for sample size [Comparative Fit Index (CFI) > 0.9], and residuals of the model [Root Mean Square Error of Approximation (RMSEA < 0.06)]. Path analyses were conducted and diagrams prepared using the R packages "lavaan" (Rosseel, 2012) and "semPlot" (Epskamp, 2013).

RESULTS

Variability in Plant Relative Growth Rates Among Genotypes (AMK6, ACZ9, GUA6, GUA8) and Irrigation Treatments

Due to the deficit irrigation, $g_{s,max}$ in the WS plants of the four genotypes selected was lower (around 37%) than that in WW plants, but only for the hottest and driest months (mid-June to September of 2016) (**Figures 1B–D**). In the remaining months, due to the lower evaporative demand of the experimental site (**Figure 1A**), the reduced irrigation applications were not sufficient to produce a marked reduction of $g_{s,max}$.

Although the irrigation protocol based on the reduction of $g_{s,max}$ provoked only moderate water stress conditions in the hottest months, it was enough to decrease RGR values of WS plants significantly and to different extents amongst genotypes compared to WW plants for the period from April 2016 (H1) to April 2017 (H2) in all genotypes (**Figure 2**). At the three levels considered, leaf, root and plant, there was a statistically significant interaction between the irrigation treatment and genotype ($p < 0.001$), i.e., the effect of irrigation depends on the genotype. Whereas GUA6 showed the highest RGR in WW plants, both in leaves ($6.54 \times 10^{-3} \pm 0.42 \times 10^{-3}$ g g^{-1} day^{-1}; **Figure 2A**) and roots ($7.90 \times 10^{-3} \pm 0.23 \times 10^{-3}$ g g^{-1} day^{-1}; **Figure 2B**), GUA8 presented the highest RGR in WS plants. Moreover the RGR_{root} of GUA8 was statistically similar ($p > 0.05$) between treatments, in contrast to the rest of the genotypes where RGR_{root} was significantly lower in WS than in WW plants ($p < 0.05$). Based on these findings, GUA8 was the genotype in which RGR was least affected by water stress.

A regression analysis was conducted to relate RGR_{plant} with each of its components at the leaf level (LMF, SLA, and NAR) and corresponding parameters at the root level (RMF and SRL) (**Figure 3**) by pooling together all genotypes and irrigation treatments. Variations in RGR_{plant} were mainly explained by changes in NAR (**Figure 3C**) based on the strong correlation between parameters ($R^2 = 0.79$; $p < 0.01$). The highest RGR_{plant} values were found for those genotypes with the highest NAR. ANCOVA revealed non-significant differences in the regression lines between WW and WS plants. The other traits studied related to carbon allocation (LMF and RMF) and anatomy (SLA and SRL), both for leaves and roots, were not significantly correlated with RGR_{plant}. While SLA and SRL showed similar patterns in each genotype, with both parameters reduced under WS conditions (**Figures 3B,E**), the different magnitude of the change for each genotype prevented a common trend from being identified.

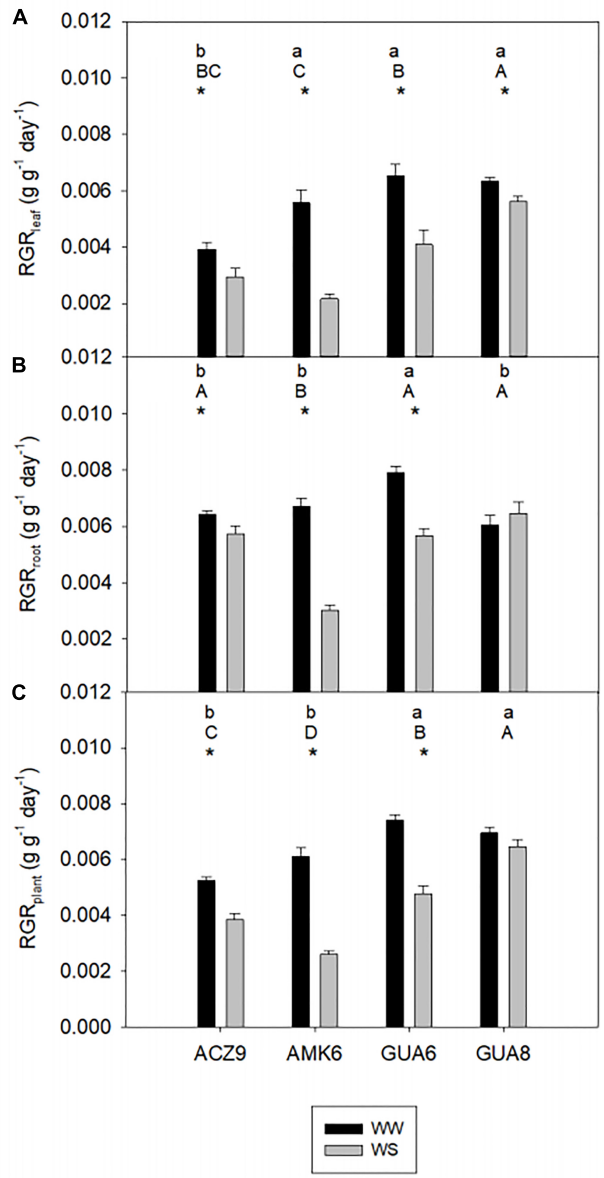

FIGURE 2 | Comparison of relative growth rate (RGR) from harvest 1 to harvest 2 of leaf **(A)**, root **(B)**, and the whole-plant **(C)** biomass for the different genotypes of well-watered plants (WW) and water-stressed plants (WS). Bars are the average of four plants ±1 SE. Lowercase letters indicate statistical differences among the genotypes for WW plants and capital letters for WS plants. The asterisks indicate significant differences ($p < 0.05$) between WW and WS plants for each genotype.

The Role of Hydraulic Traits in GUA8 and GUA6 to Explain Relative Growth Rate Patterns

To further explain the above results showing NAR as the main parameter related to changes in RGR_{plant}, we focused on gas exchange dynamics at the leaf level of the GUA6 and GUA8 genotypes, including both irrigation treatments, which provided the most contrasting results in terms of growth for the different irrigation treatments. While GUA6 had the highest RGR under the WW conditions (although not significantly so), the same was true for GUA8 under the WS conditions. Pooling together the data for GUA6 and GUA8 to conduct a Path Analysis, we found two path models (**Figures 4A,C**) that were better than the other two (**Figures 4B,D**) in terms of fit statistics (see Materials and Methods section for further details). These two best-fitting models differed from each other in terms of how LA:RA impacted on g_s. In the model shown in **Figure 4A** the effect is direct, whereas in **Figure 4C** the impact is indirect and mediated by LA:SA. Here, the total variance explained for A_N was 0.88 and 0.85 for the models in **a** and **c**, respectively. The regression between LA:RA and g_s or LA:SA was not significant in any case, meaning that LA:SA and K_{leaf} were the main variables controlling g_s. The path coefficient was lower in model **a** for K_{leaf} (0.42) than for the LA:SA path coefficient (0.49), whereas in model **c** this trend changed slightly (0.47 and 0.45 for the K_{leaf} and LA:SA path coefficients, respectively). Stomatal conductance was the variable determining A_N to the greatest extent across the models.

At the leaf level, we further assessed differences in gas exchange and related variables for the different genotypes and irrigation treatments. We observed that g_s was slightly higher in GUA6 than in GUA8 for all levels of leaf water potential (**Figure 5A**), and that A_N was similar between genotypes for all levels of g_s (**Figure 5C**). As a result, the water-use efficiency calculated for GUA8 was also higher than for GUA6, in the sense that, to assimilate 1 μmol of CO_2, GUA6 plants transpired more water than GUA8. Accordingly, g_m was higher for GUA8 than GUA6 (**Table 3**), with this difference more evident in WS plants ($p < 0.05$; GUA6: 0.15 ± 0.03 mol m^{-2} s^{-1}; GUA8 0.24 ± 0.02 mol m^{-2} s^{-1}). In addition, V_{cmax} and foliar N (**Table 3**) followed the same trends for g_m, with statistically significant differences ($p < 0.05$) seen in the foliar N of WS plants. The hydraulic vulnerability curves for both genotypes were similar over the range of Ψ_{leaf} values and followed a sigmoidal shape (**Figure 5B**). No significant differences between irrigation treatments or genotypes were seen for the other hydraulic traits (Π_0 and TLP) analyzed (**Table 3**).

At whole-plant level, values of LA:SA and LA:RA ratios were always lower for GUA8 than GUA6 and for WS compared to WW. These differences were significant ($p < 0.05$) for the LA:RA ratio between the genotypes in WS plants, and between the irrigation treatments in the case of LA:SA for GUA8 (**Table 3**).

DISCUSSION

Our results suggest that whole-plant hydraulic allometry adjustments together with shorter-term leaf physiological responses allowed the GUA8 genotype to buffer the impact of the drought stress experienced, leading to a RGR that was less-affected by water stress compared to the other olive genotypes tested. At the whole-plant level, the observed fine tuning of the supply-demand hydraulic system made this genotype more capable of extracting and transporting water. Also, as the total leaf area was lower, water transport capacity on a leaf specific

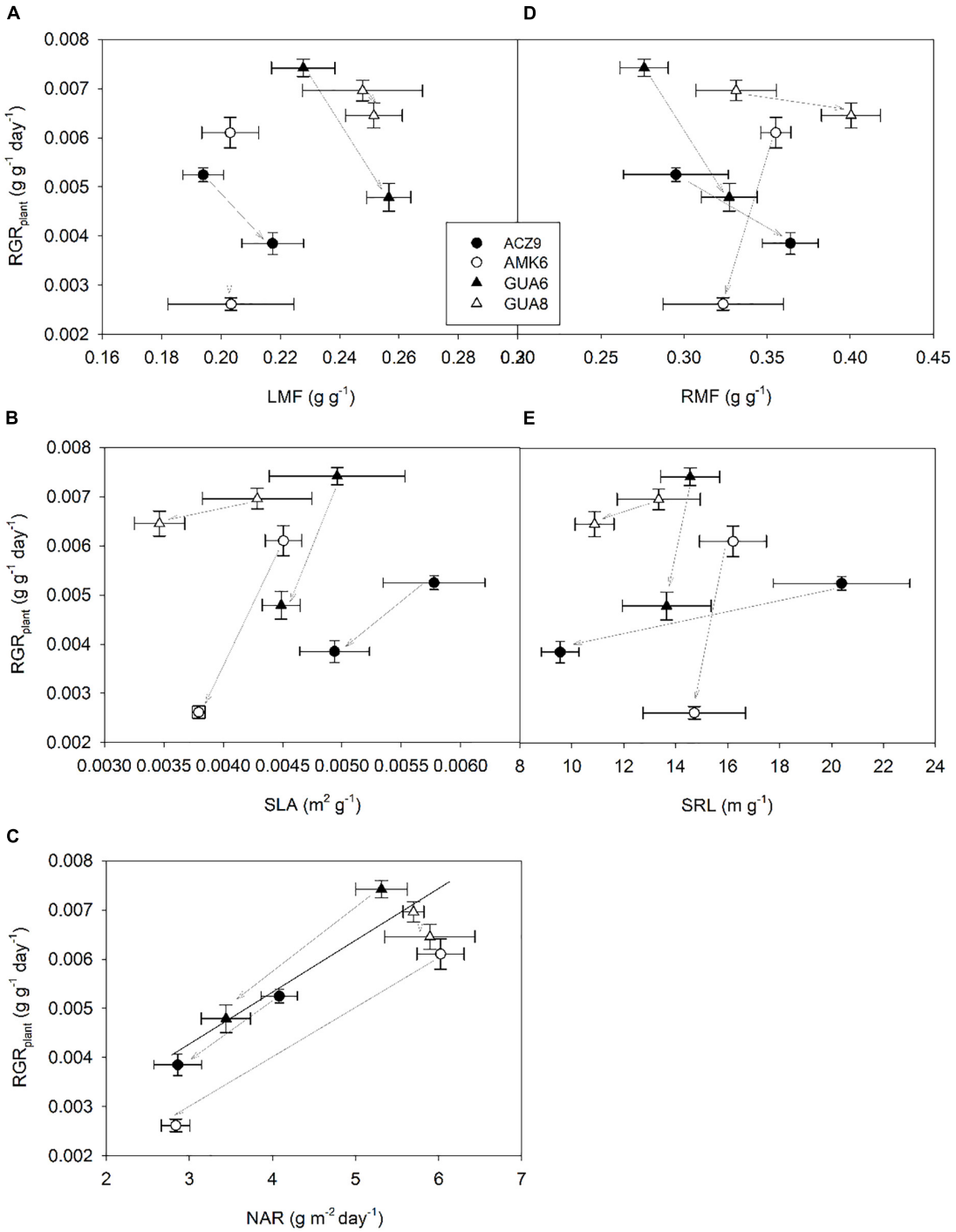

FIGURE 3 | Relationship between plant relative growth rate (RGR_{plant}) (H1 to H2) and leaf mass fraction; LMF **(A)**, specific leaf area; SLA **(B)**, net assimilation rate; NAR **(C)**, root mass fraction; RMF **(D)** and specific root length; SRL **(E)** for the different genotypes for well-watered (WW) and water-stressed (WS) plants. Each point is the average of four plants ±1 SE. Gray arrows indicate the change provoked by water stress (from WW to WS plants).

basis was higher. At the leaf level, the greater photosynthetic capacity in GUA8 WS than in GUA6 WS plants (higher g_m and V_{cmax} in WS plants, **Table 3**) also resulted in a slightly higher water-use efficiency for GUA8 under conditions of water stress (**Figure 5C**). Although it is difficult to estimate the below-ground biomass in adult trees grown under field conditions, more work is needed in adult trees to verify the patterns found in this study in juvenile olive seedlings growing in pots.

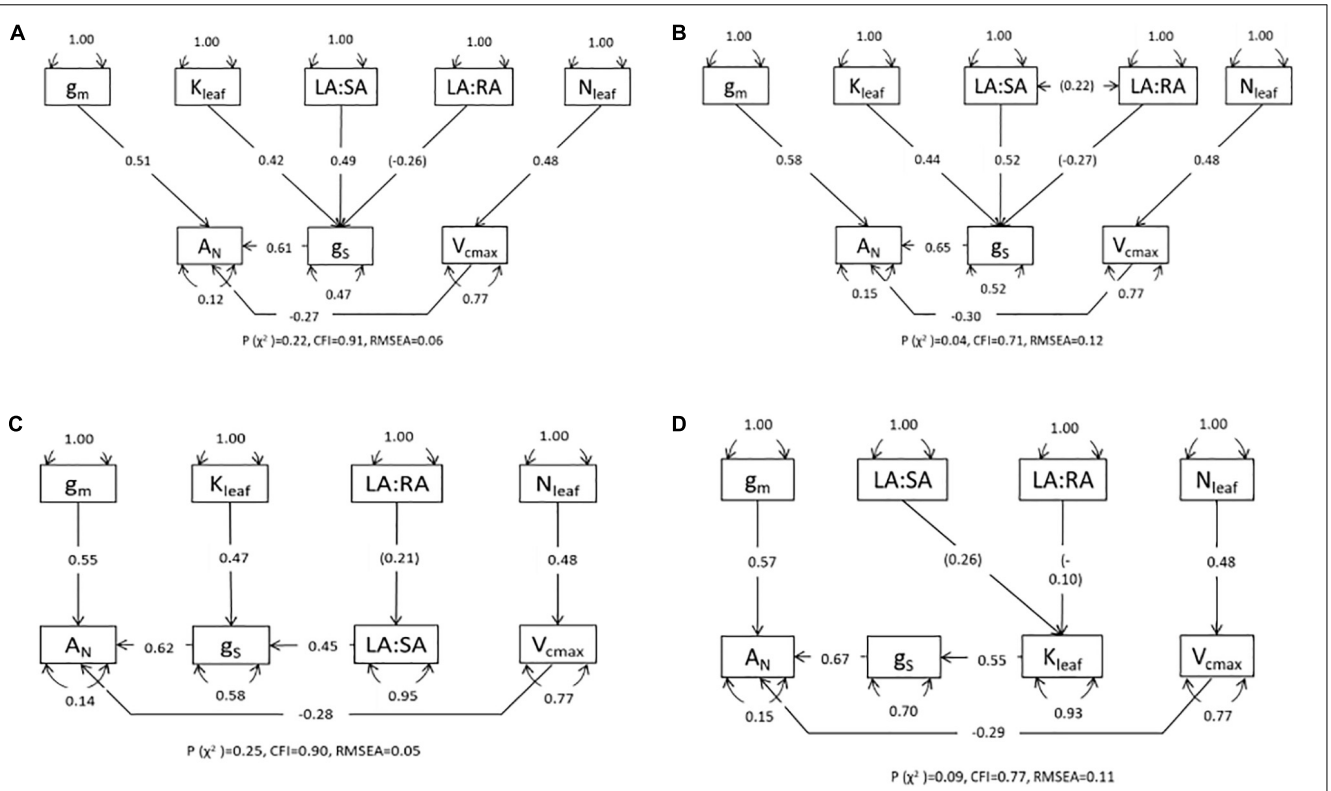

FIGURE 4 | Path diagrams for GUA6 and GUA8 from the plants measured after harvest 2 for the four models describing causal relationships with photosynthesis (A_N) mediated by stomatal conductance (g_s): **(A)** direct impact of leaf hydraulic conductance (K_{leaf}), leaf area to sapwood area ratio (LA:SA) and leaf area to root area ratio (LA:RA); **(B)** same as in **(A)** but both ratios represented as covariance; **(C)** direct effect of K_{leaf} but indirect effect of LA:RA mediated by LA:SA; and **(D)** indirect effect of LA:RA and LA:SA through their effect on K_{leaf}. Single-ended arrows and associated number indicate direct relationships and standardized parameter estimates of regression; double-ended arrows represent covariance; the curved double-ended arrows are the variances of each variable. In brackets are the non-significant parameters. V_{cmax}, maximum velocity of carboxylation; g_m, mesophyll conductance; N_{leaf}, foliar nitrogen. Overall fit statistics for each path model [p (χ^2), CFI (Comparative Fit Index) and RMSEA (Root Mean Square Error of Approximation)] are shown at the bottom of each diagram.

Differential Response of Relative Growth Rate to Water Stress in Olive Genotypes

Our results showed that although $g_{s,max}$ was only significantly reduced in summer, this decrease was sufficient to decrease RGR in different olive genotypes over a whole year (**Figure 1**). Such a long experimental period for this kind of study, coupled with long-term responses to soil and atmospheric drought as described here, are not usual. Although this experiment length adds value to the study, it could influence the results due to ontogenetic drift. As described by Rees et al. (2010), RGR is not totally size independent, because most plants become increasingly inefficient as they get larger because of self-shading, tissue aging, allocation to structural components, etc. However, such an effect is not likely to have happened in our study since there is no correspondence between the size of the plants (**Table 2**) and RGR (**Figure 2**) for either treatment. Despite belonging to the same species and sharing most of their water-stress response traits, differences were observed among the studied genotypes, with the GUA8 genotype having a significantly less-affected RGR as a result of decreased stomatal conductance in response to water stress (**Figure 2**). From the components of the RGR analysis, only physiological changes (NAR) were strongly and positively correlated to RGR_{plant} among the genotypes (**Figure 3**). Similar patterns have been found in other woody species (Galmés et al., 2005; Shipley, 2006), particularly under the high radiation of field experiments in comparison to laboratory or greenhouse experiments (Shipley, 2002). Other plant growth components did not show a common pattern of change among the genotypes analyzed, although in general denser roots and leaf tissues were found for GUA8 than for the other genotypes, which is consistent with GUA8 being less affected by water stress. The influence of the different components on the decrease in RGR imposed by drought conditions has been shown to be strongly dependent on the species in question, reflecting differences in response and adaptation to environmental constraints (Galmés et al., 2005).

Coordinated Response of Hydraulic Properties and Leaf Gas Exchange to Water Stress

We further assessed relationships between, and differences in, physiological parameters that might influence gas exchange and thereby explain why the RGR of GUA8 was less affected by water stress than GUA6. At the leaf level, and for both genotypes, the net photosynthesis rate was shown to be

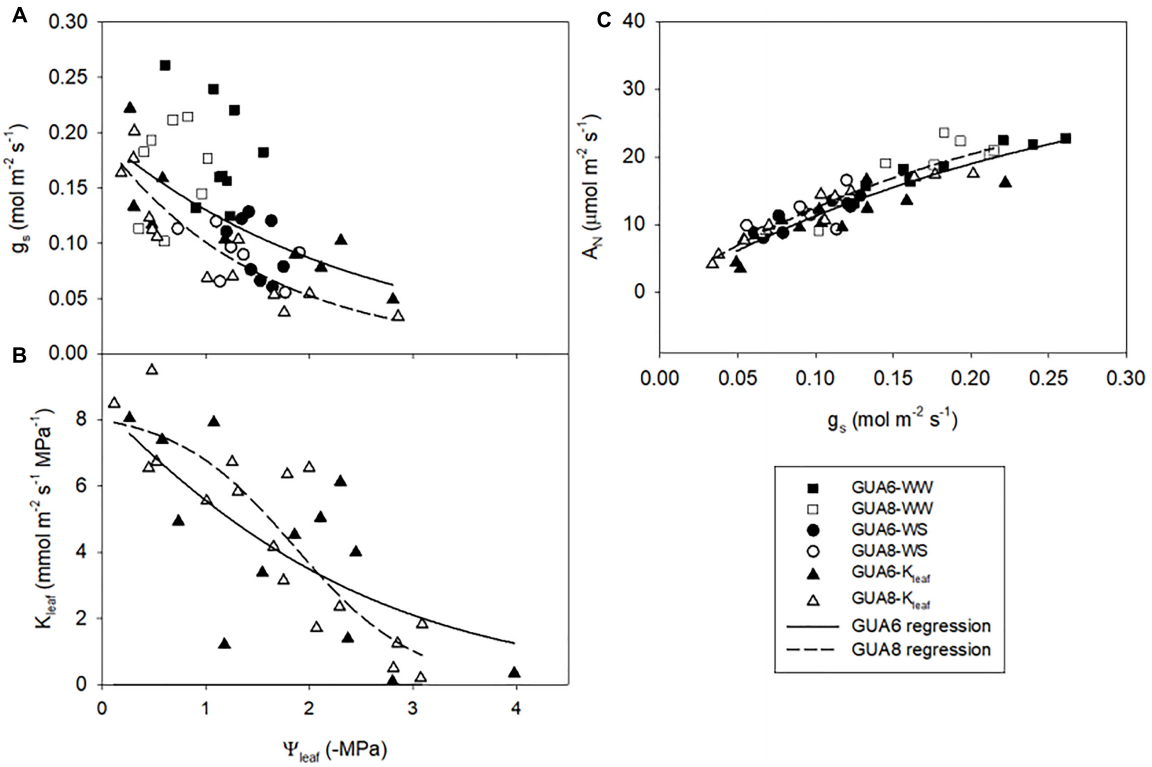

FIGURE 5 | Response curves of stomatal conductance; g_s **(A)** and leaf hydraulic conductance; K_{leaf} **(B)** to leaf water potential Ψ_{leaf}; and relationships between g_s and net photosynthesis rate; A_N **(C)** for GUA6 and GUA8 genotypes combing information for both well-watered (WW) and water-stress (WS) plants. Each point is one measurement per plant. Data in panels **(A,C)** were obtained from field-conducted A–C_i measurements with corresponding Ψ_{leaf} measurements (June and July 2017); and from the dry-down experiment to obtain the leaf hydraulic vulnerability curves shown in panel **(B)**.

TABLE 3 | Average and standard errors of different variables measured in the genotypes GUA6 and GUA8, for well-watered (WW) and water-stressed plants (WS).

	GUA6		GUA8	
	WW	**WS**	**WW**	**WS**
Foliar N	3.68 ± 0.46	**3.71 ± 0.46**	3.92 ± 0.99	**5.83 ± 0.78**
g_m	0.22 ± 0.05	**0.15 ± 0.03**	0.27 ± 0.03	**0.24 ± 0.02**
V_{cmax}	213.75 ± 41.38	165.39 ± 16.80	199.54 ± 4.92	221.97 ± 15.86
LA:RA	0.74 ± 0.12	**0.53 ± 0.08**	0.63 ± 0.24	**0.28 ± 0.07**
LA:SA	8.72 ± 1.47	5.36 ± 0.77	6.56 ± 0.51^a	3.35 ± 0.97^b
Π_o	−1.43 ± 0.37	−1.36 ± 0.39	−1.41 ± 0.18	−1.33 ± 0.10
TLP	−2.09 ± 0.29	−2.37 ± 0.45	−2.09 ± 0.12	−2.28 ± 0.19

Numbers followed by different letters indicate significant differences between WW and WS plants for one genotype and bold numbers represent significant differences between the two genotypes for one irrigation treatment. Foliar N, leaf nitrogen (gN m^{-2}); g_m, mesophyll conductance (mol m^{-2} s^{-1}); V_{cmax}, maximum velocity of carboxylation (µmol m^{-2} s^{-1}); LA:RA, leaf area divided by root area (m m^{-2}); LA:SA, ratio between leaf area and sapwood area (cm^2 mm^{-2}); Π_0, osmotic pressure at full turgor (–MPa); TLP, turgor loss point (–MPa).

mainly limited by stomatal conductance (**Figures 4**, **5**) as demonstrated for many other species, given that stomatal closure is one of the earliest responses to drought and the dominant limitation to photosynthesis under mild to moderate drought conditions (Flexas and Medrano, 2002). The relationship between stomatal conductance and leaf hydraulic conductance was strong (**Figure 4**), thus adding to a growing body of evidence reporting the coordination between water supply and demand at the leaf level (Sack and Holbrook, 2006; Scoffoni et al., 2016). Leaf hydraulic conductance determines the efficiency of the coordination between water supply and demand, and hence, it may determine the degree that the stomata can remain open to allow photosynthesis. In that sense, leaf hydraulic conductance has been increasingly recognized to play a central role in determining plant performance and productivity (Brodribb, 2009; Flexas et al., 2013).

At the plant level, we observed changes in the hydraulic allometry (as proposed by Maseda and Fernández, 2006) of WS plants compared to WW plants, with morphological adjustment being more evident in GUA8. These changes involved a decrease of leaf area to sapwood and root areas, which may reflect a tuning of the hydraulic structure of these individuals to increase water extraction and transport capacity under conditions of water deficit, thereby improving the supply of water to the leaves and the leaf-specific hydraulic conductivity of the plant (Martínez-Vilalta et al., 2009; Martin-StPaul et al., 2017). This, in turn, helps to maintain stomatal conductance (Addington et al., 2006) and photosynthesis (Zhou et al., 2016). WS GUA8 showed a significant increase in root area to leaf area ratio compared

to that seen in WS GUA6. This change could contribute to improved plant hydraulic efficiency by helping to maintain the plant water potential within a safe range, thereby reducing the risk of disruptive xylem embolism (Magnani et al., 2002) and a decline in below-ground hydraulic conductance (Johnson et al., 2018). In addition, olive plants have been shown to be very resistant to cavitation, including leaf xylem and coarse root xylem pathways (Rodriguez-Dominguez et al., 2018), so loss of xylem water transport capacity under our experimental framework were unlikely. However, pathways outside the xylem may have reduced K_{leaf} and, in turn, g_s (Scoffoni et al., 2017) under moderate water stress conditions.

Although homeostasis in response to a sudden perturbation can be achieved only through stomatal regulation, structural changes appear to play a central role in the plant's adjustment to prevailing environmental conditions over periods of months to years (Magnani et al., 2002). Indeed, the LA:SA ratio was also highly correlated to stomatal conductance, although this was not the case for the LA:RA ratio. Despite the lack of association between LA:RA and g_s, optimal allocation of resources between transpiring foliage and absorbing roots has been suggested to be coordinated with short-term regulation of g_s in response to drought (Magnani et al., 2002; Rodriguez-Dominguez and Brodribb, unpublished). A differential LA:RA response to water stress by the GUA6 and GUA8 genotypes, used in the path analysis, might underlie the lack of the relation between LA:RA and g_s, as mentioned above. New advances in root hydraulics that are just beginning to emerge (Cuneo et al., 2016; Poyatos et al., 2018; Rodriguez-Dominguez et al., 2018) will bring new possibilities to explore the impact of changes in LA:RA on stomatal conductance.

Carbon Balance at the Leaf Level

Despite g_s and A_N being very similar in the two genotypes, g_s was slightly higher in GUA6 than in GUA8, although this was not reflected in A_N. This resulted in a better instantaneous water use efficiency for GUA8 than GUA6, which could be advantageous under conditions where water is scarce. Indeed, GUA8 exhibited leaf gas exchange traits which enhanced the net photosynthesis rate for a given g_s. This was observed in terms of changes in V_{cmax} and g_m. A larger g_m is an interesting solution for plants under water stress (Barbour et al., 2010; Flexas et al., 2016), since it reduces that drawdown in CO_2 from the intercellular spaces to the chloroplastic sites of carboxylation, without an increase in transpiration. This is even more important if V_{cmax} has increased, as in the case of GUA8, since a higher V_{cmax} demands more CO_2. Therefore, an orchestrated enhancement of both V_{cmax} and g_m is necessary to yield the desired goal of increasing A_N under water stress conditions. This physiological strategy has been reported as being typical of Mediterranean species with sclerophyllous leaves (Flexas et al., 2013; Peguero-Pina et al., 2015a, 2017). Moreover, the mechanism has not only been shown in angiosperms but also in gymnosperms (Peguero-Pina et al., 2015b), and is now accepted as a typical characteristic of species living in arid and semi-arid environments.

The high concentration of leaf N, as measured in this study for GUA8, confirms that this increase in nitrogen is not a mechanism for storing this macronutrient. The prime goal of the increase in N is directed to an enhancement of V_{cmax} and subsequently the A_N. The increase of N is putatively driven by the decrease in SLA, since a larger mass is concentrated by leaf surface area. Foliar N is mainly allocated to the photosynthetic apparatus of the leaf (Rubisco, electron transport, and chloroplasts) (Evans, 1989). This obviously has a direct impact on V_{cmax} and J_{max}, but it is also likely to affect g_m. Although we have no data on the anatomy of the leaves, an increase of SLA and N have been reported to enhance the surface area of chloroplasts exposed to the intercellular spaces, thus improving the liquid component of mesophyll conductance, which is usually the most limiting factor for g_m (Tosens et al., 2012; Tomas et al., 2013; Flexas and Diaz-Espejo, 2015).

CONCLUSION

We showed here that genotypes belonging to the olive species can exhibit different RGRs in response to water stress. Although differences among genotypes within species are usually smaller than differences among species, two main adjustments to improve the net photosynthesis rate were identified in one of the genotypes (GUA8) used in this study, allowing it to maintain or even increase growth rate under mild water stress conditions. First, at the whole-plant level, a hydraulic allometry adjustment took place as a result of the decrease in the ratios of the areas of leaf-root and leaf-sapwood, the latter being also strongly related to stomatal conductance. Secondly, at the leaf level we identified an increase in CO_2 fixation for a given stomatal conductance that was brought about by an adjustment of traits optimizing CO_2 fixation (higher mesophyll conductance and leaf N favoring maximum carboxylation rate). We also found that the leaf hydraulic conductance plays an important role in controlling stomatal conductance. Multi-scale studies such as the present one can be of great help to provide information on alternative opportunities to generate more drought-tolerant varieties.

AUTHOR CONTRIBUTIONS

VH-S, AD-E, and CR-D contributed to the conception and design of the study. VH-S organized the database, performed the statistical analysis, and wrote the first draft of the manuscript. PD-R, AD-E, and JC-F wrote sections of the manuscript. All authors contributed to manuscript revision, read and approved the submitted version.

FUNDING

This work was supported by the Spanish Ministry of Science and Innovation through the research project AGL2015-71585-R and PCIN-2017-002. Funding was also received from a "RECUPERA-2020" FEDER-MINECO grant (Ref. 20134R089) and a "Grupos Operativos" FEDER-MAPAMA grant (Ref. 20160020006629). CR-D benefited from an Individual Fellowship

from the European Union's Horizon 2020 Research and Innovation Program under the Marie Skłodowska-Curie grant agreement no. 751918-AgroPHYS during the writing process of the manuscript.

ACKNOWLEDGMENTS

We thank Guillaume Besnard (University of Toulouse, CNRS, Laboratoire Évolution et Diversité Biologique, ENSFEA, IRD, UMR5174, EDB, Toulouse, France) for providing seeds of the *cuspidata* subspecies and Adrián Perez-Arcoiza, Francisco Durán, Joaquín Espartero and Carlos Rivero for valuable technical assistance.

SUPPLEMENTARY MATERIAL

The Supplementary Material for this article can be found online at: https://www.frontiersin.org/articles/10.3389/fpls.2019.00291/full#supplementary-material

FIGURE S1 | Growth and water use traits of wild olive genotypes. Water consumption relative to leaf fresh weight (FW), total FW, shoot FW, root FW, and the root *vs.* shoot (R/S) biomass ratio was quantified in potted seedlings during the 2015 screening in selected genotypes from the subspecies *europaea* (ACZ8, ARC1, ACZ27, APR1, AJA18, AJA4, AJA1, ACO15, AJA6, ACZ4, ACZ9, ACZ1, ACO18, AMK34, ACZ10, ACO14, AMK5, AMK14, AMK16, ACZ5, AMK21, and AMK6), *guanchica* (GUA7, GUA6, GUA1, GUA4, GUA5, GUA8, GUA2 and GUA9), and *cuspidata* (CEH3, CEH9, CEH24, CEH6, CEH8). Bars are the average of six plants ±1 SE. Asterisks indicate significant differences between well-watered (WW) and water-stressed (WS) plants for each genotype ($p < 0.05$).

REFERENCES

Addington, R. N., Donovan, L. A., Mitchell, R. J., Vose, J. M., Pecot, S. D., et al. (2006). Adjustments in hydraulic architecture of Pinus palustris maintain similar stomatal conductance in xeric and mesic habitats. *Plant Cell Environ.* 29, 535–545. doi: 10.1111/j.1365-3040.2005.01430.x

Anderegg, W. R. L., Klein, T., Bartlett, M., Sack, L., Pellegrini, A. F. A., Choat, B., et al. (2016). Meta-analysis reveals that hydraulic traits explain cross-species patterns of drought-induced tree mortality across the globe. *Proc. Natl. Acad. Sci. U.S.A.* 113, 5024–5029. doi: 10.1073/pnas.1525678113

Barbour, M. M., Warren, C. R., Farquhar, G. D., Forrester, G. U. Y., and Brown, H. (2010). Variability in mesophyll conductance between barley genotypes, and effects on transpiration efficiency and carbon isotope discrimination. *Plant Cell Environ.* 33, 1176–1185. doi: 10.1111/j.1365-3040.2010.02138.x

Bernacchi, C. J., Portis, A. R., Nakano, H., von Caemmerer, S., and Long, S. P. (2002). Temperature response of mesophyll conductance. Implications for the determination of Rubisco enzyme kinetics and for limitations to photosynthesis in vivo. *Plant Physiol.* 130, 1992–1998. doi: 10.1104/pp.008250

Blackman, C. J., and Brodribb, T. J. (2011). Two measures of leaf capacitance: insights into the water transport pathway and hydraulic conductance in leaves. *Funct. Plant Biol.* 38:118. doi: 10.1071/FP10183

Blum, A. (2017). Osmotic adjustment is a prime drought stress adaptive engine in support of plant production. *Plant Cell Environ.* 40, 4–10. doi: 10.1111/pce.12800

Brodribb, T. J., Holbrook, N. M., Zwieniecki, M. A., and Palma, B. (2005). Leaf hydraulic capacity in ferns, conifers and angiosperms: impacts on photosynthetic maxima. *New Phytol.* 165, 839–846. doi: 10.1111/j.1469-8137.2004.01259.x

Brodribb, T. J., Feild, T. S., and Jordan, G. J. (2007). Leaf maximum photosynthetic rate and venation are linked by hydraulics. *Plant Physiol.* 144, 1890–1898. doi: 10.1104/pp.107.101352

Brodribb, T. J. (2009). Xylem hydraulic physiology: the functional backbone of terrestrial plant productivity. *Plant Sci.* 177, 245–251. doi: 10.1016/j.plantsci.2009.06.001

Brodribb, T. J., and Holbrook, N. M. (2003). Stomatal closure during leaf dehydration, correlation with other leaf physiological traits 1. *Plant Physiol.* 132, 2166–2173. doi: 10.1104/pp.103.023879

Brodribb, T. J., and Holbrook, N. M. (2004). Diurnal depression of leaf hydraulic conductance in a tropical tree species. *Plant Cell and Environment* 27, 820–827. doi: 10.1093/treephys/tps028

Brodribb, T. J., and Holbrook, N. M. (2006). Declining hydraulic efficiency as transpiring leaves desiccate: two types of response. *Plant Cell Environ.* 29, 2205–2215. doi: 10.1111/j.1365-3040.2006.01594.x

Brodribb, T. J., and Jordan, G. J. (2008). Internal coordination between hydraulics and stomatal control in leaves. *Plant Cell Environ.* 31, 1557–1564. doi: 10.1111/j.1365-3040.2008.01865.x

Buckley, T. N. (2005). The control of stomata by water balance. *New Phytol.* 168, 275–292. doi: 10.1111/j.1469-8137.2005.01543.x

Burnett, A. C., Rogers, A., Rees, M., and Osborne, C. P. (2016). Carbon source–sink limitations differ between two species with contrasting growth strategies. *Plant Cell Environ.* 39, 2460–2472. doi: 10.1111/pce.12801

Chen, J.-W., Zhang, Q., Li, X.-S., and Cao, K.-F. (2010). Gas exchange and hydraulics in seedlings of Hevea brasiliensis during water stress and recovery. *Tree Physiol.* 30, 876–885. doi: 10.1093/treephys/tpq043.

Cuneo, I. F., Knipfer, T., Brodersen, C. R., and McElrone, A. J. (2016). Mechanical failure of fine root cortical cells initiates plant hydraulic decline during drought. *Plant Physiol.* 172, 1669–1678. doi: 10.1104/pp.16.00923

Diaz-Espejo, A., Fernández, J. E., Torres-Ruiz, J. M., Rodriguez-Dominguez, C. M., Perez-Martin, A., et al. (2018). "The olive tree under water stress: fitting the pieces of response mechanisms in the crop performance puzzle," in *Water Scarcity and Sustainable Agriculture in Semiarid Environment,* eds I. F. García Tejero and V. H. Durán Zuazo. Amsterdam: Elsevier. doi: 10.1016/B978-0-12-813164-0.00018-1

Diaz-Espejo, A., Nicolás, E., and Fernández, J. E. (2007). Seasonal evolution of diffusional limitations and photosynthetic capacity in olive under drought. *Plant Cell Environ.* 30, 922–933. doi: 10.1111/j.1365-3040.2007.001686.x

Diaz-Espejo, A., Walcroft, A. S., Fernández, J. E., Hafidi, B., Palomo, M. J., Girón, I. F., et al. (2006). Modeling photosynthesis in olive leaves under drought conditions. *Tree Physiol.* 26, 1445–1456. doi: 10.1093/treephys/26.11.1445

Epskamp, S. (2013). *semPlot: Path Diagrams and Visual Analysis of Various SEM Packages' Output. R Package Version 0.3.3.* Available at: https://github.com/SachaEpskamp/semPlot

Ethier, G. J., and Livingston, N. J. (2004). On the need to incorporate sensitivity to CO_2 transfer conductance into the Farquhar-von Caemmerer-Berry leaf photosynthesis model. *Plant Cell Environ.* 27, 137–153. doi: 10.1111/j.1365-3040.2004.01140.x

Evans, J. (1989). Photosynthesis and nitrogen relationships in leaves of C3 plants. *Oecologia* 78, 9–19 doi: 10.1007/BF00377192

Fernández, J. E. (2014). Plant-based sensing to monitor water stress: applicability to commercial orchards. *Agric. Water Manage.* 142, 99–109. doi: 10.1016/j.agwat.2014.04.017

Flexas, J., Díaz-Espejo, A., Berry, J. A., Cifre, J., Galmés, J., Kaldenhoff, R., et al. (2007). Analysis of leakage in IRGA's leaf chambers of open gas exchange systems: quantification and its effects in photosynthesis parameterization. *J Exp Bot.* 58, 1533–1543. doi: 10.1093/jxb/erm027

Flexas, J., Díaz-Espejo, A., Conesa, M. A., Coopman, R. E., Douthe, C., Gago, J., et al. (2016). Mesophyll conductance to CO2 and Rubisco as targets for improving intrinsic water use efficiency in C3 plants. *Plant Cell Environ.* 39, 965–982. doi: 10.1111/pce.12622

Flexas, J., and Medrano, H. (2002). Drought-inhibition of photosynthesis in C3 plants: stomatal and non-stomatal limitations revisited. *Ann. Bot.* 89, 183–189. doi: 10.1093/aob/mcf027

Flexas, J., Carriquí, M., Coopman, R. E., Gago, J., Galmés, J., Martorell, S., et al. (2014). Stomatal and mesophyll conductances to CO2 in different plant groups: underrated factors for predicting leaf photosynthesis responses to climate change? *Plant Sci.* 226, 41–48. doi: 10.1016/j.plantsci.2014.06.011

Flexas, J., and Diaz-Espejo, A. (2015). Interspecific differences in temperature response of mesophyll conductance: food for thought on its origin and regulation. *Plant Cell Environ.* 38, 625–628. doi: 10.1111/pce.12476

Flexas, J., Niinemets, Ü., Gallé, A., Barbou, M. M., Centritto, M., Díaz-Espejo, A., et al. (2013). Diffusional conductances to CO2 as a target for increasing photosynthesis and photosynthetic water-use efficiency. *Photosynth. Res.* 117, 45–59. doi: 10.1007/s11120-013-9844-z

Galmés, J., Cifre, J., Medrano, H., and Flexas, J. (2005). Modulation of relative growth rate and its components by water stress in Mediterranean species with different growth forms. *Oecologia* 145, 21–31. doi: 10.1007/s00442-005-0106-4

Gortan, E., Nardini, A., Gascó, A., and Salleo, S. (2009). The hydraulic conductance of *Fraxinus ornus* leaves is constrained by soil water availability and coordinated with gas exchange rates. *Tree Physiol.* 29, 529–539. doi: 10.1093/treephys/tpn053

Hernandez-Santana, V., Fernández, J. E., Rodriguez-Dominguez, C. M., Romero, R., and Diaz-Espejo, A. (2016). The dynamics of radial sap flux density reflects changes in stomatal conductance in response to soil and air water deficit. *Agric. For. Meteorol.* 218–219, 92–101. doi: 10.1016/j.agrformet.2015.11.013.

Hunt, R., Causton, D. R., Shipley, B., and Askew, A. P. (2002). A modern tool for classical plant growth analysis. *Ann. Bot.* 90, 485–488. doi: 10.1093/aob/mcf214

Jackson, R. B., Mooney, H. A., and Schulze, E. D. (1997). A global budget for fine root biomass, surface area, and nutrient contents. *Proc. Natl. Acad. Sci. U.S.A.* 94, 7362–7366. doi: 10.1073/pnas.94.14.7362

Johnson, D. M., Domec, J. C., Carter Berry, Z., Schwantes, A. M., McCulloh, K. A., Woodruff, D. R., et al. (2018). Co-occurring woody species have diverse hydraulic strategies and mortality rates during an extreme drought. *Plant Cell Environ.* 41, 576–588. doi: 10.1111/pce.13121

Lo Gullo, M. A., Nardini, A., Trifilò, P., and Salleo, S. (2005). Diurnal and seasonal variations in leaf hydraulic conductance in evergreen and deciduous trees. *Tree Physiol.* 25, 505–512. doi: 10.1093/treephys/25.4.505

López-Sampson, A., Cernusak, L. A., and Page, T. (2017). Relationship between leaf functional traits and productivity in *Aquilaria crassna* (Thymelaeaceae) plantations: a tool to aid in the early selection of high-yielding trees. *Tree Physiol.* 37, 645–653. doi: 10.1093/treephys/tpx007

Magnani, F., Grace, J., and Borghetti, M. (2002). Adjustment of tree structure in response to the environment under hydraulic constraints. *Funct. Ecol.* 16, 385–393. doi: 10.1046/j.1365-2435.2002.00630.x

Martínez-Vilalta, J., Cochard, H., Mencuccini, M., Sterck, F. J., Herrero, A., Korhonen, J. F. K., et al. (2009). Hydraulic adjustment od scots pine across Europe. *New Phytol.* 184, 353–364. doi: 10.1111/j.1469-8137.2009.02954.x

Martin-StPaul, N. K., Limousin, J. M., Vogt-Schilb, H., Rodríguez-Calcerrada, J., Rambal, S., Longepierre, D., et al. (2013). The temporal response to drought in a Mediterranean evergreen tree: comparing a regional precipitation gradient and a throughfall exclusion experiment. *Glob Chang Biol.* 19, 2413–2426. doi: 10.1111/gcb.12215

Martin-StPaul, N., Delzon, S., and Cochard, H. (2017). Plant resistance to drought relies on early stomatal closure. *Ecol. Lett.* 20, 1437–1447. doi: 10.1111/ele.12851

Maseda, P. H., and Fernández, R. J. (2006). Stay wet or else: three ways in which plants can adjust hydraulically to their environment. *J. Exp. Bot.* 57, 3963–3977. doi: 10.1093/jxb/erl127

Melcher, P. J., Michele Holbrook, N., Burns, M. J., Zwieniecki, M. A., Cobb, A. R., Brodribb, T. J., et al. (2012). Measurements of stem xylem hydraulic conductivity in the laboratory and field. *Methods Ecol. Evol.* 3, 685–694. doi: 10.1111/j.2041-210X.2012.00204.x

Mencuccini, M. (2014). Temporal scales for the coordination of tree carbon and water economies during droughts. *Tree Physiol.* 34, 439–442. doi: 10.1093/treephys/tpu029

Nardini, A., and Salleo, S. (2000). Limitation of stomatal conductance by hydraulic traits: sensing or preventing xylem cavitation? *Trees* 15, 14–24. doi: 10.1007/s004680000071

Nardini, A., Tyree, M. T., and Salleo, S. (2001). Xylem cavitation in the leaf of *Prunus laurocerasus* and its impact on leaf hydraulics. *Plant Physiol.* 125, 1700–1709. doi: 10.1104/pp.125.4.1700

Nevo, E., Fu, Y. B., Pavlicek, T., Khalifa, S., Tavasi, M., Beiles, A., et al. (2012). Evolution of wild cereals during 28 years of global warming in Israel. *Proc. Natl. Acad. Sci. U.S.A.* 109, 3412–3415. doi: 10.1073/pnas.1121411109

Niinemets, Ü. (2012). Optimization of foliage photosynthetic capacity in tree canopies: towards identifying missing constraints. *Oecologia* 32, 505–509.

Niinemets, U., Diaz-Espejo, A., Flexas, J., Galmés, J., and Warren, C. R. (2009). Role of mesophyll diffusion conductance in constraining potential photosynthetic productivity in the field. *J. Exp. Bot.* 60, 2249–2270. doi: 10.1093/jxb/erp036

Peguero-Pina, J. J., Sancho-Knapik, D., Flexas, J., Galmés, J., Niinemets, Ü., Gil-Pelegrín, E., et al. (2015b). Light acclimation of photosynthesis in two closely related firs (*Abies pinsapo* Boiss. and *Abies alba* Mill.): the role of leaf anatomy and mesophyll conductance to CO2. *Tree Physiol.* 36, 300–310. doi: 10.1093/treephys/tpv114

Peguero-Pina, J. J., Sisó, S., Flexas, J., Galmés, J., Niinemets, Ü., Sancho-Knapik, D., et al. (2017). Coordinated modifications in mesophyll conductance, photosynthetic potentials and leaf nitrogen contribute to explain the large variation in foliage net assimilation rates across Quercus ilex provenances. *Tree Physiol.* 37, 1084–1094. doi: 10.1093/treephys/tpx057

Peguero-Pina, J. J., Sisó, S., Sancho-Knapik, D., Díaz-Espejo, A., Flexas, J., Galmés, J., et al. (2015a). Leaf morphological and physiological adaptations of a deciduous oak (*Quercus faginea* Lam.) to the Mediterranean climate : a comparison with a closely related temperate species (*Quercus robur* L.). *Tree Physiol.* 36, 287–299. doi: 10.1093/treephys/tpv107

Perez-Martin, A., Michelazzo, C., Torres-Ruiz, J. M., Flexas, J., Fernández, J. E., Sebastiani, L., et al. (2014). Regulation of photosynthesis, stomatal and mesophyll conductance under water stress acclimation and recovery in olive trees: correlation with gene expression of carbonic anhydrase and aquaporins. *J. Exp. Bot.* 65, 3143–3156. doi: 10.1093/jxb/eru160

Poyatos, R., Aguadé, D., and Martínez-Vilalta, J. (2018). Below-ground hydraulic constraints during drought-induced decline in Scots pine. *Ann. For. Sci.* 75:100. doi: 10.1007/s13595-018-0778-7

Reddy, K. R., Brand, D., Wijewardana, C., and Gao, W. (2017). Temperature effects on cotton seedling emergence, growth, and development. *Agron. J.,* 109, 1379–1387 doi: 10.2134/agronj2016.07.0439

Rees, M., Osborne, C. P., Woodward, F. I., Hulme, S. P., Turnbull, L. A., Taylor, S. H., et al. (2010). Partitioning the components of relative growth rate: how important is plant size variation? *Am. Nat.* 176, E152–E161. doi: 10.1086/657037

Reich, P. B. (2014). The world-wide 'fast–slow'plant economics spectrum: a traits manifesto. *J. Ecol.* 102, 275–301. doi: 10.1111/1365-2745.12211

Rodriguez-Dominguez, C. M., Carins Murphy, M. R., Lucani, C., and Brodribb, T. J. (2018). Mapping xylem failure in disparate organs of whole plants reveals extreme resistance in olive roots. *New Phytol.* 218, 1025–1035. doi: 10.1111/nph.15079

Rosseel, Y. (2012). Lavaan: an R package for structural equation modeling. *J. Stat. Softw.* 48, 1–36. doi: 10.3389/fpsyg.2014.01521

Ruane, J., Sonnino, A., Steduto, P., and Deane, C. (2008). *Coping With Water Scarcity: What Role for Biotechnologies? Land and Water Discussion Paper*. Rome: FAO.

Rugini, E. (1984) In vitro-propagation of some olive (*Olea europaea* sativa L.) cultivars with different root-ability, and medium development using analytical data from developing shoots and embryos. *Sci. Hortic.* 24, 123–134. doi: 10.1016/0304-4238(84)90143-2

Sack, L., and Pasquet-Kok, J. (2017). PrometheusWiki contributors, "Leaf pressure-volume curve parameters," PrometheusWiki.

Sack, L., Bartlett, M., Creese, C., Guyot, G., Scoffoni, C., and PrometheusWiki contributors (2011). "Constructing and operating a hydraulics flow meter." PrometheusWiki.

Sack, L., Ball, M. C., Brodersen, C., Davis, S. D., Des Marais, D. L., Donovan, L. A., et al. (2016). Plant hydraulics as a central hub integrating plant and ecosystem function: meeting report for 'Emerging Frontiers in Plant Hydraulics' (Washington, DC, May 2015). *Plant Cell Environ.* 39, 2085–2094. doi: 10.1111/pce.12732

Sack, L., Cowan, P. D., Jaikumar, N., and Holbrook, N. M. (2003). The 'hydrology' of leaves: co-ordination of structure and function in temperate woody species. *Plant Cell Environ.* 26, 1343–1356. doi: 10.1046/j.0016-8025.2003.01058.x

Sack, L., and Holbrook, N. M. (2006). Leaf hydraulics. *Annu. Rev. Plant Biol.* 57, 361–381. doi: 10.1146/annurev.arplant.56.032604.144141

Scoffoni, C., Albuquerque, C., Brodersen, C. R., Townes, S. V., John, G. P., Bartlett, M. K., et al. (2017). Outside-Xylem vulnerability, not xylem embolism, controls leaf hydraulic decline during dehydration. *Plant Physiol.* 173, 1197–1210. doi: 10.1104/pp.16.01643

Scoffoni, C., Chatelet, D. S., Pasquet-Kok, J., Rawls, M., Donoghue, M. J., Edwards, E. J., et al. (2016). Hydraulic basis for the evolution of photosynthetic productivity. *Nat. Plants* 2:16072. doi: 10.1038/nplants.2016.72

Scoffoni, C., McKown, A. D., Rawls, M., and Sack, L. (2012). Dynamics of leaf hydraulic conductance with water status: quantification and analysis of species differences under steady state. *J. Exp. Bot.* 63, 643–658. doi: 10.1093/jxb/err270

Shipley, B. (2000). *Cause and Correlation in Biology: A User's Guide to Path Analysis, Structural Equations, and Causal Inference*. Oxford: Oxford University Press.

Shipley, B. (2002). Trade-offs between net assimilation rate and specific leaf area in determining relative growth rate: relationship with daily irradiance. *Funct. Ecol.* 16, 682–689. doi: 10.1046/j.1365-2435.2002.00672.x

Shipley, B. (2006). Net assimilation rate, specific leaf area and leaf mass ratio: which is most closely correlated with relative growth rate? A meta-analysis. *Funct. Ecol.* 20, 565–574. doi: 10.1111/j.1365-2435.2006.01135.x

Sterck, F., and Zweifel, R. (2016). Trees maintain a similar conductance per leaf area through integrated responses in growth, allocation, architecture and anatomy. *Tree Physiol.* 36, 1307–1309. doi: 10.1093/treephys/tpw100

Tomas, M., Flexas, J., Copolovici, L., Galmés, J., Hallik, L., Medrano, H., et al. (2013). Importance of leaf anatomy in determining mesophyll diffusion conductance to CO2 across species: quantitative limitations and scaling up by models. *J. Exp. Bot.* 64, 2269–2281. doi: 10.1093/jxb/ert086

Tosens, T., Niinemets, Ü., Vislap, V., Eichelmann, H., and Castro-Díez, P. (2012). Developmental changes in mesophyll diffusion conductance and photosynthetic capacity under different light and water availabilities in *Populus tremula*: how structure constrains function. *Plant Cell Environ.* 35, 839–856. doi: 10.1111/j.1365-3040.2011.02457.x

Trentacoste, E. R., Contreras-Zanessi, O., Beyá-Marshall, V., and Puertas, C. M. (2018). Genotypic variation of physiological and morphological traits of seven olive cultivars under sustained and cyclic drought in Mendoza, Argentina. *Agric. Water Manage.* 196, 48–56. doi: 10.1016/j.agwat.2017.10.018

Turner, N. C. (2017). Turgor maintenance by osmotic adjustment, an adaptive mechanism for coping with plant water deficits. *Plant Cell Environ.* 40, 1–3. doi: 10.1111/pce.12839

United Nations (2015). *Transforming Our World: The 2030 Agenda for Sustainable Development*. New York, NY: United Nations

Walcroft, A. S., Whitehead, D., Silvester, W. B., and Kelliher, F. M. (1997). The response of photosynthetic model parameters to temperature and nitrogen concentration in *Pinus radiata* D. Don. *Plant Cell Environ.* 20, 1338–1348. doi: 10.1046/j.1365-3040.1997.d01-31.x

Xiong, D., Douthe, C., and Flexas, J. (2018). Differential coordination of stomatal conductance, mesophyll conductance, and leaf hydraulic conductance in response to changing light across species. *Plant Cell Environ.* 41, 436–450. doi: 10.1111/pce.13111

Zhou, S. X., Medlyn, B. E., and Prentice, I. C. (2016). Long-term water stress leads to acclimation of drought sensitivity of photosynthetic capacity in xeric but not riparian *Eucalyptus* species. *Ann. Bot.* 117, 133–144. doi: 10.1093/aob/mcv161

Conflict of Interest Statement: The authors declare that the research was conducted in the absence of any commercial or financial relationships that could be construed as a potential conflict of interest.

frontiers in Plant Science

METHODS
published: 29 May 2019
doi: 10.3389/fpls.2019.00694

Establishment of a Sensitive qPCR Methodology for Detection of the Olive-Infecting Viruses in Portuguese and Tunisian Orchards

Maria Doroteia Campos[1], Mohamed Salem Zellama[2], Carla Varanda[1], Patrick Materatski[1], Augusto Peixe[3], Maher Chaouachi[2] and Maria do Rosário Félix[3]*

[1] ICAAM – Instituto de Ciências Agrárias e Ambientais Mediterrânicas, Instituto de Investigação e Formação Avançada, Universidade de Évora, Évora, Portugal, [2] Laboratoire de Recherche "Bioressources: Biologie Intégrative & Valorisation," Institut Supérieur de Biotechnologie de Monastir, Université de Monastir, Monastir, Tunisia, [3] Departamento de Fitotecnia, ICAAM – Instituto de Ciências Agrárias e Ambientais Mediterrânicas, Escola de Ciências e Tecnologia, Universidade de Évora, Évora, Portugal

OPEN ACCESS

Edited by:
José Manuel Martínez-Rivas, Instituto de la Grasa (IG), Spain

Reviewed by:
Eddo Rugini, Università degli Studi della Tuscia, Italy
Enrique Martinez Force, Spanish National Research Council (CSIC), Spain

***Correspondence:**
Maria Doroteia Campos
mdcc@uevora.pt

Specialty section:
This article was submitted to Crop and Product Physiology, a section of the journal Frontiers in Plant Science

Received: *06 March 2019*
Accepted: *08 May 2019*
Published: *29 May 2019*

Citation:
Campos MD, Zellama MS, Varanda C, Materatski P, Peixe A, Chaouachi M and Félix MR (2019) Establishment of a Sensitive qPCR Methodology for Detection of the Olive-Infecting Viruses in Portuguese and Tunisian Orchards. Front. Plant Sci. 10:694. doi: 10.3389/fpls.2019.00694

Sensitive detection of viruses in olive orchards is actually of main importance since these pathogenic agents cannot be treated, their dissemination is quite easy, and they can have eventual negative effects on olive oil quality. The work presented here describes the development and application of a new SYBR® Green-based real-time quantitative PCR (qPCR) analysis for specific and reliable quantification of highly spread olive tree viruses: *Olive latent virus 1* (OLV-1), *Tobacco necrosis virus D* (TNV-D), *Olive mild mosaic virus* (OMMV), and *Olive leaf yellowing-associated virus* (OLYaV). qPCR methodology revealed high specificity and sensitivity, estimated in the range of 0.8–8 copies of the virus genome, for the studied viruses. For validation of the method, total RNA and double strand RNA (dsRNA) from naturally infected trees were used. In a first trial, dsRNAs from trees of cv. "Galega vulgar" from a Portuguese orchard, were subjected to qPCR and from the 30 samples tested, 26 were TNV-D and/or OMMV-positive and 25 were OLV-1 positive. In a second trial, total RNA from trees of different cultivars from Tunisian orchards, were here tested by qPCR and all viruses were detected. From the 33 samples studied, the most prevalent virus detected in Tunisia orchards was OLV-1 (31 samples diagnosed), followed by OLYaV (20 samples diagnosed), and finally the combination in last TNV-D and/or OMMV (12 samples diagnosed). In both trials, qPCR demonstrated to be effective and sensitive, even when using total RNA as template. qPCR through the use of a SYBR® Green methodology enabled, for the first time, a reliable, sensitive, and reproducible estimation of virus accumulation in infected olive trees, in which viruses are usually in low titres, that will allow gaining new insights in virus biology essential for disease control and give an important contribution for establishment of sanitary certification of olive propagative material.

Keywords: *OLEA europaea*, qPCR, viral diseases, virus detection, sensitive detection

INTRODUCTION

Olive trees are susceptible to several pathogens that may affect the yield and quality of their products with important economic impact, such as diseases causes by fungi (i.e., *Colletotrichum* spp. and *Spilocaea oleagina*) (Salman, 2017; Materatski et al., 2018), and more recently the emergence of *Xylella fastidiosa,* first noticed in 2013, and responsible for a severe outbreak of Olive quick decline syndrome (Saponari et al., 2013). Regarding virus infection, plants infected usually present morphological and physiological alterations, which always incurs in inferior performance such as the decreased host biomass and crop yield loss, with chloroplast known to be highly involved in those processes (Zhao et al., 2016). Olive trees are affected by several viruses, with 15 olive viruses identified until now (Félix et al., 2012). Viral symptoms on olive trees include bumpy fruits, leaf yellowing, vein banding, and vein clearing, (Martelli, 1999; Albanese et al., 2012). These symptoms are non-specific and difficult to recognize, and often occur in virus-infected olive trees without apparent symptoms, which makes viral diagnosis in the field impossible to perform (Martelli et al., 2002; Alabdullah et al., 2010; Martelli, 2011; Zellama et al., 2018). A decrease in oil yield and maturity index in virus infected olives was also reported, as well as elevated total phenols in olive oil content from infected olives when compared to healthy fruits (Godena et al., 2012). Nevertheless, the *Olive leaf yellowing associated virus* (OLYaV) was not found to have a negative interference in oil yield and quality (Fontana et al., 2019).

Virus surveys carried in Mediterranean countries and others, concerning eight olive-infecting viruses (SLRSV, *Strawberry latent ringspot virus*; ArMV, *Arabis mosaic virus*; CLRV, *Cherry leafroll virus*; OLRSV, *Olive latent ringspot virus*; CMV, *Cucumber mosaic virus*; OLYaV, *Olive leaf yellowing-associated virus*; OLV-1, *Olive latent virus 1*; OLV-2, *Olive latent virus 2*), have shown high levels of infection, such as 75% in Tunisia, 51% in Syria, 33% in Italy, 31% in Lebanon, 25% in Croatia, and 31% of necroviruses infection in Portugal (Al Abdullah et al., 2005; Fadel et al., 2005; Faggioli et al., 2005; Varanda et al., 2010; Luigi et al., 2011; Zellama et al., 2018). However, the high presence of double stranded RNA (dsRNA) in olive orchards suggests even higher levels of infection (Félix et al., 2002; Saponari et al., 2002) that may be identified with new and more sensitive diagnostic techniques.

Phytosanitary certification programs depend on robust diagnostic procedures for detection of the olive viruses, since their spread will mainly depend on preventive measures such as the use of pathogen-tested propagative material (Albanese et al., 2012). Following the EU regulation on the marketing of fruit plants intended for fruit production, namely the Commission Directive 93/48/EEC (EEC Directive, 1993), the *Conformitas Agraria Communitatis* (*CAC*) category, applicable to olive plant material, demands that plants must be free of all viruses (Annex to the 93/48/EEC). The Italian certification of propagative material (DM 20/11/2006), followed by most of the Mediterranean countries, including the countries from the North of Africa, imposes the absence of several viruses such as ArMV, CLRV, SLRSV, CMV, OLV-1, OLV-2, OLYaV, and *Tobacco necrosis virus senso lato*, in which *Tobacco necrosis virus* D (TNV-D) and *Olive mild mosaic virus* (OMMV) are included (Albanese et al., 2012). The adoption of such certification programs requires the use of extremely sensitive diagnostic techniques for viral detection, which are the basis for valid programs. The low viral titres in olive tissues are the major constraint of the techniques, and do not always allow the successful, accurate and reproducible detection (Zellama et al., 2018).

Traditionally, unreliability techniques based on serology tests (ELISA) have been used for the detection of viruses (Martelli, 1999; Bertolini et al., 2001). More recently, molecular biology-based methods that include the highly laborious dsRNA analysis have been performed, once dsRNA reduces the constraint caused by the common low viral concentration in trees (Varanda et al., 2010, 2014; Zellama et al., 2018). RT-PCR has demonstrated to be the most rapid, sensitive, and reliable technique (Varanda et al., 2010; Luigi et al., 2011; Albanese et al., 2012; Zellama et al., 2018), using different templates as viral targets such as TNA, total RNA or dsRNA. The advancements of the molecular virology and biotechnology have witnessed major breakthroughs in the recent years resulting in highly sensitive and effective technologies/methods (Yadav and Khurana, 2016). In plant virology, real-time quantitative PCR (qPCR) is increasingly being used to improve sensitivity and accuracy while maintaining reliability (Poojari et al., 2016; Malandraki et al., 2017). The use of qPCR instrumentation presents several advantages, since it requires considerably short hands-on time, and detection of amplified products is automated, simple, and reproducible (Espy et al., 2006).

In the work described here, three new SYBR® Green qPCR assays were developed for reliable and sensitive detection of OLV-1, TNV-D and/or OMMV, and OLYaV. The work involved the use of specific primers for each target virus, using different templates (total RNA and dsRNA). The main performance criteria were tested such as the sensitivity of the technique and the specificity of the primers. qPCR was validated through application to plant material from different olive orchards, from Portugal and Tunisia.

MATERIALS AND METHODS

Virus Isolates and Plant Material

Virus reference isolates of OLV-1, TNV-D, and OMMV were obtained according to Varanda et al. (2014). For OLYaV, since this virus is not mechanically transmitted (van Regenmortel et al., 2000), a sequenced cDNA obtained from an infected olive tree was used as reference (Zellama et al., 2018).

For validation and comparative analysis of virus infection, two different experiments were conducted. In the first one, samples were collected from 30 symptomatic or asymptomatic olive trees from an orchard under traditional management. The cultivar studied was the native cultivar "Galega vulgar," and the orchard was located in Alentejo region (south Portugal).

The second experiment was performed in samples collected from a total of 33 symptomatic or asymptomatic olive trees. These samples were randomly selected from the 280 collected

by Zellama et al. (2018), but with the care to select 3 trees per each orchard. The sampled trees belonged to 11 orchards, under different types of management: three traditional, six semi-intensive, and two intensive. The orchards were located in several regions covering whole Tunisia. Sampled trees belonged to the Tunisian native cultivars "Chemlali," "Chétoui," "Meski," and to the introduced cultivars "Picholine," "Koroneiki," and "Arbequina." All samples consisted of four cuttings of ca. 20 cm in length collected from 2-year stems from each quadrant of the canopy of each tree, that were kept in plastic bags at 4°C, until further use.

Nucleic Acids Extraction and Reverse Transcription

In the first experiment, double stranded RNAs (dsRNAs) were extracted from 300 mg of cortical scrapings according to Morris and Dodds (1979). dsRNAs were visualized by 0.8% agarose gel electrophoresis prior to denaturation by heating at 100°C for 5 min, followed by 15 min on ice. cDNA was produced by RevertAid H Minus Reverse Transcriptase (Thermo Scientific), according to manufacturer's instructions, with random hexamers (Promega).

In the second experiment, total RNA was extracted from 25 mg of cortical scrapings from cuttings that were mixed together and homogenized using liquid nitrogen. Total RNA was extracted using the RNeasy Plant Mini Kit (Qiagen), following the manufacturer's instructions. The quantification of RNA and the evaluation of its purity were determined in a NanoDrop-2000C spectrophotometer (Thermo Scientific). RNA integrity was evaluated by denaturing gel electrophoresis. Total RNA (500 ng) was reverse transcribed with the Maxima First Strand cDNA Synthesis Kit (Thermo Scientific), according to manufacturer's instructions.

Conventional PCR Assays

For conventional PCR assays, primers used for OLV-1 and OLYaV were the same as in Zellama et al. (2018) (**Table 1**). For the detection of OMMV and TNV-D, a single set of primers that allow the amplification of both TNV-D and OMMV was used (**Table 1**; Cardoso et al., 2004). 2 μl of cDNA were used in PCR carried out in 1x DreamTaq Buffer (Thermo Scientific), 0.2 mM dNTPs, 0.5 μM of each primer and 2.5 U of DreamTaq DNA Polymerase (Thermo Scientific) in a total volume of 50 μl. Amplifications were carried out in a Thermal Cycler (Bio-Rad) at 95°C for 1 min, 35 cycles at 95°C for 30 s, 54°C (for OLV1 and both TNV-D and OMMV) or 58°C (for OLYaV) for 1 min, 72°C for 1 min, and a final extension step of 72°C for 10 min. Amplified products were analyzed by electrophoresis in 1% agarose gel.

TABLE 1 | Primers used on conventional PCR assays.

Species	Primers (5′ → 3′)	AS (bp)
OMMV and/or TNV-D	Fw: GTGTTCAGTCATATACATACC	247
	Rv: GCCTATTGTGCTGTACCAC	
OLV-1	Fw: TTTCACCCCACCAAATGGC	747
	Rv: CTCACCCATCGTTGTGTGG	
OLYaV	Fw: CGAAGAGAGCGGCTGAAGGCTC	346
	Rv: GGGACGGTTACGGTCGAGAGG	

Description of forward (Fw) and reverse (Rv) primers used for specific detection of Olive mild mosaic virus (OMMV) and/or Tobacco necrosis virus D (TNV-D) (Cardoso et al., 2004), Olive latent virus 1 (OLV-1) and Olive leaf yellowing-associated virus (OLYaV) in the conventional PCR assays (Zellama et al., 2018). AS, amplicon size.

SYBR® Green qPCR Assays

These assays were performed in both experiments. For TNV-D and/or OMMV it was used the already referred primer set (Cardoso et al., 2004). For OLV-1 a gene-specific primer set was designed in a conserved region of the capsid protein (CP), after alignment of all full-genome and CP sequences collected from NCBI GenBank database (accession n° KF804054). For OLYaV the same procedure was followed, but the primers were designed in the conserved gene coding the heat shock protein 90 (accession n° AJ844555). The Primer Express 3.0 Software (Applied Biosystems) was used for the design of the primers, using the default parameters of the software, and their specificity was tested *in silico* using basic local alignment search tool (BLAST) at the National Center for Biotechnology Information (NCBI)[1]. All qPCR primers are listed in **Table 2**.

qPCRs were carried out on a 7500 Real Time PCR System (Applied Biosystems) with SYBR Green q-PCR Master Mix (Nzytech). 5 μL of first-strand cDNA (previously diluted 1:10) and 560 nM of each specific primer were used, performing in a total 18 μl reaction volume. The quantification cycle (Cq) values were acquired for each sample with the following cycling conditions: 10 min at 95°C for initial denaturation, an amplification program of 40 cycles at 95°C for 15 s and 60°C for 1 min. Three technical replicates were considered for each sample. Virus reference isolates and no template controls were included in all plates. The fluorescence threshold was manually set above the background level. The specificity of qPCR reactions was evaluated by melting curve analysis. The identity of each amplicon was confirmed by Sanger sequencing. Specific amplification of target viral cDNA was confirmed by cloning PCR amplicons into pGem®-T Easy vector (Promega) and used to transform *Escherichia coli* JM109 (Promega) competent cells, by standard methodologies. Each amplicon, sequenced through Sanger procedure, was identified by comparison with corresponding virus sequences available from GenBank.

The specificity of each SYBR® Green assay against the cDNA of the other virus reference isolates was also tested by qPCR.

For each specific viral fragment, to determine the amplification efficiencies of the primers, standard curves were generated from 10-fold dilution series of plasmid DNA (each viral amplicon were cloned into a plasmid vector, as described above), used to draw a nine-point calibration curve to validate each assay in the dynamic range chosen (0.8 to 8E7 target copies). Amplification efficiencies were calculated through the equation $E = (10^{(-1/\text{slope})} - 1) \times 100$, as well as slope and linearity (coefficient of determination, R^2). Detection sensitivities of the assays were determined from the Cq of the lowest plasmid dilution that fell within the

[1] http://www.ncbi.nlm.nih.gov/

TABLE 2 | Primers used on qPCR assays.

Species	Accession ID	Primers (5′ → 3′)	AS (bp)	References
OMMV and/or TNV-D	AY616760	Fw: GTGTTCAGTCATATACATACC	247	Cardoso et al. (2004)
		Rv: GCCTATTGTGCTGTACCAC		
OLV-1	KF804054	Fw: GGGGTATGATGGTGCTATGG	162	This work
		Rv: ACTCCGCAATATCCGTTCTG		
OLYaV	AJ844555	Fw: GCTTATCTACTACGCCGATCTTGTC	71	This work
		Rv-AAGAGTGGATCCATCTAGATCGAAA		

Description of forward (Fw) and reverse (Rv) primers used for specific detection of Olive mild mosaic virus (OMMV) and/or Tobacco necrosis virus D (TNV-D), Olive latent virus 1 (OLV-1) and Olive leaf yellowing-associated virus (OLYaV), in the qPCR assays. AS, amplicon size.

linear standard curve. The method performed for absolute DNA quantification was based on the determination of the absolute number of target copies (TCN) previously described by Campos et al. (2018).

RESULTS

Linearity, Sensitivity, and Specificity of qPCR Assays

Standard curves of all studied olive viruses were constructed based on Cq values obtained from a 10-fold dilution series of the target plasmid DNA obtained from each reference isolate, in the dynamic range that was chosen. Linear relationships between Cq values and *log* plasmid DNA were obtained for all viruses, with regression coefficients (R^2) above 0.99 (**Figure 1**). As expected, similar standard curves were obtained when OMMV and TNV-D were used as targets, once a single set of primers for amplification of both viruses was used. The efficiencies (E) for all virus-specific primer pairs ranged from 99% to 104% (**Figure 1**).

The detection sensitivity of each assay was determined from the Cq of the lowest plasmid dilution that fell with standard curve, that enable to detect 8 target copies of OLYaV and 0.8 target copies of TNV-D/OMMV and OLV-1 (**Table 3**). The Cq values that correspond to the detected target copies are indicated in **Table 3**.

The specificity of the assays was confirmed *in silico*, performing homology search similarities against NCBI databases, and experimentally, with each reference virus isolates targeted only by the respective SYBR® Green assay (not shown). Also, the specificity of the primers and their combinations were verified via cloning and sequencing of amplified products.

Validation of Real-Time qPCR Assays Using Field Samples

To evaluate the practical robustness and accuracy of the qPCR assays, two experiments were conducted to test the presence of the viruses using field samples. Additionally, conventional PCR assays were also performed. It was also studied if total RNA template as viral target was suitable for virus detection through qPCR.

In the first experiment, concerning the use of dsRNA from 30 field-collected samples from a Portuguese olive orchard, OLYaV was not detected with neither qPCR nor conventional PCR. For the other studied viruses, qPCR revealed 26 positive samples for TNV-D and/or OMMV and 25 positive samples for OLV-1

TABLE 3 | Detection limits of each of the three qPCR assays based on determination of copy numbers.

Virus	Cq value	Copy number
TNV-D/OMMV	33.27	0.8
OLV-1	33.36	0.8
OLYaV	32.07	8

The detection range was determined from standard curves generated from the dilution series of respective recombinant plasmid DNA. The mean Cq values of positive samples were represented with respective copy numbers. TNV-D, Tobacco necrosis virus D; OMMV, Olive mild mosaic virus; OLV-1, Olive latent virus 1; OLYaV, Olive leaf yellowing-associated virus.

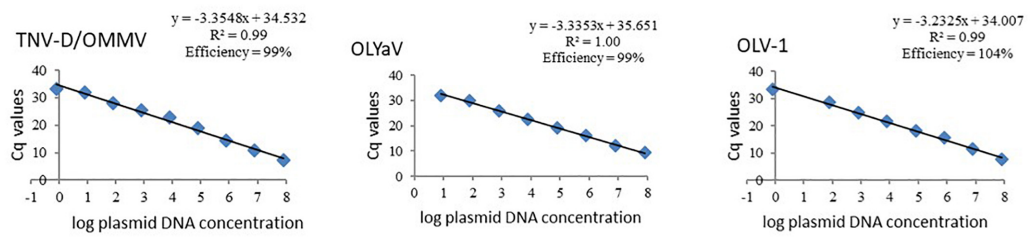

FIGURE 1 | Standard curves of olive viruses constructed based on Cq values obtained from a ten-fold dilution series of each target plasmid DNA in the dynamic range of 0.8 to 8E7 target copies. TNV-D, *Tobacco necrosis virus*; OMMV, *Olive mild mosaic virus*; OLV-1, *Olive latent virus 1*; OLYaV, *Olive leaf yellowing-associated virus*; R^2, regression coefficients.

(**Table 4** and **Supplementary Table 1**). Using conventional PCR, only six samples were positive for TNV-D and/or OMMV and three samples were positive to OLV-1.

To demonstrate the suitability of the qPCR methodology in different olive material and corroborate qPCR sensitivity, a second experiment was performed in 33 field-collected samples from 11 olive orchards, in several regions of Tunisia. For the qPCR experiment it was used as template total RNA from cortical scrapings from cuttings, instead of the highly laborious protocol for extraction of dsRNA used for conventional PCR. The results revealed that through qPCR and using total RNA as template, it was possible to detect all the studied viruses (**Table 5** and **Supplementary Table 1**). qPCR revealed that the most prevalent virus detected in Tunisia orchards was OLV-1 (31 samples diagnosed), followed by OLYaV (20 samples diagnosed), and finally the combination in last TNV-D and/or OMMV (12 samples diagnosed). Results on conventional PCR revealed that 11 samples were OLV-1 positive, 10 samples were TNV-D and/or OMMV-positive and 10 samples were OLYaV positive, as determined by Zellama et al. (2018).

Both experiments performed here demonstrate qPCR tests as suitable for detection of virus infecting olive.

DISCUSSION

Since there is no known source of genetic resistance to olive viruses, a key component of viral disease management is the propagation of virus-free plant materials. The main approach used to obtain, propagate and commercialize plants free from harmful pathogens is through phytosanitary selection and certification programs. The obtention of pathogen-free material from infected trees is possible to achieve through sanitation treatments such as heat therapy, meristem tip culture and micrografting, although the use of these methodologies for virus elimination in olive is still limited (Albanese et al., 2012). Thus, sensitive, reliable and cost-effective assays for the detection of olive viruses are critical and of major importance to guarantee a sustainable production of the orchards. The use of the highly sensitive qPCR arises as an extremely useful tool for studying various agents of infectious. In plant pathology, this technology is increasingly being used for studying various causal agents of plant diseases, including viruses (Poojari et al., 2016; Malandraki et al., 2017; Abdullah et al., 2018; Baaijens et al., 2018; Campos et al., 2019).

The work performed here, describes for the first time the use of a SYBR® Green-based qPCR methodology for specific and reliable quantitative detection of highly spread olive viruses. Moreover, despite the low viral titres of the olive viruses (Martelli, 1999), qPCR turns possible the use of total RNA for the detection of viruses, instead of the highly laborious dsRNA extraction essential for RT-PCR (Varanda et al., 2010, 2014; Félix et al., 2012; Zellama et al., 2018). The primers used in the experiments successfully differentiated the target pathogens, and the results obtained show that qPCR is not only a faster method, but most importantly, a sensitive method for the detection and quantification of olive viruses directly from woody plant material. It was used a primer set that allow the simultaneous detection of TNV-D and OMMV (designed in the CP gene, see Cardoso et al., 2004), and newly designed primers targeting OLV-1 and OLYaV, that revealed E, R^2 and slope consistent with the acceptance criteria (Broeders et al., 2014), confirming the accuracy and linear response of the assays over a wide range of dilutions, and suggesting absence of PCR inhibitors. These performance criteria further demonstrate that the developed assays, additionally to detection, constitute a reliable quantitative tool suitable for population or competition studies among the studied viruses in mixed infections in a variety of olive hosts. Conventional PCR conditions are different from qPCR conditions, with different optimized protocols and primers (only TNV-D and/or OMMV primer set was common to both methodologies), and consequently with not comparable results. Nevertheless, the idea of the higher sensitivity qPCR methodology, even with the low viral titres in olive tissues, is here reinforced. In the Portuguese cv. "Galega vulgar" the viruses OLV-1, TNV-D and/or OMMV were identified while OLYaV was not detected. OLV-1, TNV-D and/or OMMV were already identified in Portugal by RT-PCR methodology, although with lower rates (Cardoso et al., 2004, 2009; Varanda et al., 2010). In Tunisian orchards, independently of the cultivar, type of management or region, OLYaV, OLV-1, TNV-D and/or OMMV were detected, confirming previous RT-PCR results (Zellama et al., 2018), although qPCR registered a higher level of infection for the viruses under study. These results reinforce the idea of the sensitivity of the qPCR methodology, regardless of cultivar or region.

TABLE 4 | Comparison of SYBR® Green-based real-time quantitative reverse transcription PCR assays with conventional PCR, for virus detection in field-collected samples from a Portuguese olive orchard, with cv. "Galega vulgar."

Virus	SYBR Green-based PCR (qPCR) (Virus-positive/total number of samples)	Conventional PCR (RT-PCR) (Virus-positive/total number of samples)
TNV-D and/or OMMV	26/30	6/30
OLV-1	25/30	3/30
OLYaV	0/30	0/30

TNV-D, Tobacco necrosis virus D; OMMV, Olive mild mosaic vírus; OLV-1, Olive latent virus 1; OLYaV, Olive leaf yellowing-associated virus.

TABLE 5 | Comparison of SYBR® Green-based real-time quantitative reverse transcription PCR assays with conventional PCR, for virus detection in field-collected samples from 11 olive orchards, in several regions of Tunisia.

Virus	SYBR Green-based PCR (qPCR) (Virus-positive/total number of samples)	Conventional PCR (RT-PCR) (Virus-positive/total number of samples)
TNV-D and/or OMMV	12/33	10/33
OLV-1	31/33	11/33
OLYaV	20/33	10/33

Conventional PCR results included in Zellama et al. (2018). TNV-D, Tobacco necrosis virus D; OMMV, Olive mild mosaic vírus; OLV-1, Olive latent virus 1; OLYaV, Olive leaf yellowing-associated virus.

qPCR combined with the SYBR® Green methodology enabled, for the first time, a high level of reliability, sensitivity and reproducibility regarding the estimation of virus accumulation in infected olive trees, being an efficient tool for the early diagnosis of the diseases, and for the improvement of the viral diagnosis. The results achieved will allow gaining new insights in virus biology, essential for disease control. Furthermore, this robust diagnostic procedure will give an important contribute for the establishment of phytosanitary certification programs of olive and high-quality productions.

DATA AVAILABILITY

The datasets generated for this study are available on request to the corresponding author.

AUTHOR CONTRIBUTIONS

MDC and MRF: conceptualization. MDC: formal analysis. MDC and AP: funding acquisition. MDC, MZ, and CV: methodology. MDC, MZ, CV, and PM: resources. MRF and MC: supervision. MDC: writing, original draft preparation. MDC, MZ, CV, PM, AP, MC, and MRF: writing, review and editing.

FUNDING

This work was financially supported by FEDER and National Funds through the ALENTEJO 2020 (Regional Operational Program of the Alentejo), Operação ALT20-03-0145-FEDER-000014 – "Valorização das Variedades de Oliveira Portuguesas (OLEAVALOR)", and by National Funds through FCT – Foundation for Science and Technology under the Project UID/AGR/00115/2019.

SUPPLEMENTARY MATERIAL

The Supplementary Material for this article can be found online at: https://www.frontiersin.org/articles/10.3389/fpls.2019.00694/full#supplementary-material

REFERENCES

Abdullah, A. S., Turo, C., Moffat, C. S., Lopez-Ruiz, F. J., Gibberd, M. R., Hamblin, J., et al. (2018). Real-time PCR for diagnosing and quantifying co-infection by two globally distributed fungal pathogens of wheat. *Front. Plant Sci.* 9:1086. doi: 10.3389/fpls.2018.01086

Al Abdullah, A., El Beaino, T., Saponari, M., Hallak, H., and Digiaro, M. (2005). Preliminary evaluation of the status of olive-infecting viruses in Syria. *EPPO Bull.* 35, 249–252. doi: 10.1111/j.1365-2338.2005.00818.x

Alabdullah, A., Minafra, A., Elbeaino, T., Saponari, M., Savino, V., and Martelli, G. P. (2010). Complete nucleotide sequence and genome organization of olive latent virus 3, a new putative member of the family Tymoviridae. *Virus Res.* 152, 10–18. doi: 10.1016/j.virusres.2010.05.010

Albanese, G., Saponari, M., and Faggioli, F. (2012). "Phytosanitary certification," in *Olive Germoplasm-The Olive Cultivation, Table Olive and Olive Oil Industry in Italy*, ed. I. Muzzalupo (Rijeka: InTech), 107–132.

Baaijens, R., Urbez-Torres, J. R. R., Liu, M., Ayres, M., Sosnowski, M. R., and Savocchia, S. (2018). Molecular methods to detect and quantify botryosphaeriaceae inocula associated with grapevine dieback in Australia. *Plant Dis.* 102, 1489–1499. doi: 10.1094/PDIS-11-17-1854-RE

Bertolini, E., Olmos, A., Martínez, M. C., Gorris, M. T., and Cambra, M. (2001). Single-step multiplex RT-PCR for simultaneous and colourimetric detection of six RNA viruses in olive trees. *J. Virol. Methods* 96, 33–41. doi: 10.1016/S0166-0934(01)00313-5

Broeders, S., Huber, I., Grohmann, L., Berben, G., Taverniers, I., Mazzara, M., et al. (2014). Guidelines for validation of qualitative real-time PCR methods. *Trends Food Sci. Technol.* 37, 115–126. doi: 10.1016/j.tifs.2014.03.008

Campos, M. D., Patanita, M., Campos, C., Materatski, P., Varanda, C. M. R., Brito, I., et al. (2019). Detection and quantification of Fusarium spp. (F. oxysporum, F. verticillioides, F. graminearum) and magnaporthiopsis maydis in maize using real-time PCR targeting the ITS region. *Agronomy* 9:45. doi: 10.3390/agronomy9010045

Campos, M. D., Valadas, V., Campos, C., Morello, L., Cardoso, G., Braglia, L., et al. (2018). A TaqMan real-time PCR method based on alternative oxidase genes for detection of plant species in animal feed samples. *PLoS One* 13:e0190668. doi: 10.1371/journal.pone.0190668

Cardoso, J. M. S., Félix, M. R., Clara, M. I., and Oliveira, S. (2009). Complete genome sequence of a tobacco necrosis virus D isolate from olive trees. *Arch. Virol.* 154, 1169–1172. doi: 10.1007/s00705-009-0414-9

Cardoso, J. M. S., Félix, M. R., Oliveira, S., and Clara, M. I. E. (2004). A tobacco necrosis virus D isolate from Olea europaea L.: viral characterization and coat protein sequence analysis. *Arch. Virol.* 149, 1129–1138. doi: 10.1007/s00705-003-0258-7

Espy, M. J., Uhl, J. R., Sloan, L. M., Buckwalter, S. P., Jones, M. F., Vetter, E. A., et al. (2006). Real-time PCR in clinical microbiology: applications for routine routine laboratory testing. *Clin. Microbiol. Rev.* 19, 165–256. doi: 10.1128/CMR.00022-06

Fadel, C., Digiaro, M., Choueiri, E., El Beaino, T., Saponari, M., Savino, V., et al. (2005). On the presence and distribution of olive viruses in Lebanon. *OEPP EPPO Bull.* 35, 33–36. doi: 10.1111/j.1365-2338.2005.00776.x

Faggioli, F., Ferretti, L., Albanese, G., Sciarroni, R., Pasquini, G., Lumia, V., et al. (2005). Distribution of olive tree viruses in italy as revealed by one-step RT-PCR. *J. Plant Pathol.* 87, 49–55.

Félix, M., Clara, M., Leitão, F., and Fernandes Serrano, J. (2002). Virus incidence in four olea europaea cultivars evaluated by mechanical inoculation and immunological assays. *Acta Hortic.* 586, 721–724. doi: 10.17660/ActaHortic.2002.586.154

Félix, R., Varanda, C. M. R., and Clara, M. I. E. (2012). Biology and molecular characterization of necroviruses affecting olea europaea L.: a review. *Eur. J. Plant Pathol.* 133, 247–259. doi: 10.1007/s10658-011-9907-y

Fontana, A., Piscopo, A., Bruno, A., De Tiberini, A., Muzzalupo, I., and Albanese, G. (2019). Impact of olive leaf yellowing associated virus on olive (Olea europaea L.) oil. *Eur. J. Lipid Sci. Technol.* 121:1800472. doi: 10.1002/ejlt.201800472

Godena, S., Bendini, A., Giambanelli, E., Cerretani, L., Ermić, D., and Ermić, E. (2012). Cherry leafroll virus: impact on olive fruit and virgin olive oil quality. *Eur. J. Lipid Sci. Technol.* 114, 535–541. doi: 10.1002/ejlt.201100277

Luigi, M., Godena, S., Dermić, E., Barba, M., and Faggioli, F. (2011). Detection of viruses in olive trees in Croatian Istria. *Phytopathol. Mediterr.* 50, 150–153.

Malandraki, I., Beris, D., Isaioglou, I., Olmos, A., Varveri, C., and Vassilakos, N. (2017). Simultaneous detection of three pome fruit tree viruses by one-step multiplex quantitative RT-PCR. *PLoS One* 12:e0180877. doi: 10.1371/journal.pone.0180877

Martelli, G. P. (1999). Infectious diseases and certification of olive: an overview. *Bull. OEPP EPPO* 29, 127–133. doi: 10.1111/j.1365-2338.1999.tb00806.x

Martelli, G. P. (2011). "Infectious diseases of olive," in *Olive Diseases and Disorders*, eds L. Schena, G. E. Agosteo, and S. O. Cacciola (Tri-vandrum: Transworld Research Network), 71–78.

Martelli, G. P., Salerno, M., Savino, V., and Prota, U. (2002). An appraisal of diseases and pathogens of olive. *Acta Hortic.* 586, 701–708. doi: 10.17660/ActaHortic.2002.586.150

Materatski, P., Varanda, C., Carvalho, T., Campos, M. D., and Rei, F. (2018). Diversity of colletotrichum species associated with olive anthracnose and new perspectives on controlling the disease in Portugal. *Agronomy* 8:301. doi: 10.3390/agronomy8120301

Morris, T. J., and Dodds, J. A. (1979). Isolation and analysis of double-stranded RNA from virus-infected plant and fungal tissue. *Phytopathology* 69, 854–858. doi: 10.1094/Phyto-69-854

Poojari, S., Alabi, O. J., Okubara, P. A., and Naidu, R. A. (2016). SYBR® Green-based real-time quantitative reverse-transcription PCR for detection and discrimination of grapevine viruses. *J. Virol. Methods* 235, 112–118. doi: 10.1016/j.jviromet.2016.05.013

Salman, M. (2017). Biological control of spilocaea oleagina, the causal agent of olive leaf spot disease, using antagonistic bacteria. *J. Plant Pathol.* 99, 741–744.

Saponari, M., Alkowni, R., Grieco, F., Pantaleo, V., Savino, V., Martelli, G. P., et al. (2002). Detection of olive-infecting viruses in the mediterranean basin. *Acta Hortic.* 586, 787–790. doi: 10.17660/ActaHortic.2002.586.170

Saponari, M., Boscia, D., Nigro, F., and Martelli, G. P. (2013). Fungal species associated with a severe decline of olive in identification of dna sequences related to xylella fastidiosa in oleander, almond and olive trees exhibiting leaf scorch symptoms in apulia (southern italy). *J. Plant Pathol.* 95, 659–668.

van Regenmortel, M. H. V., Fauquet, C. M., Bishop, D. H. L., Carstens, E. B., Estes, M. K., Lemon, S. M., et al. (2000). *Virus Taxonomy. Seventh Report of the International Committee on Taxonomy of Viruses*. San Diego, CA: Academic Press.

Varanda, C., Cardoso, J. M. S., do Rosário Félix, M., Oliveira, S., and Clara, M. I. (2010). Multiplex RT-PCR for detection and identification of three necroviruses that infect olive trees. *Eur. J. Plant Pathol.* 127, 161–164. doi: 10.1007/s10658-010-9593-1

Varanda, C. M. R., Nolasco, G., Clara, M. I., and Félix, M. R. (2014). Genetic diversity of the coat protein of olive latent virus 1 isolates. *Arch. Virol.* 159, 1351–1357. doi: 10.1007/s00705-013-1953-7

Yadav, N., and Khurana, S. M. P. (2016). "Plant Virus Detection and Diagnosis: Progress and Challenges," in *Frontier Discoveries and Innovations in Interdisciplinary Microbiology*, ed. P. Shukla (New Delhi: Springer).

Zellama, M. S., Varanda, C. M. R., Materatski, P., Nabi, N., Hafsa, A. B., Saamali, B. M., et al. (2018). *An Integrated Approach for Understanding the High Infection Rates of Olive Viruses in Tunisia*. Amsterdam: Springer Netherlands, doi: 10.1007/s10658-018-01620-y

Zhao, J., Zhang, X., Hong, Y., Liu, Y., and Liu, Y. (2016). Chloroplast in plant-virus interaction. *Front. Microbiol.* 7:1565. doi: 10.3389/fmicb.2016.01565

Conflict of Interest Statement: The authors declare that the research was conducted in the absence of any commercial or financial relationships that could be construed as a potential conflict of interest.

frontiers in Nutrition

ORIGINAL RESEARCH
published: 04 July 2019
doi: 10.3389/fnut.2019.00094

Oil Content, Fatty Acid and Phenolic Profiles of Some Olive Varieties Growing in Lebanon

Milad El Riachy[1], Athar Hamade[2], Rabih Ayoub[2], Faten Dandachi[1] and Lamis Chalak[2]*

[1] Department of Olive and Olive Oil, Lebanese Agricultural Research Institute, Tal Amara, Lebanon, [2] Faculty of Agronomy, The Lebanese University, Beirut, Lebanon

Olive growing in Lebanon plays an important role at both a social and economic level. Nevertheless, the quality of olive oil produced in the country is rarely addressed. In this study, oil content, fatty acid, and phenolic profiles were studied along four different ripening stages for 11 varieties of olives, including two clones of the local variety "Baladi," in addition to nine foreign varieties ("Ascolana Tenera," "Bella di Cerignola," "Itrana," "Jabaa," "Kalamata," "Nabali," "Salonenque," "Sigoise," and "Tanche"). Oil content was determined using the Soxhlet method and Abencor system. Fatty acid composition was determined using a GC-FID, total phenols using spectrophotometry, and the phenolic profile using HPLC-DAD. Results showed that variety, fruit ripening and their interaction have a significant effect on the overall studied oil parameters. Among the studied varieties, "Kalamata" presented the higher oil content on dry matter (OCDM = 48.24%), "Baladi 1" the highest oil content on humid matter (OCHM = 27.86%), and "Tanche" the highest oil industrial yield (OIY = 19.44%). While "Tanche" recorded the highest C18:1 (71.75%), "Ascolana Tenera" showed the highest total phenols (TP = 539 mg GAE/Kg of oil), "Salonenque" the highest oleacein (121.57 mg/Kg), and "Itrana" the highest oleocanthal contents (317.68 mg/Kg). On the other hand, oil content together with C18:2 and C18:0 increased along ripening while C18:1, total phenols and the main individual phenols decreased. Although preliminary, this study highlights the good quality of olive oil produced from both local and foreign varieties growing in Lebanon and encourages further investigations on the characterization and authentication of Lebanese olive oil.

Keywords: ***Olea europaea*** **L., variety characterization, fruit ripening, oil yield, oil quality attributes**

OPEN ACCESS

Edited by:
Wenceslao Moreda, Spanish National Research Council (CSIC), Spain

Reviewed by:
Susana Casal, University of Porto, Portugal
Susana P. Alves, University of Lisbon, Portugal

****Correspondence:***
Milad El Riachy
mriachy@lari.gov.lb

Specialty section:
This article was submitted to Food Chemistry, a section of the journal Frontiers in Nutrition

Received: *07 March 2019*
Accepted: *06 June 2019*
Published: *04 July 2019*

Citation:
El Riachy M, Hamade A, Ayoub R, Dandachi F and Chalak L (2019) Oil Content, Fatty Acid and Phenolic Profiles of Some Olive Varieties Growing in Lebanon. Front. Nutr. 6:94. doi: 10.3389/fnut.2019.00094

INTRODUCTION

Edible olives originate from areas along the eastern Mediterranean shore in what is now southern Turkey, Syria, Lebanon, and Palestine since 5,000–6,000 years ago (1, 2). Lebanon is rich in indigenous and ancient olive trees and its history of olive traditions is as old as its cultural history (3, 4). The Lebanese groves are dominated by the main traditional denomination "Baladi." Other old varieties are still found in some ancient groves e.g., "Ayrouni," "Sorani," "Dal," "Jlot," and "Abou Chawkeh" across the country (5, 6). A few other varieties, introduced from neighboring Arab countries, are also found such as "Nabali" which is one of the oldest olive varieties in the Middle East. During the last few decades, grooves of foreign varieties have been planted, imported from Italy ("Frantoio," "Leccino," "Ascolana Tenera," "Nocellara Del Belice"), Spain ("Manzanilla de

Sevilla," "Arbequina"), Greece ("Kalamata," "Koroneiki"), France ("Salonenque," "Picholine"), and Algeria ("Sigoise") (7, 8).

The interest in olive varieties with higher oil content (OC), improved fatty acid composition, mainly high monounsaturated fatty acids (MUFAs) and a high content of phenolic compounds, has increased due to its stability and health benefits (9, 10). While OC is associated with oil quantity and olive growing profitability; the proportions of the different fatty acids and phenolic compounds are associated with oil quality. For example, a high percentage of MUFA, mainly oleic acid, is a primordial factor in determining the nutritional value of the oil as it reduces the risk of atherosclerosis (11) and protects against different kinds of cancers (12). In addition, fatty acid composition influences the stability of the oil through the contribution of polyunsaturated fatty acids (PUFAs) to oil rancidity (13). On the other hand, the amount of olive oil phenolic compounds, such as oleuropein derivatives is of primary importance when evaluating its quality, as these natural antioxidants improve oil resistance to oxidation and are responsible for its sharp bitter taste (14). The pharmacological interest of olive phenolic compounds is also well-known (15, 16).

Several agro-industrial parameters may modify the OC, the fatty acid composition and phenolic content of virgin olive oil (VOO). Indeed, previous studies showed that OC, fatty acid and phenolic profiles are a built-in genetic factor. Values between 10 and 30% of oil were reported when evaluating the different accessions of the World Olive Germplasm Bank in Cordoba-Spain (17). Moreover, in the Germplasm Banks of Catalonia and Cordoba, Tous et al. (18) and Uceda et al. (19), respectively, showed that more than 70% of the variation in the fatty acids (except for linolenic acid) and several minor components, such as phenolic compounds, bitter index (K225), and oil stability, was due to genetic effects. In addition, evaluation of new varieties obtained by breeding programs showed that genotypic variance was the main contributor to the total variance of fatty acids (20, 21) and of phenolic compounds (21, 22). In addition, fruit ripening affects oil quantity and composition as early harvested olives, especially green olives, give lower oil quantity but higher content in MUFAs and antioxidants than late harvested ones (23–25). Additionally, OC and composition may vary according to the climatic conditions of the year, the irrigation regimes and the processing systems among others (23, 25–27).

In the past few years, authenticity and characterization of olive oils have been the object of numerous studies due to the importance of the protection of consumers. Various physico-chemical determinations in association with chemometric analyses have been applied: fatty acids (28–31), fatty acids and triacylglycerols (32, 33), sterols (34), phenolic compounds (35), and aromas (36). Yet little attention has been given to the authentication and characterization of Lebanese olive oils. Chehade et al. (6, 37) described some oil traits for eight Lebanese olive varieties; however, many other varieties cultivated in Lebanon are still not comprehensively assessed. In this manuscript, we report the characterization of monovarietal olive oils for 11 varieties cultivated in northern Lebanon for their OC, fatty acid and phenolic composition along fruit ripening with the perspective of evaluating and valorizing Lebanese olive oil. Expected findings will allow the development of a set of practical recommendations providing farmers with knowledge of the best varieties to be grown and the best time for olive harvesting, to further improve Lebanese production of olive oil in terms of quantity and quality.

Abbreviations: GAE, Gallic acid equivalent; MC, Moisture content; OC, Oil content; OCDM, Oil content on dry matter; OCHM, Oil content on humid matter; OIY, Oil industrial yield; PCA, Principal component analysis; RI, Ripening index; TP, Total phenols.

MATERIALS AND METHODS

Plant Material and Extraction of Olive Oil

Olive fruits were collected from 11 varieties growing in Abdeh station of the Lebanese Agricultural Research Institute (LARI) during the 2015 olive harvest season. This station, located at 18 m a.s.l., 34°31'0" N and 35°58'0" E, has been hosting an international olive collection of 72 olive varieties, initially collected from Lebanon, Arabic, and European countries, since the early seventies. The Abdeh region is characterized by a typical Mediterranean climate with a dry summer from June to September. The average annual precipitation sums 870 mm, the soil is a clay type soil with 25% sand, 15% silt, and 60% clay with 2% organic matter content. The olive trees in the Abdeh collection are rainfed.

The 11 genotypes considered included two clones of the local traditional variety, "Baladi 1" and "Baladi 2," as previously differentiated by Chalak et al. (38), in addition to nine foreign varieties i.e., "Nabali" and "Jabaa" (from Palestine), "Kalamata" (derived from Greece), "Salonenque" and "Tanche" (from France), "Ascolana Tenera," "Bella di Cerignola" and "Itrana" (originating from Italy), and "Sigoise" (derived from Algeria) (2, 39–41). For each variety, three fruit samples were collected from three trees, at different harvesting dates, based on fruit skin color (0= deep or dark green; 1 = yellowish-green; 2 = yellowish with reddish spots; 3 = reddish or light violet; and 4 = black), and the ripening index (RI). RI was determined on samples of 100 fruits according to the method described by Uceda and Hermoso (42) and modified by El Riachy et al. (43), following the formula:

$$RI = \frac{((0 \times n_0) + (1 \times n_1) + (2 \times n_2) + (3 \times n_3) + (4 \times n_4))}{100};$$

where, n_0 to n_4, is the total number of olive fruits in each category. Then, RI was categorized to the following five categories: RI $\leq$ 0.5 (RI0), 0.5 $\geq$ RI $\leq$ 1.5 (RI1), 1.5 $\geq$ RI $\leq$ 2 (RI2), 2.5 $\geq$ RI $\leq$ 3.5 (RI3), and finally RI $\geq$ 3.5 (RI4).

The olive oil was obtained using the Abencor system (MC2 Ingenierías y Sistemas, Sevilla, Spain). For each sample, ~500 g of fruits were ground to a paste using a hammer mill, stirred in the thermobeater for 30 min at 28 ± 1°C, and then centrifuged for 2 min to separate the oil, which was collected and left to decant in graduated cylinders. OIY was calculated using the following formula (44):

$$OIY = \frac{V \times 0.915 \times 100}{W};$$

where, V is the volume of oil obtained; and W is the weight of the processed olive paste. Finally, the oil extracted was collected and stored in glass vials in darkness at −20°C until analysis.

Chemical Reagents

The chemical reagents used for VOO characterization were of GC or HPLC grade. Methanol, acetonitrile, *o*-phosphoric acid and the Folin-Ciocateu (F-C) reagent were provided from Sigma-Aldrich (Steinheim, Germany), *n*-hexane from Hipersolv Chromanorm (Pennsylvania, USA), Na_2CO_3 anhydrous from Acros organics (New Jersey, USA) and KOH from Fisher Scientific (Loughborough, UK). Regarding the commercial standards, methyl palmitate, methyl palmitoleate, methyl stearate, methyl oleate, methyl linoleate, methyl linolenate, hydroxytyrosol, tyrosol, *p*-coumaric acid, luteolin, and apigenin were purchased from Sigma-Aldrich (Steinheim, Germany) and Fluka (Steinheim, Germany), vanillic and syringic acid standards were obtained from Acros organics (New Jersey, USA), gallic acid from Fisher Scientific (Loughborough, UK), and oleacein and oleocanthal were supplied by Prof. Prokopios Magiatis (Athens, Greece). Finally, deionized water (18 MΩ cm) from a Milli-Q water purification system (Millipore, Bedford, MA, USA) was used to prepare the mobile phases for HPLC analysis.

Determination of the Oil Content (OC) in the Olive Paste Using Soxhlet Method

OC in the olive paste was determined using a Gerhardt Soxhlet instrument (Gerhardt Soxtherm SE−416, Germany) (45). From each sample, an aliquot of 50–60 g of the olive paste was dried at 105°C to weight stability using a rapid moisture analyzer (Metler Toledo HS 153, Switzerland). One gram of the dry paste was placed on a filter paper which was folded and closed tightly using a cotton wire. Each prepared sample was placed in previously weighed soxhlet beakers containing three boiling chips. Petroleum benzene was used as a solvent. The total program length was 2 h and 20 min. When the process ended, the samples were thrown out, and the remaining solvent was eliminated by placing the beakers under a fume hood overnight, then, the beakers were dried in an oven at 105°C for 1.5 h in a desiccator for 45 min before being weighed. OC was calculated from both dry matter (OCDM) and humid matter basis (OCHM) as follows:

$$\text{Oil content on dry matter (OCDM)} = \frac{m_2 - m_1}{\text{Sample weight}} \times 100$$

$$\text{Oil content on humid matter (OCHM)} = \frac{(100 - \text{MC}) \times \text{OCDM}}{100}$$

where, m_1 = beaker weight before extraction; m_2 = beaker weight after extraction and MC = moisture content.

Determination of Fatty Acid Profile

Fatty acid methyl esters (FAMEs) were prepared based on a cold transmethylation reference method (46). A sample of 0.1 g oil was shaken manually with 2 mL *n*-hexane for 2 s then 0.2 mL of methanolic solution (2 N) of potassium hydroxide was added. The sample was mixed with a vortex for 1 min (1,400 rpm), before resting for 5 min. A volume of 975 μL of the upper phase that contains the FAME was transferred to 1.5 mL vials with 25 μL of external standard (nonadecanoate methyl ester 1,000 ppm). The separation of FAMEs was carried out using a Shimadzu gas chromatograph (GC-2010 Plus) equipped with a flame ionization detector (FID). A fused silica capillary column (DB-wax; Agilent Technologies, Wilmington, DE; 30 m length × 0.25 mm i.d. and 0.25 μm of film thickness) was used. Nitrogen was used as a carrier gas with a flow rate of 1.69 mL/min. As for the chromatographic gradient, the initial oven temperature was kept at 165°C for 15 min and then programmed to rise at 5°C/min up to 200°C, maintained for 2 min, and followed by a second gradient of 5°C/min to a final temperature of 240°C, which was held for 5 min. The injector and detector temperatures were 250 and 280°C, respectively. Hydrogen and compressed air were used for the flame detector. Finally, the injection volume was 1 μL with a split ratio of 50. Identification of the different fatty acids was achieved by a comparison of their retention times with those of authentic standards. Results were expressed as percentages of total fatty acids. Finally, the calculated sums and ratios were; saturated fatty acid (SFA), MUFA, PUFA, MUFA/PUFA, MUFA/SFA, PUFA/SFA, C16:0/C18:2, C18:1/C18:2, and C18:2/C18:3.

Extraction of Phenolic Compounds

Prior analysis samples were left to thaw at room temperature. Meanwhile, an internal standard solution was prepared by dissolving 15 mg of syringic acid in 10 mL of 60:40 v/v methanol–water. Then, 1 mL from this solution was diluted in a 25 mL volumetric flask with 60:40 v/v methanol–water.

The phenolic compounds in the olive oil were extracted using a modification of the procedure described by Montedoro et al. (47). An amount of 3 g of olive oil was shaken manually with 2 mL of *n*-hexane for 15 s. Then, a volume of 1.75 mL of 60:40 (v/v) methanol–water mixture was added together with 0.25 mL of the internal standard solution and shaken for 2 min to undergo the first extraction. For the second extraction, 2 mL of methanol/water (60/40) was added and shaken for 2 min. The extracts from both extractions were combined and placed in the dark at −20°C for further determinations.

Spectrophotometric Estimation of Total Phenols

The total phenols (TP) content of the oil extracts was determined according to the Folin-Ciocalteu spectrophotometric method (48). Briefly, 20 μL of the sample (with prior 1:50 dilution with water) was, in this order, mixed with 1.58 mL of water, 0.3 mL of 20% (w/v) Na_2CO_3 aqueous solution, and 0.1 mL of F–C reagent, and heated in an oven for 5 min at 50°C. Then, the resulting solution was allowed to stand for 30 min. The reaction product was spectrophotometrically monitored at 765 nm by a jenway UV/Vis spectrophotometer (Staffordshire, ST15 OSA, UK). A nine level calibration curve was prepared using gallic acid as a commercial standard ($r^2 = 0.998$), and the results were expressed as mg gallic acid equivalent (GAE)/Kg of oil.

Chromatographic Analysis of Phenols by HPLC-DAD

The produced extract was also used to determine the following eight individual phenolic compounds: hydroxytyrosol, tyrosol, vanillic acid, *p*-coumaric acid, oleacein, oleocanthal, luteolin, and apigenin. The extracted phenolic fraction was injected in triplicate in a Shimadzu High Performance Liquid Chromatograph (HPLC) equipped with an automatic injector, a column oven and a diode array UV detector (DAD). Separation of individual phenols was achieved on a Microsorb-MV 100 C18 column (250 × 4.6 id mm, 5 µ particle size), maintained at 40°C. The injection volume was 20 µL and the flow rate 1.0 mL/min. Mobile phases were 0.2% *o*-phosphoric acid in water (mobile phase A) and a mixture methanol-acetonitrile (50:50, v/v) (B). The initial concentrations were 96% of A and 4% of B and the gradient was changed as follows: the concentration of B was increased to 50% in 40 min, increased to 60% in 5 min, and to 100% in 15 min, and maintained for 10 min. Initial conditions were reached in 7 min. The identification of individual olive oil phenols was performed at 280 nm, on the basis of their maximum absorption and retention times compared to those of commercial standard compounds. Phenolic compounds quantification was achieved using syringic acid as an internal standard and 9 point calibration curves of authentic standards. Results were expressed as mg of the target analyte per Kg of oil.

Statistical Analysis

The total number of samples was 129 samples. Each sample was loaded in triplicate for individual phenol analysis, in duplicate for fat content and for fatty acid determination, and just once for the TP estimation. Multivariate analysis of variance (MANOVA) was used to assess the combined effect of variety, fruit ripening, and their interaction on the different sets of variables; and one-way analysis of variance (ANOVA) was used to test the significance of the effect of the studied factors and their interaction on each parameter studied. For all traits studied, trait means, coefficient of variation, and standard error were calculated; while means were compared using Tukey's HSD test at ($p < 0.05$). A principal component analysis (PCA) was also performed in order to determine the degree of contribution of each of the characters to the total variation and to highlight the effect of the studied factors on those traits (49). Data processing was performed using the Statistics (Analytical Software, Tallahasse, FL, USA) and Unscrambler (CAMO A/S, Trodheim, Norway) statistical packages.

RESULTS

The combined effects of the variety, the fruit ripening and their interaction were assessed for the sets of variables related to OC, fatty acids and phenolic composition. The results of the MANOVA (**Table 1**) showed a highly significant effect of the interaction variety × fruit ripening ($p < 0.001$) on the three sets of variables. Similarly, each factor alone also showed a highly significant effect ($p < 0.001$) on these sets of variables. In this case, the variety and its associated error exhibited a more remarkable effect, expressed as partial η^2, while 64% of the change in the OC set can be accounted for by the variety and its associated error; 83% in the fatty acid composition set; and 69% in the phenolic composition set. Moreover, the two studied factors and their interaction showed a very high power (=1) sufficient to detect such effects.

To have more advanced information about the effects of the variety, the fruit ripening and their interaction on each of the studied variables, the Tests of Between-Subjects Effects, which are similar to many ANOVAs, were used (**Table 2**). Results highlighted the relative importance, expressed as percentages of the total sum of squares, of variety (29.38–92.32%), fruit ripening (0.38–55.07%), and their interaction (1.91–39.27%); with however, a greater contribution attributed to variety except in case of C16:0/C18:2 where fruit ripening recorded the greater contribution and in case of apigenin where the interaction variety × fruit ripening showed the greater contribution. The interaction variety × fruit ripening significantly affected MC and OIY ($p < 0.0125$); C16:0, C16:1, SFA, MUFA/PUFA, MUFA/SFA, PUFA/SFA, C16:0/C18:2, and C18:1/C18:2 ($p < 0.003$); and TP and all individual phenols studied ($p < 0.005$). As per each factor alone, significant differences were observed between varieties for OC traits, fatty acids, and phenolic composition. Similarly, significant differences were observed according to the fruit ripening for OC traits, C16:1, C18:1, C18:2, MUFA, PUFA, MUFA/PUFA, PUFA/SFA, C16:0/C18:2, C18:1/C18:2, C18:2/C18:3, TP, vanillic acid, oleacein, oleocanthal, and apigenin.

Mean comparisons (**Table 3**) showed that "Kalamata" recorded the highest OCDM (48.24%), "Baladi 1" the highest OCHM (27.86%), and "Tanche" the highest OIY (19.44%). As per the fatty acid composition, "Tanche" was characterized by the highest percentage of MUFA (72.43%) as it recorded the highest C18:1 (71.75%), the most important fatty acid characteristic of olive oil. On the other hand, "Jabaa" was characterized by higher percentages of PUFA (20.59%) due to the high percentages of C18:2 (19.47%) and C18:3 (1.12%) recorded in this variety. As per the SFA, "Saloneque" presented the highest percentage of C16:0 (17.34%) and "Bella di Cerignola" the highest C18:0 (4.35%), while the highest SFA was recorded in "Saloneque" (20.48%). Regarding the different ratios that strongly influence olive oil oxidative stability and health benefits, "Tanche" presented the highest MUFA/PUFA (7.02), the highest C18:1/C18:2 (7.64) and together with "Sigoise" the highest MUFA/SFA (4.62 and 4.74, respectively); and "Nabali" recorded the lowest PUFA/SFA (0.64). Regarding phenolic compounds, "Ascolana Tenera" presented the highest content of TP (539 mg/Kg), hydroxytyrosol (9.1 mg/Kg), tyrosol (8.97 mg/Kg), and vanillic acid (3.46 mg/Kg); "Itrana" the highest values of *p*-coumaric acid (2.59 mg/Kg) and oleocanthal (317.68 mg/Kg); "Saloneque" the highest content of oleacein (121.57 mg/Kg); and "Jabaa" the richest in Apigenin (7.93 mg/Kg).

OC traits and the majority of fatty acids and phenolic compounds appeared to be significantly affected by the fruit ripening (**Table 4**). OC assessed as OCDM, OCHM, and OIY, showed a general increase along the ripening process; although, OCHM and OIY decreased with the increase of moisture

TABLE 1 | Results of the Multivariate Analysis of Variance (MANOVA) of the three sets of variables: oil content (OC), fatty acids, and phenolics composition.

Parameters	Interaction	Wilk's Λ	F	Partial η^2	Power
OC	Variety	0.02	14.84***	0.64	1
	Fruit ripening	0.15	18.18***	0.47	1
	Variety × fruit ripening	0.12	2.01***	0.41	1
Fatty acids	Variety	0.00	36.07***	0.83	1
	Fruit ripening	0.02	15.81***	0.74	1
	Variety × fruit ripening	0.00	4.20***	0.60	1
Phenolic compounds	Variety	0	21.17***	0.69	1
	Fruit ripening	0.14	7.85***	0.49	1
	Variety × Fruit ripening	0	5.34***	0.66	1

***$P < 0.001$.

content after rainfall. Indeed, OCDM increased progressively from 37.27% at RI = 1 to 45.75 at RI = 4; however, OCHM and OIY, increased from RI = 1 (19.88 and 9.51%, respectively) to RI = 3 (23.42 and 15.30%, respectively) before decreasing at RI = 4 (22.52 and 13.96%, respectively). Among fatty acids, C16:0 and C18:1 decreased; although the difference was only significant in case of C18:1 ($p < 0.003$). In contrast, C16:1, C18:0, and C18:2 increased with a significant difference only in the case of C16:1 and C18:2. Similarly, the studied phenolic compounds displayed different tendencies along ripening too. TP, oleacein and oleocanthal significantly decreased from 387 mg GAE/Kg, 61.87 mg/Kg, and 136.28 mg/Kg, respectively at RI = 1 to 250 mg GAE/Kg, 46.57 mg/Kg, and 81.13 mg/Kg, respectively at RI = 4. The rest of the phenols increased until RI = 2 in case of hydroxytyrosol, *p*-coumaric acid, luteolin, and apigenin and until RI = 3 in case of tyrosol and vanillic acid, before decreasing at RI = 4; although the difference was only significant ($p < 0.005$) in the case of vanillic acid and apigenin.

The general evolution pattern described above along ripening was in some studied traits different between varieties (**Figure 1**). For instance, OIY increased along ripening in "Baladi 2," "Itrana," and "Nabali"; however, it increased until RI = 2 in case of "Ascolana," "Baladi 1," "Jabaa," and Salonenque" and until RI = 3 in "Bella di Cerignola," "Tanche," "Kalamata," and "Sigoise" before decreasing later on. Among fatty acids, C16:0 decreased along ripening in "Ascolana," "Baladi 1," "Baladi 2," "Kalamata," "Sigoise," and "Tanche"; decreased until RI = 3 and then increased in "Bella di Cerignola" and "Nabali"; but increased until RI = 3 and then decreased slightly in "Itrana," and "Salonenque." While TP generally decreased along ripening in almost all varieties; it increased in "Bella di Cerignola" and Jabaa. The evolution of TP was noticeable in "Baladi 1," "Baladi 2," "Itrana," and "Kalamata" as it increased from RI = 1 to RI = 2 and then decreased to values lower than those recorded at RI = 1. As per the most concentrated individual phenols, oleacein decreased in "Sigoise"; decreased in "Bella di Cerignola" till RI = 2 and then increased; decreased in "Baladi 1" and "Nabali" till RI = 3 and then increased; and decreased till RI = 2, increased till RI = 3 and then decreased in "Kalamata." In contrast, oleacein content increased in "Baladi 2"; increased till RI=2 in "Ascolana Tenera," "Itrana," and "Jabaa" and then decreased; and increased till RI = 3 and then decreased in "Salonenque" and "Tanche." Oleocanthal showed the same evolution pattern as oleacein in the case of "Ascolana Tenera," "Baladi 2," "Bella di cerigonala," "Itrana," "Nabali," and "Sigoise." However, it increased till RI = 2, decreased at RI = 3 and increased beyond in "Baladi 1" and "Jabaa"; increased till RI = 2 and then decreased in "Salonenque"; increased till RI = 3 and then decreased in "Kalamata"; and decreased till RI = 2, increased at RI = 3 and then decreased beyond in "Tanche."

A Principal component analysis (PCA) was performed for fatty acid traits which are recognized as the most stable indicators for characterizing a given VOO (39). The results showed that the first two PCs explained 78.25% of the total variance (**Figure 2**). PC1 accounted for 58.49% of the total variance with a high positive correlation with PUFA and C18:2; and a high negative correlation with MUFA and C18:1. However, PC2 accounted for 19.76%, with a high positive correlation with SFA and C16:0. In addition, in the correlation circle, a negative correlation was observed between C18:1 and MUFA from one side and C18:2 and PUFA from the other side (data not shown).

The PCA was able to differentiate more between harvesting times rather than between varieties, as it can be seen that in the individual score plot (**Figure 2**) the samples from harvest 1, with higher content of C16:0 and C18:1 in comparison with other harvests, are all grouped in the negative side of the PC1 and in the positive side of PC2 except the samples of "Jabaa" and "Salonenque" as these varieties are characterized by the lowest content of C18:1 (57.14 and 57.59%, respectively) and the highest content of C18:2 (19.47 and 17.94%, respectively) among all varieties studied.

DISCUSSION

In this study, the characterization of 11 olive varieties cultivated in Lebanon was reported at different ripening stages using 28 traits relevant to OC, fatty acid, and phenolic profile. Results showed the strong effects of variety, fruit ripening and their interaction on the majority of the studied traits. This strong genetic variability revealed here is in parallel with the results previously reported for advanced selections of the olive breeding program in Cordoba (Spain) (43, 50). Moreover,

TABLE 2 | Relative importance of varieties and ripening index expressed as percentages of total sum of squares and significance in the ANOVA for different traits under study.

Parameters	Variety	Fruit ripening	Interaction	Error	CV	Mean	SE
MC (%)	54.03*	18.79*	11.57*	15.61	15.38	46.72	1.84
OCDM (%)	50.16*	20.33*	7.57	21.94	15.44	41.61	2.24
OCHM (%)	64.37*	9.92*	8.57	17.14	23.83	22.20	1.33
OIY (%)	51.95*	20.16*	12.94*	14.95	31.75	13.41	1.41
C16:0 (%)	77.95**	1.74	8.46**	11.85	13.83	14.98	0.49
C16:1 (%)	78.41**	3.52**	14.5**	3.57	68.46	0.97	0.08
C18:0 (%)	92.32**	0.48	1.91	5.29	36.32	3.00	0.15
C18:1 (%)	75.97**	12.7**	3.89	7.45	7.79	65.97	1.04
C18:2 (%)	58.16**	31.42**	4.02	6.40	30.22	12.80	0.69
C18:3 (%)	79.82**	0.50	6.72	12.96	19.21	0.88	0.05
SFA (%)	77.37**	1.15	10.27**	11.21	8.26	18.85	0.45
MUFA (%)	75.86**	13.2**	3.19	7.76	6.91	67.47	0.99
PUFA (%)	59.55**	29.9**	4.04	6.51	28.80	13.68	0.71
MUFA/PUFA	48.29**	38.18**	7.02**	6.51	33.20	5.46	0.32
MUFA/SFA	83.38**	0.38	7**	9.24	18.67	3.68	0.14
PUFA/SFA	48.41**	37.48**	7.51**	6.61	31.03	0.74	0.04
C16:0/C18:2	29.38**	55.07**	8.39**	7.16	28.44	1.27	0.07
C18:1/C18:2	46.75**	39.38**	7.56**	6.31	35.95	5.78	0.36
C18:2/C18:3	49.16**	39.77**	4.03	7.04	28.93	14.90	0.76
TP (mg GAE/Kg of oil)	46.95***	9.81***	31.77***	11.46	42.81	363	37.55
Hydroxytyrosol (mg/Kg)	39.8***	2.21	25.69***	32.31	102.26	6.80	1.00
Tyrosol (mg/Kg)	56.26***	1.25	27.7***	14.78	82.24	3.75	0.74
Vanillic acid (mg/Kg)	88.18***	1.27***	5.81***	4.73	36.98	3.20	0.24
P-coumaric acid (mg/Kg)	39.09***	0.21	30.68***	30.01	136.72	2.73	0.26
Oleacein (mg/Kg)	55.4***	1.86***	34.37***	8.36	76.14	46.20	8.99
Oleocanthal (mg/Kg)	65.26***	5.07***	25.19***	4.48	69.75	132.66	13.68
Luteolin (mg/Kg)	37.39***	4.18	33.12***	25.31	52.77	4.33	0.86
Apigenin (mg/Kg)	34.1***	4.31***	39.27***	22.31	66.05	6.89	1.00

MC, moisture content; OCDM, oil content on dry matter; OCHM, oil content on humid matter; OIY, oil industrial yield; C16:0, palmitic; C16:1, palmitoleic; C18:0, stearic; C18:1, oleic; C18:2, linoleic; C18:3, linolenic; SFA, saturated fatty acid; MUFA, monounsaturated fatty acid; PUFA, polyunsaturated fatty acid; TP, total phenols; GAE, Gallic acid equivalent; RI, ripening index; $^{*}p < 0.0125$; $^{**}p < 0.003$; $^{***}p < 0{,}005$ *(Considering the Bonferroni corrections).*

these results confirm the physical and chemical modifications occurring during fruit ripening, affecting OC, fatty acid and phenolic composition and consequently oil quality and oxidative stability (24, 51).

The OC traits, mainly OCDM (31.42–48.24%), OCHM (14.18–27.86%), and OIY (7.14–19.44%), showed high variability among varieties. Similar wide ranges of variation were observed by Chehade et al. (37) while characterizing the oil content and composition of five main Lebanese olive cultivars ("Aayrouni," "Abou Chawkeh," "Baladi," "Del," and "Soury"). These authors reported an OCHM between 17.8 and 36.4% and an OCDM between 42.5 and 56.2% in olives at spotted stage of ripening, with comparable values recorded for "Baladi" (28 ± 1% and 42.5 ± 1.8%, respectively). OCDM values increased along ripening reaching a significantly higher value at RI = 4; however, OCHM and OIY reached the maximum values at RI = 3 before decreasing later on probably due to rainfall in this period. This pattern of evolution of OC traits along ripening was also similar to the one described in other olive varieties in Spain (23, 24) and Tunisia (25, 52).

Regarding fatty acid profile, all percentages of fatty acids obtained in the present study fit, more or less, with the requirements established by the IOC for VOO, except for C18:3 which slightly exceeded the limit of IOC ($C18:3 < 1\%$) in case of "Ascolana Tenera" (1.02%), "Jabaa" (1.12%), "Salonenque" (1.10%), and "Sigoise" (1.08%). Similarly, previous work found that the amounts of some fatty acids could be outside the ranges listed by IOC such as in French (53), Tunisian (54, 55), Moroccan (56), Argentinian (57), New Zealandian (58), and Italian olive varieties (59). On the other hand, our study revealed a wide variability in the percentages of the main fatty acids of olive oil in parallel with the findings of León et al. (20), Boskou (9), Diraman et al. (60), Sánchez de Medina et al. (50), and Chehade et al. (37). Oleic acid is well-recognized to be the most important fatty acid in olive oil, associated with its high nutritional value and oxidative stability (61, 62). An olive variety is considered

TABLE 3 | OC, fatty acids and phenolic compounds traits variability among the studied varieties cultivated in Lebanon.

Variables	"Ascolana Tenera"	"Baladi 1"	"Baladi 2"	"Bella di Cerignola"	"Itrana"	"Jabaa"	"Kalamata"	"Nabali"	"Saloneque"	"Sigoise"	"Tanche"	IOC limits
MC (%)	53.22^{a}	38.92^{f}	42.15^{ef}	47.04^{cd}	43.60^{de}	54.77^{a}	51.59^{ab}	48.39^{bc}	47.41^{bcd}	44.93^{cde}	42.55^{ef}	–
OCDM (%)	38.09^{cd}	45.72^{a}	44.57^{ab}	38.56^{cd}	37.19^{d}	31.42^{e}	48.24^{a}	43.4^{abc}	45.67^{a}	40.02^{bcd}	44.05^{ab}	–
OCHM (%)	17.78^{f}	27.86^{a}	25.56^{ab}	20.38^{ef}	20.91^{def}	14.18^{g}	23.29^{bcde}	22.23^{cde}	23.89^{bcd}	22.11^{de}	25.36^{abc}	–
OIY (%)	11.06^{cd}	18.19^{a}	17.17^{ab}	11.40^{cd}	14.47^{bc}	8.37^{de}	14.47^{bc}	9.57^{de}	14.18^{bc}	7.14^{d}	19.44^{a}	–
C16:0 (%)	17.08^{a}	13.88^{b}	14.03^{b}	12.89^{b}	16.59^{a}	17.29^{a}	13.19^{b}	16.25^{a}	17.34^{a}	12.87^{b}	13.5^{b}	7.5–20
C16:1 (%)	2.04^{a}	0.47^{g}	0.47^{g}	0.34^{g}	1.32^{c}	1.64^{b}	0.76^{ef}	0.96^{d}	1.19^{c}	0.94^{de}	0.68^{f}	0.3–3.5
C18:0 (%)	1.97^{d}	4.05^{a}	4.17^{a}	4.35^{a}	2.19^{d}	1.88^{d}	2.25^{d}	2.74^{c}	3.14^{b}	2.16^{d}	2.21^{d}	0.5–5
C18:1 (%)	63.94^{d}	67.63^{bc}	67.07^{c}	70.14^{ab}	66.49^{c}	57.14^{e}	68.08^{bc}	66.98^{c}	57.59^{e}	70.08^{ab}	71.75^{a}	55–83
C18:2 (%)	12.5^{bc}	11.77^{cd}	12.03^{cd}	10.70^{cd}	11.54^{cde}	19.47^{a}	13.75^{b}	11.36^{cde}	17.94^{a}	11.99^{cd}	9.96^{e}	3.5–21
C18:3 (%)	1.02^{ab}	0.64^{d}	0.64^{d}	0.94^{bc}	0.83^{c}	1.12^{a}	0.83^{c}	0.70^{d}	1.10^{a}	1.08^{a}	0.9^{c}	<1
SFA (%)	19.05^{b}	17.93^{cd}	18.21^{bcd}	17.24^{d}	18.78^{bc}	19.17^{b}	15.44^{e}	19^{bc}	20.48^{a}	15.03^{e}	15.71^{e}	–
MUFA (%)	65.98^{e}	68.10^{cde}	67.54^{de}	70.48^{abc}	67.8^{de}	58.78^{f}	68.84^{bcd}	67.94^{de}	58.79^{f}	71.02^{ab}	72.43^{a}	–
PUFA (%)	13.52^{bc}	12.41^{cde}	12.67^{cd}	11.64^{de}	12.37^{cde}	20.59^{a}	14.58^{b}	12.07^{cde}	19.03^{a}	13.08^{bcd}	10.85^{e}	–
MUFA/PUFA	5.07^{cd}	5.8^{bc}	5.65^{cd}	6.54^{ab}	5.7^{cd}	2.96^{e}	4.99^{d}	5.76^{cd}	3.17^{e}	5.71^{cd}	7.02^{a}	–
MUFA/SFA	3.47^{c}	3.63^{c}	3.57^{c}	4.11^{b}	3.61^{c}	3.07^{e}	4.5^{a}	3.59^{c}	2.88^{e}	4.74^{a}	4.62^{a}	–
PUFA/SFA	0.71^{c}	0.66^{c}	0.66^{c}	0.67^{c}	0.66^{c}	1.07^{a}	0.96^{b}	0.64^{c}	0.93^{b}	0.89^{b}	0.7^{c}	–
C16:0/C18:2	1.42^{ab}	1.24^{c}	1.21^{c}	1.29^{bc}	1.49^{a}	0.91^{e}	1.02^{de}	1.46^{a}	0.98^{e}	1.17^{cd}	1.44^{ab}	–
C18:1/C18:2	5.34^{c}	6.06^{bc}	5.88^{bc}	7.15^{a}	6.04^{bc}	3.06^{d}	5.26^{c}	6.04^{bc}	3.3^{d}	6.23^{b}	7.64^{a}	–
C18:2/C18:3	12.28^{cd}	18.38^{a}	19.05^{a}	11.4^{d}	14.02^{c}	17.47^{ab}	16.5^{b}	16.19^{b}	16.34^{b}	11.31^{d}	11.07^{d}	–
TP (mg GAE/Kg of oil)	539^{a}	321^{cd}	301^{cd}	207^{ef}	469^{ab}	384^{bc}	285de	176^{f}	157^{f}	275de	276de	–
Hydroxytyrosol (mg/Kg)	9.1^{a}	4.3^{bcd}	3.69^{bcd}	2.95^{d}	4.86^{bcd}	5.92^{b}	3.09^{cd}	5.51^{bc}	3.28^{cd}	3.31^{cd}	4.92^{bcd}	
Tyrosol (mg/Kg)	8.97^{a}	3.25^{c}	2.19^{cd}	0.98^{d}	6.04^{b}	1.89^{cd}	3.04^{c}	2.31^{cd}	2.36^{cd}	3.12^{c}	2.09^{cd}	–
Vanillic acid (mg/Kg)	3.46^{a}	2.8^{bc}	2.72^{cd}	2.87^{bc}	2.88^{bc}	3.34^{ab}	2.4^{cd}	2.16^{d}	2.21^{d}	2.36^{cd}	2.72^{cd}	
p-Coumaric acid (mg/Kg)	1.74^{bcd}	2.22^{ab}	1.95^{abc}	1.58^{cd}	2.59^{a}	1.38^{cd}	1.69^{bcd}	1.62^{bcd}	1.47^{cd}	1.15^{d}	2.42^{a}	–
Oleacein (mg/Kg)	51.41^{bc}	26.97^{d}	27.78^{d}	49.62^{bc}	108.03^{a}	14.3^{d}	32.54^{cd}	58.2^{b}	121.57^{a}	62.75^{b}	62.49^{b}	–
Oleocanthal (mg/Kg)	109.89^{cd}	73.53^{efgh}	48.36^{h}	132.81^{bc}	317.68^{a}	102.98^{cde}	156.24^{b}	90.03^{def}	87.43^{defg}	55.26^{gh}	59.21^{fgh}	–
Luteolin (mg/Kg)	2.98^{def}	7.19^{a}	3.94^{bcdef}	2.65^{ef}	4.4^{bcde}	5.35^{abc}	4.87^{bcd}	3.33^{cdef}	1.96^{f}	5.81^{ab}	3.02^{def}	–
Apigenin (mg/Kg)	4.71^{bcde}	6.82^{ab}	4.18^{cde}	3.7^{cde}	7.89^{a}	7.93^{a}	2.79^{e}	5.03^{bcde}	3.12^{de}	5.25^{bcd}	6.08^{abc}	–

IOC, international olive council; MC, moisture content; OCDM, oil content on dry matter; OCHM, oil content on humid matter; OIY, oil industrial yield; C16:0, palmitic acid; C16:1, palmitoleic acid; C18:0, stearic acid; C18:1, oleic acid; C18:2, linoleic acid; C18:3, linolenic acid; SFA, saturated fatty acid; MUFA, monounsaturated fatty acid; PUFA, polyunsaturated fatty acid; TP, total phenols; GAE, gallic acid equivalent. Different letters in a row indicate significant differences (Tukey's HSD test).

TABLE 4 | Evolution of OC, fatty acids and phenolic compounds traits along ripening.

Variables	RI			
	1	2	3	4
MC (%)	44.15^{b}	43.65^{c}	45.61^{bc}	50.81^{a}
OCDM (%)	37.27^{c}	40.98^{b}	43.01^{b}	45.75^{a}
OCHM (%)	19.88^{b}	23.10^{a}	23.42^{a}	22.52^{a}
OIY (%)	9.51^{b}	15.11^{a}	15.30^{a}	13.96^{a}
C16:0 (%)	15.41^{a}	15.22^{ab}	14.78^{bc}	14.5^{c}
C16:1 (%)	0.87^{b}	0.92^{b}	1.02^{a}	1.06^{a}
C18:0 (%)	2.73^{b}	2.90^{ab}	2.88^{ab}	2.94^{a}
C18:1 (%)	68.92^{a}	66.03^{b}	64.46^{c}	64.41^{c}
C18:2 (%)	9.79^{c}	12.75^{b}	14.65^{a}	15.38^{a}
C18:3 (%)	0.91^{a}	0.86^{a}	0.88^{a}	0.90^{a}
SFA (%)	18.13^{a}	18.12^{a}	17.66^{ab}	17.45^{b}
MUFA (%)	69.79^{a}	66.95^{b}	65.48^{c}	65.46^{c}
PUFA (%)	10.69^{c}	13.60^{b}	15.53^{a}	16.29^{a}
MUFA/PUFA	7.00^{a}	5.27^{b}	4.44^{c}	4.31^{c}
MUFA/SFA	3.85^{a}	3.72^{a}	3.76^{a}	3.82^{a}
PUFA/SFA	0.58^{d}	0.74^{c}	0.88^{b}	0.93^{a}
C16:0/C18:2	1.65^{a}	1.24^{b}	1.04^{c}	0.97^{c}
C18:1/C18:2	7.61^{a}	5.57^{b}	4.65^{c}	4.49^{c}
C18:2/C18:3	11.02^{c}	15.07^{b}	16.93^{a}	17.45^{a}
TP (mg GAE/Kg of oil)	387^{a}	305^{b}	268^{bc}	250^{c}
Hydroxytyrosol (mg/Kg)	4.21^{ab}	5.16^{a}	4.93^{ab}	3.84^{b}
Tyrosol (mg/Kg)	2.8^{a}	3.5^{a}	3.53^{a}	2.82^{a}
Vanillic acid (mg/Kg)	2.67^{a}	2.79^{a}	2.93^{a}	2.37^{b}
p-Coumaric acid (mg/Kg)	1.82^{a}	1.91^{a}	1.79^{a}	1.74^{a}
Oleacein (mg/Kg)	61.87^{a}	60.95^{a}	54.12^{ab}	46.57^{b}
Oleocanthal (mg/Kg)	136.28^{a}	130.72^{a}	104.59^{b}	81.13^{c}
Luteolin (mg/Kg)	4.48^{ab}	4.56^{a}	3.81^{ab}	3.53^{b}
Apigenin (mg/Kg)	5.49^{ab}	6.07^{a}	4.84^{b}	4.47^{b}

RI, ripening index; MC, moisture content; OCDM, oil content on dry matter; OCHM, oil content on humid matter; OIY, oil industrial yield; C16:0, palmitic acid; C16:1, palmitoleic acid; C18:0, stearic acid; C18:1, oleic acid; C18:2, linoleic acid; C18:3, linolenic acid; SFA, saturated fatty acid; MUFA, monounsaturated fatty acid; PUFA, polyunsaturated fatty acid; TP, total phenols; GAE, gallic acid equivalent. Different letters in a row indicate significant differences (Tukey's HSD test).

as having a high content of oleic acid if C18:1 is about 65% and above (39). In the present study, eight of the 11 studied varieties including the local "Baladi" ones could be categorized as having high oleic acid content. In addition, "Baladi 1" and "Baladi 2" presented the lowest percentages of C18:3 (0.64%), and medium percentages of C18:2 (11.77 and 12.03%, respectively) which also increase their oxidative stability. These results are partially in agreement with those obtained by Chehade et al. (37) on the same variety (65.95% of C18:1 in 2011 but 62.44% in 2010; and 11.30% of C18:2 in 2011 but 16.39% in 2010). In addition, the results are close to those described by El Riachy et al. (63) who reported values of C18:1 between 69.42 and 71.46%, of C18:2 between 10.37 and 11.34%, and of C18:3 between 0.59 and 0.63%. These discrepancies are possibly due to the fact that the latter authors collected the samples from different altitudes (200–1,050 m a.s.l.), while, in the present study the samples were collected only from one site at a low altitude (18 m a.s.l.); and it is well known that C18:1 increases with altitude (63, 64). Regarding foreign varieties, "Sigoise" showed higher percentages of C18:1 and C18:2 in Lebanon (70.08 and 11.99%, respectively) than in Tunisia (around 68.5 and 10.02%, respectively) (65). However, "Salonenque" in Lebanon recorded higher percentages of C16:0 (17.34%) and C18:2 (17.94%) but a lower value for C18:1 (57.59%) in comparison to those recorded by Ollivier et al. (39) in France (14.55, 12.59, and 64.76%, respectively). This data variation could be attributed to the geographical area of growing and its climatic conditions which affect olive oil fatty acid profile (24).

Besides the individual fatty acids, several sums and ratios were evaluated in this study because of their importance in olive oil quality such as MUFA (61, 66). For instance, "Tanche," "Sigoise," and "Bella di Cerignola" presented the highest MUFA values. The local varieties "Baladi 1" and "Baladi 2" recorded lower values (68.1 and 67.54%, respectively) including values lower than those reported by Merchak et al. (64) who also collected the samples from different altitudes (0 to more than 700 m a.s.l.). The high ratios of MUFA/PUFA and C18:1/C18:2 recorded in "Tanche" and MUFA/SFA recorded in "Sigoise"; and the low PUFA/SFA ratio registered in "Nabali" are linked to the high oxidative stability and low rancidity of olive oil (13), and affects, in combination with other minor compounds, the organoleptic and health properties of VOO (9, 67).

Concerning the evolution of the different fatty acids along ripening, the results of this study showed a general decrease of C16:0 and C18:1 together with a significant increase of C18:2; in concordance with several previous studies (24, 64, 68). According to Gutiérrez et al. (23), the C16:0 level fell during the ripening process, possibly as a result of a dilution effect. However, the increase in C18:2 content could be linked to the activity of the enzyme oleate desaturase, transforming oleic acid into linoleic acid (23, 69). These changes will produce a decrease of the ratio C18:1/C18:2 together with an increase of the ratio PUFA/SFA which will have a detrimental effect on the oil oxidative stability reducing the shelf-life of olive oils obtained from late harvest.

Results of total and individual phenols also expressed a large variability among the varieties studied. These results are in agreement with previous works indicating that genetic variability is the main factor affecting the phenolic composition (22, 70). The TP values obtained for "Baladi 1" and "Baladi 2" are higher than those reported by Chehade et al. (37) and El Riachy et al. (63) for the same variety (167–249 mg GAE/kg of oil and 194–236 mg GAE/kg of oil, respectively). It is worth pointing out here the low content of secoiridoids in the local varieties in comparison to the foreign ones, which highlights the need for breeding to improve the traditional local varieties as these phenolic compounds have a detrimental effect on olive oil quality and nutraceutical properties and are very useful as selection criteria in breeding programs. Additionally, several works indicate a significant decrease of TP content during ripening (43, 54, 71) similar to the pattern described in the present paper. This decrease was most likely correlated with the increased activity of hydrolytic enzymes observed during ripening (72). In parallel, oleacein and oleocanthal also decreased from 61.87 to 46.57 mg/Kg and from 136.28 to 81.13 mg/Kg, respectively. It is worth noting that, the other studied individual phenols recorded the

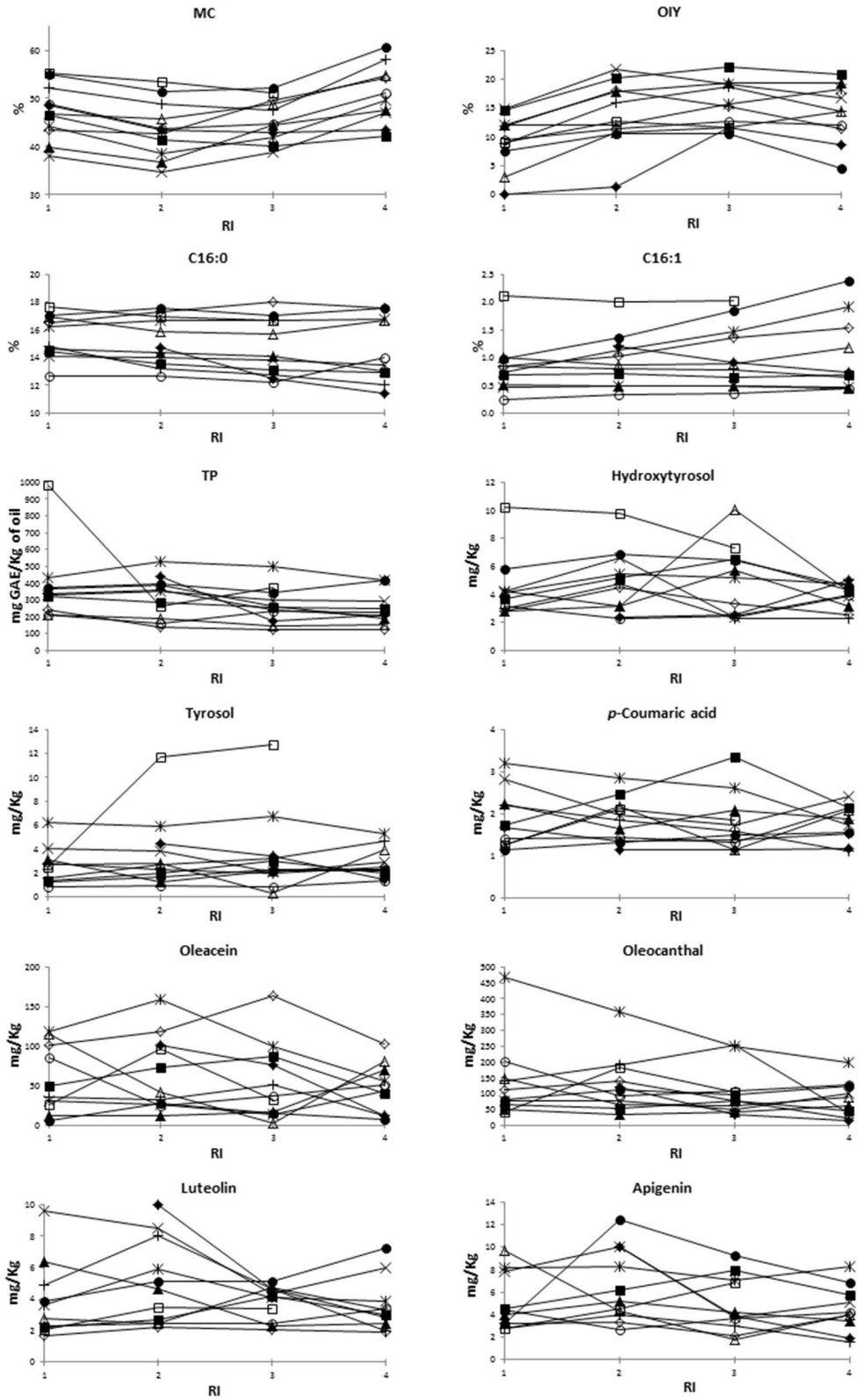

FIGURE 1 | Evolution pattern along ripening of the different studied traits. MC, moisture content; OIY, oil industrial yield; TP, total phenols; RI, ripening index. □, "Ascolana Tenera;" ×, "Baladi 1;" ▲, "Baladi 2;" ○, "Bella di Cerignola;" *, "Itrana;" ●, "Jabaa;" +, "Kalamata;" △, "Nabali;" ◇", "Salonenque;" ♦, "Sigoise;" ■, "Tanche".

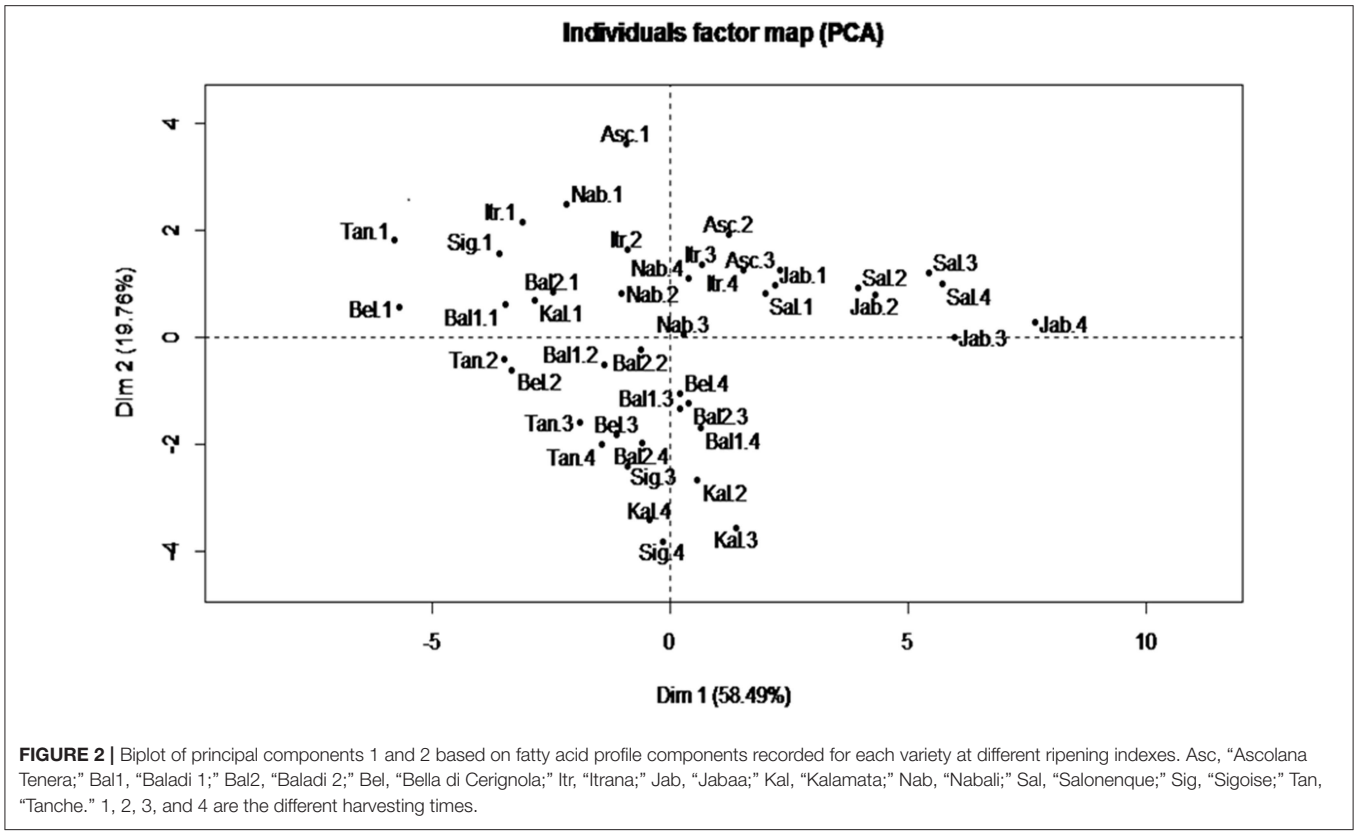

FIGURE 2 | Biplot of principal components 1 and 2 based on fatty acid profile components recorded for each variety at different ripening indexes. Asc, "Ascolana Tenera;" Bal1, "Baladi 1;" Bal2, "Baladi 2;" Bel, "Bella di Cerignola;" Itr, "Itrana;" Jab, "Jabaa;" Kal, "Kalamata;" Nab, "Nabali;" Sal, "Salonenque;" Sig, "Sigoise;" Tan, "Tanche." 1, 2, 3, and 4 are the different harvesting times.

maximum values at RI between 2 and 3 before decreasing later on. Therefore, early harvesting (before black pigmentation, RI = 4) should be recommended to obtain higher content of phenolic compounds in addition to higher content of C18:1. These results are in partial agreement with other studies that reported an increase in TP content to a maximum level at the "spotted" and "purple" pigmentation, the content decreasing drastically as ripening progressed (24, 52).

Finally, PCA analysis showed that PC1 and PC2 explained the highest total variance (78%) when using the set of 15 traits related to fatty acid composition alone. This PCA allowed the classification of the samples according to the ripening stage with samples at RI = 1, having higher percentages of C16:0, C18:1, and MUFA, clustering together in the negative side of PC1 and positive side of PC2 (**Figure 2**). These results are in line with those obtained by León et al. (73) who separated 18 varieties growing in the World Olive Germplasm Bank (WOGB) of IFAPA (Cordoba, Spain) into four groups according to their fatty acid composition and to the country of origin, where the percentages of C18:1, C18:2, and saturated fatty acids were the main contributors of variation.

In conclusion, the present study reports the characterization of 11 local and foreign varieties growing under Lebanon climatic conditions. In comparison to foreign varieties, the local "Baladi 1" showed outstanding OCHM; however, both "Baladi 1" and "Baladi 2" recorded similar fatty acid composition but low phenolic composition. Indeed, many of the studied foreign varieties presented several outstanding characteristics such as "Kalamata" in terms of higher OCHM; "Tanche" in terms of higher OIY; "Tanche" and "Sigoise" in terms of higher C18:1, higher MUFA, higher MUFA/PUFA ratio, higher C18:1/C18:2, higher MUFA/SFA, and higher C18:1/C18:2; "Ascolana Tenera" and "Itrana" in terms of higher total phenols content; "Itrana" in terms of oleocanthal; and "Salonenque" in terms of oleacein. Taking into consideration that the appropriate time for harvesting is when a good balance between oil quality and oil quantity is achieved, and based on the fact that OCHM and OIY increased significantly until RI = 2 while C18:1, MUFA, MUFA/PUFA, C16:0/C18:2, C18:1/C18:2, TP, oleacein, and oleocanthal decreased along ripening, we can conclude that the best time for harvesting is at RI = 2 (when the color is yellowish green with reddish spots). This is true for all studied varieties, except "Sigoise" that must be harvested later at RI = 3 for better oil extractability. These findings on monovarietal olive oils should be confirmed over years in order to evaluate and valorize the local olive germplasm compared to the foreign one, and for the characterization and authentication of Lebanese olive oil. This is also critical in identifying the main default of the local varieties in order to start their genetic improvement through breeding programs.

DATA AVAILABILITY

The raw data supporting the conclusions of this manuscript will be made available by the authors, without undue reservation, to any qualified researcher.

AUTHOR CONTRIBUTIONS

MR and LC contributed to the conception and design of the experiment, statistical analysis, and paper preparation. AH and RA performed sample collection and all chemical analyses. AH also contributed to the statistical analysis and data elaboration. FD participated in sample collection and experiment design.

ACKNOWLEDGMENTS

The Lebanese Agricultural Research Institute (LARI) is gratefully acknowledged for having provided the financial support for this study. The authors are also grateful to colleagues in the olive oil department and the feed lab at LARI, namely: Eng. Joseph Kahwaji, Ghina Jebbawi, Ghinwa Al Hawi, Celine Berbari, Maria Karam, and Ayat Ayoub.

REFERENCES

1. Civantos Lopez-Villalta L. *The Olive Tree, the Oil, the Olive*. International Olive Oil Council. Madrid: ADICOM (1998).
2. Bartolini G, Messeri C, Prevost G. Olive tree germplasm: descriptor list of cultivated varieties in the world. *Acta Hortic*. (1994) 356:116–8. doi: 10.17660/ActaHortic.1994.356.25
3. Chalak L. Following olive footprints in Lebanon. In: El-Kholy M, editor. *Following Olive Footprints Olea europaea L.): Cultivation and Culture, Folklore and History, Traditions and Uses*. Leuven: ISHS, IOC and AARINENA (2012). p. 209–21.
4. Chalak L, Haouane H, Essalouh L, Santoni S, Besnard G, Khadari B. Extent of the genetic diversity in Lebanese olive (*Olea europaea* L.) trees: a mixture of an ancient germplasm with recently introduced varieties. *Genet Resour Crop Evol*. (2015) 62:621–33. doi: 10.1007/s10722-014-0187-1
5. Chalak L, Chehade A, Elbitar B, Hamadeh B, Youssef H, Nabbout R, et al. Morphological characterization of cultivated olive trees in Lebanon. In: *Proceedings of the 4th International Conference on Olive Culture, Biotechnology and Quality of Olive Tree Products, (OLIVEBIOTEQ), Vol. 1*. Chania (2011). p. 51–6.
6. Chehade A, ElBittar A, Choueiri E, Kadri A, Nabbout R, Youssef H, et al. *Characterization of the Main Lebanese Olive Germplasm*. The Italian cooperation project "Social and economic support for the families of producers in the olive-growing marginal regions of Lebanon (L'Olio del Libano).": Beirut (2012).
7. Salibi A. *Marketing Study for Olive, Olive oil and Apple in Lebanon*. Beirut: Ministry of agriculture (2007).
8. Ministry of Agriculture. *Agricultural Development Project "Olive" (ADP-Olive), A European Union (EU) Project*. Beirut: Ministry of Agriculture (2003).
9. Boskou D. *Olive Oil Chemistry and Technology*. Champaign, IL: AOCS Press (1996).
10. Kiritsakis AK. *Olive Oil: From the Tree to the Table*. Trumbull, CT: Food & Nutrition Press (1998).
11. Moreno JJ, Mitjavilab MT. The degree of unsaturation of dietary fatty acids and the development of atherosclerosis (Review). *J Nutr Biochem*. (2003) 14:182–95. doi: 10.1016/S0955-2863(02)00294-2
12. García-González D, Aparicio-Ruiz R, Aparicio R. Virgin olive oil – chemical implications on quality and health. *Eur J Lipid Sci Technol*. (2008) 110:602–7. doi: 10.1002/ejlt.200700262
13. Tous J, Romero A. *Variedades de Olivo*. Barcelona: Fundación 'La Caixa' (1993).
14. Baldioli M, Servili M, Perretti G, Montedoro GF. Antioxidant activity of tocopherols and phenolic compounds of virgin olive oil. *J Am Oil Chem Soc*. (1996) 73:1589–93. doi: 10.1007/BF02523530
15. Cortesi N, Azzolini M, Rovellini P, Fedeli E. Minor polar components of virgin olive oils: a hypothetical structure by LC-MS. *Riv Ital Sos Gra*. (1995) 72:241–51.
16. Visioli F, Galli C. Olive oil phenols and their potential effects on human health. *J Agric Food Chem*. (1998) 46:4292–6. doi: 10.1021/jf980049c
17. Del Rio C, Caballero JM, García-Fernández MD. Contenido graso (Banco de Germoplasma de Cordoba). In: Rallo L, Barranco D, Caballero J, Martín A, Del Río C, Tous J, et al., editors. *Las Variedades de Olivo Cultivadas en España, Libro II: Variabilidad y Selección* (Madrid: Junta de Andalucía/MAPA/Ediciones Mundi-Prensa) (2005). p. 348–56.
18. Tous J, Romero A, Díaz I. Composición del aceite (Banco de Germoplasma de Cataluña). In: Rallo L, Barranco D, Caballero J, Martín A, Del Río C, Tous J, et al., editors. *Las Variedades de Olivo Cultivadas en España, Libro II: Variabilidad y Selección* (Madrid: Junta de Andalucía/MAPA/Ediciones Mundi-Prensa) (2005). p. 357–64.
19. Uceda M, Beltrán G, Jiménez A. "Composición del aceite (Banco de Germoplasma de Córdoba). In: Rallo L, Barranco D, Caballero J, Martín A, Del Río C, Tous J, et al., editors. *Las Variedades de Olivo Cultivadas en España, Libro II: Variabilidad y Selección* (Madrid: Junta de Andalucía/MAPA/Ediciones Mundi-Prensa) (2005). p. 365–72.
20. León L, Uceda M, Jiménez A, Marten LM, Rallo L. Variability of fatty acid composition in olive (*Olea europaea*, L.) progenies. *Span J Agric Res*. (2004) 2:353–9. doi: 10.5424/sjar/2004023-89
21. Ripa V, De Rose F, Caravita MA, Parise MR, Perri E, Rosati A, et al. Qualitative evaluation of olive oils from new olive selections and effects of genotype and environment on oil quality. *Adv Hort Sci*. (2008) 22:95–103.
22. El Riachy M, Priego-Capote F, Rallo L, Luque de Castro MD, León L. Phenolic composition of virgin olive oils from cross breeding segregating populations. *Eur J Lipid Sci Technol*. (2012) 114:542–51. doi: 10.1002/ejlt.201100129
23. Gutiérrez F, Jímenez B, Ruíz A, Albi MA. Effect of olive ripeness on the oxidative stability of virgin olive oil extracted from the varieties Picual and Hojiblanca and on the different components involved. *J Agric Food Chem*. (1999) 47:121–7. doi: 10.1021/jf980684i
24. Salvador MD, Aranda F, Fregapane G. Influence of fruit ripening on 'Cornicabra' virgin olive oil quality A study of four successive crop seasons. *Food Chem*. (2001) 73:45–53. doi: 10.1016/S0308-8146(00)00276-4
25. Bouaziz M, Jemai H, Khaboub W, Sayadia S. Oil content, phenolic profiling and antioxidant potential of Tunisian olive drupes. *J Sci Food Agric*. (2010) 90:1750–8. doi: 10.1002/jsfa.4013
26. Di Giovacchino L, Costantini N, Ferrante ML, Serraiocco A. Influence of malaxation time of olive paste on the technological results and qualitative characteristics of virgin olive oil obtained by a centrifugal decanter at water saving. *Grasas Aceites*. (2002) 53:179–86. doi: 10.3989/gya.2002.v53.i2.302
27. Lavee S. The effect of predetermined deficit irrigation on the performance of cv. Muhasan olives (*Olea europaea* L) in the eastern coastal plain of Israel. *Sci Horticult*. (2007) 112:156–63. doi: 10.1016/j.scienta.2006.12.017
28. Alonso García MV, Aparicio López R. Characterization of European virgin olive oils using fatty acids. *Grasas Aceites*. (1993) 44:18–24. doi: 10.3989/gya.1993.v44.i1.1115
29. Tsimidou M, Karakostas KX. Geographical classification of Greek virgin olive oils by non-parametric multivariate evaluation of fatty acid composition. *J Sci Food Agric*. (1993) 62:253–7. doi: 10.1002/jsfa.2740620308
30. Stefanoudaki E, Kotsifaki F, Koutsaftakis A. Classification of virgin olive oils of the two major cretan cultivars based on their fatty acid composition. *J Am Oil Chem Soc*. (1999) 76:623–6. doi: 10.1007/s11746-999-0013-7

31. Bucci R, Magri AD, Magri AL, Marini D, Marini F. Chemical authentification of extra virgin olive oil varieties by supervised chemometric procedures. *J Agric Food Chem*. (2002) 50:413–8. doi: 10.1021/jf010696v
32. Tsimidou M, Macrae M, Wilson I. Authentification of virgin olive oils using principal component analysis of triglyceride and fatty acid profiles. Part I classification of Greek oils. *Food Chem*. (1987) 25:227–39. doi: 10.1016/0308-8146(87)90148-8
33. Aranda F, Gómez-Alonso S, Rivera del Alamo RM, Salvador MD, Fregapane G. Triglyceride, total and 2-position fatty acid composition of Cornicabra virgin olive oil: comparaison with other spanish cultivars. *Food Chem*. (2004) 86:485–92. doi: 10.1016/j.foodchem.2003.09.021
34. Leardi R, Paganuzzi V. Characterization of the origin of extra virgin olive oils by chemometric methods applied to the sterols fraction. *Riv Ital Sos Gra*. (1987) 64:131–6.
35. Bajoub A, El Amin A, Fernández-Gutiérrez A, Carrasco-Pancorbo A. Evaluating the potential of phenolic profiles as discriminant features among extra virgin olive oils from Moroccan controlled designations of origin. *Food Res Int*. (2016) 84:41–51. doi: 10.1016/j.foodres.2016.03.010
36. Ollivier D, Artaud J, Pinatel C, Durbec JP, Guérère M. Differentiation of French virgin olive oil RDOs by sensory characteristics, fatty acid and triacylglycerol compositions and chemometrics. *Food Chem*. (2006) 97:382–93. doi: 10.1016/j.foodchem.2005.04.024
37. Chehade A, El Bitar A, Kadri A, Choueiri E, Nabbout R, Youssef H, et al. *In situ* evaluation of the fruit and oil characteristics of the main Lebanese olive germplasm. *J Sci Food Agric*. (2015) 96:2532–8. doi: 10.1002/jsfa.7373
38. Chalak L, Haouane H, Chehade A, Elbitar A, Hamadeh B, Youssef H, et al. Morphological and molecular characterization for assessment of genetic variation within the "Baladi" olive variety. *Acta Hortic*. (2014) 1057:741–8. doi: 10.17660/ActaHortic.2014.1057.95
39. Ollivier D, Artaud J, Pinatel C, Durbec JP, Guérère M. Triacylglycerol and fatty acid compositions of French virgin olive oils. Characterization by chemometrics. *J Agric Food Chem*. (2003) 51:5723–31. doi: 10.1021/jf034365p
40. Mendil M, Sebai A. *Catalogue of Algerian Variety of the Olive Tree*. ITAF; Ministry of Agriculture and Rural Development (2006).
41. Miller K. *Greece*. ebook ed. Oakland, CA: Lonely Planet (2018).
42. Uceda M, Hermoso M. Maduración. In: Barranco D, Fernández-Escobar R, Rallo L, editors. *El Cultivo del Olivo*. Madrid: Coedición Junta de Andalucía-Mundiprensa (1998).
43. El Riachy M, Priego-Capote F, Rallo L, Luque de Castro MD, León L. Phenolic profile of virgin olive oil from advanced breeding selections. *Span J Agric Res*. (2012) 10:443–53. doi: 10.5424/sjar/2012102-264-11
44. Martínez-Suarez JM, Muñoz E, Alba J, Lanzón A. Informe sobre la utilización del Analizador de Rendimientos "Abencor". *Grasas Aceites*. (1975) 26:379–85.
45. Aenor. Asociación Española de Normalización y certificación. *Materias Grasas. Determinación del Contenido en Materia Grasa Total de la Aceituna*. Madrid: Norma UNE 55030 (1961).
46. European Union Commission Regulation EEC/2568/91. *On the Characteristics of Olive and Olive Pomace Oils and Their Analytical Methods* (1991).
47. Montedoro GF, Servili M, Baldioli M, Miniati E. Simple and hydrolysable compounds in virgin olive oil. 1. Their extraction, separation and quantitative and semi quantitative evaluation by HPLC. *J Agric Food Chem*. (1992) 40:1571–6. doi: 10.1021/jf00021a019
48. Singleton VL, Rossi JA. Colorimetry of total phenolics with phosphomolybdic-phosphotungstic acid reagents. *Am J Enol Vitic*. (1965) 16:144–58.
49. Saporta G. Simulatenous analysis of qualitative and quantitative data. In: *Societa Italiana Di Statistica. Atti Della XXXV Riunione Scientifica*. Padova (1990). p. 62–72.
50. Sánchez de Medina V, Calderón-Santiago M, El Riachy M, Priego-Capote F, Luque de Castro MD. Influence of genotype on the fatty acids composition of virgin olive oils from advanced selections obtained by crosses between Arbequina, Picual, and Frantoio cultivars along the ripening process. *Eur J Lipid Sci Technol*. (2015) 117:954–66. doi: 10.1002/ejlt.201400265
51. Arslan D. Physico-chemical characteristics of olive fruits of Turkish varieties from the province of Hatay. *Grasas Aceites*. (2012) 63:158–66. doi: 10.3989/gya.071611
52. Chimi H, Atouati Y. Determination of the optimal stage for harvesting Moroccan Picholine olives by monitoring change in total polyphenols. *Olivae*. (1994) 54:56–60.
53. Pinatel C, Ollivier D, Artaud J. Qualité, sécurité alimentaire, traçabilité et typicité de nos productions. *Le Nouvel Olivier*. (2006) 52:22–3.
54. Baccouri O, Cerretani L, Bendini A, Caboni MF, Zarrouk M, Pirrone L, et al. Preliminary chemical characterization of Tunisian monovarietal virgin olive oils and comparison with Sicilian ones. *Eur J Lipid Sci Technol*. (2007) 109:1208–17. doi: 10.1002/ejlt.200700132
55. Laroussi-Mezghani S, Vanloot P, Molinet J, Dupuy N, Hammami MN, et al. Authentication of Tunisian virgin olive oils by chemometric analysis of fatty acid compositions and NIR spectra. Comparison with Maghrebian and French virgin olive oils. *Food Chem*. (2015) 173:122–32. doi: 10.1016/j.foodchem.2014.10.002
56. El Antari A, El Moudni A, Ajana H. Étude de la composition lipidique de deux compartiments du fruit d'olive (pulpe et amande) de six variétés d'oliviers cultivées au Maroc. *Olivae*. (2003) 98:20–8.
57. Ravetti L. Caracterización preliminar de variedades y aceites de oliva vírgenes de la provincia de Catamarca. *Grasas Aceites*. (1999) 36:361–9.
58. Meehan CK. *The quality of New Zealand olive oil* (BhortSc (Hons) thesis), Lincoln University, New Zealand (2001).
59. Dettori S, Russo G. Influence du cultivar et du régime hydrique sur le volume de production et la qualité de l'huile d'olive. *Olivae*. (1993) 49:36–43.
60. Diraman H, Saygi H, Hisil Y. Relationship between geographical origin and fatty acid composition of Turkish virgin olive oils from two harvest years. *J Am Oil Chem Soc*. (2010) 87:781–9. doi: 10.1007/s11746-010-1557-2
61. Aparicio M, Cano N, Chauveau P, Azar R, Canaud B, Flory A, et al. Nutritional status of haemodialysis patients: a French national cooperative study. French Study Group for Nutrition in Dialysis. *Nephrol Dial Transplant*. (1999) 14:1679–86. doi: 10.1093/ndt/14.7.1679
62. Frankel EN. Nutritional and biological properties of extra virgin olive oil. *J Agric Food Chem*. (2011) 59:785–92. doi: 10.1021/jf103813t
63. El Riachy M, Bou-Mitri C, Youssef A, Andary R, Skaff W. Chemical and sensorial characteristics of olive oil produced from the Lebanese olive variety 'Baladi'. *Sustainability*. (2018) 10:4630. doi: 10.3390/su10124630
64. Merchak N, El Bacha E, Bou Khouzam R, Rizk T, Akoka S, Bejjani J. Geoclimatic, morphological, and temporal effects on Lebanese olive oils composition and classification: a ^{1}H NMR metabolomics study. *Food Chem*. (2017) 217:379–88. doi: 10.1016/j.foodchem.2016.08.110
65. Dabbou S, Sifi S, Rjiba I, Esposto S, Taticci A, Servili M, et al. Effect of pedoclimatic conditions on the chemical composition of the sigoise olive cultivar. *Chem Biodivers*. (2010) 7:898–908. doi: 10.1002/cbdv.200900215
66. Mensink RP, Katan MB. Effect of dietary fatty acids on serum lipid and lipoproteins. A meta-analysis of 27 trials. *Arterioscler Thromb*. (1992) 12:911–9. doi: 10.1161/01.ATV.12.8.911
67. Maestro-Durán R, Borja-Padilla R. Relationship between the quality of the oil and the composition and ripening of the olive. *Grasas Aceites*. (1990) 41:171–8. doi: 10.17660/ActaHortic.1990.286.91
68. Baccouri O, Guerfel M, Baccouri B, Cerretani L, Bendini A, Lercker G, et al. Chemical composition and oxidative stability of Tunisian monovarietal virgin olive oils with regard to fruit ripening. *Food Chem*. (2008) 109:743–54. doi: 10.1016/j.foodchem.2008.01.034
69. Damak N, Bouaziz M, Ayadi M, Sayadi S, Damak M. Effect of the maturation process on the phenolic fractions, fatty acids, and antioxidant activity of the Chétoui olive fruit cultivar. *J Agric Food Chem*. (2008) 56:1560–6. doi: 10.1021/jf072273k
70. Brenes M, García A, García P, Ríos JJ, Garrido A. Phenolic compounds in Spanish olive oil. *J Agric Food Chem*. (1999) 47:3535–40. doi: 10.1021/jf990009o

71. Rotondi A, Bendini A, Cerretani L, Mari M, Lercker G, Gallina-Toschi T. Effect of olive ripening degree on the oxidative stability and organoleptic properties of cv. Nostrana di Brisighella extra virgin olive oil. *J Agric Food Chem*. (2004) 52:3649–54. doi: 10.1021/jf049845a
72. Amiot MJ, Fleuriet A, Macheix JJ. Accumulation of oleuropein derivatives during maturation. *Phytochem*. (1989) 28:67–9. doi: 10.1016/0031-9422(89)85009-5
73. León L, de la Rosa R, Gracia A, Barranco D, Rallo L. Fatty acid composition of advanced olive selections obtained by crossbreeding. *J Sci Food Agric*. (2008) 88:1921–6. doi: 10.1002/jsfa.3296

Conflict of Interest Statement: The authors declare that the research was conducted in the absence of any commercial or financial relationships that could be construed as a potential conflict of interest.

frontiers in Plant Science

ORIGINAL RESEARCH
published: 05 July 2019
doi: 10.3389/fpls.2019.00867

Behavior of Four Olive Cultivars During Salt Stress

Luca Regni[1], Alberto Marco Del Pino[1], Soraya Mousavi[2], Carlo Alberto Palmerini[1]*, Luciana Baldoni[2], Roberto Mariotti[2], Hanene Mairech[1], Tiziano Gardi[1], Roberto D'Amato[1] and Primo Proietti[1]*

[1] Department of Agricultural, Food and Environmental Sciences, University of Perugia, Perugia, Italy, [2] Institute of Biosciences and Bioresources, National Research Council, Perugia, Italy

Olive is considered as a moderately salt tolerant plant, however, tolerance to salt appears to be cultivar-dependent and genotypic responses have not been extensively investigated. In this work, saline stress was induced in four olive cultivars: Arbequina, Koroneiki, Royal de Cazorla and Fadak 86. The plants were grown in 2.5 l pots containing 60% peat and 40% of pumice mixture for 240 days and were irrigated three times a week with half-strength Hoagland solution containing 0, 100 and 200 mM NaCl. The effects of salt stress on growth, physiological and biochemical parameters were determined after 180, 210, and 240 days of treatment. Saline stress response was evaluated in leaves by measuring the activity of GSH and CAT enzymatic activity, as well as proline levels, gas exchanges, leaves relative water content and chlorophyll content, and proline content. All the studied cultivars showed a decrease in Net Photosynthesis, leaves chlorophyll content and plant growth (mainly leaves dry weight) and an increase in the activity of GSH and CAT. In addition, the reduction of proline content in leaf tissues, induced an alteration of osmotic regulation. Among the studied cultivars Royal and Koroneiki better counteracting the effects of saline stress thanks to a higher activity of two antioxidant enzymes.

Keywords: salt stress, olive, photosynthesis, proline, antioxidant enzyme

OPEN ACCESS

Edited by:
Antonio Diaz Espejo, Institute of Natural Resources and Agrobiology of Seville (CSIC), Spain

Reviewed by:
Enrique Mateos-Naranjo, University of Seville, Spain
Peter A. Roussos, Agricultural University of Athens, Greece

****Correspondence:***
Luca Regni
regni.luca.agr@gmail.com
Carlo Alberto Palmerini
carlo.palmerini@unipg.it

Specialty section:
This article was submitted to Crop and Product Physiology, a section of the journal Frontiers in Plant Science

Received: *18 December 2018*
Accepted: *18 June 2019*
Published: *05 July 2019*

Citation:
Regni L, Del Pino AM, Mousavi S, Palmerini CA, Baldoni L, Mariotti R, Mairech H, Gardi T, D'Amato R and Proietti P (2019) Behavior of Four Olive Cultivars During Salt Stress. Front. Plant Sci. 10:867. doi: 10.3389/fpls.2019.00867

INTRODUCTION

Environmental conditions may strongly impact plant crop growth (Kachaou et al., 2010; Feller and Vaseva, 2014; Pandolfi et al., 2017). In particular, abiotic constraints, such as drought, soil salinity and extreme temperatures, which cause water depletion in cells, are responsible for a large proportion of losses in agricultural productivity (Bose et al., 2014).

In order to overcome water shortages and to satisfy the increasing water demand for agricultural development, the use of water of low quality (brackish, reclaimed, drainage) that frequently has an high salinity level is becoming important in many countries (Chartzoulakis, 2005).

In particular, plants under high salinity conditions are subject to significant physiological and biochemical changes, for example a marked decrease in photosynthesis rate and transport of salt ions from roots to shoots (Ben Ahmed et al., 2009; Anjum et al., 2011; Singh and Reddy, 2011; Goltsev et al., 2012; Abdallah et al., 2018). A major biochemical alteration, also induced by other types of stress, is the production of reactive oxygen species (ROS) (Gill and Tuteja, 2010; Boguszewska and Zagdańska, 2012; Ozgur et al., 2013; Bose et al., 2014). An excess of ROS leads to lipid peroxidation, inhibition of enzymes, and modifications of nucleic acids (Proietti et al., 2013; Bose et al., 2014; Tedeschini et al., 2015). Under stress conditions, plants can nonetheless

develop tolerance, that is, the ability to adequately survive, and often prosper, under an unfavorable environment, following a robust production of antioxidant enzymes (Ben Ahmed et al., 2009; Bhaduri and Fulekar, 2012; Keunen et al., 2013). Among these enzyme, superoxide dismutase (SOD), ascorbate peroxidase (APX), and glutathione reductase (GSH) are localized in chloroplasts and mitochondria (Pang and Wang, 2010; Del Buono et al., 2011; Proietti et al., 2013), whereas catalase (CAT) and guaiacol peroxidase (GPX) are generally present within microbodies and cytosol, respectively (Bhaduri and Fulekar, 2012; Hameed et al., 2013; Nath et al., 2016).

Mechanistically, tolerance may also include osmotic adjustments at cellular level (Ayala-Astorga and Alcaraz-Meléndez, 2010). Some plants implement this process by increasing the amount of solutes and lowering the water potential of root cells, thereby counteracting the water outflow. These substances, reported as osmolytes, can accumulate in large amount, but do not generally interfere with enzymatic activities and cytoplasmic pH, due to their zwitterionic nature. Osmolytes commonly used by plants are sugars, alcohols, quaternary amines, betaine, glycine and proline (Warren, 2014). In this regard, the concentration of proline in leaves and roots was reported as a response by the olive tree to saline stress (Ayala-Astorga and Alcaraz-Meléndez, 2010; Hayat et al., 2012; Iqbal et al., 2014; Abdallah et al., 2018). In fact, proline facilitates water retention in the cytoplasm and, therefore, its concentration is indicative of response to saline stress (Ben Ahmed et al., 2009; Gupta and Huang, 2014). Cultivated olive (*Olea europaea* subsp. europaea var. europaea) is a long-living, evergreen, thermophilic species. In the Mediterranean basin where olive is mostly cultivated salinity is becoming a relevant problem due to high rates of evaporation and insufficient leaching (Mousavi et al., 2019). In addition in costal areas the need for water of good quality for urban use is increasing while there is a large amount of low quality water mostly saline (EC $>$ 2.0 dS m^{-1}) that can be use for irrigation (Chartzoulakis, 2005). Olive is considered as a moderately salt tolerant plant and the tolerance appear to be cultivar dependent (Rugini and Fedeli, 1990). The olive crop counts a very rich varietal heritage (Mousavi et al., 2017) but genotypic responses of olive to NaCl salinity have not been extensively investigated, and only few works have been published (Al-Absi et al., 2003; Chartzoulakis, 2005). In this context it's important to select cultivars that may give good performance when cultivated in soil with salinity problems or irrigated with saline water. Among the cultivars studied in the present work Arbequina and Koroneiki cultivars are the subject of increasing interest given their adaptability to super-intensive cultivation systems (Proietti et al., 2015). The identification of saline-resistant cultivars is of particular interest, especially for those cultivation systems, such as the super-intensive, which require large quantities of water as the availability of non-saline water will decrease dramatically in the future due to climate change.

The purpose of this work was to study the behavior of different olive cultivars during saline stress by analyzing the activity of the GSH and CAT enzymes, the proline content and the plant growth parameters.

MATERIALS AND METHODS

Plant Material, Growing Conditions and Salt Treatments

Sixty own-rooted plants for each olive cultivar Fadak 86, Royal de Cazorla (referred along the text as "Royal"), Koroneiki and Arbequina were used (20 plant replicates per treatment). Two-years old plants, approximately 1.3–1.5 m tall, were grown in greenhouse in black plastic pots (volume 2.5 L) containing a substrate composed of 60% peat and 40% pumice (w/w). Plants were irrigated three times a week, for 3 months, using half-strength Hoagland solution in the absence of salt. Subsequently, for the following 8 months from February, plants were irrigated three times a week with half-strength Hoagland solution containing 0, 100, and 200 mM NaCl, respectively. The salinity levels used were high since 137 mM NaCl has been is the tolerance limit for olive trees (Rugini and Fedeli, 1990) and were chosen accordingly to previous studies on salt stress in olive (Therios and Misopolinos, 1988; Tattini et al., 1995; Ben Ahmed et al., 2008). At beginning of treatment, to prevent osmotic shock, salt was added using daily increments of 25 mM up to the target levels. Electrical conductivity was determined weekly in the leaching solution with the conductometer "Hanna Instruments-HI 9033," giving values of about 1.2, 12.4, and 21.4 dS m^{-1} in relation to the 0, 100, and 200 mM NaCl group, respectively, thus confirming that an irrigation rate with a leaching fraction of 20–30%, ensures a stable salinity level in pots throughout the course of the experiment (Perica et al., 2008).

Plants were exposed to natural light inside the greenhouse, and a ventilation system was automatically engaged by air temperature not exceeding 35°C.

During the entire course of the experiment, minimum and maximum daily temperatures ranged between 9.4 and 15.2°C, and 10.4–30.4°C, respectively.

Plant Growth

At the beginning of the experiment and at 240 days after treatment (DAT), five plants for each treatment (including control plants) were removed from the substrate, roots were washed with deionized water and separated into different parts. For each plant, basal diameter, total height, number of lateral shoots, total length of lateral shoots, total leaf area and fresh and dry weight (FW and DW) of roots, lateral shoots (after removing the leaves) and stems (principal axis) were determined. DW was obtained by oven-drying at 95°C until constant weight was achieved.

At the end of the experiment the relative growth rate (RGR) was calculated as follows (Hoffmann and Poorter, 2002):

$$RGR = \frac{\ln(v_2) - \ln(v_1)}{t_2 - t_1}$$

where: ln = natural logarithm; v_2 e v_1 = plant DW at the end (t_2) and at the beginning (t_1) of the experiment.

Leaf Net Photosynthesis (Pn), Stomatal Conductance (gs), Leaf Transpiration Rate (E), and Sub-Stomatal CO_2 Concentration (Ci)

Photosynthesis, gs, E and Ci were determined at 180, 210 and 240 DAT in 15 leaves for each combination (cultivar + treatment). Leaf gas exchange rates were measured using a portable IRGA (ADC-LCA-3, Analytical Development, Hoddesdon, United Kingdom) and a Parkinson-type assimilation leaf chamber. Leaves were enclosed in the leaf chamber and perpendicularly exposed to sun's rays inside the greenhouse. PPFD was always higher than 1,200 μmol m^{-2} s^{-1} (within the 1,500–1,900 range), which is known to be over the saturation point in olive (Proietti and Famiani, 2002). The flow rate of air passing through the chamber was kept at 5 cm^3 s^{-1}. During gas-exchange measurements, the external CO_2 concentration was about 385 cm^3 m^{-3} and the air temperature inside the leaf chamber was 2–4°C higher than outside. Measurements were taken under steady state conditions (about 30 s). Leaves were then returned to the laboratory for area measurements using a Delta-T Image Analysis System ("Delta-T Devices," Cambridge, United Kingdom) and Pn, gs and E were expressed in relation to the leaf area.

Leaf Water Status and Chlorophyll Content

For each treatment, relative water content (RWC) was determined from leaves of five plants (three leaves each), collected at 180, 210, and 240 DAT. Leaves were detached, sealed in a plastic bag, and taken immediately to the laboratory to determine leaf water status according to the procedure previously described (Proietti et al., 2013).

Total chlorophyll content was determined by the portable SPAD-502 chlorophyll meter, which allows rapid, non-destructive measurements (Boussadia et al., 2011).

Chemical Analysis

Glutathione Reductase (GSH)

The enzymatic activity was measured by a modification of the previously published method (Flohé and Günzler, 1984) using H_2O_2 as substrate. GSH activity was measured in olive leaves (five leaves of about 1 g total for each combination cultivar+treatment) homogenized in 5 ml of $KNaHPO_4$ (0.1 M) buffer at pH 7.0 containing EDTA 1 mM, with an ultra-Turrax T25 homogenizer (Tanke and Kunkel Ika Labortechnik) for 3 min in ice. The supernatant obtained by centrifugation (10 min at 3,000 rpm) was used as the source of enzyme activity.

The reaction mixture consisted of 0.2 mL of the extract supernatant, 0.4 ml of GSH (0.1 mM) and 0.2 ml of $KNaHPO_4$ (0.067 M) containing EDTA 1 mM. The reaction mixture was kept at 25°C for 5 min, after which the reaction was started by adding 0.2 ml of H_2O_2 (1.3 mM), and then stopped 10 min later with 1 ml of trichloroacetic acid.

The mixture was cooled in ice for 30 min and centrifuged at 3000 rpm for 10 min; the supernatant (0.48 ml) was placed in a cuvette containing 2.2 ml of 0.32 M Na_2HPO_4 and 0.32 ml of 1 mM DTNB (Sigma-Aldrich), and read after 5 min in a Beckman spectrophotometer set at 412 nM.

Catalase (CAT)

Catalase activity was carried out in olive leaves (five leaves for each combination cultivar+treatment) homogenized for 3 min in ice by an ultra-Turrax T25 in 5 ml of 0.2 M Tris buffer (pH 7.8) containing 0.13 mM EDTA and 80 mM PVP. The homogenates were centrifuged at 3,000 × g for 10 min, after which the supernatants were used to measure CAT activity. CAT activity was determined based upon the consumption of hydrogen peroxide (coefficient of extinction 39.4 M^{-1} cm^{-1}) at 240 nM for 2 min (Kraus et al., 1995).

The reaction mixture contained 2 ml of a 100 mM NaH_2PO_4/Na_2HPO_4 buffer (pH 6.5), and 0.05 ml of the extract. The reaction was started by adding 0.01 ml of 30% (w/v) hydrogen peroxide.

Proline

The determination of proline in leaves (five leaves for each combination cultivar + treatment of about 1 g total) was performed by HPLC using a Jasco 880-PU instrument equipped with a Jasco 821-FP fluorometric detector. The HPLC procedure was carried out according to the method described (Palmerini et al., 1985). Proline was measured in leaves homogenized in 5 mL of ultra-pure H_2O with an ultra-TurraxT25 for 3 min in ice.

The extract supernatant (1 ml) was deproteinized with 0.2 ml of $HClO_4$ (20% v/v) in ice, centrifuged at 8000 rpm for 5 min, and finally neutralized with 0.2 ml of KOH (20% by weight).

The supernatant (0.05 ml) was mixed with 0.15 ml (0.4 M) of borate pH 9, 0.05 ml of o-phthalide chloride (OPA) (150 mM) in methanol and 0.1 ml of 7-chloro-4-nitrobenzo 2 ossa-1,3-diazolo (NBD-Cl) (25 mM) in methanol. The reaction, set at 60°C for 3 min, was stopped in ice with 0.1 ml HCl (1 M).

The derivatized sample (0.02 ml) was injected into a HPLC Lichrosor RP-18 column (15 cm × 4.6 mm ID) and eluted under isocratic conditions with H_2O/CH_3CN (93/7), used as the mobile phase. The solvents used were previously passed through a 0.22-micron filter (Millipore Corporation).

NBD-derivatives were determined at 470 nM (excitation) and 530 nM (emission). NBD-proline was eluted in 6.5 min and quantified using a standard proline solution. Proline (0.043 M) and hydroxy-proline (0.038 M) standards were diluted 1 to 100 in H_2O, derivatized with NBD-Cl and analyzed by the same HPLC method to generate reference data.

Statistical Analysis

All statistical analyses of data were performed using Graph Pad Prism 6.03 software for Windows (La Jolla, CA, United States). Tests for variance assumptions were conducted (homogeneity of variance by the Levene's test, normal distribution by the D'Agostino-Pearson omnibus normality test). Significance of differences were analyzed by Fisher's least significant differences test, after the analysis of variance according to the randomized complete factorial design. Differences with $p < 0.05$ were

TABLE 1 | Gas exchanges in four cultivars treated with 0, 100, and 200 mM NaCl.

	Pn $\mu mol(CO_2)\ m^{-2}\ s^{-1}$	E mmo $l(H_2O)\ m^{-2}\ s^{-1}$	gs $mmol(H_2O)\ m^{-2}\ s^{-1}$	Ci $\mu mol\ mol^{-1}$
180 DAT				
Fadak 86-0	12.14 a	3.50 a	246.50 a	297.21 a
Fadak 86–100	11.67 a	3.55 a	236.38 a	284.46 a
Fadak 86–200	11.40 a	3.60 a	232.47 a	281.67 a
Royal-0	13.80 a	2.93 a	147.97 a	209.54 a
Royal-100	12.03 a	2.43 a	127.96 b	213.80 a
Royal-200	10.15 b	2.25 a	128.62 b	201.41 a
Koroneiki-0	14.10 a	3.85 a	252.65 a	260.69 b
Koroneiki-100	10.69 b	3.81 a	209.77 b	312.56 a
Koroneiki-200	9.31 b	3.51 a	180.34 b	359.19 a
Arbequina-0	13.05 a	3.38 a	184.47 a	254.94 a
Arbequina-100	11.63 b	2.32 b	174.70 b	244.43 a
Arbequina-200	11.01 b	2.33 b	170.79 b	251.64 a
210 DAT				
Fadak 86-0	11.75 a	2.12 a	162.53 a	288.21 b
Fadak 86–100	7.20 b	1.38 b	72.04 b	346.47 a
Fadak 86–200	5.47 b	1.35 b	68.78 b	332.03 a
Royal-0	6.72 a	0.69 a	21.60 a	112.07 a
Royal-100	6.02 a	0.72 a	27.06 a	101.43 a
Royal-200	5.17 b	0.70 a	22.18 a	117.32 a
Koroneiki-0	9.30 a	2.12 a	90.75 a	241.55 b
Koroneiki-100	5.54 b	1.61 a	57.79 b	279.20 a
Koroneiki-200	4.47 b	1.30 b	45.85 b	295.43 a
Arbequina-0	7.96 a	1.83 a	108.32 a	329.36 b
Arbequina-100	4.60 b	1.85 a	105.90 a	394.26 a
Arbequina-200	4.79 b	1.86 a	53.47 b	368.24 ab
240 DAT				
Fadak 86-0	5.01 a	2.11 a	72.66 a	266.25 b
Fadak 86–100	−0.68 b	1.28 b	37.53 b	341.68 a
Royal-0	7.77 a	2.34 a	86.55 a	265.92 b
Royal-100	1.78 b	1.55 b	50.04 b	371.09 a
Royal-200	−0.45 b	1.37 b	36.37 b	393.99 a
Koroneiki-0	4.06 a	2.96 a	95.40 a	296.85 b
Koroneiki-100	−0.16 b	1.94 b	53.15 b	375.65 a
Koroneiki-200	−0.83 b	2.11 b	59.32 b	395.95 a
Arbequina-0	2.70 a	4.57 a	167.90 a	333.34 b
Arbequina-100	−0.86 b	3.03 a	95.16 b	383.40 a

Mean values followed by different letters are significantly different ($P < 0.05$). Tests were performed inside each cultivar for three treatments (0, 100, and 200 mM NaCl) and separately for each time point.

considered significant (**Supplementary Tables S1–S14**). The coefficient of variation (CV) was determined for each trait.

RESULTS

Leaf Net Photosynthesis (Pn), Stomatal Conductance (gs), Leaf Transpiration Rate (E), and Sub-Stomatal CO_2 Concentration (Ci)

Plants treated with 100 and 200 mM NaCl showed lower values of Pn compared to control, especially at 210 and 240 days after treatment start (DAT). The Pn decrease in stressed plants started from 180 DAT, and the most significant impact was observed in "Arbequina," and "Fadak 86" treated withf Pn compared to control, 100 and 200 mM NaCl and the plants of the same cultivars treated with 200 mM NaCl died at 220 DAT. Ci increased at 100 and 200 mM NaCl and the higher values were observed in Arbequina and Fadak 86 gs and E decreased at 200 mM.

As a general trend, in stressed plant, the decrease in Pn was accompanied by a decrease in gs. On the other hand, gs decrease is related with an increase in Ci and a decrease in E (**Table 1**).

TABLE 2 | Relative water content of leaves in four olive cultivars treated with 0, 100, and 200 mM NaCl.

	RWC (%)		
	180 DAT	**210 DAT**	**240 DAT**
Fadak 86-0	84.36 a	84.36 a	70.40 a
Fadak 86–100	84.15 a	84.15 a	56.65 b
Fadak 86–200	83.37 a	83.37 a	0
Royal-0	82.72 a	74.89 a	76.06 a
Royal-100	83.43 a	76.15 a	66.23 b
Royal-200	79.05 a	77.47 a	64.58 b
Koroneiki-0	88.43 a	77.84 a	75.13 a
Koroneiki-100	84.04 a	81.46 a	72.01 a
Koroneiki-200	83.49 a	78.33 a	64.67 b
Arbequina-0	86.03 a	85.53 a	78.75 a
Arbequina-100	82.73 b	77.44 b	68.51 b
Arbequina-200	80.09 b	73.95 b	0

Mean values followed by different letters are significantly different ($P < 0.05$). Tests were performed inside each cultivar for three treatments (0, 100, and 200 mM NaCl) and separately for each time point.

TABLE 3 | Chlorophyll content of leaves of different olive cultivars treated with 0, 100, and 200 mM of NaCl.

	SPAD		
	180 DAT	**210 DAT**	**240 DAT**
Fadak 86-0	85.75 a	88.02 a	82.10 a
Fadak 86–100	85.70 a	80.78 b	65.23 b
Fadak 86–200	84.48 a	79.84 b	0
Royal-0	90.74 a	91.29 a	90.40 a
Royal-100	93.08 a	83.22 b	68.00 b
Royal-200	92.14 a	84.39 b	66.99 b
Koroneiki-0	92.99 a	93.18 a	89.53 a
Koroneiki-100	90.54 a	80.96 b	77.18 b
Koroneiki-200	93.44 a	82.33 b	62.51 b
Arbequina-0	95.94 a	93.11 a	94.35 a
Arbequina-100	95.36 a	82.86 b	50.99 b
Arbequina-200	96.78 a	85.62 ab	0

Mean values followed by different letters are significantly different ($P < 0.05$). Tests were performed inside each cultivar for three treatments (0, 100, and 200 mM NaCl) and separately for each time point.

Relative Water Content (RWC) and Chlorophyll Content

In general in stressed plants, RWC was lower than control starting from 210 DAT without differences between 100 and 200 mM NaCl (**Table 2**).

In all plants under saline stress of the four cultivars, low values of chlorophyll content than control were observed at 240 DAT, however, the major impact was observed in stressed plants of "Fadak 86" (**Table 3**).

Plant Growth

Salt treatments reduced dry weight (DW) in all plant parts of all examined cultivars at 100 and 200 mM NaCl. The larger DW reductions were observed in leaves while roots and shoots DW decreased only at 200 mM (**Table 4** and **Supplementary Figures S1–S4**). The major DW reduction was observed in "Fadak 86." Moreover, "Fadak 86" and "Arbequina" showed the lowest RGR values (data not shown).

Enzymatic Activity

In leaves of plants treated with 100 and 200 mM NaCl, GSH, and CAT activities systematically increased in relation to controls across the four cultivars and regardless of the duration of NaCl treatment (**Figure 1**). CAT increased more markedly with extended exposure to saline stress in "Fadak 86," "Royal" and, less evidently, in "Koroneiki" and '"Arbequina," whereas GSH activity exhibited higher values in "Royal" plants.

Catalase increased more markedly with prolonged exposure to salt stress in "Fadak 86," "Arbequina," and "Koroneiki," less

TABLE 4 | Dry weight (DW) (g) of different parts of olive plants treated with 100 and 200 mM NaCl at 240 DAT.

	Roots DW	**Shoots DW**	**Leaves DW**	**Stem DW**	**Plant DW**
Fadak 86-0	28.81 a	2.63 a	8.19 a	9.85 a	49.48 a
Fadak 86–100	19.06 b	2.66 a	8.36 a	10.56 a	40.64 a
Fadak 86–200	9.52 c	2.51 a	0.03 b	11.10 a	23.16 b
Royal-0	32.24 a	9.30 a	23.14 a	19.11 a	83.79 a
Royal-100	17.40 b	5.20 b	10.19 b	14.99 b	47.78 b
Royal-200	18.52 c	3.84 c	2.78 c	12.11 c	37.25 b
Koroneiki-0	33.54 a	11.87 a	21.75 a	21.64 a	88.80 a
Koroneiki-100	11.38 b	3.83 b	5.81 b	11.26 b	32.28 b
Koroneiki-200	15.61 b	5.03 c	3.21 b	12.30 b	36.15 b
Arbequina-0	25.75 a	9.81 a	24.41 a	21.70 a	81.67 a
Arbequina-100	20.24 b	4.42 b	8.98 b	15.25 b	30.89 b
Arbequina-200	12.35 c	2.16 c	0.02 c	11.99 c	26.52 b

Mean values followed by different letters are significantly different ($P < 0.05$). Tests were performed inside each cultivar for three treatments (0, 100, and 200 mM NaCl).

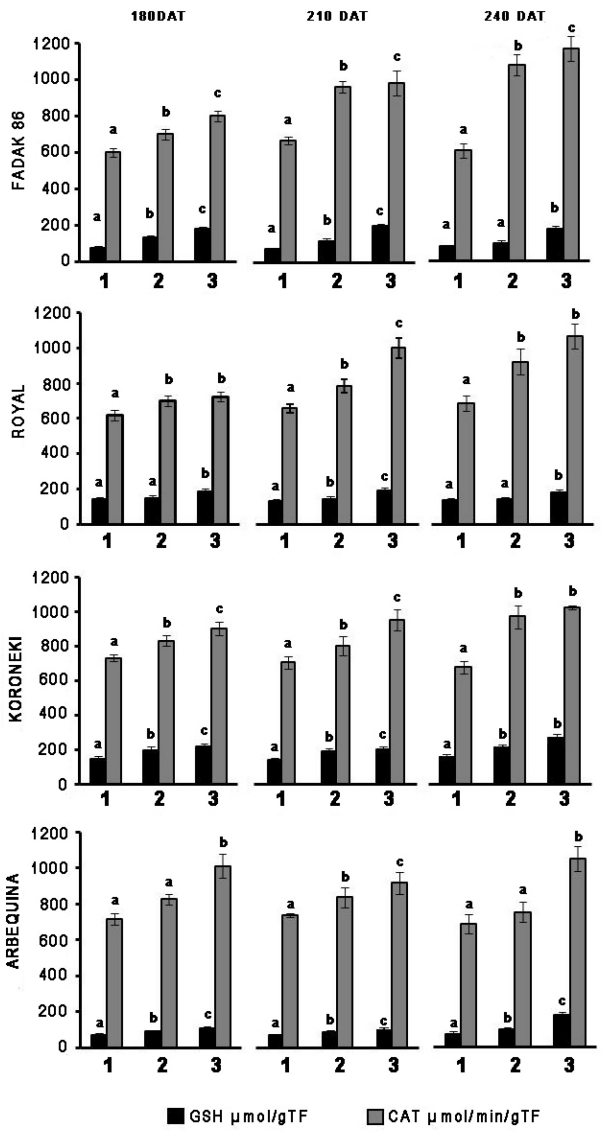

FIGURE 1 | Time-points of glutathione reductase (GSH) and catalase (CAT) activity in leaves of four olive cultivars under saline stress. (1) control, (2) 100 mM NaCl, and (3) 200 mM NaCl. Each value represents the average of five experiments ± SEM. Mean values followed by different letters are significantly different ($P < 0.05$).

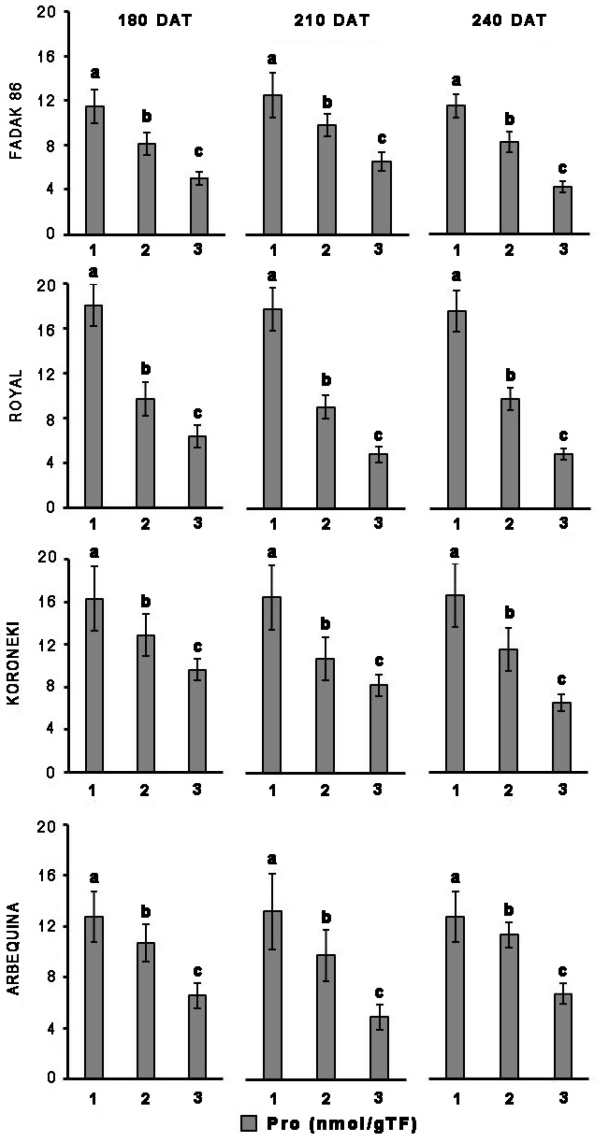

FIGURE 2 | Proline levels in leaves of four olive cultivars under saline stress. (1) control, (2) 100 mM NaCl, and (3) 200 mM NaCl. Each value represents the average of five experiments ± SEM. Mean values followed by different letters are significantly different ($P < 0.05$).

noticeably, in "Royal," while GSH activity showed higher values in plants "Koroneiki."

At 240 DAT the enzymatic activity was determined in the leaves of "Arbequina," and "Fadak 86" of the few survived trees treated with 200 mM NaCl.

Proline

Upon salt stress, proline concentration decreased in all four cultivars, and more evidently at the higher dose of NaCl (**Figure 2**). Notably, proline reduction did not correlate with duration of the induced stress. In control plants, the concentration of proline in leaves was higher in "Royal" and "Koroneiki" compared to "Arbequina" and "Fadak 86." At 240 DAT the proline concentration was determined in the leaves of "Arbequina," and "Fadak 86" of the few survived trees treated with 200 mM NaCl.

DISCUSSION

In all the four cultivars considered in this study, Pn reduction in leaves under stress conditions was associated with an increase in Ci. This is in agreement with Chartzoulakis (2005) who reports that low and moderate salinity is associated

with reduction of CO_2 assimilation rate. The increase in Ci due to reduction of Pn caused stomatal closure, with a consequent decrease in gs and E and this is in agreement with what postulated by Proietti et al., 2013. The Ci increase is likely indicative that Pn reduction is mainly caused by non-stomatal effects, and could be the result of a damage in the photosystem under saline stress (Proietti and Famiani, 2002; Ben Ahmed et al., 2010; Singh and Reddy, 2011; Proietti et al., 2012).

The reduction of the photosynthetic rate in plants exposed to salt stress togheter with the reduction in Leaf area caused a reduction of plant's growth (Chartzoulakis et al., 2002; Karimi and Hasanpour, 2014; Pandolfi et al., 2017; Abdallah et al., 2018). In this regard, we noted that saline stressed plants clearly displayed, with time, a lower DW than controls. The DW reduction, mainly localized in leaves was observed also by Karimi and Hasanpour (2014), who found that if the amount of salt rises to a toxic level in the leaves, it causes premature leaf senescence and abscission.

Catalase and GSH enzymes were both investigated in light of their different cellular localization, since CAT is expressed in peroxisomes and removes H_2O_2 produced by the conversion of superoxide anion (Guerfel et al., 2009; Huang et al., 2012), while GSH is mainly present in chloroplasts and mitochondria, where it maintains a high ratio between reduced (GSH) and oxidized (GSSG) glutathione, despite formation of GSSG as a result of exposure to the superoxide anion (Bray, 2000; Yousuf et al., 2012; Keunen et al., 2013).

In the absence of stress, "Fadak 86," "Koroneiki," and "Arbequina" plants showed a greater activity of CAT, while only the cultivar "Koroneiki" expressed GSH. This may explain the greater resistance of 'Koroneiki' to saline stress also confirmed by a lower reduction of Pn compared to "Fadak 86" and "Arbequina."

Decrease in Pn and chlorophyll content after treatments with 100 and 200 mM NaCl, could be related to a greater catalytic activity of both CAT and GSH in the leaves of the four cultivars (Yasar et al., 2008; Sevengor et al., 2011; Keshavkant et al., 2012).

Overall, obtained results indicated significant increase in CAT and GSH enzymatic activities according to the increase of NaCl concentrations across the four cultivars, excepting for GSH at low salt level (100 mM) in "Royal." The increased activity of CAT and GSH in response to the reduction of Pn indicates an altered redox state in the different cellular compartments of leaves of the four cultivars and can be considered an important marker of cellular response to saline stress, as also reported by Hernández et al. (2000). Indeed a low chlorophyll content in leaves of stressed plants, as observed in the olive plants, is a typical effect of NaCl exposure, associated with an increase of oxidative stress and, at the same time, an increase in ROS scavenging enzymes as a physiological response (Yasar et al., 2008; Gill and Tuteja, 2010; Saha et al., 2010; Din et al., 2011; Arjenaki et al., 2012).

Other reports on olive response to salt stress have shown that the concentration in leaves and roots of osmolytes such as proline, may refer to a possible mechanism of adaptation to unfavorable conditions (Feller and Vaseva, 2014; Iqbal et al., 2014). Proline promotes water retention in the cytoplasm and its higher content appears to represent a specific mechanism engaged by the plants to better tolerate stress conditions (Parida and Das, 2005; Ben Ahmed et al., 2010; Hayat et al., 2012; Iqbal et al., 2014). However, the involvement of osmolytes in carrying out a protective action under unfavorable environmental conditions is currently widely debated and has not yet been elucidated and clarified, considering that tolerance to dehydration also depends on the ability of cells to keep membranes intact and prevent protein denaturation (Munns and Tester, 2008; Iqbal et al., 2014; Cardi et al., 2015). Proline concentration in the four cultivars examined under non-stress conditions was different, that is, higher in "Royal" and "Koroneiki" and less pronounced in "Fadak 86" and "Arbequina." In saline stressed plants, proline decrease was statistically significant across the four cultivars. This finding is in agreement with the observations of some authors (Ayala-Astorga and Alcaraz-Meléndez, 2010), however, it does not parallel what is reported by others, since in some cases it was shown an increase in proline during saline stress (Ben Ahmed et al., 2009). In this regard, it must be noted that the trend affecting proline concentration is likely associated with NaCl doses higher than 100 mM, usually used to evoke a saline stress (Ayala-Astorga and Alcaraz-Meléndez, 2010). Furthermore, a number of observations concerning proline and saline stress were made under different experimental conditions (e.g., NaCl doses), and by the application of different assay methods, such as non-specific, colorimetric determinations (e.g., ninhydrin), that might impact specificity and sensitivity of the determinations (Bates et al., 1973).

In conclusion, the increase of CAT and GSH in salt stress, induced by high levels of NaCl on the cultivars examined, indicates the presence of a high oxidative stress in progress.

In particular, the Koroneiki cultivar showed a greater response to saline stress, probably due to the prevalence of CAT and GSH in control coditions.

Therefore, it will be interesting to investigate whether the increased activity of CAT, GSH and proline, in basal conditions, may represent a possible prognostic marker of olive trees in the salt stress response.

AUTHOR CONTRIBUTIONS

PP, LB, CP, LR, and SM: conceptualization. PP, LR, SM, RD'A, ADP, RM, and HM: investigation. LR, SM, ADP, PP, LB, and CP: methodology and writing original draft. PP, LB, CP, and TG: supervision.

FUNDING

This research was partially funded by the EU project LIFE OLIVE4CLIMATE (LIFE15 CCM/IT/000141), by the "BeFOre – Bioresources for Oliviculture," H2020-MSCA-RISE (G.A. 645595), and by the Fondazione Cassa di Risparmio di Perugia (2017.0217.021).

ACKNOWLEDGMENTS

We would like to thank Sanat Zeytoon Fadak Saraj olive grove in Qom Province (Iran). We are grateful to Mrs. Massimo Pilli and Paolo Tancini for their technical support.

SUPPLEMENTARY MATERIAL

The Supplementary Material for this article can be found online at: https://www.frontiersin.org/articles/10.3389/fpls.2019.00867/full#supplementary-material

FIGURE S1 | Arbequina trees at 240 DAT.

FIGURE S2 | Fadak86 trees at 240 DAT.

FIGURE S3 | Koroneiki trees at 240 DAT.

FIGURE S4 | Royal trees at 240 DAT.

TABLE S1 | Gas exchanges – variable Pn.

TABLE S2 | Gas exchanges – variable E.

TABLE S3 | Gas exchanges – variable gs.

TABLE S4 | Gas exchanges – variable Ci.

TABLE S5 | Variable RWC.

TABLE S6 | Variable chlorophyll content.

TABLE S7 | Variable roots DW.

TABLE S8 | Variable shoots DW.

TABLE S9 | Variable stem DW.

TABLE S10 | Variable leaves DW.

TABLE S11 | Variable total plant DW.

TABLE S12 | Variable GSH.

TABLE S13 | Variable CAT.

TABLE S14 | Variable proline.

REFERENCES

Abdallah, M. B., Trupiano, D., Polzella, A., De Zio, E., Sassi, M., Scaloni, A., et al. (2018). Unraveling physiological, biochemical and molecular mechanisms involved in olive (*Olea europaea* L. *cv. Chétoui)* tolerance to drought and salt stresses. *J. Plant Physiol.* 220, 83–95. doi: 10.1016/j.jplph.2017.10.009

Al-Absi, K., Qrunfleh, M., and Abu-Sharar, T. (2003). Mechanism of salt tolerance of two olive (*Olea europaea* L.) cultivars as related to electrolyte concentration and toxicity. *Acta Hortic.* 618, 281–290. doi: 10.17660/actahortic.2003.618.32

Anjum, S. A., Xie, X., Wang, L., Saleem, M. F., Man, C., and Lei, W. (2011). Morphological, physiological and biochemical responses of plants to drought stress. *Afr. J. Agric. Res.* 6, 2026–2032.

Arjenaki, F. G., Jabbari, R., and Morshedi, A. (2012). Evaluation of drought stress on relative water content, chlorophyll content and mineral elements of wheat (Triticum aestivum L.) varieties. *Int. J. Agric. Crop Sci.* 4, 726–729.

Ayala-Astorga, G. I., and Alcaraz-Meléndez, L. (2010). Salinity effects on protein content, lipid peroxidation, pigments, and proline in Paulownia imperialis (Siebold and Zuccarini) and *Paulownia fortunei* (Seemann and Hemsley) grown in vitro. *Electr. J. Biotechnol.* 13, 13–14.

Bates, L. S., Waldren, R. P., and Teare, I. D. (1973). Rapid determination of free proline for water-stress studies. *Plant Soil* 39, 205–207. doi: 10.1016/j.dental.2010.07.006

Ben Ahmed, C., Ben Rouina, B., Sensoy, S., Boukhriss, M., and Abdullah, F. B. (2009). Saline water irrigation effects on antioxidant defense system and proline accumulation in leaves and roots of field-grown olive. *J. Agric. Food Chem.* 57, 11484–11490. doi: 10.1021/jf901490f

Ben Ahmed, C., Ben Rouina, B., Sensoy, S., Boukhriss, M., and Ben Abdullah, F. (2010). Exogenous proline effects on photosynthetic performance and antioxidant defense system of young olive tree. *J. Agric. Food Chem.* 58, 4216–4222. doi: 10.1021/jf9041479

Ben Ahmed, C., Rouina, B. B., and Boukhris, M. (2008). Changes in water relations, photosynthetic activity and proline accumulation in one-year-old olive trees (*Olea europaea* L. *cv. Chemlali)* in response to NaCl salinity. *Acta Physiol. Plant.* 30, 553–560. doi: 10.1007/s11738-008-0154-6

Bhaduri, A. M., and Fulekar, M. H. (2012). Antioxidant enzyme responses of plants to heavy metal stress. *Rev. Environ. Sci. Biotechnol.* 11, 55–69. doi: 10.1007/s11157-011-9251-x

Boguszewska, D., and Zagdańska, B. (2012). "ROS as signaling molecules and enzymes of plant response to unfavorable environmental conditions," in *Oxidative Stress-Molecular Mechanisms and Biological Effects*, eds V. Lushchak and H. M. Semchyshyn (Rijeka: InTech), doi: 10.5772/33589

Bose, J., Rodrigo-Moreno, A., and Shabala, S. (2014). ROS homeostasis in halophytes in the context of salinity stress tolerance. *J. Exp. Bot.* 65, 1241–1257. doi: 10.1093/jxb/ert430

Boussadia, O., Steppe, K., Zgallai, H., Ben El Hadj, S., Braham, M., Lemeur, R., et al. (2011). Nondestructive determination of nitrogen and chlorophyll content in olive tree leaves and the relation with photosynthesis and fluorescence parameters. *Photosynthetica* 49, 149–153. doi: 10.1007/s11099-011-0019-x

Bray, E. A. (2000). "Responses to abiotic stresses," in *Biochemistry and Molecular Biology of Plants*, eds B. B. Buchanan, W. Gruissem, and R. L. Jones (Rockville, MD: American Society of Plant Physiologists), 1158–1203.

Cardi, M., Castiglia, D., Ferrara, M., Guerriero, G., Chiurazzi, M., and Esposito, S. (2015). The effects of salt stress cause a diversion of basal metabolism in barley roots: possible different roles for glucose-6-phosphate dehydrogenase isoforms. *Plant Physiol. Biochem.* 86, 44–54. doi: 10.1016/j.plaphy.2014.11.001

Chartzoulakis, K. (2005). Salinity and olive: growth, salt tolerance, photosynthesis and yield. *Agric. Water Manag.* 78, 108–121. doi: 10.1016/j.agwat.2005.04.025

Chartzoulakis, K., Loupassaki, M., Bertaki, M., and Androulakis, I. (2002). Effects of NaCl salinity on growth, ion content and CO2 assimilation rate of six olive cultivars. *Sci. Hortic.* 96, 235–247. doi: 10.1016/s0304-4238(02)00067-5

Del Buono, D., Ioli, G., Nasini, L., and Proietti, P. (2011). A comparative study on the interference of two herbicides in wheat and Italian ryegrass and on their antioxidant activities and detoxification rates. *J. Agric. Food Chem.* 59, 12109–12115. doi: 10.1021/jf2026555

Din, J., Khan, S. U., Ali, I., and Gurmani, A. R. (2011). Physiological and agronomic response of canola varieties to drought stress. *J. Anim. Plant Sci.* 21, 78–82.

Feller, U., and Vaseva, I. I. (2014). Extreme climatic events: impacts of drought and high temperature on physiological processes in agronomically important plants. *Front. Environ. Sci.* 2:39. doi: 10.3389/fenvs.2014.00039

Flohé, L., and Günzler, W. A. (1984). Assays of glutathione peroxidase. *Methods Enzymol.* 105, 114–120. doi: 10.1016/s0076-6879(84)05015-1

Gill, S. S., and Tuteja, N. (2010). Reactive oxygen species and antioxidant machinery in abiotic stress tolerance in crop plants. *Plant Physiol. Biochem.* 48, 909–930. doi: 10.1016/j.plaphy.2010.08.016

Goltsev, V., Zaharieva, I., Chernev, P., Kouzmanova, M., Kalaji, H. M., Yordanov, I., et al. (2012). Drought-induced modifications of photosynthetic electron transport in intact leaves: analysis and use of neural networks as a tool for a rapid non-invasive estimation. *Biochim. Biophys. Acta* 1817, 1490–1498. doi: 10.1016/j.bbabio.2012.04.018

Guerfel, M., Baccouri, O., Boujnah, D., Chaïbi, W., and Zarrouk, M. (2009). Impacts of water stress on gas exchange, water relations, chlorophyll content and leaf structure in the two main Tunisian olive (*Olea europaea* L.) cultivars. *Sci. Hortic.* 119, 257–263. doi: 10.1016/j.scienta.2008.08.006

Gupta, B., and Huang, B. (2014). Mechanism of salinity tolerance in plants: physiological, biochemical, and molecular characterization. *Int. J. Genomics* 2014:701596.

Hameed, A., Goher, M., and Iqbal, N. (2013). Drought induced programmed cell death and associated changes in antioxidants, proteases, and lipid peroxidation in wheat leaves. *Biol. Plant.* 57, 370–374. doi: 10.1007/s10535-012-0286-9

Hayat, S., Hayat, Q., Alyemeni, M. N., Wani, A. S., Pichtel, J., and Ahmad, A. (2012). Role of proline under changing environments: a review. *Plant Signal. Behav.* 7, 1456–1466. doi: 10.4161/psb.21949

Hernández, J. A., Jiménez, P., Mullineaux, P., and Sevilla, F. (2000). Tolerance of pea (*Pisum sativum L.*) to long-term salt stress is associated with induction of antioxidant defences. *Plant Cell Environ.* 23, 853–862. doi: 10.1046/j.1365-3040.2000.00602.x

Hoffmann, W. A., and Poorter, H. (2002). Avoiding bias in calculations of relative growth rate. *Ann. Bot.* 90, 37–42. doi: 10.1093/aob/mcf140

Huang, G. T., Ma, S. L., Bai, L. P., Zhang, L., Ma, H., Jia, P., et al. (2012). Signal transduction during cold, salt, and drought stresses in plants. *Mol. Biol. Rep.* 39, 969–987. doi: 10.1007/s11033-011-0823-1

Iqbal, N., Umar, S., Khan, N. A., and Khan, M. I. R. (2014). A new perspective of phytohormones in salinity tolerance: regulation of proline metabolism. *Environ. Exp. Bot.* 100, 34–42. doi: 10.1016/j.envexpbot.2013.12.006

Kachaou, H., Larbi, A., Gargouri, K., Chaieb, M., Morales, F., and Msallem, M. (2010). Assessment of tolerance to NaCl salinity of five olive cultivars, based on growth characteristics and Na+ and Cl- exclusion mechanisms. *Sci. Hortic.* 124, 306–315. doi: 10.1016/j.scienta.2010.01.007

Karimi, H. R., and Hasanpour, Z. (2014). Effects of salinity and water stress on growth and macro nutrients concentration of pomegranate (*Punica granatum* L.). *Plant Nutr.* 37, 1937–1951. doi: 10.1080/01904167.2014.920363

Keshavkant, S., Padhan, J., Parkhey, S., and Naithani, S. C. (2012). Physiological and antioxidant responses of germinating Cicer arietinum seeds to salt stress. *Russ. J. Plant Physiol.* 59, 206–211. doi: 10.1134/s1021443712010116

Keunen, E. L. S., Peshev, D., Vangronsveld, J., Van Den Ende, W. I. M., and Cuypers, A. N. N. (2013). Plant sugars are crucial players in the oxidative challenge during abiotic stress: extending the traditional concept. *Plant Cell Environ.* 36, 1242–1255. doi: 10.1111/pce.12061

Kraus, T. E., McKersie, B. D., and Fletcher, R. A. (1995). Paclobutrazol-induced tolerance of wheat leaves to paraquat may involve increased antioxidant enzyme activity. *J. Plant Physiol.* 145, 570–576. doi: 10.1016/s0176-1617(11)81790-6

Mousavi, S., Mariotti, R., Regni, L., Nasini, L., Bufacchi, M., Pandolfi, S., et al. (2017). The first molecular identification of an olive collection applying standard simple sequence repeats and novel expressed sequence tag markers. *Front. Plant Sci.* 8:1283. doi: 10.3389/fpls.2017.01283

Mousavi, S., Regni, L., Bocchini, M., Mariotti, R., Cultrera, N. G. M., Mancuso, S., et al. (2019). Physiological, epigenetic and genetic regulation in some olive cultivars under salt stress. *Sci. Rep.* 9:1093. doi: 10.1038/s41598-018-37496-5

Munns, R., and Tester, M. (2008). Mechanisms of salinity tolerance. *Annu. Rev. Plant Biol.* 59, 651–681. doi: 10.1146/annurev.arplant.59.032607.092911

Nath, M., Bhatt, D., Prasad, R., Gill, S. S., Anjum, N. A., and Teteja, N. (2016). Reactive oxygen species generation-scavenging and signaling during plant-arbuscular mycorrhizal and *Piriformospora indica* interaction under stress condition. *Front. Plant Sci.* 7:1574. doi: 10.3389/fpls.2016.01574

Ozgur, R., Uzilday, B., Sekmen, A. H., and Turkan, I. (2013). Reactive oxygen species regulation and antioxidant defence in halophytes. *Funct. Plant Biol.* 40, 832–847.

Palmerini, C. A., Fini, C., Floridi, A., Morelli, A., and Vedovelli, A. (1985). High-performance liquid chromatographic analysis of free hydroxyproline and proline in blood plasma and of free and peptide-bound hydroxyproline in urine. *J. Chromatogr. B Biomed. Sci. Appl.* 339, 285–292. doi: 10.1016/s0378-4347(00)84655-1

Pandolfi, C., Bazihizina, N., Giordano, C., Mancuso, S., and Azzarello, E. (2017). Salt acclimation process: a comparison between a sensitive and a tolerant *Olea europaea* cultivar. *Tree Physiol.* 37, 380–388. doi: 10.1093/treephys/tpw127

Pang, C.-H., and Wang, B.-S. (2010). "Role of ascorbate peroxidase and glutathione reductase in ascorbate–glutathione cycle and stress tolerance in plants," in *Ascorbate-Glutathione Pathway and Stress Tolerance in Plants*, eds N. Anjum, M. T. Chan, and S. Umar (Dordrecht: Springer), 91–113. doi: 10.1007/978-90-481-9404-9_3

Parida, A. K., and Das, A. B. (2005). Salt tolerance and salinity effects on plants: a review. *Ecotoxicol. Environ. Saf.* 60, 324–349. doi: 10.1016/j.ecoenv.2004.06.010

Perica, S., Goreta, S., and Selak, G. V. (2008). Growth, biomass allocation and leaf ion concentration of seven olive (*Olea europaea* L.) cultivars under increased salinity. *Sci. Hortic.* 117, 123–129. doi: 10.1016/j.scienta.2008.03.020

Proietti, P., and Famiani, F. (2002). Diurnal and seasonal changes in photosynthetic characteristics in different olive (*Olea europaea* L.) cultivars. *Photosynthetica* 40, 171–176.

Proietti, P., Nasini, L., Del Buono, D. D., Amato, R., Tedeschini, E., and Businelli, D. (2013). Selenium protects olive (*Olea europaea* L.) from drought stress. *Sci. Hortic.* 164, 165–171. doi: 10.1016/j.scienta.2013.09.034

Proietti, P., Nasini, L., and Ilarioni, L. (2012). Photosynthetic behavior of Spanish Arbequina and Italian Maurino olive (*Olea europaea* L.) cultivars under super-intensive grove conditions. *Photosynthetica* 50, 239–246. doi: 10.1007/s11099-012-0025-7

Proietti, P., Nasini, L., Reale, L., Caruso, T., and Ferranti, F. (2015). Productive and vegetative behavior of olive cultivars in super high-density olive grove. *Sci. Agricola* 72, 20–27. doi: 10.1590/0103-9016-2014-0037

Rugini, E., and Fedeli, E. (1990). "Olive (Olea europea L.) as an oilseed crop," in *Biotechnology in Agriculture and Forestry Legume and Oilseed Crops I*, Vol. 1, ed. Y. P. S. Bajaj (Berlin: Springer), 593–641. doi: 10.1007/978-3-642-74448-8_29

Saha, P., Chatterjee, P., and Biswas, A. K. (2010). NaCl pretreatment alleviates salt stress by enhancement of antioxidant defense system and osmolyte accumulation in mungbean (*Vigna radiata* L. *Wilczek). Indian J. Exp. Biol.* 48, 593–600.

Sevengor, S., Yasar, F., Kusvuran, S., and Ellialtioglu, S. (2011). The effect of salt stress on growth, chlorophyll content, lipid peroxidation and antioxidative enzymes of pumpkin seedling. *Afr. J. Agric. Res.* 6, 4920–4924.

Singh, S. K., and Reddy, K. R. (2011). Regulation of photosynthesis, fluorescence, stomatal conductance and water-use efficiency of cowpea (*Vigna unguiculata* [L.] *Walp.*) under drought. *J. Photochem. Photobiol. B Biol.* 105, 40–50. doi: 10.1016/j.jphotobiol.2011.07.001

Tattini, M., Gucci, R., Coradeschi, M. A., Ponzio, C., and Everarard, J. D. (1995). Growth, gas exchange and ion content in *Olea europaea* plants during salinity and subsequent relief. *Physiol. Plant.* 95, 203–210. doi: 10.1034/j.1399-3054.1995.950205.x

Tedeschini, E., Proietti, P., Timorato, V., D'Amato, R., Nasini, L., Del Buono, D., et al. (2015). Selenium as stressor and antioxidant affects pollen performance in *Olea europaea*. *Flora Morphol. Distrib. Funct. Ecol. Plants* 215, 16–22. doi: 10.1016/j.flora.2015.05.009

Therios, I. N., and Misopolinos, N. D. (1988). Genotypic response to sodium chloride salinity of four major olive cultivars (*Olea europaea* L.). *Plant Soil* 106, 105–111. doi: 10.1007/bf02371201

Warren, C. R. (2014). Response of osmolytes in soil to drying and rewetting. *Soil Biol. Biochem.* 70, 22–32. doi: 10.1016/j.soilbio.2013.12.008

Yasar, F., Ellialtioglu, S., and Yildiz, K. (2008). Effect of salt stress on antioxidant defense systems, lipid peroxidation, and chlorophyll content in green bean. *Russ. J. Plant Physiol.* 55, 782–786. doi: 10.1134/s1021443708060071

Yousuf, P. Y., Hakeem, K. U. R., Chandna, R., and Ahmad, P. (2012). "Role of glutathione reductase in plant abiotic stress," in *Abiotic Stress Responses in Plants*, eds P. Ahmad and M. Prasad (New York, NY: Springer), 149–158. doi: 10.1007/978-1-4614-0634-1_8

Conflict of Interest Statement: The authors declare that the research was conducted in the absence of any commercial or financial relationships that could be construed as a potential conflict of interest.

frontiers in Nutrition

ORIGINAL RESEARCH
published: 04 September 2019
doi: 10.3389/fnut.2019.00134

Extra-Virgin Olive Oil Extracted Using Pulsed Electric Field Technology: Cultivar Impact on Oil Yield and Quality

Gianluca Veneziani[1], Sonia Esposto[1], Agnese Taticchi[1], Roberto Selvaggini[1], Beatrice Sordini[1], Antonietta Lorefice[1], Luigi Daidone[1], Mauro Pagano[2], Roberto Tomasone[2] and Maurizio Servili[1]*

[1] Department of Agricultural, Food and Environmental Sciences, University of Perugia, Perugia, Italy, [2] Council for Agricultural Research and Economics Research Centre for Engineering and Agro-Food Processing, Monterotondo, Italy

OPEN ACCESS

Edited by:
Wenceslao Moreda, Spanish National Research Council (CSIC), Spain

Reviewed by:
Alam Zeb, University of Malakand, Pakistan
Marco Iammarino, Istituto Zooprofilattico Sperimentale di Puglia e Basilicata (IZSPB), Italy
Enzo Perri, Council for Agricultural and Economics Research, Italy

***Correspondence:**
Gianluca Veneziani
gianluca.veneziani@unipg.it;
gianluca.veneziani@gmail.com

Specialty section:
This article was submitted to Food Chemistry, a section of the journal Frontiers in Nutrition

Received: *29 April 2019*
Accepted: *09 August 2019*
Published: *04 September 2019*

Citation:
Veneziani G, Esposto S, Taticchi A, Selvaggini R, Sordini B, Lorefice A, Daidone L, Pagano M, Tomasone R and Servili M (2019) Extra-Virgin Olive Oil Extracted Using Pulsed Electric Field Technology: Cultivar Impact on Oil Yield and Quality. Front. Nutr. 6:134. doi: 10.3389/fnut.2019.00134

The main operators of the olive oil sector are continuously involved in the development of the olive oil mechanical extraction process with the common aim of increasing both the quality and the oil extraction yield coupled with the potential enhancement of the working efficiency of the olive mill. The pulsed electric field (PEF) is a recently studied technological innovation for the improvement of olive oil extraction technology. The impact of the PEF on the diffusion of oil and microconstituents, determined by the disruption effects on olive cell tissues carried out by the non-thermal method, was evaluated. A PEF can increase the permeability and breaking of the cell membranes with a consequent positive result on oil extractability and quality, mainly related to the compounds involved in the health and sensory properties of extra virgin olive oil. The PEF was tested on three Italian olive cultivars (Carolea, Coratina, and Ottobratica). The results showed a positive impact of the new technology on the oil yield, with an increase ranging from 2.3 to 6%, and on the concentration of hydrophilic phenols, with an increase ranging from 3.2 to 14.3%, with respect to the control tests. The data of the main compounds related to the health and sensory notes also showed high variability as a consequence of the genetic origins of the olive cultivars.

Keywords: extraction process, pulsed electric field, cultivar, oil yield, phenols, quality

INTRODUCTION

The technological evolution of the olive oil mechanical extraction process in recent decades has been mainly based on the improvement of extra-virgin olive oil (EVOO) quality, which is strictly connected with compounds characterized by their health and sensory properties (phenolic and volatile compounds). The activities concerning the control of the main technological parameters (time, temperature, and oxygen) and the critical steps of the crushing and malaxation phases (1–4) benefitted from the introduction of heat exchangers that could easily and rapidly regulate the temperature of the crushed olive paste in relation to the climatic conditions of the harvesting period and the specific needs of the olive mill to achieve a better quality product (5–9).

In contrast, the recent technologies applied to the extraction system, such as microwaves, ultrasounds, and pulsed electric fields (PEFs), are mainly focused on increasing oil extractability

and improving plant working efficiency with little attention on their impacts on the legal, commercial, and quality parameters of EVOO (10–15). All of these recent technologies are based on the degradation of the olive fruit cells through thermal and non-thermal treatments that enable pore formation, membrane permeability alterations, water influx, swelling, and deflation with an overall consequence of rupturing the cell walls and membranes. Cell lysis results in an abundant release of micro- and macro-intracellular components into the water phase that leads to an increase in free olive droplets characterized by different qualitative and quantitative chemical compositions due to the destructive effects on the olive tissues altering the solubilization phenomena and improving the mass transfer rate (16–18). The use of PEFs for the improvement of the quality characteristics of different foods and beverages is mainly linked to the enhancement of quality attributes, such as color, texture, flavor, phenolic compounds, carotenoids, and vitamins, and bioactive compound extractability, and thus, PEFs have been investigated in recent years (19–25). The application of the PEF system to the virgin olive oil extraction process, and to the valorization opportunities of by-product (26, 27), is still very limited, and there are only a few preliminary studies concerning its effects on oil yield and quality. Both Abenoza et al. (10) and Puértolas and Martínez de Marañón (14) analyzed the impact of the new technology on the oil extractability and chemical and sensory parameters by processing Arbequina and Arroniz olives and carrying out PEF treatment on the olive pastes before and after the malaxation phase, respectively. The first author used a laboratory-scale extraction system equipped with a PEF system set up at an electric field strength of 1 and 2 kV cm^{-1} and a frequency of 125 Hz. The treatment of the crushed paste did not result in any significant increase in oil yield but was able to guarantee the same extractability at a reduced malaxation temperature with a consequent positive impact on the EVOO sensory notes. The other study (14) investigated the activity of PEF of 2 kV cm^{-1} applied to the olive paste at a frequency of 25 Hz before the horizontal centrifuge using an industrial oil extraction plant. The non-thermal treatment resulted in an increase in the oil extraction yield and an improvement in the VOO quality related to the enhancement of the polyphenol, phytosterol and tocopherol contents. However, both studies highlighted the need for further research to evaluate the influences of external factors, such as the cultivar, maturity index, temperature, and other process parameters, on the performance of PEF applied to the olive oil mechanical extraction system.

Based on the information from these recent studies, the cultivar impact on the yield and quality of EVOOs using a different PEF system, characterized by a different set up, was investigated. This study reports detailed data of the trials carried out for processing the olives belonging to different Italian cultivars with particular attention to the olive cell destruction process and the subsequent release of larger amounts of oil and the main components connected to the sensory and quality parameters of the olive oils, such as the contents of hydrophilic and lipophilic phenols and volatile compounds.

MATERIALS AND METHODS

EVOO Mechanical Extraction Process

Control and PEF treated EVOO samples were extracted from the olives of the Carolea, Ottobratica, and Coratina cultivars (**Figure 1**). The olive batches of the Carolea (fruit weight: medium-high, high; stone size: large; fruit-flesh/pit ratio: medium, medium-high; oil content: medium, medium-high; tree-harvest time: medium, medium-late) and Ottobratica (fruit weight: medium-low, low; stone size: small; oil content: medium; tree-harvest time: early) cultivars were harvested in October 2017 in the Calabria region, whereas the olives of Coratina (fruit weight: medium, medium-high; stone size: large; fruit-flesh/pit ratio: low; oil content: high; tree-harvest time: medium-late) belonging to the Apulia region were purchased in the area of Bari during the first week of November 2017 (28). All olives were harvested at a medium-low maturity index ranging from 0.8 to 1.5 (29). The control and PEF EVOO samples were obtained in triplicate using an industrial plant TEM 200 system (Toscana Enologica Mori, Tavarnelle Val di Pesa, Florence, Italy) consisting of a hammer mill, a malaxer with a gas controller system and a working capacity of 200 kg of olives and a two-phase decanter; additionally a vertical centrifuge [UVPX 305 AGT 14 (Alfa Laval S.p.A., Tavarnelle Val di Pesa, Florence, Italy)] was used to separate the olive oil from the residual water phase. Single trials of 180 kg of olives each were carried out using a heat exchanger to determine the rapid thermal conditioning of olive pastes at 25°C ± 0.5 after the crushing phase. The oil extraction system was equipped with an oliveCEPT Model 6.2 (Arcaroma Pure AB, Lund, Sweden), which is a PEF system based on closed environment PEF treatment (CEPT) technology and positioned after the malaxation phase. The PEF was set up at an electric field strength of 1.7 kV cm^{-1} and a specific energy of 17 kJ kg^{-1}.

EVOO Analyses

During the experimental study, the main quality parameters potentially influenced by the introduction of the technological innovation of the olive oil mechanical extraction process were evaluated without analyzing other characteristics of EVOO rarely modified by olive oil mechanical extraction process such as fatty acid composition, sterols, and waxes (10, 14, 15).

Chemicals

Phenolic alcohols such as hydroxytyrosol (3,4-DHPEA) and tyrosol (*p*-HPEA) were supplied by Cabru s.a.s. (Arcore, Milan, Italy) and Fluka (Milan, Italy), respectively. Lignans [(+)-1-acetoxypinoresinol and (+)-pinoresinol)] and the secoiridoid derivatives [dialdehydic forms of elenolic acid linked to 3,4-DHPEA and *p*-HPEA (3,4-DHPEA-EDA and *p*-HPEA-EDA), isomer of oleuropein aglycon (3,4-DHPEA-EA) and ligstroside aglycone] were obtained as quoted in the study of Veneziani et al. (8). The analytical standards of volatile compounds [pentanal, (*E*)-2-pentenal, hexanal, (*E*)-2-hexenal, (*E*, *E*)-2,4-hexadienal, 2,4-hexadienal (i), 1-pentanol, 1-penten-3-ol, (*E*)-2-penten-1-ol, (*Z*)-2-penten-1-ol, 1-hexanol, (*E*)-2-hexen-1-ol, (*Z*)-3-hexen-1-ol, (*E*)-3-hexen-1-ol, hexyl acetate], α-tocopherol and all the

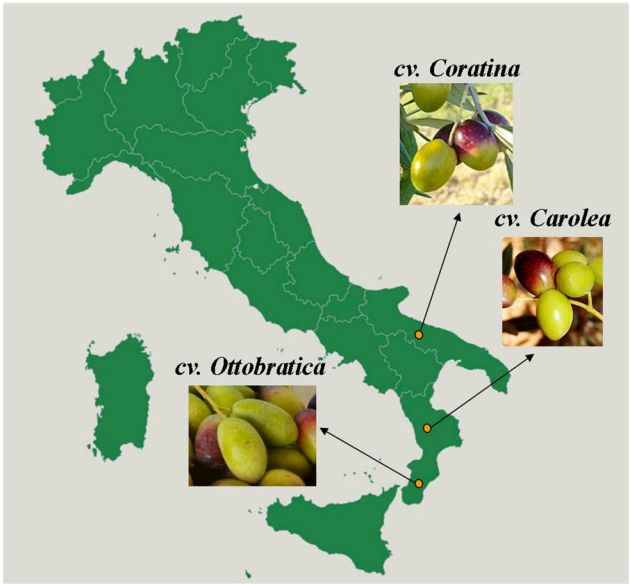

FIGURE 1 | Geographical origin of three different Italian olive cultivars.

reagents used in the analysis were purchased from Merck (Merck KGaA, Darmstadt, Germany).

Legal Quality Parameters

The main legal quality parameters (free acidity, peroxide value, and the UV absorption characteristics) of the EVOOs were determined by the European Official Methods (30).

Moisture Content of Pomace

The moisture contents of the control and PEF EVOOs were evaluated following the method described by International Organization for Standardization (45). Five grams of each oil sample was weighed in an aluminum capsule and placed in a BINDER oven (BINDER GmbH, Tuttlingen, Germany) at 105°C for ∼5 h until a constant weight was obtained.

Oil Content of Pomace

A Soxhlet extractor was utilized to analyze the pomace oil content; 10 g of dried sample and 5 g of pumice stone were loaded into a thimble made from thick filter paper and placed in the main compartment of the Soxhlet extractor. The process was carried out for 6 h using hexane as the extraction solvent. The solvent was removed by means of a rotary evaporator [Rotavapor R-210 (BUCHI Italia s.r.l, Cornaredo, Italy)], and the residual oil content was detected afterwards (31).

Phenolic Compounds

The phenolic fraction was recovered by a liquid-liquid extraction method mixing 20 g of EVOOs with 10 mL of methanol/water solution (80/20 v/v) using Ultra-Turrax T 25 homogenizer (IKA Labortechnik, Staufen, Germany) at 17,000 rpm for 2 min. The mixture was centrifuged at 935 × g for 10 min at room temperature (Andreas Hettich GmbH & Co.KG, Tuttlingen, Germany) than the supernatant was recovered (32). The extraction was repeated twice. The quantitative and qualitative phenolic concentrations of the EVOOs were determined by high-performance liquid chromatography (HPLC) using an Agilent Technologies model 1100 controlled by ChemStation (Agilent Technologies, Palo Alto, CA, USA). A C18 column, Spherisorb ODS-1 (250 × 4.6 mm), with a particle size of 5 μm (Phase Separation Ltd., Deeside, UK) was used. The mobile phase was composed of 0.2% acetic acid (pH 3.1) in water (solvent A) with methanol (solvent B). The gradient was changed as follows: 95% A/5% B for 2 min, 75% A/25% B in 8 min, 60% A/40% B in 10 min, 50% A/50% B in 16 min, 0% A/100% B in 14 min. This composition was maintained for 10 min and was then returned to the initial conditions and equilibration in 13 min. The final running time was 73 min with a flow rate of 1 mL min^{-1} (**Figure 2**). The phenolic compounds were identified and quantified according to the procedure reported by Selvaggini et al. (33).

Volatile Compounds

The headspace, solid-phase microextraction followed by gas chromatography mass spectrometry (HS-SPME/GC-MS) technique was used to detect and quantify the volatile compounds in the control and PEF EVOOs of the Carolea, Ottobratica, and Coratina cultivars.

The SPME was carried out holding the vials, with 3 g of EVOO and 50 μL of a standard methanolic solution, at 35°C and then the SPME fiber (a 50/30 μm 1 cm long DVB/Carboxen/PDMS, Stableflex; Supelco, Inc., Bellefonte, PA, USA) was exposed to the vapor phase for 30 min to detect the volatile compounds.

The GC-MS analysis were conducted using a Varian 4000 GC-MS equipped with a 1079 split/splitless injector (Varian). The fused-silica capillary column (DB-Wax-ETR, 50 m, 0.32 mm i.d., 1 μm film thickness; J&W Scientific, Folsom, CA, USA) was operated with helium regulated by an electronic flow controller (EFC) at a constant flow rate (1.7 ml min^{-1}). All the operative conditions was set following the method described by Veneziani et al. (7) without any modifications. The data of the peak areas were evaluated on the basis of calibration curve of each different compound and expressed in μg kg^{-1} of EVVO (**Figure 3**).

α-Tocopherol

The α-Tocopherol EVOOs were evaluated by HPLC–DAD–FLD analysis: 1 g of oil was dissolved in 10 mL of n-hexane, filtered with a 5-μm polyvinylidene difluoride (PVDF) syringe filter (Whatman, Clifton, NJ) and injected into the HPLC system. The HPLC analysis was conducted using the Agilent Technologies Model 1100, and the α-Tocopherol was detected at an excitation wavelength of 294 nm and at an emission wavelength of 300 nm as described by Esposto et al. (34).

Oxidative Stability

The oxidative stability of the control and PEF EVOO of Coratina was assessed using a Rancimat (Methrom Ltd., Herisau, Switzerland) as described by Baldioli et al.

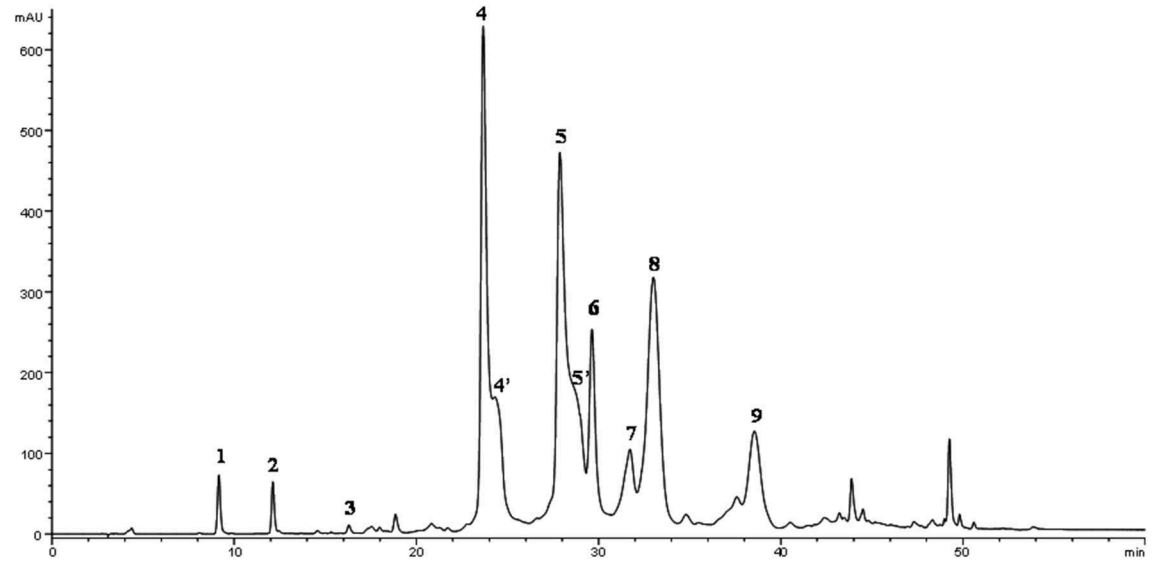

FIGURE 2 | HPLC chromatogram of EVOO methanolic extract of cv. Peranzana recorded with DAD at 278 nm. Peak numbers: 1, 3,4-DHPEA; 2, p-HPEA; 3, vanillic acid; 4, 3,4-DHPEA-EDA; 5, p-HPEA-EDA; 6, (+)-1-acetoxypinoresinol; 7, (+)-pinoresinol; 8, 3,4-DHPEA-EA; 9, ligustroside aglycone [4′ and 5′ structures identified by Rovellini et al. (44)].

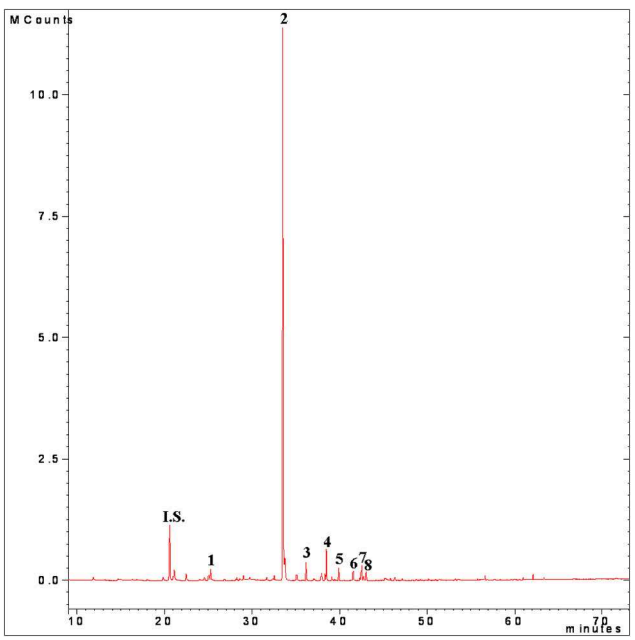

FIGURE 3 | HS-SPME-GC-MS volatile fraction total ion current chromatogram of virgin olive oil cv. Peranzana. Peak numbers: I.S., internal standard (Isobutyl acetate); 1, hexanal; 2, (*E*)-2-hexenal; 3, hexyl acetate; 4, (*Z*)-3-hexenyl acetate; 5, 1-hexanol, 6, (*Z*)-3-hexen-1-ol; 7, (*E*)-2-hexen-1-ol; 8, (*E*, *E*)-2,4-hexadienal.

(35). The oils were treated with a flow of purified air (20 L h^{-1}) at 120°C for 24 h. The oxidative stability was detected as the oxidation induction time (OIT), expressed in hours.

RESULTS AND DISCUSSION

A PEF system was applied to the olive oil mechanical extraction process to evaluate its technological performance on the oil extractability and its impact on the main quality parameters of EVOO. Compared to the others previous studies on the effect of PEF applied to the oil mechanical extraction process, the trials were carried out by processing three different Italian olive cultivars to better understand the effects of the technology in relation to the different genetic origins of the three olive varieties. As reported by Bartolini et al. (28), Carolea, Ottobratica, and Coratina are characterized by different geographical, morphological and agronomical characters that could influence the performance of PEF system in the improvement of oil yield and EVOO quality, mainly related to phenolic and volatile compounds.

The EVOOs obtained from the PEF-assisted extraction showed an increase in the oil yield for all of the processed cultivars, indicating the efficient degradation of the olive tissues to guarantee an improvement in the oil extractability of the mechanical extraction plant. The release of a large amount of oil in the free water phase of the olive paste enhanced the total oil extracted at the end of the mechanical separation process with a variability that is a function of the different genetic origins of the olives (**Table 1**), with enhancement values ranging from 2.3 to 6.0%. The data were also confirmed by the analysis of oil content of pomaces that showed a lower values in the PEF samples compared to the control tests (**Table 1**). The above statement is in accordance with the results presented in a previous work (36), which showed that the impacts of different settings of PEF on oil extraction yields were also influenced by the cultivar and the dimension of the olive fruits. The PEF trials highlighted a putative, cultivar-dependent effect that was probably due to the

TABLE 1 | EVOOs extraction yield, moisture and oil contents of pomaces obtained from olives Control and treated using PEF of three different cultivar[a].

	cv. Carolea		cv. Ottobratica		cv. Coratina	
	Control	**PEF**	**Control**	**PEF**	**Control**	**PEF**
Extraction yield (%)	15.0 ± 0.3	15.9 ± 0.3	12.8 ± 0.2	13.1 ± 0.1	15.8 ± 0.4	16.6 ± 0.1
Moisture content (%)	66.8 ± 0.5	66.9 ± 0.1	59.1 ± 0.1	59.0 ± 0.2	58.7 ± 0.01	58.8 ± 0.1
Oil content (%)	7.02 ± 0.1	5.95 ± 0.2	6.01 ± 0.1	5.89 ± 0.04	5.72 ± 0.0	5.44 ± 0.1

[a] *The data are the mean values of four independent experiments analyzed in duplicate, ± standard deviation.*

TABLE 2 | Legal quality parameters of Control and PEF EVOOs of three Italian cultivar.

	Acidity (g of oleic acid 100 g of oil^{-1})	**Peroxide value (meq of O_2 kg of oil^{-1})**	**K_{232}**	**K_{270}**	**ΔK**
cv. Carolea[a]					
Control	0.27 ± 0.01	5.6 ± 0.1	1.668 ± 0.003	0.106 ± 0.001	−0.002 ± 0.0002
PEF	0.26 ± 0.002	6.0 ± 0.4	1.691 ± 0.01	0.111 ± 0.002	−0.002 ± 0.0001
cv. Ottobratica					
Control	0.28 ± 0.01	6.0 ± 0.1	1.701 ± 0.004	0.166 ± 0.005	−0.002 ± 0.0001
PEF	0.30 ± 0.01	6.2 ± 0.2	1.747 ± 0.02	0.153 ± 0.004	−0.003 ± 0.0003
cv. Coratina					
Control	0.27 ± 0.02	3.0 ± 0.07	1.817 ± 0.01	0.187 ± 0.02	−0.004 ± 0.0002
PEF	0.28 ± 0.01	3.1 ± 0.1	1.828 ± 0.02	0.185 ± 0.002	−0.005 ± 0.0001

[a] *The data are the mean values of four independent experiments analyzed in duplicate, ± standard deviation.*

different fruit-flesh/pit ratios and the moisture and oil contents of the olives, which were able to modify the power and activity levels of the electric field on the fruit cells, reducing or increasing the degradation process. Olive paste is a very complex matrix composed of different ratios of water, wood, pulp, and oil that is primarily related to the cultivar and secondarily to agronomic factors, such as the growing area, irrigation, climatic season, ripening stage, and soil management (7, 37, 38). The different elements that form the olive fruit can interfere with and influence the homogeneous diffusion of the electric field into the olive paste, altering the effects of treatment.

The PEF treatment did not significantly alter the free acidity, peroxide value, or UV spectrophotometric indices of the EVOOs of any of the cultivars compared to the respective control test (**Table 2**).

The evaluation of hydrophilic phenols in the experimental trials showed an increase in phenolic compounds in all of the EVOOs extracted from different cultivars compared to the control test, which was confirmed by Puértolas and Martínez de Marañón (14). The overall positive effect of the PEF system on the phenolic fraction of the EVOOs led to the conclusion that the non-thermal treatment applied to the malaxed olive paste improves the release of phenols and solubilization into the oily phase. **Figure 4** shows the percentage increases in the phenolic fractions of the PEF-EVOOs expressed as total phenols, oleuropein derivatives (sum of 3,4-DHPEA, 3,4-DHPEA-EDA, and 3,4-DHPEA-EA), ligstroside derivatives (*p*-HPEA, *p*-HPEA-EDA, and ligstroside aglycone) and lignans (sum of (+)-1-acetoxypinoresinol and (+)-pinoresinol). The phenolic enhancement was qualitatively due to the amount of 3,4-DHPEA-EDA and 3,4-DHPEA-EA, which are the main phenolic compounds influenced by technological processes, whereas ligstroside derivatives and lignans seemed more stable than the other molecules (4, 5, 9, 10, 39). The significant increases of total phenol, 14.3, 7.05, and 3.2% for Carolea, Ottobratica, and Coratina, respectively, showed a high variability, probably due to the different genetic origins of the olive cultivars, even if the lowest enhancement, which was detected during the extraction of the Coratina EVOOs, could be the result of saturation phenomena in the oil as a consequence of the high amount of phenols detected (∼1.5 g kg^{-1}), which is probably very close to the limit value of the product.

In contrast, the content of α-tocopherol was not influenced by the PEF treatment and did not show any significant differences in concentration in any of the cultivars. The concentration of lipophilic phenols was 204.2 and 203.3 mg kg^{-1} (cv. Carolea), 313.5 and 314.7 mg kg^{-1} (cv. Ottobratica), 261.3 and 266.3 mg kg^{-1} (cv. Coratina) for control, and PEF EVOOs, respectively.

The same trend was detected for the volatile fractions of the EVOOs treated using PEF technology that did not modify the concentration of the main aldehydes, alcohols, and esters involved in the flavor of the olive oils (**Figure 5**). The PEF system was performed in the oil extraction phase, during which the largest amount of volatile compounds were already produced and probably did not have time to interfere with the activity of the enzymes of the lipoxygenase pathway. In addition, the non-thermal treatment did not negatively alter the concentrations of the developed volatile compounds in the EVOOs, as reported by other authors in several food products (40–43).

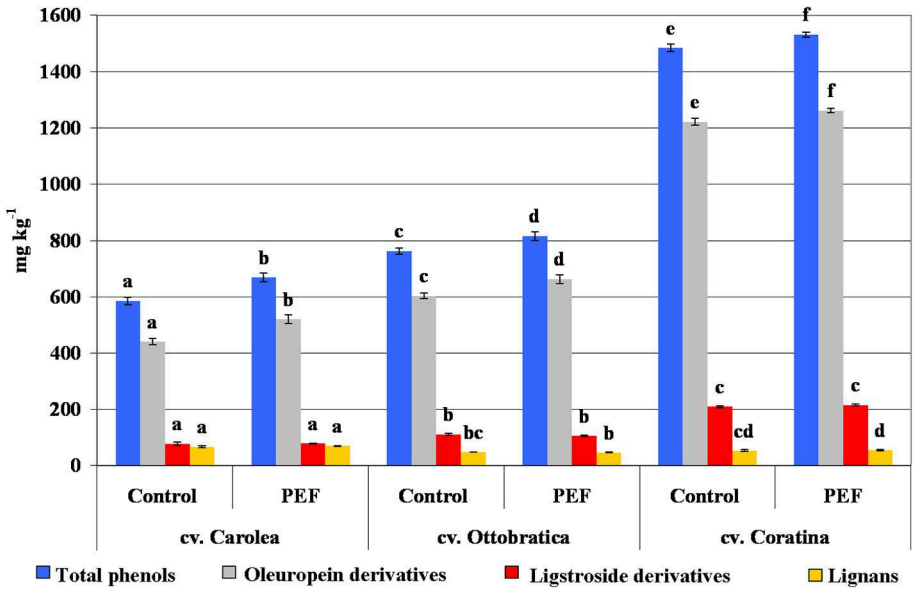

FIGURE 4 | Phenolic composition (mg kg^{-1}) of the PEF and control EVOOs of the three different Italian olive cultivars. Phenolic content was expressed as total phenols, oleuropein derivatives (sum of 3,4-DHPEA, 3,4-DHPEA-EDA, and 3,4-DHPEA-EA), ligstroside derivatives (*p*-HPEA, *p*-HPEA-EDA and ligstroside aglycone) and lignans [sum of (+)-1-acetoxypinoresinol and (+)-pinoresinol]. The data are the mean values of three independent extractions analyzed in duplicate, ± standard deviation. The values of each phenolic group with different letters (a–f) are significantly different from one another ($p < 0.05$).

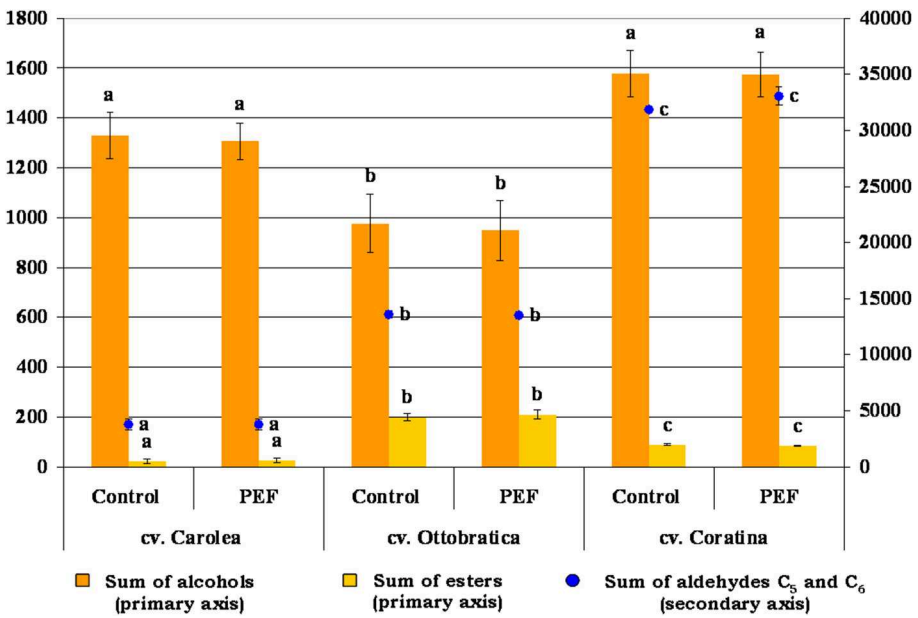

FIGURE 5 | Volatile composition (μg kg^{-1}) of the PEF and control EVOOs of the three different Italian olive cultivars responsible for oil flavor. Volatile content was expressed as alcohols [sum of 1-pentanol, 1-penten-3-ol, (*E*)-2-penten-1-ol, (*Z*)-2-penten-1-ol, 1-hexanol, (*E*)-2-hexen-1-ol, (*Z*)-3-hexen-1-ol, and (*E*)-3-hexen-1-ol], esters [sum of hexyl acetate and (*Z*)-3-hexenyl acetate] and C_5 and C_6 saturated and unsaturated aldehydes [sum of pentanal, (*E*)-2-pentenal, hexanal, (*E*)-2-hexenal, (*E,E*)-2,4-hexadienal and 2,4-hexadienal (i)]. The data are the mean values of three independent extractions analyzed in duplicate, ± standard deviation. The values of each volatile compound group with different letters (a–c) are significantly different from one another ($p < 0.05$).

The electrodes that generated the pulsed electric field (PEF) could release traces of metals, such as iron and cupper, characterized by pro-oxidant activities into the product, which could possibly negatively impact the oxidative stability of the food matrices. No data were found in the literature about this possible effect of PEF treatment of olive paste and its

potential consequences on the EVOO quality. For that reason, the oxidative stability, analyzed by the Rancimat test, was also detected in the EVOOs extracted from the Coratina olives to evaluate the differences in the oxidation induction time (OIT). The data showed a longer OIT of the EVOO from the PEF sample (21.1 h) compared to the control (20.3 h), highlighting the absence of possible metals issued by the electrodes in the PEF oil, which should increase the rate of oil oxidation. The higher OIT for the PEF sample was due to the major concentration of antioxidant compounds (**Figure 4**).

CONCLUSION

The impact of the PEF technology applied to the olive oil mechanical extraction process showed a significant effect on the EVOO yield for the tests conducted on Carolea, Ottobratica, and Coratina olives. The percent increase in the oil yield (ranging from 2.3 to 6%) should be cultivar dependent, probably in relation to the different ratios of the constituent parts of the fruits, which is mainly influenced by the genetic origins of the olive drupes and by the ripening stage. As also supposed in a previous study (14), the different fruit-flesh/pit ratios and the moisture and oil contents influenced PEF extraction performance. The PEF also showed a positive impact on the quality of the EVOO characterized by an enhancement of the phenolic compounds responsible for health-promoting benefits, with an increase ranging from 3.2 to 14.3% that is a function of the different olive cultivars and their maturity index.

The alteration of the olive tissue structure induced by the PEF treatment and the subsequent release of intracellular matrices into the water phase did not affect the legal quality parameters or the oxidative stability of the product as a consequence of the possible release of pro-oxidant metals from the PEF chamber. The concentrations of α-tocopherol and the main classes of volatile compounds responsible for the EVOO flavor were not significantly modified compared to the control test. The new technology improved the oil extractability and the antioxidant contents of the EVOO without altering the main qualitative and organoleptic characteristics of the product.

DATA AVAILABILITY

The raw data supporting the conclusions of this manuscript will be made available by the authors, without undue reservation, to any qualified researcher.

AUTHOR CONTRIBUTIONS

GV: extraction process, data processing, and conclusion. SE and AT: data processing. RS and BS: chemical analysys. AL and LD: sampling and chemical analysys. MP and RT: engineering technical support. MS: research plan and supervision.

ACKNOWLEDGMENTS

The authors wish to thank Arcaroma Pure AB (Lund, Sweden) for financial support and technical assistance.

REFERENCES

1. Inarejos-Garcia AM, Fregapane G, Desamparados Salvador M. Effect of crushing on olive paste and virgin olive oil minor components. *Eur Food Res and Technol.* (2011) 232:441–51. doi: 10.1007/s00217-010-1406-4
2. Jimenez B, Sanchez-Ortiz A, Rivas A. Influence of the malaxation time and olive ripening stage on oil quality and phenolic compounds of virgin olive oils. *Int J Food Sci and Tech.* (2014) 49:2521–7. doi: 10.1111/ijfs.12592
3. Polari JJ, Garci-Aguirre D, Olmo-Garcia L, Carrasco-Pancorbo A, Wang SC. Interactions between hammer mill crushing variables and malaxation time during continuous olive oil extraction. *Eur J Lipid Sci Technol.* (2018) 120:1800097. doi: 10.1002/ejlt.201800097
4. Selvaggini R, Esposto S, Taticchi A, Urbani S, Veneziani G, Di Maio I, et al. Optimization of the temperature and oxygen concentration conditions in the malaxation during the oil mechanical extraction process of four Italian olive cultivars. *J Agric Food Chem.* (2014) 62:3813–22. doi: 10.1021/jf405753c
5. Esposto S, Veneziani G, Taticchi A, Selvaggini R, Urbani S, Di Maio I, et al. Flash thermal conditioning of olive pastes during the olive oil mechanical extraction process: impact on the structural modifications of pastes and oil quality. *J Agric Food Chem.* (2013) 61:4953–60. doi: 10.1021/jf400037v
6. Leone A, Esposto S, Tamborrino A, Romaniello R, Taticchi A, Urbani S, et al. Using a tubular heat exchanger to improve the conditioning process of the olive paste: evaluation of yield and olive oil quality. *Eur J Lipid Sci Technol.* (2016) 118:308–17. doi: 10.1002/ejlt.201400616
7. Veneziani G, Esposto S, Taticchi A, Selvaggini R, Urbani S, Di Maio I, et al. Flash thermal conditioning of olive pastes during the oil mechanical extraction process: cultivar impact on the phenolic and volatile composition of virgin olive oil. *J Agric Food Chem.* (2015) 63:6066–74. doi: 10.1021/acs.jafc.5b01666
8. Veneziani G, Esposto S, Taticchi A, Urbani S, Selvaggini R, Di Maio I, et al. Cooling treatment of olive paste during the oil processing: impact on the yield and extra virgin olive oil quality. *Food Chem.* (2017) 221:107–13. doi: 10.1016/j.foodchem.2016.10.067
9. Veneziani G, Esposto S, Taticchi A, Urbani S, Selvaggini R, Sordini B, et al. Characterization of phenolic and volatile composition of extra virgin olive oil extracted from six Italian cultivars using a cooling treatment of olive paste. *LWT Food Sci Technol.* (2018) 87:523–8. doi: 10.1016/j.lwt.2017.09.034
10. Abenoza M, Benito M, Saldana G, Alvarez I, Raso J, Sanchez-Gimeno AC. Effects of pulsed electric field on yield extraction and quality of olive oil. *Food Bioprocess Technol.* (2013) 6:1367–73. doi: 10.1007/s11947-012-0817-6
11. Bejaoui MA, Sanchez-Ortiz A, Aguilera MP, Ruiz-Moreno MJ, Sanchez S, Jimenez A, et al. High power ultrasound frequency for olive paste conditioning: effect on the virgin olive oil bioactive compounds and sensorial characteristics. *Innov Food Sci Emerg Technol.* (2018) 47:136–145. doi: 10.1016/j.ifset.2018.02.002
12. Clodoveo ML, Durante V, La Notte D, Punzi R, Gambacorta G. Ultrasound-assisted extraction of virgin olive oil to improve the process efficiency. *Eur J Lipid Sci Technol.* (2013) 115:1062–9. doi: 10.1002/ejlt.201200426
13. Leone A, Romaniello R, Tamborrino A, Xu X-Q, Juliano P. Microwave and megasonics combined technology for a continuous olive oil process with enhanced extractability. *Innov. Food Sci Emerg Technol.* (2017) 42:56–63. doi: 10.1016/j.ifset.2017.06.001
14. Puértolas E, Martínez de Marañón I. Olive oil pilot-production assisted by pulsed electric field: impact on extraction yield, chemical parameters and sensory properties. *Food Chem.* (2015) 167:497–502. doi: 10.1016/j.foodchem.2014.07.029
15. Taticchi A, Selvaggini R, Esposto S, Sordini B, Veneziani G, Servili M. Physicochemical characterization of virgin olive oil obtained using an ultrasound-assisted extraction at an industrial scale: influence of olive maturity index and malaxation time. *Food Chem.* (2019) 289:7–15. doi: 10.1016/j.foodchem.2019.03.041

16. Gabrić D, Barba F, Roohinejad S, Mohammad S, Gharibzahedi T, Radojčin M, et al. Pulsed electric fields as an alternative to thermal processing for preservation of nutritive and physicochemical properties of beverages: a review. *J Food Process Eng.* (2018) 41:e12638. doi: 10.1111/jfpe.12638
17. Kumari B, Tiwari BK, Hossain MB, Brunton NP, Rai DK. Recent advances on application of ultrasound and pulsed electric field technologies in the extraction of bioactives from agro-industrial by-products. *Food Bioprocess Technol.* (2018) 11:223–41. doi: 10.1007/s11947-017-1961-9
18. Puértolas E, Luengo E, Álvarez I, Raso J. Improving mass transfer to soften tissues by pulsed electric fields: fundamentals and applications. *Annu Rev Food Sci Technol.* (2012) 3:263–82. doi: 10.1146/annurev-food-022811-101208
19. Arroyo C, Lascorz D, O'Dowd L, Noci F, Arimi J, Lyng JG. Effect of pulsed electric field treatments at various stages during conditioning on quality attributes of beef longissimus thoracis et lumborum muscle. *Meat Sci.* (2015) 99:52–9. doi: 10.1016/j.meatsci.2014.08.004
20. González-Casado S, Martín-Belloso O, Elez-Martínez P, Soliva-Fortuny R. Enhancing the carotenoid content of tomato fruit with pulsed electric field treatments: effects on respiratory activity and quality attributes. *Postharvest Biol Tec.* (2018) 137:113–8. doi: 10.1016/j.postharvbio.2017.11.017
21. Ignat A, Manzocco L, Brunton NP, Nicoli MC, Lyng JG. The effect of pulsed electric field pre-treatments prior to deep-fat frying on quality aspects of potato fries. *Innov Food Sci Emerg Technol.* (2015) 29:65–9. doi: 10.1016/j.ifset.2014.07.003
22. Ricci A, Parpinello GP, Versari A. Recent advances and applications of Pulsed Electric Fields (PEF) to improve polyphenol extraction and color release during red winemaking. *Beverages.* (2018) 4:18. doi: 10.3390/beverages4010018
23. Turk MF, Vorobiev E, Baron A. Improving apple juice expression and quality by pulsed electric field on an industrial scale. *LWT Food Sci Technol.* (2012) 49:245–50. doi: 10.1016/j.lwt.2012.07.024
24. Yilmaz M, Evrendilek GA. Impact of the pulsed electric field treatment on bioactive food compounds: bioaccessibility and bioavailability. *J Nutr Food Sci.* (2017) 7:3. doi: 10.4172/2155-9600.1000605
25. Zeng X, Zhong H, Zi Z. Effects of pulsed electric field treatments on quality of peanut oil. *Food Control.* (2010) 21:611–4. doi: 10.1016/j.foodcont.2009.09.004
26. Roselló-Soto E, Koubaa M, Moubarik A, Lopes RP, Saraiva JA, Boussetta N, et al. Emerging opportunities for the effective valorization of wastes and by-products generated during olive oil production process: nonconventional methods for the recovery of high-added value compounds. *Trends Food Sci Technol.* (2015) 45:296–310. doi: 10.1016/j.tifs.2015.07.003
27. Roselló-Soto E, Barba FJ, Parniakov O, Galanakis CM, Lebovka N, Grimi N, et al. High voltage electrical discharges, pulsed electric field, and ultrasound assisted extraction of protein and phenolic compounds from olive kernel. *Food Bioprocess Technol.* (2015) 8:885–94. doi: 10.1007/s11947-014-1456-x
28. Bartolini G, Cerretti S, Petruccelli R, Stefani F, Briccoli BC, Zelasco S, et al. *Data From: Olive Germplasm (Olea europaea L.) - Cultivars, Synonyms, Cultivation Area, Collections, Descriptors*. National Research Council ITALY – IVALSA (2008).
29. Beltran G, Uceda M, Jimenez A, Aguilera MP. Olive oil extractability index as a parameter for olive cultivar characterisation. *J Sci Food Agric.* (2003) 83:503–6. doi: 10.1002/jsfa.1369
30. European Commission. *Regulation 1989/03 Amending Regulation (EEC) No 2568/91 on the Characteristics of Olive Oil and Olive-Pomace Oil and on the Relevant Methods of Analysis Modifies the CEE n. 2568/91 on Olive Oils and Pomace Olive Oils Characteristics and Relative Analysis Method*s. Official Journal L. 295/57 13/11/2003 (2003).
31. AOAC. *Official Methods of Analysis Lipids, Fats and Oils Analysis Total Fat Animal Feed, 17th Edn*. AOAC (2006).
32. Antonini E, Farina A, Leone A, Mazzara E, Urbani S, Selvaggini R, et al. Phenolic compounds and quality parameters of family farming versus protected designation of origin (PDO) extra-virgin olive oils. *J Food Compos Anal.* (2015) 43:75–81. doi: 10.1016/j.jfca.2015.04.015
33. Selvaggini R, Servili M, Urbani S, Esposto S, Taticchi A, Montedoro GF. Evaluation of phenolic compounds in virgin olive oil by direct injection in high-performance liquid chromatography with fluorometric detection. *J Agric Food Chem.* (2006) 54:2832–8. doi: 10.1021/jf0527596
34. Esposto S, Taticchi A, Di Maio I, Urbani S, Veneziani G, Selvaggini R, et al. Effect of an olive phenolic extract on the quality of vegetable oils during frying. *Food Chem.* (2015) 176:184–92. doi: 10.1016/j.foodchem.2014.12.036
35. Baldioli M, Servili M, Perretti G, Montedoro GF. Antioxidant activity of tocopherols and phenolic compounds of virgin olive oil. *J Am Oil Chem Soc.* (1996) 73:1589–93. doi: 10.1007/BF02523530
36. Andreou V, Dimopoulos G, Alexandrakis Z, Katsaros G, Oikonomoub D, Toepfl S, et al. Shelf-life evaluation of virgin olive oil extracted from olives subjected to non thermal pretreatments for yield increase. *Innov Food Sci Emerg Technol.* (2017) 40:52–57. doi: 10.1016/j.ifset.2016.09.009
37. Fuentesa E, Paucar F, Tapia F, Ortiz J, Jimenez P, Romero N. Effect of the composition of extra virgin olive oils on the differentiation and antioxidant capacities of twelve monovarietals. *Food Chem.* (2018) 243:285–94. doi: 10.1016/j.foodchem.2017.09.130
38. Gucci R, Caruso G, Gennai C, Esposto S, Urbani S, Servili M. Fruit growth, yield and oil quality changes induced by deficit irrigation at different stages of olive fruit development. *Agric. Water Manag.* (2019) 212:88–98. doi: 10.1016/j.agwat.2018.08.022
39. Leone A, Romaniello R, Tamborrino A, Urbani S, Servili M, Amarillo M, et al. Application of microwaves and megasound to olive paste in an industrial olive oil extraction plant: impact on virgin olive oil quality and composition. *Eur J Lipid Sci Technol.* (2018) 120:1700261. doi: 10.1002/ejlt.201700261
40. Garde-Cerdán T, González-Arenzana L, López N, López R, Santamaría P, López-Alfaro I. Effect of different pulsed electric field treatments on the volatile composition of Graciano, Tempranillo and Grenache grape varieties. *Innov Food Sci Emerg Technol.* (2013) 20:91–9. doi: 10.1016/j.ifset.2013.08.008
41. Gualberto Sotelo KA, Hamid N, Oey I, Gutierrez-Maddox N, Ma Q, Leong SY. Effect of pulsed electric fields on the flavour profile of red-fleshed sweet cherries (*Prunus avium* var. Stella). *Molecules.* (2015) 20:5223–38. doi: 10.3390/molecules20035223
42. Sampedro F, Geveke DJ, Fan X, Zhang HQ. Effect of PEF, HHP and thermal treatment on PME inactivation and volatile compounds concentration of an orange juice–milk based beverage. *Innov Food Sci Emerg Technol.* (2009) 10:463–9. doi: 10.1016/j.ifset.2009.05.006
43. Zhang S, Yang R, Zhao W, Hua X, Zhang W, Zhang Z. Influence of pulsed electric field treatments on the volatile compounds of milk in comparison with pasteurized processing. *J Food Sci.* (2011) 76:127–32. doi: 10.1111/j.1750-3841.2010.01916.x
44. Rovellini P, Cortesi N, Fedeli E. Analysis of flavonoids from Olea Europaea by HPLC-UV and HPLC-electrospray-MS. *Riv Ital Sostanze Gr.* (1997) 74:273–9.
45. International Organization for Standardization. *ISO 662 (1998). Animal and Vegetable Fats and Oils. Determination of Moisture and Volatile Matter Content*. International Organization for Standardization (1998).

Conflict of Interest Statement: The authors declare that the research was conducted in the absence of any commercial or financial relationships that could be construed as a potential conflict of interest.

frontiers in Sustainable Food Systems

ORIGINAL RESEARCH
published: 06 September 2019
doi: 10.3389/fsufs.2019.00064

Dittrichia viscosa (Asterales: Asteraceae) as an Arthropod Reservoir in Olive Groves

Rafael Alcalá Herrera[1]*, *Juan Castro-Rodríguez*[2], *María Luisa Fernández-Sierra*[1] and *Mercedes Campos*[1]

[1] Plant Protection Group, Department of Environmental Protection, Estación Experimental del Zaidín (EEZ-CSIC), Granada, Spain, [2] IFAPA Centro Camino del Purchil de Granada, Granada, Spain

Non-crop cultivated plants can provide agriculture with ecosystem services, such as biological pest control and, a sound knowledge of the relationships between these plants and arthropod communities is important. Given its entomophilous characteristics, *Dittrichia viscosa*, a plant commonly found in the Mediterranean region, could potentially be used in integrated pest management systems. The aim of this study is to investigate arthropofauna associated with *D. viscosa* in olive groves during its pre-flowering, flowering and post-flowering stages and to determine the possible relationships between different groups of arthropods. Using vacuum-sampling, the study was carried out on *D. viscosa* plants bordering and inside olive groves. The plants produced new leaves in April and flowered between August and October. Miridae, Aphididae, Hymenoptera parasitoids, Formicidae, Araneae, and Aleyrodidae were the most abundant groups of arthropods collected during the pre-flowering and flowering stages. Plant phenology differentially influenced the arthropod populations of the different groups, with the Aleyrodidae family found to be more abundant during the pre-flowering stage, while Hymenoptera parasitoids were more numerous during the flowering stage. During the post-flowering stage, the number of arthropods captured was very low. Numerous correlations between and within the different functional groups were observed throughout the life cycle of *D. viscosa*. Our results clearly show that *D. viscosa* plants in olive groves have great potential as a reservoir of different predators and Hymenoptera parasitoids and that these olive groves were not attacked by any *D. viscosa*-related phytophages.

Keywords: ecological infrastructure, *Olea europaea*, Hymenoptera parasitoids, Miridae, Araneae, Formicidae, Aleyrodidae

OPEN ACCESS

Edited by:
José Manuel Martínez-Rivas, Instituto de la Grasa (IG), Spain

Reviewed by:
Agnieszka Barbara Najda, University of Life Sciences of Lublin, Poland
Mark Paul Running, University of Louisville, United States

***Correspondence:**
Rafael Alcalá Herrera
rafa.alcala@eez.csic.es

Specialty section:
This article was submitted to Crop Biology and Sustainability, a section of the journal Frontiers in Sustainable Food Systems

Received: *07 May 2019*
Accepted: *29 July 2019*
Published: *06 September 2019*

Citation:
Alcalá Herrera R, Castro-Rodríguez J, Fernández-Sierra ML and Campos M (2019) Dittrichia viscosa (Asterales: Asteraceae) as an Arthropod Reservoir in Olive Groves. Front. Sustain. Food Syst. 3:64. doi: 10.3389/fsufs.2019.00064

INTRODUCTION

The intensification of agriculture has led to a simplification of the landscape and a reduction in biodiversity, which have affected various ecosystem services, such as natural pest control and pollination (Zhang et al., 2007). The agroecological strategy of habitat management could help to reverse this situation by enhancing conservation biological control, as the presence of semi-natural habitats increases landscape diversity and supplies resources (pollen, nectar, alternative hosts, refuge, and oviposition sites) to natural enemies and pollinators which provide these ecosystem services (Landis et al., 2000; Bianchi et al., 2006; Holland et al., 2016, 2017). However, as the effect of landscape and vegetation on arthropod populations (pests and natural enemies) is based on

complex mechanisms, the conditions that contribute to increasing and reducing biological control need to be investigated. It is also crucial to determine how key plant species are managed (Simon et al., 2010; Carrié et al., 2012; Chaplin-Kramer et al., 2013; Miñarro and Prida, 2013). To do this, it is necessary to explore the relationships between available resources in each type of habitat and its associated arthropod community, the spatial-temporal distribution of resources in the landscape and interactions with other factors that play a role in pest regulation (Holland et al., 2016).

Dittrichia viscosa (L.) Greuter (Asterales: Asteraceae) is a plant of considerable interest, given its distribution throughout the Mediterranean region, its adaptation to a wide range of stress conditions, and its various uses including phytoremediation, as well as its role as a bioaccumulator and bioindicator (Parolin et al., 2014). In addition, given its entomophilous character, it has great potential for use in the integrated pest management of Mediterranean agroecosystems (Parolin et al., 2014). Indeed, *D. viscosa* has been proven to play an outstanding role in maintaining and expanding predatory mirid populations in different agroecosystems (Alomar et al., 2002; Perdikis et al., 2007; Lambion, 2011; Lykouressis et al., 2012) and as a reservoir of aphid parasitoids (Kavallieratos et al., 2002) and phytoseiid mites (Tixier et al., 2000). However, it is also worth noting that *D. viscosa* can boost the presence of phytophages, such as whiteflies (Homoptera: Aleyrodidae) (Parolin et al., 2013) and can act as a reservoir of tomato infectious chlorosis viruses (Orfanidou et al., 2016).

In olive groves, numerous studies are being carried out on the role played by different types of vegetation in biological pest control and other regulatory ecosystem services, such as fertility, erosion and pollination (Villa Serrano, 2016; Alcántara et al., 2017; Paredes et al., 2017; Porcel et al., 2017; Gómez et al., 2018). The plant species *D. viscosa* associated with olive groves, is of considerable interest in relation to its role in olive pest control, as its flowers are attacked by the gall-producing *Myopites stylatus* (Fabricius, 1974) (Diptera: Tephritidae). Its larvae are parasitized by *Eupelmus urozonus* (Hymenoptera: Eupelmidae), which, in turn, parasitizes the olive fly *Bactrocera oleae* (Rossi, 1790) (Diptera: Tephritidae), one of the principal olive pests (Warlop, 2006; Franco-Micán et al., 2010; Mota et al., 2011). It is also important to note that the flowering period of *D. viscosa* lasts from September to October (Parolin et al., 2014), when floral resources in olive groves are scarce and crop vegetation cover has been eliminated due to soil management requirements (Alcántara et al., 2017). This explains why, among native Mediterranean plants, *D. viscosa* is considered a potential source of food for natural enemies of olive pests (Nave et al., 2017). Its floral architecture has been found to facilitate access to pollen and nectar for four of the principal parasitoids of *Prays oleae* (Bernard, 1788) (Lepidoptera: Plutellidae), another important olive pest. However, it also prevents access to adults of this phytophage and *Chrysoperla carnea,* one of its most notable predators (Nave et al., 2016).

Before floral resources are introduced into an agroecosystem to improve or expand ecosystem services, such as biological control, in-depth entomological and agronomic studies need to be carried out (Araj and Wratten, 2015), as the arthropod community can respond in different ways to environmental factors at the local and spatial level, as previously observed in the case of spiders in olive groves (Picchi et al., 2016).

Thus, the objective of this study is to investigate arthropofauna associated with *D. viscosa* present in olive groves during its pre-flowering, flowering and post-flowering stages and to determine the possible relationships between different groups of arthropods.

MATERIALS AND METHODS

Area of Study

The study was carried out in two olive (*Olea europaea* L.) groves (Granada 37°10′34″N; 3°34′51″W; 880 m and Jaén 37°40′49″N; 3°48′3″W; 872 m) in Andalusia (Spain). The olive variety was "Picual," with a planting layout of 10 × 10 m. *D. viscosa* natural plants can be found in these olive groves, some bordering and others inside the crop. In the latter case, there are also cultivated *D. viscosa* plants between the rows of olive trees. As in the case of ditches and trenches in roads, this plant, which is attracted by unstable and collapsed lateral walls, has colonized most of the gullies in the olive groves (Simões et al., 2013; Parolin et al., 2014).

The natural plants bordering the olive groves are surrounded by olive trees, grazing land, such as *Daucus carota* L., *Convolvulus arvensis* L., *Taraxacum sp.* F. H. Wigg., and *Foeniculum vulgare* Mill., and forest mainly composed of *Pinus sp.* L., *Quercus coccifera* L., and *Quercus rotundifolia* Lam. The cultivated *D. viscosa* plants located inside the crop are placed one meter apart and are surrounded by olive trees and others plant species, such as *Capparis spinosa* L., *Daucus carota* L., *Cichorium intybus* L., *Convolvulus arvensis* L., *Psoralea bituminosa* L., *Bromus rubens* L., and *Foeniculum vulgare* Mill. The distance between the natural plants, which are in gullies, varies from one to three meters and are surrounded by olive trees and different herbaceous and shrub species, such as Rubus idaeus L., *Spartium junceum* L., *Asparragus acutifolius* L., *Smilax aspera* L., *Aristolochia baetica* L., *Cynodon dactylon* L., and *Carduus* sp. L.

Both olive groves have a meso-Mediterranean climate, with an average temperatures ranging from 15 to 18°C and an average rainfall of between 477 and 560 mm (Valle Tendero et al., 2005).

Collection of Arthropods

The study was carried out between June and December 2014. In order to analyze the arthropods in the different phenological stages of *D. viscosa*, sampling was carried out in June during the pre-flowering stage, in September during the flowering stage and in November during the post-flowering stage in the three areas studied: bordering (natural plants) and inside the olive grove (cultivated and natural plants). In each area, five sites were sampled, and the plants were vacuum-sampled for 40 s with the aid of an entomological aspirator (Modified CDC Backpack Aspirator Model 1412, John W. Hock Co., Gainsville, FL, USA). After vacuuming, the samples were labeled and cold-stored to avoid any interactions between the arthropofauna captured before going to the laboratory where they were stored at −20°C.

Under a stereomicroscope (Nikon SMZ800 Model CP-S, Nikon Co., Tokyo, Japan), the samples were cleaned and the

arthropods were separated from vegetal material, which were then conserved in 70% alcohol. All the material was identified using Hymenoptera of the World (Goulet and Huber, 1993), Heteroptera Families of the Iberian Peninsula (Mata and Goula, 2011) and Bases para un Curso Práctico de Entomología (Barrientos, 1988) as keys. We also used molecular analysis to identify the mirid species *Macrolophus* (Castañé et al., 2013).

The phenological states of *D. viscosa* were noted at each sampling and subsequent visits.

Statistical Analysis

All analyses were carried out using the R program version 3.5.0 (R Development Core Team, 2017). Analysis began with a data exploration (Zuur et al., 2010). We analyzed differences in the abundance of the majority taxonomic groups of phytophages (Aphididae and Aleyrodidae), predators (Araneae, Formicidae, Miridae) and Hymenoptera parasitoids according to their location (bordering or inside the olive grove) and the phenological stage of *D. viscosa* (pre-flowering, flowering, and post-flowering). In the case of plants situated inside the olive groves, we needed to pinpoint any differences between cultivated and natural *D. viscosa* plants. Depending on whether or not abundance data followed a normal distribution pattern, we opted for the Least Significant Difference test (Fisher-LSD) or the Kruskal-Wallis test, with a Bonferroni adjustment in both cases, using the "*agricolae*" software package (De Mendiburu, 2017). Additionally, we performed Pearson correlations with a confidence level of 95% ($\alpha = 0.05$) between the taxonomic groups in all cases.

RESULTS

Phenology of *D. viscosa*

Following the winter rest period, with the appearance of new leaves, *D. viscosa* emerged in early April, continued to grow until mid-June and stopped growing with the arrival of summer and drought conditions. The plants began to produce flower buds at the end of July and then flowered from August until October. In September, the first fruits were observed which matured between October and November. Galls formed in the plants during the months of October to November and remained during winter. The arrival of cold weather led to some leaf senescence in the plant (**Figure 1**).

Arthropods Collected

A total of 2,249 individuals were collected, corresponding to 11 Orders of arthropods (**Tables 1**, **2**). The most abundant family was Miridae (968 individuals), in which *Macrolophus melanotoma* (Costa, 1853) predominated, followed by the Aphididae family (364 individuals) represented by *Brachycaudus sp*. Hymenoptera parasitoids (222 individuals), composed of 15 families, were the third most abundant group, followed by the Formicidae family (167 individuals), with six genera (predominantly *Plagiolepis sp.*), the Order Araneae (149 individuals), with seven families, being (predominantly Oxyopidae and Thomisidae), and the family Aleyrodidae (142 individuals), mostly made up of *Trialeurodes sp*.

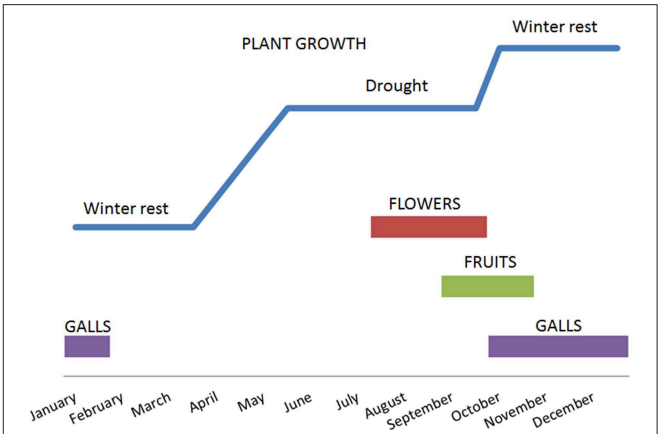

FIGURE 1 | Evolution of the phenology of *D. viscosa* in 2014 in the olive groves studied.

Impact of Phenological Stage and Location of *D. viscosa* on Arthropod Abundance and Its Relationship Between Different Groups of Arthropods

The post-flowering period was not analyzed due to the small number of captures, which accounted for 3.7% (83 individuals) of total arthropods collected.

We studied the most abundant groups of arthropods (Aphididae, Aleyrodidae, Araneae, Formicidae, Miridae and Hymenoptera parasitoids), which accounted for 89.5% (2,012 individuals) of total captures.

D. viscosa Bordering Olive Groves

During the pre-flowering stage, in the most abundance taxonomic groups, a total of 196 arthropods were captured, while the number of arthropods captured dropped to 100 during the flowering stage.

The various groups of arthropods responded differently to the phenological changes in *D. viscosa*. The Aleyrodidae family occupied a predominant position during the pre-flowering period, although the presence of flowers led to a significant reduction in their populations (Kruskal-Wallis $\chi^2 = 6.31$; d.f. = 1; $p < 0.05$). The abundance of the other groups (Hymenoptera parasitoids, aphids, and predators) was not found to be affected by phenological changes in *D. viscosa*. Populations of the Miridae family remained high in the pre-flowering and flowering stages (**Table 3**).

In the pre-flowering stage, we observed a significantly negative correlation between the abundance levels of Araneae and Aphididae (Pearson cor $= -0.94$, $p < 0.05$), while the correlation between Aleyrodidae and Formicidae was positive (Pearson cor $= 0.97$, $p < 0.01$) (**Table 4**). During the flowering period, a significantly negative correlation between abundances of spiders and parasitoids was observed (Pearson cor $= -0.96$, $p < 0.05$).

D. viscosa Inside Olive Groves

The number of individual arthropods captured in the most abundance taxonomic groups during the pre-flowering period

TABLE 1 | Number of individuals collected during sampling period in bordering and inside olive grove.

Subclass or order	Family	Inside olive groves	Bordering olive groves	Total
Acari		3	0	3
Araneae		91	58	149
Coleoptera		32	9	41
Dictioptera		1	0	1
Diptera		34	6	40
Hemiptera	Aleyrodidae	48	94	142
	Anthocoridae	8	2	10
	Aphididae	360	4	364
	Cicadellidae	17	5	22
	Miridae	883	85	968
	Pentatomidae	1	3	4
Hymenoptera	Aphelinidae	38	13	51
	Apidae	1	18	19
	Braconidae	12	0	12
	Ceraphronidae	3	0	3
	Cynipidae	4	0	4
	Elasmidae	1	0	1
	Encyrtidae	0	2	2
	Eulophidae	42	0	42
	Eupelmidae	3	1	4
	Formicidae	137	30	167
	Ichneumonidae	2	0	2
	Mymaridae	24	0	24
	Platygastridae	2	0	2
	Pteromalidae	16	2	18
	Scelionidae	48	7	55
	Torymidae	1	0	1
	Trichogrammatidae	1	0	1
Lepidoptera		1	3	4
Neuroptera		2	0	2
Orthoptera		11	4	15
Thysanoptera		71	5	76
Total		1,898	351	2,249

TABLE 2 | Number of individuals collected to the Order Araneae and the family Formicidae during sampling period inside and bordering olive groves.

Taxonomic identification		Inside olive groves	Bordering olive groves	Total
Araneae	Araneidae fam.	18	6	24
	Dictynidae fam.	0	2	2
	Lycosidae fam.	1	0	1
	Oxyopidae fam.	34	19	53
	Pisauridae fam.	3	4	7
	Salticidae fam.	14	2	16
	Thomisidae fam.	19	25	44
	Unidentified	2	0	2
	Total	91	58	149
Formicidae	*Camponotus sp.*	1	19	20
	Cataglyphis sp.	0	1	1
	Pheidole sp.	1	0	1
	Plagiolepis sp.	127	10	137
	Tapinoma sp.	2	0	2
	Tetramorium sp.	5	0	5
	Unidentified	1	0	1
	Total	137	30	167

reached 794, which increased to 904 individuals during the flowering period.

The populations of Aleyrodidae and Aphididae, the principal phytophage families present, were found to be affected in opposite ways by flowering. In the case of the Aleyrodidae family, as observed in *D. viscosa* plants bordering the olive groves, its populations diminished significantly (Kruskal-Wallis $\chi^2 = 9.15$; d.f. $= 1$; $p < 0.01$), while Aphididae populations were observed to rise considerably in this period (Kruskal-Wallis $\chi^2 = 10.74$; d.f. $= 1$; $p < 0.01$) (**Table 4**). Hymenoptera parasitoid populations, which multiplied 5-fold, were significantly higher during the flowering period (Kruskal-Wallis $\chi^2 = 13.25$; d.f. $= 1$; $p < 0.001$). As for the response of the different predator groups, the abundance of spiders was observed to diminish significantly in this period (Kruskal-Wallis $\chi^2 = 8.81$; d.f. $= 1$; $p < 0.01$); populations of the Formicidae family were similar in both periods, while those of the Miridae family, which reached high levels in both periods, declined, with no significant inter-period differences being observed (**Table 4**).

In the pre-flowering period, we noted a significantly positive correlation between Aphididae and Miridae (Pearson cor $= 0.86$, $p < 0.01$). During the flowering stage, a positive correlation was observed between Formicidae and Hymenoptera parasitoids (Pearson cor $= 0.73$, $p < 0.05$).

With respect to the comparison between cultivated and naturally growing *D. viscosa* plants, we observed that, among the majority taxonomic groups, during the pre-flowering and flowering periods in the cultivated plants, 354 and 353 individuals were captured, respectively; on the other hand, in the naturally growing plants, the numbers rose to 440 and 551 individuals, respectively. During the pre-flowering period, the abundances of the Aleyrodidae and Aphididae families were low, although Aleyrodidae populations were significantly higher in the cultivated plants (Fisher-LSD MSerror $= 16.55$; $p < 0.05$), while Aphididae populations were higher in the natural plants (Kruskal-Wallis $\chi^2 = 6.91$; d.f. $= 1$; $p < 0.01$). Populations of the other groups were similar in both types of plants (**Figure 2**). In addition, during the pre-flowering stage of natural *D. viscosa* plants, a positive correlation was observed between Aphididae and Miridae (Pearson cor $= 0.91$, $p < 0.05$), while no significant correlation in cultivated plants was found.

During the flowering period, the abundance of the Formicidae family in cultivated plants was higher than that in natural plants (Kruskal-Wallis $\chi^2 = 6.99$; d.f. $= 1$; $p < 0.01$). The other groups analyzed (Aphididae, Aleyrodidae, Araneae, Miridae and Hymenoptera parasitoids) did not show any significant differences between the two types of plants (**Figure 2**). With respect to relationships between the groups in the natural

TABLE 3 | Average number (mean ± SE) of individuals of different taxonomic groups captured during the pre-flowering and flowering stages of *D. viscosa* bordering olive groves.

Phenological stage	*n*	Aphididae	Aleyrodidae	Araneae	Formicidae	Miridae	Hymenoptera parasitoids
Pre-flowering	5	0.2 ± 0.2^{a}	18 ± 9.6^{a}	7.4 ± 1.2^{a}	3 ± 1.8^{a}	8.2 ± 3.2^{a}	3 ± 0.9^{a}
Flowering	5	0.6 ± 0.2^{a}	0.8 ± 0.8^{b}	4.2 ± 1.3^{a}	3 ± 1.4^{a}	8.8 ± 1.9^{a}	2 ± 0.9^{a}

The letters representing superindices indicate differences between the flowering stages for each taxonomic group.

TABLE 4 | Average number (mean ± SE) of individuals of different taxonomic groups captured before and during the flowering period of *D. viscosa* located inside the olive groves.

Phenology	*n*	Aphididae	Aleyrodidae	Araneae	Formicidae	Miridae	Hymenoptera parasitoids
Pre-flowering	10	1.3 ± 0.5^{a}	4.6 ± 1.6^{a}	6.7 ± 1.2^{a}	8 ± 2^{a}	56.1 ± 10.1^{a}	3.2 ± 0.6^{a}
Flowering	10	33.9 ± 15.8^{b}	0.2 ± 0.2^{b}	2.2 ± 0.6^{b}	6 ± 3^{a}	31.9 ± 3.3^{a}	16 ± 2.9^{b}

The letters representing superindices indicate differences between the flowering stages for each taxonomic group.

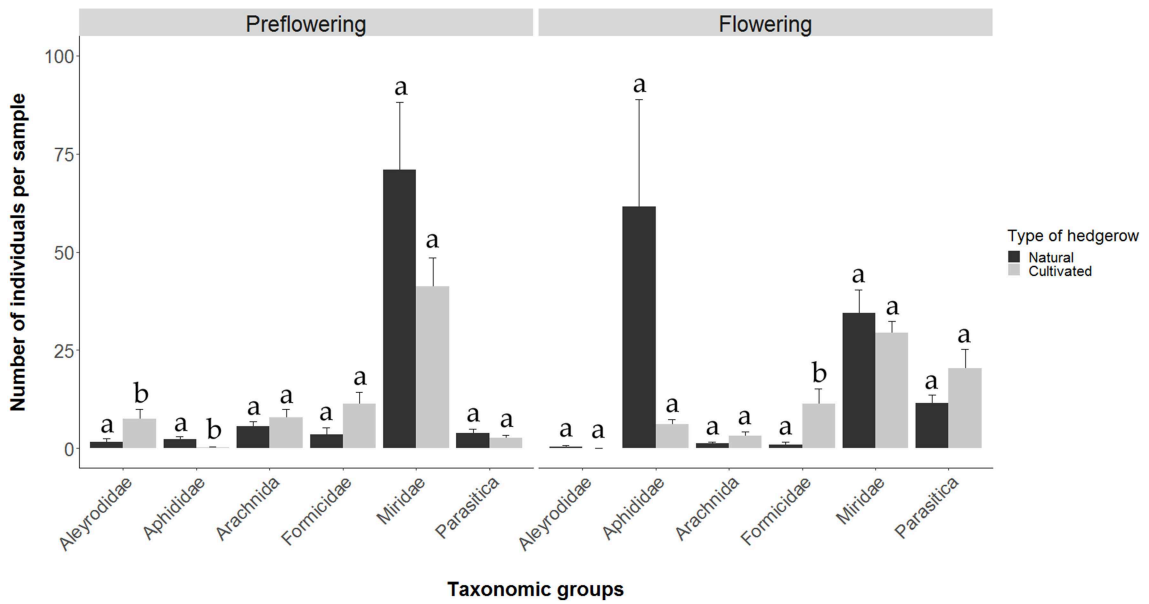

FIGURE 2 | Number of individuals (media ± SE) of the different taxonomic groups during the pre-flowering and flowering periods of *D. viscosa* plants in natural and cultivated hedgerows inside olive groves.

plants, a negative correlation between aphids and Hymenoptera parasitoids was observed (Pearson cor = −0.89, $p < 0.05$). In cultivated plants, we found positive correlations between Aleyrodidae and Araneae (Pearson cor = 41, $p < 0.05$), between Araneae and Formicidae (Pearson cor = 0.64, $p < 0.001$) and Miridae (Pearson cor = 0.6, $p < 0.001$) and between Miridae and Hymenoptera parasitoids (Pearson cor = 0.47, $p < 0.01$).

DISCUSSION

D. viscosa plants adapted well to conditions in the areas studied, and their phenology did not differ significantly from other Mediterranean regions (Parolin et al., 2013). However, their phenology can be affected by agricultural vegetation cover management, as the timing and frequency of clearance can affect the plant's growth and floral development. Thus, late vegetation cover management in summer reduces the quantity of flowers (Simões et al., 2013) and prevents leaf senescence in winter (Parolin et al., 2013).

Throughout its life cycle, *D. viscosa* is colonized by numerous arthropods from different functional groups, whose populations can vary depending on requirements. The leaves, present from the beginning of April to December, can be used as food, whose importance for arthropod colonizers has not been analyzed (Parolin et al., 2014). The pollen and nectar of its open flowers are important sources of food for beneficial arthropods, as the nectar contains high concentrations of sugars (Hidalgo and Cabezudo, 1995), which, together with the scarcity of other flowering plants

at that time of year in different agroecosystems, make *D. viscosa* a plant of considerable importance (Nave et al., 2017). Due to gall production by *M. stylatus,* the numerous larvae inside the flower during winter can be used as hosts by different families of Hymenoptera parasitoids, whose adults begin to emerge during the month of May (Franco-Micán et al., 2010; Mota et al., 2011).

Aleyrodidae are an abundant family in the group of phytophages associated with *D. viscosa* (Parolin et al., 2013; Rodríguez et al., 2018). In our study, *Trialeurodes sp.* was found to be present in both olive groves studied, preferentially during the pre-flowering period. This is in line with the finding of Rodríguez et al. (2018), who reported that no whiteflies were captured during the flowering period, which explains why *Trialeurodes sp.* may mostly feed on leaves during the pre-flowering period. Its positive correlation with the Formicidae family could be due to honeydew secreted by this aleyrodid. Another noteworthy phytophage is the aphid, belonging to the genus *Brachycaudus sp.*, whose populations increased during the flowering period of *D. viscosa* plants located inside the olive groves. In the pre-flowering stage, we observed a positive correlation with the Miridae family, one of the principal enemies of the family Aphididae (Perdikis et al., 2007). Although an extract of *D. viscosa* showed aphid antifeedant activity (Mamoci et al., 2012), this plants species was colonized by various aphid species. These aphids can be parasitized by individuals belonging to the Aphelinidae family, as *D. viscosa* is considered a reservoir of aphid parasitoids (Kavallieratos et al., 2002).

The group of Hymenoptera parasitoids associated with *D. viscosa* in our study is highly complex, with 15 families, notably Scelionidae, Aphelinidae, and Eulophidae, having been identified. Their presence during both the pre-flowering and flowering stages of plants bordering and inside the olive groves points to their potential role in maintaining these natural enemies together with others associated with *D. viscosa* galls in different locations (Alcalá Herrera et al., 2017). In plants located inside olive groves, Hymenoptera parasitoid populations increased significantly during the flowering period. This could be due to the ability of adult Hymenoptera parasitoids to feed on pollen and nectar as well as to find possible hosts; although *D. viscosa* flowers have protected nectaries, the size of their corolla (5.91 mm deep and 1.19 mm wide) permits parasitoids, such as *Ageniaspis fuscicollis* (Hymenoptera: Encyrtidae) and *Elasmus flabellatus* (Hymenoptera: Eulophidae), to enter the corolla in order to feed (Nave et al., 2016).

Predators belonging to the Miridae family, principally *M. melanotoma,* were highly abundant in *D. viscosa* plants both bordering and inside olive groves; however, in other studies, mirid bugs were found to be more abundant in outer rows with higher whitefly densities (Alomar et al., 2002). *M. melanotoma* is present during pre-flowering and flowering periods. In Greece, *Macrolophus sp.* is present throughout the year in *D. viscosa*, reaching maximum levels in June and July, as it can feed on the plant and different types of prey (Perdikis et al., 2007). The small number of mirids found in the post-flowering stage were mirid nymphs, which is in line with the situation observed in the north of Spain, where winter populations of *M. melanotoma* are mostly composed of nymphs (Alomar et al., 1994). In pre-flowering plants situated inside the olive groves, mirid populations correlated with the Aphididae family, which constitutes the best prey for the development of mirids, while predator numbers were found to respond to the presence of aphids, such as *Capitophorus inulae* in spring (Perdikis et al., 2007). Another group of predators, spiders, was present in the areas studied, particularly during the pre-flowering stage in plants located inside the olive groves, possibly because they usually respond to fluctuations in their prey, as availability of food is a critical factor in their relationships (Picchi et al., 2016). The spiders present in olive groves are highly diverse, and, although most are generalist, some species specialize in certain prey (Cárdenas et al., 2011). Ants, whose populations vary throughout the year and are affected by vegetation cover management, are known to constitute a highly abundant group in olive groves (Redolfi et al., 1999). In our study, ant populations captured in *D. viscosa* did not differ significantly between the pre-flowering and flowering stages in either location, possibly due to their capacity to feed on many different types of food (Way and Khoo, 1992).

Differences between cultivated and natural plants were mainly observed in the pre-flowering stage, which affected both phytophage groups, with the Aphididae family showing the highest abundance in natural plants and the Aleyrodidae family in cultivated plants. This could be due to differences in existing plant diversity surrounding *D. viscosa* plants.

Our findings clearly show that arthropod communities associated with *D. viscosa* and the relationships between different groups of arthropods can vary during the pre-flowering and flowering stages. However, in all locations studied (inside and bordering olive groves) and in cultivated and natural plants, *D. viscosa* is still potentially of considerable interest as a reservoir of different predators and Hymenoptera parasitoids, although it is important to point out that none of the phytophages present affected the olive trees. Nevertheless, it should be noted that, in olive groves and commercial plantations, *D. viscosa*, which is very difficult to remove using herbicides and has significant resprouting capacity, is considered to be a problematic plant (Simões et al., 2013); these two factors should therefore be taken into account when *D. viscosa* is incorporated into the ecological infrastructure.

DATA AVAILABILITY

All relevant data generated and anlyzed for this study are included in the manuscript.

AUTHOR CONTRIBUTIONS

MC obtained the funding. MC and JC-R conceived and designed the study. MC, MF-S carried out the sampling. RA and MF-S identified the arthropod. RA carried out the formal analyses. MC, JC-R, and RA wrote, reviewed, and edited the

manuscript. The manuscript was revised and approved by all the authors.

FUNDING

This study was funded within the framework of a Spanish National Research Council (CSIC) intramural funding program (Project 201540E007) and by the Junta de Andalucía (Project P12-AGR-1419). The Spanish Council for Scientific Research CSIC Open Access Publication Support Initiative through its Unit of Information Resources for Research (URICI) assisted with the payment of the publication fee.

ACKNOWLEDGMENTS

We wish to thank Nuria Agustí who identified the *Macrolophus* specimen using molecular techniques. Joaquin Moreno Chocano for his help to sampling in field. The manuscript was translated by Michael O'Shea.

REFERENCES

Alcalá Herrera, R., Castro Rodríguez, J., Fernández-Sierra, M. L., Moreno-Chocano, J., and Campos Aranda, M. (2017). "Incidencia de la localización de *Dittrichia viscosa* (Asteraceae) en el olivar sobre el complejo parasitario asociados a las agallas producidas por *Myopites stylata* (Diptera: Tephritidae)," in *XVIII Symposium Científico-Técnico Expoliva del 10 al 12 de mayo de 2017* (Jaén: Fundación Olivar), 1–3.

Alcántara, C., Soriano, A., Saavedra, M., and Gómez, J. A. (2017). "Sistemas de manejo del suelo," in *El cultivo del olivo, 7th Edn.*, eds D. Barranco Navero, R. Fernández Escobar, and L. Rallo Romero (Madrid: Mundi-Prensa), 335–417.

Alomar, O., Goula, M., and Albajes, R. (1994). Mirid bugs for biological control: identification, survey in non-cultivated winter plants, and colonization of tomato fields. *IOBC/WPRS Bull.* 17, 217–223.

Alomar, O., Goula, M., and Albajes, R. (2002). Colonisation of tomato fields by predatory mirid bugs (Hemiptera: Heteroptera) in northern Spain. *Agric. Ecosyst. Environ.* 89, 105–115. doi: 10.1016/S0167-8809(01)00322-X

Araj, S. E., and Wratten, S. D. (2015). Comparing existing weeds and commonly used insectary plants as floral resources for a parasitoid. *Biol. Control* 81, 15–20. doi: 10.1016/j.biocontrol.2014.11.003

Barrientos, J. A. (1988). *Bases para un curso práctico de entomología.* Barcelona: Asociación Española de Entomología.

Bianchi, F. J., Booij, C. J., and Tscharntke, T. (2006). Sustainable pest regulation in agricultural landscapes: a review on landscape composition, biodiversity and natural pest control. *Proc. Biol. Sci.* 273, 1715–1727. doi: 10.1098/rspb.2006.3530

Cárdenas, M., Campos, M., and Pascual, F. (2011). Roles de las arañas (Orden Araneae) en el agroecosistema del olivar. *Phytoma España* 229, 1–6.

Carrié, R. J., George, D. R., and Wäckers, F. L. (2012). Selection of floral resources to optimise conservation of agriculturally-functional insect groups. *J. Insect Conserv.* 16, 635–640. doi: 10.1007/s10841-012-9508-x

Castañé, C., Agustí, N., Arnó, J., Gabarra, R., Riudavets, J., Comas, J., et al. (2013). Taxonomic identification of *Macrolophus pygmaeus* and *Macrolophus melanotoma* based on morphometry and molecular markers. *Bull. Entomol. Res.* 103, 204–215. doi: 10.1017/S0007485312000545

Chaplin-Kramer, R., De Valpine, P., Mills, N. J., and Kremen, C. (2013). Detecting pest control services across spatial and temporal scales. *Agric. Ecosyst. Environ.* 181, 206–212. doi: 10.1016/j.agee.2013.10.007

De Mendiburu, F. (2017). *Agricolae: Statistical Procedures for Agricultural Research*. R package version 1.2-8 Edn.

Franco-Micán, S. X., Castro, J., and Campos, M. (2010). Preleminary study of the parasitic complex associated with *Dittrichia viscosa* in Andalusia (Spain). *Integrated Protection of Olive Crops. IOBC/WRPS Bulletin* 53, 139–143.

Gómez, J. A., Campos, M., Guzman, G., Castillo-Llanque, F., Vanwalleghem, T., Lora, A., et al. (2018). Soil erosion control, plant diversity, and arthropod communities under heterogeneous cover crops in an olive orchard. *Environ. Sci. Pollut. Res.* 25, 977–989. doi: 10.1007/s11356-016-8339-9

Goulet, H., and Huber, J. T. (1993). *Hymenoptera of the World: An Identification Guide to Families.* Ottawa, ON: Centre for Land and Biological Resources Research.

Hidalgo, M. I., and Cabezudo, B. (1995). Producción de néctar en matorrales del sur de España (Andalucía). *Acta Botanica Malacitana* 20, 123–132.

Holland, J. M., Bianchi, F. J. J. A., Entling, M. H., Moonen, A. C., Smith, B. M., and Jeanneret, P. (2016). Structure, function and management of semi-natural habitats for conservation biological control: a review of European studies. *Pest Manag. Sci.* 72, 1638–1651. doi: 10.1002/ps.4318

Holland, J. M., Douma, J. C., Crowley, L., James, L., Kor, L., Stevenson, D. R. W., et al. (2017). Semi-natural habitats support biological control, pollination and soil conservation in Europe. A review. *Agron. Sustain. Dev.* 37:31. doi: 10.1007/s13593-017-0434-x

Kavallieratos, N. G., Stathas, G. J., Athanassiou, C. G., and Papadoulis, G. T. (2002). *Dittrichia viscosa* and *Rubus ulmifolius* as reservoirs of aphid parasitoids (Hymenoptera: Braconidae: Aphidiinae) and the role of certain coccinellid species. *Phytoparasitica* 30, 231–242. doi: 10.1007/BF03039992

Lambion, J. (2011). "Functional biodiversity in Southern France: a method to enhance predatory mirid bug populations," in *I International Conference on Organic Greenhouse Horticulture. Acta Horticulturae 915*, eds M. Dorais and S. D. Bishop (Bleiswijk: International Society for Horticultural Science), 165–170. doi: 10.17660/ActaHortic.2011.915.20

Landis, D. A., Wratten, S. D., and Gurr, G. M. (2000). Habitat management to conserve natural enemies of arthropod pests in agriculture. *Ann. Rev. Entomol.* 45, 175–201. doi: 10.1146/annurev.ento.45.1.175

Lykouressis, D., Perdikis, D., and Kallioras, C. (2012). Selection of Macrolophus melanotoma between its main non-crop host plant (*Dittrichia viscosa*) and eggplant, pepper and tomato, in choice experiments. *Entomol. Hellenica* 21, 3–12. doi: 10.12681/eh.11513

Mamoci, E., Cavoski, I., Andres, M. F., Díaz, C. E., and Gonzalez-Coloma, A. (2012). Chemical characterization of the aphid antifeedant extracts from Dittrichia viscosa and Ferula communis. *Biochem. Syst. Ecol.* 43, 101–107. doi: 10.1016/j.bse.2012.02.012

Mata, L., and Goula, M. (2011). *Clave de Familias de Heterópteros de la Península Ibérica (Insecta, Hemiptera, Heteroptera). Versión 1.* Barcelona, ES: Centre de Recursos de Biodiversitat Animal, Facultat de Biologia, Universitat de Barcelona.

Miñarro, M., and Prida, E. (2013). Hedgerows surrounding organic apple orchards in north-west Spain: potential to conserve beneficial insects. *Agric. For. Entomol.* 15, 382–390. doi: 10.1111/afe.12025

Mota, L., Bento, A., Porcel, M., Campos, M., and Pereira, J. A. (2011). "O papel de Dittrichia viscosa (L.) W. Greuter no olival: estudo da influencia dos parámetros biométricos das galhas no número Myopites stylatus (Fabricius) e seus parasitoides," in *VII Congreso Nacional de Entomología Aplicada* (Baeza), de 24 al 28 de Octubre de 2011, 128.

Nave, A., Crespi, A. L., Goncalves, F., Campos, M., and Torres, L. (2017). Native Mediterranean plants as potential food sources for natural enemies of insect pests in olive groves. *Ecol. Res.* 32, 459–459. doi: 10.1007/s11284-017-1460-5

Nave, A., Gonçalves, F., Crespí, A. L., Campos, M., and Torres, L. (2016). Evaluation of native plant flower characteristics for conservation biological control of *Prays oleae*. *Bull. Entomol. Res.* 106, 249–257. doi: 10.1017/S0007485315001091

Orfanidou, C. G., Maliogka, V. I., and Katis, N. I. (2016). False Yellowhead (*Dittrichia viscosa*), a banker plant as source of tomato infectious chlorosis virus in Greece. *Plant Dis.* 100, 869–869. doi: 10.1094/PDIS-10-15-1201-PDN

Paredes, D., Cayuela, L., and Campos, M. (2017). "Potential of ecological infrastructures to restore conservation biological control: case study in Spanish

olive groves," in *Natural Enemies. Identification Protection Strategies and Ecological Impacts,* ed. *S. A. P. Santos* (New York, NY: Nova Publishers), 153.

Parolin, P., Scotta, M. I., and Bresch, C. (2014). Biology of *Dittrichia viscosa*, a Mediterranean ruderal plant: a review. *Phyton-Int. J. Exp. Bot.* 83, 251–262.

Parolin, P., Scotta, M. I., and Bresh, C. (2013). Notes on the phenology of *Dittrichia viscosa*. *J. Mediterr. Ecol.* 12, 27–35.

Perdikis, D., Favas, C., Lykouressis, D., and Fantinou, A. (2007). Ecological relationships between non-cultivated plants and insect predators in agroecosystems: the case of *Dittrichia viscosa* (Asteraceae) and *Macrolophus melanotoma* (Hemiptera: Miridae). *Acta Oecol. Int. J. Ecol.* 31, 299–306. doi: 10.1016/j.actao.2006.12.005

Picchi, M. S., Bocci, G., Petacchi, R., and Ending, M. H. (2016). Effects of local and landscape factors on spiders and olive fruit flies. *Agric. Ecosyst. Environ.* 222, 138–147. doi: 10.1016/j.agee.2016.01.045

Porcel, M., Cotes, B., Castro, J., and Campos, M. (2017). The effect of resident vegetation cover on abundance and diversity of green lacewings (Neuroptera: Chrysopidae) on olive trees. *J. Pest Sci.* 90, 195–196. doi: 10.1007/s10340-016-0748-5

R Development Core Team (2017). *R: A Language and Environment for Statistical Computing*. Vienna: R Foundation for Statistical Computing.

Redolfi, I., Tinaut, A., Pascual, F., and Campos, M. (1999). Qualitative aspects of myrmecocenosis (Hym., Formicidae) in olive orchards with different agricultural management in Spain. *J. Appl. Entomol. Zeitschr. Angew. Entomol.* 123, 621–627. doi: 10.1046/j.1439-0418.1999.00411.x

Rodríguez, E., González, M., Paredes, D., Campos, M., and Benítez, E. (2018). Selecting native perennial plants for ecological intensification in Mediterranean greenhouse horticulture. *Bull. Entomol. Res.* 108, 694–704. doi: 10.1017/S0007485317001237

Simões, P. M., Belo, A. D. F., and Souza, C. (2013). Effects of mowing regime on diversity of mediterranean roadside vegetation – implications for management. *Pol. J. Ecol.* 61, 241–255.

Simon, S., Bouvier, J. C., Debras, J. F., and Sauphanor, B. (2010). Biodiversity and pest management in orchard systems. A review. *Agron. Sustain. Dev.* 30, 139–152. doi: 10.1051/agro/2009013

Tixier, M. S., Kreiter, S., Auger, P., Sentenac, G., Salva, G., and Weber, M. (2000). Phytoseiid mites located in uncultivated areas surrounding vineyards in three French regions. *Acarologia* 41, 127–140.

Valle Tendero, F., Navarro Reyes, F. B., Jiménez Morales, M. N., Algarra Ávila, J. A., Arrojo Agudo, E., Asensi Marfil, A., et al. (2005). *Datos botánicos aplicados a la gestión del medio natural andaluz I: Bioclimatología y Biogeografía.* Sevilla: Consejería de Medio Ambiente, Junta de Andalucía.

Villa Serrano, A. M. (2016). *Ecological infrastructures in sustainable olive growing: studies about Prays oleae (Bernard) and its natural enemies* (Doctoral thesis), University of Lisboa, Lisbon, Portugal.

Warlop, F. (2006). Limitation of olive pest populations through the development of conservation biocontrol. *Cah. Agric.* 15, 449–455.

Way, M. J., and Khoo, K. C. (1992). Role of ants in pest management. *Ann. Rev. Entomol.* 37, 479–503. doi: 10.1146/annurev.en.37.010192.002403

Zhang, W., Ricketts, T. H., Kremen, C., Carney, K., and Swinton, S. M. (2007). Ecosystem services and dis-services to agriculture. *Ecol. Econ.* 64, 253–260. doi: 10.1016/j.ecolecon.2007.02.024

Zuur, A. F., Ieno, E. N., and Elphick, C. S. (2010). A protocol for data exploration to avoid common statistical problems. *Methods Ecol. Evol.* 1, 3–14. doi: 10.1111/j.2041-210X.2009.00001.x

Conflict of Interest Statement: The authors declare that the research was conducted in the absence of any commercial or financial relationships that could be construed as a potential conflict of interest.

frontiers in Plant Science

ORIGINAL RESEARCH
published: 19 September 2019
doi: 10.3389/fpls.2019.01149

Generation of Superoxide by OeRbohH, a NADPH Oxidase Activity During Olive (*Olea europaea* L.) Pollen Development and Germination

María José Jimenez-Quesada[1], José Angel Traverso[1†], Martin Potocký[2], Viktor Žárský[2,3] and Juan de Dios Alché[1]*

[1] Plant Reproductive Biology and Advanced Microscopy Laboratory, Department of Biochemistry, Cellular and Molecular Biology of Plants, Estación Experimental del Zaidín (CSIC), Granada, Spain, [2] Institute of Experimental Botany of the Czech Academy of Sciences, Prague, Czechia, [3] Department of Experimental Plant Biology, Faculty of Science, Charles University in Prague, Prague, Czechia

OPEN ACCESS

Edited by:
Antonio Diaz Espejo, Institute of Natural Resources and Agrobiology of Seville (CSIC), Spain

Reviewed by:
Anna Dobritsa, The Ohio State University, United States
Ki-Hong Jung, Kyung Hee University, South Korea

***Correspondence:**
Juan de Dios Alché
juandedios.alche@eez.csic.es

†Present address:
José Angel Traverso
Department of Cell Biology, University of Granada, Granada, Spain

Specialty section:
This article was submitted to Crop and Product Physiology, a section of the journal Frontiers in Plant Science

Received: *19 February 2019*
Accepted: *22 August 2019*
Published: *19 September 2019*

Citation:
Jimenez-Quesada MJ, Traverso JA, Potocký M, Žárský V and Alché JdD (2019) Generation of Superoxide by OeRbohH, a NADPH Oxidase Activity During Olive (Olea europaea L.) Pollen Development and Germination. Front. Plant Sci. 10:1149. doi: 10.3389/fpls.2019.01149

Reactive oxygen species (ROS) are produced in the olive reproductive organs as the result of intense metabolism. ROS production and pattern of distribution depend on the developmental stage, supposedly playing a broad panel of functions, which include defense and signaling between pollen and pistil. Among ROS-producing mechanisms, plasma membrane NADPH-oxidase activity is being highlighted in plant tissues, and two enzymes of this type have been characterized in *Arabidopsis thaliana* pollen (RbohH and RbohJ), playing important roles in pollen physiology. Besides, pollen from different species has shown distinct ROS production mechanism and patterns of distribution. In the olive reproductive tissues, a significant production of superoxide has been described. However, the enzymes responsible for such generation are unknown. Here, we have identified an Rboh-type gene (OeRbohH), mainly expressed in olive pollen. OeRbohH possesses a high degree of identity with RbohH and RbohJ from *Arabidopsis*, sharing most structural features and motifs. Immunohistochemistry experiments allowed us to localize OeRbohH throughout pollen ontogeny as well as during pollen tube elongation. Furthermore, the balanced activity of tip-localized OeRbohH during pollen tube growth has been shown to be important for normal pollen physiology. This was evidenced by the fact that overexpression caused abnormal phenotypes, whereas incubation with specific NADPH oxidase inhibitor or gene knockdown lead to impaired ROS production and subsequent inhibition of pollen germination and pollen tube growth.

Keywords: NADPH oxidase, NOX, pollen, Rboh, sexual plant reproduction, olive

INTRODUCTION

Pollen–pistil interaction is recognized as a key aspect of sexual plant reproduction. The pollen grains must undergo a tightly controlled sequence of physiological events after landing on compatible stigmatic papillae. These processes involve the initial pollen rehydration and germination, the pollen tube growth through the female tissues, and the final interaction with the embryo sac to eventually achieve the double fertilization and generate the progeny. To assure the success of the sexual plant reproduction, pollen and the female tissues of the pistil must accomplish an efficient cross

talk, which involves a large number of signaling mechanisms. Redox regulation and signaling are now proposed as a crucial mechanism able to manage different aspects of the sexual plant reproduction, where ROS and NO molecules seem to act as mediators in such an interchange of information between pollen and pistil tissues (Traverso et al., 2013b; Domingos et al., 2015).

NADPH oxidase enzymes are eukaryotic proteins able to catalyze the physiological generation of the short-lived superoxide radical ($O_2^{\bullet-}$) throughout membranes (Lambeth, 2004), which is rapidly dismutated leading to H_2O_2 accumulation (Lamb and Dixon, 1997). This protein family shares six transmembrane central domains, two heme-binding sites, and a long cytoplasmic C-terminal end owning FAD- and NADPH-binding domains. In addition, Ca^{2+}-binding EF-hand motifs in the N-terminus are a distinctive feature of plant NADPH oxidases as well as NOX5 and DUOX human NADPH oxidases (Bedard et al., 2007). In *Arabidopsis thaliana*, 10 NADPH oxidase homologues are encoded (Torres et al., 1998; Dangl and Jones, 2001), which are also designed as "*respiratory burst oxidase homologs*" (*Rbohs*).

Rbohs play crucial roles in a broad range of responses to biotic interaction (pathogenic or symbiotic) as well as in the response to different kinds of abiotic stresses and adaptation mechanisms. Moreover, Rbohs have been shown to be involved in cell growth (diffuse or polarized) and other developmental events (Marino et al., 2012). Cell-to-cell communication over long distances in plants has also been shown to be mediated by Rboh-derived $O_2^{\bullet-}$ (Miller et al., 2009). Among these enzymes, *Arabidopsis* RbohH and RbohJ seem to be specifically expressed in pollen and stamens (Sagi and Fluhr, 2006). Moreover, NADPH oxidase-produced ROS are detected through pollen tube growth, subsequently to pollen rehydration (Speranza et al., 2012) and seem to be essential for pollen apical elongation (Potocky et al., 2007) and then upon fertilization (Kaya et al., 2015).

The activity of plant Rboh proteins has been shown to be highly regulated by multiple factors. Diverse studies have described specific regulatory mechanism involving the N-terminus of these proteins (Suzuki et al., 2011), such as the activation by Ca^{2+} (Takeda et al., 2008) and phosphorylation in a synergistic way (Ogasawara et al., 2008; Drerup et al., 2013). Also, small GTPases from the Rop family and phosphatidic acid (PA) have been shown to stimulate NADPH oxidase production of ROS (Ono et al., 2001; Zhang et al., 2009). These regulatory interactions have been progressively confirmed for pollen Rbohs as well (Potocky et al., 2012; Boisson-Dernier et al., 2013; Kaya et al., 2014; Lassig et al., 2014; Jimenez-Quesada et al., 2016).

Recent studies point to RbohH and RbohJ as the source for most ROS produced at the pollen tube apex in *Arabidopsis*, since the corresponding double mutant shows defective *in vivo* and *in vitro* ROS generation (Boisson-Dernier et al., 2013; Kaya et al., 2014). However, different species seem to show distinct patterns for ROS production. Thus, the generation of ROS in lily (*Lilium formosanum*) pollen tubes was previously proposed to have a mitochondrial origin, showing an alternative localization in the subapical zone, instead of at the tip (Cardenas et al., 2006). In the cucumber (*Cucumis sativus* cv. Marketer) pollen tube, ROS are first detected at the tip but progressively become extended to the entire tube (Sirova et al., 2011). Superoxide production in kiwifruit pollen does not exhibit a clear tip localization (Speranza et al., 2012). In the growing pollen tubes of *Picea meyeri*, different ROS sources—mitochondria in the pollen tube shank and NADPH oxidase at the apex—are considered (Liu et al., 2009). Concerning their subcellular localization, and besides the expected occurrence in the plasma membrane associated to lipid microdomain (Liu et al., 2009), pollen Rbohs have been also localized at the cytoplasm (Lassig et al., 2014). Wide differences in timing, developmental patterns, and localization of ROS also occur in the stigma of numerous plant species (Zafra et al., 2016).

The study of *RbohH/RbohJ* double mutants of *Arabidopsis* suggests that RbohH and RbohJ modulate and stabilize pollen tube growth and are involved in maintenance of cell-wall integrity (Boisson-Dernier et al., 2013; Kaya et al., 2014; Lassig et al., 2014). Also, the involvement of flavoenzymes others than Rbohs in pollen tube growth cannot be excluded (Lassig et al., 2014).

Most studies carried out to date in pollen have been performed in model plants such as *Arabidopsis*, tobacco, or lily with a variety of results. This raises the question about how NADPH oxidase-produced ROS behave in pollen from other species, like the agronomically important and allergy relevant species *Olea europaea* L. (olive tree). Olive pollination is preferentially allogamous, and this plant shows genotypes with different degrees of self-incompatibility (SI), which is likely of the gametophytic type, although the precise mechanism underlying this system remains unclear (Mookerjee et al., 2005; Díaz et al., 2006; Vuletin Selak et al., 2014). Previously, ROS have been involved in gametophytic SI systems in *Angiosperms* (McInnis et al., 2006). The production of ROS and NO has also been analyzed in olive reproductive tissues along floral development (Zafra et al., 2010). However, the biochemical and molecular pathways governing and regulating the specific production of superoxide in the reproductive tissues of this plant have not been yet determined.

In this paper, we characterize the ROS-producing activity in olive pollen. For this purpose, we have cloned an *Rboh*-type gene from olive, designated as *OeRbohH*. It is mainly expressed in pollen, both during the ontogeny and the subsequent germination and tube growth. OeRbohH is a plasma membrane protein of the pollen tip. The use of specific NADPH oxidase inhibitors as well as antisense oligodeoxynucleotides (ODNs) to manage gene knockdown have demonstrated that OeRbohH is probably a tightly regulated protein required for ROS production in olive pollen. Furthermore, this ROS-producing OeRbohH activity has been revealed to be crucial for olive pollen germination and tube growth.

MATERIALS AND METHODS

Plant Material and Growing Conditions

Olea europaea L. plant material was collected from selected olive trees of the cultivar "Picual," located at the Estación Experimental del Zaidín (CSIC, Granada, Spain) or from 2-week *in vitro* germinated plantlets from embryos of the same cultivar, according to Zienkiewicz et al. (2011a). Olive pollen samples were collected during anthesis in large paper bags by vigorously

shaking the inflorescences and were sequentially sieved through 150- and 50-µm mesh nylon filters to eliminate debris. All biological samples were immediately used or stored at −80°C. Tobacco (*Nicotiana tabacum*) pollen was collected as previously described (Potocky et al., 2003).

Olive pollen *in vitro* germination was initiated by a pre-hydration step in a humid chamber at room temperature for 30 min. Pollen was then transferred to the germination medium (10% [w/v] sucrose, 0.03% [w/v] $Ca[NO_3]_2$, 0.01% [w/v] KNO_3, 0.02% [w/v] $MgSO_4$, and 0.03% [w/v] boric acid), as described previously (M'rani-Alaoui et al., 2002). Pollen was maintained at room temperature in the dark, and samples were taken after hydration and at different times of germination (5 min; 1, 2, 4, 6, and 8 h). Germinated and non-germinated pollen grains from each sample were separated by filtration through 50-µm and 20-µm meshes. Tobacco pollen was *in vitro* germinated according to Kost et al. (1998).

The NADPH oxidase inhibitor diphenylene iodonium chloride (DPI, Sigma) was added to the germination medium when indicated (50 µM final concentration stocked in 2% DMSO) either at the beginning of the process (to study germination inhibition) or when pollen grain had already germinated, that is, at the beginning of third hour of *in vitro* germination (to analyze the effect on the elongation). Negative control samples were treated with DMSO, in the same proportion (2% v/v). Pollen tube length was measured using ImageJ software (http://rsb.info.nih.gov/ij/).

Molecular Biology

Determination of OeRbohH Sequences

Total RNA was obtained from olive mature pollen (untreated pollen obtained immediately after anther dehiscence) using the RNeasy Plant Total RNA Kit (Qiagen). cDNA was synthesized with 1 µg of total RNA, $oligo(dT)_{19}$ primer and M-MLV reverse transcriptase (Fermentas), according to the manufacturer's instructions. Taq (BioTools) or Pfu (Promega) polymerases were used for PCR amplification purposes. RACE 3' and 5' were performed following manufacturer's specifications (SMARTer RACE, Clontech).

Gene Expression Analysis

Semi-quantitative PCRs for gene expression analysis were performed using specific primers designed at the 3′-untranslated region, with Oe18S as housekeeping gene. The number of cycles was optimized for both genes to avoid reactive depletion. For quantitative PCR (qPCR), total RNA was reverse transcribed using Transcriptor High Fidelity cDNA Synthesis Kit (Roche) according to manufacturer's instruction. Specific primers for qPCR were designed using the Primer3 software (http://frodo.wi.mit.edu/primer3/). Samples were prepared according to the LightCycler 480 SYBR Green I Master protocol, and a LightCycler 480 Instrument (Roche) was used for quantification. Relative gene expression was monitored and quantified after normalization with actin expression as the internal control. Fold variation over a calibrator was calculated using a method with kinetic PCR efficiency correction (Pfaffl, 2001), operating the relative expression ratio $R = (E_{target})^{\Delta CP\ target\ (control-sample)}/(E_{ref})^{\Delta CP\ ref\ (control-sample)}$, where E is the efficiency of target or reference amplification, and CP is the cycle number at the target or reference detection threshold (crossing point). PCR efficiencies were estimated from the calibration curves generated from the serial dilution of cDNAs.

Obtaining Upstream Regulatory Sequences

Genomic DNA was obtained using a NucleoSpin Tissue Kit (Macherey-Nagel). The upstream regulatory sequences were obtained by PCR walking, using an olive genomic DNA library generated according to Devic et al. (1997) as the template. Olive pollen genomic DNA libraries were generated by digestion with restriction enzymes (DraI, EcoRV, PvuII, ScaII, SspI, StuI, and HpaI) and ligation of known sequence adaptors in both extremes. MBLong polymerase (MOLBIOLAB) was used. A fragment of 1.8 kb from the start codon of *OeRbohH* was obtained.

Construction of the OeRbohH Promoter-β-Glucuronidase (GUS) Fusion

The fragment of 1.8-kb upstream the start codon of *OeRbohH* was amplified with specific primers incorporating a restriction site (**Supplementary Table 1**) to allow cloning into the binary vector pBI101.1 (Clontech) at the initiation codon of the promoterless *GUS* gene.

Construction of OeRbohH-GFP and OeRbohH-YFP Fusions

YFP fusion proteins were constructed in vectors pWen240 for (N-terminal fusion) and pHD32 (C-terminal fusion), under the control of the pollen-specific Lat52 promoter. Sequences were obtained using the specific forward oligonucleotide OeRboh-Ngo-F and the reverse oligonucleotides OeRboh-Xma-RS or OeRboh-Xma-RNS, to incorporate the appropriate restriction site.

Construction of OeRbohH Expression Vector

For open reading frame (ORF) cloning purpose, 2,502-bp-long cDNA of OeRbohH was cloned into the expression vector pET51b+ expression vector (Novagen). The sequence was amplified using the specific forward oligonucleotide OeXbaRbohF and the reverse OeSacRbohR, to incorporate in the appropriate restriction site (XbaI/SacI).

All primers used in this work are described in **Supplemental Data, Table S1**.

Biochemistry

Protein Extracts

For protein extraction, pollen was powdered in liquid nitrogen and re-suspended in extraction buffer [50 mM phosphate buffer (pH 7.8), 1mM PMSF] to a proportion of 15 ml solution per gram of fresh tissue, and proteins were eluted by stirring for 2 h at 4°C. After centrifugation at 13,000 ×g for 20min at 4°C, the supernatants were filtered through a 0.22-µm mesh and used for activity assays and Western blot analysis. The protein concentration in each sample was measured following the Bradford (1976) method, using the Bio-Rad reagent and bovine serum albumin (BSA) as standard.

Native PAGE and In-Gel NADPH Oxidase Activity Assay

Samples prepared as above were loaded into a 7.5% native acrylamide gel (80 µg protein per lane) as described by Davis and Ornstein (1964). Proteins were separated using a Mini-PROTEAN II system (Bio-Rad, U.S.A.).

The presence of NADPH-dependent production of $O_2^{\bullet-}$ was tested in gels by the NBT (Nitroblue tetrazolium) reduction method as previously described (Potocky et al., 2007). The gel was incubated in the developing solution [50mM Tris-HCL (pH 7.4), 0.2mM MgCl2, 1mM $CaCl_2$, 0.5 mg/ml NBT (Sigma), and 0.2 mM NADPH (Sigma)] and incubated at RT overnight under gentle shaking. The reaction was stopped by immersing the gel in distilled water. To test the effects of specific inhibitors, DPI (50 µM) and sodium azide (10 mM) were added to the developing solution.

In Vitro Expression of OeRbohH in *Escherichia coli* and Rise of an OeRbohH Antibody

Recombinant protein carrying a 10-His tag in N-terminus was over-expressed in *Escherichia coli* strain *BL21 Rosetta 2* (Novagen) according to Traverso et al. (2013a). An overnight pre-inoculum (1ml) was added to LB medium supplemented with 50 mg/ml of ampicillin and 34 mg/ml of chloramphenicol and incubated at 21–22°C until OD_{600} of 0.6 was reached. Expression was then induced with 0.4 mM isopropylthio-b-galactoside (IPTG), and cells were incubated for another 12 h. Finally, cells were harvested by centrifugation. Crude protein extracts corresponding to the disrupted bacteria, both from the expression construct and the negative control, were subjected to SDS-PAGE analysis. Differential bands were excised, digested with trypsin, and subjected to LC-ESI-MS/MS in the proteomic facilities of CNB-CSIC (Madrid, Spain). Mass data collected were used to search using a local Mascot server (Matrix Science, London, UK) against an in-house-generated protein database composed of protein sequences of *Viridiplantae*. Carbamidomethylation of cysteine (+57Da) and oxidation of methionine (+16Da) were set as variable modifications. Protein identification was confirmed using a Mascot's threshold score of identity at a 95% confidence level.

One of the fragments (corresponding to a 35-kDa band) was used to immunize hens in order to obtain a polyclonal antibody against OeRbohH (Davids Biotechnologie GmbH).

Immunoblotting of OeRbohH

Total protein per sample was loaded on 12% (w/v) polyacrylamide gels and electrophoresed using a Mini-PROTEAN 3 apparatus (Bio-Rad). After electrophoresis, proteins were electroblotted onto a polyvinylidene fluoride (PVDF) membrane in a Semi-Dry Transfer Cell (Bio-Rad) at 100V during 1h. For immunodetection, membranes were incubated in blocking buffer [3% (w/v) milk in Tris-buffered saline (TBS) buffer] at RT during 1 h, followed by incubation in primary antibody (anti-OeRbohH), diluted 1:1,000 in TBS buffer (pH 7.4) containing 0.1% (v/v) Tween-20 overnight at 4°C under shaking. Incubation in secondary antibody (1:2,000 dilution) conjugated to Alexa Fluor 488 (Invitrogen) was performed at RT during 1 h under agitation. The fluorescent signal was detected in a Pharos FX Molecular Imager (Bio-Rad).

Nucleic Acid Transfection

Arabidopsis thaliana Transformation and GUS Assays

Binary constructions were introduced into *Agrobacterium tumefaciens* (C58pMP90). *Arabidopsis* (*Arabidopsis thaliana*; ecotype Columbia) was transfected by the floral dip method (Clough and Bent, 1998). T1, T2, and T3 seedlings were selected *in vitro* on Murashige and Skoog medium supplemented with 1% (w/v) sucrose, 0.8% (w/v) agar, and 30 μg/ml kanamycin under a 16-h-light/8-h-dark regime at 22°C. Plants were cultivated in soil and under the same conditions as described above. GUS histochemical staining was performed according to Jefferson et al. (1987).

Biolistic Transformation

Germinated pollen grains from olive and tobacco were bombarded with gold particles alternatively coated with two different in-frame constructs of OeRbohH and the fluorescent yellow protein (YFP either at the amino- or the caboxi-terminus of the construct) and with the YFP alone (control), using the PDS-1000/He instrument (Bio-Rad) as previously described (Traverso et al., 2013a; Potocký et al., 2014).

Design of Antisense Oligodeoxynucleotides (ODNs) and Delivery Into Growing Pollen Tubes

OeRbohH sequence was tested for accessibility prediction and effective design of antisense ODNs with Soligo software (http://sfold.wadsworth.org/cgi-bin/soligo.pl). Proposed antisense and corresponding sense control ODNs were synthesized with phosphorothioate modifications in both the 5′- and 3′ terminus. Three antisense/sense ODNs pairs were essayed, and the most effective pair was selected (antisense: TAAGCAATCTTCGC CTGGTG; sense: CACCAGGCGAAGATTGCTTA). For the transfection, ODN-cytofectin complexes were prepared as described previously (Moutinho et al., 2001; Bezvoda et al., 2014) and incorporated to the germination medium. Control samples were incubated as described; however, no ODNs were used.

Microscopy Analyses

Immunocytochemistry

For immunocytochemistry, fresh anthers at different stages of development were prepared as described previously (Zienkiewicz et al., 2011b). Germinated pollen samples were fixed, and tube walls were digested as described before (Zienkiewicz et al., 2010). Slides containing semi-thin sections of olive anthers at different developmental stages and germinated pollen samples were incubated in blocking solution containing 1% (w/v) BSA in phosphate buffered saline (PBS) solution (pH 7.2) for 1 h at room temperature. OeRbohH was immunodetected by incubation of slides overnight at 4°C with the anti-OeRbohH primary Ab (diluted 1:10 in blocking solution) followed by an anti-chicken IgG-Alexa Fluor 488–conjugated secondary antibody (Ab) (Molecular Probes, USA) (diluted 1:100 in blocking solution) for

1 h at 37°C. In control sections, the preimmune serum was used. A few drops of an anti-fading solution of Citifluor (Sigma-Aldrich) were added, and samples were observed with a Zeiss Axioplan epifluorescence microscope under blue light irradiation.

Detection of $O_2^{\bullet-}$ Production

Detection of $O_2^{\bullet-}$ production in growing pollen tubes was determined by incubation in growth medium containing 1 mg ml^{-1} NBT for 5 min. Negative control experiments were carried out the same; however, no NBT was added to the growth medium. Inhibition experiments were performed by incubating pollen tubes in growth medium containing 50 μM DPI (30 min) before NBT staining. Alternatively, the effect of sodium azide (10 mM) was also tested. Samples were observed with a Zeiss Axioplan microscope under bright field. Quantification of the intensity of the dark purple-colored precipitate was performed in the pollen tubes through 50 μm along the apical region of the pollen tubes starting at the pollen tube apex. Quantification was achieved by using the Nikon EZ-C1 viewer (3.30) software, selecting the region of interest (ROI) and analyzing pixel intensity, which was referred to the area of the ROI, therefore calculating the ratio color intensity/area in arbitrary units. Both average and standard deviation were calculated after measurement of a minimum of 10 images of pollen tubes per experiment, along three independent experiments.

Bioinformatic Tools

Protein amino acid sequences were aligned using Clustal Omega multiple alignment tool with default parameters (McWilliam et al., 2013). Phylogenetic trees were constructed with the aid of the software SeaView (Gouy et al., 2010) using the maximum likelihood (PhyML) method and implementing the most probable amino acid substitution model (LG) previously calculated by the ProtTest 2.4 server (Darriba et al., 2011). The branch support was estimated by bootstrap resampling with 100 replications. OeRbohH motifs were predictively analyzed by the software "PredictProtein" according to the proteins HsNox2 (Sumimoto, 2008; von Lohneysen et al., 2010) and OsRbohB (Oda et al., 2010).

Statistical Analysis

Statistical significance was determined by Kruskal–Wallis one-way analysis of variance followed by Kruskal–Wallis Multiple-Comparison Z-Value Test (Dunn's Test).

RESULTS

OeRbohH Is an Rboh-Type Gene Present in the Olive Tree, Which Is Mainly Expressed in Pollen

Considering that superoxide ($O_2^{\bullet-}$) generation in mature pollen is described as mainly produced by the physiological activity of NADPH oxidases (Potocky et al., 2007); we decided to investigate the occurrence of NADPH oxidases in the olive (*O. europaea* L.) tree. For such purpose, we initially obtained the sequence of an olive Rboh gene expressed in pollen. Several pairs of degenerated primers were designed on conserved domains identified in other species (**Supplemental Data, Figure S1**). Using primers OeRboh804F and OeRboh2286R, we initially sequenced a 300-bp fragment. From this nucleotide sequence, two primers were designed and used to obtain the 5' and 3'UTR (untranslated) sequences by RACE (rapid amplification of cDNA ends) (OeRbohRW2 and OeRbohFW2, respectively). This enabled us to obtain the whole coding sequence (CDS) of 2,502bp (GenBank KX648357).

The corresponding translated amino acid sequence was denominated OeRbohH according to its identity with AtRbohH (62.11%), which was higher than that displayed with AtRbohJ (60.77%). It also contained all the characteristics structural and catalytic motifs to be considered as a plant Rboh (**Figures 1A, B**). Secondary structural motifs and domains were identified *in silico* accordingly to the proteins HsNox2 (Sumimoto, 2008; von Lohneysen et al., 2010) and OsRbohB (Oda et al., 2010), and the predictive software "PredictProtein." Thus, OeRbohH enzyme was predicted to contain six α-helix transmembrane domains—which included the conserved heme-coordinating His residues—together with two terminal cytosolic extensions. The C-terminus contained four sites for NADPH binding and two sites for FAD binding, and the N-terminal end was predicted to contain two EF-hand Ca^{2+}-binding motifs (**Figures 1A, B**).

Moreover, a phylogenetic analysis among OeRbohH and other available plant Rboh sequences showed OeRbohH clustered in a subgroup containing the pollen specific Rbohs from *A. thaliana* and tobacco (**Figure 1C**), which are the unique pollen-specific Rbohs identified so far (Potocky et al., 2007; Boisson-Dernier et al., 2013). In addition, primers OeRbohF and OeRbohR were designed and used to amplify the genomic sequence (GenBank KX648358) corresponding to the whole ORF (4,025 bp). Alignment between the obtained genomic sequence and the corresponding ORF allowed us to identify 13 introns (**Supplemental Data, Figure S2**) whose positions relative to the ORF were conserved within the plant Rboh family (**Supplemental Data, Figure S3**).

With the purpose of studying gene expression pattern of OeRbohH, a pair of primers was designed in the 3'UTR region of OeRbohH, and cDNAs from different vegetative and reproductive organs were synthesized to be used as template. Semiquantitative PCRs were carried out in a first approach, and OeRbohH expression was almost exclusively detected in flowers (**Figure 2A**, see discussion). Within the flower, expression was detected in pollen (**Figure 2A**) and not in the gynoecium.

We also measured the gene expression level of OeRbohH throughout pollen ontogeny by using cDNA from anthers at different stages. OeRbohH was expressed both during microsporogenesis (pollen mother cells to the tetrad stage) and microgametogenesis (**Figure 2A**). Evidently, this result does not allow us to discriminate whether the expression of OeRbohH in the anther takes place in the sporophytic or the gametophytic tissues. In addition, taking into account that pollen Rbohs has been suggested to be involved in pollen tube growth (Kaya et al., 2014; Lassig et al., 2014); qPCR analysis was performed in the course of pollen *in vitro* germination. Variations of gene

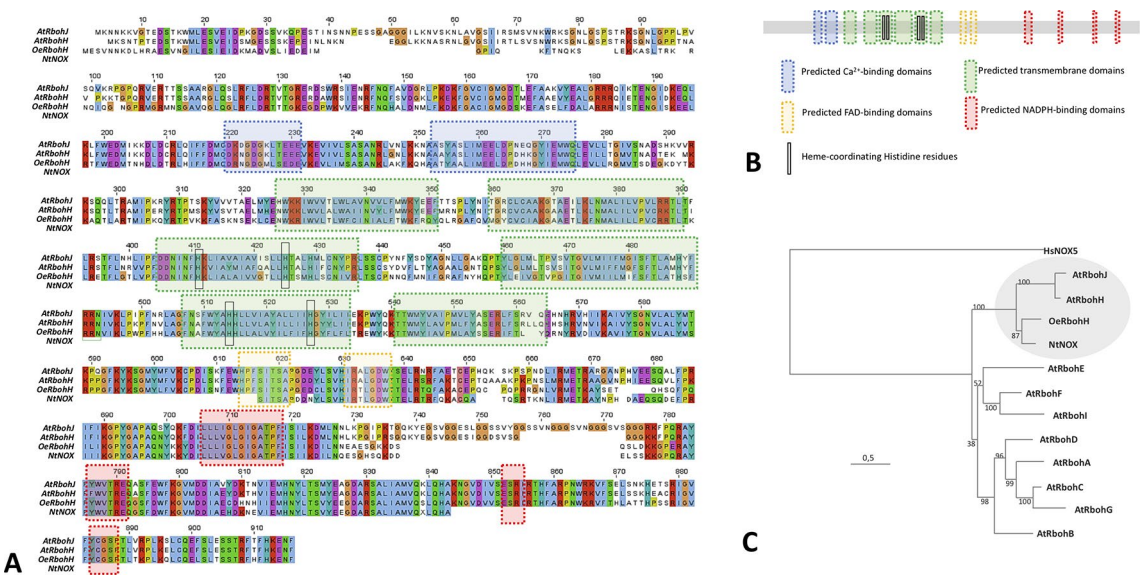

FIGURE 1 | (A) Amino acid sequence alignment and predicted motifs of OeRbohH, AtRbohH, AtRbohJ, and NtNOX. Conserved residues are highlighted in red. The blue boxes indicate the predicted calcium-binding domains (2). Predicted transmembrane domains (6) are boxed in green, including the conserved heme-coordinating histidine residues (4) highlighted with black circles. The predicted FAD-binding sites are marked with purple boxes (2). Predicted sites for NADPH binding (4) are indicated with red boxes. **(B)** Analogous color coding was used to show domains/motifs in a simplified diagram of OeRbohH. **(C)** Phylogenetic relationships of the 10 NADPH oxidase proteins from *Arabidopsis* (AtRbohA-J), together with olive pollen OeRbohH and a partial tobacco pollen sequence Rboh NtNOX. The tree was constructed by the maximum likelihood (ML) from Clustal Omega multiple alignment and rooted with human NOX isoform HsNOX5. Numbers at nodes indicate bootstrap values. The circle marks the putative pollen-Rboh subgroup.

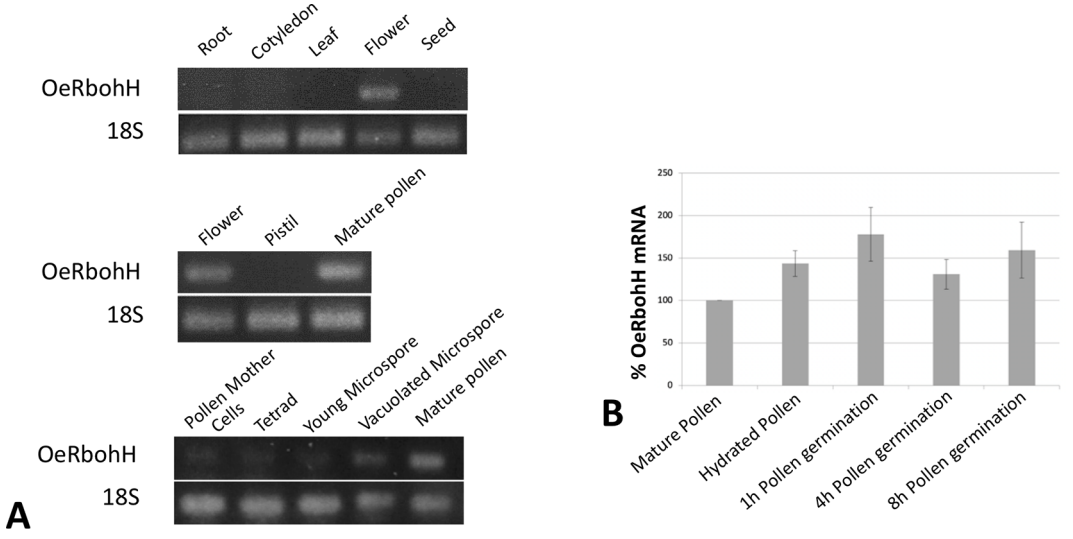

FIGURE 2 | (A) OeRbohH expression analysis using semiquantitative PCR of seedling and tree tissues (upper panel), floral tissues (medium panel), and pollen ontogeny (lower panel). **(B)** mRNA levels of OeRboh determined by real-time PCR in pollen along *in vitro* germination, expressed as percentages compared to the mRNA level of the mature pollen (100%). Averages of three biological replicates ± SD are presented. No significant differences were found. ANOVA test ($p < 0.05$).

expression at these stages would differently involve OeRbohH in different aspects of pollen physiology. However, the expression level of OeRbohH during pollen tube growth was rather stable, with a relative, although not statistically, significant peak of expression at 1 h of *in vitro* germination (**Figure 2B**).

In order to improve our knowledge about OeRbohH, we also decided to analyze the expression pattern of the reporter gene β-glucuronidase (GUS; UidA) under the control of a 1.8-Kb fragment from the upstream regulatory sequences of OeRbohH in *Arabidopsis thaliana* transgenic lines. However,

in these lines, we were unable to detect UidA expression (data not shown), which is in good agreement with the low expression level found during the semi-quantitative analyses (see discussion).

Bacterial Expression of OeRbohH and Determination of the Specificity of the Risen Antibody

In vitro expression of OeRbohH in *E. coli* as a recombinant protein tagged with a multiple His was monitored by SDS-PAGE. The *E. coli* strain expressed OeRbohH efficiently, although the extracts of the induced cultures displayed three differential bands of c.a. 100, 80, and 35 kDa in the insoluble fraction, the latter showing reactivity to an anti-His Tag antibody in further Western blotting experiments (**Supplemental Data, Figure S4, A, B**).

The three bands were excised from gels and subjected to mass spectrometry (MS) analysis. They were identified by LC-ESI-MS/MS (liquid chromatography–electroSpray ionization–tandem mass spectrometry) as different fragments corresponding to translated product of OeRbohH (**Supplemental Data, Table S2**). Fragment 3 was used to obtain the antibody (see material and methods).

The binding specificity of the anti-OeRbohH antibody developed in hen was tested by immunoblotting (**Supplemental Data, Figure S4, C**). The antibody recognizes a single band in the membranes resulting from the transference of native gels with electrophoresed extracts of both mature pollen and pollen during *in vitro* germination. These bands were coincident in electrophoretic mobility with the activity bands revealed by in-gel NADPH oxidase activity assay (**Supplemental Data, Figure S4, D**).

Using this anti-OeRbohH antibody, we performed the immunoanalysis to investigate the protein expression during pollen ontogeny and *in vitro* pollen germination (**Figure 3A**). One band was detected in all of the developmental stages analyzed, although cross-reactivity with other Rboh isoforms expressed in anthers could not be rejected. We then probed pollen protein extracts at different times after the onset of the *in vitro* germination, and a single band was detected during the process (**Figure 3B**).

OeRbohH Protein Localizes in Both the Developing Pollen Grains and the Sporophytic Tissues of the Anther

Immunohistochemical experiments were performed to localize OeRBOH *in situ* along pollen ontogeny. OeRbohH antibody signals were evident not only in the developing pollen grains but also in some cell types from the sporophytic surrounding tissues (**Figure 4**).

Young anthers containing pollen mother cells were barely labeled (**Figure 4A**). Anti-OeRbohH labeling was detected during microsporogenesis at spots placed in the vicinity of the plasma membrane within the tetrad. In addition, signal was likewise detected in a low level in both the anther wall layers (**Figure 4B**). These anther tissues showed a more evident OeRbohH labeling after microspore release (**Figure 4C**). OeRbohH signal was located at the plasma membrane of young free microspores

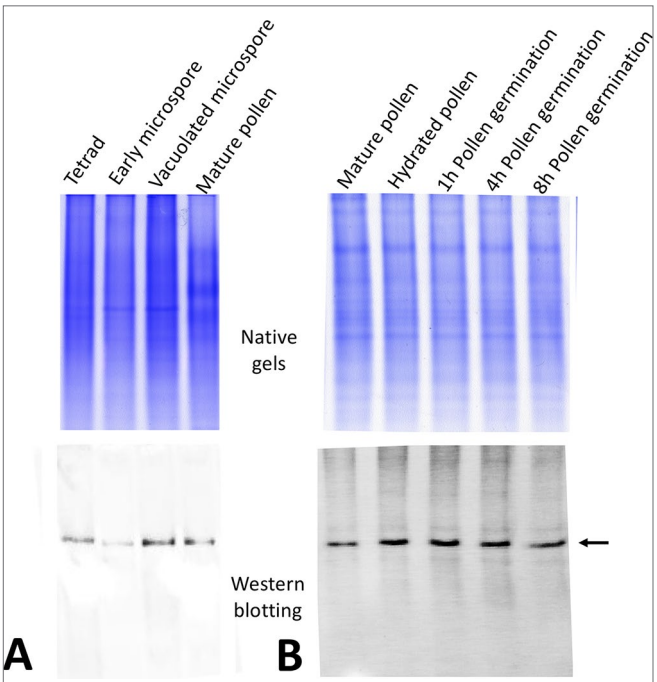

FIGURE 3 | OeRbohH protein expression along pollen ontogeny **(A)** and *in vitro* pollen germination **(B)**. Western blot using the anti-OeRbohH antibody (lower panel) was performed after native-PAGE (upper panel).

(**Figure 4C**, magnification) and vacuolated microspores which were also labeled intracellularly at unidentified spots/rings (**Figure 4D**). The mature pollen grain showed signal at the plasma membrane and also at cytoplasmic spots (**Figure 4E**). During pollen maturation, fluorescence was present in both the endothecium and the tapetum remnants (**Figures 4D**, **E**, magnifications). Negative control sections, treated with the preimmune serum instead of the anti-OeRbohH antibody, showed no relevant fluorescent signal (**Figure 4F**).

OeRbohH Is a Plasma Membrane Protein With Enhanced Activity at the Pollen Tip, Whose Activity Must Be Highly Regulated

OeRbohH localization during olive pollen tube growth was carried out by immunohistochemistry. *In vitro* germinated pollen displayed enhanced fluorescence at the pollen tube tip since tube emergence, and until the tube reaches high lengths (**Figure 4G–I**), in contrast with the samples subjected to the control treatment (**Figure 4J**), which displayed no signal.

We also used an *in vivo* strategy to analyze the subcellular localization of OeRbohH. The fluorescent chimeras OeRbohH-YFP or YFP-OeRbohH were transiently expressed in growing pollen tubes of a heterologous system (tobacco) by biolistic transformation driven by the control of the pollen-specific Lat52 promoter, whereas olive pollen transformants were barely found. Pollen tubes expressing YFP only showed homogenous fluorescence signal all-through the pollen tube cytoplasm (**Figure 5A**). Alternatively, growing pollen tubes transformed with the YFP-OeRbohH (**Figure 5B**) or

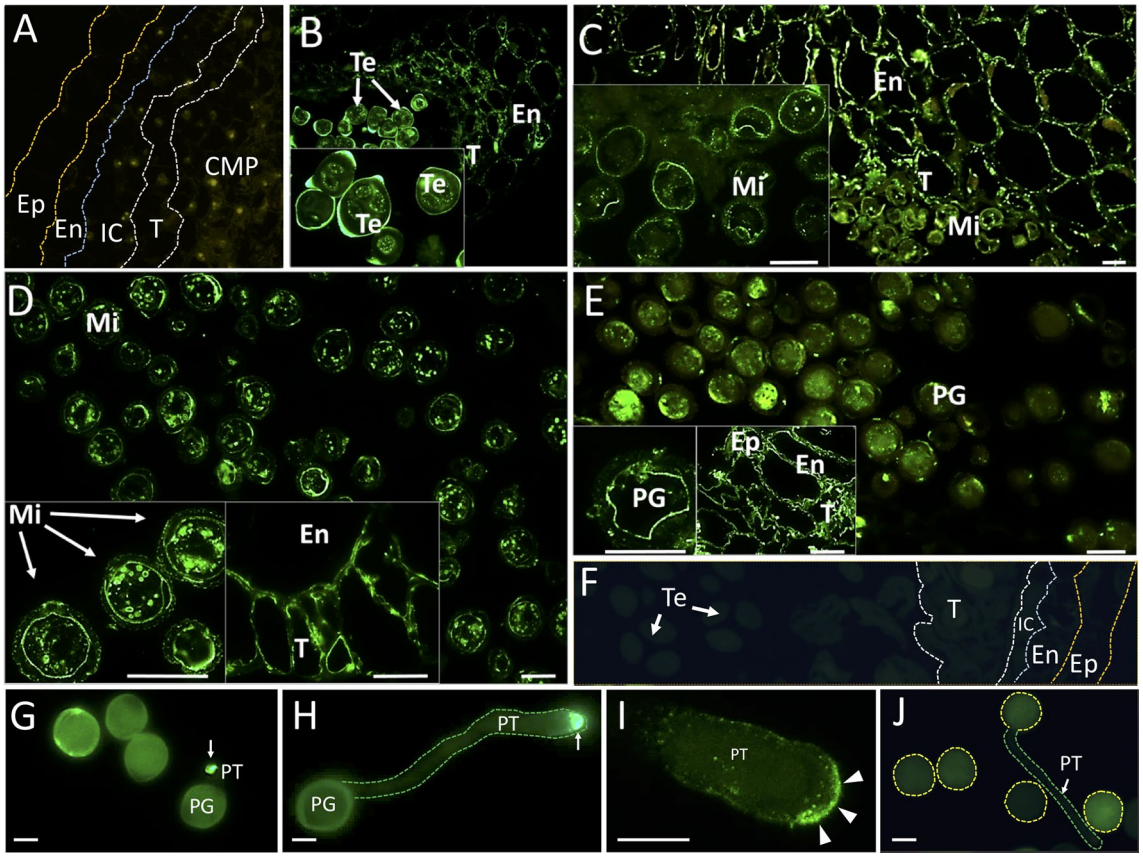

FIGURE 4 | Fluorescence microscopy localization of OeRbohH in the olive anther and *in vitro* germinated pollen grains. Sections from olive anthers at the following stages: pollen mother cells prior to meiosis **(A)**, tetrads **(B)**, young microspores **(C)**, vacuolated microspores **(D)**, and mature pollen **(E)** were incubated with an anti-OeRbohH Ab, followed by an anti-chicken IgG-Alexa Fluor 488–conjugated secondary Ab. In insets, detailed view of gametophytic tissue is shown in B-E. Right insets in D and E show a detailed view of the sporophytic tissues of the anther. Negative control sections (anthers at the tetrad stage) were treated with the preimmune serum **(F)**. *In vitro* germinated pollen grains were also used for fluorescence microscopy localization of OeRbohH. Recently emerged pollen tube showed intense labeling at the pollen tube tip (**G**, arrow). Elongated pollen tubes also showed intense labeling at the tip (**H**, arrow). High magnification of the pollen tube apex after immunolocalization of OeRbohH **(I)**. The protein accumulates at the very tip, although it can be also weakly localized at the plasma membrane (arrowheads). Negative control (using the preimmune serum as the primary antibody) did not show labeling **(J)**. Note the autofluorescence of the exine. En, endothecium; Ep, epidermis; IC, intermediate cells; Mi, microspore; MP, mature pollen grain; T, tapetum; Te, tetrad; YP, young pollen. Bar = 20μm. Boundaries of the anther layers and the pollen grain/pollen tube contour are shown for reference in several pictures **(A, F, H, J)**.

OeRbohH-YFP (**Figures 5C–F**) constructs were preferentially labeled at the tip plasma membrane along with signal detected in the cytoplasm and the endomembrane system (**Figures 5B, C**), as it has been previously reported in *Arabidopsis* pollen (Boisson-Dernier et al., 2013; Lassig et al., 2014). Accumulation of fluorescence also occurred at the proximal boundary of the callose plugs (referred to the pollen grain) in the OeRbohH-YFP transformed pollen tubes (**Figure 5D**). Several morphological alterations, i.e., accumulations in the endomembrane system and presence of accumulation spots (**Figures 5E, F**), suggest a physiological unbalance due to an excess of OeRbohH in the transformants. Furthermore, pollen tube elongation was reduced in the transformant grains (**Figure 5G**).

OeRbohH is an Rboh-type protein from olive, which localizes to the plasma membrane and endomembranes in the growing pollen tube tip and whose over-expression affects pollen tube integrity and physiological growth.

Oxidative Burst in the Olive Pollen Tube Tip Depends Mainly on NADPH Oxidase Activity

To provide empirical evidence supporting the involvement of NADPH oxidase activities during the germination of olive pollen, as it has been previously proposed for model plants such as *Arabidopsis* or tobacco (Potocky et al., 2007; Boisson-Dernier et al., 2013), a set of experiments were carried out during olive pollen *in vitro* germination. The short-lived superoxide radical was preferentially produced at the tip of the growing pollen tube as it was revealed by the NBT staining (**Figures 6A, B, D**). Occasionally, the cytoplasm in the proximity of the proximal end of the callose plugs (referred to the pollen grain) was also labeled (**Figures 6C, D**).

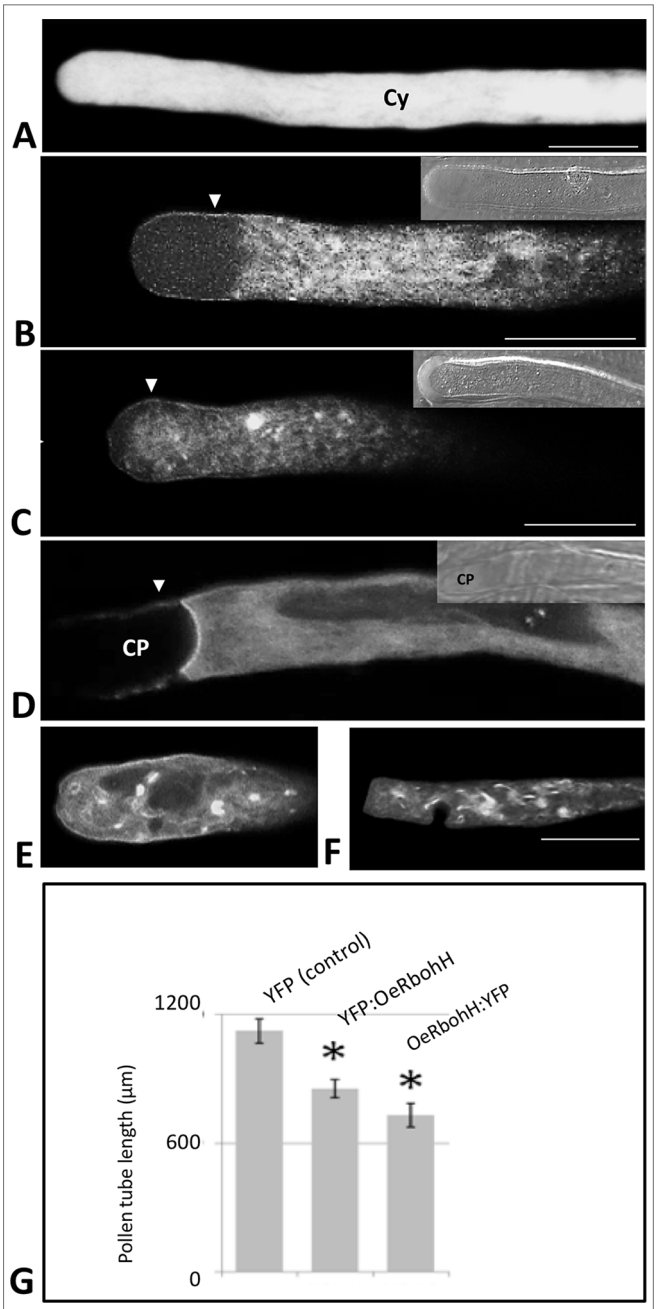

FIGURE 5 | Transient expression of OeRbohH in tobacco pollen tubes as YFP fusions, observed by CLSM. **(A)** YFP construction alone (control) showed homogeneous yellow fluorescence throughout the cytoplasm of the pollen tube. **(B)** YFP : OeRbohH and **(C–F)** OeRbohH : YFP transformants showed labeling in the plasma membrane (arrowheads) as well as in the cytoplasm without significant differences among both constructs. **(D)** Fluorescence was also observed at the edge of callose plugs in their proximal side (referred to the pollen grain). The majority of transformed pollen tubes showed accumulation spots **(C, E, F)** and abnormal phenotypes (i.e., swelling) at the tip **(E–F)**, and their growth was significantly inhibited after 4h *in vitro* culture **(G)**. Insets at pictures **B**, **C**, and **D** show bright field images of the pollen tubes for reference. CP, callose plug; Cy, cytoplasm. *indicates that the mean is significantly different from the control at $P < 0.05$. n = 100 from three independent experiments. Bars = 20 µm.

In addition, with the aim of determining the physiological role of NADPH oxidases in germination and pollen tube growth, the NOX inhibitor DPI, which has been shown to inhibit both mammalian and plant oxidases (Frahry and Schopfer, 1998; Chen et al., 2013; Altenhöfer et al., 2015), was added to the germination medium. Such addition led to a dramatic reduction in the staining due to superoxide radical. In order to discriminate between NADPH oxidase and peroxidase activities as $O_2^{\bullet-}$ sources (Carter et al., 2007), we assayed the sensitivity of the staining to sodium azide, which has been described to inhibit different peroxidases (Ortiz de Montellano et al., 1988; Tuisel et al., 1991; Gabison et al., 2014). In this case, no inhibition of the staining was detected (**Figure 6E**). Likewise, germination ratio was 4-fold reduced when the samples were treated with DPI at the very beginning of the *in vitro* germination process (**Figure 7**). NADPH oxidase activity resulted equally critical for pollen tube growth as tube length effectively decreased when the inhibitor was added during the *in vitro* germination process (**Figure 7**). In agreement with the results described above, NADPH oxidase enzymatic activity observed after native PAGE (**Figures 8A, C**) experienced some decrease upon pollen hydration and then was progressively enhanced throughout olive pollen *in vitro* germination when compared to the mature pollen grain. The DPI addition inhibited this activity, while the in-gel activity was not affected by azide (**Figures 8B, D**).

We also carried out olive pollen transfections with specific sense/antisense ODNs corresponding to the OeRbohH ORF sequence. Although a slight difference in pollen tube length average was observed when germinated pollen grains were treated with sense ODNs, this difference was not statistically significant. Alternatively, the treatment with antisense ODNs produced a relevant and statistically significant reduction in both the pollen tube growth and the superoxide production, which visualized as a decrease in NBT staining (**Figure 9**).

DISCUSSION

In this work, we have carried out a complex characterization of a superoxide-producing Rboh-homologous protein from olive pollen (OeRbohH), which allowed us to identify it as a key protein involved in both pollen germination and pollen tube growth.

Studies focused on ROS production in pollen from different species have revealed that the enzymatic origin of these chemicals is controversial, as well as the localization of these oxygen metabolism products. In fact, it has been suggested that the classically used NOX-inhibitor DPI may cause tube growth inhibition not just because it could be affecting NADPH oxidase activity but also inhibition of other flavoenzymes (Lassig et al., 2014). According to this view, the activity of mitochondrial NAD(P)H dehydrogenases has been suggested to be involved in ROS production in lily (*L. formosanum*) pollen (Cardenas et al., 2006). The presence of different sources of ROS may also suggest different localizations of the product. In lily, ROS are detected in the subapical region of the pollen tube, a cell position also coincidental with most of mitochondria present

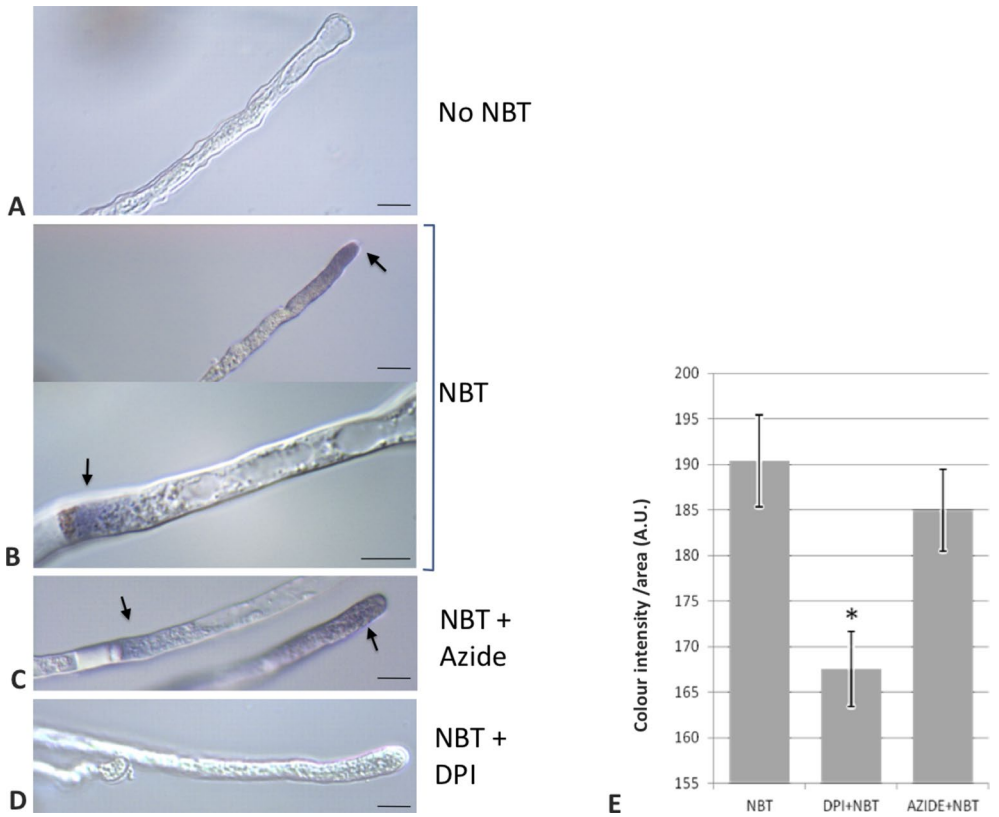

FIGURE 6 | Detection of $O_2^{\bullet-}$ putatively generated by NADPH oxidase activity in pollen tubes. **(A)** Control sample incubated in growth medium in the absence of NBT. **(B)** NBT precipitate is observed in the pollen tube near the apex and in the proximity of callose plugs. **(C)** NBT stain remains even in the presence of sodium azide, an inhibitor of NADPH peroxidase. **(D)** Addition of NBT in the presence of DPI, an inhibitor of NADPH oxidases, did not lead to staining. **(E)** Quantification of the precipitate intensity along 50 µm of the apical region of the pollen tubes. Data represent means ± SEM. *indicates that the mean value is significantly different from the control at $P < 0.001$. n = 100 from three independent experiments. Bars = 10 µm. NBT, NBT-treated samples; DPI+NBT, samples treated with NBT and DPI; AZIDE+NBT, samples treated with NBT and sodium azide; A.U., arbitrary units.

in this structure. Contrary to that, in tobacco growing pollen tubes, ROS are concentrated at the pollen tube tip (Potocky et al., 2007), and NADPH oxidase has been proposed as the source for superoxide. Moreover, in *Arabidopsis* pollen, and although NADPH oxidase-produced ROS were detected at the tip, the signal was higher in the shank of the pollen tube (Boisson-Dernier et al., 2013), and the authors suggested mitochondria as well as peroxisomes as the possible origins for these chemical species. This dual pollen-ROS source was also suggested in other study carried out in *P. meyeri* (Liu et al., 2009). Furthermore, in kiwifruit pollen tube, there is not a clear tip pattern of ROS generation (Speranza et al., 2012), whereas in cucumber, ROS are detected at the apex during germination onset but in the whole tube throughout the progress of the pollen tube growth (Sirova et al., 2011). Also, a double localization is proposed for pollen specific Rbohs: RbohH and J are both detected in the subapical region, but RbohJ was also located in the pollen shank (Lassig et al., 2014). Thus, further analyses are needed to clarify these potential species-related differences.

We decided to investigate the involvement of Rboh proteins in the sexual plant reproduction of the non-model species *O. europaea* L., not only due to its economic importance but also considering the proposed link between the ROS produced by pollen-intrinsic NADPH oxidase activity and the allergic inflammatory response (Bacsi et al., 2005; Dharajiya et al., 2008). Olive pollen allergy is an especially important disease in the case of olive in Mediterranean countries (Liccardi et al., 1996). This possible pollen NADPH oxidase ability to trigger allergy symptoms (Pazmandi et al., 2012) has already been suggested for other allergenic pollen grains owning NADPH oxidase activity (Boldogh et al., 2005; Wang et al., 2009), although disagreeing studies are also found (Shalaby et al., 2013). OeRbohH must be also considered the first Rboh protein involved in sexual plant reproduction characterized in a tree (Potocky et al., 2007; Kaya et al., 2014).

One of the first challenges to develop this work was the lack of available genomic databases from olive at the time of the onset of the study. This fact forced us to identify conserved domains from different plant Rbohs to design degenerated primers. These included three Rboh sequences, which were decisive for such propose. We initially isolated a first coding fragment, and then, using a variety of PCR-based methodologies, we were able

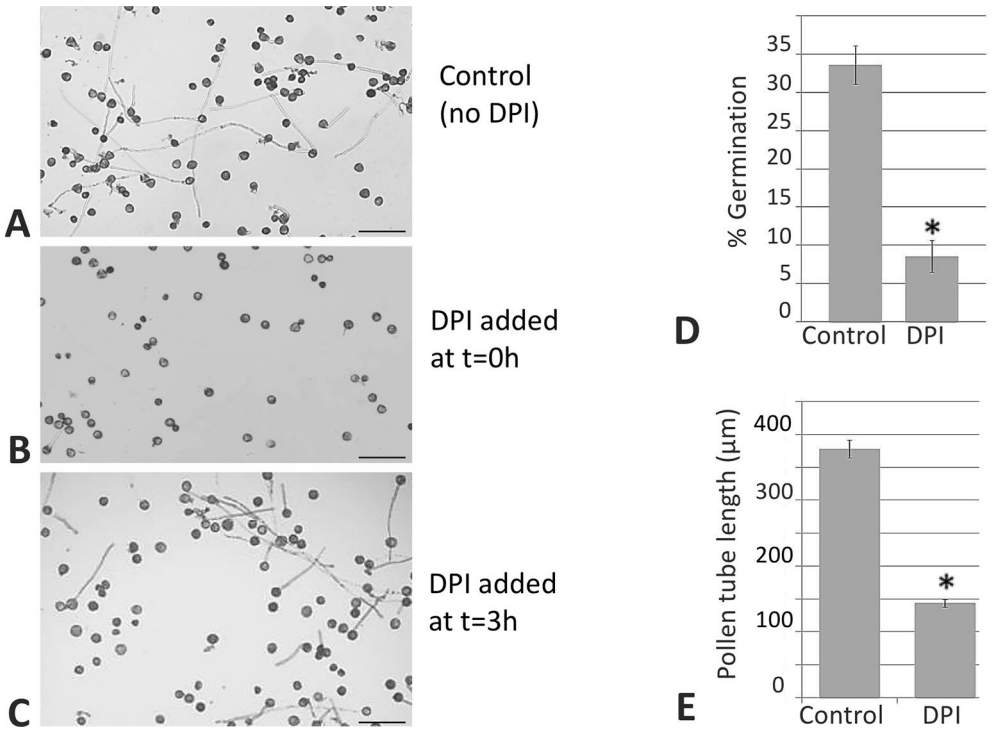

FIGURE 7 | DPI inhibits germination and pollen tube elongation. Control sample **(A)**. When the NADPH oxidase inhibitor was added at the beginning of the process, the *in vitro* germination percentage was affected **(B)**. When the inhibitor was added during the germination, the length of the pollen tube was affected **(C)** in both cases when compared to the control. Representative pictures from three independent experiments are shown. Quantification of the germination rate **(D)** and pollen tube lengths **(E)**. Data represent means ± SEM. n = 100. *indicates that the mean is significantly different from the control at $P < 0.05$. Bars = 100 µm.

to obtain both the coding and the whole genomic sequences of a Rboh-homologous protein from olive pollen. According to sequence similarity and intron positions, our translated protein can be clustered in the subgroup of plant Rboh proteins showing preferential expression in pollen grain, where AtRbohJ and AtRbohH from *A. thaliana* and a NtNOX from tobacco are included (Potocky et al., 2007; Boisson-Dernier et al., 2013). According to this similarity, the olive sequence was also named as OeRbohH, due to the high level of identity with pollen AtRbohH from *A. thaliana*. These results will be reviewed after the recent release of an olive genome draft (Cruz et al., 2016), which allowed retrieving 12 genomic sequences similar to Rboh (unpublished results), together with the implementation of an improved olive reproductive transcriptome, now underway after the generation of new Illumina sequencing reactions and RNA-Seq analysis. Such new data will allow assessing the possibility of other OeRboh genes being expressed in the anther tissues at prior stages of pollen development or even at the mature pollen grain itself, as the result of the higher reliability and the increased number of readings.

Using a PCR-walking approach, we also obtained a fragment of 1.8kb from the 5-upstream region of OeRbohH. However, this regulatory fragment was not able to yield detectable GUS activity in the generated transgenic lines of *A. thaliana*. Although this result was initially intriguing, we thought it was due to a low gene level expression of OeRbohH. This suggestion agrees with the low-level expression that we found during the PCR quantification experiments. According to this fact, it must be mentioned that a pollen-specific Rboh promoter analysis was included in a study focused on low expressed genes in *Arabidopsis* (Xiao et al., 2010). This low expression was also revealed for OsRbohH in a previous study (Wong et al., 2007). In addition, several Rboh genes from *Medicago truncatula* were not included in a promoter study by GUS fusion approach, because of their very low gene expression levels (Marino et al., 2011). We have attempted different approaches focused to the detection of low GUS activity in order to improve histochemical detection (Rech et al., 2003), with identical negative results.

OeRbohH was almost exclusively expressed in pollen and anthers. Similarly, Kaya et al. (2014) showed that AtRbohH as well as AtRbohJ are specifically expressed in the pollen grain and pollen tubes of *Arabidopsis* flowers. Curiously, we also noticed a very low level of expression in seeds and seedling roots, which were only observed when a high number of PCR cycles were used (not shown).

We have also shown here the occurrence of OeRbohH during olive pollen ontogeny. The results are in accordance with a previous study where superoxide production was detected in the rice anther in a stage-dependent way, with the localization restricted to tapetal cells and microspores (Hu et al., 2011). These authors detected a low level of superoxide anion before meiosis, followed by a noticeable increase during the

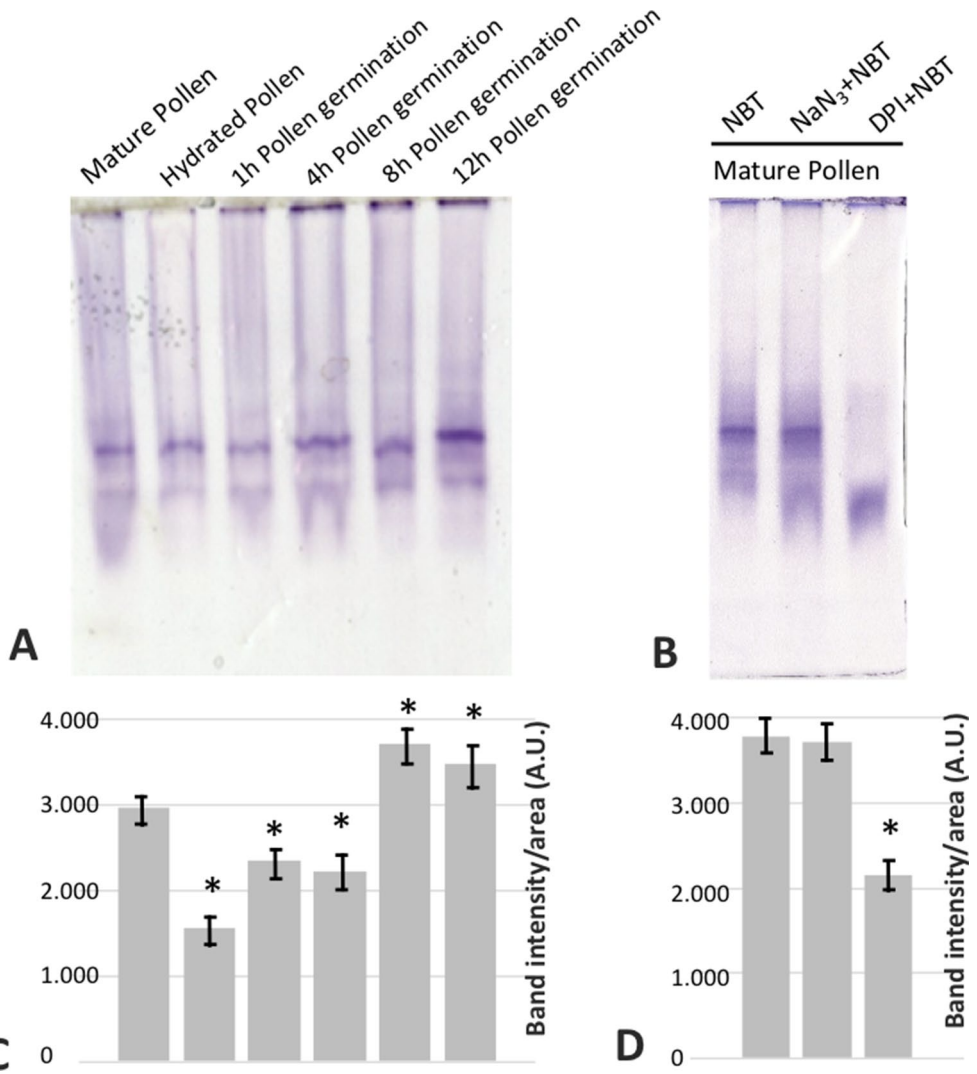

FIGURE 8 | (A) In gel NADPH oxidase activity of mature (MP), hydrated (H), and germinated pollen extracts at different times (1, 4, 8, and 12 h) fractionated by native PAGE (50 μg/lane). **(B)** In mature pollen, the activity revealed by NBT was challenged by the addition of sodium azide or DPI during the incubation. **(C, D)** Densitometry quantification of NADPH oxidase activity as in **(A)** and **(B)**, respectively. *indicates that the mean from three independent experiments is significantly different from the control (mature pollen) at $P < 0.05$.

formation of the tetrads (anther developmental stage 8), and especially when the free microspores were released (stage 9). The following stages showed again a low amount of superoxide, until the rise of mature pollen (stage 12), exhibiting increased superoxide content once again. This pattern is in line with our results regarding superoxide localization (Zafra et al., 2010) in the olive anthers through flower development and indirectly supports our findings concerning OeRbohH gene expression and immunohistochemistry.

OeRbohH immunolocalization during pollen ontogeny is in good agreement with the results obtained by PCR. However, we cannot exclude that the signal may also correspond to cross-reaction with other Rboh proteins present in gametophytic and/or sporophytic germlines. In fact, the importance of the Rboh homologous *RbohE* in the tapetal programmed cell death to proper pollen development has been recently highlighted (Xie et al., 2014).

In addition, different transcriptomic data also indicated that AtRbohH and AtRbohJ increased their expression levels throughout the microgametogenesis, mainly after the second pollen mitosis originating tricellular pollen (Honys and Twell, 2004). According to our results, the present work would be the first evidence about the presence of pollen RbohH proteins during pollen ontogeny in both the gametophytic and sporophytic tissues of the anther.

The presence of transmembrane domains as well as the protein size initially represented a challenge for the recombinant expression of OeRbohH and the subsequent purification process. A recombinant Rboh-type protein from *Arabidopsis* was successfully obtained by Zhang et al. (2009), and we were

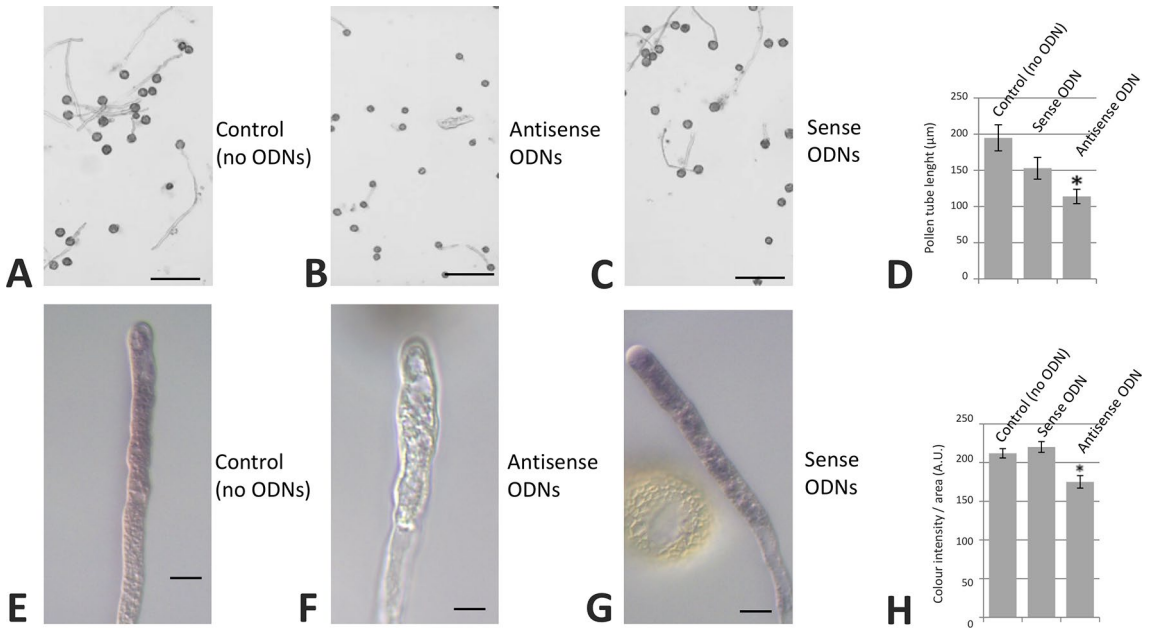

FIGURE 9 | Transfection of olive pollen tubes with OeRbohH-specific antisense oligodeoxynucleotides (ODNs). The OeRbohH sequence obtained was used to design antisense ODNs. Control samples **(A, E)**. Transfection of olive pollen tubes with such antisense ODNs resulted in pollen tube growth inhibition **(B)** as well as in a reduction of the production of tip-localized $O_2^{\bullet-}$ **(F)** when compared with the control samples or the sense ODNs **(C, G)**. Quantification of pollen tube lengths **(D)** and precipitate intensity **(H)**. Data represent means ± SEM; n = 300. *indicates that the mean value is significantly different from the control at $P < 0.05$. Bars in upper panel = 100 µm. Bars in bottom panel = 10 µm.

encouraged to carry out a similar approach. However, the obtained results were different, as RbohH was *in vivo* digested by the host (*E. coli*) during the recombinant expression, yielding three protein fragments mainly identified in the non-soluble protein fraction. This fact was used (after band identifications) to obtain a polyclonal antibody, which ultimately helped us to obtain several important results and conclusions.

Using the polyclonal antibody anti-OeRbohH as well as the YFP fusions, we have shown the occurrence of RbohH in plasma membrane, as it has previously been described for other Rboh isoforms (Keller et al., 1998; Sagi and Fluhr, 2001; Wong et al., 2007; Takeda et al., 2008) and for AtRbohH and J (Boisson-Dernier et al., 2013; Kaya et al., 2014). YFP fluorescence was detected at the plasma membrane and also intracellularly in the endomembrane system with analogous pattern for both constructs, suggesting that the position of the tag does not affect fusion protein localization. Together with the plasma membrane localization, the isoform RbohF is associated with internal membranes (Drerup et al., 2013). Intracellular presence of NtRbohD was also reported in the form of what the authors (Noirot et al., 2014) called rings (identified as Golgi) and dots (suggested to be exocytic compartment). In addition, Lassig et al. (2014) localized *Arabidopsis* pollen Rbohs also at the cytoplasm. Previous Western blotting assays of Rbohs after membrane fractionation drove to a weak signal in internal membrane fractions, which was considered a contamination by the authors (Heyno et al., 2008). In mammals, NOX2 was found at the plasma membrane as well as in endosomes, and NOX4 was described to accumulate in intracellular membranes, the endoplasmic reticulum, and the nuclear compartment (Ushio-Fukai, 2006). However, the presence of NADPH oxidases associated with endomembrane system is not as well documented in plant as in animals.

Our data indicate a critical role of OeRbohH in the control of pollen germination and pollen tube elongation. Initially, we detected a decrease of NADPH oxidase activity when olive mature pollen became hydrated and this activity then raised during the whole process of germination. This activity has been suggested to be involved in changes in the mechanical features of the pollen cell wall during pollen elongation (Smirnova et al., 2014). Contrary to the NADPH oxidase activity, no significant differences were found in OeRbohH gene expression with a relative rise after 1 h of *in vitro* germination. These steady gene expression levels are in good agreement with the data extracted from transcriptome analysis previously achieved in *Arabidopsis* pollen *in vivo* and through semi-*in vivo* germination, and pollen tube growth (Wang et al., 2008; Qin et al., 2009).

The presence and activity of regulatory molecules and networks able to modulate OeRbohH activity are likely to be behind the differences between enzyme RNA expression and enzyme activity. As mentioned before, the production of superoxide by OeRbohH and other RbohHs has been demonstrated to be modulated by multiple factors including Ca^{2+} signaling, acidic signaling phospholipids, and small GTP-binding proteins from the Rac/Rop family (Potocky et al., 2012). Moreover, we have evidence of OeRbohH regulation by *S*-nitrosylation events, which may exert

changes in its function (Jimenez-Quesada et al., 2017a; Jimenez-Quesada et al., 2017b). Such PTM is highly dependent on the levels of NO (GSNO) (Corpas et al., 2013), which are critically acting on olive pollen germination physiology (Jimenez-Quesada et al., 2017a; Jimenez-Quesada et al., 2017b).

We established a link between RbohH-produced superoxide and pollen tube growth using specific antisense ODNs and DPI, indicating a key role of RbohH in pollen physiology. NADPH oxidase inhibitor DPI was able to prevent olive pollen germination and superoxide production. This is in agreement with previous results described in tobacco (Potocky et al., 2007), although it does not take place in cucumber, where the NADPH oxidase inhibitor was, on the contrary, able to promote the germination (Sirova et al., 2011). During olive pollen tube growth, we detected superoxide at the tip, with a minor fraction of tubes lacking the NBT stain (about 20% of them), as it has been previously noted also in tobacco pollen tubes (Potocky et al., 2007). The occurrence of NBT staining close to the callose plugs, and in their proximal side only (as referred to the pollen grain), which is described here for the first time, occurred in a significant proportion of such structures. Different explanations for this localization can be proposed. First of all, NBT staining might be the result of superoxide accumulation rather than indicative of superoxide production, as the result of the physical impediment of superoxide transit caused by the callose plugs. Callose synthases have been localized in close proximity to these structures, taking part in their synthesis (Cai et al., 2011). Also, it has been suggested that the activity of callose synthases is enhanced by GTPases like RabA4c, at least during pathogen-induced callose biosynthesis (Ellinger et al., 2014). Because GTPases (at least small GTPases) have been also proposed to induce positively the activity of Rbohs (Potocky et al., 2012), an accumulation of superoxide concomitant to callose synthesis might be foreseen. However, these hypotheses have to be further analyzed experimentally. Our results may also indicate that both the presence of the NADPH oxidase enzyme and likely its activity and consequent superoxide accumulation are polarized, as they occur in the proximal side of the callose plugs in reference to the pollen grain (and in parallel, at the pollen tube tip), likely addressing pollen tube metabolism and direction of growth.

Antisense ODN knockdown strategy inhibited both superoxide production and olive pollen tube growth, as it occurred with the NADPH oxidase inhibitor, indicating a key role of RbohH in such processes. These observations support the hypothesis of OeRbohH as the main responsible of the NADPH oxidase activities and signals found in all previous experiments, and the most important source of $O_2^{\bullet-}$ during olive pollen germination and tube growth. However, we cannot reject the hypothesis of other flavoenzymes also prone to inhibition by DPI, which might be involved in pollen tube growth. This idea is consistent with the proposal of mitochondria or peroxisomes as ROS sources in other pollen species (Cardenas et al., 2006; Boisson-Dernier et al., 2013).

The idea of RbohH as a mere pollen tube growth promoter is incomplete according to our opinion, considering that the over-expression analysis was able to produce plasma membrane invaginations and abnormal pollen tubes and, finally, tube growth prevention. Furthermore, onion cells expressing the GFP-RbohH fusion were severely disturbed, probably due to the toxic effect of the protein (data not shown). Alterations of pollen tube tip integrity by pollen-Rboh over-expression have been recently reported and connected to over accumulation of cell-wall material (Boisson-Dernier et al., 2013). Altogether, our data are consistent with the idea of RbohH as source of ROS in olive growing pollen tube, and as a key element in controlling tube expansion, interacting with a plethora or other numerous factors, including cGMP, Ca^{2+}, ions, and the multitasked signaling gas nitric oxide (Domingos et al., 2015).

DATA AVAILABILITY

The datasets generated for this study can be found in GenBank and ReprOlive database (http://reprolive.eez.csic.es/olivodb/), GenBank KX648357.

AUTHOR CONTRIBUTIONS

JA, VŽ, and MJ-Q designed the work. JA, MJ-Q, JT, and MP performed most of the experimental contributions and data acquisition. JA, VŽ, and MP implemented interpretation of the results and critical review and reprogramming of experiments. All authors contributed to drafting the work, revised the final manuscript and approved submission.

FUNDING

This study was supported by the following European Regional Development Fund (ERDF) co-funded grants: BFU2011-22779, BFU2016-77243-P, CSIC 201840E055 and RTC-2017-6654-2, the Ministry of Education, Youth and Sports of CR from ERDF-Project "Centre for Experimental Plant Biology": No. CZ.02.1.01/0.0/0.0/16_019/0000738, Czech Science Foundation GACR 18-18290J, and by a bilateral research agreement between the Spanish National Research Council (CSIC) and the Academy of Sciences of the Czech Republic (AVCR), Ref. 2010CZ0001.

ACKNOWLEDGMENTS

The authors thank Dr. AJ Castro and Dr. JC Jimenez-Lopez (EEZ-CSIC, Granada, Spain) for critical comments about the manuscript and advice, and Dr. Lima-Cabello for providing germinated pollen.

SUPPLEMENTARY MATERIAL

The Supplementary Material for this article can be found online at: https://www.frontiersin.org/articles/10.3389/fpls.2019.01149/full#supplementary-material

REFERENCES

Altenhöfer, S., Radermacher, K. A., Kleikers, P. W. M., Wingler, K., and Schmidt, H. H. H. W. (2015). Evolution of NADPH oxidase inhibitors: selectivity and mechanisms for target engagement. *Antioxid. Redox Signaling* 23, 5. doi: 10.1089/ars.2013.5814

Bacsi, A., Dharajiya, N., Choudhury, B. K., Sur, S., and Boldogh, I. (2005). Effect of pollen-mediated oxidative stress on immediate hypersensitivity reactions and late-phase inflammation in allergic conjunctivitis. *J. Allergy Clin. Immunol.* 116, 836–843. doi: 10.1016/j.jaci.2005.06.002

Bedard, K., Lardy, B., and Krause, K. H. (2007). NOX family NADPH oxidases: not just in mammals. *Biochimie* 89, 1107–1112. doi: 10.1016/j.biochi.2007.01.012

Bezvoda, R., Pleskot, R., Zarsky, V., and Potocky, M. (2014). Antisense oligodeoxynucleotide-mediated gene knockdown in pollen tubes. *Methods Mol. Biol.* 1080, 231–236. doi: 10.1007/978-1-62703-643-6_19

Boisson-Dernier, A., Lituiev, D. S., Nestorova, A., Franck, C. M., Thirugnanarajah, S., and Grossniklaus, U. (2013). ANXUR receptor-like kinases coordinate cell wall integrity with growth at the pollen tube tip *via* NADPH oxidases. *PLoS Biol.* 11, e1001719. doi: 10.1371/journal.pbio.1001719

Boldogh, I., Bacsi, A., Choudhury, B. K., Dharajiya, N., Alam, R., Hazra, T. K., et al. (2005). ROS generated by pollen NADPH oxidase provide a signal that augments antigen-induced allergic airway inflammation. *J. Clin. Invest.* 115, 2169–2179. doi: 10.1172/JCI24422

Bradford, M. (1976). A rapid and sensitive method for the quantitation of microgram quantities of protein utilizing the principle of protein-dye binding, *Anal. Biochem.* 72, (1–2), 1976, 248-254, ISSN 0003-2697. doi: 10.1016/0003-2697(76)90527-3

Cai, G., Faleri, C., Del Casino, C., Emons, A. M., and Cresti, M. (2011). Distribution of callose synthase, cellulose synthase, and sucrose synthase in tobacco pollen tube is controlled in dissimilar ways by actin filaments and microtubules. *Plant Physiol.* 155, 1169–1190. doi: 10.1104/pp.110.171371

Cardenas, L., McKenna, S. T., Kunkel, J. G., and Hepler, P. K. (2006). NAD(P)H oscillates in pollen tubes and is correlated with tip growth. *Plant Physiol.* 142, 1460–1468. doi: 10.1104/pp.106.087882

Carter, C., Healy, R., O'Tool, N. M., Naqvi, S. M., Ren, G., Park, S., et al. (2007). Tobacco nectaries express a novel NADPH oxidase implicated in the defense of floral reproductive tissues against microorganisms. *Plant Physiol.* 143, 389–399. doi: 10.1104/pp.106.089326

Chen, H. J., Huang, C. S., Huang, G. J., Chow, T. J., and Lin, Y. H. (2013). NADPH oxidase inhibitor diphenyleneiodonium and reduced glutathione mitigate ethephon-mediated leaf senescence, H_2O_2 elevation and senescence-associated gene expression in sweet potato (*Ipomoea batatas*). *J. Plant Physiol.* 170, 1471–1483. doi: 10.1016/j.jplph.2013.05.015

Clough, S. J., and Bent, A. F. (1998). Floral dip: a simplified method for *Agrobacterium*-mediated transformation of *Arabidopsis thaliana*. *Plant J.* 16, 735–743. doi: 10.1046/j.1365-313x.1998.00343.x

Corpas, F. J., Alché, J. D., and Barroso, J. B. (2013). Current overview of S-nitrosoglutathione (GSNO) in higher plants. *Front. Plant Sci.* 4, 126. doi: 10.3389/fpls.2013.00126

Cruz, F., Julca, I., Gómez-Garrido, J., Loska, D., Marcet-Houben, M., Cano, E., et al. (2016). Genome sequence of the olive tree, *Olea europaea*. *GigaScience* 5, 29. doi: 10.1186/s13742-016-0134-5

Dangl, J. L., and Jones, J. D. (2001). Plant pathogens and integrated defence responses to infection. *Nature* 411, 826–833. doi: 10.1038/35081161

Darriba, D., Taboada, G. L., Doallo, R., and Posada, D. (2011). ProtTest 3: fast selection of best-fit models of protein evolution. *Bioinformatics*. 2011 Apr 15; 27(8): 1164–1165. doi: 10.1093/bioinformatics/btr088

Davis, B. J., and Ornstein, L. (1964). "Disc Electrophoresis 1. Background and Theory," *Ann. N. Y. Acad. Sci.* 121, 321–349.

Devic, M., Albert, S., Delseny, M., and Roscoe, T. J. (1997). Efficient PCR walking on plant genomic DNA. *Plant Physiol. Biochem. (Paris)* 35, 331–339.

Dharajiya, N., Boldogh, I., Cardenas, V., and Sur, S. (2008). Role of pollen NAD(P)H oxidase in allergic inflammation. *Curr. Opin. Allergy Clin. Immunol.* 8, 57–62. doi: 10.1097/ACI.0b013e3282f3b5dc

Díaz, A., Martín, A., Rallo, P., Barranco, D., and De la Rosa, R. (2006). Self-incompatibility of arbequina and picual olive assessed by SSR markers. *J. Am. Soc. Hortic. Sci.* 131, 250–255. doi: 10.21273/JASHS.131.2.250

Domingos, P., Prado, A. M., Wong, A., Gehring, C., and Feijo, J. A. (2015). Nitric oxide: a multitasked signaling gas in plants. *Mol. Plant* 8, 506–520. doi: 10.1016/j.molp.2014.12.010

Drerup, M. M., Schlucking, K., Hashimoto, K., Manishankar, P., Steinhorst, L., Kuchitsu, K., et al. (2013). The calcineurin B-like calcium sensors CBL1 and CBL9 together with their interacting protein kinase CIPK26 regulate the *Arabidopsis* NADPH oxidase RBOHF. *Mol. Plant* 6, 559–569. doi: 10.1093/mp/sst009

Ellinger, D., Glöckner, A., Koch, J., Naumann, M., Stürtz, V., Schütt, K., et al. (2014). Interaction of the *Arabidopsis* GTPase RabA4c with its effector PMR4 results in complete penetration resistance to powdery mildew. *The Plant Cell Online.* 2014 Jul; 26(7): 3185–3200. doi: 10.1105/tpc.114.127779

Frahry, G., and Schopfer, P. (1998). Inhibition of O_2-reducing activity of horseradish peroxidase by diphenyleneiodonium. *Phytochemistry* 48, 223–227. doi: 10.1016/S0031-9422(98)00004-1

Gabison, L., Colloc'h, N., and Prangé, T. (2014). Azide inhibition of urate oxidase. *Acta Cryst.* 70, 896–902. doi: 10.1107/S2053230X14011753

Gouy, M., Guindon, S., and Gascuel, O. (2010). SeaView Version 4: a multiplatform graphical user interface for sequence alignment and phylogenetic tree building. *Mol. Biol. Evol.* 27, 221–224. doi: 10.1093/molbev/msp259

Heyno, E., Klose, C., and Krieger-Liszkay, A. (2008). Origin of cadmium-induced reactive oxygen species production: mitochondrial electron transfer versus plasma membrane NADPH oxidase. *New Phytol.* 179, 687–699. doi: 10.1111/j.1469-8137.2008.02512.x

Honys, D., and Twell, D. (2004). Transcriptome analysis of haploid male gametophyte development in *Arabidopsis*. *Genome Biol.* 5, R85. doi: 10.1186/gb-2004-5-11-r85

Hu, L., Liang, W., Yin, C., Cui, X., Zong, J., Wang, X., et al. (2011). Rice MADS3 regulates ROS homeostasis during late anther development. *Plant Cell* 23, 515–533. doi: 10.1105/tpc.110.074369

Jefferson, R. A., Kavanagh, T. A., and Bevan, M. W. (1987). GUS fusions: beta-glucuronidase as a sensitive and versatile gene fusion marker in higher plants. *EMBO J.* 6, 3901–3907. doi: 10.1002/j.1460-2075.1987.tb02730.x

Jimenez-Quesada, M. J., Carmona, R., Lima-Cabello, E., Traverso, J. A., Castro, A. J., Claros, M. G., et al. (2017a). Generation of nitric oxide by olive (*Olea europaea* L.) pollen during *in vitro* germination and assessment of the S-nitroso- and nitro-proteomes by computational predictive methods. *Nitric Oxide Biol. Chem.* 68, 23–37. doi: 10.1016/j.niox.2017.06.005

Jimenez-Quesada, M. J., Carmona, R., Lima-Cabello, E., Traverso, J. A., Castro, A. J., Claros, M. G., et al. (2017b). S-nitroso- and nitro- proteomes in the olive (*Olea europaea* L.) pollen. Predictive versus experimental data by nano-LC-MS. *Data in Brief* 15, 474–477. doi: 10.1016/j.dib.2017.09.058

Jimenez-Quesada, M. J., Traverso, J. A., and Alche, J. D. (2016). NADPH oxidase-dependent superoxide production in plant reproductive tissues. *Front. Plant Sci.* 7, 359. doi: 10.3389/fpls.2016.00359

Kaya, H., Iwano, M., Takeda, S., Kanaoka, M. M., Kimura, S., Abe, M., et al. (2015). Apoplastic ROS production upon pollination by RbohH and RbohJ in *Arabidopsis*. *Plant Signal Behav.* 10, e989050. doi: 10.4161/15592324.2014.989050

Kaya, H., Nakajima, R., Iwano, M., Kanaoka, M. M., Kimura, S., Takeda, S., et al. (2014). Ca^{2+}-activated reactive oxygen species production by Arabidopsis RbohH and RbohJ is essential for proper pollen tube tip growth. *Plant Cell* 26, 1069–1080. doi: 10.1105/tpc.113.120642

Keller, T., Damude, H. G., Werner, D., Doerner, P., Dixon, R. A., and Lamb, C. (1998). A plant homolog of the neutrophil NADPH oxidase gp91phox subunit gene encodes a plasma membrane protein with Ca^{2+} binding motifs. *Plant Cell* 10, 255–266. doi: 10.1105/tpc.10.2.255

Kost, B., Spielhofer, P., and Chua, N.-H. (1998). A GFP-mouse talin fusion protein labels plant actin filaments in vivo and visualizes the actin cytoskeleton in growing pollen tubes. *Plant J.* 16, 393–401. doi: 10.1046/j.1365-313x.1998.00304.x

Lamb, C., and Dixon, R. A. (1997). The oxidative burst in plant disease resistance. *Annu. Rev. Plant Physiol. Plant Mol. Biol.* 48, 251–275. doi: 10.1146/annurev.arplant.48.1.251

Lambeth, J. D. (2004). NOX enzymes and the biology of reactive oxygen. *Nat. Rev. Immunol.* 4, 181–189. doi: 10.1038/nri1312

Lassig, R., Gutermuth, T., Bey, T. D., Konrad, K. R., and Romeis, T. (2014). Pollen tube NAD(P)H oxidases act as a speed control to dampen growth rate oscillations during polarized cell growth. *Plant J.* 78, 94–106. doi: 10.1111/tpj.12452

Liccardi, G., D'Amato, M., and D'Amato, G. (1996). Oleaceae pollinosis: a review. *Int. Arch. Allergy Immunol.* 111, 210–217. doi: 10.1159/000237370

Liu, P., Li, R. L., Zhang, L., Wang, Q. L., Niehaus, K., Baluska, F., et al. (2009). Lipid microdomain polarization is required for NADPH oxidase-dependent ROS signaling in *Picea meyeri* pollen tube tip growth. *Plant J.* 60, 303–313. doi: 10.1111/j.1365-313X.2009.03955.x

M'rani-Alaoui, M., Castro, A., Alché, J. D., Wang, W., Fernández, M. C., and Rodríguez-García, M. I., (2002). *Expression of ole E 1, the major olive pollen allergen, during in-vitro pollen germination*, *Acta Hortic*. 586, 465–468. doi: 10.17660/ActaHortic.2002.586.96

Marino, D., Andrio, E., Danchin, E. G., Oger, E., Gucciardo, S., Lambert, A., et al. (2011). A *Medicago truncatula* NADPH oxidase is involved in symbiotic nodule functioning. *New Phytol.* 189, 580–592. doi: 10.1111/j.1469-8137.2010.03509.x

Marino, D., Dunand, C., Puppo, A., and Pauly, N. (2012). A burst of plant NADPH oxidases. *Trends Plant Sci.* 17, 9–15. doi: 10.1016/j.tplants.2011.10.001

McInnis, S. M., Desikan, R., Hancock, J. T., and Hiscock, S. J. (2006). Production of reactive oxygen species and reactive nitrogen species by angiosperm stigmas and pollen: potential signalling crosstalk? *New Phytol.* 172, 221–228. doi: 10.1111/j.1469-8137.2006.01875.x

McWilliam, H., Li, W., Uludag, M., Squizzato, S., Park, Y. M., Buso, N., et al. (2013). Analysis Tool Web Services from the EMBL-EBI. *Nucleic Acids Res.* 41, W597–W600. doi: 10.1093/nar/gkt376

Miller, G., Schlauch, K., Tam, R., Cortes, D., Torres, M. A., Shulaev, V., et al. (2009). The plant NADPH oxidase RBOHD mediates rapid systemic signaling in response to diverse stimuli. *Sci. Signal* 2, ra45. doi: 10.1126/scisignal.2000448

Mookerjee, S., Guerin, J., Collins, G., Ford, C., and Sedgley, M. (2005). Paternity analysis using microsatellite markers to identify pollen donors in an olive grove. *Theor. Appl. Genet.* 111, 1174–1182. doi: 10.1007/s00122-005-0049-5

Moutinho, A., Hussey, P. J., Trewavas, A. J., and Malho, R. (2001). cAMP acts as a second messenger in pollen tube growth and reorientation. *Proc. Natl. Acad. Sci. U. S. A.* 98, 10481–10486. doi: 10.1073/pnas.171104598

Noirot, E., Der, C., Lherminier, J., Robert, F., Moricova, P., Kieu, K., et al. (2014). Dynamic changes in the subcellular distribution of the tobacco ROS-producing enzyme RBOHD in response to the oomycete elicitor cryptogein. *J. Exp. Bot.* 65, 5011–5022. doi: 10.1093/jxb/eru265

Oda, T., Hashimoto, H., Kuwabara, N., Akashi, S., Hayashi, K., Kojima, C., et al. (2010). Structure of the N-terminal regulatory domain of a plant NADPH oxidase and its functional implications. *J. Biol. Chem.* 285, 1435–1445. doi: 10.1074/jbc.M109.058909

Ogasawara, Y., Kaya, H., Hiraoka, G., Yumoto, F., Kimura, S., Kadota, Y., et al. (2008). Synergistic activation of the *Arabidopsis* NADPH oxidase AtrbohD by Ca^{2+} and phosphorylation. *J. Biol. Chem.* 283, 8885–8892. doi: 10.1074/jbc.M708106200

Ono, E., Wong, H. L., Kawasaki, T., Hasegawa, M., Kodama, O., and Shimamoto, K. (2001). Essential role of the small GTPase Rac in disease resistance of rice. *Proc. Natl. Acad. Sci. U. S. A.* 98, 759–764. doi: 10.1073/pnas.021273498

Ortiz de Montellano, P. R., David, S. K., Ator, M. A., and Tew, D. (1988). Mechanism-based inactivation of horseradish peroxidase by sodium azide. Formation of meso-azidoprotoporphyrin IX. *Biochemistry* 27, 5470–5476. doi: 10.1021/bi00415a013

Pazmandi, K., Kumar, B. V., Szabo, K., Boldogh, I., Szoor, A., Vereb, G., et al. (2012). Ragweed subpollen particles of respirable size activate human dendritic cells. *PLoS One* 7, e52085. doi: 10.1371/journal.pone.0052085

Pfaffl, M. W. (2001). A new mathematical model for relative quantification in real-time RT-PCR. *Nucleic Acids Res.* 29, e45. doi: 10.1093/nar/29.9.e45

Potocky, M., Elias, M., Profotova, B., Novotna, Z., Valentova, O., and Zarsky, V. (2003). Phosphatidic acid produced by phospholipase D is required for tobacco pollen tube growth. *Planta* 217, 122–130.

Potocky, M., Jones, M. A., Bezvoda, R., Smirnoff, N., and Zarsky, V. (2007). Reactive oxygen species produced by NADPH oxidase are involved in pollen tube growth. *New Phytol.* 174, 742–751. doi: 10.1111/j.1469-8137.2007.02042.x

Potocky, M., Pejchar, P., Gutkowska, M., Jimenez-Quesada, M. J., Potocka, A., Alche Jde, D., et al. (2012). NADPH oxidase activity in pollen tubes is affected by calcium ions, signaling phospholipids and Rac/Rop GTPases. *J. Plant Physiol.* 169, 1654–1663. doi: 10.1016/j.jplph.2012.05.014

Potocký, M., Pleskot, R., Pejchar, P., Vitale, N., Kost, B., and Žárský, V. (2014). Live-cell imaging of phosphatidic acid dynamics in pollen tubes visualized by Spo20p-derived biosensor. *New Phytol.* 203, 483–494. doi: 10.1111/nph.12814

Qin, Y., Leydon, A. R., Manziello, A., Pandey, R., Mount, D., Denic, S., et al. (2009). Penetration of the stigma and style elicits a novel transcriptome in pollen tubes, pointing to genes critical for growth in a pistil. *PLoS Genet.* 5, e1000621. doi: 10.1371/journal.pgen.1000621

Rech, P., Grima-Pettenati, J., and Jauneau, A. (2003). Fluorescence microscopy: a powerful technique to detect low GUS activity in vascular tissues. *Plant J.* 33, 205–209. doi: 10.1046/j.1365-313X.2003.016017.x

Sagi, M., and Fluhr, R. (2001). Superoxide production by plant homologues of the gp91(phox) NADPH oxidase. Modulation of activity by calcium and by tobacco mosaic virus infection. *Plant Physiol.* 126, 1281–1290. doi: 10.1104/pp.126.3.1281

Sagi, M., and Fluhr, R. (2006). Production of reactive oxygen species by plant NADPH oxidases. *Plant Physiol.* 141, 336–340. doi: 10.1104/pp.106.078089

Shalaby, K. H., Allard-Coutu, A., O'Sullivan, M. J., Nakada, E., Qureshi, S. T., Day, B. J., et al. (2013). Inhaled birch pollen extract induces airway hyperresponsiveness *via* oxidative stress but independently of pollen-intrinsic NADPH oxidase activity, or the TLR4-TRIF pathway. *J. Immunol.* 191, 922–933. doi: 10.4049/jimmunol.1103644

Sirova, J., Sedlarova, M., Piterkova, J., Luhova, L., and Petrivalsky, M. (2011). The role of nitric oxide in the germination of plant seeds and pollen. *Plant Sci* 181, 560–572. doi: 10.1016/j.plantsci.2011.03.014

Smirnova, A. V., Matveyeva, N. P., and Yermakov, I. P. (2014). Reactive oxygen species are involved in regulation of pollen wall cytomechanics. *Plant Biol. (Stuttg.)*. 2014 Jan; 16(1): 252–257. doi: 10.1111/plb.12004

Speranza, A., Crinelli, R., Scoccianti, V., and Geitmann, A. (2012). Reactive oxygen species are involved in pollen tube initiation in kiwifruit. *Plant Biol. (Stuttg.)* 14, 64–76. doi: 10.1111/j.1438-8677.2011.00479.x

Sumimoto, H. (2008). Structure, regulation and evolution of Nox-family NADPH oxidases that produce reactive oxygen species. *FEBS J.* 275, 3249–3277. doi: 10.1111/j.1742-4658.2008.06488.x

Suzuki, N., Miller, G., Morales, J., Shulaev, V., Torres, M. A., and Mittler, R. (2011). Respiratory burst oxidases: the engines of ROS signaling. *Curr. Opin. Plant Biol.* 14, 691–699. doi: 10.1016/j.pbi.2011.07.014

Takeda, S., Gapper, C., Kaya, H., Bell, E., Kuchitsu, K., and Dolan, L. (2008). Local positive feedback regulation determines cell shape in root hair cells. *Science* 319, 1241–1244. doi: 10.1126/science.1152505

Torres, M. A., Onouchi, H., Hamada, S., Machida, C., Hammond-Kosack, K. E., and Jones, J. D. (1998). Six *Arabidopsis thaliana* homologues of the human respiratory burst oxidase (gp91phox). *Plant J.* 14, 365–370. doi: 10.1046/j.1365-313X.1998.00136.x

Traverso, J. A., Micalella, C., Martinez, A., Brown, S. C., Satiat-Jeunemaitre, B., Meinnel, T., et al. (2013a). Roles of N-terminal fatty acid acylations in membrane compartment partitioning: *Arabidopsis* h-type thioredoxins as a case study. *Plant Cell* 25, 1056–1077. doi: 10.1105/tpc.112.106849

Traverso, J. A., Pulido, A., Rodriguez-Garcia, M. I., and Alche, J. D. (2013b). Thiol-based redox regulation in sexual plant reproduction: new insights and perspectives. *Front. Plant Sci.* 4, 465. doi: 10.3389/fpls.2013.00465

Tuisel, H., Grover, T. A., Lancaster, J. R., Bumpus, J. A., and Aust, S. D. (1991). Inhibition of lignin peroxidase H2 by sodium azide. *Arch. Biochem. Biophys.* 288, 456–462. doi: 10.1016/0003-9861(91)90220-D

Ushio-Fukai, M. (2006). Localizing NADPH oxidase-derived ROS. *Sci. STKE* 2006, re8. doi: 10.1126/stke.3492006re8

von Lohneysen, K., Noack, D., Wood, M. R., Friedman, J. S., and Knaus, U. G. (2010). Structural insights into Nox4 and Nox2: motifs involved in function and cellular localization. *Mol. Cell Biol.* 30, 961–975. doi: 10.1128/MCB.01393-09

Vuletin Selak, G., Cuevas, J., Goreta Ban, S., and Perica, S. (2014). Pollen tube performance in assessment of compatibility in olive (*Olea europaea* L.) cultivars. *Sci. Hort.* 165, 36–43. doi: 10.1016/j.scienta.2013.10.041

Wang, X. L., Takai, T., Kamijo, S., Gunawan, H., Ogawa, H., and Okumura, K. (2009). NADPH oxidase activity in allergenic pollen grains of different plant species. *Biochem. Biophys. Res. Commun.* 387, 430–434. doi: 10.1016/j.bbrc.2009.07.020

Wang, Y., Zhang, W.-Z., Song, L.-F., Zou, J.-J., Su, Z., and Wu, W.-H. (2008). Transcriptome analyses show changes in gene expression to accompany pollen

germination and tube growth in *Arabidopsis*. *Plant Physiol.* 148, 1201–1211. doi: 10.1104/pp.108.126375

Wong, H. L., Pinontoan, R., Hayashi, K., Tabata, R., Yaeno, T., Hasegawa, K., et al. (2007). Regulation of rice NADPH oxidase by binding of Rac GTPase to its N-terminal extension. *Plant Cell* 19, 4022–4034. doi: 10.1105/tpc.107.055624

Xiao, Y.-L., Redman, J., Monaghan, E., Zhuang, J., Underwood, B., Moskal, W., et al. (2010). High throughput generation of promoter reporter (GFP) transgenic lines of low expressing genes in *Arabidopsis* and analysis of their expression patterns. *Plant Methods* 6, 18. doi: 10.1186/1746-4811-6-18

Xie, H. T., Wan, Z. Y., Li, S., and Zhang, Y. (2014). Spatiotemporal production of reactive oxygen species by NADPH oxidase is critical for tapetal programmed cell death and pollen development in *Arabidopsis*. *Plant Cell* 26, 2007–2023. doi: 10.1105/tpc.114.125427

Zafra, A., Rejón, J. D., Hiscock, S. J., and Alché, J. D. (2016). Patterns of ROS accumulation in the stigmas of Angiosperms and visions into their multi-functionality in plant reproduction. Frontiers in Plant Science. Special Topic: recent insights into the double role of hydrogen peroxide in plants. *Front Plant Sci.* 2016 (7), 1112. Published online 2016 Aug 5. doi: 10.3389/fpls.2016.01112

Zafra, A., Rodriguez-Garcia, M. I., and Alche, J. D. (2010). Cellular localization of ROS and NO in olive reproductive tissues during flower development. *BMC Plant Biol.* 10, 36. doi: 10.1186/1471-2229-10-36

Zhang, Y., Zhu, H., Zhang, Q., Li, M., Yan, M., Wang, R., et al. (2009). Phospholipase dalpha1 and phosphatidic acid regulate NADPH oxidase activity and production of reactive oxygen species in ABA-mediated stomatal closure in *Arabidopsis*. *Plant Cell* 21, 2357–2377. doi: 10.1105/tpc.108.062992

Zienkiewicz, A., Jiménez-López, J., Zienkiewicz, K., Alché, J. D., and Rodríguez-García, M. (2011a). Development of the cotyledon cells during olive (*Olea europaea* L.) *in vitro* seed germination and seedling growth. *Protoplasma* 248, 751–765. doi: 10.1007/s00709-010-0242-5

Zienkiewicz, K., Castro, A. J., Alché, J. D., Zienkiewicz, A., Suárez, C., and Rodríguez-García, M. I. (2010). Identification and localization of a caleosin in olive (*Olea europaea* L.) pollen during *in vitro* germination. *J. Exp. Bot.* 61, 1537–1546. doi: 10.1093/jxb/erq022

Zienkiewicz, K., Zienkiewicz, A., Rodriguez-Garcia, M., and Castro, A. (2011b). Characterization of a caleosin expressed during olive *(Olea europaea* L.) pollen ontogeny. *BMC Plant Biol.* 11, 122. doi: 10.1186/1471-2229-11-122.

Conflict of Interest Statement: The authors declare that the research was conducted in the absence of any commercial or financial relationships that could be construed as a potential conflict of interest.

frontiers in Plant Science

MINI REVIEW
published: 24 September 2019
doi: 10.3389/fpls.2019.01151

Olive Nutritional Status and Tolerance to Biotic and Abiotic Stresses

*Ricardo Fernández-Escobar**

Departamento de Agronomía, ETSIAM, Universidad de Córdoba, Cordova, Spain

The role of nutrients in plant growth is generally explained in terms of their functions in plant metabolism. Nevertheless, there is evidence that plant tolerance or resistance to biotic or abiotic stresses could be affected by the nutritional status. Although not well studied, an adequate nutritional status for optimal plant growth is thought to also be optimal for plant tolerance to stress. Considering the current global trend toward sustainability, studies that clarify the relationships between nutrition and stress are of great interest. For example, potassium plays an important role in the regulation of water status in the olive, improving drought tolerance, while calcium is involved in sodium exclusion mechanism, which can increase tolerance to salinity. Nitrogen excess, in contrast, increases susceptibility to spring frost and olive leaf spot. Silicon is not an essential element for plant growth, but it is considered a beneficial element; among its roles in the control of pests and diseases is the formation of a physical barrier that occurs through silicon deposition in the epidermal cells of the leaves. The presence of soluble silicon also facilitates the deposition of phenolic and other compounds at sites of infection, which is a general defense mechanism to pathogen attack. In olive, silicon application, either by foliar sprays or through irrigation water, reduces the incidence of olive leaf spot. This review summarizes the current status of olive nutrition, the relationships with biotic and abiotic stresses, and the effects of silicon.

Keywords: potassium, calcium, nitrogen, silicon, drought, salinity, temperature, olive leaf spot

OPEN ACCESS

Edited by:
José Enrique Fernández, Institute of Natural Resources and Agrobiology of Seville (CSIC), Spain

Reviewed by:
Arnon Dag, Agricultural Research Organization (ARO), Israel
Rodney Thompson, University of Almería, Spain

***Correspondence:**
Ricardo Fernández-Escobar
rfernandezescobar@uco.es

Specialty section:
This article was submitted to Crop and Product Physiology, a section of the journal Frontiers in Plant Science

Received: *24 March 2019*
Accepted: *23 August 2019*
Published: *24 September 2019*

Citation:
Fernández-Escobar R (2019) Olive Nutritional Status and Tolerance to Biotic and Abiotic Stresses. Front. Plant Sci. 10:1151. doi: 10.3389/fpls.2019.01151

CURRENT STATUS OF OLIVE NUTRITION

The olive, as with other perennial, woody plants, usually requires lower nutrient application than annual plants because it has nutrient storage organs and the ability to reuse these nutrients to support new growth. In mature olive trees growing under rainfed conditions, the amounts of nitrogen, potassium, and calcium removed annually by fruit yield, and pruning were 54.4, 45.5, and 57.9 kg.ha^{-1}, respectively (Fernández-Escobar et al., 2015). The amounts of other macronutrients removed, such as phosphorus and magnesium, were less than 7 kg.ha^{-1}, while those of micronutrients were less than 0.12 kg.ha^{-1}. Under irrigated cultivation, estimations of fruit removal of N, P, and K showed similar or slightly elevated values (Erel et al., 2018). Considering that the current practice in many orchards is to leave a mulch of pruning material, nutrient removal from olive orchards will be lower than the above values.

The small amounts of nutrients removed suggest that, in orchards established on fertile soils, the need for fertilization of olive trees is relatively low. Even with nitrogen, the mineral element required in the greatest amounts by plants, the balance in unfertilized orchards, i.e., the difference between

nitrogen input and output that represents the gain or loss of nitrogen in an orchard, was positive (Fernández-Escobar et al., 2012). In contrast, nutrient deficiencies can occur when olive orchards are established on unfertile soils with low availability of a specific nutrient, or when a specific nutrient is blocked due to the physical or chemical characteristics of the soil. Potassium deficiency represents the major nutritional disorder in olives growing both in drylands and on calcareous soils, due to its interaction with water shortage and calcium, respectively (Parra et al., 2003; Restrepo-Díaz et al., 2008). Calcium deficiency is also expected in acidic soils, and deficiencies of other nutrients are occasional and localized. Iron deficiency chlorosis has been reported in calcareous soils in Spain (Fernández-Escobar et al., 1993; Sánchez-Alcalá et al., 2012) and Israel (Zipori et al., 2011). Boron deficiency, meanwhile, has been described in California (Hartmann et al., 1966) and Italy (Sanzani et al., 2012), whereas an excess of boron was observed in some areas of Greece (Chatzissavvidis and Therios, 2010). Zinc deficiency is very rare, although it has been observed in some areas of Turkey (Başar and Gürel, 2016), Sicily (Sanzani et al., 2012), and Israel (Zipori et al., 2018). No references to other nutritional disorders have been reported for olives cultivated under field conditions.

Despite this, large amounts of nutrients are applied annually in many olive orchards. The perception that the annual application of large amounts of fertilizer ensures a good crop, even in orchards established on fertile soils, as well as the low cost of fertilizers in relation to the crop value, has led to unnecessarily high levels of fertilizer application. This practice results in environmental hazards, negative effects on the tree and the crop, and increased costs. **Table 1** shows the negative effects of excess nitrogen application. Nitrogen is the most commonly applied element in olive orchards and is usually applied in excess (Fernández-Escobar, 2011), as also occurs for other fruit tree species (Weinbaum et al., 1992; Faqi et al., 2008). The case of phosphorus is unique. Phosphorus deficiency is very rare in mature fruit trees (Shear and Faust, 1980; Erel et al., 2016), and although there is normally a lack of response to phosphorus application in olive orchards (Hartmann et al., 1966; Jiménez-Moreno and Fernández-Escobar, 2016; Ferreira et al., 2018), phosphorus is still applied in many fertilization programs. However, the reserves of phosphate rock, the main source of phosphorus fertilizer, are finite and could disappear this century (Dawson and Hilton, 2011; Gilbert, 2009), indicating the need for a more responsible and efficient use of phosphorus fertilizers, particularly for woody crops. In contrast, potassium fertilization has been frequently ignored, even though it represents the major nutritional disorder in rainfed olives. This indicates that olive nutrition is based mainly in tradition, repeating the same fertilization program, and also in the testimony of the neighbors. In a study comparing the environmental impacts of several olive-growing systems in Spain, Romero-Gámez et al. (2017) found that the manufacture and application of fertilizers were the primary contributors in all impact categories and cropping systems. These authors concluded that the reduction and optimization of fertilizers would be the most efficient way to improve the sustainability of fertilization practices.

Performing a rational and sustainable fertilization program is simple. A nutrient should be supplied only when there is evidence that it is needed to assure normal growth and productivity, and when an economic gain is expected from the application of the fertilizer. For this, leaf nutrient analysis is currently the best method available for diagnosing tree nutritional status and the need for fertilization (Shear and Faust, 1980; Benton Jones, 1985; Fernández-Escobar et al., 2009b). Fully expanded leaves from the middle to the basal portion of the current season's growth must be collected for leaf analysis in July in the northern hemisphere. The analytical results must then be compared with standard values established for these samples, which are shown in **Table 2**. The strategy is to maintain all the nutrients at the adequate levels indicated in the table. When this is achieved, nutrients should not be applied the following season. A nutrient must be applied only if leaf analysis shows values below the sufficiency (adequate) threshold. But if a nutrient is below that threshold because another element interacts with it, usually because it is in excess or deficient, the action should be concentrated on this element. If several nutrients are low (between deficient and adequate) or deficient, application of the lowest or most deficient element

TABLE 1 | Negative effects of excess nitrogen on olive trees.

Effect	Reference
Increase soil pollution	Fernández-Escobar et al., 2009a
Decrease oil quality	Fernández-Escobar et al., 2006 Dag et al., 2018
Reduce flower fertility	Fernández-Escobar et al., 2008
Affects frost tolerance	Fernández-Escobar et al., 2011
Reduce rooting and cutting survival	Dag et al., 2012
Delays fruit maturation	Fernández-Escobar et al., 2014a
Reduce root and shoot growth	Othman and Leskovar, 2019
Reduce nitrogen uptake efficiency	Fernández-Escobar et al., 2014b
Reduce potassium uptake	Antonaya-Baena and Fernández-Escobar, 2012
Increase susceptibility to *Fusicladium oleagineum*	Roca et al., 2018

TABLE 2 | Interpretation of nutrient levels in olive leaves sampled in July in the northern hemisphere, expressed as dry matter. Adapted from Fernández-Escobar (2018).

Element	Deficient	Adequate	Toxic
Nitrogen, N (%)[1]	1.4 (1.2)	1.5-2.0 (1.3-1.7)	(>1.7)
Phosphorus, P (%)[2]	0.05	0.1-0.3	–
Potassium, K (%)	0.4	>0.8	–
Calcium, Ca (%)	0.3	>1	–
Magnesium, Mg (%)	0.08	>0.1	–
Manganese, Mn (ppm)	–	>20	–
Zinc, Zn (ppm)	–	>10	–
Copper, Cu (ppm)	–	>4	–
Boron, B (ppm)	14	19-150	185
Sodium, Na (%)	–	–	>0.2
Chloride, Cl (%)	–	–	>0.5

[1]In brackets, nitrogen levels proposed by Molina-Soria and Fernández-Escobar (2012).
[2]Toxicity symptoms were observed at 0.21% in young plants (Jiménez-Moreno and Fernández-Escobar, 2016).

is usually enough to correct the problem. If leaf analysis in the following season shows that one of these nutrients is still below sufficiency, it may then be necessary to apply that nutrient. A detailed description of the procedure can be found in Fernández-Escobar (2017) and Fernández-Escobar (2007).

Estimating the amount of fertilizer required when leaf analysis indicates the need for fertilization is not simple. It should be based on judgments of tree nutritional status, crop demand, nutrient availability, and other site-specific variables. Nutrient removal of a deficient element is a simple first approach to determine the amount of that nutrient to be applied. Additionally, Fernández-Escobar (2017) suggests application rates that can be used to correct deficiencies.

The timing of nutrient application must consider that the uptake and use of a nutrient are usually not simultaneous processes. Thus, the aim of fertilization is to maximize nutrient uptake efficiency to increase its content in the tree, which normally occurs when the tree is active. Once taken up, the nutrient may be stored in the tree or used for growth.

RELATIONSHIPS WITH BIOTIC AND ABIOTIC STRESSES

The roles of nutrients in plant growth can usually be explained in terms of their functions in plant metabolism. However, there is evidence that plant tolerance or resistance to biotic or abiotic stresses can be affected by the nutritional status (Huber et al., 2012; Sanzani et al., 2012). These relationships have not been well studied, particularly in woody plants, but it is generally assumed that an adequate nutritional status for optimal plant growth is also optimal for plant tolerance to these stresses. Consequently, good management of olive nutrition, as described above, may mitigate the negative effects of some biotic or abiotic stresses.

Some abiotic factors are well known to influence tolerance to pests and disease (Sanzani et al., 2012). In contrast, it is still unclear how global warming affects the incidence of current olive pests or pathogens, or the emergence of new ones. Nevertheless, all practices in olive culture should encourage sustainability, and studies that clarify the relationships between olive nutrition and biotic and abiotic stresses will be of great interest, particularly considering that European regulations have led to a drastic reduction in the number of authorized active materials for olive pest and disease control.

The Role of Mineral Nutrients in the Tolerance to Abiotic Stresses

The olive is a crop that is commonly subjected to various stress situations (Sanzani et al., 2012). It is traditionally cultivated in marginal areas, often on calcareous soils, and usually under rainfed conditions, but is sometimes also irrigated with low-quality water. Although cultivated almost exclusively under Mediterranean conditions, olive orchards can be found in many different regions with diverse climates. Many older olive orchards are still based on traditional growing systems, but new plantations are based on more intensive growing methods. The use of new varieties, different cultural practices, and new environments may influence the effects of abiotic stresses.

Since most olive orchards are cultivated in drylands, K deficiencies can be expected (Restrepo-Díaz et al., 2008). There is insufficient information available to fully understand the role of nutritional status on drought tolerance. However, it is well known that K-deficient plants lose water more easily than well-nourished ones (Hsiao and Läuchli, 1986; Fournier et al., 2005). One plausible explanation may be that K plays an important role in stomatal opening and closure (Poffenroth et al., 1992) and, consequently, in the regulation of plant water status. In the olive, stomatal conductance under drought conditions is reportedly higher in K-deficient plants than in well-nourished ones displaying lower water-use efficiency (Arquero et al., 2006; Benlloch-González et al., 2008). Erel et al. (2014) reported that, under these conditions, the addition of Na^+ increases stomatal conductance. Since K plays an important role in the regulation of water status in olive trees, maintaining leaf K concentrations above the sufficiency threshold is highly recommended. However, it has also been reported that K uptake by olive trees is restricted by both K deficiency of the tree and water stress (Restrepo-Díaz et al., 2008), indicating that K fertilizer must be applied before the deficiency threshold is reached, and when trees present a good water status, usually in spring if growing in drylands.

Water demand for irrigation is increasing in olive orchards because of increased yields. Since olive trees are considered moderately tolerant to salinity (Maas and Hoffman, 1977; Rugini and Fedeli, 1990; Marin et al., 1995) and water resources in the Mediterranean basin are scarce, irrigation with saline water is often used. As in other glycophytic species (Greenway and Munns, 1980), salt tolerance in the olive is associated with ion exclusion mechanisms located in the roots (Benlloch et al., 1991; Tattini et al., 1995; Melgar et al., 2006), which reduce translocation and accumulation of Na^+ and Cl^- to the aerial part. Olive trees are less sensitive to leaf Cl^- than Na^+ (Bongi and Loreto, 1989; Tattini et al., 1992), and the Cl^- ion does not cause toxicity in olive trees (Melgar et al., 2009). In contrast, Na^+ toxicity is usually a concern when Ca^{2+} concentrations are relatively low (Bañuls et al., 1991; Maas, 1993). Indeed, when Ca^{2+} was applied to saline irrigation water, leaf Ca^{2+} concentrations increased with the amount of Ca^{2+} applied, but with a concomitant decrease in leaf Na^+ concentrations (Melgar et al., 2006). This indicates that Ca^{2+} plays an important role in the Na^+ exclusion mechanism, and that maintaining adequate Ca^{2+} nutrition can protect olive trees against Na^+ toxicity (Melgar et al., 2007; Tattini and Traversi, 2009; Methenni et al., 2018). The results obtained from a long-term experiment under field conditions (Melgar et al., 2009) suggest that supplying Ca^{2+} in irrigation water to prevent Na^+ toxicity using drip irrigation until winter rest, as well as growing a tolerant cultivar, can allow the use of high-saline irrigation water for extended periods without affecting olive tree growth or yield.

The olive is more tolerant to high than low temperatures (Sebastiani, 2018). Damage due to high temperatures is very rare in the olive and is often associated with drought or dry, hot winds (Sanzani et al., 2012). Under these conditions, Benlloch-González et al. (2016) found that the olive tree has a great capacity to accumulate K in the root, which is used by the tree to maintain the growth of the aerial part since, as mentioned previously, K plays an important role in the regulation of water status in the

olive. However, when high temperatures affect both the aerial part and root system, both K transport from the roots and tree growth are inhibited.

Low temperatures in winter and spring are limiting for olive growth. According to Sanzani et al. (2012), the extent of frost damage depends on the time of the year when the frost occurs. Little damage is expected during the fall, but in winter, the aerial part of the plant can be damaged at temperatures below −7°C (Palliotti and Bongi, 1996), and tree death can occur at −12°C (Larcher, 1970). In spring, olive trees are susceptible to frost injury. The threshold temperature below which symptoms of cold damage appear depends on numerous factors, including the nutritional status of the tree. Nitrogen has been associated with frost tolerance in many crops, although the study results are controversial. Depending on the species and/or the reference, increasing plant N may increase, decrease, or have no influence on cold tolerance (Pellett and Carter, 1981). In a study developed to determine the influence of N status on the frost tolerance of olive trees under field conditions, Fernández-Escobar et al. (2011) found that, in October, before the onset of dormancy, excess N resulted in increased frost tolerance. During dormancy, all the trees exhibited greater tolerance to low temperatures, and no differences were observed among them. In April, after budbreak, trees become more sensitive, and those with an excess of N were more sensitive to low temperatures. These results may explain some of the controversial results reported in the literature for other species. In Italy, K fertilization is recommended to reduce frost damage in the spring (Proietti and Famiani, 2005), likely due to the role of K in the regulation of water status.

Interactions among mineral nutrients are frequent, particularly in the soil. For instance, it is well known that K, Ca, and Mg interact in the soil exchange complex, sometimes inducing deficiencies in one element through an excess of another. Interactions also occur at the plant level, such that a deficiency or excess of one element may affect the uptake or utilization of another. However, the exact nature of some of these interactions remains unclear. As mentioned above, the main nutritional concerns in many olive orchards growing in the Mediterranean area, particularly in Spain, are low or deficient levels of plant K as well as N overfertilization. Reports regarding N and K interactions are scarce and mostly refer to annual plants. In the olive, preliminary results obtained with potted plants showed a significant interaction between N and K. Plants well-nourished with K increased both K content and vegetative growth, depending on the amount of N applied. In contrast, plants poorly nourished with K exhibited decreased K content and vegetative growth at the highest amounts of N applied (Antonaya-Baena and Fernández-Escobar, 2012). These results indicate that K uptake could be reduced in K-deficient plants with an excess of N. Moreover, leaf K concentrations are low in many Spanish olive orchards growing in soils with high levels of available K but subjected to N overfertilization.

The Role of Mineral Nutrients in the Tolerance to Biotic Stresses

Although plant tolerance to pests and disease is a genetic characteristic, it can also be affected by environmental factors like plant nutrition. The effect depends on the nutrient, plant species, and parasite, although it may be small in very tolerant or very susceptible cultivars.

Many studies have been carried out on the effects of N and K, and their interaction, on plant tolerance to pests and disease (Huber et al., 2012), although the results have sometimes been controversial. However, overall, excess N tends to favor disease development (Huber and Thompson, 2007), while K deficiency increases susceptibility to parasites (Huber and Arny, 1985). The efficiency of disease control also depends on the N:K ratio, since the effect of K may vary depending on the plant N nutritional status (Prabhu et al., 2007). The role of Ca is also well documented, particularly its effects on disease control during fruit storage (Shear, 1975; Scott and Wills, 1979; Rahman and Punja, 2007). Other mineral nutrients can also affect disease incidence, but to a lesser extent (Datnoff et al., 2007; Marchner, 2012), although Cu is used extensively as a fungicide for many species, including the olive. In addition, the role of phosphite (PO_3^{3-}) in the control of *Phytophthora cinnamomi* in many tree species is well documented (Fenn and Coffey, 1984; Fernández-Escobar et al., 1999).

Reports relating to olive nutrition and tolerance to biotic stresses are limited. Recent studies showed the effect of N on the incidence of olive leaf spot, the most common foliar disease in the olive, which is caused by the fungus *Fusicladium oleagineum* (currently *Venturia oleaginea*). Experiments developed under different growing conditions, including hydroponic culture, potted plants, and mature trees growing under field conditions, showed that disease incidence was significantly higher in plants subjected to a high-N treatment than in those subjected to a low-N treatment under all conditions (Roca et al., 2018). These results suggest that N excess increases susceptibility to olive leaf spot.

Mycorrhization of nursery olive plants has become common practice as it results in increased plant tolerance to biotic and abiotic stresses (Castillo et al., 2006; Porras-Soriano et al., 2009). However, mycorrhization of young olive plants with *Glomus intraradices* (currently *Rhizophagus irregularis*) has recently been observed to interact with the presence of high levels of P in the substrate (Jiménez-Moreno et al., 2018), resulting in reduced plant growth. In contrast, when the substrate contained low P concentrations, root growth increased compared to a control without mycorrhization. These results suggest that P should not be supplied to the substrate if plants are to be mycorrhized.

Tree tolerance to pest attack often depends more on the presence of repellents or toxic compounds than the effect of a nutrient (Huber et al., 2012). However, young plants or those with rapid vegetative growth are generally more susceptible to pest attack. In the olive, excessive N fertilizer application may increase the incidence of *Saissetia oleae*, likely due to the emergence of numerous new shoots that facilitates a suitable place for nymphs to settle (Ben-Dov and Hodgson, 1997).

The Role of Non-Essential Elements: Silicon

Some elements are not essential for plant growth, but are considered to have beneficial effects on plants, particularly due

to their roles in plant tolerance to biotic and abiotic stresses. One such element is silicon (Si), the second most abundant element in the earth's crust after oxygen. Silicon in soils can be found in a solid phase composed mainly of silica (SiO_2) and silicates adsorbed to soil particles and Fe and Al oxides and hydroxides, or in a liquid phase mainly in the form of monosilicic acid (H_4SiO_4) (Tubana et al., 2016). Monosilicic acid does not dissociate at pHs below 9 and plants uptake Si from the soil solution in this form (Epstein, 1994; Ma and Takahashi, 2002). All plants growing in soil contain Si in their tissues, and the concentration of Si in plant tissues depends on the soil and plant species (Tubana et al., 2016; Debona et al., 2017).

The Si taken up by plants is transported from the roots to shoots, either actively or passively, *via* the transpiration stream. In the shoot, silicic acid is concentrated through loss of water due to transpiration and is polymerized into insoluble silica, forming a silica gel layer between the cuticle and epidermal cells (Debona et al., 2017; Wang et al., 2017) and preventing Si translocation to new, growing leaves. This silica layer constitutes a physical barrier that is believed to reduce the incidence of pests and disease, as well as to improve photosynthetic rates and tolerance to water stress, drought conditions, and other abiotic stresses (Marchner, 2012). Silicon also forms a chemical barrier, inducing the production of phenolic compounds, phytoalexins, and other products that activate plant defense mechanisms (Debona et al., 2017; Wang et al., 2017).

Consequently, plants supplied with Si may have enhanced resistance to multiple biotic and abiotic stresses (Luyckx et al., 2017). Ma (2004) suggests that the more Si accumulates in the shoots, the larger the effect. Therefore, although Si is abundant in the soil, many plants cannot take up enough Si to increase their tolerance to biotic and abiotic stresses. Since Si deposited in the leaves is immobile, a continuous supply of Si is required in newly formed leaves for optimal tolerance to these stresses (Huber et al., 2012). Silicon can be applied by foliar sprays, directly to the soil, or through irrigation water, although Savva and Ntatsi (2015) indicated that application through the soil is more effective than foliar application in increasing Si levels in plant tissues.

Although many studies investigating the effect of Si application in plants have recently been undertaken, limited information is available on Si application in fruit tree crops. In the olive, recent studies reported that continuous Si application in young olive plants significantly reduces symptoms in leaves inoculated with *V. oleaginea*, even at low doses (Nascimento-Silva et al., 2018). Cultivar differences were evident in the responses to Si application, and the effect was more pronounced in 'Arbequina', a moderately susceptible cultivar, than in the more susceptible cultivar 'Picual'. Additionally, this study clearly showed that both foliar spray and application through irrigation water were effective in increasing leaf Si concentrations. However, at the highest doses applied, foliar sprays were more effective at increasing leaf Si concentrations in 'Arbequina', but not 'Picual'. These results are interesting because most olive trees are grown in drylands, and foliar spraying is the method commonly used for agrochemical applications.

AUTHOR CONTRIBUTIONS

The author confirms being the sole contributor of this work and has approved it for publication.

FUNDING

This work was supported by project AGL2017-85246-R financed by the Agencia Estatal de Investigación and European Regional Development Funds (AEI/FEDER, UE).

REFERENCES

Antonaya-Baena, M. F., and Fernández-Escobar, R. (2012). Nitrogen and potassium interaction on olive cutting growth, N and K content and nutrients use efficiency. *Proc. of 4th Int. Conf. Olivebioteq* vol. II, 455–458.

Arquero, O., Barranco, D., and Benlloch, M. (2006). Potassium starvation increases stomatal conductance in olive trees. *HortScience* 41, 433–436. doi: 10.21273/HORTSCI.41.2.433

Bañuls, J., Legaz, F., and Primo-Millo, E. (1991). Salinity-calcium interactions on growth and ionic concentrations of *Citrus* plants. *Plant Soil* 133, 39–46. doi: 10.1007/BF00011897

Başar, H., and Gürel, S. (2016). The influence of Zn, Fe and B applications on leaf and fruit absorption of table olive 'Gemlik' based on phonological stages. *Sci. Hortic.* 198, 336–343. doi: 10.1016/j.scienta.2015.12.001

Ben-Dov, Y., and Hodgson, C. (1997). *Soft scale insects: their biology, natural enemies and control*. Amsterdam: world crop pest, Vol. 7b. Elsevier Science B. V.

Benlloch, M., Arboleda, F., Barranco, D., and Fernández-Escobar, R. (1991). Response of young olive trees to sodium and boron excess in irrigation water. *HortScience* 26, 867–870. doi: 10.21273/HORTSCI.26.7.867

Benlloch-González, M., Arquero, O., Fournier, J. M., Barranco, D., and Benlloch, M. (2008). K^+ starvation inhibits water-stress-induced stomatal closure. *J. Plant Physiol.* 165, 623–630. doi: 10.1016/j.jplph.2007.05.010

Benlloch-González, M., Quintero, J. M., Suárez, M. P., Sánchez-Lucas, R., Fernández-Escobar, R., and Benlloch, M. (2016). Effect of moderate high temperature on the vegetative growth and potassium allocation in olive plants. *J. Plant Physiol.* 207, 22–29. doi: 10.1016/j.jplph.2016.10.001

Benton Jones, J. (1985). Soil testing and plant analysis: guides to the fertilization of horticultural crops. *Hort. Rev.* 7, 1–68. doi: 10.1002/9781118060735.ch1

Bongi, G., and Loreto, F. (1989). Gas-exchange properties of salt-stressed olive (*Olea europaea* L.) leaves. *Plant Physiol.* 90, 1408–1416. doi: 10.1104/pp.90.4.1408

Castillo, P., Nico, A. I., Azcón-Aguilar, C., Del Río Rincón, C., Calvet, C., and Jiménez-Díaz, R. M. (2006). Protection of olive planting stocks against parasitism of root-knot nematodes by arbuscular mycorrhizal fungi. *Plant Pathol.* 55, 705–713. doi: 10.1111/j.1365-3059.2006.01400.x

Chatzissavvidis, C., and Therios, I. (2010). Response of four olive (*Olea europaea* L.) cultivars to six B concentrations: growth performance, nutrient status and gas exchange parameters. *Sci. Hortic.* 127, 29–38. doi: 10.1016/j.scienta.2010.09.008

Dag, A., Erel, R., Ben-Gal, A., Zipori, I., and Yermiyahu, U. (2012). The effect of olive tree stock plant nutritional status on propagation rates. *HortScience* 47 (2), 307–310. doi: 10.21273/HORTSCI.47.2.307

Dag, A., Erel, R., Kerem, Z., Ben-Gal, A., Stern, N., Bustan, A., et al. (2018). Effect of nitrogen availability on olive oil quality. *Acta Hortic.* 1199, 465–469. doi: 10.17660/ActaHortic.2018.1199.74

Datnoff, L. E,. Elmer, W. H., Huber, D. M., editors. (2007). *Mineral Nutrition and Plant Disease*. Minnesota: The American Phytopathological Society Press.

Dawson, C. J., and Hilton, J. (2011). Fertiliser availability in a resource-limited world: production and recycling of nitrogen and phosphorus. *Food Policy* 36, S14–S22. doi: 10.1016/j.foodpol.2010.11.012

Debona, D., Rodrigues, F. A., and Datnoff, L. E. (2017). Silicon's role in abiotic and biotic plant stresses. *Annu. Rev. Phytopathol.* 55, 85–107. doi: 10.1146/annurev-phyto-080516-035312

Epstein, E. (1994). The anomaly of silicon in plant biology. *Proc. Natl. Acad. Sci. U.S.A.* 91, 11–17. doi: 10.1073/pnas.91.1.11

Erel, R., Ben-Gal, A., Dag, A., Schwartz, A., and Yermiyahu, U. (2014). Sodium replacement of potassium in physiological processes of olive trees (var. Barnea) as affected by drought. *Tree Physiol.* 34, 1102–1117. doi: 10.1093/treephys/tpu081

Erel, R., Yermiyahu, U., Yasuor, H., Cohen Chamus, D., Schwartz, A., Ben-Gal, A., et al. (2016). Phosphorous nutritional level, carbohydrate reserves, and flower quality in olives. *PLoS One* 11 (12), e0167591. doi: 10.1371/journal.pone.0167591

Erel, R., Yermiyahu, U., Ben-Gal, A., and Dag, A. (2018). Olive fertilization under intensive cultivation management. *Acta Hortic.* 1217, 207–224. doi: 10.17660/ActaHortic.2018.1217.27

Faqi, W., Haibin, L., Baosheng, S., Jian, W., and Gale, W. J. (2008). Net primary production and nutrient cycling in an apple orchard-annual crop system in the Loess Plateau, China: a comparison of Qinguan apple, Fuji apple, corn and millet production systems. *Nutr. Cycl. Agroecosyst.* 81, 95–105. doi: 10.1007/s10705-007-9155-x

Fenn, M. E., and Coffey, M. D. (1984). Studies on the *in vitro* and *in vivo* antifungal activity of fosetil-Al and phosphorous acid. *Phytopathology* 74, 606–611. doi: 10.1094/Phyto-74-606

Fernández-Escobar, R. (2007). *"Fertilization" in production techniques in olive growing*. Madrid: International Olive Council, 145–164.

Fernández-Escobar, R. (2011). Use and abuse of nitrogen in olive fertilization. *Acta Hortic.* 888, 249–257. doi: 10.17660/ActaHortic.2011.888.28

Fernández-Escobar, R. (2017). "Fertilización," in *El Cultivo del Olivo*. Eds. D. Barranco, R. Fernández-Escobar, and L. Rallo (Madrid: Ediciones Mundi-Prensa), 419-460.

Fernández-Escobar, R. (2018). Trends in olive nutrition (*a review*). *Acta Hortic.* 1199, 215–223. doi: 10.17660/ActaHortic.2018.1199.35

Fernández-Escobar, R., Barranco, D., and Benlloch, M. (1993). Overcoming iron chlorosis in olive and peach trees using a low-pressure trunk-injection method. *HortScience* 28 (3), 192–194. doi: 10.21273/HORTSCI.28.3.192

Fernández-Escobar, R., Gallego, F. J., Benlloch, M., Membrillo, J., Infante, J., and Pérez de Algaba, A. (1999). Treatment of oak decline using pressurized injection capsules of antifungal materials. *Eur. J. For. Path.* 29, 29–38. doi: 10.1046/j.1439-0329.1999.00127.x

Fernández-Escobar, R., Beltrán, G., Sánchez-Zamora, M. A., García-Novelo, J., Aguilera, M. P., and Uceda, M. (2006). Olive oil quality decreases with nitrogen over-fertilization. *HortScience* 41, 215–219. doi: 10.21273/HORTSCI.41.1.215

Fernández-Escobar, R., Ortiz-Urquiza, A., Prado, M., and Rapoport, H. F. (2008). Nitrogen status influence on olive tree flower quality and ovule longevity. *Environ. Exp. Bot.* 64, 113–119. doi: 10.1016/j.envexpbot.2008.04.007

Fernández-Escobar, R., Marin, L., Sánchez-Zamora, M. A., García-Novelo, J. M., Molina-Soria, C., and Parra, M. A. (2009a). Long-term effects of N fertilization on cropping and growth of olive trees and on N accumulation in soil profile. *Europ. J. Agron.* 31, 223–232. doi: 10.1016/j.eja.2009.08.001

Fernández-Escobar, R., Parra, M. A., Navarro, C., and Arquero, O. (2009b). Foliar diagnosis as a guide to olive fertilization. *Span. J. Agric. Res.* 7, 212–223. doi: 10.5424/sjar/2009071-413

Fernández-Escobar, R., Navarro, S., and Melgar, J. C. (2011). Effect of nitrogen status on frost tolerance of olive trees. *Acta Hortic.* 924, 41–44. doi: 10.17660/ActaHortic.2011.924.3

Fernández-Escobar, R., García-Novelo, J. M., Molina-Soria, C., and Parra, M. A. (2012). An approach to nitrogen balance in olive orchards. *Sci. Hortic.* 135, 219–226. doi: 10.1016/j.scienta.2011.11.036

Fernández-Escobar, R., Braz Frade, R., Beltrán Maza, G., and Lopez Campayo, M. (2014a). Effect of nitrogen fertilization on fruit maturation of olive trees. *Acta Hortic.* 1057, 101–105. doi: 10.17660/ActaHortic.2014.1057.10

Fernández-Escobar, R., Antonaya-Baena, M. F., Sánchez-Zamora, M. A., and Molina-Soria, C. (2014b). The amount of nitrogen applied and nutritional status of olive plants affect nitrogen uptake efficiency. *Sci. Hortic.* 167, 1–4. doi: 10.1016/j.scienta.2013.12.026

Fernández-Escobar, R., Sánchez-Zamora, M. A., García-Novelo, J. M., and Molina-Soria, C. (2015). Nutrient removal from olive trees by fruit yield and pruning. *HortScience* 50 (3), 1–5. doi: 10.21273/HORTSCI.50.3.474

Ferreira, I. Q., Rodrigues, M. A., Moutinho-Pereira, J. M., Correia, C. M., and Arrobas, M. (2018). Olive response to applied phosphorus in field and pot experiments. *Sci. Hortic.* 234, 236–244. doi: 10.1016/j.scienta.2018.02.050

Fournier, J. M., Roldán, A. M., Sánchez, C., Alexandre, G., and Benlloch, M. (2005). K^+ starvation increases water uptake in whole sunflower plants. *Plant Sci.* 168, 823–829. doi: 10.1016/j.plantsci.2004.10.015

Gilbert, N. (2009). The disappearing nutrient. *Nature* 461 (7265), 716–718. doi: 10.1038/461716a

Greenway, H., and Munns, R. (1980). Mechanisms of salt tolerance in nonhalophytes. *Ann. Rev. Plant Physiol.* 31, 149–190. doi: 10.1146/annurev.pp.31.060180.001053

Hartmann, H. T., Uriu, K., and Lilleland, O. (1966). "Olive nutrition," in *temperate to tropical fruit nutrition*. Ed. N. F. Childers (New Brunswick, NJ, USA: Rutgers University Horticultural Publications), 252–261.

Hsiao, T. C., and Läuchli, A. (1986). "Role of potassium in plant-water relation," in *Advances in plant nutrition*, vol. 2. Eds. B. Tinker and A. Läuchli (New York: Praeger Scientific), 281–312.

Huber, D., Römheld, V., and Weinmann, M. (2012). "Relationship between nutrition, plant diseases and pests," in *Marschner's mineral nutrition of higher plants*. Ed. P. Marchner (USA: Elservier Ltd), 283–298. doi: 10.1016/B978-0-12-384905-2.00010-8

Huber, D. M., and Thompson, I. A. (2007). *Nitrogen and plant disease" in Mineral nutrition and plant disease*. Eds. L. E. Datnoff, W. H. Elmer, and D. M. Huber. Minnesota: The American Phytopathological Society Press, 3–44.

Huber, D. M., and Arny, D. C. (1985). "Interactions of potassium with plant diseases," in *Potassium in agriculture*. Ed. R. D. Munson (Madison, Wisconsin: American Society of Agronomy).

Jiménez-Moreno, M. J., and Fernández-Escobar, R. (2016). Response of young olive plants (*Olea europaea* L.) to phosphorus application. *HortScience* 51 (9), 1167–1170. doi: 10.21273/HORTSCI11032-16

Jiménez-Moreno, M. J., Moreno-Márquez, M. C., Moreno-Alías, I., Rapoport, H., and Fernández-Escobar, R. (2018). Interaction between mycorrhization with Glomus intraradices and phosphorus in nursery olive plants. *Sc. Hortic.* 233, 249–255. doi: 10.1016/j.scienta.2018.01.057

Larcher, W. (1970). Kälteresistenz und Uberwinterungsvermögen mediterraner Holzpflanzen. *Oecologia Plant* 5, 267–286.

Luyckx, M., Hausman, J. F., Lutts, S., and Guerriero, G. (2017). Silicon and plants: current knowledge and technological perspectives. *Front. Plant Sci.* 8, 411. doi: 10.3389/fpls.2017.00411

Ma, J. F., and Takahashi, E. (2002). *Soil, fertilizer and plant silicon research in Japan*. Dordrecht: Elsevier Science. doi: 10.1016/B978-044451166-9/50009-9

Ma, J. F. (2004). Role of silicon in enhancing the resistance of plants to biotic and abiotic stresses. *Soil Sci. Plant Nutr.* 50 (1), 11–18. doi: 10.1080/00380768.2004.10408447

Maas, E. V. (1993). Salinity and citriculture. *Tree Physiol.* 12, 195–216. doi: 10.1093/treephys/12.2.195

Maas, E. V., and Hoffman, G. J. (1977). Crop salt tolerance-current assessment. *J. Irr. Drain. Div., ASCE* 103, 115–134.

Marchner, P. (2012). *Marschner's mineral nutrition of higher plants*. USA: Elservier Ltd.

Marin, L., Benlloch, M., and Fernández-Escobar, R. (1995). Screening of olive cultivars for salt tolerance. *Sci. Hortic.* 64, 113–116. doi: 10.1016/0304-4238(95)00832-6

Melgar, J. C., Benlloch, M., and Fernández-Escobar, R. (2006). Calcium increases sodium exclusion in olive plants. *Sci. Hortic.* 109, 303–305. doi: 10.1016/j.scienta.2006.04.013

Melgar, J. C., Benlloch, M., and Fernández-Escobar, R. (2007). Calcium starvation increases salt susceptibility in olive plants but has no effect on susceptibility to water stress. *J. Hortic. Sci. Biotech.* 82 (4), 622–626. doi: 10.1080/14620316.2007.11512282

Melgar, J. C., Mohamed, Y., Serrano, N., García-Galavís, P. A., Navarro, C., Parra, M. A., et al. (2009). Long term responses of olive trees to salinity. *Agr. Water Manage.* 96, 1105–1113. doi: 10.1016/j.agwat.2009.02.009

Methenni, K., Ben Abdallah, M., Nouairi, I., Smaoui, A., Ben Ammar, w., Zarrouk, M., et al. (2018). Salicylic acid and calcium pretreatments alleviate the toxic effect of salinity in the Oueslati olive variety. *Sci. Hortic.* 233, 349–358. doi: 10.1016/j.scienta.2018.01.060

Molina-Soria, C., and Fernández-Escobar, R. (2012). A proposal of new critical leaf nitrogen concentrations in olive. *Acta Hortic.* 949, 283–286. doi: 10.17660/ActaHortic.2012.949.41

Nascimento-Silva, K., Roca, L. F., Benlloch-González., M., and Fernández-Escobar, R. (2018). Effect of silicon on the incidence of Fusicladium Oleagineum in the olive. In: Fernández, JE, editor. 6th International Conference on Olive Tree and Olive Products Olivebioteq'18. Book of Abstracs; Oct 15-19; Seville, Spain. p. 116

Othman, Y. A., and Leskovar, D. (2019). Nitrogen management influenced root length intensity of young olive trees. *Sci. Hortic.* 246, 726–733. doi: 10.1016/j.scienta.2018.11.052

Palliotti, A., and Bongi, G. (1996). Freezing injury in the olive leaf and effects of mefluidide treatment. *J. Hort. Sci.* 71, 57–63. doi: 10.1080/14620316.1996.11515382

Parra, M. A., Fernández-Escobar, R., Navarro, C., and Arquero, O. (2003). *Los suelos y la fertilización del olivar cultivado en zonas calcáreas*. Madrid: Mundi-Prensa.

Pellett, H. M., and Carter, J. V. (1981). Effect of nutritional factors on cold hardiness of plants. *Hort. Rev.* 3, 144–171. doi: 10.1002/9781118060766.ch4

Poffenroth, M., Green, D. B., and Tallman, G. (1992). Sugar concentrations in guard cells of *Vicia faba* illuminated with red or blue light. *Plant Physiol.* 98, 1460–1471. doi: 10.1104/pp.98.4.1460

Porras-Soriano, A., Soriano-Martín, M. L., Porras-Piedra, A., and Azcón, R. (2009). Arbuscular mycorrhizal fungi increased growth, nutrient uptake and tolerance to salinity in olive trees under nursery conditions. *J. Plant Physiol.* 166, 1350–1359. doi: 10.1016/j.jplph.2009.02.010

Prabhu, A. S., Fageria, N. K., Huber, D. M., and Rodrigues, F. A. (2007). "Potassium and plant disease," in *Mineral nutrition and plant disease*. Eds. L. E. Datnoff, W. H. Elmer, and D. M. Huber (Minnesota: The American Phytopathological Society Press).

Proietti, P., and Famiani, F. (2005). Cultural choices and olive health. *Inf. Fitopatol.* 55 (11), 4–11.

Rahman, M., and Punja, Z. K. (2007). *Calcium and plant disease" in Mineral nutrition and plant disease*. Eds. L. E. Datnoff, W. H. Elmer, and D. M. Huber. Minnesota: The American Phytopathological Society Press.

Restrepo-Díaz, H., Benlloch, M., Navarro, C., and Fernández-Escobar, R. (2008). Potassium fertilization of rainfed olive orchards. *Sci. Hortic.* 116, 399–403. doi: 10.1016/j.scienta.2008.03.001

Roca, L. F., Romero, J., Bohórquez, J. M., Alcántara, E., Fernández-Escobar, R., and Trapero, A. (2018). Nitrogen status affects growth, chlorophyll content and infection by *Fusicladium oleagineum* in olive. *Crop Prot.* 109, 80–85. doi: 10.1016/j.cropro.2017.08.016

Romero-Gámez, M., Castro-Rodriguez, J. C., and Suárez-Rey, E. M. (2017). Optimization of olive growing practices in Spain from a life cycle assessment perspective. *J. Clean. Prod.* 149, 25–37. doi: 10.1016/j.jclepro.2017.02.071

Rugini, E., and Fedeli, E. (1990). "Olive (*Olea europaea* L.) as an oilseed crop," in *Biotechnology in Agriculture and Forestry*. Ed. Y. P. S. Bajai (Berlin: Springer-Verlag), 563–641. doi: 10.1007/978-3-642-74448-8_29

Sánchez-Alcalá, I., Bellón, F., Del Campillo, M. C., Barrón, V., and Torrent, J. (2012). Application of synthetic siderite (FeCO3) to the soil is capable of alleviating iron chlorosis in olive trees. *Sci. Hortic.* 138, 17–23. doi: 10.1016/j.scienta.2012.02.001

Sanzani, S. M., Schena, L., Nigro, F., Sergeeva, V., Ippolito, A., and Salerno, M.-G. (2012). Abiotic diseases of olive. *J. Plant Pathol.* 94 (3), 469–491.

Savva, D., and Ntatsi, G. (2015). Biostimulant activity of silicon in horticulture. *Sci. Hortic.* 196, 66–81. doi: 10.1016/j.scienta.2015.09.010

Scott, K. J., and Wills, R. B. H. (1979). Effects of vacuum and pressure infiltration of calcium chloride and storage temperature on the incidence of bitter pit and low temperature breakdown of apples. *Aust. J. Agric. Res.* 30, 917–928. doi: 10.1071/AR9790917

Sebastiani, L. (2018). Abiotic stresses in olive: physiological and molecular mechanisms. *Acta Hortic.* 1199, 47–55. doi: 10.17660/ActaHortic.2018.1199.8

Shear, C. B. (1975). Calcium related disorders of fruits and vegetables. *HortScience* 10, 361–365.

Shear, C. B., and Faust, M. (1980). Nutritional ranges in deciduous tree fruits and nuts. *Hortic. Rev.* 2, 142–163. doi: 10.1002/9781118060759.ch3

Tattini, M., Bertoni, P., and Caselli, S. (1992). Genotypic responses of olive plants to sodium chloride. *J. Plant Nutrit.* 15, 1467–1485. doi: 10.1080/01904169209364412

Tattini, M., Gucci, R., Coradeschi, M. A., Ponzio, C., and Edward, J. D. (1995). Growth, gas exchange and ion content in *Olea europaea* plants during salinity stress and subsequent relief. *Physiol. Plant.* 95, 203–210. doi: 10.1111/j.1399-3054.1995.tb00828.x

Tattini, M., and Traversi, M. L. (2009). On the mechanism of salt tolerance in olive (*Olea europaea* L.) under low- or high-Ca^{2+} supply. *Environ. Exper. Bot.* 65, 72–81. doi: 10.1016/j.envexpbot.2008.01.005

Tubana, B. S., Babu, T., and Datnoff, L. E. (2016). A review of silicon in soils and plants and its role in US agriculture: history and future perspectives. *Soil Sci.* 181 (9/10), 393–411. doi: 10.1097/SS.0000000000000179

Wang, M., Gao, L., Dong, S., Sun, Y., Shen, Q., and Guo, S. (2017). Role of silicon on plant–pathogen interactions. *Front. Plant Sci.* 8, 701. doi: 10.3389/fpls.2017.00701

Weinbaum, S. A., Johnson, R. S., and De Jong, T. M. (1992). Causes and consequences of overfertilization in orchards. *Horttechnology* 2, 112–121. doi: 10.21273/HORTTECH.2.1.112b

Zipori, I., Yermiyahu, U., Ben-Gal, A., and Dag, A. (2011). Response of olive trees to iron application. *Acta Hortic.* 888, 295–300. doi: 10.17660/ActaHortic.2011.888.34

Zipori, I., Yermiyahu, U., Tugendhaft, Y., Ben-Gal, A., and Dag, A. (2018). The response of olive (*Olea europaea*) trees to zinc nutrition. *Acta Hortic.* 1199, 351–356. doi: 10.17660/ActaHortic.2018.1199.55

Conflict of Interest Statement: The author declares that the research was conducted in the absence of any commercial or financial relationships that could be construed as a potential conflict of interest.

frontiers in Plant Science

ORIGINAL RESEARCH
published: 02 October 2019
doi: 10.3389/fpls.2019.01199

Sap Flow Responses to Warming and Fruit Load in Young Olive Trees

Andrea Miserere[1,2], *Peter S. Searles*[1], *Guadalupe Manchó*[3], *Pablo H. Maseda*[3] *and Maria Cecilia Rousseaux*[1,4*†]

[1] Centro Regional de Investigaciones Científicas y Transferencia Tecnológica de La Rioja (CRILAR-Provincia de La Rioja-UNLaR- SEGEMAR-UNCa-CONICET), Anillaco, Argentina, [2] Departamento de Ciencias y Tecnologías Aplicada, Universidad Nacional de La Rioja, La Rioja, Argentina, [3] Facultad de Agronomía, Universidad de Buenos Aires, Buenos Aires, Argentina, [4] Departamento de Ciencias Exactas, Físicas y Naturales, Universidad Nacional de La Rioja, La Rioja, Argentina

Global warming will likely lead to temperature increases in many regions of South America where temperatures are already considered to be high for olive production. Thus, experimental studies are needed to assess how water use in olive trees may be affected by global warming. The objectives of this study were to (i) evaluate the response of olive tree sap flow, stomatal conductance, and xylem anatomy to elevated temperature and (ii) determine whether fruit load may affect the temperature responses. A warming experiment using well-irrigated olive trees (cv. Arbequina) in open-top chambers (OTCs) with two temperature levels was performed from fruit set to the end of fruit growth in two seasons. Temperature levels were a near ambient control (T0) and a treatment 4°C above the control (T+). Trees were in the chambers for either one (2015–2016) or two seasons (2014–2015, 2015–2016) and were evaluated only in the second season when all trees were 3 years old. Whole-tree sap flow on leaf area basis, stomatal conductance, and aspects of xylem anatomy were measured. Sap flow was slightly higher in T+ than T0 trees heated for one season early in fruit development (summer) likely due to the elevated temperature and increase in vapor pressure deficit. Later in fruit development (fall), sap flow was substantially higher in the T+ trees heated for one season. Total vessel number per shoot was greater in the T+ than the T0 trees at this time due to more small-diameter vessels in the T+ trees, but this did not appear to explain the greater sap flow. The T+ trees that were heated for two seasons had less fruit load than the T0 trees due to little flowering. In contrast to trees heated for one season, sap flow was less in T+ than controls late in fruit development the second season, which was likely related to lower fruit load. An independent experiment using untreated trees confirmed that sap flow decreases when fruit load is below a threshold value. The results emphasize that multiple, interacting factors should be considered when predicting warming effects on water use in olive orchards.

Keywords: fruit load, global warming, heating, open-top chamber, sap flow, xylem anatomy

OPEN ACCESS

Edited by:
José Enrique Fernández, Institute of Natural Resources and Agrobiology of Seville (CSIC), Spain

Reviewed by:
Álvaro López-Bernal, Universidad de Córdoba, Spain
Dirk Vanderklein, Montclair State University, United States

****Correspondence:***
María Cecilia Rousseaux
crousseaux@conicet.gov.ar;
crousseaux2@gmail.com

†ORCID:
María Cecilia Rousseaux
orcid.org/0000-0001-8761-8839

Specialty section:
This article was submitted to Crop and Product Physiology, a section of the journal Frontiers in Plant Science

Received: *11 June 2019*
Accepted: *30 August 2019*
Published: *02 October 2019*

Citation:
Miserere A, Searles PS, Manchó G, Maseda PH and Rousseaux MC (2019) Sap Flow Responses to Warming and Fruit Load in Young Olive Trees. Front. Plant Sci. 10:1199. doi: 10.3389/fpls.2019.01199

INTRODUCTION

Global warming has already led to temperature increases around 1°C, and further increases are expected at an increasing rate for the coming decades (IPCC, 2014). This temperature increase together with changes in rainfall patterns will likely have a negative impact on crop production in semiarid and arid environments (Fereres et al., 2011; De Ollas et al., 2019). Olive (*Olea europaea*) is a widely cultivated fruit

tree species in the semiarid Mediterranean Basin and has expanded considerably over the last few decades to new warm, dry regions in the southern hemisphere including parts of Argentina and Australia (Torres et al., 2017). In such regions, current high temperatures are associated with little flowering in some cultivars (Ayerza and Sibbett, 2001; Aybar et al., 2015), as well as reductions in oil yield and quality (Mailer et al., 2010; Rondanini et al., 2014; García-Inza et al., 2014, García-Inza et al., 2016). Manipulative, warming experiments have also shown that increasing temperatures by 3°C to 4°C above current levels is likely to be detrimental for yields in southern Spain and northwest Argentina (Benlloch-González et al., 2018; Miserere et al., 2018; Benlloch-González et al., 2019).

In semiarid and arid regions, competition for water between agriculture and other sectors of the society is of critical importance and will likely only increase in the future as water scarcity intensifies (Fernández and Torrecillas, 2012). Regional climate modeling has indicated that the combination of increasing temperature and decreased rainfall in much of the Mediterranean Basin will lead to a greater need for irrigation (Tanasijevic et al., 2014). Further modeling suggests that increasing CO_2 concentrations may lessen expected increases in crop water use under high temperature conditions by reducing stomatal conductance (Lorite et al., 2018). Due to the number of uncertainties involved, manipulative field experiments of water use under increased temperatures would provide much needed information.

Tree transpiration depends on the available soil water, leaf area, and the atmospheric demand. In a 2-year field experiment using open-top chambers (OTCs), sap flow of heated grapevines was higher than that of control plants the first season due to greater chamber vapor pressure deficit (VPD) and leaf area (Bonada et al., 2018). However, sap flow was less in the heated grapevines the second season due to depletion of soil water. In 30-year-old Scots pine trees, sap flow was higher under long-term warming conditions because of increases in stomatal conductance and needle area (Kellomäki and Wang, 2000). In olive, the sap flow response to prolonged warming has not yet been addressed to the best of our knowledge.

Whole-tree transpiration in olive has been observed to be sensitive to current air temperature conditions in the field. Transpiration under well-irrigated conditions was found to represent approximately 70% to 80% of crop evapotranspiration in 7-year-old cv. Manzanilla fina trees in northwest Argentina with sap flow increasing linearly over a wide range of daily mean temperatures (13°C–32°C) (Rousseaux et al., 2009). Below mean daily values of 13°C, sap flow was minimal. Similarly, transpiration values in a mature cv. Picual orchard showed a linear relationship with mean daily air temperature when normalized for intercepted solar radiation (Orgaz et al., 2007). Under rainfed conditions or deficit irrigation, low soil water content would likely alter such relationships due to reductions in stomatal conductance and water potentials (Fernández et al., 1997; Cuevas et al., 2013; Chebbi et al., 2018).

Water lost from trees including olive is regulated in large part by stomatal aperture (Jones, 1998; Hernández-Santana et al., 2016). In the short term, stomatal conductance (g_s) increased with temperature in poplar and loblolly pine when measured at a similar VPD under controlled conditions in well-watered plants (Urban et al., 2017). However, increases in temperature under field conditions are often accompanied by greater VPD. When atmospheric demand increases, g_s has been consistently shown to decrease in olive trees (Moriana et al., 2002; Rousseaux et al., 2008). During a 2-week-long heat wave event in Italy, g_s dropped considerably in young trees when midday temperatures reached 40°C and recovered quickly following the heat wave (Haworth et al., 2018). Nevertheless, information is lacking as to how g_s in olive trees responds to more prolonged warming.

In the long term, changes in xylem anatomy in response to growth conditions can modify hydraulic conductivity and ultimately transpiration rates (Maseda and Fernández, 2006; Hacke et al., 2017). Elevated temperature increased the stem conduit area and hydraulic conductivity of saplings from several temperate and boreal species in a prolonged field experiment, particularly in species that were near the colder limit of their natural distribution (McCulloh et al., 2016). Furthermore, an increase in vein density and a decrease in vein diameter were observed in leaves of *Arabidopsis* ecotypes from different latitudes with increasing growth temperature (Adams et al., 2016). In this same study, leaf transpiration increased linearly with vein density when plants were evaluated under similar growing conditions. Olive is a species with small-diameter vessels compared to some other fruit trees species such as orange (*Citrus sinensis*) (Fernández et al., 2006) and has a low vulnerability to xylem embolisms and loss of hydraulic conductivity under moderate water stress (Tognetti et al., 2009; Torres-Ruiz et al., 2013). Yet, the effects of warming on the xylem anatomy of olive are not currently known.

Fruit load is important to consider in fruit tree studies because fruit are a significant carbon sink and affect plant water relations (Grossman and DeJong, 1994; Naor et al., 2008). In olive, whole-tree transpiration measured using lysimeters increased linearly with fruit load (Bustan et al., 2016). Stomatal conductance has also been shown to increase with fruit load in olive field studies in some cases (Martín-Vertedor et al., 2011; Naor et al., 2013), but not in others (Proietti et al., 2006; Bustan et al., 2016). In a warming experiment, g_s was higher in heated grapevines compared to controls on days with high g_s (Sadras et al., 2012b). However, low fruit load may have reduced the positive impact of elevated temperature on g_s. Given that warming can affect flowering in olive, fruit load should be carefully considered in whole-tree warming experiments.

The objectives of the present study were to (i) evaluate the responses of olive tree sap flow, stomatal conductance, and xylem anatomy to prolonged elevated temperature and (ii) determine whether fruit load may have affected the temperature responses. A warming experiment was conducted in which olive trees were grown either in control OTCs with near ambient air temperature or in heated OTCs that were several degrees above the control temperature for 5 months. An independent experiment using plants with a wide range of fruit load allowed for a more rigorous interpretation of the warming experiment.

MATERIALS AND METHODS

Plant Material

Cv. Arbequina olive trees were grown in an open, field nursery at the experimental field station of CRILAR-CONICET in Anillaco, La Rioja, in northwestern Argentina (28° 48′ S, 66° 56′ W, 1325 masl). The region is adjacent to the Andes mountains and is hot and dry with an annual evapotranspiration of about 1,600 mm and annual precipitation of 100 to 400 mm (Gómez-del-Campo et al., 2010; Searles et al., 2011). Own-rooted trees obtained from cuttings of a mother tree (San Gabriel Nursery S.A.; La Rioja) were transplanted when they were 14 months old in October 2013 to 30-L plastic pots filled with a 5:2 sandy soil:perlite mix and irrigated using 2 L h^{-1} drip emitters. The estimated water requirements were based on a previously derived function between mean daily temperature and sap flow (Rousseaux et al., 2009). Additional irrigation (30%) was provided in order to account for water losses from soil evaporation. Fertilization with macronutrients (15 N: 15 P: 15 K) was performed manually at a monthly interval, and micronutrients (B, 0.02% by weight; Cu, 0.01%; Fe, 3%; Mn, 1%; Zn, 1%, Mo 0.007%) + nitrogen (2.8%) + magnesium (0.5%) were applied weekly (Aminoquelant minors, Brometan, Spain).

Warming Experiment—Treatments

The warming experiment was conducted from final fruit set (December 1) to the end of fruit and vegetative growth (early May) during two growing seasons (2014–2015 and 2015–2016). The trees were warmed during either one or both growing seasons in OTCs (**Table 1**). All measurements presented in this study were performed the second season (2015–2016) when all trees were 3 years old. Trees receiving two seasons of temperature treatment were transferred to the OTCs for the first season of warming on December 2014. After approximately 5 months of warming, these trees returned to the adjacent field nursery in May 2015. The same group of trees was heated again in 2015–2016 along with a second group of previously unheated trees of the same age. Control trees were also placed in the OTCs in a similar manner both seasons.

The two temperature levels evaluated using the OTCs were a control slightly above ambient air temperature (T0) and a warming treatment with a target temperature set at 4°C above the control (T+). There were four OTCs per temperature level in a randomized complete block design with two factors (temperature and number of seasons heated in the OTCs). Blocks were used to account for any variability between OTCs in plant response that could have been related to the prevailing wind direction or minor differences in the heating system setup. Each OTC was designed to hold up to four trees, but only two trees per OTC were utilized in this study. One tree received its first season of warming, and the other received its second season. All trees were placed in cavities of about 30-cm soil depth with the soil surface in the pot being at the same level as the surrounding soil to avoid an increase in root temperature.

All OTC sidewalls (1.5 m each side and 2 m tall) were covered with 150-μm-thick, translucent polyethylene with low infrared transmittance (Premium Thermal Agrotileno PLDT221510; AgroRedes, Argentina). The T0 OTCs had some passive heating from the sidewalls but were not actively heated. The T+ OTCs had two complementary, active heating methods to increase temperature: a 6-m-long plastic sleeve with blackened stones through which heated air was sucked into the OTCs by fans during the daylight hours and an electric space heater (model AX-CA-1900 W; Axel, Argentina) whose operation was crucial during the night. Heated air from both methods entered into the OTCs *via* a PVC pipe with the pipe outlet positioned in the middle of the chamber at a height of 30 cm from the ground surface. Air flow from the outlet was redirected throughout the chamber by an air baffle. The electric heater was regulated by an electronic control system to avoid overheating (Cavadevices, Argentina). Shielded temperature sensors (TC1047A, Microchip Inc., China) were placed in each OTC at tree crown height (1.0 m), and the sensors were attached to a data logger recording every 15 min. The control program turned on or off the electric heater according to the 4°C differential target between T0 and T+ OTCs. Further details of the OTC design and function can be found in Miserere et al. (2019).

In addition to the air temperature readings from each OTC, relative humidity (RH) was recorded every 30 min using one sensor located at tree crown height in a T0 OTC and another in a T+ OTC. The sensors were moved every 2 to 3 days to a new pair of OTCs, and VPD was calculated based on the RH and temperature data (Allen et al., 1998). Outside of the chambers, air temperature and photosynthetic photon flux density (PPFD) were also monitored every hour in the field nursery adjacent to the OTCs. The PPFD was measured at a height of 3 m above the nursery trees (sensorPAR; Cavadevices), and air temperature was measured at tree crown height as was done within the OTCs. The PPFD inside the OTCs was measured periodically with a 1-m-long light bar (Cavadevices) and was about 75% of the PPFD above the field nursery due to absorption by the polyethylene walls and metal OTC structure with no differences between T0 and T+ OTCs.

Warming Experiment—Plant Measurements

All fruit on each tree were harvested at the end of the season (April 29 2016) to determine fruit number and total fresh fruit weight per tree. On May 10, all leaves were removed from each tree to obtain leaf biomass after drying at 70°C until constant weight was reached in an oven, and specific leaf mass was calculated from leaf disks of known area sampled from 50 leaves per tree. Leaf area per tree was then estimated by dividing leaf dry weight per tree by specific leaf mass. Lastly, fruit load was calculated as fruit number per tree divided by leaf area.

Sap flow of the main trunk was determined using the heat balance method (Flow 32, Dynamax Inc., TX, USA). This method consists of applying a known amount of heat (Pin) to the entire trunk perimeter and measuring the vertical (up and down; Qu and Qd) and radial (Qr) dissipation of heat using several sets of thermocouples. The heat dissipated by sap flux (Qf) is then calculated by subtraction (Equation 1). The flux rate (F) is Qf divided by the average difference in temperature (dT) between

upstream and downstream thermocouples and the heat capacity of water (Cp) (Equation 2).

$$Qf = Pin - Qu - Qd - Qr \quad (1)$$

$$F = Qf / (Cp * dT) \quad (2)$$

Given that the above method integrates the entire trunk, azimuth variations that often occur in sap flux measurements (López-Bernal et al., 2010) should be largely eliminated.

Measurements were conducted in both January (summer) and April (fall) (**Table 1**). In January, sap flow was measured for 10 consecutive days in the trees heated two seasons (2014–2015; 2015–2016) and their corresponding controls. One tree per OTC was measured including a total of four trees in T+ OTCs and four trees in T0 OTCs. Because only eight sensors were available due to economic limitations, the trees heated one season were measured for a similar 10-day period immediately following the two-season trees. In April, similar measurements were conducted, but the one-season trees were measured first. Measurements on the same tree were conducted over a limited number of consecutive days in order to better allow for comparisons between one- and two-season trees and to avoid possible damage to the trunk given that olive tree trunks can be damaged by heating (i.e., cracking) over extended periods (Rousseaux et al., 2009). Sensors were installed on trees with trunk diameters ranging from 20 to 30 mm (model SGB 16 and SGB25). The trunks were cleaned prior to installation, and canola oil was sprayed lightly on the trunk to improve contact between the trunk and the sensor. Power supply was adjusted daily by changing the heater input (0.25–0.3 W) to keep the average difference in temperature between upstream and downstream thermocouples (dT) between 0.7°C and 5°C. The dT was minimum at midday when sap flow was high and maximum at dawn when sap flow was negligible. Although the trunk was heated at night, this occurred in both the control and T+ trees. All sensors were heavily insulated and at least 15 cm from the soil surface to reduce heat flux from the soil. The sensors were connected to a Campbell CR10X data logger (Campbell Scientific, Logan, UT, USA) with readings taken every 60 s and averaged over 15 min. Daily sap flow was calculated as the accumulation of sap flow values along the day and expressed on a leaf area basis.

Stomatal conductance (g_s) was measured at least once during each measurement period on leaves from both the trees heated one or two seasons using a portable porometer (model AP4; Delta-T Devices Ltd, UK). Two sunlit, fully expanded leaves were measured per tree on shoots with no fruit (i.e., vegetative shoots) for each measurement date. Additionally, leaves from shoots with fruit (reproductive shoots) were measured on some occasions. Measurements were performed at midday (13:00 to 14:00 h solar time) when temperatures were near their maximum daily values to coincide with the time of day when sap flow was likely highest, although it is recognized that maximum g_s most often occurs at midmorning (Moriana et al., 2002). The porometer was calibrated on each measurement date within both the T0 and T+ OTCs to properly reflect the temperature and humidity conditions. Potential oscillations in g_s were not directly considered (López-Bernal et al., 2018), but sap flow monitored at 5-min intervals on one day did not detect any significant oscillations.

Xylem anatomy including the diameter and number of vessels was evaluated in one current-year shoot from each of the one- and two-season trees heated in the 2015–2016 growing season. The shoots were collected at predawn in the OTCs at the end of the season (2015–2016). In the laboratory, the shoots were introduced in humidified labeled nylon bags and kept in the refrigerator until processing. Four cross sections from each shoot were submerged in a 10% sodium hypochlorite solution, washed with distilled water, and stained with safranin (1%) (Zarlavsky, 2014). Then, the cross sections were mounted on a slide with Canadian balsam. The cross sections were observed with an optical microscope (Carl Zeiss Axiostar Plus, Germany) connected to a digital camera (Canon Power Shot G9, Japan). ImageJ software was used for the image processing (version 1.50i; National Institutes of Health, USA).

Fruit Load Experiment

To better interpret the warming experiment, eight olive trees from the field nursery with a wide range of fruit number per tree (33–900 fruit tree^{-1}) were used to evaluate sap flow and g_s responses to fruit load (# m^{-2} leaf area). The different fruit numbers per tree were naturally obtained because of differences in flowering intensity and fruit set. The trees in the nursery were of the same age and characteristics as those used in the warming experiment. To determine fruit load, fruit and leaf number were counted visually on the field nursery trees in February 2016. These values were corroborated at the end of the season (April 20, 2016) by harvesting the fruit and removing the leaves from each of the eight trees.

Sap flow was measured on each tree between February 23 and March 13 in 2016. Only 13 days were included in the analyses because of electrical outages. Protocol for the measurements was the same as that of the warming experiment. On March 1, g_s was measured on three sunlit, fully expanded leaves of both

TABLE 1 | Description of the warming experiment in the open-top chambers (OTCs) during two growing seasons (2014–2015, 2015–2016).

Seasons heated in OTCs (#)	Location during the season (December–May)			Sap flow measurements
	2013–2014	2014–2015	2015–2016	Day of the year
One season	Nursery	Nursery	OTC	25–35, 74–82
Two seasons	Nursery	OTC	OTC	14–24, 83–108

Trees were transplanted to 30-L plastic pots on October 2013 and heated either one or two seasons. All physiological measurements were performed in 2015–2016 when the trees were 3 years old.

vegetative and reproductive shoots per tree between 13:00 and 14:00 h solar time.

At the end of the season (April 20, 2016), a number of yield-related variables were measured in the eight trees including total fresh fruit weight, individual fruit dry weight, maturity index, and oil concentration (%). Individual fruit weight and maturity index were obtained using 50 fruit per tree when sufficient fruit were available. The fruit maturity index was calculated using the standard color evaluation of the skin and flesh with a 0- to 7-point scale (Uceda and Hermoso, 2001). Oil concentration (%) was ascertained from dried fruit (50) by nuclear magnetic resonance (model SLK-200; Spinlock, Argentina).

Statistical Analyses

Most variables from the warming experiment such as fruit number, leaf area, g_s, and number of vessels were analyzed using an ANOVA for fixed effects and a Duncan post-test to determine differences among treatment means ($p \leq 0.05$). Assumptions of homogeneity of variances and normality of the data were previously confirmed using Levene and Shapiro-Wilk tests, respectively. The analysis of variance was performed in InfoStat statistical software (Di Rienzo et al., 2016). Linear and bilinear functions between mean daily temperature and response variables such as daily sap flow were determined in the warming experiment. Differences between the slopes of mean daily temperature and sap flow were evaluated using the Student *t* test. The significant functions presented in the tables and figures correspond to the highest r^2 value for a particular variable. A similar approach was utilized in the fruit load experiment. Linear regression or bilinear regressions were analyzed with GraphPad Prism version 6.01 software (GraphPad Prism Software, Inc., LaJolla, CA, USA).

RESULTS

Warming Experiment

Mean daily, ambient air temperature outside the OTCs was high during the January sap flow measurement period in the summer (18°C–32°C) and somewhat lower in April in the fall (13°C–26°C) (**Figure 1A**). The daily temperature in the experimental OTCs varied in accordance with the ambient air temperatures, and the daily mean temperature was 0.4°C and 3.9°C above the ambient temperature in the T0 and T+ OTCs, respectively. Mean daily VPD values were about 0.4 to 0.5 kPa greater in the T+ OTCs than in the T0 OTCs in both January and April (**Figure 1B**). Maximum VPD values were 6.3 in T+ and 5.0 kPa in T0 during the early afternoon of January 23. Daily PPFD values outside of the OTCs during the sap flow measurements varied between 20 and 53 mol m^{-2} d^{-1} in January and 16 to 42 mol m^{-2} d^{-1} in April for the dates available (**Figure 1C**). The lower values in April were due to the combined effect of lower solar elevation and shorter days.

At final harvest, fruit number averaged 750 fruit per tree in both T0 and T+ OTCs for trees that were treated only one season in 2015–2016 (**Figure 2A**). In contrast, trees growing in the OTCs for two seasons (2014–2015, 2015–2016) had significantly lower

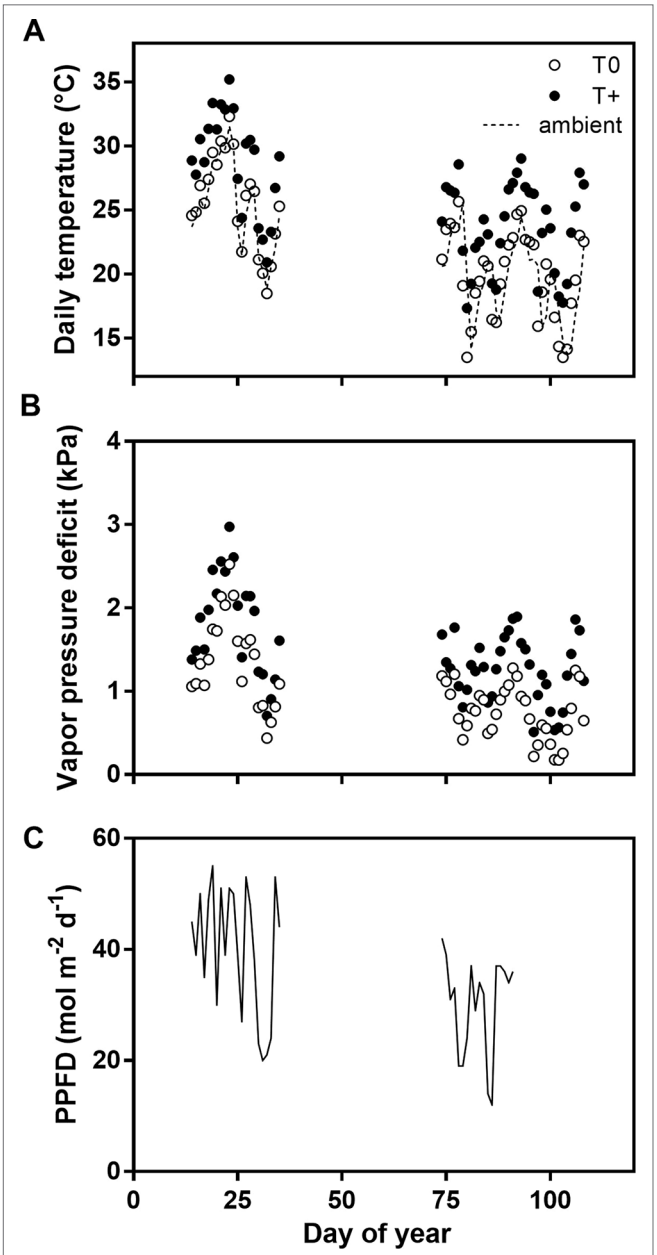

FIGURE 1 | Mean daily temperature **(A)**, mean daily vapor pressure deficit **(**VPD; **B)**, and daily integrated photosynthetic photon flux density **(**PPFD; **C)** during the sap flow measurement periods of the warming experiment from January to April 2016. The daily temperature and VPD values were measured inside the control (T0) and heated (T+) open-top chambers (OTCs). Symbols represent the average of four independent OTCs. Ambient temperature values outside the OTCs are also shown with a dotted lined, and PPFD was measured only outside the OTCs. PPFD values were not available for the latter part of April.

fruit numbers following the first season. Average fruit number was 540 fruit $tree^{-1}$ in T0 and only 200 fruit $tree^{-1}$ in T+. Given that fruit number was similar in the T0 and T+ trees in the first season since warming started after final fruit set in the summer, the reduced flowering intensity in the T+ trees the second season did not appear to be directly related to differences associated with

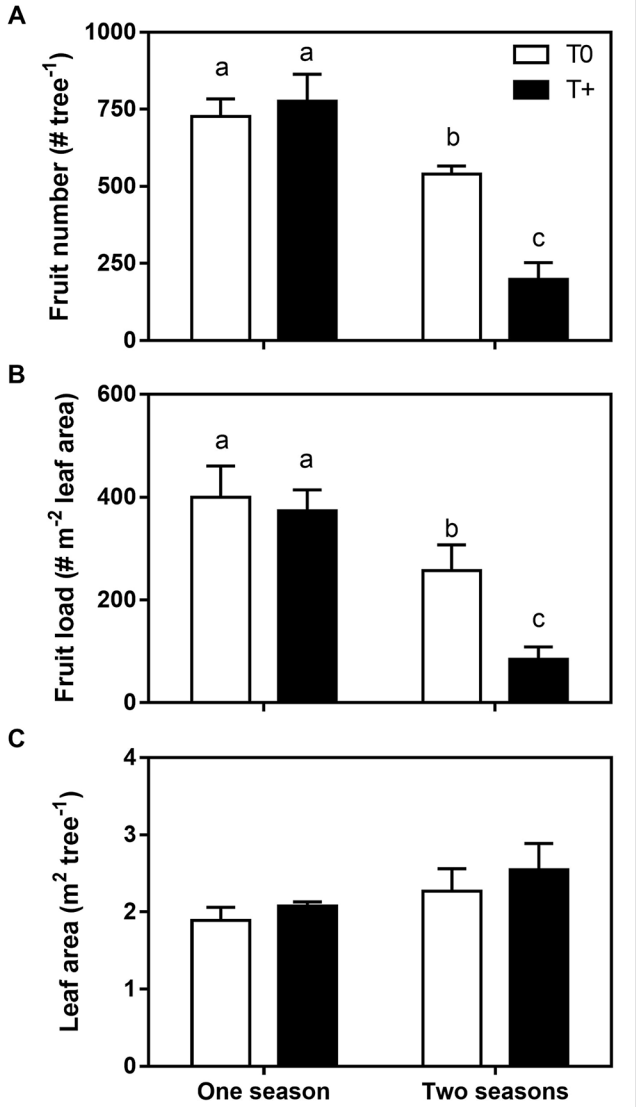

FIGURE 2 | Fruit number per tree **(A)**, fruit load **(B)**, and leaf area per tree **(C)** at harvest in 2016 for trees in the control (T0) and heated (T+) open-top chambers (OTCs). The trees were treated in the OTCs either one (2015–2016) or two seasons (2014–2015, 2015–2016). All trees were 3 years old during 2015–2016. Bars represent the averages ± one standard error (n = 4). Different letters indicate statistical significant differences between means ($p \leq 0.05$).

alternate bearing. Fruit load (# m^{-2} leaf area) showed a similar pattern (**Figure 2B**) since leaf area at the end of the season was not affected by warming in either trees with one or two seasons of temperature treatment (**Figure 2C**).

Diurnal sap flow patterns per unit of leaf area showed a sharp increase in the early morning with maximum rates between 10 and 16 h solar time, followed by a decrease until 20 h when sap flow became negligible ($p \leq 0.05$; **Figure 3**). Regardless of being in either T0 or T+ OTCs, trees with one season in the OTCs and high fruit load (**Figure 3A**) had consistently higher sap flow values at midday than trees with two seasons in the OTCs and lower fruit load in January (**Figure 3C**; $p \leq 0.01$). Although these measurements were conducted on different dates, mean ambient daily temperature was similar for the one- (25.7°C) and two-season (25.9°C) trees (**Figure 1**). With respect to warming, the T+ trees had slightly higher sap flow rates than T0 trees in January early in fruit development for both trees in the OTCs either one or two seasons (**Figures 3A**, **C**; $p \leq 0.10$). Later in fruit development (April), the results were different. T+ had much higher sap flow than T0 in the one-season trees despite fruit load being the same in both OTC types (**Figure 3B**; $p \leq 0.01$), while T+ had lower sap flow than T0 in the two-season trees (**Figure 3D**; $p \leq 0.01$). In this latter case, fruit load was significantly lower in the T+ trees.

Daily sap flow per unit leaf area of T0 and T+ trees was explained by a single linear relationship with mean daily temperature in January in both one- and two-season trees (**Figures 4A**, **C**). In contrast, daily sap flow of T+ trees increased linearly at twice the rate of T0 plants (0.048 vs. 0.023 kg m^{-2} d^{-1} $°C^{-1}$; $p \leq 0.05$) in one-season trees in April (**Figure 4B**). Thus, T+ sap flow was higher than that of T0 for a given mean daily temperature. However, as suggested by the diurnal sap flow pattern in **Figure 3D**, the daily sap flow of T+ trees increased linearly with mean daily temperature in April, but at a rate three times less than T0 trees (0.021 vs. 0.068 kg m^{-2} d^{-1} $°C^{-1}$; $p \leq 0.05$) (**Figure 4D**). Lastly, mean daily temperature was highly correlated with mean daily VPD ($r = 0.93$), maximum daily temperature ($r = 0.91$), and maximum daily VPD ($r = 0.90$). For this reason, relationships between daily sap flow and these variables were similar to the relationships shown for mean temperature (data not shown).

Stomatal conductance of leaves from vegetative and reproductive shoots was similar between T0 and T+ for one-season trees, which all had high fruit load (**Table 2**). In contrast, g_s of leaves from vegetative and reproductive shoots was generally lower in T+ than T0 for two-season trees ($p \leq 0.05$). As mentioned earlier, fruit load was low in the T+ trees and intermediate in the T0 trees. However, no differences were apparent in g_s values between the two shoot types for these same trees.

With respect to xylem anatomy, T+ trees had a greater number of small-diameter vessels than T0 in both one- and two-season trees (**Figure 5**; $p \leq 0.05$), and only T0 had vessels in the largest size classes. Furthermore, the total number of vessels per shoot was significantly greater in the T+ trees (634 vessels for the entire cross-sectional area of the shoot) than the T0 trees (561) for one season (**Figure 5A**). Shoot cross-sectional areas averaged 3.15 and 3.65 mm^2 in the T0 and T+ trees, respectively. A similar response occurred for the two-season trees (T+, 715; T0, 571) with cross-sectional areas of 2.86 in T+ and 3.51 mm^2 in T0 (**Figure 5B**).

Fruit Load Experiment

As was expected, the wide range of fruit load on these young trees strongly affected most yield-related variables (**Table 3**). Total fresh weight per tree increased with fruit load up to reaching a plateau at 200 fruit m^{-2} of leaf area above which no further increase occurred. Fruit maturity index decreased bilinearly with increasing fruit load, while individual fruit dry weight decreased linearly. Fruit oil concentration (%) was constant with fruit loads lower than 145 fruit m^{-2} and then decreased linearly as fruit load increased.

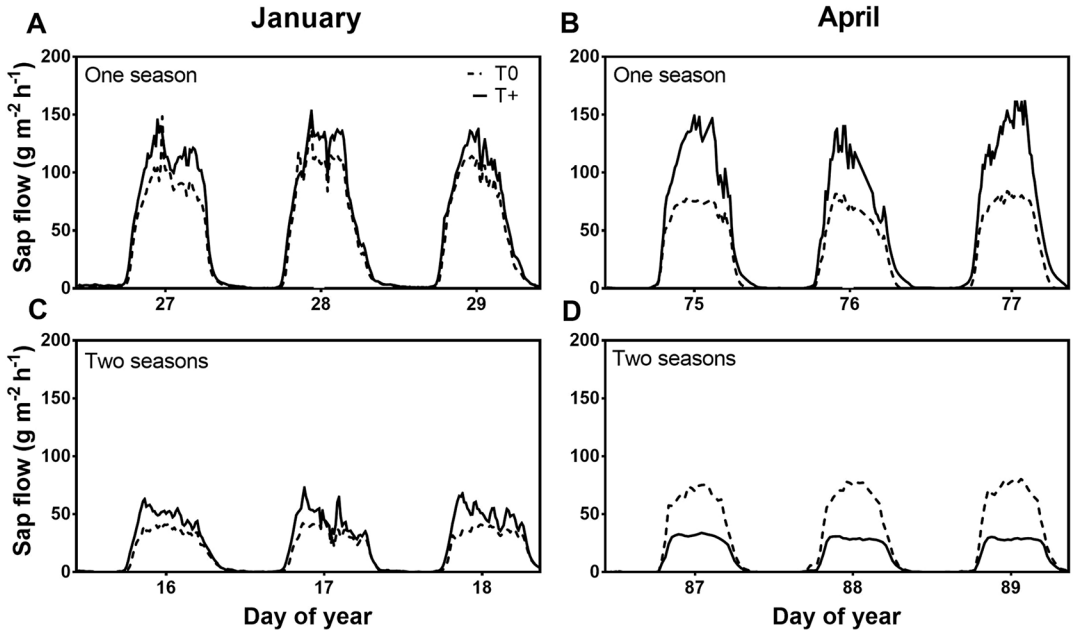

FIGURE 3 | Diurnal sap flow per tree in January **(A**, **C)** and April **(B**, **D)** 2016 for 3 consecutive days in control (T0) and heated (T+) open-top chambers (OTCs). The trees were treated in the OTCs either one (2015–2016) or two seasons (2014–2015, 2015–2016). All trees were 3 years old during 2015–2016. Each line represents the average of four OTCs.

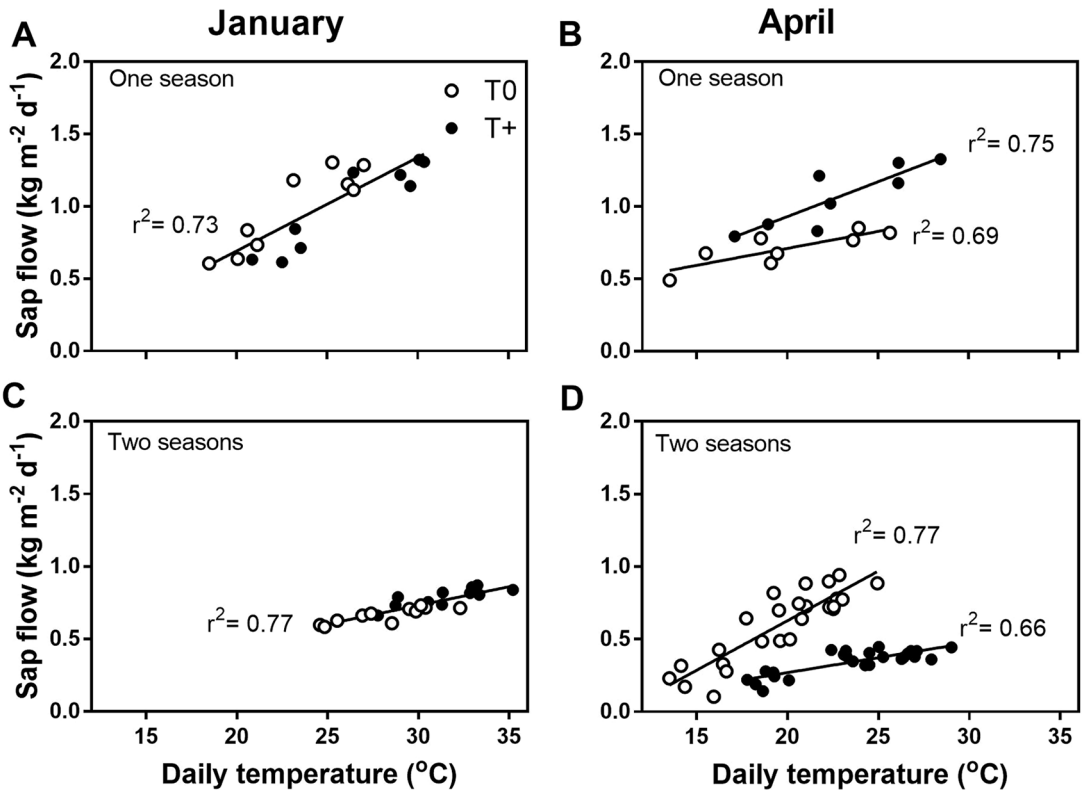

FIGURE 4 | Daily sap flow per tree in January **(A**, **C)** and April **(B**, **D)** 2016 as a function of mean daily temperature in control (T0) and heated (T+) open-top chambers (OTCs). The trees were treated in the OTCs either one (2015–2016) or two seasons (2014–2015, 2015–2016). All trees were 3 years old during 2015–2016. Each point represents the average of four OTCs. Different regression lines are shown when the slopes are significantly different between the T0 and T+ data ($p \leq 0.05$).

TABLE 2 | Stomatal conductance (mmol m^{-2} s^{-1}) at midday of leaves on vegetative and reproductive shoots in control (T0) or heated (T+) open-top chambers.

		Vegetative shoots		Reproductive shoots	
		One season	Two seasons	One season	Two seasons
January	T0	329 ± 22	405 ± 32 a	320 ± 11	371 ± 62
	T+	379 ± 26	269 ± 41 b	365 ± 59	191 ± 10
April	T0	377 ± 25	460 ± 50 a	318 ± 9.5	465 ± 12 a
	T+	325 ± 22	258 ± 78 b	290 ± 2.5	131 ± 30 b

The trees in the OTCs were heated one or two seasons. Means are shown ± standard error (n = 4). Different letters indicate statistically significant differences between means ($p \leq 0.05$).

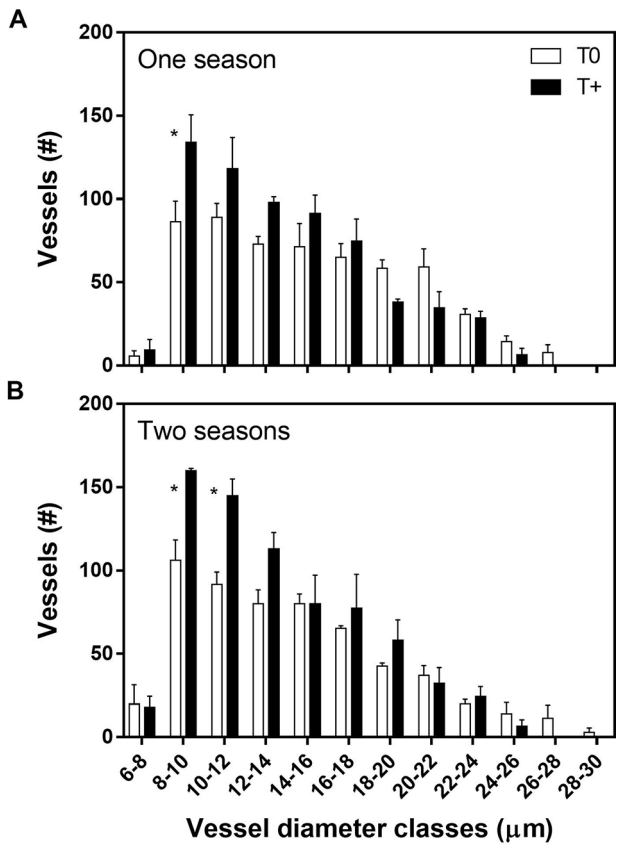

FIGURE 5 | Vessel diameter distribution in 2016 for current-season shoots in control (T0) and heated (T+) open-top chambers (OTCs). The trees were treated in the OTCs either one (2015–2016; **A**) or two seasons (2014–2015, 2015–2016; **B**). All trees were 3 years old during 2015–2016. Bars represent the averages ± one standard error (n = 4). Asterisks between bars indicate statistically significant differences between means for a given vessel diameter class ($p \leq 0.05$).

Daily sap flow increased with fruit load up to a threshold of 400 fruit m^{-2} leaf area with no further increase above that value (**Figure 6A**). A rate of increase of 0.3 kg m^{-2} d^{-1} for each increase of 100 fruit m^{-2} leaf area occurred with sap flow being three times greater in trees at 400 or more fruit m^{-2} leaf area than those at minimal fruit loads. Similarly, g_s increased with fruit load up to 180 fruit m^{-2} in leaves on vegetative shoots and 250 fruit m^{-2} in leaves on reproductive shoots, with a higher dispersion of the data for reproductive shoots (**Figures 6B**, **C**). Differences in the fruit load values at which the plateau was reached for sap flow and g_s are likely attributable to the limited number of trees measured.

Modeling Sap Flow Responses to Warming With Fruit Load

Sap flow responses to warming during the later stages of fruit development (April) were reanalyzed using bilinear models to account for fruit load (**Figure 7**). Daily sap flow increased significantly with fruit load up to a threshold of 280 fruit m^{-2} leaf area (**Figure 7A**). Above this threshold, sap flow values were highly variable, which resulted in a modeled r^2 value of 0.39 between fruit load and sap flow. In part, this was likely a consequence of sap flow being measured on different dates in one- and two-season trees (**Table 1**). Stomatal conductance, which was measured on the same dates in all trees, showed a similar bilinear function, but a much larger percentage of the variability was explained by fruit load (**Figures 7B**, **C**). The values of r^2 were approximately 0.60 between fruit load and g_s for both vegetative and reproductive shoots.

DISCUSSION

This study employed an experimental approach for determining the water use of young olive trees under prolonged, elevated temperature (+4°C) conditions using OTCs. A modest increase in VPD accompanied the temperature increase in the heated OTCs as has been seen in other studies (Norby et al., 1997; Sadras et al., 2012a), but other microclimate variables such as PPFD were similar to the control OTCs. Our experimental approach is consistent with regional climate models, which predict that aridity will increase by midcentury in our Andean region (Penalba and Rivera, 2013; Zaninelli et al., 2019). The active heating system also allowed for maintaining the high level of heating necessary to obtain a +4°C temperature increase. More open systems using infrared heaters provide more natural microclimate conditions, but obtaining large temperature differences is difficult under windy conditions (Kimball et al., 2018).

Whole-tree sap flow in young olive trees was slightly higher in the heated than the control trees early in fruit development in January for both trees in the OTCs either one or two seasons (**Figures 3A**, **C**). Leaf photosynthetic gas exchange measurements also indicated higher transpiration rates in the

TABLE 3 | Yield-related variables at harvest of the fruit load experiment in 2016. Fruit load was measured as the fruit number divided by the leaf area per tree (# m^{-2}).

Fruit load (# m^{-2})	Total fruit fresh weight (g $tree^{-1}$)	Maturity index (0–7)	Fruit dry weight (g $fruit^{-1}$)	Fruit oil concentration (%)
8	58	6.5	1.37	43.8
9	96	6.0	1.25	42.0
49	450	5.1	1.21	43.9
144	1200	4.5	1.26	44.3
180	1348	4.2	1.19	42.7
250	1348	2.6	0.97	41.0
446	1808	1.5	0.78	36.8
613	1608	2.1	0.61	35.6
Function	Bilinear	Bilinear	Linear	Bilinear
r^2	0.96	0.82	0.94	0.96

The data in each row represent an individual tree. The r^2 values for the best modeled functions between fruit load and a given variable are shown when significant ($p \leq 0.05$) at the bottom of the table.

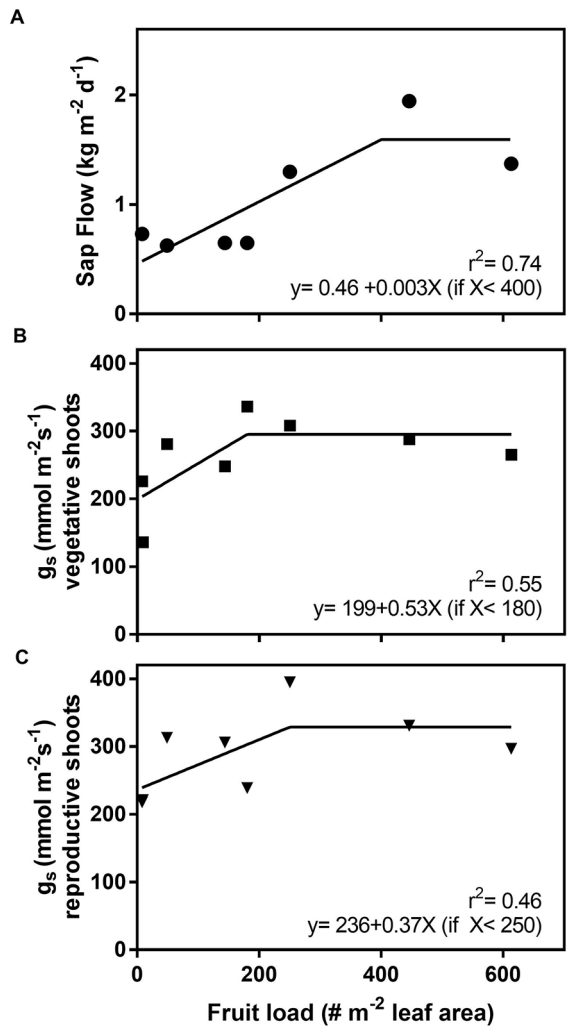

FIGURE 6 | Daily sap flow **(A)**, stomatal conductance of leaves on vegetative shoots (g_s; **B)**, and stomatal conductance of leaves on reproductive shoots **(C)** as a function of fruit load in the independent fruit load experiment. Each point represents the average sap flow for 13 days for an individual tree with mean daily temperature ranging from 17°C to 27°C. Stomatal conductance was measured on March 1. A data point is not shown for the tree with 9.1 fruit m^{-2} leaf area in panel A due to a technical malfunction of the sap flow sensor. Data points shown for all trees are present in the other two panels.

T+ trees (Miserere, unpublished results). In grapevines, even a modest warming between 1°C and 2°C resulted in higher sap flow due to both greater leaf area and slightly higher VPD in heated vines than control vines under field conditions (Bonada et al., 2018). Aspen trees also showed significant increases in water use when heated by 5°C under growth chamber conditions because of greater growth and whole-tree hydraulic conductance in heated seedlings (Way et al., 2013). In the current study, leaf area per tree was similar between T+ and T0 trees (**Figure 2C**) most likely because the trees were heated either one or two seasons in the summer and fall when shoot growth was fairly low. Even in young olive trees, vegetative growth at that time of the year is very limited due to fruit growth and oil accumulation (Rosati et al., 2018). Also, root biomass did not show any differences between T0 and T+ trees (data not shown). Thus, it did not appear that differences in root biomass contributed to the sap flow responses.

The higher sap flow of the heated trees was explained by a single linear relationship with mean daily temperature early in fruit development (January) in both trees heated either one or two seasons (**Figures 4A**, **C**). Given that neither leaf area nor g_s (**Table 2**) was affected by heating for one season, it appears likely that elevated temperature accompanied by greater VPD led to the higher daily sap flow in these trees. In the trees heated for two seasons, g_s tended to be lower in January, although sap flow was somewhat higher in these same trees. Stomatal conductance has been shown to decrease with increasing instantaneous VPD values up to approximately 3.5 kPa in some previous olive field studies, but to be largely unresponsive to higher VPD values (Fernández et al., 1997; Rousseaux et al., 2008). In the present study, midday VPD values when g_s was measured were substantially higher than the 3.5 kPa threshold in both T+ and T0 trees. Thus, it is suggested that the decrease in g_s at midday may have been an early response to the low fruit load rather than VPD in the T+ trees. As will be discussed further, g_s often decreases with fruit load (Martín-Vertedor et al., 2011; Naor et al., 2013).

Later in fruit development (April), T+ trees had much higher diurnal values of sap flow than T0 trees for trees heated during the current season (i.e., one-season trees) (**Figure 3B**). Higher sap flow values in the T+ trees were even apparent for a given mean daily temperature (**Figure 4B**). This response could be explained by acclimation to temperature after several months

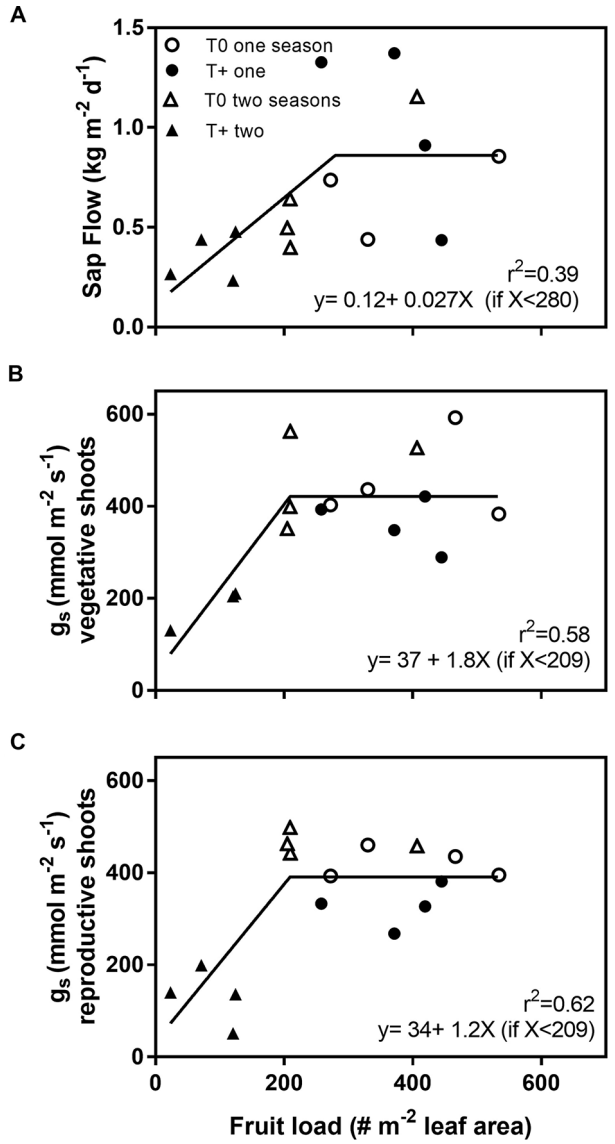

FIGURE 7 | Daily sap flow **(A)**, stomatal conductance of leaves on vegetative shoots (g_s; **B)**, and stomatal conductance of leaves on reproductive shoots **(C)** as a function of fruit load in control (T0) and heated (T+) open-top chambers (OTCs). The trees were treated in the OTCs either one (2015–2016) or two seasons (2014–2015, 2015–2016). All trees were 3 years old during 2015–2016 when measurements were performed. Sap flow data correspond to the average of 9 (one season; March 14–22) and 24 (two seasons; March 23– April 17) measurement dates. Stomatal conductance is the average of two measurement dates (March 17, April 4) with similar weather conditions. Each point represents one tree per OTC.

of warming. In addition to greater tree sap flow, current season shoots of T+ trees had a higher total vessel number than the T0 trees due to more small-diameter vessels (**Figure 5A**). In olive, modifications in vessel density and diameter of current season shoots have been previously reported in response to deficit irrigation (Torres-Ruiz et al., 2013; Rossi et al., 2013), but not as a function of growth temperature. An increase in vessel number can be indicative of greater shoot water transport capacity in trees (Way et al., 2013), although this is not always the case. Further analysis shows that the theoretical specific hydraulic conductivity of the T+ trees was actually somewhat lower than that of the T0 trees based on the Hagen-Poiseuille equation (data not shown) (Tyree and Ewers, 1991). This occurred because the increase in vessel number in the T+ trees was due to more small-diameter vessels, which have little conductivity, and some tendency to have fewer large vessels that have very high conductivities. Thus, it does not appear that changes in vessel number in our study and their distribution resulted in the greater sap flow in the T+ trees. López-Bernal et al. (2010) also did not find a good correlation between the theoretical specific conductivity and sap velocity in mature olive trees. Other mechanisms in T+ trees such as lower leaf water potential due to osmotic adjustment as occurs under water stress in olive trees (Dichio et al., 2005; Lo Bianco and Scalisi, 2017) or less sap viscosity at higher temperature (Cochard et al., 2000) might explain the greater sap flow. Further research is needed in this regard. Lastly, the increase in small-diameter vessel number could suggest a safer water transport system based on redundancy and potentially less vulnerability to cavitation as reviewed by Hacke et al. (2017).

In contrast to the T+ trees heated for one season, sap flow was lower in T+ trees heated for two seasons compared to T0 trees late in fruit development for any given temperature (**Figure 4D**). The T+ trees had high fruit loads similar to the T0 trees the first season, but fruit load was much lower in the T+ trees than the controls the second season due to less flowering (**Figure 2B**). Moreover, total fruit dry weight was also lower in T+ than T0 (148 vs. 547 g tree^{-1}) because of the combined effect of a lower fruit load and smaller individual fruit size (0.8 vs. 1.01 g fruit^{-1}) due to the temperature treatment. Whole-tree water use using lysimeters has previously been shown to be low under low fruit loads with water use increasing markedly as fruit load increased, and the response to fruit load was much greater late in the season when fruit size was near maximum (Bustan et al., 2016). In the present study, the g_s was also lower in the T+ trees in April during the second season of heating. As mentioned previously, similar changes in g_s with fruit load have been reported in some other olive field studies (Martín-Vertedor et al., 2011; Naor et al., 2013), although this is not always the case (Proietti et al., 2006; Bustan et al., 2016). Sap flow and g_s in our study also showed a strong response to increasing fruit load when trees with a wide range of fruit loads were evaluated in an independent experiment in our field nursery (**Figure 6**).

A reanalysis of the warming experiment corroborated that fruit load explained a significant portion of the sap flow and g_s results in the warming experiment (**Figure 7**). Bilinear models best fit the relationship between sap flow and g_s with fruit load, although sap flow was variable at high fruit loads. Such information may be of use in predicting complex responses to global warming using simulation models in olive (Morales et al., 2016). One future scenario is that if flowering and subsequent fruit load are reduced by warming in olive trees (Vuletin Selak et al., 2014; Benlloch-González et al., 2018), warming would lead to less whole-tree transpiration and lower irrigation needs

in olive orchards. Alternatively, different cultivars may respond differently to warming (De Ollas et al., 2019), and responses may vary due to regional climate. Such possibilities suggest a wider range of future scenarios.

CONCLUSIONS

Sap flow of young olive trees appeared to increase due to elevated temperature and accompanying increases in VPD in the short term with further increases apparent over several months in the first season of warming. In contrast, trees heated for more than one season had lower fruit loads, which decreased sap flow in heated trees late in the season when fruit were near full size. These results provide a further understanding of the ecophysiological responses of olive trees to temperature and emphasize that multiple, interacting factors should be considered when predicting warming effects on water use in olive orchards.

DATA AVAILABILITY STATEMENT

The datasets generated for this study are available on request to the corresponding author.

AUTHOR CONTRIBUTIONS

AM, PS, and MR designed the measurements and sampling protocols. PM and GM performed the anatomical measurements. MR and AM performed most of the data collection, data processing, and statistical analyses. All authors contributed to the overall intellectual development of the study and the writing of the manuscript.

FUNDING

This research was supported by grants from the Ministerio de Ciencia, Tecnología e Innovación Productiva de Argentina (ANPCyT, PICT2015 0195) and CONICET (PUE 2016 0125).

ACKNOWLEDGMENTS

Carlos Herrera, Diego Castro, Ana Ailén Federico, and Romina Zabaleta provided technical assistance in the field. Fabian Teran of San Gabriel nursery donated the olive trees and Santiago Brizuela of Agropecuaria Norte S.A. provided advice on the irrigation system design. AM held a doctoral fellowship from CONICET. MR and PS are members of CONICET.

REFERENCES

Adams, W. W., Stewart, J. J., Cohu, C. M., Muller, O., and Demmig-Adams, B. (2016). Habitat temperature and precipitation of *Arabidopsis thaliana* ecotypes determine the response of foliar vasculature, photosynthesis, and transpiration to growth temperature. *Front. Plant Sci.* 7, 1026. doi: 10.3389/fpls.2016.01026

Allen, R. G., Pereira, L. S., Raes, D., and Smith, M. (1998). *Crop evapotranspiration: guidelines for computing crop water requirements. FAO Irrigation and Drainage Paper No. 56*. Rome: FAO.

Aybar, V. E., De Melo-Abreu, J. P., Searles, P. S., Matias, A. C., Del Río, C., Caballero, J. M., et al. (2015). Evaluation of olive flowering at low latitude sites in Argentina using a chilling requirement model. *Spanish J. Agric. Res.* 13, 1–10. doi: 10.5424/sjar/2015131-6375

Ayerza, R., and Sibbett, G. S. (2001). Thermal adaptability of olive (*Olea europaea* L.) to the Arid Chaco of Argentina. *Agric. Ecosyst. Environ.* 84, 277–285. doi: 10.1016/S0167-8809(00)00260-7

Benlloch-González, M., Sánchez-Lucas, R., Aymen, M., Benlloch, M., and Fernández-Escobar, R. (2019). Global warming effects on yield and fruit maturation of olive trees growing under field conditions. *Sci. Hortic.* 249, 162–167. doi: 10.1016/j.scienta.2019.01.046

Benlloch-González, M., Sánchez-Lucas, R., Benlloch, M., and Fernández-Escobar, R. (2018). An approach to global warming effects on flowering and fruit set of olive trees growing under field conditions. *Sci. Hortic.* 240, 405–410. doi: 10.1016/j.scienta.2018.06.054

Bonada, M., Buesa, I., Moran, M. A., and Sadras, V. O. (2018). Interactive effects of warming and water deficit on Shiraz vine transpiration. *OENO One* 52, 189–202. doi: 10.20870/oeno-one.2018.52.2.2141

Bustan, A., Dag, A., Yermiyahu, U., Erel, R., Presnov, E., Agam, N., et al. (2016). Fruit load governs transpiration of olive trees. *Tree Physiol.* 36, 380–391. doi: 10.1093/treephys/tpv138

Chebbi, W., Boulet, G., Le Dantec, V., Lili Chabaane, Z., Fanise, P., Mougenot, B., et al. (2018). Analysis of evapotranspiration components of a rainfed olive orchard during three contrasting years in a semi-arid climate. *Agric. For. Meteorol.* 257, 159–178. doi: 10.1016/j.agrformet.2018.02.020

Cochard, H., Martin, R., Gross, P., and Bogeat-Triboulot, M. B. (2000). Temperature effects on hydraulic conductance and water relations of *Quercus robur* L. *J. Exp. Bot.* 51, 1255–1259. doi: 10.1093/jexbot/51.348.1255

Cuevas, M. V., Martín-Palomo, M. J., Díaz-Espejo, A., Torres-Ruiz, J. M., Rodriguez-Dominguez, C. M., Perez-Martin, A., et al. (2013). Assessing water stress in a hedgerow olive orchard from sap flow and trunk diameter measurements. *Irrig. Sci.* 31, 729–746. doi: 10.1007/s00271-012-0357-x

De Ollas, C., Morillón, R., Fotopoulos, V., Puértolas, J., Ollitrault, P., Gómez-Cadenas, A., et al. (2019). Facing climate change: biotechnology of iconic Mediterranean woody crops. *Front. Plant Sci.* 10, 427. doi: 10.3389/fpls.2019.00427

Dichio, B., Xiloyannis, C., Sofo, A., and Montanaro, G. (2005). Osmotic regulation in leaves and roots of olive trees during a water deficit and rewatering. *Tree Physiol.* 26, 179–185. doi: 10.1093/treephys/26.2.179

Di Rienzo, J. A., Casanoves, F., Balzarini, M. G., Gonzalez, L., Tablada, M., and Robledo, C. W. (2016). *InfoStat versión 2016*. Argentina: Grupo InfoStat, FCA, Universidad Nacional de Córdoba.

Fereres, E., Orgaz, F., and Gonzalez-Dugo, V. (2011). Reflections on food security under water scarcity. *J. Exp. Bot.* 62, 4079–4086. doi: 10.1093/jxb/err165

Fernández, J. E., Moreno, F., Girón, I. F., and Blázquez, O. M. (1997). Stomatal control of water use in olive tree leaves. *Plant Soil* 190, 179–192. doi: 10.1023/A:1004293026973

Fernández, J. E., Durán, P. J., Palomo, M. J., Diaz-Espejo, A., Chamorro, V., and Girón, I. F. (2006). Calibration of sap flow estimated by the compensation heat pulse method in olive, plum and orange trees: relationships with xylem anatomy. *Tree Physiol.* 26, 719–728. doi: 10.1093/treephys/26.6.719

Fernández, J. E., and Torrecillas, A. (2012). For a better use and distribution of water: an introduction. *Agric. Water Manage.* 114, 1–3. doi: 10.1016/j.agwat.2012.07.004

García-Inza, G. P., Castro, D. N., Hall, A. J., and Rousseaux, M. C. (2014). Responses to temperature of fruit dry weight, oil concentration, and oil fatty acid composition in olive (*Olea europaea* L. var. 'Arauco'). *Eur. J. Agron.* 54, 107–115. doi: 10.1016/j.eja.2013.12.005

García-Inza, G. P., Castro, D. N., Hall, A. J., and Rousseaux, M. C. (2016). Opposite oleic acid responses to temperature in oils from the seed and mesocarp of the olive fruit. *Eur. J. Agron.* 76, 138–147. doi: 10.1016/j.eja.2016.03.003

Gómez-del-Campo, M., Morales-Sillero, A., Vita Serman, F., Rousseaux, M. C., and Searles, P. S. (2010). Olive growing in the arid valleys of northwest Argentina (provinces of Catamarca, La Rioja and San Juan). *Olivae* 114, 23–45.

Grossman, Y. L., and DeJong, T. M. (1994). PEACH: a simulation model of reproductive and vegetative growth in peach trees. *Tree Physiol.* 14, 329–345. doi: 10.1093/treephys/14.4.329

Hacke, U. G., Spicer, R., Schreiber, S. G., and Plavcová, L. (2017). An ecophysiological and developmental perspective on variation in vessel diameter. *Plant Cell Environ.* 40, 831–845. doi: 10.1111/pce.12777

Haworth, M., Marino, G., Brunetti, C., Killi, D., De Carlo, A., and Centritto, M. (2018). The impact of heat stress and water deficit on the photosynthetic and stomatal physiology of olive (*Olea europaea* L.)—a case study of the 2017 heat wave. *Plants* 7, 1–13. doi: 10.3390/plants7040076

Hernández-Santana, V., Fernández, J. E., Rodriguez-Dominguez, C. M., Romero, R., and Díaz-Espejo, A. (2016). The dynamics of radial sap flux density reflects changes in stomatal conductance in response to soil and air water deficit. *Agric. For. Meteorol.* 218 (219), 92–101. doi: 10.1016/j.agrformet.2015.11.013

IPCC. (2014). *Climate change 2014: synthesis report. Contribution of Working Groups I, II and III to the fifth assessment report of the Intergovernmental Panel on Climate Change*. Geneva, Switzerland: IPCC.

Jones, H. (1998). Stomatal control of photosynthesis and transpiration. *J. Exp. Bot.* 49, 387–398. doi: 10.1093/jxb/49.Special_Issue.387

Kellomäki, S., and Wang, K. Y. (2000). Modelling and measuring transpiration from Scots pine with increased temperature and carbon dioxide enrichment. *Ann. Bot.* 85, 263–278. doi: 10.1006/anbo.1999.1030

Kimball, B. A., Alonso-Rodríguez, A. M., Cavaleri, M. A., Reed, S. C., González, G., and Wood, T. E. (2018). Infrared heater system for warming tropical forest understory plants and soils. *Ecol. Evol.* 8, 1932–1944. doi: 10.1002/ece3.3780

Lo Bianco, R., and Scalisi, A. (2017). Water relations and carbohydrate partitioning of four greenhouse-grown olive genotypes under long-term drought. *Trees* 31, 717–727. doi: 10.1007/s00468-016-1502-6

López-Bernal, A., Alcántara, E., Testi, L., and Villalobos, F. J. (2010). Spatial sap flow and xylem anatomical characteristics in olive trees under different irrigation regimes. *Tree Physiol.* 30, 1536–1544. doi: 10.1093/treephys/tpq095

López-Bernal, A., García-Tejera, O., Testi, L., Orgaz, F., and Villalobos, F. J. (2018). Stomatal oscillations in olive trees: analysis and methodological implications. *Tree Physiol.* 38, 531–542. doi: 10.1093/treephys/tpx127

Lorite, I. J., Gabaldón-Leal, C., Ruiz-Ramos, M., Belaj, A., de la Rosa, R., León, L., et al. (2018). Evaluation of olive response and adaptation strategies to climate change under semi-arid conditions. *Agric. Water Manage.* 204, 247–261. doi: 10.1016/j.agwat.2018.04.008

Mailer, R. J., Ayton, J., and Graham, K. (2010). The influence of growing region, cultivar and harvest timing on the diversity of Australian olive oil. *J. Am. Oil Chem. Soc.* 87, 877–884. doi: 10.1007/s11746-010-1608-8

Martín-Vertedor, A. I., Pérez-Rodríguez, J. M., Prieto Losada, H., and Fereres Castiel, E. (2011). Interactive responses to water deficits and crop load in olive (*Olea europaea* L., cv. Morisca) I.—growth and water relations. *Agric. Water Manage.* 98, 941–949. doi: 10.1016/j.agwat.2011.01.002

Maseda, P. H., and Fernández, R. J. (2006). Stay wet or else: three ways in which plants can adjust hydraulically to their environment. *J. Exp. Bot.* 57, 3963–3977. doi: 10.1093/jxb/erl127

McCulloh, K. A., Petitmermet, J., Stefanski, A., Rice, K. E., Rich, R. L., Montgomery, R. A., et al. (2016). Is it getting hot in here? Adjustment of hydraulic parameters in six boreal and temperate tree species after 5 years of warming. *Glob. Chang. Biol.* 22, 4124–4133. doi: 10.1111/gcb.13323

Miserere, A., Searles, P. S., García-Inza, G. P., and Rousseaux, M. C. (2018). Elevated temperature affects vegetative growth and fruit oil concentration in olive trees (*Olea europaea*). *Acta Hortic.* 1199, 523–528. doi: 10.17660/ActaHortic.2018.1199.83

Miserere, A., Searles, P. S., Hall, A. J., García-Inza, G. P., and Rousseaux, M. C. Complementary active heating methods for evaluating the responses of young olive trees to warming. *Sci. Hortic* (in press) (2019). 257, 108754. doi: 10.1016/j.scienta.2019.108754

Morales, A., Leffelaar, P. A., Testi, L., Orgaz, F., and Villalobos, F. J. (2016). A dynamic model of potential growth of olive (*Olea europaea* L.) orchards. *Eur. J. Agron.* 74, 93–102. doi: 10.1016/j.eja.2015.12.006

Moriana, A., Villalobos, F. J., and Fereres, E. (2002). Stomatal and photosynthetic responses of olive (*Olea europaea* L.) leaves to water deficits. *Plant Cell Environ.* 25, 395–405. doi: 10.1046/j.0016-8025.2001.00822.x

Naor, A., Naschitz, S., Peres, M., and Gal, Y. (2008). Responses of apple fruit size to tree water status and crop load. *Tree Physiol.* 28, 1255–1261. doi: 10.1093/treephys/28.8.1255

Naor, A., Schneider, D., Ben-Gal, A., Zipori, I., Dag, A., Kerem, Z., et al. (2013). The effects of crop load and irrigation rate in the oil accumulation stage on oil yield and water relations of 'Koroneiki' olives. *Irrig. Sci.* 31, 781–791. doi: 10.1007/s00271-012-0363-z

Norby, R. J., Edwards, N. T., Riggs, J. S., Abner, C. H., Wullschleger, S. D., and Gunderson, C. A. (1997). Temperature-controlled open-top chambers for global change research. *Glob. Chang. Biol.* 3, 259–267. doi: 10.1046/j.1365-2486.1997.00072.x

Orgaz, F., Villalobos, F. J., Testi, L., and Fereres, E. (2007). A model of daily mean canopy conductance for calculating transpiration of olive canopies. *Funct. Plant Biol.* 34, 178–188. doi: 10.1071/FP06306

Penalba, O., and Rivera, J. A. (2013). Future changes in drought characteristics over southern South America projected by a CMIP5 multi-model ensemble. *Am. J. Clim. Change* 2, 173–182. doi: 10.4236/ajcc.2013.23017

Proietti, P., Nasini, L., and Famiani, F. (2006). Effect of different leaf-to-fruit ratios on photosynthesis and fruit growth in olive (*Olea europaea* L.). *Photosynthetica* 44, 275–285. doi: 10.1007/s11099-006-0019-4

Rondanini, D. P., Castro, D. N., Searles, P. S., and Rousseaux, M. C. (2014). Contrasting patterns of fatty acid composition and oil accumulation during fruit growth in several olive varieties and locations in a non-Mediterranean region. *Eur. J. Agron.* 52, 237–246. doi: 10.1016/j.eja.2013.09.002

Rosati, A., Paoletti, A., Al Hariri, R., Morelli, A., and Famiani, F. (2018). Resource investments in reproductive growth proportionately limit investments in whole-tree vegetative growth in young olive trees with varying crop loads. *Tree Physiol.* 38, 1–11. doi: 10.1093/treephys/tpy011

Rossi, L., Sebastiani, L., Tognetti, R., d'Andria, R., Morelli, G., and Cherubini, P. (2013). Tree-ring wood anatomy and stable isotopes show structural and functional adjustments in olive trees under different water availability. *Plant Soil* 372, 567–579. doi: 10.1007/s11104-013-1759-0

Rousseaux, M. C., Benedetti, J. P., and Searles, P. S. (2008). Leaf-level responses of olive trees (*Olea europaea*) to the suspension of irrigation during the winter in an arid region of Argentina. *Sci. Hortic.* 115, 135–141. doi: 10.1016/j.scienta.2007.08.005

Rousseaux, M. C., Figuerola, P. I., Correa-Tedesco, G., and Searles, P. S. (2009). Seasonal variations in sap flow and soil evaporation in an olive (*Olea europaea* L.) grove under two irrigation regimes in an arid region of Argentina. *Agric. Water Manage.* 96, 1037–1044. doi: 10.1016/j.agwat.2009.02.003

Sadras, V. O., Bubner, R., and Moran, M. A. (2012a). A large-scale, open-top system to increase temperature in realistic vineyard conditions. *Agric. For. Meteorol.* 154 (155), 187–194. doi: 10.1016/j.agrformet.2011.11.005

Sadras, V. O., Montoro, A., Moran, M. A., and Aphalo, P. J. (2012b). Elevated temperature altered the reaction norms of stomatal conductance in field-grown grapevine. *Agric. For. Meteorol.* 165, 35–42. doi: 10.1016/j.agrformet.2012.06.005

Searles, P. S., Agüero Alcarás, M., and Rousseaux, M. C. (2011). Consumo del agua por el cultivo del olivo (*Olea europaea* L.) en el Noroeste de Argentina: una comparación con la Cuenca Mediterránea. *Ecol. Aus.* 21, 15–28.

Tanasijevic, L., Todorovic, M., Pereira, L. S., Pizzigalli, C., and Lionello, P. (2014). Impacts of climate change on olive crop evapotranspiration and irrigation requirements in the Mediterranean region. *Agric. Water Manage.* 144, 54–68. doi: 10.1016/j.agwat.2014.05.019

Tognetti, R., Giovannelli, A., Lavini, A., Morelli, G., Fragnito, F., and D'Andria, R. (2009). Assessing environmental controls over conductances through the soil-plant-atmosphere continuum in an experimental olive tree plantation of southern Italy. *Agric. For. Meteorol.* 149, 1229–1243. doi: 10.1016/j.agrformet.2009.02.008

Torres, M., Pierantozzi, P., Searles, P., Rousseaux, M. C., García-Inza, G., Miserere, A., et al. (2017). Olive cultivation in the southern hemisphere: flowering, water requirements and oil quality responses to new crop environments. *Front. Plant Sci.* 8, 1–12. doi: 10.3389/fpls.2017.01830

Torres-Ruiz, J. M., Diaz-Espejo, A., Morales-Sillero, A., Martín-Palomo, M. J., Mayr, S., Beikircher, B., et al. (2013). Shoot hydraulic characteristics, plant water status and stomatal response in olive trees under different soil water conditions. *Plant Soil* 373, 77–87. doi: 10.1007/s11104-013-1774-1

Tyree, M. T., and Ewers, F. W. (1991). The hydraulic architecture of trees and other woody plants. *New Phytol.* 119, 345–360. doi: 10.1111/j.1469-8137.1991.tb00035.x

Uceda, M., and Hermoso, M. (2001). "La calidad del aceite de oliva," in *El cultivo del olivo*. Eds. D. Barranco, R. Fernández-Escobar, and L. Rallo (Madrid: Ediciones Mundi-Prensa), 589–614.

Urban, J., Ingwers, M., McGuire, M. A., and Teskey, R. O. (2017). Stomatal conductance increases with rising temperature. *Plant Signal. Behav.* 12, doi: 10.1080/15592324.2017.1356534

Vuletin Selak, G., Cuevas, J., Goreta Ban, S., Pinillos, V., Dumicic, G., and Perica, S. (2014). The effect of temperature on the duration of the effective pollination period in 'Oblica' olive (*Olea europaea*) cultivar. *Ann. Appl. Biol.* 164, 85–94. doi: 10.1111/aab.12082

Way, D. A., Domec, J., and Jackson, R. B. (2013). Elevated growth temperatures alter hydraulic characteristics in trembling aspen (*Populus tremuloides*) seedlings: implications for tree drought tolerance. *Plant Cell Environ.* 36, 103–115. doi: 10.1111/j.1365-3040.2012.02557.x

Zaninelli, P. G., Menéndez, C. G., Falco, M., Franca, N. L., and Carril, A. F. (2019). Future hydroclimatological changes in South America based on an ensemble of regional climate models. *Clim. Dyn.* 52, 819–830. doi: 10.1007/s00382-018-4225-0

Zarlavsky, G. E. (2014). *Histología Vegetal: técnicas simples y complejas*. Buenos Aires: Sociedad Argentina de Botánica.

Conflict of Interest: The authors declare that the research was conducted in the absence of any commercial or financial relationships that could be construed as a potential conflict of interest.

frontiers in Plant Science

ORIGINAL RESEARCH
published: 08 October 2019
doi: 10.3389/fpls.2019.01260

Green Olive Browning Differ Between Cultivars

*Shiri Goldental-Cohen, Iris Biton, Yair Many, Sivan Ben-Sason, Hanita Zemach, Benjamin Avidan and Giora Ben-Ari**

Institute of Plant Science Volcani Center, ARO, Bet-Dagan, Israel

Currently, table olives, unlike oil olives, are harvested manually. Shortage of manpower and increasing labor costs are the main incentives to mechanizing the harvesting of table olives. One of the major limiting factors in adopting mechanical harvest of table olives is the injury to fruit during mechanical harvest, which lowers the quality of the final product. In this study, we used the Israeli germplasm collection of olive cultivars at the Volcani Institute to screen the sensitivity of many olive cultivars to browning in response to injury. The browning process after induced mechanical injury was characterized in 106 olive cultivars. The proportional area of brown coloring after injury, compared to the total fruit surface area, ranged from 0 to 83.61%. Fourteen cultivars were found to be resistant to browning and did not show any brown spot 3 h after application of pressure. Among them, there are some cultivars that can serve as table olives. The different response to mechanical damage shown by the cultivars could be mainly due to genetic differences. Mesocarp cells in the fruits of the sensitive cultivars were damaged and missing the cell wall as a result of the applied pressure. The cuticles of resistant cultivars were thicker compared to those of susceptible cultivars. Finally, we showed that the browning process is enzymatic. We suggest cuticle thickness as an indicator of table olive cultivars suitable for mechanical harvest. A shift to browning-resistant cultivars in place of the popular cultivars currently in use will enable the mechanical harvest of table olive without affecting fruit quality.

Keywords: ***Olea europaea*, browning, table olive, mechanical harvest, germplasm collection**

OPEN ACCESS

Edited by:
José Manuel Martínez-Rivas, Instituto de la Grasa (IG), Spain

Reviewed by:
Marilena Ceccarelli, University of Perugia, Italy
Gabriela Vuletin Selak, Institute for Adriatic Crops and Karst Reclamation, Croatia

****Correspondence:***
Giora Ben-Ari
giora@agri.gov.il

Specialty section:
This article was submitted to Crop and Product Physiology, a section of the journal Frontiers in Plant Science

Received: *07 May 2019*
Accepted: *11 September 2019*
Published: *08 October 2019*

Citation:
Goldental-Cohen S, Biton I, Many Y, Ben-Sason S, Zemach H, Avidan B and Ben-Ari G (2019) Green Olive Browning Differ Between Cultivars. Front. Plant Sci. 10:1260. doi: 10.3389/fpls.2019.01260

INTRODUCTION

Worldwide production of table olives has risen steadily over the last 30 years from 0.95 million tons in 1990 to 2.9 million tons in 2018. Consumption of table olives has not been far behind, rising from about 1 million tons worldwide in 1996 to 2.7 million tons in 2018 (IOOC, 2019).

Oil olives are harvested when a light green to purple coloration is achieved and fruit softening begins. In contrast to this, most table olives are harvested toward the end of the mesocarp development stage (before physiological maturation), when fruit detachment force (DF) is very high. This hinders fruit harvesting and increases the effort necessary in carrying out this task. Currently, table olives are still harvested manually. Shortage of manpower for hand harvesting and increasing labor costs are the major reasons for mechanizing the harvesting of table olives. At present, manual harvesting is the most expensive phase of table olive production (Ferguson et al., 2010; Zipori et al., 2014). The two major obstacles involved in shifting from manual to mechanical harvesting of table olives are harvesting efficiency and fruit injury.

Abscission agents currently in use for lowering fruit DF before harvest, as a pretreatment for mechanical harvesting of oil olives, are ethylene-releasing compounds such as ethephon (2-chloroethyl phosphonic acid), which achieve consistent fruit loosening. However, ethephon application also resulted in attendant leaf loss coincident with fruit loosening (Hartmann et al., 1970; Martin, 1994; Burns et al., 2008). Recently, we have shown that treating olive-bearing trees with a combination of ethephon and antioxidants reduces DF fruit without weakening that of the leaves (Goldental-Cohen et al., 2017). However, mechanical harvesting technologies used for harvesting oil olives cannot be applied to table olives, due to the high percentage of fruit damaged during mechanical harvesting (Gambella et al., 2013; Jiménez-Jiménez et al., 2013b; Zipori et al., 2014; Jiménez et al., 2016).

As in other fruits, bruising of olives causes changes in the fruit skin color (Samim and Banks, 1993; Conway et al., 2003). The current food industry demands high-quality products. In small fruits such as olives, classification is based on visual characteristics such as the color of the skin or the presence of external defects. Currently, most factories use automatic machines for sorting defective olives by color, and defective fruits are rejected and cause considerable financial loss (Diaz et al., 2000; Diaz et al., 2004; Garrido Fernández, 2006).

Olive fruit is characterized by a thin exocarp surrounding fleshy mesocarp tissue, which makes up the edible portion of the table olive.

The damage caused by impact during mechanical harvesting of olives appears as brown spots on the fruit's exterior (Castro-Garcia et al., 2009). The browning process begins with a darkening of a section of the green color on the olive fruit surface. After a while, depending on the severity of the impact, the browning spreads over the exocarp and the mesocarp as well and can even affect the endocarp (Jiménez et al., 2011; Jiménez-Jiménez et al., 2013b). The browning process in olive, as in many other fruits, is produced by oxidation of phenolic compounds by different enzymes, particularly polyphenol oxidase (PPO) (Segovia-Bravo et al., 2007; Segovia-Bravo et al., 2009; Segovia-Bravo et al., 2011). Susceptibility to browning in other fruits was reported to be dependent on multiple factors such as fruit size, fruit shape, firmness, cell wall strength, and others (Studman, 1997; Grotte et al., 2000; Berardinelli et al., 2005; Bollen, 2005). Produce type and cultivar differences account for most of the differences in browning susceptibility. However, it is still not yet clear which factors mostly contribute to the potential of susceptible cultivars to bruising (Opara and Pathare, 2014). In olives, susceptibility to browning was seen to vary among different cultivars. For example, "Manzanillo," the main table olive in Israel and in other countries, was shown to be relatively sensitive to browning in response to impact (Jiménez-Jiménez et al., 2013a; Jiménez et al., 2016).

Jiménez et al. (2016) described and quantified anatomical changes in the olive mesocarp in response to bruising in olive fruits after an induced impact. They studied the browning characteristics of the cultivars "Manzanillo" and "Hojiblanca" at two time points, 4 and 24 h after induced impact. In response to the impact, fruits exhibited damaged mesocarp tissue, including ruptured cells, loss of cell wall thickness, and discoloration of the damaged areas. These changes were greater in the more sensitive cultivar, "Manzanillo," compared to the more resistant cultivar, "Hojiblanca."

As mentioned above, mechanical harvest of green olives, particularly of table olives, can cause brown spots on the fruits. Rejection of these fruits represents financial loss to the farmer. Pre-harvest treatment of olives by an anti-browning agent has been very limited to date, and the inhibitory effect of anti-browning agents on reducing PPO activity was found to be cultivar-dependent (Mohsenabadi et al., 2017). Assuming that cultivar susceptibility is the main factor contributing to browning in response to impact, large scale screening of various cultivars has not been performed, neither the factors causing some cultivars to be more resistant than others to browning have been indicated.

The aim of this study was to evaluate the variation in susceptibility to browning among olive cultivars in order to identify those more resistant and to understand the main factors influencing browning resistance. Olive fruits from 106 olive cultivars in the Israeli germplasm collection were subject to mechanical injury. Elasticity as well as browning level were characterized for all cultivars at 3 and 24 h after impact. Exocarp cells remained unharmed after the impact even in the more susceptible cultivars. However, mesocarp cells were damaged only in the susceptible cultivars. We suggest that the major factor contributing to the variation in susceptibility to browning among cultivars is the thickness of the cuticle.

MATERIALS AND METHODS

Plant Material

The Israeli germplasm collection consists of 119 cultivars, each represented by three 23-year-old trees growing in an irrigated olive orchard. It is located at the Volcani Center (ARO) in Bet Dagan, Israel (31°58'57.7"N 34°49'47.4"E). This collection includes oil producing strains, as well as table olive cultivars from different geographic origins, and represents the most popular varieties grown around the world.

Once a week, beginning September 1st 2016, we visually screened the olive orchard containing the Israeli germplasm collection, in order to identify cultivars in which fruit color changed from green to yellow indicating the physiological stage suitable for the harvest of table olives. Ten fruits from three trees (3–4 fruits from each tree) of each cultivar showing color change were sampled and the fruit immediately taken for analysis of their response to applied mechanical pressure. Out of the 119 cultivars, 13 bore no fruit; therefore, fruits from only 106 cultivars were analyzed. Damage induction and elasticity evaluation of the 20 cultivars whose response to mechanical pressure registered at the two extremes of the scale (10-resistant and 10-sensitive) were analyzed once again a year later.

Damage Induction and Elasticity Evaluation

At the time of the table olive harvest, 10 fruits from each cultivar were sampled as described above and immediately subjected to mechanical pressure. Monitoring of pressure and

elasticity was done by a force gauge FG-5000A (MRC, Holon, Israel). We used a flat circle pinhead, 8-mm diameter, for both damage induction and elasticity evaluation. Five fruits per cultivar were subjected to damage induction. Each fruit was placed on a metal base and pressed with the force gauge at 3 kg of pressure. Each group of five fruits from the same cultivar was placed in a small plastic tray and incubated at room temperature for 24 h. Fruits were photographed 3 and 24 h after being pressed. Images were collected by Fujifilm FinePix S4300 digital camera (FujiFilm, Ramat Gan, Israel) fixed on a metal stand 10 cm above the fruits. The remaining five fruits from each cultivar were used for evaluating elasticity as follows: fruits were placed on a metal base and pressed 3 mm from the surface of the fruits toward the fruit endocarp. We measured the force needed to move the pinhead 3 mm toward the inner part of the fruit.

Brown Spot Area

We used Adobe Photoshop software (Onstott, 2012) to calculate the proportion of brown spot resulting from injury to the fruit, relative to the surface area of the fruit. The proportion of brown area was calculated as follow: brown area (cm^2) = brown pixels/(total pixels/cm^2). For each cultivar, the average proportion of brown area on five fruits was calculated 3 and 24 h after pressure was applied.

Fruit Mesocarp and Exocarp Structures

Mesocarp and exocarp structures as well as the cuticle thickness of four resistant and four sensitive cultivars were analyzed. Tissue blocks (approx. 3.0 mm × 1.5 mm × 1.5 mm sizes) were cut revealing the mesocarp and exocarp in longitudinal view. The samples were fixed in 70% ethanol followed by dehydration in gradual ethanol series (90, 95, 100, and 100%). Samples were dried in critical point dryer (K850 Quorom). The dry tissues were attached to a metal stub by double-sided carbon tape and coated with gold palladium (Quorum SC7620 Mini Sputter Coater). Images were taken with a JEOL JCM-6000 benchtop scanning electron microscope (SEM). Analysis was performed using the SEM software. The thickness of the cuticular flange wedged between epidermal cells was measured (Lanza and Di Serio, 2015).

Penetration force was measured using Lutron fruit hardness tester model FR 5105 (Scientific Instrument & Optical Sales, Brisbane, Queensland, Australia) with a 3-mm measuring tip. From each of eight cultivars (four resistant and four sensitive), we tested 20 fruits and measured the force needed to penetrate the exocarp.

Enzyme Inactivation

In order to test whether the brown spots which appeared in response to the injury caused by mechanical pressure applied to the fruit are enzyme-dependent, we used 10 fruits of the sensitive cultivar "Koroneiki." All 10 fruits were pressed with the force gauge, and five of these were immediately incubated in a water bath at 65°C for 10 min enclosed in a covered plastic container. All 10 fruits were exposed for 3 h at room temperature then photographed as described above.

Statistical Analysis

The ratio between brown area and total surface area (after arcsine transformation), elasticity coefficient, thickness of the cuticular flange, and penetration force among cultivars were measured and subjected to one-way analysis of variance (ANOVA) with Tukey–Kramer test using JMP Software (SAS Institute, 2007). The damaged areas as appeared 3 and 24 h after pressing were compared using linear regression and Pearson correlation, in order to derive the regression coefficient (slope) and correlation coefficient. The same analysis was carried out to compare the degree of browning 3 h after pressing and the elasticity coefficient of each cultivar. The degree of browning of the genetic clusters was subjected to a one-way ANOVA and a Tukey–Kramer test. The same procedure was carried out for the elasticity coefficients. The delineation of the various genetic clusters was determined visually according to the dendrogram characterizing the phylogenetic relationships among 119 cultivars of the Israeli germplasm collection, based on a set of 138 SNPs (Biton et al., 2015).

RESULTS

Distribution of the Degree of Browning in the Germplasm Collection, as a Result of Mechanical Injury to Olive Fruit

After deliberately injuring fruits of the cultivars composing our germplasm collection, the damaged outer area was measured. Some cultivars proved to be more sensitive to injury than others, and their color began changing from green to brown in the area surrounding the injury (**Supplementary Clip**). The proportional area of the brown spots was measured. Significant variations among cultivars were found. In addition, browning level measured 3 and 24 h after pressing was similar in all cultivars but three. We performed regression analysis between the damaged outer areas 3 and 24 h after pressing. The regression coefficient was 1.033. The proportional area of brown coloring of 3 out of the 106 cultivars, "Dolce de Marocain," "Memecik," and "Gemlik," was much higher 24 h after pressing (54.83, 54.6, and 50.86, respectively) compared to 3 h after pressing (16.94, 18.09, and 19.37%, respectively). However, regression analysis for all cultivars other than the three mentioned above resulted in a regression coefficient of 1.02 and a correlation coefficient of 0.956 ($P < 9.34X10^{-37}$). On this basis, we used the browning level 3 h after pressing to evaluate the variation among cultivars.

The proportional area of brown coloring 3 h after injury, compared to the fruit surface as measured by the two dimensional photograph of the fruit, ranged from 0% in certain cultivars to 83.61% in cultivar UC13A6, with an average of 16.8% (**Figure 1A** and **Table 1**).

In order to evaluate the variation in hardness of different cultivars, we also measured the elasticity coefficient of the fruits of each cultivar. Elasticity coefficient of the various cultivars ranged between 4.75 and 20 N/mm, with an average of 12.67 N/mm (**Figure 1B** and **Table 1**). The degree of browning and the elasticity coefficient of each cultivar was found to be significantly and negatively correlated with a correlation coefficient of −0.526

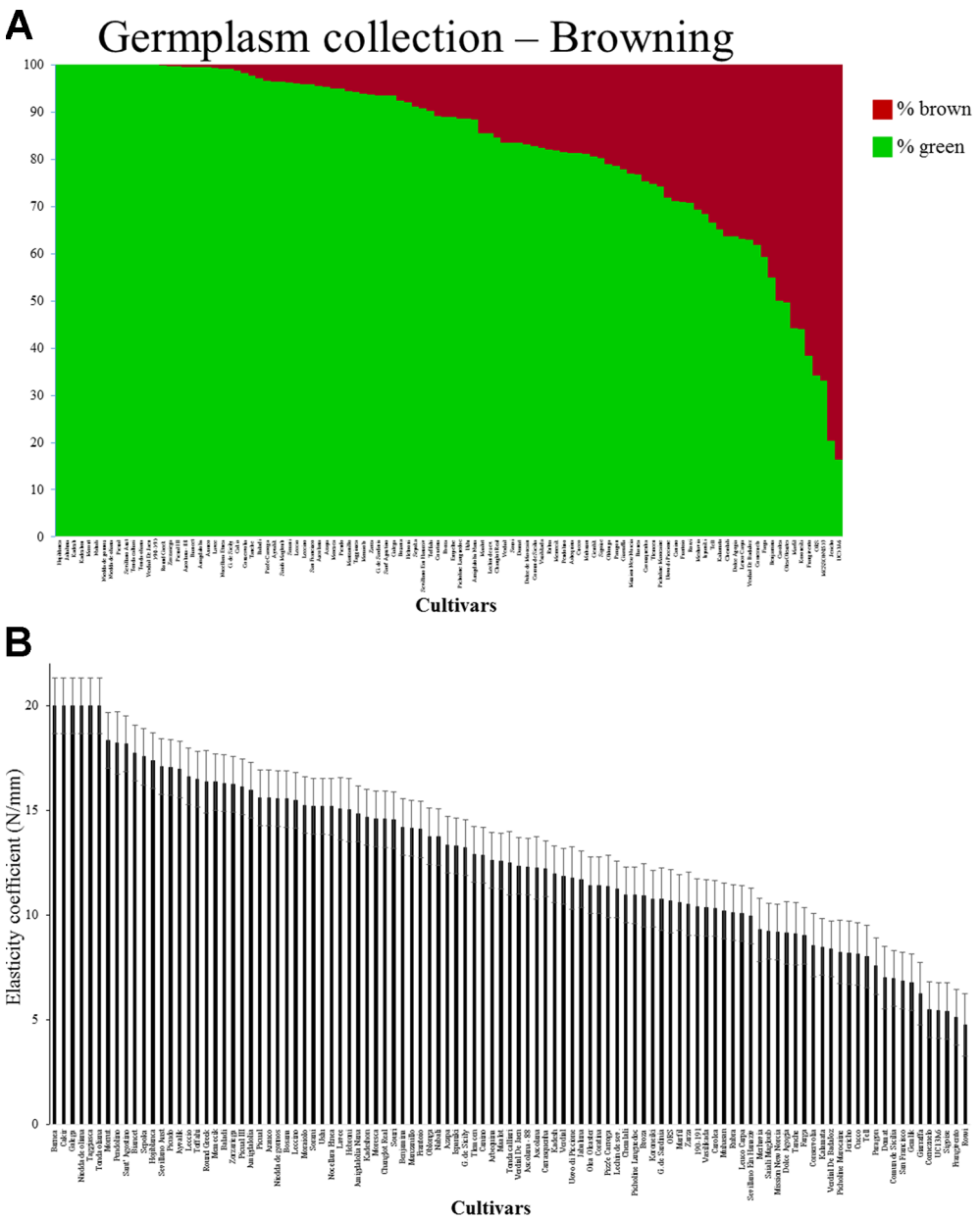

FIGURE 1 | (A) Proportional area (expressed in percentage) of the olive surface turned brown as a result of injury. This was measured by a two-dimensional photograph of the fruit of each cultivar. The values were plotted as a column graph. The green and brown column bars at each segment represent the percentage of green and brown colors, respectively, on the surface of the fruit. **(B)** Elasticity coefficient of each cultivar. Error bars represent confidence limits (n = 5; $\alpha = 0.05$).

($P < 1.16X10^{-8}$). As part of the Israeli breeding program, we tested the average fruit weight and oil content of all cultivars composing the Israeli germplasm collection during 5 consecutive years (data not shown). No significant correlation was found between degree of browning and fruit weight ($r = -0.09$; $P = 0.39$) or to oil percentage ($r = 0.05$; $P = 0.65$).

Fourteen cultivars were found to be resistant to browning and did not show any brown spot 3 h after application of pressure. Among them, there are several table olives such as the cultivars "Sevillano Australia," "Kadesh," and "Kadeshon." The latter two are table olive cultivars developed as part of the Israeli olive breeding program. Some of the resistant cultivars are dual purpose and can be used either as table or oil olives; these include the cultivars "Hojiblanca," "Nabali," "Niedda de gonnos," "Picual," "Tonda calliari," and "Tonda oliana." Finally, among the resistant cultivars, there are typical oil cultivars such as "Jabaluna," "Morrut," and "Verdial de Jaen" (**Figure 2A**). At the other end of our scale, several cultivars exhibited severe browning in response to injury by the 3-kg press. The most sensitive cultivars were the table olive cultivars "UC13A6"

TABLE 1 | For each cultivar of the germplasm collection, the table describes country of origin, the purpose of the olive cultivar (O, oil cultivar; T, table cultivar; D, dual purpose cultivar), the proportion of brown area 3 h after induced pressure, and the elasticity coefficient (n = 5).

Cultivar	Origin	Purpose	% green	% brown	E(N/mm)
Hojiblanca	Spain	D	100	0	17.38
Jabaluna	Spain	O	100	0	11.71
Kadesh	Israel	T	100	0	11.96
Kadeshon	Israel	T	100	0	14.68
Morrut	Spain	O	100	0	18.33
Nabali	Palestine	D	100	0	13.73
Niedda de gonnos	Italy	D	100	0	15.57
Niedda de oliana			100	0	20.00
Picual	Spain	D	100	0	15.61
Sevillano Aust	Spain	T	100	0	17.09
Tonda calliari	Italy	D	100	0	12.48
Tonda oliana	Italy	D	100	0	20.00
Verdial De Jaen	Spain	O	100	0	12.35
190-191	Israel		100	0	10.39
Round Greek	Greece	T	99.92	0.08	16.36
Zorzariega	Spain	D	99.71	0.29	16.25
Picual III	Spain	O	99.69	0.31	16.12
Ascolana - 88	Italy	T	99.56	0.44	12.31
Biancet	?	O	99.48	0.52	17.73
Amigdalolia	Greece	D	99.47	0.53	15.97
Arauco	Argentina	T	99.43	0.57	15.59
Lavee	Israel	D	99.34	0.66	15.08
Nocellara Etnea	Italy	D	99.24	0.76	15.18
G. de Sicily	Italy	T	99.17	0.83	13.23
Cakir	Turkey	D	98.81	1.19	20.00
Conservolia	Greece	T	98.29	1.71	8.57
Tanche	France	D	97.64	2.36	9.12
Baladi	Lebanon	O	97.12	2.88	16.30
Pizz'e Carroga	Italy	O	96.64	3.36	11.37
Ayvalik	Turkey	O	96.41	3.59	16.96
Saiali Magloub	Tunisia		96.40	3.60	9.24
Sorani	Syria	D	96.26	3.74	15.19
Leccio	Italy	O	95.99	4.01	16.62
Leccino	Italy	O	95.91	4.09	15.48
San Francisco	Italy	O	95.81	4.19	6.87
Ascolana	Italy	T	95.50	4.50	12.26
Azapa	Chile	T	95.41	4.59	13.36
Moresca	Italy	D	94.93	5.07	14.60
Picudo	Spain	O	94.89	5.11	17.06
Manzanillo	Spain	T	94.50	5.50	14.14
Taggiasca	Italy	O	94.22	5.78	20.00
Moraiolo	Italy	O	93.84	6.16	15.26
Zarza	Spain		93.76	6.24	10.54
G. de Sardinia	Italy	T	93.47	6.53	10.78
Sant' Agostino	Italy	T	93.47	6.53	18.17
Galega	Portugal	O	93.45	6.55	20.00
Bosana	Italy	O	92.43	7.57	15.54
Hebroni	Palestine	T	91.98	8.02	15.02
Sepoka	Israel	T	91.13	8.87	17.56
Sevillano Ein Hanaziv	Israel	T	90.70	9.30	9.97
Toffahi	Egypt	T	90.22	9.78	16.48
Coratina	Italy	O	89.18	10.82	11.43
Broza	Israel	T	89.05	10.95	10.94
Empeltre	Spain	O	88.96	11.04	
Picholine Languedoc	France	D	88.65	11.35	10.95
Uslu	Turkey	D	88.60	11.40	15.19
Amigdalolia Nana	Greece	D	88.34	11.66	14.83
Maalot	Israel	O	85.53	14.47	12.58
Lechin de sev.	Spain	O	85.51	14.49	11.24
Changlot Real	Spain	O	84.62	15.38	14.58
Verdial	Spain	O	83.51	16.49	11.86
Souri	Israel	D	83.47	16.53	14.54
Domat	Turkey	T	83.43	16.57	7.03
Dolce de Marocain	Morocco		83.06	16.94	
Comun de Sicilia	Italy		82.79	17.21	6.98
Vasilikada	Greece		82.48	17.52	10.35
Rubra	?	O	82.14	17.86	10.11
Memecik	Turkey	D	81.91	18.09	16.35
Pendolino	Italy	O	81.52	18.48	18.21
Arbequina	Spain	O	81.36	18.64	12.62
Cucco	Italy	T	81.35	18.65	8.15
Muhasan	Palestine	D	81.08	18.92	10.19
Gemlik	Turkey	D	80.63	19.37	6.79
Sigoise	Algeria	D	80.18	19.82	5.42
Oblonga	USA	O	78.88	21.12	13.76
Paragon	Australia	O	78.67	21.33	7.57
Giarraffa	Italy	T	77.87	22.13	6.25
Mission New Norcia	?	O	76.92	23.08	9.20
Barnea	Israel	O	76.70	23.30	20.00
Carrasquenha	Portugal	T	75.36	24.64	12.23
Tlemcen	Algeria	D	74.78	25.22	12.90
Picholine Marocaine	Morocco	D	74.25	25.75	8.24
Uovo di Piccione	Italy	T	71.83	28.17	11.78
Canino	Italy	O	71.06	28.94	12.87
Frantoio	Italy	O	70.93	29.07	14.10
Rowi	?		70.80	29.20	4.75
Merhavia	Israel	T	69.28	30.72	9.30
Ispaniki	Spain	O	68.40	31.60	13.31
Tell	Algeria	D	66.68	33.32	8.02
Kalamata	Greece	T	65.18	34.82	8.49
Chemlali	Tunisia	O	63.74	36.26	10.97
Dolce Agogia	Italy	O	63.67	36.33	9.15
Leuco Carpa	Italy	O	63.14	36.86	10.09
Verdial De BadaJoz	Spain		62.86	37.14	8.39
Cornezuelo	Spain	T	61.77	38.23	5.48
Farga	Spain	O	59.37	40.63	9.02
Benjamina	Palestine	O	55.01	44.99	14.20
Carolea	Italy	T	50.00	50.00	10.33
Olea Oleaster	Italy		49.65	50.35	11.43
Marfil	Spain	O	44.14	55.86	10.60
Koroneiki	Greece	O	43.94	56.06	10.78
Frangivento	Italy	O	38.30	61.70	5.12
ORS	Australia	O	34.12	65.88	10.67
MCSSON 0517	?		33.19	66.81	
Jericho	Palestine	T	20.28	79.72	8.20
UC13A6	USA	T	16.39	83.61	5.44

and "Jericho," which showed 83.61 and 79.72% brownings, respectively. In addition, the oil cultivars "ORS," "Frangivento," "Koroneiki," "Marfil," "Benjamina," and "Farga" showed browning proportions greater than 40%. Last are the table olive cultivars "Carolea" and "Cornezuelo," which showed 50 and 38.23% brownings, respectively (**Figure 2B**).

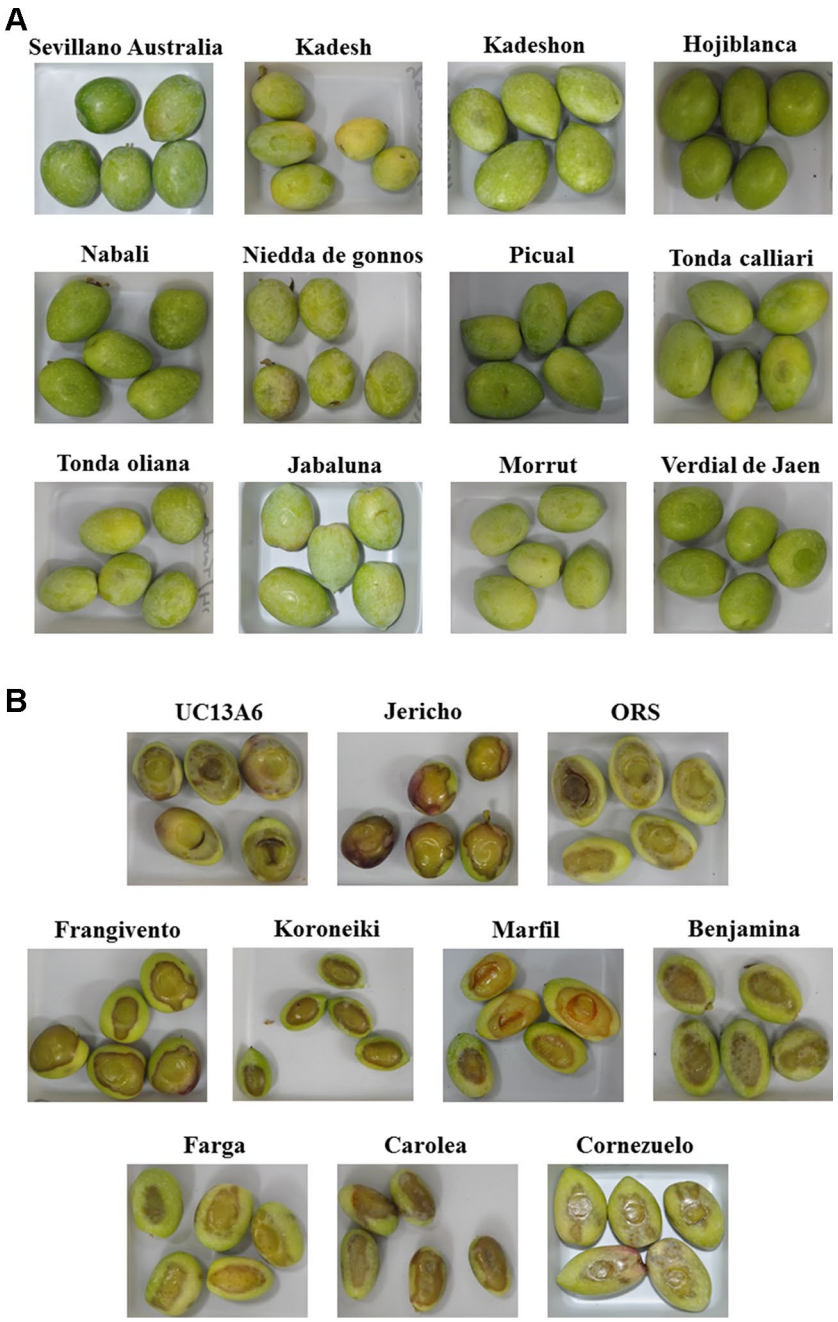

FIGURE 2 | Photographs of five fruits from each of the most resistant **(A)** or susceptible **(B)** cultivars to browning, 3 h after induced mechanical pressure.

No significant differences were detected between browning degree or cuticle elasticity among cultivars on the basis of their geographical origin.

The genetic relationships between the 119 cultivars making up the major part of the Israeli germplasm collection had been analyzed by means of a set of 138 SNPs (Biton et al., 2015). According to the dendrogram previously obtained, we clustered the olive cultivars into 13 genetic groups. We then analyzed the differences in browning level and elasticity coefficient among the 13 groups. The average browning level and elasticity coefficient of the cultivars from each of the 13 genetic groups were significantly different ($P < 1.17X10^{-15}$ and $P < 0.008$, respectively) (**Figure 3**). Many cultivars that are closely related genetically showed similar browning characteristics. For example, the cultivars "UC13A6," "MCSSON 0517," and "ORS" are part of the same genetic cluster and show high browning levels (83.61, 66.81, and 65.88%, respectively). The cultivars "Fragivento" and

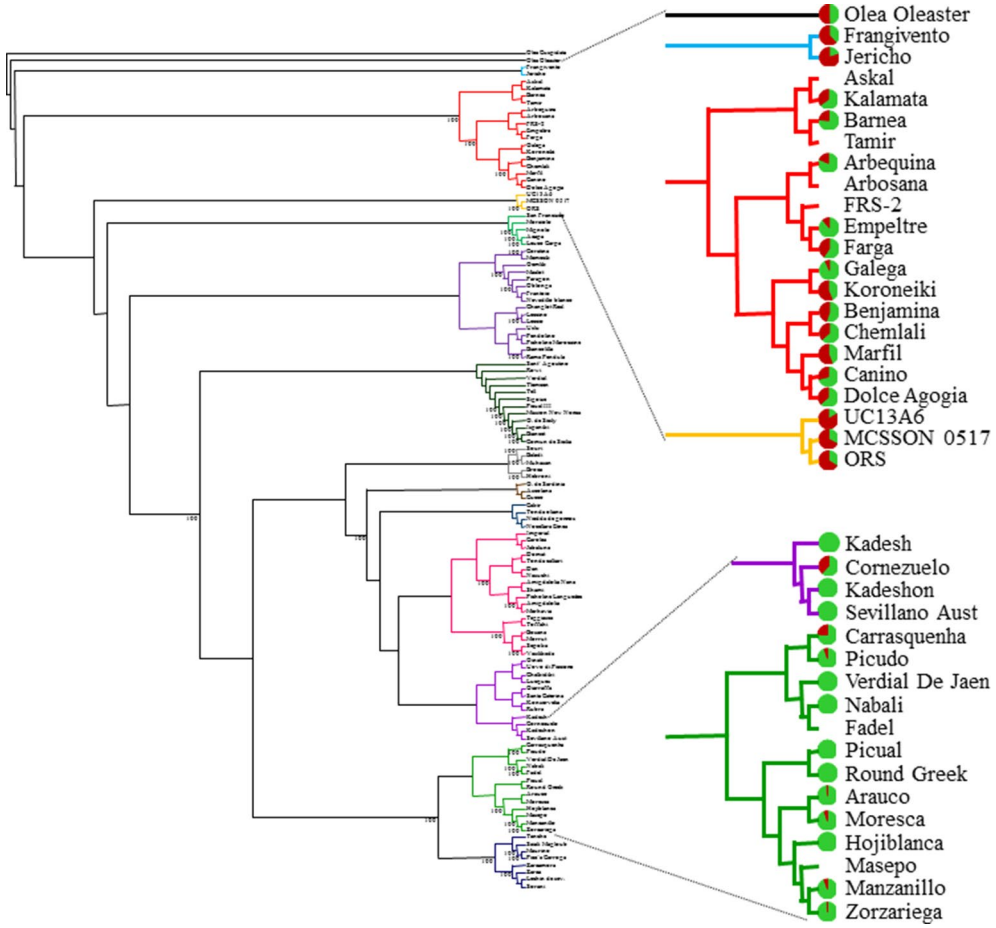

FIGURE 3 | Neighbor-joining tree of 119 cultivars making up most of the Israeli germplasm collection, based on a set of 138 SNPs (Biton et al., 2015). The branches of different clusters appear in different colors. Sub-clusters are enlarged, including the names of the relevant cultivars. For each of the enlarged clusters, the proportion of brown area appears next to the cultivar name, as a pie chart with green and brown areas representing the green and brown proportions of the cultivar fruits as a response to mechanical injury.

"Jericho" are also genetically close and exhibit high rates of browning (61.7 and 79.72%, respectively). At the other end of the cluster distribution, "Kadesh," "Kadeshon," and "Sevillano Australia" are on the same genetic cluster and are all resistant to browning. Although some cultivars showed a unique pattern of browning, unlike other cultivars of the same genetic cluster, such as the browning-sensitive cultivar "Cornezuelo" or the semiresistant cultivar "Galega," most of the cultivars showed a similar browning pattern as their neighbors, in all clusters (**Figure 3**).

Fruit Mesocarp Cells Are Damaged by the Press

In order to understand the relationship between the damage caused by the simulated injury to the fruit and the browning phenomenon, the exocarp and mesocarp cells of the pressed fruits were screened using a scanning electron microscope. Tissue and cell structure were compared after the application of pressure in four sensitive cultivars ('ORS," "Carolea," "Benjamina," and "Farga") and four resistant ones ("Hojiblanca," 'Morrut," "Nabali," and "Kadesh"). Exocarp cells of both groups suffered any damage from the applied pressure. However, some of the mesocarp cells in the fruits of the sensitive cultivars were totally disrupted, and their cell walls were missing as a result of the applied pressure (**Figure 4**).

The Cuticle of the Resistant Cultivars Is Thicker Than That of Sensitive Cultivars

In order to understand the factors which cause some cultivars to be resistant while others are sensitive to pressure, we measured the thickness of the cuticle of fruits from various cultivars. The thickness of the cuticular flange that is wedged between epidermal cells was measured by SEM and compared in fruits sampled from sensitive ("ORS," "Carolea," "Benjamina," and "Farga") *versus* resistant ("Hojiblanca," "Morrut," "Nabali," and "Kadesh") cultivars. The average thickness of the cuticle of the resistant cultivars, whose mesocarp cells remained intact, was 28.21 μm, while the cuticle thickness of the sensitive cultivars

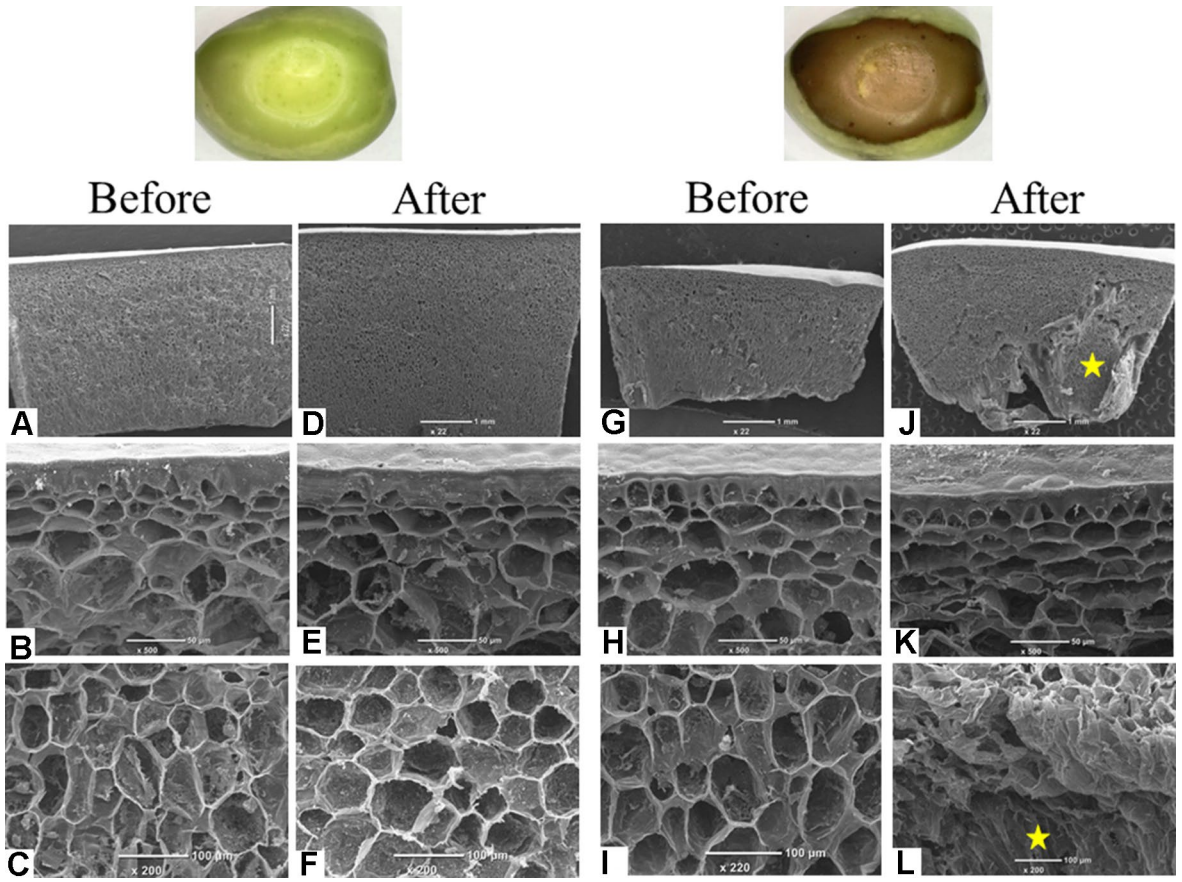

FIGURE 4 | Images before and 3 h after the induced pressure of a representative fruit of browning-resistant ("Nabali"; **A**–**F**) and browning-susceptible ("ORS"; **G**–**L**) cultivars. For each fruit, before **(A**–**C**, **G**–**I)** and after **(D**–**F**, **J**–**L)** exposures to mechanical pressure, three images are presented representing a comprehensive view **(A**, **B**, **G**, **J)**, a zoom in on the exocarp cells **(B**, **E**, **H**, **K**) and a zoom in on the mesocarp cells **(C**, **F**, **L**, **L)**. Mesocarp cell rupture is marked by a yellow star.

was 21.49 µm. This difference in cuticle thickness between resistant and sensitive cultivars was significant ($P < 6.66X10^{-5}$) (**Figure 5A**).

We also measured the penetration force of the cuticle. The average penetration force in the resistant cultivars was 2.5 kg, while the penetration force in the sensitive cultivars was significantly less, 1.6 kg ($P < 1.3X10^{-35}$) (**Figure 5B**).

The Browning Is an Enzyme-Dependent Response

In order to test if the browning response to fruit injury is enzyme-dependent, we sampled fruits from "Koroneiki," a cultivar of proven sensitivity to pressure. Fruits were pressed by the force gauge, and half the fruits were dipped in boiling water for 10 min, while the other half was incubated at room temperature. The fruits were photographed 3 h after passing through the press. Heated fruits had no brown spots, while control fruits clearly showed large brown spots in response to the applied pressure (**Supplementary Figure 1**).

DISCUSSION

Mechanical harvesting of oil olives, mostly by trunk shaker or by harvester, is now a common practice in orchards. However, mechanical harvest of table olives is still very limited (Tous and Tous, 2011; Zipori et al., 2014). Recently, we published a study suggesting the use of ethephon and ascorbic acid as a pretreatment to facilitate mechanical harvest of green table olives (Goldental-Cohen et al., 2017). This pretreatment was shown to decrease the DF of the fruits without causing defoliation. However, in order to enable mechanical harvest of table olives, it is also necessary to prevent external fruit color change or browning. In this study, we used our germplasm collection to screen for browning-susceptible and -resistant cultivars. The various olive cultivars differ in their degree of browning in response to injury. Fruits of some cultivars are completely resistant and remained green 24 h after impact, while others developed a large brown spot around the point of impact. We also found that the browning process in response to impact begins with damage to the mesocarp cells while a thick cuticle inhibits this process.

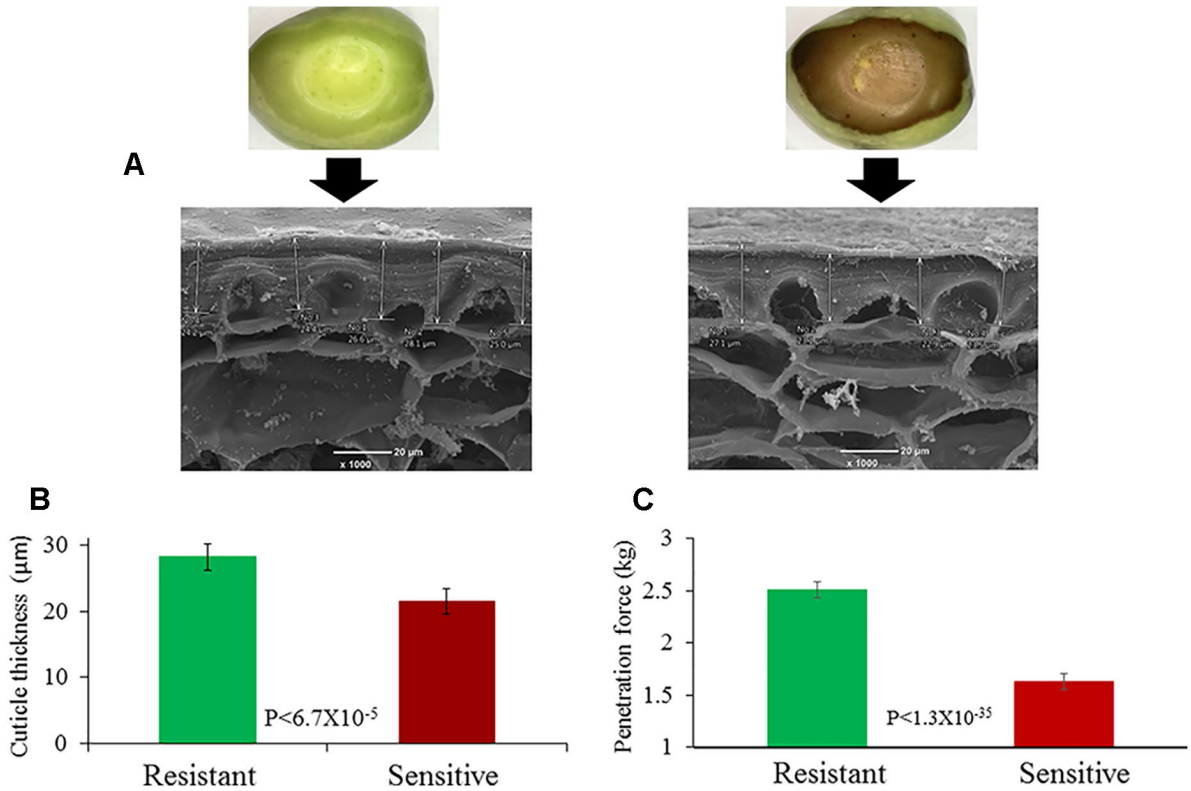

FIGURE 5 | Cuticle thickness measured by SEM. **(A)** Cuticle of a browning-resistant ("Nabali," left) and a browning-susceptible cultivar ("ORS," right). **(B)** Average cuticle thickness of browning-resistant and -susceptible cultivars (green and brown columns, respectively). **(C)** Penetration force of browning-resistant and -susceptible cultivars (green and brown columns, respectively). Error bars are confidence limits (n = 5; $\alpha = 0.05$).

Some Cultivars Are Resistant to Browning

In this study, the parameter used to evaluate the differences among cultivars was the two-dimensional proportion of the brown area around the impact point in relation to the surface area of the whole fruit. Although this parameter may be inaccurate in evaluating total damage to the fruit, because it takes into account only two dimensions, it should provide enough information to be used as a fast and easy method for screening commercial quantities of fruit. Using this parameter, we were easily able to screen the damaged area of each of 5 fruits from 106 cultivars for a total of 530 fruits. Jiménez et al. (2016) quantitatively defined bruising damage to olives by 11 parameters. Of these, they recommended the use of three parameters as the most discriminant, the easiest to assess and the most useful for the evaluation of susceptibility to bruising. One of them is the total damaged area of the mesocarp. In contrast, we focused on the visible outer layer of the fruit to quantify browning. Since most factories currently use automatic machines for sorting defective olives by color, the parameter of visual color of the skin, which was measured in this study, is the relevant parameter based on which defective drupes are discarded, causing financial losses.

There was significant variation in the different cultivars susceptibility to browning. Some were completely green after impact whereas others were extremely brown several hours after impact. In apples, it has been suggested that variation in bruise size for a given impact energy occurs across cultivars and depends on a number of factors such as maturity and temperature (Samim and Banks, 1993). We tested the cultivars at their "green maturity" stage (table olive harvest time). However, observation of the developmental stage for all cultivars was performed visually and may not always have been accurate. In addition, since each cultivar was tested on a different day, according to its stage of development, the temperature at harvest was not identical. However, the temperature at this season (during September) is fairly stable in Israel. In addition, extreme cultivars were retested, and validation of their susceptibility/resistance to browning was performed. Comparison of the phylogenetic relationships among cultivars analyzed in a previous study (Biton et al., 2015) with the browning pattern and elasticity coefficient of the various cultivars revealed that genetically close cultivars tend to show a similar browning level and elasticity coefficient (**Figure 3**). Therefore, although our analysis may contain some biased results, we are convinced that, in general, and especially for the extreme cultivars, the level of browning presented here for each cultivar is mainly due to genetic differences among cultivars.

Timing of the Browning Phenomenon

Brown spots appeared on the fruits immediately after the induced pressure and spread over time, until they reached their

final size 3 h after pressure was applied. The differences in most cultivars between 3 and 24 h after the induced pressure were not significant. The regression coefficient between the browning proportion at 3 and 24 h after injury was found to be 1.033. This is very close to a regression coefficient of 1, corresponding to equality between the two tested variables. Apart from the three cultivars, "Dolce de Marocain," "Memecik," and "Gemlik," in which the browning process continued after 3 h, in the remaining 103 cultivars, the browning process reached its full extent during the first 3 h after injury. Other studies reported that discoloration continued spreading and reached its final size 24 after the induced pressure (Jiménez-Jiménez et al., 2013a; Jiménez et al., 2016; Jiménez et al., 2017). However, these studies used methods of simulating injury such as dropping the fruits from a height of 1 m to induce damage, whereas we used direct pressure on the fruits. The different methods used could explain the differences in spreading time of the bruising.

The "Manzanillo" cultivar is the most popular table olive in Israel, as well as in other countries (Diego and Rallo, 2000). In this study, the "Manzanillo" showed 5.5% browning 3 h after application of pressure. Other cultivars used as table olives showed resistance to browning, such as "Hojiblanca," "Kadesh," "Kadeshon," "Nabali," "Niedda de gonnos," "Picual," "Sevillano," "Tonda calliari," and "Tonda oliana." Other studies have also shown that there are cultivars more resistant to bruising than the "Manzanillo," such as "Hojiblanca" (Jiménez et al., 2016) and "Manzanillo Cacerena" (Jiménez et al., 2017). Switching to mechanical harvest of table olives with minimum injury to the harvested fruits can be achieved by replacing sensitive trees with a browning-resistant cultivar.

A Thick Cuticle Promotes Resistance to Browning

Injuries incurred during mechanical harvesting can be either from blows received from canes used to assist the mechanical shaker in helping the fruit drop from the tree or from fruitshitting the ground after falling from the tree. In both cases, the impact is flat and not sharp. Therefore, we used a force gauge with a flat rounded pinhead to mimic the impact inflicted on the fruit by the mechanical harvester. Not surprisingly, the flat pressure did not damage the exocarp tissue. However, damage was found in the mesocarp layer. Jiménez et al. (2016) also found that no damage was observed in the exocarp as a result of olive fruits falling to the ground. However, mesocarp cells were injured from this treatment. When the penetration force needed to damage the exocarp with a sharp pinhead was measured, significant differences in the resistance of susceptible cultivars were found. Not surprisingly, the susceptible cultivars were characterized by a lower penetration force (**Figure 5**). This validated our presumption that the cuticle of the resistant cultivars may be thicker than that of the susceptible cultivars. It has already been suggested that cuticle thickness is one of the major factors influencing susceptibility to browning (Hammami and Rapoport, 2012). However, this was never tested on several cultivars. A significant difference was found between the cuticle thickness of the cultivars susceptible to browning and that of the resistant cultivars (**Figure 5**). This significant disparity, together with the observation that the exocarp cells remain unharmed after induced pressure even in the susceptible cultivars, while the mesocarp cells were clearly damaged in response to this pressure, suggests that the main factor in determining the difference among cultivars in their susceptibility to browning is the thickness of their cuticle. We used the cuticular flange wedged between epidermal cells to evaluated cuticle thickness. A difference of 31% was found between the average cuticle thickness of the susceptible compare to the resistant cultivars (21.49 and 28.21 μm, respectively). Our results are in agreement with other studies that found thicker cuticles in the more resistant cultivars (Hammami and Rapoport, 2012; Jiménez et al., 2017).

The Browning Process in Green Olives

Browning of olive fruits after induced injury can be prevented by dipping the fruits in boiling water (**Supplementary Figure 1**).

It was important to ascertain, as suggested by other studies, that the parameter we evaluated—the proportion of brown color on the fruit skin—is the result of an enzymatic process. Several studies have found that dipping the olives in NaOH also inhibits the browning process (Ben-Shalom et al., 1978; Sánchez et al., 2006; Zipori et al., 2014). In plants, PPOs known for their role in post-harvest browning of fruits and vegetables are localized into plastids (Sullivan, 2015). It has also been suggested that this class of enzymes is involved in the browning process of green olives after damage (Ben-Shalom et al., 1978; Sciancalepore and Longone, 1984). PPOs and their potential phenolic substrates have been considered to be physically separated from one another, with most PPOs targeted to the chloroplasts, while phenolic compounds accumulate primarily in the vacuole and cell wall (Vaughn et al., 1988; Steffens et al., 1994). Postharvest browning occurs in damaged plant tissues due to the contact between phenolic compounds and PPOs, leading to transformation of phenolic compounds to colored polymers (Araji et al., 2014; Croguennec, 2016). Based on the results of other studies mentioned above and the conclusions we have reached from our present study, we would like to suggest that the browning process in olives is driven by the PPOs enzymes. We suggest that, as a result of the injury, physical contact between the PPOs and phenolic compounds leads to the brown spots appearing on the surface of the fruit. In the resistant cultivars identified in this study, the mesocarp cells were not harmed by the induced pressure; the PPO and the phenolic compounds remained localized in different cell components, and therefore, no brown spots appeared on the fruits of these cultivars.

CONCLUSIONS

This study describes the variation found in olive cultivars regarding their susceptibility to fruit browning in response to injury occurred during mechanical harvest. The varied browning

level as a response to mechanical damage shown by the cultivars could be mainly due to genetic differences among cultivars. Many cultivars can be characterized as browning-resistant due to their thick cuticle. We therefore suggest this simple method of induced pressure described above, in order to screen for new browning-resistant table olive cultivars as the first step in a breeding program aimed at identifying table olive phenotypes suitable for mechanical harvesting.

The two major factors involved in shifting from manual to mechanical harvesting of table olives are harvesting efficiency and prevention of injury to fruit. High harvesting efficiency demands pretreatment which will enable fruit abscission without defoliation. In a recent study, added antioxidants such as ascorbic acid or butyric acid to ethephon spray as a pretreatment to green olive harvest inhibited leaf abscission while enhancing fruit abscission (Goldental-Cohen et al., 2017). In our present study, we have identified 14 cultivars that showed resistance to browning after induced pressure. Among them, nine cultivars are known to produce table olives or to serve as dual purpose. Work is in progress to screen these nine cultivars regarding their response to ethephon and ascorbic acid. Those that respond similarly to "Manzanillo" to ethephon and ascorbic acid then could be used as table olive cultivars suitable for mechanical harvest.

DATA AVAILABILITY STATEMENT

All datasets generated for this study are included in the manuscript/**Supplementary Files**.

AUTHOR CONTRIBUTIONS

SG-C, IB, YM, SB-S, HZ, BA, and GB-A performed the experiments. SG-C and GB-A were involved in data analysis. GB-A wrote the manuscript.

FUNDING

This work was supported by the Israeli Ministry of Agriculture and Rural Development (Grant No. 203-0858).

ACKNOWLEDGMENTS

The authors would like to thank Yehuda Ben-Ari for valuable assistance in editing this paper.

SUPPLEMENTARY MATERIAL

The Supplementary Material for this article can be found online at: https://www.frontiersin.org/articles/10.3389/fpls.2019.01260/full#supplementary-material

SUPPLEMENTARY CLIP | Fast-forward play of the three hours following induced pressure, as the browning-sensitive cultivar fruit changes color from green to brown in the area surrounding the point of injury.

SUPPLEMENTARY FIGURE 1 | Illustration of induced pressure by the force gauge, the dipping of fruits in a bath of boiling water and the images taken 3 hours after incubation of the browning-sensitive cultivar 'Koroneiki' fruits with and without treatment in boiling water (right and left images, respectively). Boiling the fruits for ten minutes prevented appearance of brown spots on the surface of the fruits.

REFERENCES

Araji, S., Grammer, T. A., Gertzen, R., Anderson, S. D., Mikulic-Petkovsek, M., Veberic, R., et al. (2014). Novel roles for the polyphenol oxidase enzyme in secondary metabolism and the regulation of cell death in walnut. *Plant Physiol.* 164 (3), 1191–1203. doi: 10.1104/pp.113.228593

Ben-Shalom, N., Harel, E., and Mayer, A. M. (1978). Enzymic browning in green olives and its prevention. *J. Sci. Food Agric.* 29 (4), 398–402. doi: 10.1002/jsfa.2740290415

Berardinelli, A., Donati, V., Giunchi, A., Guarnieri, A., and Ragni, L. (2005). Damage to pears caused by simulated transport. *J. Food Eng.* 66 (2), 219–226. doi: 10.1016/j.jfoodeng.2004.03.009

Biton, I., Doron-Faigenboim, A., Jamwal, M., Mani, Y., Eshed, R., Rosen, A., et al. (2015). Development of a large set of SNP markers for assessing phylogenetic relationships between the olive cultivars composing the Israeli olive germplasm collection. *Mol. Breed.* 35 (4), 107. doi: 10.1007/s11032-015-0304-7

Bollen, A. F. (2005). Major factors causing variation in bruise susceptibility of apples (malus domestica) grown in New Zealand. *N. Z. J. Crop Hortic. Sci.* 33 (3), 201–210. doi: 10.1080/01140671.2005.9514351

Burns, J. K., Ferguson, L., Glozer, K., Krueger, W. H., and Rosecrance, R. C. (2008). Screening fruit loosening agents for black ripe processed table olives. *HortScience* 43 (5), 1449–1453. doi: 10.21273/HORTSCI.43.5.1449

Castro-Garcia, S., Rosa, U. A., J. Gliever, C., Smith, D., K. Burns, J., Krueger, W., et al. (2009). Video evaluation of table olive damage during harvest with a canopy shaker. *HortTechnology* 19 (2), 260–266. doi: 10.21273/HORTSCI.19.2.260

Conway, W. S., Faust, M., and Sams, C. E. (2003). "*Encyclopedia of Food Sciences and Nutrition*," in *Fruits of temperate climates | factors affecting quality*, 2nd. Ed. B. Caballero. (Oxford: Academic Press), 2768–2774. doi: 10.1016/B0-12-227055-X/00532-0

Croguennec, T. (2016). "Enzymatic Browning," in *Handbook of Food Science and Technology 1*. ISTE Ltd and (John Wiley & Sons, Inc.), 159–181. doi: 10.1002/9781119268659.ch6

Diaz, R., Faus, G., Blasco, M., Blasco, J., and Moltó, E. (2000). The application of a fast algorithm for the classification of olives by machine vision. *Food Res. Int.* 33 (3), 305–309. doi: 10.1016/S0963-9969(00)00041-7

Diaz, R., Gil, L., Serrano, C., Blasco, M., Moltó, E., and Blasco, J. (2004). Comparison of three algorithms in the classification of table olives by means of computer vision. *J. Food Eng.* 61 (1), 101–107. doi: 10.1016/S0260-8774(03)00191-2

Diego, B., and Rallo, L. (2000). Olive cultivars in spain. *HortTechnology* 10 (1), 107–110. doi: 10.21273/HORTTECH.10.1.107

Ferguson, L., Rosa, U. A., Castro-Garcia, S., Lee, S. M., Guinard, J. X., Burns, J., et al. (2010). Mechanical harvesting of California table and oil olives. *Adv. Hortic. Sci.* 24 (1), 53–63.

Gambella, F., Dimauro, C., and Paschino, F. (2013). Evaluation of fruit damage caused by mechanical harvesting of table olives. *Trans. ASABE* 56 (4), 1267–1272. doi: 10.13031/trans.56.9553

Garrido Fernández, A. (2006). Special issue: trends in table olive and olive oil processing. *GRASAS ACEITES* 57 (1), 86–94. doi: 10.3989/gya.2006.v57.i1.22

Goldental-Cohen, S., Burstein, C., Biton, I., Ben Sasson, S., Sadeh, A., Many, Y., et al. (2017). Ethephon induced oxidative stress in the olive leaf abscission zone enables development of a selective abscission compound. *BMC Plant Biol.* 17 (1), 87–87. doi: 10.1186/s12870-017-1035-1

Grotte, M., Duprat, F., Loonis, D., and Piétri, E. (2000). Bruising appearance of apples: Involved parameters. *Sci. Aliments* 20 (6), 575–590. doi: 10.3166/sda.20.575-590

Hammami, S. B. M., and Rapoport, H. F. (2012). Quantitative analysis of cell organization in the external region of the olive fruit. *Int. J. Plant Sci.* 173 (9), 993–1004. doi: 10.1086/667610

Hartmann, H. T., Tombesi, A., and Whisler, J. (1970). Promotion of ethylene evolution and fruit abscission in the olive by 2-chloroethanephosphonic acid and cycloheximide. *J. Amer. Soc. Hort. Sci.* 95, 635–640.

IOOC (2019). *World Table Olive Figures* [Online]. http://www.internationaloliveoil.org/estaticos/view/132-world-table-olive-figures. [Accessed].

Jiménez-Jiménez, F., Castro-García, S., Blanco-Roldán, G. L., Ferguson, L., Rosa, U. A., and Gil-Ribes, J. A. (2013a). Table olive cultivar susceptibility to impact bruising. *Postharvest Biol. Technol.* 86, 100–106. doi: 10.1016/j.postharvbio.2013.06.024

Jiménez-Jiménez, F., Castro-Garcia, S., Blanco-Roldan, G. L., González-Sánchez, E. J., and Gil-Ribes, J. A. (2013b). Isolation of table olive damage causes and bruise time evolution during fruit detachment with trunk shaker. *Span. J. Agricultural Res.* 11 (1), 65–71. doi: 10.5424/sjar/2013111-3399

Jiménez, M. R., Casanova, L., Suárez, M. P., Rallo, P., and Morales-Sillero, A. (2017). Internal fruit damage in table olive cultivars under superhigh-density hedgerows. *Postharvest Biol. Technol.* 132, 130–137. doi: 10.1016/j.postharvbio.2017.06.003

Jiménez, M. R., Rallo, P., Rapoport, H. F., and Suárez, M. P. (2016). Distribution and timing of cell damage associated with olive fruit bruising and its use in analyzing susceptibility. *Postharvest Biol. Technol.* 111, 117–125. doi: 10.1016/j.postharvbio.2015.07.029

Jiménez, R., Rallo, P., Suarez, M.-P., Morales-Sillero, A., Casanova, L., and Rapoport, H. (2011). Cultivar susceptibility and anatomical evaluation of table olive fruit bruising. *Acta Hortic.* 924 (924), 419–424. doi: 10.17660/ActaHortic.2011.924.53

Lanza, B., and Di Serio, M. G. (2015). SEM characterization of olive (Olea europaea L.) fruit epicuticular waxes and epicarp. *Sci. Hortic.* 191, 49–56. doi: 10.1016/j.scienta.2015.04.033

Martin, G. C. (1994). Mechanical olive harvest: use of fruit loosening agents. *Acta Hortic.* 356, 284–291. doi: 10.17660/ActaHortic.1994.356.60

Mohsenabadi, M., Ghasemnezhad, M., Hashempour, A., and Sajedi, R. H. (2017). Inhibition of polyphenol oxidases and peroxidase activities in green table olives by some anti-browning agents. *Agric. Conspec. Sci.* 82 (4), 375–381.

Onstott, S. (2012). *Adobe Photoshop CS6 Essentials*. (Berkley, California, USA: SYBEX Inc.).

Opara, U. L., and Pathare, P. B. (2014). Bruise damage measurement and analysis of fresh horticultural produce—a review. *Postharvest Biol. Technol.* 91, 9–24. doi: 10.1016/j.postharvbio.2013.12.009

Samim, W., and Banks, N. H. (1993). Color changes in bruised apple fruit tissue. *N. Z. J. Crop Hortic. Sci.* 21 (4), 367–372. doi: 10.1080/01140671.1993.9513795

Sánchez, A. H., García, P., and Rejano, L. (2006). Elaboration of table olives. *GRASAS ACEITES* 57 (1), 86–94. doi: 10.3989/gya.2006.v57.i1.24

SAS Institute. (2007). *JMP® version 7 User's Guide*. NC: SAS Institute Inc. Cary.

Sciancalepore, V., and Longone, V. (1984). Polyphenol oxidase activity and browning in green olives. *J. Agric. Food Chem.* 32 (2), 320–321. doi: 10.1021/jf00122a035

Segovia-Bravo, K. A., García-García, P., López-López, A., and Garrido-Fernández, A. (2011). Effect of bruising on respiration, superficial color, and phenolic changes in fresh Manzanilla olives (olea europaea pomiformis): development of treatments to mitigate browning. *J. Agric. Food Chem.* 59 (10), 5456–5464. doi: 10.1021/jf200219u

Segovia-Bravo, K. A., Jarén-Galán, M., García-García, P., and Garrido-Fernández, A. (2007). Characterization of polyphenol oxidase from the Manzanilla cultivar (olea europaea pomiformis) and prevention of browning reactions in bruised olive fruits. *J. Agric. Food Chem.* 55 (16), 6515–6520. doi: 10.1021/jf063675f

Segovia-Bravo, K. A., Jarén-Galán, M., García-García, P., and Garrido-Fernández, A. (2009). Browning reactions in olives: mechanism and polyphenols involved. *Food Chem.* 114 (4), 1380–1385. doi: 10.1016/j.foodchem.2008.11.017

Steffens, J. C., Harel, E., and Hunt, M. D. (1994). "Genetic Engineering of Plant Secondary Metabolism," in Polyphenol oxidase. Eds. B. E. Ellis, G. W. Kuroki, and H. A. Stafford (Boston, MA: Springer US), 275–312. doi: 10.1007/978-1-4615-2544-8_11

Studman, C. J. (1997). "Proceedings of the 2nd International Conference of Plant Biomechanics," in *Factors affecting the bruise susceptibility of fruit*. Eds. G. Jeronimidis and J. F. V. Vincent (University of Reading: Centre for Biomimetics), 273–281.

Sullivan, M. L. (2015). Beyond brown: polyphenol oxidases as enzymes of plant specialized metabolism. *Front. Plant Sci.* 5, 783–783. doi: 10.3389/fpls.2014.00783

Tous, J., and Tous, J. (2011). Olive production systems and mechanization. *Acta Hortic.* 924, 169–184. doi: 10.17660/ActaHortic.2011.924.22

Vaughn, K. C., Lax, A. R., and Duke, S. O. (1988). Polyphenol oxidase: the chloroplast oxidase with no established function. *Physiol. Plant.* 72 (3), 659–665. doi: 10.1111/j.1399-3054.1988.tb09180.x

Zipori, I., Dag, A., Tugendhaft, Y., and Birger, R. (2014). Mechanical harvesting of table olives: harvest efficiency and fruit quality. *HortScience* 49 (1), 55–58. doi: 10.21273/HORTSCI.49.1.55

Conflict of Interest: The authors declare that the research was conducted in the absence of any commercial or financial relationships that could be construed as a potential conflict of interest.

frontiers in Plant Science

ORIGINAL RESEARCH
published: 09 October 2019
doi: 10.3389/fpls.2019.01243

Ripening Indices, Olive Yield and Oil Quality in Response to Irrigation With Saline Reclaimed Water and Deficit Strategies

Cristina Romero-Trigueros[1], Gaetano Alessandro Vivaldi[1], Emilio Nicolás Nicolás[2], Antonello Paduano[1], Francisco Pedrero Salcedo[2] and Salvatore Camposeo[1]*

[1] Dipartimento di Scienze Agro-Ambientali e Territoriali, Università degli Studi di Bari Aldo Moro, Bari, Italy, [2] Department of Irrigation, Centro de Edafología y Biología Aplicada del Segura (CEBAS-CSIC), Murcia, Spain

OPEN ACCESS

Edited by:
Antonio Diaz Espejo, Institute of Natural Resources and Agrobiology of Seville (CSIC), Spain

Reviewed by:
Maria Cecilia Rousseaux, Centro Regional de Investigaciones Científicas y Transferencia Tecnológica de La Rioja (CRILAR CONICET), Argentina
Gregorio Egea, University of Seville, Spain

***Correspondence:**
Emilio Nicolás Nicolás
emilio@cebas.csic.es

Specialty section:
This article was submitted to Crop and Product Physiology, a section of the journal Frontiers in Plant Science

Received: *14 June 2019*
Accepted: *06 September 2019*
Published: *09 October 2019*

Citation:
Romero-Trigueros C, Vivaldi GA, Nicolás EN, Paduano A, Salcedo FP and Camposeo S (2019) Ripening Indices, Olive Yield and Oil Quality in Response to Irrigation With Saline Reclaimed Water and Deficit Strategies. Front. Plant Sci. 10:1243. doi: 10.3389/fpls.2019.01243

The 70% worldwide surface of olive orchards is irrigated. The evaluation of non-conventional water resources and water-saving techniques has gained importance during the last decades in arid and semiarid environments. This study evaluated the effects of irrigation with two water sources: low-cost water DEsalination and SEnsoR Technology (DESERT) desalinated water (DW) EC_w ~1 dS m^{-1}) and reclaimed water (RW) (EC_w ~ 3 dS m^{-1}) combined with two irrigation strategies: full irrigation (FI) (100% of ET_c) and regulated deficit irrigation (RDI, 50% of ET_c) on fruit yield, ripening indices, and oil yield and quality of olive trees cv Arbosana planted in Mediterranean conditions. Our results showed that RW without water restrictions increased the fruit yield by 35% due to a slight increase in the fruit weight and, mainly, to a greater fruit set than the control trees; although this did not result in a higher oil yield (g $tree^{-1}$) since the oil content per fruit dry weight was reduced. The RDI strategy did not decrease the fruit yield despite the fact that olive weight tended to decrease, and it increased the oil yield by ~14.5%. The combination of both stresses (RW and RDI) neither decreased the fruit yield; however, it significantly reduced oil yield (25% less in 2018) since oil content per fruit dry weight was strongly reduced (40%) compared to control trees. Both RDI treatments, regardless water source, determined acidity levels in olive paste lower than in FI treatments; however, it reduced oil extractability and fatty yield. The finding about oil quality indicated that olive exposure to RW, regardless of the water amount, decreased oil quality mainly due to the reduction of oleic acid and the increase of C18:2/C18:3 ratio and peroxides; on the contrary, both RW and RDI improved the total polyphenols. In all cases, the parameters met the legislation. In short, with appropriate management, RW and RDI have great potential to manage oil olive production; nevertheless, studies subjected to long-term use of these techniques should be experienced to ensure the sustainability of oil yields and quality.

Keywords: acidity, Arbosana, fruit weight, oil extractability, oleic acid, polyphenol, peroxide, total production

INTRODUCTION

Water is essential for agricultural production and food security. Our freshwater resources are dwindling at an alarming rate. It is estimated that by 2025, around 2 billion people will be affected by absolute water scarcity (Riemenschneider et al., 2016). Thus, growing water scarcity is now one of the leading challenges for sustainable development. This challenge will become more pressing as the world's population continues to grow, their living standards increase, diets change, and the effects of climate change intensify, increasing temperatures across the world. In this context, more frequent and severe droughts are already having an impact on agricultural production, where rising temperatures translate into increased crop water demand.

Agriculture, which is the most water-demanding economic sector worldwide, is both a major cause and casualty of water scarcity. Farming accounts for almost 70% of all water withdrawals, and up to 95% in some developing countries, with freshwater resources heavily stressed by irrigation and food production (FAO, 2018). In Italy, the dimensions of economic loss in the farming sector were predicting losses of 2 billion Euros (EC, 2018) due to the droughts of summer 2017. In particular, Apulia region (southeast of Italy), which exhibits a Mediterranean climate characterized by hot, dry summer, requires a high volume of irrigation water because many hectares of fruit tree crops (olive, grapes, almond, sweet cherry) account for 80% of the region's irrigated land (Arborea et al., 2017). Besides, extensive exploitation of wells by Apulian regional farmers is causing the progressive salinization and depletion of relevant portions of the regional aquifers reducing the water available for agriculture (Vivaldi et al., 2019).

Thus, techniques for optimizing water productivity as the regulated deficit irrigation (RDI), where water deficits are imposed during phenological periods when the tree is the least sensitive to water stress, and with little impact on fruit yield (Romero-Trigueros et al., 2017) or the use of non-conventional water sources in agriculture as a component of effective water conservation strategies, are required in regions with water scarcity (Romero-Trigueros et al., 2019). Doing so will not prevent a drought from occurring, but it can help in preventing droughts to result in famine and socioeconomic disruption (FAO, 2018).

With respect to non-conventional water sources, reused reclaimed water (RW) is considered non-expensive and reliable, particularly for irrigation in agriculture. It is estimated that, globally, the market for reuse was on the verge of expansion and expected to outpace desalination in the future. It is foreseen that, by 2030, water reuse will represent about 1.7% (26 billion m^3 $year^{-1}$) of the total water use (Global Water Market, 2017). RW usually may contain not only essential nutrients, which are beneficial for crop growth and economy of the growers, but also salts, toxic ions, and micropollutants, which discharge into the environment and can accumulate in the soil and crops over time, affecting plants, soils, and underground water bodies (Romero-Trigueros et al., 2014). For this reason, reducing salt concentrations in these water sources, leading to desalinated water, using technologies, could be an imperative need. Nevertheless, the technologies used must be adequately validated in real crops, ensuring their sustainability, and knowing how it affects the fruit yield and quality. Olive crop is considered moderately tolerant to salinity (Gucci and Tattini, 1997; Erel et al., 2019) with water electrical conductivity (EC_w) between 3 and 6 dS m^{-1}, causing no effect to growth or yields (Ayers and Westcot, 1985). In addition, in the Mediterranean region, olive is a major tree crop, and more than 90% of the world's olive oil is produced. Concretely, in Apulia region, olive is the most representative fruit tree crop irrigated with 383,650 ha cultivated (33 % of total olive orchards in Italy) and with a production of 205,983 t of olive (48% of total Italian production) (ISTAT, 2017; ISMEA, 2018). Salinity tolerance mechanisms of olive trees apparently include a strong ability to exclude potentially toxic ions from above-ground tissues (Kchaou et al., 2010). There are some studies where the saline RW has been used to irrigate olive trees in Mediterranean countries (Greece, Israel, Italy, Spain, Jordan, Egypt, and Tunisia), which reported that the tolerance to salinity depends on the olive varieties. Most of the works evaluated soil properties and leaf nutrients (Aragüés et al., 2005; Ben Rouina et al., 2011; Segal et al., 2011; Petousi et al., 2015; Bourazanis et al., 2016; Erel et al., 2019), root nutrient (Bedbabis et al., 2014), vegetative growth (Kchaou et al., 2010; Ben-Gal et al., 2017), fruit nutrient (Melgar et al., 2009; Batarseh et al., 2011; Bedbabis et al., 2014), and oil yield and quality (Melgar et al., 2009; Ayoub et al., 2016; Tietel et al., 2019).

Regarding the effects of RDI in olive crop, recent works showed that linoleic acid content in olive oil (Hernández et al., 2018), the vegetative growth (Rosecrance et al., 2015; Hernández-Santana et al., 2018), the fruit yield (Gucci et al., 2019) were decreased by water stress. However, a moderate water stress can increase olive oil yield and quality and accelerate fruit maturity (Rosecrance et al., 2015).

To our knowledge, however, nothing has been published about the effects of (i) the irrigation with desalinized water (DW) or of the combination of both water sources (DW and RW) with the RDI strategy and (ii) the strategies on cultivar Arbosana, which is the variety object of study of this work. This cultivar is characterized by early bearing (2nd year after planting), low vigor, and slow canopy growth so that it is the most suitable cultivar to new super high-density olive (SHD) cropping systems (Godini et al., 2011; Rallo and Provenzano, 2013; Vivaldi et al., 2015). SHD olive orchards are spread on over 200,000 ha all over the world on five continents (Olint, 2018). Arbosana, despite being a cultivar widely cultivated has been under-assessed; only Kchaou et al. (2010) studied it in a greenhouse pot experiment with nutrient solution. Indeed, most of works used other olive cultivated varieties, such as Barnea, Leccino (Segal et al., 2011; Ben-Gal et al., 2017; Erel et al., 2019; Tietel et al., 2019), Arbequina (Aragüés et al., 2005; Rosecrance et al., 2015; Hernández et al., 2018; Hernandez-Santana et al., 2018), Chemlali (Ben Rouina et al., 2011; Bedbabis et al., 2014; Bedbabis and Ferrara, 2018), Koroneiki (Petousi et al., 2015; Bourazanis et al., 2016), Nabali Muhassan (Ayoub et al., 2016), Frantoio (Gucci et al., 2019), and Picual (Melgar et al., 2009).

This work intends to assess the effects of the use of desalinated and saline RW combined with two irrigation strategies, full

irrigation (FI) and RDI on (i) fruit yield and ripening indices and (ii) oil yield and quality of olive trees cv Arbosana.

MATERIALS AND METHODS

Experimental Site and Plant Material

The study was conducted at an experimental site located in the southeast of Italy (Bari, Apulia Region) (41°06′41′′N, 16°52′57′′E) (5 m above sea level) during 2017 and 2018. The crop used was 2 years self-rooted olive trees (cv Arbosana) planted on not covered 100-L polyethylene pots (diameter, 50 cm; height, 65 cm). Pots were on the ground with a 1.85 × 2.10 m planting system in rows oriented N-NE to S-SW. The soil texture within the first 90 cm depth was classified as loam (44.78 % sand, 12.32 % clay, and 42.90 % silt) (USDA textural soil classification).

Irrigation Treatments

Two irrigation water sources were examined. First was low-cost water DEsalination and SEnsoR Technology (DESERT) DW, obtained by treating secondary wastewater coming from Bari secondary wastewater treatment plant with EC_w 1.2 dS m^{-1} by ultrafiltration, active carbon, and reverse osmosis till reaching an EC_w of 1.0 dS m^{-1}. DESERT is an innovative water desalination and sensor technology compact module for continuously monitoring water quality that has been developed in the framework of the DESERT European project (Water JPI, 2016) with participating partners from Italy, Spain, and Belgium. DESERT technology, to contrast water scarcity and to increase the water quality, enhances the energy savings using solar energy to treat the non-conventional water. The second one is saline RW, which is obtained by mixing the secondary wastewater (EC_w 1.2 dS m^{-1}) with the brine produced on the DESERT prototype till reaching an EC_w of 3 dS m^{-1}).

Two irrigation treatments were established for each water source. The first treatment was FI treatment throughout the growing season to fully satisfy crop water requirements (100% ET_c). The second one was an RDI treatment with an irrigation regime similar to FI, except during the initiation of the first stage of oil accumulation, when it received half the water as applied to the FI (50% ET_c). This RDI period was chosen because it corresponded to approximately the end of maximum rate of pit hardening and before the rapid phase of fruit growth and oil accumulation begins, thus avoiding the fruit set period (Stage 1), when olive trees are more sensitive to water stress (Gucci et al., 2019; Rosecrance et al., 2015). The DW-RDI was considered as the control treatment. The irrigation was scheduled on the basis of daily evapotranspiration of the crop (ET_c) accumulated during the previous week. ET_c values were estimated by multiplying reference evapotranspiration (ET_0) (Equation 1) as recommended by FAO (Allen et al., 1998):

$$ET_c = Kr \cdot Kc \cdot ET_0 \quad (1)$$

where Kr is reduction coefficient (Kr = 0.75) and Kc (0.40 Kc_{ini}, 0.90 Kc_{mid}, 0.65 Kc_{end}) is crop coefficient. ET_0 was calculated by Penman–Monteith methodology, and all data were provided by a climate station located 100 m far from the experimental

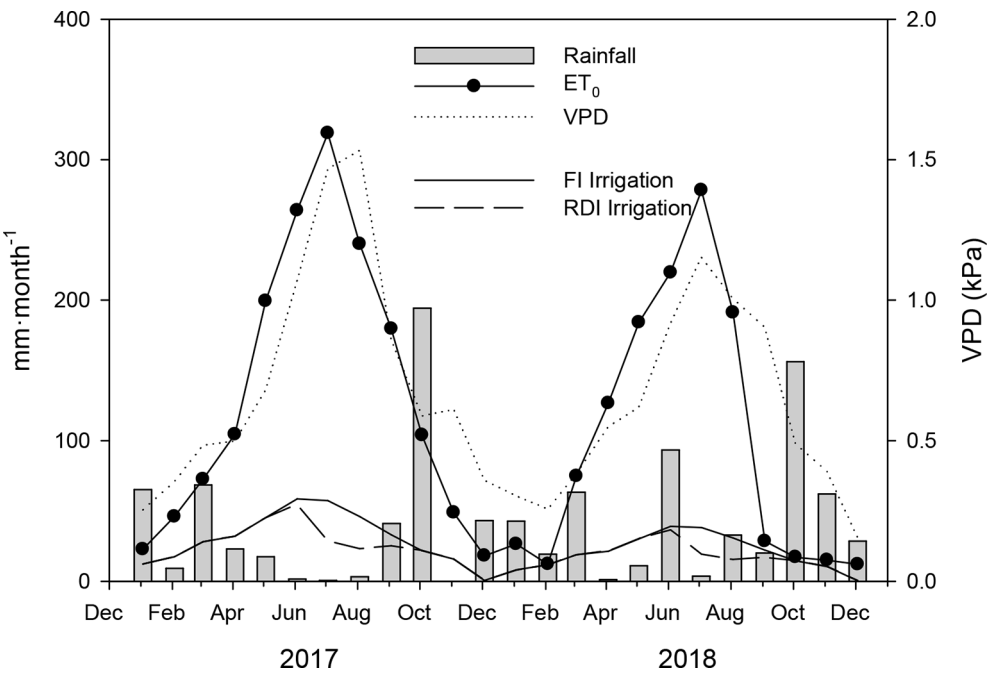

FIGURE 1 | Seasonal evolution of rainfall (mm·month^{-1}), reference evapotranspiration (ET_0, mm·month^{-1}), vapor pressure deficit (VPD, kPa), and full (FI) and regulated deficit (RDI) irrigation depths (mm·month^{-1}) during 2017 and 2018.

platform. The monthly evolution of the ET_0 during the experiment is shown in **Figure 1**. The water was supplied by drip irrigation with three pressure compensated drippers per tree, each with a flow rate of 2 L h^{-1}.

All trees received the same amount of NPK macronutrients through a drip irrigation system. Integrated pest management and pruning were those commonly used by growers in the area, and no weeds were allowed to develop within the orchard.

Water Quality and Plant Water Status

The inorganic solute content, pH and EC_w of each irrigation water source were assessed monthly during the irrigation seasons in 2017 and 2018. The samples were collected in glass bottles, transported in an ice chest to the laboratory, and stored at 5°C before being processed for chemical and physical analyses. The concentrations of macronutrients (N, K, P, Ca, and Mg) and micronutrients including B were determined by inductively coupled plasma optical emission spectrometer (ICP-ICAP 6500 DUO Thermo, England). Anions (Cl^-, NO_3^-, PO_4^{3-}, and SO_4^{2-}) were analyzed by ion chromatography with a liquid chromatograph (Metrohm, Switzerland). EC_w was determined using a PC-2700 meter (Eutech Instruments, Singapore), and pH was measured with a pH-meter Crison-507 (Crison Instruments S.A., Barcelona, Spain).

Stem water potential (SWP) was determined weekly during the irrigation periods at midday, using a pressure chamber (model 3000, Soil Moisture Equipment Corp., California, USA), according to Scholander et al. (1965), on one fully expanded leaf per tree from the mid-shoot area, which were bagged within foil-covered aluminum envelopes at least 2 h before the measurement (Shackel et al., 1997).

Fruit Yield and Ripening Indices

The harvesting was made on October 31, 2017, and November 21, 2018, at the appropriate ripening stage, when detachment index reached at least 2 N g^{-1}. All olives were manually and separately collected and weighed to determine the fruit yield (g $tree^{-1}$). The fruit number per tree was calculated by dividing the fruit yield by average single fruit weight.

Fifty olives from each tree of each treatment were randomly sampled immediately after harvest to determine the different fruit ripening indices, following the methodology reported by Camposeo et al. (2013). For fresh weight (FWe), dry weight (DWe), and water content (WC) calculated as (FWe-DWe)·FWe−1·100, fruits were brought to the laboratory to determine the FWe on a digital balance (XS105 Dual Range, Mettler Toledo, Greifensee, Switzerland). Then, these were oven-dried for 48 h at 65°C, cooled for 30 min in a desiccator and again weighted. The detachment index (DI; N g^{-1}) was calculated as: DI = DF·FWe^{-1} where DF is the detachment force (N) measured using a manual dynamometer (Somfy Tec). Fruit firmness was measured with a penetrometer ADEMVA (mod.TR) using a tip Ø 2 mm on the equatorial zone.

Fruit color was determined as pigmentation index (PI) calculated in Equation (2):

$$PI = \sum_{i=0}^{5} \frac{i \times ni}{N} \quad (2)$$

where i is the number of the group, ni is the number of fruits per group, N is the total number of fruits in the sample. The procedure consisted in distributing the sample of olives in six groups, according to the following characteristics: group 0, green skin; group 1, <50% black skin with white flesh; group 2, ≥50% black skin with white flesh; group 3, 100% black skin with white flesh; group 4, 100% black skin with <50% purple flesh; and group 5, 100% black skin and ≥50% purple flesh ($0 \leq PI \leq 5$).

Oil Extraction and Quality

Fatty yield (%), humidity (%), and acidity (%) were determined by near-infrared spectroscopy in part of fruits which were crushed in a hammer mill (FOSS Olivia™, Barcelona, Spain), the resulting olive paste malaxed at 25°C for 30 min (Servili et al., 2007).

To determine oil industrial extractability (%) after olive paste was obtained, the oil was extracted and separated by vertical centrifugation, collected, and left to decant. The oil samples were filtered and stored at 14°C in a dark and cool place in amber glass bottles until analysis. Results were also expressed as oil content per dry and fresh fruit weight (%) and oil yield (g_{oil} tree).

Olive oil free acidity (FA), given as percent of oleic acid (C18:1), (% C18:1 per 100 g olive oil), peroxide value (meq O_2 kg^{-1} oil), and UV determinations (K_{232}, K_{270}, and ΔK) were carried out according to the European Union Commission Reg. 61/2011 (EEC, 2011) and International Olive Council (IOC) standard methods. The parameters or extinction coefficients, K_{232} and K_{270}, have oil absorbance at 232 and 270 nm, respectively, and ΔK was calculated from the absorbances at 232, 268, and 274 nm. Spectrophotometric determinations, K_{232}, K_{270}, and ΔK analyses, were carried out using a Shimadzu UV-1601 spectrophotometer (Shimadzu, Kyoto, Japan).

Profiles of fatty acids methyl esters (FAME) were determined by gas chromatography (EEC, 2011). Olive oil was diluted in hexane (1% oil) and 0.4-ml solution was added to 0.2-ml methanol solution with KOH 2 N. The mixture was vigorously shaken for 1 min and 2 µL of the hexane organic phase was collected for the GC injection. A Shimadzu mod. GC-17A equipped with flame ionization detected (FID) (Shimadzu Italia, Milan, Italy) was used for the analysis. The acquisition software was Class-VP Chromatography data system 4.6 (Shimadzu Italia, Milano, Italy). A FAME capillary column, 60 m, 0.25 mm i.d. with 0.25 mm 50% cyanopropyl-methyl phenyl silicone, was used (Quadrex Corporation, New Heave, USA). Chamber was held at 170°C for 20 min using a rate of 10°C min^{-1} until 220°C, held for 5 min. Injector temperature and FID temperature was 250°C; carrier gas, Helium; column flow, 2 ml min^{-1}; split ratio, 1/60; injected volume, 20 µl. Peaks identification was performed by comparing retention times of fatty acids with those of pure compounds (mixture of pure methyl esters of fatty acids; Larodan, Malmoe, Sweden) injected in the same condition.

Phenolic compounds were extracted and determined according to Caponio et al. (2015) with slight modifications. Extraction was carried out on 1 g of oil by adding 1 ml of hexane and 5 ml of methanol/water (60:40v/v). After vortexing for 1 min and centrifuging at 4000 rpm for 10 min, the hydroalcoholic phase was recovered and filtered through nylon filters (pore size 0.45 µm, Sigma-Aldrich, Milan, Italy). Then, 100 ml of extract were mixed with 100 ml of Folin–Ciocalteu reagent by Folin and Ciocalteau (1927) and after 4 min, with 800 ml of a 5% (w/v) solution of sodium carbonate. The mixture was stored in the dark for 30 min, and the total phenol content was determined at 750 nm by a Shimadzu UV-1601 spectrophotometer (Shimadzu, Kyoto, Japan). The total phenolic content was expressed as gallic acid equivalents ($mg \cdot kg^{-1}$).

Chlorophyll and carotenoids determination was carried out by measuring the absorption of the oil/hexane solution (1:1 v/v) at wavelengths of 670 nm for chlorophyll and 450 nm for carotenoids using a Shimadzu UV-1601 spectrophotometer (Shimadzu, Kyoto, Japan) (Minguez et al., 1991).

Experimental Design and Statistical Analysis

A total of 40 trees were used in this study (10 per treatment). The experimental design of each irrigation treatment was five replicates distributed following a completely randomized design. Each replica consisted of two trees. To evaluate the fruit yield and ripening indices, all trees per treatment (10 trees per treatment) were used. For the study of the SWP, oil yield and quality five trees per treatment (one per replicate) were evaluated.

A weighted analysis of variance (ANOVA) followed by Tukey's test ($P \leq 0.05$) was used for assessing differences among treatments. Linear regressions among the different variables measured were calculated. Pearson's correlation coefficients were used to assess the significance of these relationships. These statistical analyses were performed using SPSS (vers. 23.0 for Windows, SPSS Inc., Chicago, IL). To discriminate significant differences among parameters of different linear regressions (slope and intercept) analysis of covariance (ANCOVA) were performed using Statgraphics software (Statgraphics Plus for Windows Version 4.1). The data also were analyzed using a two-way ANOVA with water quality and water amount as the main factors.

RESULTS

Climatic Data

Climate conditions at the experimental site followed typical Mediterranean patterns, with hot and dry weather from May to September, reaching ET_0 values of 318.81 and 278.28 $mm \cdot month^{-1}$ in 2017 and 2018, respectively, and being mild and wet for the rest of the year. The total rainfall was 467 and 535 mm in 2017 and 2018, respectively. Most of the annual rainfall occurred between September and May (**Figure 1**). The daily average vapor pressure deficit (VPD) values reached 1.53 and 1.15 kPa in August of 2017 and 2018, respectively (**Figure 1**). There was a clear different climatic pattern between years. The first year was hotter and more arid than the second one. In particular, during the ripening period (from September to November), the sum of ET0 values was much higher in 2017 than in 2018 (332.5 mm vs 60.6 mm, respectively).

TABLE 1 | Physical and chemical properties for DESERT desalinated water (DW) and reclaimed water (RW) in 2017 and 2018.

Property	Units	2017		2018		Limits D.L. 185/2003
		DW	RW	DW	RW	
pH		7.53 ± 0.31	8.15 ± 0.20	8.11 ± 0.32	8.44 ± 0.34	6–9.5
EC_w	$dS \cdot m^{-1}$	1.00 ± 0.15	3.00 ± 0.45	1.13 ± 0.61	3.00 ± 0.89	3
SAR		3.7 ± 0.42	7.2 ±1.52	4.79 ± 1.94	5.69 ± 1.62	10
Ca	$mg\ L^{-1}$	56.28 ± 11.30	121.3 ± 22.1	50.76 ± 21.52	108.05 ± 57.15	–
Mg	$mg\ L^{-1}$	20.9 ± 5.40	35.5 ± 6.10	18.31 ± 8.12	35.96 ± 16.82	–
K	$mg\ L^{-1}$	20.67 ± 8.81	42.76 ± 6.30	20.37 ± 9.77	33.54 ± 12.60	–
Na	$mg\ L^{-1}$	148.4 ± 53.2	353.2 ± 48.7	160.10 ± 85.67	270.66 ± 126.36	–
B	$mg\ L^{-1}$	0.14 ± 0.06	0.15 ± 0.07	0.13 ± 0.05	0.14 ± 0.04	1.00
Mn	$mg\ L^{-1}$	0.08 ± 0.01	0.16 ± 0.02	0.09 ± 0.03	0.17 ± 0.06	–
Zn	$mg\ L^{-1}$	0.03 ± 0.00	0.05 ± 0.01	0.03 ± 0.02	0.04 ± 0.01	
Fe	$mg\ L^{-1}$	0.04 ± 0.01	0.04 ± 0.01	0.07 ± 0.06	0.13 ± 0.12	–
Cu	$mg\ L^{-1}$	0.000 ± 0.000	0.009 ± 0.004	0.009 ± 0.005	0.015 ± 0.001	
Al	$mg\ L^{-1}$	0.04 ± 0.01	0.05 ± 0.02	0.06 ± 0.03	0.09 ± 0.06	
Ni	$mg\ L^{-1}$	0.012 ± 0.000	0.026 ± 0.001	0.022 ± 0.023	0.114 ± 0.176	
NO_3^-	$mg\ L^{-1}$	15.83 ± 2.53	36.16 ± 9.28	28.39 ± 25.08	42.70 ± 19.93	–
PO_4^{3-}	$mg\ L^{-1}$	1.3 ± 0.61	3.1 ± 0.52	2.01 ± 0.52	2.51 ± 1.45	2
SO_4^{-2}	$mg\ L^{-1}$	97.98 ± 16.2	227.4 ± 37.5	92.37 ± 66.11	144.92 ± 92.15	500
F^-	$mg\ L^{-1}$	0.22 ± 0.09	0.38 ± 0.11	0.22 ± 0.12	0.30 ± 0.17	–
Cl^-	$mg\ L^{-1}$	198.1 ± 54.1	379.5 ± 72.3	199.77 ± 184.71	380.18 ± 181.33	250

Values are averages ± SD of 12 individual samples taken throughout the crop cycle. EC_w, water electrical conductivity; RW, reclaimed water; DW, DESERT desalinized water.

Irrigation Water Quality and Plant Water Status

The results of the chemical analysis of both irrigation water sources used in the experiment, DW and RW, during 2017 and 2018, are presented in **Table 1**. In general, both waters were characterized by a slight alkaline; within the range of proper irrigation water (Bedbabis et al., 2010). The pH values were weakly higher in RW than in DW, and both within the limits allowed by the D.L. 185/2003. RW had significantly higher salinity than DW (31 ds·m^{-1} versus 1 ds·m^{-1}). The sodium absorption ratio (SAR) also was higher in RW than DW, and both sources presented values below the limit. The Cl^- concentrations were around 200 mg·L^{-1} for DW and almost double (380 mg·L^{-1}) for RW, exceeding, in this last case, the threshold values indicated in D.L. 185/2003. Likewise, Na presented higher levels in the RW than in the DW, mainly in 2017. Regarding nutrients and elements considered essential for plant growth and development, RW contained higher amounts of NO_3^-, PO_4^{3-}, and K, with respect to DW. Similarly, Mg and Ca concentrations in RW were around the double in comparison with DW. Boron, an important micronutrient for olive tree production (Saadati et al., 2013) was found in both sources at a quite similar concentration. The micronutrients as Fe, Mn, and Zn also were slightly higher in RW than in DW (Fe, only in 2018, and Mn presented values about almost double both years). Others toxic heavy metals as Cd, Cr, and Pb were not detected in any of the water sources, whereas the highest Al and Ni levels were in RW.

The irrigation season lasted from May 1 to October 31 and from May 15 to November 9 for 2017 and 2018, respectively. The amounts of water applied were 3679.63 and 3062.34 m^3·ha^{-1} for FI and RDI treatments in 2017 and 2460.49 and 2011.23 m^3·ha^{-1} for FI and RDI treatments in 2018, respectively (**Figure 1**). Therefore, the RDI treatment saved about 21% of irrigation water. The RDI period in 2017 began on DOY 180 (29th June 2017) and ended on 213 (August 1, 2017). The RDI period in 2018 started on DOY 180 (June 29, 2018) and ended on DOY 243 (August 31, 2018). The RDI period in 2017 lasted 1 month less than in 2018 for two reasons: (i) the trees were very young and (ii) the trees were shortly transplanted (1 year).

The water quality did not affect the SWP. However, the RDI treatments reached SWP values significantly more negative (−1.90 and −3.05 MPa in 2017 and 2018, respectively) than the control treatment (−1.02 and −1.29 MPa in 2017 and 2018, respectively) during the RDI periods. The SWP was lower in the water stressed trees during the second year than in the first one because the RDI period was longer.

Properties of the Fruit Production

Harvest data for each year are shown in **Figure 2**. In general, the fruit yield was very low in the first year of the experiment with an average value of 218 g per tree. In the following year, Arbosana trees started to bearing, with a yield of 2.01 kg per tree. The average individual fruit weight ranged between 2.2 and 2.5 g and between 2.0 and 2.6 g for 2017 and 2018, respectively. The fruit number per tree ranged from 81.3 to 110.3 in 2017 and from 734.3 to 972.0 in 2018. Considering the different treatments, there were no differences among them neither in yield, nor in fruit weight or number of fruit in 2017. However, the RW-FI treatment had a fruit yield significantly higher than the rest of treatments, about 35% more than DW-FI (**Figure 2A**) in 2018. This was mainly due to an increase in the olive weight (7%) and to a greater number of fruits per tree (21%), although there were no significant differences in these two parameters (**Figures 2B**, **C**). Water stress caused by the RDI strategies did not affect significantly the fruit yield, regardless of the water quality, although we observed an increase in the number of fruits per tree (32.4% and 23.5% for

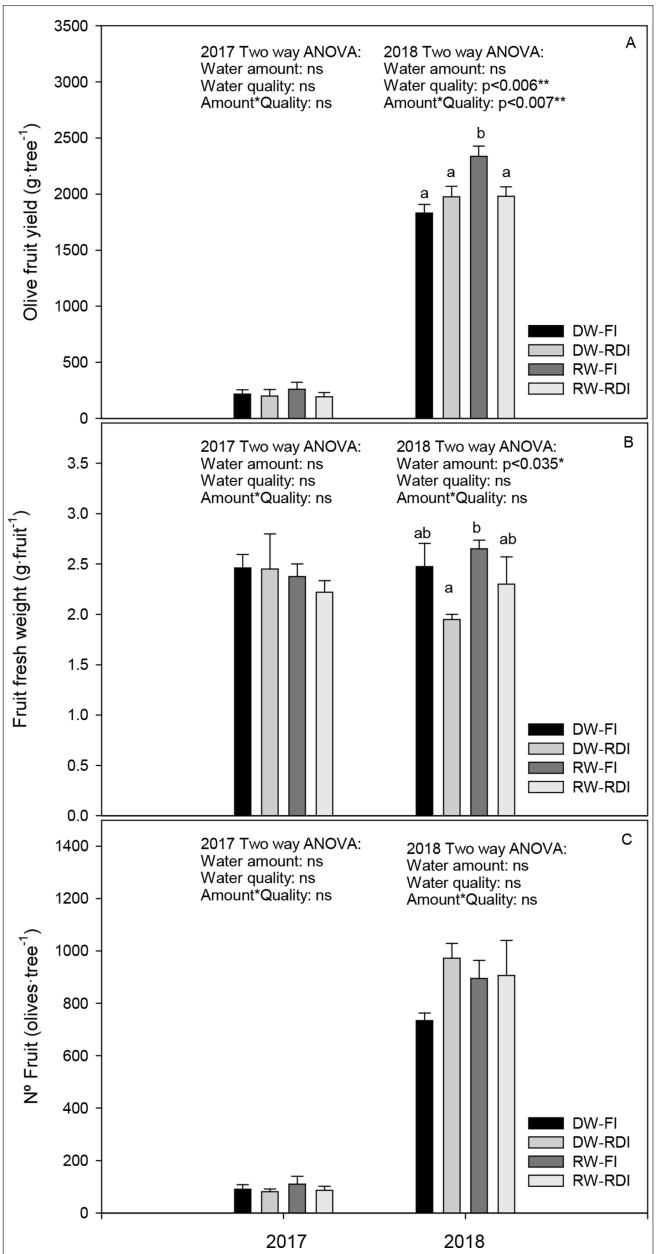

FIGURE 2 | (A) Olive fruit yield (g tree−1), **(B)** fruit fresh weight (g fruit−1) and **(C)** number of fruit (olives tree−1) for each treatment: DW-FI (DESERT water-full irrigation), DW-RDI (DESERT water-regulated deficit irrigation), RW-FI (reclaimed water-full irrigation), and RW-RDI (reclaimed water-regulated deficit irrigation) for 2017 and 2018.

TABLE 2 | Ripening indices: water content, detachment index, fruit firmness and pigmentation index for each treatment: DW-FI (DESERT water-full irrigation), DW-RDI (DESERT water-regulated deficit irrigation), RW-FI (reclaimed water-full irrigation) and RW-RDI (reclaimed water-regulated deficit irrigation) in 2017 and 2018.

	Water content (%)		Detachment Index (N·g^{-1})		Fruit firmness (N)		Pigmentation Index	
	2017	2018	2017	2018	2017	2018	2017	2018
DW-FI	58.2 ± 0.7a	56.9 ± 0.7a	2.28 ± 0.12a	2.23 ± 0.15a	6.54 ± 0.55a	7.68 ± 0.43a	1.32 ± 0.24a	0.84±0.29a
DW-RDI	59.3 ± 1.9a	59.6 ± 0.3b	2.25 ± 0.25a	2.25 ± 0.24a	5.50 ± 0.40a	7.57 ± 0.14a	1.25 ± 0.04a	0.93±0.17a
RW-FI	58.0 ± 1.2a	58.4 ± 0.1ab	2.13 ± 0.13a	2.10 ± 0.13a	5.75 ± 0.47a	7.70 ± 0.29a	2.15 ± 0.25a	0.80±0.27a
RW-RDI	59.9 ± 0.5a	59.2 ± 0.4b	2.42 ± 0.17a	2.23 ± 0.22a	6.02 ± 0.17a	7.73 ± 0.14a	1.34 ± 0.24a	0.88±0.26a
Water amount	ns	$p < 0.001$***	ns	ns	ns	ns	ns	ns
Water quality	ns	ns	ns	ns	ns	ns	ns	ns
Amount*quality	ns	$p < 0.041$*	ns	ns	ns	ns	ns	ns

Different letters within the same column indicate significant differences among treatments according to Tukey's Test ($p < 0.005$).
ns, not significant.

DW-RDI and RW-RDI, respectively) and a decrease in the fruit weight (21% and 6.8% for DW-RDI and RW-RDI, respectively) with respect to the DW-FI, mainly in the DW-RDI.

Regarding fruit ripening indices at harvest (**Table 2**), neither quality water (RW treatments) nor water amount (RDI treatments) affected significantly detachment index, fruit firmness, and PI. Nevertheless, some trends were observed. Fruits from RW trees (i) were detached more easily than control trees, although the fruit detachment force was not significantly lower in the RW-FI versus the DW-FI (**Table 2**), and (ii) had a higher PI than the DW-FI in the first year (63%). Besides, in 2017, the mean PI was 1.5 and in the second one decreased about 0.9. During the RDI period, DW-RDI fruits looked wrinkled. When such period ended, fruits visually recovered the firmness; although the lowest values of firmness were observed in this treatment at harvest. Finally, the fruit WC was significantly higher in the RDI treatments in 2018 (4.9% and 4.2% for DW-RDI and RW-RDI, respectively).

Oil Determination

The fatty yield was affected by water stress in 2018 because both RDI treatments had less fatty performance than the DW-FI (a reduction of 15.2 and 11.0% for DW-RDI and RW-RDI, respectively) (**Figure 3A**). Similarly, oil industrial extractability also was decreased by RDI strategies in 2018 (a reduction of 16.2%

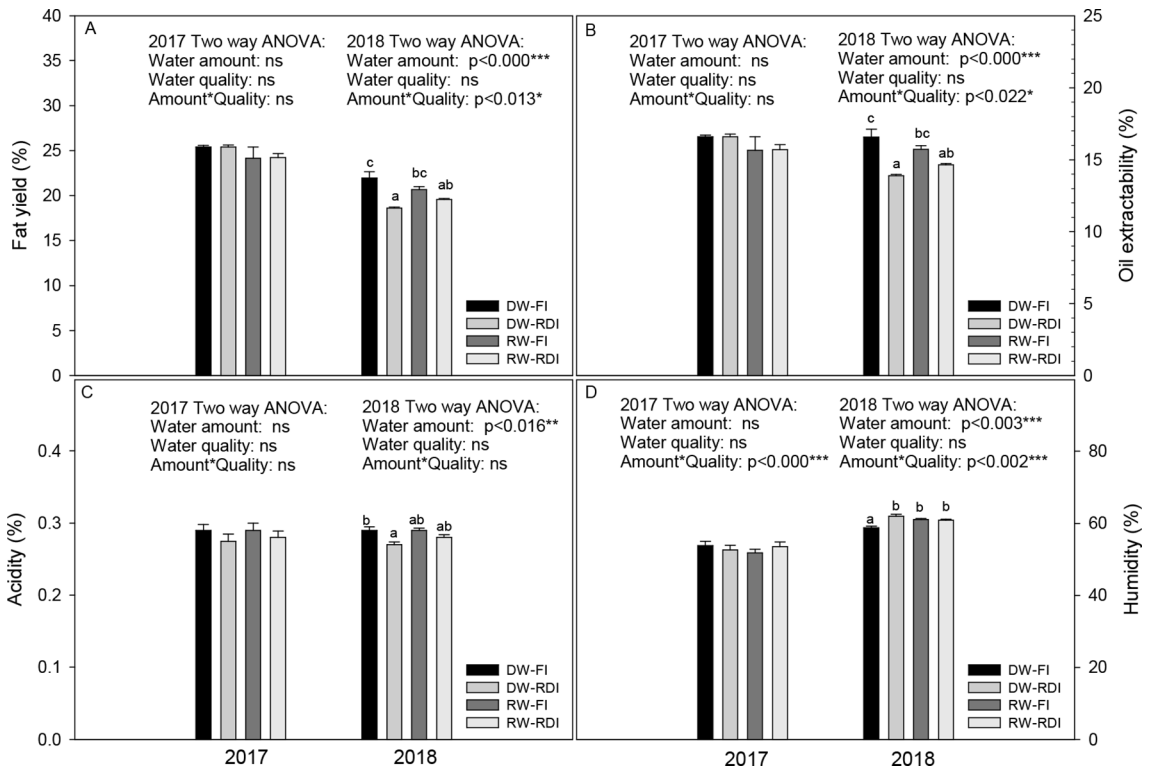

FIGURE 3 | (A) Fatty yield (%), **(B)** oil extractability (%), **(C)** acidity (%) and **(D)** humidity (%) for each treatment: DW-FI (DESERT water-full irrigation), DW-RDI (DESERT water-regulated deficit irrigation), RW-FI (reclaimed water-full irrigation), and RW-RDI (reclaimed water-regulated deficit irrigation) in 2017 and 2018.

and 11.6% for DW-RDI and RW-RDI, respectively) (**Figure 3B**). Humidity percentage in olive paste was higher in all stressed treatments compared with DW-FI in the second year. With respect to acidity, olive paste of RDI treatments also presented a mild reduction in its levels in both years, being significant for the DW-RDI in 2018 (6.1%) (**Figure 3C**). Moreover, taking into account all the treatments, humidity was significantly correlated to fatty yield ($R = 0.82$, $p < 0.005$***) and oil extractability ($R = 0.80$, $p < 0.005$***), so that as humidity increased, the fatty yield and oil extractability decreased. With less significance, humidity also correlated negatively with acidity ($R = 0.60$, $p < 0.01$**). In this sense, overall, the levels of fatty yield and oil extractability decreased by 4% and 1.2%, respectively, from 2017 to 2018. The fatty yield average values were around 24% in 2017 and decreased about 20% in 2018 and, like the oil extractability averages, were 16.4% in 2017 and 15.2% in 2018. On the contrary, humidity was higher in 2018 (61%) than 2017 (53%).

There were no significant differences among treatments for the oil content per fresh and dry fruit weight and for the oil yield in the first year of the experiment. However, oil content was affected by the water quality in the next year by two-way ANOVA (**Figures 4A**, **B**). Concretely, the oil content based on fresh fruit weight ranged from 8.20% to 13.50% and in the RW-FI and RW-RDI a reduction by 25% and 33%, respectively, was found (**Figure 4A**). In DW-RDI, on the contrary, a tendency to increase (10.6%) was observed. Oil content based on dry fruit weight showed the same behavior than oil content based on fresh weight in 2018, with values between 20% and 33%. A decrease by 22.9% in RW-FI and also a strong decrease by 39.93% in the RW-RDI, with respect to the DW-FI, were observed. Contrary, we observed a slight increase by 18.3% in the DW-RDI (**Figure 4B**).The oil yield was 0.22, 0.25, 0.21, and 0.16 g_{oil} $tree^{-1}$ for DW-FI, DW-RDI, RW-FI, and RW-RDI, respectively, in 2018. Despite the two-way ANOVA indicating that this parameter was not affected by the quality or quantity of water (**Figure 4C**), Tukey's test did show a tendency, that is, the oil yield decreased by 1.72% in RW-FI, despite such treatment having the highest olive fruit production, and markedly decreased by 24.8% in trees with the combination RWRDI. An increase by 14.5% in the DW-RDI was also found.

Oil Quality

The most nutritional and chemical quality parameters accepted in oil evaluation were evaluated (**Tables 3** and **4**, and **Figure 5**).

Taking into account the different irrigation treatments, the FA had no clear tendency (**Table 3**). We observed that it slightly decreased in DW-RDI in 2 years, similar to the data found for the acidity during industrial extraction (**Figure 3**). The peroxides decreased in DW-RDI in both years and increased in RW treatments in 2017, with respect to the control trees. The RW-RDI did not show a clear tendency for both years. The K_{232} and K_{270} indices are also indicators of the presence of oxidation compounds in oil, other than peroxides. The mean values of the specific extinction coefficients ranged from 1.51 to 2.41 and from 0.12 to 0.18, respectively, for K_{232} and K_{270}. K_{232} had the highest values in the RDI treatments, mainly in DW-RDI, but was only significant in 2017. As for K_{270}, it increased in the DW-RDI and decreased in the RW-RDI, being statistically significant only in 2017. The delta K index showed the highest values in RW treatments in 2017. In general, it is also important to highlight, that in the second year, the values of peroxides and K_{232} were higher than in the first year in all cases.

On the other hand, significant effects among treatments on the fatty acid (FAME) composition of the major fraction of the olive oil, also known as saponifiable fraction, were observed (**Table 4**). The saturated and monounsaturated acids palmitic (C16:0)

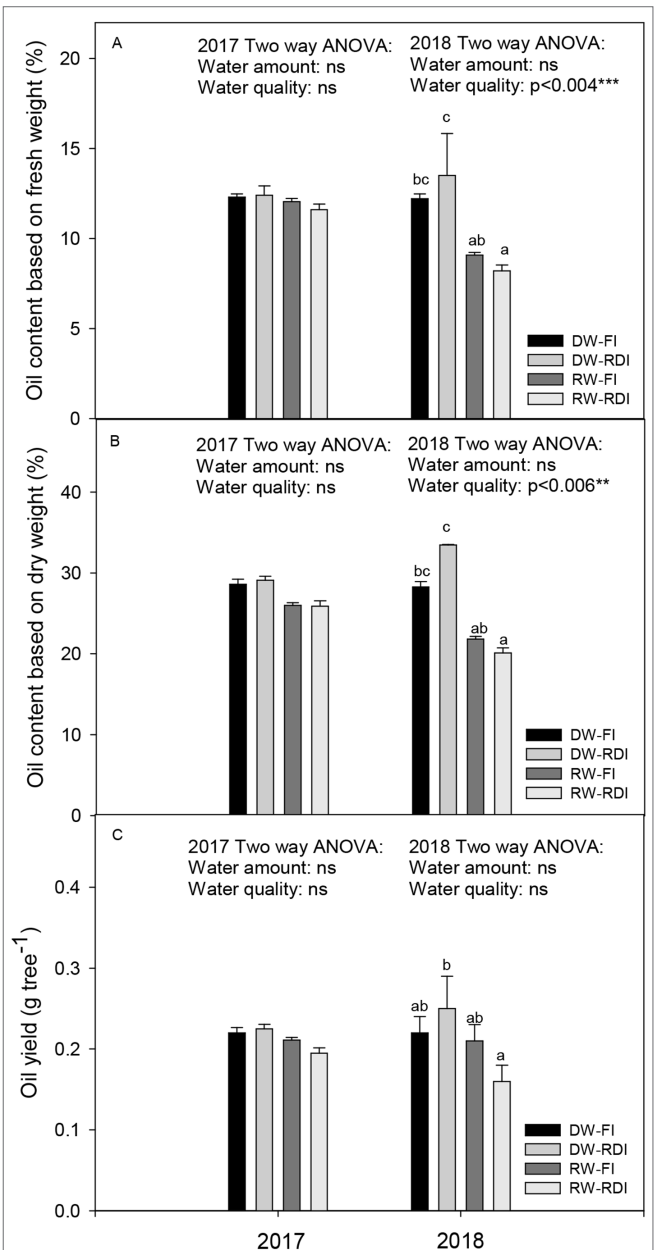

FIGURE 4 | Oil content based on **(A)** fresh fruit weight (%), **(B)** oil content based on dry fruit weight (%) and **(C)** oil yield (g tree–1) for each treatment: DW-FI (DESERT water-full irrigation), DW-RDI (DESERT water-regulated deficit irrigation), RW-FI (reclaimed water-full irrigation) and RW-RDI (reclaimed water-regulated deficit irrigation) in 2017 and 2018.

TABLE 3 | Oil quality chemical parameters: free acidity (FA), peroxides, K_{232}, K_{270} and ΔK for each treatment: DW-FI (DESERT water-full irrigation), DW-RDI (DESERT water-regulated deficit irrigation), RW-FI (reclaimed water-full irrigation) and RW-RDI (reclaimed water-regulated deficit irrigation) in 2017 and 2018.

		DW-FI	DW-RDI	RW-FI	RW-RDI	Water amount	Water quality	Amount *Quality
FA (%)	2017	0.23 ± 0.01ab	0.20 ± 0.01a	0.23 ± 0.01ab	0.25 ± 0.01b	ns	**	*
	2018	0.33 ± 0.06b	0.28 ± 0.03ab	0.25 ± 0.03ab	0.20 ± 0.00a	ns	ns	ns
Peroxides	2017	7.80 ± 0.01b	7.64 ± 0.05a	8.52 ± 0.01c	8.81 ± 0.01d	*	***	***
(meq O_2·kg^{-1})	2018	10.93 ± 0.13c	10.00 ± 0.09ab	10.33 ± 0.18bc	9.60 ± 0.17a	***	***	ns
K_{232}	2017	1.55 ± 0.00a	1.62 ± 0.00c	1.54 ± 0.00a	1.58 ± 0.00b	***	***	***
	2018	2.29 ± 0.05a	2.31 ± 0.08a	2.18 ± 0.13a	2.41 ± 0.03a	ns	ns	ns
K_{270}	2017	0.14 ± 0.00b	0.18 ± 0.00c	0.16 ± 0.00b	0.12 ± 0.00a	ns	***	***
	2018	0.17 ± 0.01a	0.18 ± 0.02a	0.16 ± 0.01a	0.15 ± 0.02a	ns	ns	ns
ΔK	2017	–0.004 ± 0.000b	–0.005 ± 0.000a	–0.004 ± 0.000c	–0.003 ± 0.000d	ns	***	***
	2018	–0.004 ± 0.001a	–0.002 ± 0.000a	–0.005 ± 0.001a	–0.004 ± 0.001a	ns	ns	ns

*Different letters within the same row indicate significant differences among treatments for the different parameters and years according to Tukey's test (*p < 0.005 ; **p < 0.01; ***p < 0.005). ns, not significant.*

TABLE 4 | Profiles of fatty acids methyl esters in the oil samples of each treatment: DW-FI (DESERT water-full irrigation), DW-RDI (DESERT water-regulated deficit irrigation), RW-FI (reclaimed water-full irrigation) and RW-RDI (reclaimed water-regulated deficit irrigation) in 2017 and 2018.

Parameter		DW-FI	DW-RDI	RW-FI	RW-RDI	Water amount	Water quality	Amount *quality
C16:0 (%)	2017	15.34 ± 0.00a	15.37 ± 0.01a	15.66 ± 0.01b	15.71 ± 0.01c	***	***	ns
	2018	15.69 ± 0.02a	15.74 ± 0.12a	15.55 ± 0.09a	15.70 ± 0.07a	ns	ns	ns
C16:1 (%)	2017	1.81 ± 0.01b	1.72 ± 0.01a	1.78 ± 0.01b	1.87 ± 0.01c	ns	***	***
	2018	1.68 ± 0.03a	1.72 ± 0.01ab	1.68 ± 0.02a	1.79 ± 0.03b	*	ns	ns
C17:0 (%)	2017	0.11 ± 0.00a	0.11 ± 0.00a	0.11 ± 0.00a	0.13 ± 0.00a	ns	ns	ns
	2018	0.12 ± 0.01a	0.11 ± 0.00a	0.12 ± 0.00a	0.11 ± 0.01a	ns	ns	ns
C17:1 (%)	2017	0.27 ± 0.00b	0.36 ± 0.00c	0.26 ± 0.00b	0.25 ± 0.00a	***	***	***
	2018	0.27 ± 0.01ab	0.35 ± 0.00c	0.24 ± 0.01a	0.28 ± 0.01b	***	***	***
C18:0 (%)	2017	2.12 ± 0.01c	2.11 ± 0.01c	2.08 ± 0.01b	2.03 ± 0.02a	*	***	ns
	2018	2.17 ± 0.02b	2.15 ± 0.04ab	2.07 ± 0.03a	2.11 ± 0.02ab	ns	*	ns
C18:1 (%)	2017	70.48 ± 0.02c	70.45 ± 0.01c	69.76 ± 0.13b	69.42 ± 0.06a	*	***	ns
	2018	70.17 ± 0.13bc	70.57 ± 0.14c	69.56 ± 0.29ab	69.03 ± 0.15a	ns	***	*
C18:2 (%)	2017	8.43 ± 0.01b	8.33 ± 0.01a	8.93 ± 0.02c	9.10 ± 0.00d	*	***	***
	2018	8.48 ± 0.05a	8.24 ± 0.03a	9.26 ± 0.21b	9.16 ± 0.16b	ns	***	ns
C18:3 (%)	2017	0.67 ± 0.01a	0.66 ± 0.01a	0.63 ± 0.01a	0.67 ± 0.01a	ns	ns	*
	2018	0.65 ± 0.01a	0.66 ± 0.01a	0.65 ± 0.01a	0.64 ± 0.01a	ns	ns	ns
C20:0 (%)	2017	0.36 ± 0.01a	0.41 ± 0.01b	0.44 ± 0.01c	0.39 ± 0.01b	ns	**	***
	2018	0.42 ± 0.01ab	0.42 ± 0.01ab	0.40 ± 0.00a	0.43 ± 0.01c	*	ns	ns
C20:1 (%)	2017	0.33 ± 0.01b	0.27 ± 0.01a	0.32 ± 0.00b	0.36 ± 0.01b	ns	***	***
	2018	0.28 ± 0.01a	0.33 ± 0.01a	0.34 ± 0.01a	0.27 ± 0.03a	ns	ns	**
C22:0 (%)	2017	0.12 ± 0.00a	0.15 ± 0.00c	0.14 ± 0.00b	0.13 ± 0.00ab	***	ns	***
	2018	0.15 ± 0.01a	0.13 ± 0.00a	0.25 ± 0.01b	0.18 ± 0.03a	**	***	ns
C24:0 (%)	2017	0.066 ± 0.001a	0.075 ± 0.000b	0.060 ± 0.001a	0.061 ± 0.003a	ns	***	*
	2018	0.072 ± 0.002a	0.063 ± 0.003a	0.060 ± 0.002a	0.061 ± 0.001a	ns	ns	ns
C18:2/C18:3	2017	12.62 ± 0.12a	12.71 ± 0.27a	14.25 ± 0.17b	13.65 ± 0.16b	ns	***	ns
ratio	2018	12.95 ± 0.26a	12.41 ± 0.12a	14.21 ± 0.58b	14.28 ± 0.16b	ns	***	ns

*Different letters within the same row indicate significant differences among treatments for the different parameters and year according to Tukey's Test (*p < 0.005 ; **p < 0.01; ***p < 0.005). ns, not significant.*

and palmitoleic (C16:1) were affected by quality and amount of water. C16:0 increased by RW (FI and RDI) only in 2017 and C16:1 by the combination of water and saline stress (RW-RDI). The saturated stearic acid (C18:0) and monounsaturated oleic acid (C18:1) significantly decreased in the RW treatments, mainly in the RW-RDI, this last one ranging between 69.03% and 70.57%. The polyunsaturated linoleic (C18:2), known as ω6, increased by RW around 9.2% and 7.1% in 2017 and 2018, respectively, being more marked again in the RW-RDI for 2017. However, linolenic acid (C18:3, ω3) was not affected by any treatment, ranging between 0.63% and 0.67%. Consistently, the C18:2/C18:3 ratio increased about 10.3% in both RW treatments (FI and RDI). As for the acids with hydrocarbon chain of 20 or more carbons, C20:0 was higher in all treatments, with respect to the DW-FI in 2017 and only in the RW-RDI in the next year. The acid C20:1 decreased by RDI (DW-RDI) in 2017. C22:0 obtained the higher values in the DW-RDI and the RW-FI. Finally, C24:0 increased in the DW-RDI and tended to decrease by effect of RW in the first year.

The main FAME of olive oil was oleic acid consisting around 70% of the FAMEs found (**Table 4**). The second most abundant FAME was palmitic, and the third one was the polyunsaturated

FAME linoleic. The order from higher to lower concentration of the different acids was as follows:

C18:1>C16:0>C18:2>C18:0>C16:1>C18:3>C20:0>C20:1>C17:1>C22:0>C17:0>C24:0

Within the unsaponifiable minority fraction of olive oil, polyphenols and pigments were evaluated (**Figure 5**). Total polyphenols content ranged between 390 and 460 ppm and between 562 and 772 ppm in the first and second year, respectively. Their levels significantly improved in all treatments, with respect to the control trees, mainly in RW-RDI. The increases were 12.9%, 4.0%, and 17.5% in 2017 and 20.9%, 29.3%, and 37.3% in 2018 for DW-RDI, RW-FI, and RW-RDI, respectively. The differences among treatments were higher in 2018 than in 2017. This response can be explained by the highest values of 2018 (**Figure 5A**).

Regardless of the treatments, the chlorophilic and carotenoids levels were lower in the second year than the first one (**Figures 5B**, **C**). The RW irrigation increased chlorophyll and decreased carotenoid contents; the combination of both stresses (RW-RDI) strongly decreased the two pigments by in the first experimental year: 47.7% less chlorophyll and 27.0% of carotenoids than the rest of treatments. In 2018, a tendency to decrease both pigments by DW-RDI was observed.

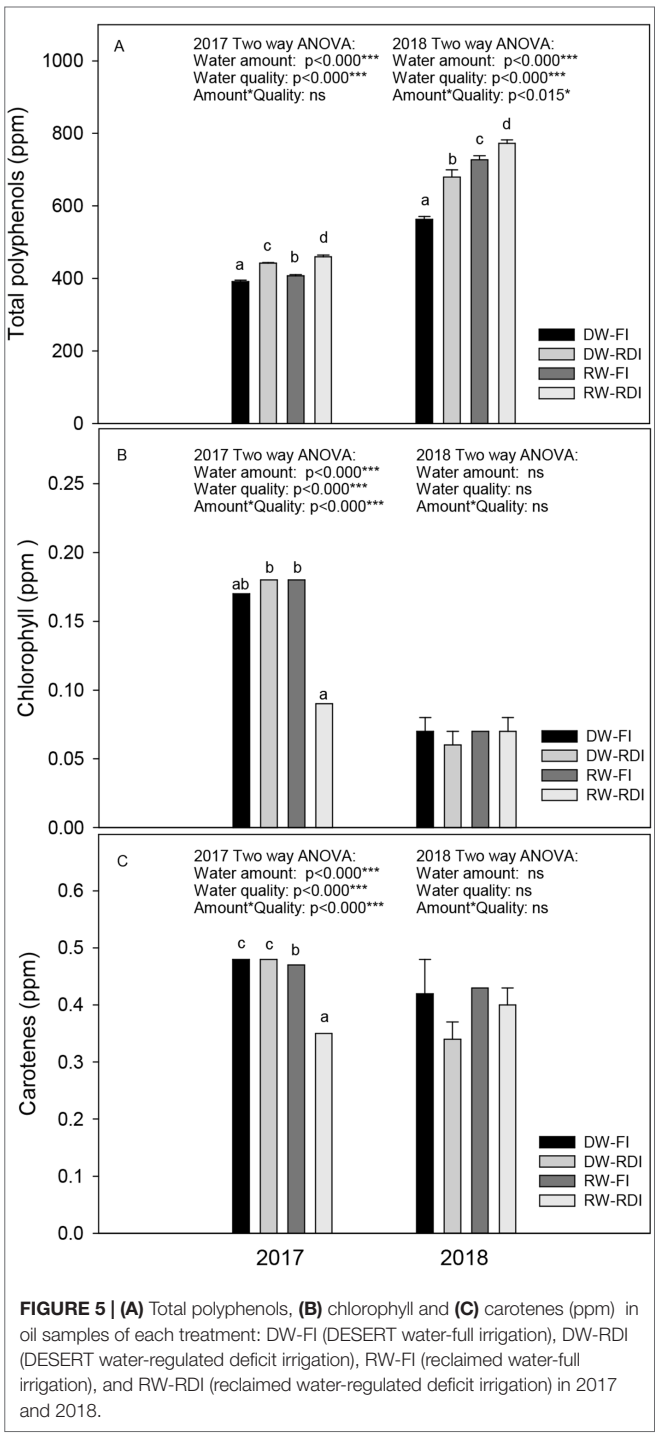

FIGURE 5 | (A) Total polyphenols, **(B)** chlorophyll and **(C)** carotenes (ppm) in oil samples of each treatment: DW-FI (DESERT water-full irrigation), DW-RDI (DESERT water-regulated deficit irrigation), RW-FI (reclaimed water-full irrigation), and RW-RDI (reclaimed water-regulated deficit irrigation) in 2017 and 2018.

DISCUSSION

Water Quality

Treated RW contain soluble minerals which depend quantitatively and qualitatively on the original source of the water and the type of treatment (Petousi et al., 2015). Our results were roughly in line with what we would expect from a properly performing secondary wastewater treatment plant. Although the EC and SAR values of RW were relatively higher than DW, they met the limits of the D.L. 185/2003. Besides, it is known that olive trees can tolerate irrigation water salinity of up to 5 $dS{\cdot}m^{-1}$ with a SAR of 18 (Tattini et al., 1992). The phytotoxic Cl^- and Na also were higher in RW, with respect to DW and the Cl^- levels exceed the limit. Moreover, RW contained quantities of nutrients as well as essential elements higher than DW source, although it also showed elevated levels of Al and Ni, according to Rosecrance et al. (2015).

Effects of the Water Quality and Amount on the Olive Production Properties

In the first year of our experiment, trees were still under juvenile phase, giving a very low fruit yield response. In the second year, Arbosana trees started to bear, confirming what was well stated in the literature (Camposeo and Vivaldi, 2018). Water quality was key in terms of fruit yield. The higher yield obtained in RW full-irrigated trees was a consequence of the increasing in fruit weight and number due to the presence of nutrient elements. Thus, RW irrigation worked as fertigation. In the RDI treatments, the fruit yield was not affected by water stress although the percent of fruit set was higher and fruit weight was lower than in the control, mainly in DW-RDI, without any significant differences (**Figure 2**). Our results are in agreement with the finding of other researchers who reported that olive irrigation with treated wastewater significantly increased the fruit yield (Bedbabis et al., 2010; Bourazanis et al., 2016; Ayoub et al., 2016). A long-term experiment of 8 years conducted in Israel with "Barnea" and "Leccino" trees irrigated with saline wastewater of lower EC than ours (EC_w~1.7 $dS{\cdot}m^{-1}$) and fresh water reported that fruit yield was not significantly different among treatments in any individual season; however, the highest values of total yield in "Barnea" olives for the entire experiment was found in the wastewater

treatment (Erel et al., 2019). . In other experiments carried out in Córdoba (Spain) under field conditions with Picual olive, two saline treatments (EC_w = 5 dS·m^{-1} and EC_w = 10 dS·m^{-1}), without using wastewater from treatment plants, did not change annual yield in any of the 9-year studies (Melgar et al., 2009). In contrast, authors Gucci and Tattini, (1997) reported that a significant yield reduction occurs in olives cultivated under high-saline conditions (EC_w >7.5 dS·m^{-1}). Ben-Gal et al. (2017) also informed that fruit yield decreased with increasing salinity in "Barnea" trees irrigated with water of different EC_w (from 2 to 11 dS·m^{-1}). Other studies, such as Ben Ahmed et al. (2007) and Chartzoulakis (2011), reported that saline waters might reduce yield compared with good quality water. Concerning fruit characteristics like fruit weight, Bourazanis et al. (2016) found that treated wastewater produced heavier fruit than those irrigated with fresh water, as in our results. However, Melgar et al. (2009) showed that salinity did not affect fruit weight.

Regarding water amount, a decrease in biomass production due to deficit irrigation for many fruit trees does not necessarily lead to a parallel reduction in fruit yield because of changes in biomass partitioning between the different organs (Gucci et al., 2019). As a result, no reductions in yield have been reported for peach (Gelly et al., 2003), plum (Intrigliolo and Castel, 2010), almond (Stewart et al., 2011), pear-jujube (Cui et al., 2009), apricot (Perez-Pastor et al., 2014) when the stress applied during the irrigation season was moderate. In olive trees, the water volume can be reduced well below the level of full satisfaction of water needs with limited or no effects on fruit yield (Moriana et al., 2003; Gucci et al., 2007; Lavee et al., 2007; Gómez del Campo, 2013), as in our results.

As for ripening indices, the detachment index and the fruit firmness are usually used to detect the optimal harvesting time for cultivars with a long maturation period, as "Arbosana" (Camposeo et al., 2013). The lowest detachment index was found in RW-FI with values about 2.1 N·g^{-1}, being this really positive for the mechanical harvesting efficiency, which is maximum (90–95%) when the detachment index is around 2 N·g^{-1} (Farinelli et al., 2012; Camposeo et al., 2013). The RDI strategies did not affect the detachment index, unlike Rosecrance et al. (2015) who reported that the RDI had a lower fruit detachment force, contributing to greater percentage fruit removal. A low fruit firmness was presented by water stress with DW (DW-RDI), contrary to another study that did not observe differences on fruit firmness by deficit irrigation (Rinaldi et al., 2011). In the case of the RW-RDI, a low fruit firmness was not observed likely due to the salinity from RW. Regarding fruit WC, it is known that moisture levels below 50% and about 60% are difficult for the mill to extract the oil (Rosecrance et al., 2015). In our study, all treatments are within that range, although the RDI had the highest values, in contrast with Rosecrance et al. (2015) who found that water stress decreased fruit WC. Finally, crop load could explained the higher PI in 2017 (1.5; very low bearing year), with respect to 2018 (bearing year) since it is known that fruit ripening strongly depends on crop load, among other factors as the climatic conditions (Camposeo et al., 2013).

Effects of the Water Quality and Amount on Oil Industrial Variables

In the process of oil extraction, the irrigation water amount was more decisive than water quality. The treatments under water stress (RDI) presented the lowest fatty yield and oil extractability, which is probably caused by the increase in humidity in the olive paste which hindered the oil extraction, as García et al. (2013) explained. Other researchers have also found that too high fruit humidity content decreases oil extraction (Gómez-del-Campo, 2013). The acidity levels, however, improved with the RDI.

Concerning oil yield, it is known that it is a function of the fruit yield as well as the percent of oil (Ben-Gal et al., 2017). In our study, the water quality was a more determining factor than the amount of water. The lowest values of oil content per dry or fresh weight were found in RW trees. Thus, although the RW-FI had the highest fruit yield, the oil yield did not improve, with respect to the control. So far, nothing has been published accordingly with our results about effects of RW-FI on the oil yield. Ayoub et al. (2016) did not find differences on oil content per dry fruit weight basis among fresh water and RW. Ben-Gal et al. (2017) cited that oil content in fruit is increased with the water EC during two years in Barnea trees irrigated with saline water. Bourazanis et al. (2016) also indicated that Koroneiki trees irrigated during two years with treated water produced more oil per tree than those irrigated with fresh water. Similar results have been also described by Segal et al. (2011), reporting a slight but non-significant increase in olive and oil yield in Barnea and Leccino. With regard both stresses combined (RW-RDI), there is nothing mentioned in the literature.

Moreover, as for water amounts, oil content dry weight-based slightly increased in the treatment with water stress (20% more in DW-RDI respect to the control), leading to the highest oil yield, despite its low oil extractability. Water stress could indirectly increase oil yield in many ways including: (1) improving the light environment for oil accumulation, (2) hastening fruit maturity at harvest, and (3) increasing fruit removal percentages from the trees (Rosecrance et al., 2015). In this work, only the first hypothesis would be possible. Trees growing under water stress (DW-RDI) had lower branches length than control trees (data not shown), and although light environments were not measured, these smaller trees likely had a greater proportion of the fruit exposed to high irradiance which likely contributed to increased oil yields. Other authors already found that to maximize olive oil yield, high irradiance is needed (Gómez-del-Campo et al., 2009; Cherbiy-Hoffmann et al., 2013).

There is dispersion in the literature about the effects of water stress on oil yield. Similar results to ours were found by a number of authors who reported curvilinear relationships between oil yields and water application, indicating that oil yields are maximized at water application rates below 100% of FI (Moriana et al., 2003). This is, the oil percentages can be increased with moderate water stress (Gucci et al., 2009; Caruso et al., 2013; Gómez-del-Campo, 2013; Rosecrance et al., 2015). Other authors cited the water volume can be reduced well below the level of full satisfaction of water needs with limited or no effects on fruit yield and oil yield (Gucci et al., 2007; Gispert et al., 2013; Gómez-del-Campo, 2013; Hernández et al., 2018).

Contrary to our results, in Fernández et al. (2013), a small reduction in oil yield by 26% was observed when the water applications were reduced by 72% in an olive orchard of "Arbequina."

Effects of the Water Quality and Amount on Oil Quality Parameters

In many parameters, differences between the two experimental years of the study were found as a consequence of the different duration of the RDI period as well as of environmental factors and fruit load, which are known to affect oil quality (Ayoub et al., 2016).

FA, Peroxides, K_{232}, K_{270}, Delta K Index

As for oil quality legal attributes, water quality (RW-FI and RW-RDI) did not affected the FA, according to Bedbabis and Ferrara (2018) who showed that acidity values were not significantly increased by saline water, as also reported by Bourazanis et al. (2016) using wastewater. However, the RW source accelerated the oxidation of the oil causing elevations in the peroxides and ΔK in 2017. Other works affirmed that these parameters were not affected by RW (Bourazanis et al., 2016).

The reduction of water amount combined with DW (DW-RDI), slightly decreased FA and peroxides, improving oil quality; however, it increased the K_{232} and K_{270} characteristics compared with the control, although only in the first year. A high value of these coefficients results in a lower resistance to oxidation of the oil and with a greater degree of oxidation. Changes in oil quality due to water deficit have been reported for many olive cultivars (Servili et al., 2007; Gómez-del-Campo and García, 2013; Caruso et al., 2014, Caruso et al., 2017; Hernández et al., 2018). Although most of these studies have shown that the irrigation regime had negligible or no effects on parameters as FA, peroxide values, spectrophotometric indices (K_{232}, K_{270} and ΔK) (Gucci et al., 2019).

In general, the values of FA, peroxides, and K_{232} and K_{270} for all oil samples examined here were lower than the maximum limits established by the cited EU legislation for the extra virgin olive oil (EVOO) category (FA ≤ 0.8; Peroxides Index ≤ 20; $K_{232} \leq 2.5$; $K_{270} \leq 0.22$; $\Delta K \leq 0.01$).

Fatty Acid Profile

When we evaluated the FAME profile, oleic acid was the dominant acid in the olive oil obtained in all irrigation treatments (ranging from 69% to 71%), followed by palmitic (15.34–15.74%), linoleic (8.24–9.26%), and stearic acid (2.03–2.17%), with their concentration falling within the range of the values for characterizing it as EVOO.

The FAME composition was more affected by water quality than by water amount. Previous studies reported increases in palmitoleic (Ben Brahim et al., 2016) and linoleic (Bedbabis and Ferrara et al., 2018) acids in treatment irrigated with saline water, as in our results. The important increase (7–9%) of the linoleic acid was probably due to the fatty synthase enzymes stimulation as fruit maturity progressed in RW treatments. Since linolenic acid were not affected by RW, according to Bourazanis et al. (2016), the ω6/ω3 ratio of oil from RW treatments increased around 10%, as also Tietel et al. (2019) indicated. Furthermore, other important acids as oleic and stearic reduced their percentages when the olive trees were irrigated with RW.

Moreover, in our experiment the reduction of the water amount (DW-RDI) only affected a few minority fatty acids as C20:1, C22:0, and C24:0 and decreased the linoleic acid respect to the DW-FI, although only in 2017. Accordingly, Hernández et al. (2018) found a decrease in linoleic acid under severe RDI conditions. Moreover, several studies for many cultivars have shown that the water deficit had negligible or no effects on FAME composition (Gómez-del-Campo and García, 2013; Caruso et al., 2014, Caruso et al., 2017).

As for the effects of the combination of both stresses (RW-RDI) on fatty acid, we observed that the reduction of oleic acid and the increase of linoleic were more pronounced than in RW-FI. It is not possible to discuss these results with other work because, so far, nothing has been published about the combination of RW and RDI strategies.

The effects reported here regarding FAME profile did not show very great differences among treatment from an agronomical point of view. However, they have a large nutritional significance, since they reflect a trend of declining nutritional and health quality of olive oil as a result of irrigation with RW. Many of the health-promoting traits of olive oil are ascribed to its monounsaturated fatty acid content, mainly the oleic acid. This has been clinically proven to enhance cardiovascular health and improve blood-lipid profile, in addition to other metabolic-syndrome-related advantages (Tietel et al., 2019). In addition, the low levels of saturated fatty acids and the ω6/ω3 ratio play a key role in the bioactivity of olive oil as a functional food (Tietel et al., 2019). Specifically, higher ω6/ω3 ratios, as occurred in this experiment with the use of RW, increase the risk for obesity (Simopoulos, 2016).

Parameters of the Minority Unsaponificable Fraction

Both water quality and amount affected the polyphenol levels, which play a role in the stress response and defense mechanism of the tree. In our experiment, saline RW (RW-FI) increased oil polyphenols , probably due to stress response to high salt levels, as reported by Chartzoulakis (2011). Salinity stress causes subsequent water deficit, which has been shown to be involved in the activation of phenylalanine ammonia lyase (PAL) (Ben Ahmed et al., 2009), a key enzyme directly involved in polyphenol biosynthesis in fruit, which causes an accumulation of phenolic compounds in the oil (Patumi et al., 2002).

Regarding RDI strategy (DW-RDI), it also improved the polyphenols content in oil, consistent with many studies (Gómez-del-Campo and García, 2013; Rosecrance et al., 2015; Caruso et al., 2017) due to water deficit enhanced synthesis of these compounds in the fruit, according to Alagna et al. (2012). Severe conditions trigger antioxidation mechanisms activated by the plant in response to oxidative stress, and hence accumulate in oil (Tietel et al., 2019). Others findings

suggest that the catabolism of phenolic substances in the fruit is likely influenced by water stress too (Cirilli et al., 2017). Moreover, RW-RDI was the treatment that showed the greatest increases in polyphenols both years. As far as we know, it is the first time that data are reported respect to the combination of water and saline stresses and nothing has been published in the literature.

From the point of view of food quality, the irrigation effects on the polyphenols levels are relevant for oil sensory quality and for the health-promoting effects of the oil (Clodoveo et al., 2015; Tietel et al., 2019) as the prevention of the formation of cancer cells, so that European Food Safety Authority (EFSA) launched a specific health claim (EU, 2012). In addition, polyphenols are also key contributors to oxidative stability, mainly 3,4-DHPEA and its secoiridoid derivatives (Servili et al., 2004). Thus, irrigation with RW and RDI and mainly the combination of both might also greatly positively affect oil shelf life and nutraceutical claim.

Finally, the climatic pattern during ripening period could explain the strong increase of 25% of total oil polyphenols contents in 2018 with respect to 2017. Indeed the second year was colder than the former. In the literature, it has been stated that low temperature stimulates polyphenol accumulation in olive oil (Artajo et al., 2006).

Color is a basic attribute for determining the characteristics of olive oil although analysis of the pigmentation is not required in the corresponding EU Regulation. The trees full irrigated with RW increased chlorophyll levels in 2017, being a positive aspect since most consumers associate the presence of chlorophyll with quality. Nevertheless, our results are contradictory with other studies (Ghrab et al., 2014; Bedbabis et al., 2015). As for carotenoids, their levels decreased in RW-FI, as Ghrab et al. (2014) also cited.

In summary, the trees full irrigated with RW improved the fruit yield although it did not increase the oil yield since the oil content dry weight-based was lower than control trees. The changes in oil fatty acid composition of these trees demonstrated tendencies that are undesirable, including increased unsaturated acids, as well as the ratio ω6/ω3. The peroxides also increased. On the contrary, higher levels of the polyphenols in oil were presented. The deficit irrigation, with DW, did not affect the fruit yield, although there was an increase in the number of fruits which showed less weight and firmness during the RDI period. Despite the reduction of the fatty yield and oil extractability due to the high fruit WC, this treatment presented the highest oil yield since oil content fruit dry weight-based improved by 20%. Furthermore, there was a reduction in the acidity and peroxides and an increase in the polyphenols of the oil by water stress. Some negative aspect were also found: an increase in K_{232} and K_{270}, although within the legal limit, and in some minority acid as C20:0, C22:0, and C24:0. Finally, the combination of RW and RDI neither reduced fruit yield. Besides, its fruits did not lose as much weight or firmness as in DW-RDI. However, although the fatty yield and oil extractability decreased less than in DW-RDI, the oil yield values of these trees under both stresses were the lowest compared with the rest of treatments since the low oil content fruit dry weight-based. As for the oil quality of RW-RDI, similar results as in RW-FI were observed, plus an important decrease of pigments in the first year. It is important to highlight also that the highest levels of polyphenols were displayed in this treatment. These aspects described about the combination of both stresses in this paper are reported in the literature for the first time. These findings could help optimize crop management of cv Arbosana in new olive cropping system, where environmental sustainability represent a key factor.

DATA AVAILABILITY STATEMENT

All datasets generated for this study are included in the manuscript/supplementary files.

AUTHOR CONTRIBUTIONS

Data curation: GV, CR-T, AP. Formal analysis: GV, AP, CR-T. Investigation: GV, CR-T, EN. Methodology: GV, FS. Project administration: SC, GV. Resources: SC, GV. Supervision: SC, GV, EN. Writing – original draft: CR-T. Writing – review and editing: SC, GV, EN.

FUNDING

The research involved in this work has been supported by the EU and Water JPI for funding, in the frame of the collaborative international Consortium DESERT, financed under the ERA-NET WaterWorks 2014 Cofunded Call. This ERA-NET is an integral part of the 2015 Joint Activities developed by the Water Challenges for a Changing World Joint Programme Initiative (Water JPI), and "Fondo di Sviluppo e Coesione" 2007-2013 e APQ Ricerca Regione Puglia "Programma regionale a sostegno della specializzazione intelligente e della sostenibilita sociale ed ambientale e FutureInResearch."

ACKNOWLEDGMENTS

CR-T acknowledges the financial support for Postdoctoral training and development fellowship (20363/PD/17) of Consejería de Empleo, Universidades y Empresa (CARM) by the Fundación Séneca-Agencia de Ciencia y Tecnología de la Región de Murcia.

REFERENCES

Alagna, F., Mariotti, R., Panara, F., Caporali, S., Urbani, S., Veneziani, G., et al. (2012). Olive phenolic compounds: metabolic and transcriptional profiling during fruit development. *BMC Plant Biol.* 12, 162. doi: 10.1186/1471-2229-12-162

Allen, R. G., Pereira, J. S., Raes, D., and Smith, M. (1998). "Food and Agriculture Organization of the United Nations," in *Crop Evapotranspiration: Guidelines for Computing Crop Water Requirements* (Rome).

Aragüés, R., Puy, J., Royo, A., and Espada, J. L. (2005). Three-year field response of young olive trees (*Olea europaea* L., cv. Arbequina) to soil salinity: trunk growth and leaf ion accumulation. *Plant Soil* 271, 265–271. doi: 10.1007/s11104-004-2695-9

Arborea, S., Giannoccaro, G., De Gennaro, B., Iacobellis, V., and Piccinni A. F. (2017). Cost–benefit analysis of wastewater reuse in Puglia, Southern Italy. *Water* 9, 175.

Artajo, L. S., Romero, M. P., Tovar, M. J., and Motilva, M. J. (2006). Effect of irrigation applied to olive trees (*Olea europaea* L.) on phenolic compound transfer during olive oil extraction. *Eur. J. Lipid Sci. Technol.* 108, 19–27. doi: 10.1002/ejlt.200500227

Ayers, R. S., and Westcot, D. W. (1985). *Water quality for agriculture*. (Rome: FAO Irrigation and Drainage), 174.

Ayoub, S., Al-Ahdiefat, S., Rawashdeh, H., and Bahabsheh, I. (2016). Utilization of reclaimed wastewater for olive irrigation: effect on soil properties, tree growth, yield and oil content. *Agric. Water Manag.* 176, 163–169. doi: 10.1016/j.agwat.2016.05.035

Batarseh, M. I., Rawajfeh, B. A., Kalavrouziotis, I., and Prodromos, H. (2011). Treated Municipal Wastewater Irrigation Impact on Olive Trees (*Olea Europaea* L.) at Al-Tafilah, Jordan. *Water Air Soil Pollut.* 217, 185–196. doi: 10.1007/s11270-010-0578-7

Bedbabis, S., Clodoveo, M. L., Rouina, B. B., and Boukhris, M. (2010). Influence of irrigation with moderate saline water on 'chemlali' extra virgin olive oil composition and quality. *J Food Qual.* 33, 228–247. doi: 10.1111/j.1745-4557.2010.00310.x

Bedbabis, S., Ben Rouina, B., Boukhris, M., and Ferrara, G. (2014). Effects of irrigation with treated wastewater on root and fruit mineral elements of Chemlali Olive cultivar. *Scien. World J.* 2014, Article ID 973638, 8. doi: 10.1155/2014/973638

Bedbabis, S., Trigui, D., Ben Ahmed, C., Clodoveo, M. L., Camposeo, S., Vivaldi, G. A., et al. (2015). Long-terms effects of irrigation with treated municipal wastewater on soil, yield and olive oil quality. *Agric. Water Manag.* 160, 14–21. doi: 10.1016/j.agwat.2015.06.023

Bedbabis, S., and Ferrara, G. (2018). Effects of long term irrigation with treated wastewater on leaf mineral element contents and oil quality in olive cv. Chemlali. *J. Hort. Sci. Biotech.* 93 (2), 216–223. doi: 10.1080/14620316.2017.1354729

Ben Ahmed, C., Ben Rouina, B., and Boukhriss, M. (2007). Effects of water deficit on olive trees cv. Chemlali under field conditions in arid region in Tunisia. *Sci. Hort.* 133 (3), 267–277. doi: 10.1016/j.scienta.2007.03.020

Ben Ahmed, C., Ben Rouina, B., Sensoy, S., and Boukhriss, M. (2009). Saline water irrigation effects on fruit development, quality, and phenolic composition of virgin olive oils, cv. Chemlali. *J. Agric. Food Chem.* 57, 2803–2811. doi: 10.1021/jf8034379

Ben Brahim, S., Gargouri, B., Marrakchi, F., and Bouaziz, M. (2016). The effects of different irrigation treatments on olive oil quality and composition: a comparative study between treated and olive mill wastewater. *J. Agric. Food Chem.* 64, 1223–1230. doi: 10.1021/acs.jafc.5b05030

Ben-Gal, A., Beiersdorf, I., Yermiyahu, U., Soda, N., Presnov, E., Zipori, I., et al. (2017). Response of young bearing olive trees to irrigation-induced salinity. *Irrig. Sci.* 35, 99–109. doi: 10.1007/s00271-016-0525-5

Ben Rouina, B., Ben Ahmed, Ch., Bedbabis, S., Baccari, M., and Boukhris, M. (2011). "Chapter in Book Environment and Ecology in the Mediterranean Region," in *Effects of long-term irrigation with treated wastewater on soil chemical properties, plant nutrient status, growth and oil quality of olive tree* (UK: Cambridge Scholars Publishing), 147–156. Chapter Thirteen.

Bourazanis, G., Roussos, P. A., Argyrokastritis, I., Kosmas, C., and Kerkides, P. (2016). Evaluation of the use of treated municipal waste water on the yield, oil quality, free fatty acids' profile and nutrient levels in olive trees cv Koroneiki, in Greece. *Agric. Water Manag.* 163, 1–8. doi: 10.1016/j.agwat.2015.08.023

Camposeo, S., and Vivaldi, G. A. (2018). Yield, harvesting efficiency and oil chemical quality of cultivars 'Arbequina' and 'Arbosana' harvested by straddle machine in two Apulian growing areas. *Proceed. Paper Acta Hortic. of VIII Int. Olive Symp*. 1199, 397–402. doi: 10.17660/ActaHortic.2018.1199.63

Camposeo, S., Vivaldi, G. V., and Gattull, C. E. (2013). Ripening indices and harvesting times of different olive cultivars for continuous harvest. *Sci. Hortic.* 151, 1–10. doi: 10.1016/j.scienta.2012.12.019

Caruso, G., Rapoport, H. F., and Gucci, R. (2013). Long-term evaluation of yield components of young olive trees during the onset of fruit production under different irrigation regimes. *Irrig. Sci.* 31, 37–47. doi: 10.1007/s00271-011-0286-0

Caruso, G., Gucci, R., Urbani, S., Esposto, S., Taticchi, A., Di Maio, I., et al. (2014). Effect of different irrigation volumes during fruit development on quality of virgin olive oil of cv Frantoio. *Agric. Water. Manag.* 134, 94–103. doi: 10.1016/j.agwat.2013.12.003

Caruso, G., Gucci, R., Sifola, M. I., Selvaggini, R., Urbani, S., Esposto, S., et al. (2017). Irrigation and fruit canopy position modify oil quality of olive trees (cv Frantoio). *J. Sci. Food Agric.* 97, 3530–3539. doi: 10.1002/jsfa.8207

Caponio, F., Squeo, G., Monteleone, J. I., Paradiso, V. M., Pasqualone, A., and Summo, C. (2015). First and second centrifugation of olive paste: influence of talc addition on yield, chemical composition and volatile compounds of the oils, LWT. *Food Sci.Technol.* 64, 439–445. doi: 10.1016/j.lwt.2015.05.007

Chartzoulakis, K. (2005). Salinity and olive: growth, salt tolerance, photosynthesis and yield. *Agric. Water Manag.* 78, 108–121. doi: 10.1016/j.agwat.2005.04.025

Chartzoulakis, K. (2011). The use of saline water for irrigation of olives: effects on growth, physiology, yield and oil quality. *Acta Hortic.* 888, 97–108. doi: 10.17660/ActaHortic.2011.888.10

Cherbiy-Hoffmann, S. U., Hall, A. J., and Rousseaux, M. C. (2013). Fruit, yield, and vegetative growth responses to photosynthetically active radiation during oil synthesis in olive trees. *Sci. Hortic.* 150, 110–116. doi: 10.1016/j.scienta.2012.10.027

Cirilli, M., Caruso, G., Gennai, C., Urbani, S., Frioni, E., Ruzzi, M., et al. (2017). The role of polyphenoloxidase peroxidase and β-Glucosidase in phenolics accumulation in *Olea europaea* L. fruits under different water regimes. *Front. Plant Sci.* 8, 717. doi: 10.3389/fpls.2017.00717

Clodoveo, M. L., Camposeo, S., Amirante, R., Dugo, G., Cicero, N., and Boskou, D. (2015). "Olives and Olive Oil Bioactive Constituents," in *Research and innovative approaches to obtain virgin olive oils with a higher level of bioactive constituents*. Ed. D. Boskou (Urbana, IL – USA: AOCS Press), 179–216. ISBN: 978-1-630670-41-2. 7 cit. doi: 10.1016/B978-1-63067-041-2.50013-6

Cui, N., Du, T., Li, F., Tong, L., Kang, S., Wang, M., et al. (2009). Response of vegetative growth and fruit development to regulated deficit irrigation at different growth stages of pear-jujube tree. *Agric. Water Manag.* 96, 1237–1246. doi: 10.1016/j.agwat.2009.03.015

D.L. 185/2003. Decreto Ministeriale 12 giugno, and 2003, n. 185. Regolamento recante norme tecniche per il riutilizzo delle acque reflue in attuazione dell'articolo 26, comma 2, del D.Lgs. 11 maggio 1999, n. 152.

EC. (2018). Regulation of the European parliament and of the council on minimum requirements for water reuse. European Community (EC). Brussels, 28.5.2018 COM 337.

EEC. (2011). European Commission Regulation No 61/2011 of 24 January 2011 amending Regulation (EEC) No 2568/91 on the characteristics of olive oil and olive-residue oil and on the relevant methods of analysis. Official Journal of the European Union. L 23/1, 27.1.

Erel, R., Eppel, A., Yermiyahu, U., Ben-Gal, A., Levy, G., Zipori, I., et al. (2019). Long-term irrigation with reclaimed wastewater: Implications on nutrient management, soil chemistry and olive (*Olea europaea* L.) performance. *Agric. Water Manag.* 213 (1), 324–335. doi: 10.1016/j.agwat.2018.10.033

EU (2012). Commision regulation (EU) No 432/2012 of 16 May 2012 establishing a list of permitted health claims made on foods, other than those referring to the reduction of disease risk and to children's development and health. European Commision.

FAO. (2018). "Coping with Water Scarcity in Agriculture: a Global Framework for Action in a Changing Climate," in *Water Scarcity – One of the greatest challenges of our time*(Rome, Italy), 4. ISBN: No ISBN. Job Number: I5604E; available online: http://www.fao.org/fao-stories/article/en/c/1185405/?utm_source=facebook&utm_medium=social+media&utm_campaign=fao.

Farinelli, D., Ruffolo, M., Boco, M., and Tombesi, A. (2012). Yield efficiency and mechanical harvesting with trunk shaker of some International olive cultivars. *Acta Hortic.* 949, 379–384. doi: 10.17660/ActaHortic.2012.949.55

Fernández, J., Perez-Martin, A., Torres-Ruiz, J., Cuevas, M., Rodriguez-Dominguez, C., Elsayed-Farag, S., et al. (2013). A regulated deficit irrigation strategy for hedgerow olive orchards with high plant density. *Plant Soil* 372, 295–297. doi: 10.1007/s11104-013-1704-2

Folin, O., and Ciocalteau, V. (1927). On tyrosine and tryptophan determination in protein. *J. Biol. Chem.* 73, 627–650.

García, J. M., Cuevas, M. V., and Fernández, J. E. (2013). Production and oil quality in 'Arbequina' olive (*Olea eurpoaea* L.) trees under two deficit irrigation strategies. *Irrig. Sci.* 31 (3), 359–370. doi: 10.1007/s00271-011-0315-z

Gelly, M., Recasens, I., Girona, J., Mata, M., Arbones, A., Rufat, J., et al. (2003). Effects of water deficit during stage II of peach fruit development and post harvest on fruit quality and ethylene production. *J. Hortic. Sci. Biotechnol.* 78, 324–330. doi: 10.1080/14620316.2003.11511626

Ghrab, M., Ayadi, M., Gargouri, K., Chartzoulakis, K., Gharsallaoui, M., Bentaher, H., et al. (2014). Long-term effects of partial root-zone drying (PRD) on yield, oil composition and quality of olive tree (cv. Chemlali) irrigated with saline water in arid land. *J. Food Compos. Anal.* 36, 90–97. doi: 10.1016/j.jfca.2014.05.005

Gispert, J. R., Ramírez de Cartagena, F., Villar, J. M., and Girona, J. (2013). Wet soil volume and strategy effects on drip-irrigated olive trees (cv. 'Arbequina'). *Irrig. Sci.* 31, 479–489. doi: 10.1007/s00271-012-0325-5

Global Water Market. (2017). Meeting the world's water and wastewater needs until 2020. *Global Water Intell.* 15.

Godini, A., Vivaldi, G. A., and Camposeo, S. (2011). Olive cultivars field-tested in super high-density system in southern Italy. *Calif. Agric.* 65 (1), 39–40. doi: 10.3733/ca.v065n01p39

Gómez-del-Campo, M., Centeno, A., and Connor, D. J. (2009). Yield determination in olive hedgerow orchards. I. Yield and profiles of yield components in north–south and east–west oriented hedgerows. *Crop Pasture Sci.* 60, 434–442. doi: 10.1071/CP08252

Gómez-del-Campo, M. (2013). Summer deficit-irrigation strategies in a hedgerow olive orchard cv 'Arbequina': effect on fruit characteristics and yield. *Irrig. Sci.* 31, 259–269. doi: 10.1007/s00271-011-0299-8

Gómez-del-Campo, M., and García, J. M. (2013). Summer deficit-irrigation strategies in a Hedgerow Olive cv. Arbequina orchard: effect on oil quality. *J. Agric. Food Chem.* 61 (37), 8899–8905. doi: 10.1021/jf402107t

Gucci, R., and Tattini, M. (1997). Salinity tolerance in olive. *Hortic. Rev.* 21, 177–214. doi: 10.1002/9780470650660.ch6

Gucci, R., Lodolini, E. M., and Rapoport, H. F. (2007). Productivity of olive trees with different water status and crop load. *J. Hortic. Sci. Biotechnol.* 82, 648–656. doi: 10.1080/14620316.2007.11512286

Gucci, R., Lodolini, E. M., and Rapoport, H. F. (2009). Water deficit-induced changes in mesocarp cellular processes and the relationship between mesocarp and endocarp during olive fruit development. *Tree Physiol.* 29, 1575–1585. doi: 10.1093/treephys/tpp086

Gucci, R., Caruso, G., Gennai, C., Esposto, S., Urbani, S., and Servili, M. (2019). Fruit growth, yield and oil quality changes induced by deficit irrigation at different stages of olive fruit development. *Agric. Water Manag.* 212, 88–98. 212. doi: 10.1016/j.agwat.2018.08.022

Hernández, M. L., Velázquez-Palermo, D., Sicardo, M. D., Fernández, J. E., Díaz-Espejo, A., and Marínez-Rivas, J. M. (2018). Effect of a regulated deficit irrigation strategy in a hedgerow 'Arbequina' olive orchard on the mesocarp fatty acid composition and desaturase gene expression with respect to olive oil quality. *Agric. Water Manag.* 204, 100–106. doi: 10.1016/j.agwat.2018.04.002

Hernandez-Santana, V., Fernandes, R. D. M., Perez-Arcoiza, A., Fernández, J. E., Garcia, J. M., and Diaz-Espejo, A. (2018). Relationships between fruit growth and oil accumulation with simulated seasonal dynamics of leaf gas exchange in the olive tree. *Agric. For. Meteorol.* 256–257, 458–469. doi: 10.1016/j.agrformet.2018.03.019

Intrigliolo, D. S., and Castel, J. R. (2010). Response of plum trees to deficit irrigation under two crop levels: tree growth yield and fruit quality. *Irrig. Sci.* 28, 525–534. doi: 10.1007/s00271-010-0212-x

ISTAT. (2017). Istituto Nazionale di Statistica (http://agri.istat.it).

ISMEA. (2018). Istituto di Servizi per il Mercato Agricolo Alimentare. (http://ismea.it).

Kchaou, H., Larbi, A., Gargouri, K., Chaieb, M., Morales, F., and Msallem, M. (2010). Assessment of tolerance to NaCl salinity of five olive cultivars based on growth characteristics and Na^+ and Cl^- exclusion mechanisms. *Sci. Hort.* 124 (3), 306–315. doi: 10.1016/j.scienta.2010.01.007

Lavee, S., Hanoch, E., Wodner, M., and Abramowitch, H. (2007). The effect of predetermined deficit irrigation on the performance of the cv. Muhasan olive (*Olea europaea* L.) in the eastern coastal plain of Israel. *Sci. Hortic.* 112, 156–163. doi: 10.1016/j.scienta.2006.12.017

Melgar, J., Mohamed, Y., Serrano, N., García-Galavís, P., Navarro, C., Parra, M., et al. (2009). Long term responses of olive trees to salinity. *Agric. Water Manag.* 96, 1105–1113. doi: 10.1016/j.agwat.2009.02.009

Minguez, M. I., Rejano, L., Gandul, B., Higinio, A., and Garrido, J. (1991). Color pigment correlation in virgin olive oil. *J. Am. Oil Chem. Soc.* 68, 332–336. doi: 10.1007/BF02657688

Moriana, A., Orgaz, F., Pastor, M., and Fereres, E. (2003). Yield responses of a mature olive orchard to water deficits. *J. Am. Soc. Hortic. Sci.* 128 (3), 425–431. doi: 10.21273/JASHS.128.3.0425

Olint (2018). Plantaciones de olivar y almendro. Olint Megazine. *Span. Ed. Tech. J.* 33.

Patumi, M., D'Andria, R., Marsilio, V., Fontanazza, G., Morelli, G. and Lanza, B. (2002). Olive and olive oil quality after intensive monocone olive growing (Oleaeuropaea L., cv. Kalamata) in different irrigation regimes. *Food Chem.* 77, 27–34.

Petousi, I., Fountoulakis, M., Saru, M., Nikolaidis, N., Fletcher, L., Stentiford, E., et al. (2015). Effects of reclaimed wastewater irrigation on olive (*Olea europaea* L. cv 'Koroneiki') trees. *Agric. Water Manag.* 160, 33–40. doi: 10.1016/j.agwat.2015.06.003

Perez-Pastor, A., Ruiz-Sanchez, M. C., and Domingo, R. (2014). Effects of timing and intensity of deficit irrigation on vegetative and fruit growth of apricot trees. *Agric. Water Manag.* 134, 110–118. doi: 10.1016/j.agwat.2013.12.007

Rallo, G., and Provenzano, G. (2013). Modelling eco-physiological response of table olive trees (*Olea europaea* L.) to soil water deficit conditions. *Agric. Water Manage.* 120, 79–88. doi: 10.1016/j.agwat.2012.10.005

Riemenschneider, C., Al-Raggad, M., Moeder, M., Seiwert, B., Salameh, E., and Reemtsma, T. (2016). Pharmaceuticals, their metabolites, and other polar pollutants in field-grown vegetables irrigated with treated municipal wastewater. *J. Agric. Food Chem.* 64 (29), 5784–5792. doi: 10.1021/acs.jafc.6b01696

Rinaldi, R., Amodio, M. L., Colelli, G., Nanos, G. D., and Pliakoni, E. (2011). Effect of deficit irrigation on fruit and oil quality of 'Konservolea' Olives. *Acta Hortic.* 924, 445–451. doi: 10.17660/ActaHortic.2011.924.57

Romero-Trigueros, C., Nortes Tortosa, P. A., Alarcon Cabañero, J. J., and Nicolas Nicolás, E. (2014). Determination of 15N stable isotope natural abundances for assessing the use of saline reclaimed water in grapefruit. *Environ. Eng. Manag. J.* 13, 2525–2530. doi: 10.30638/eemj.2014.282

Romero-Trigueros, C., Parra, M., Bayona Gambín, J. M., Nortes Tortosa, P., Alarcon Cabañero, J. J., and Nicolás Nicolás, E. (2017). Effect of deficit irrigation and reclaimed water on yield and quality of grapefruits at harvest and postharvest. *LWT – Food Sci. Technol.* 85, 405–411. doi: 10.1016/j.lwt.2017.05.001

Romero-Trigueros, C., Bayona Gambín, J. M., Nortes Tortosa, P., Alarcón Cabañero, J. J., and Nicolás Nicolás, E. (2019). Determination of crop water stress index byi thermometry in grapefruit trees irrigated with saline reclaimed water combined with deficit irrigation. *Remote Sens.* 11 (7), 757. doi: 10.3390/rs11070757

Rosecrance, R. C., Krueger, W. H., Milliron, L., Bloese, J., Garcia, C., and Mori, B. (2015). Moderate regulated deficit irrigation can increase olive oil yields and decrease tree growth in super high density 'Arbequina' olive orchards. *Sci. Hortic.* 190, 75–82. doi: 10.1016/j.scienta.2015.03.045

Saadati, S., Moallemi, N., Mortazavi, S. M. H., and Seyyednejad, S. M. (2013). Effects of zinc and boron foliar application on soluble carbohydrate and oil contents of three olive cultivars during fruit ripening. *Sci. Hortic.* 164, 30–34. doi: 10.1016/j.scienta.2013.08.033

Scholander, P. F., Hammel, H. T., Bradstreet, E. D., and Hemmingsen, E. A. (1965). Sap pressure in vascular plants: negative hydrostatic pressure can be measured in plants. *Sci.* 148, 339–346. doi: 10.1126/science.148.3668.339

Segal, E., Dag, A., Ben-Gal, A., Zipori, I., Erel, R., Suryano, S., et al. (2011). Olive orchard irrigation with reclaimed wastewater: agronomic and environmental

considerations. *Agric. Ecosyst. Environ.* 140, 454–461. doi: 10.1016/j.agee.2011.01.009

Servili, M., Selvaggini, R., Esposto, S., Taticchi, A., Montedoro, G., and Morozzi, G. (2004). Health and sensory properties of virgin olive oil hydrophilic phenols: agronomic and technological aspects of production that affect their occurrence in the oil. *J. Chromatogr. A.* 1054, 113–127. doi: 10.1016/S0021-9673(04)01423-2

Servili, M., Esposto, S., Lodolini, E. M., Selvaggini, R., Taticchi, A., Urbani, S., et al. (2007). Irrigation effects on quality phenolic composition and selected volatiles of virgin olive oil cv Leccino. *J. Agric. Food Chem.* 55, 6609–6618. doi: 10.1021/jf070599n

Shackel, K. A., Ahmadi, H., Biasi, W., Buchner, R., Goldhamer, D., and Gurusinghe, S. (1997). Plant water status as an index of irrigation need in deciduous fruit trees. *Horttechnology* 7, 23–29. doi: 10.21273/HORTTECH.7.1.23

Simopoulos, A. P. (2016). An increase in the omega-6/omega-3 fatty acid ratio increases the risk for obesity. *Nutrients* 8, 128. doi: 10.3390/nu8030128

Stewart, W. L., Fulton, A. E., Krueger, W. H., Lampinen, B. D., and Shackel, K. A. (2011). Regulated deficit irrigation reduces water use of almonds without affecting yield. *Calif. Agric.* 65, 90–95. doi: 10.3733/ca.v065n02p90

Tietel, Z., Dag, A., Yermiyahu, U., Zipori, I., Beiersdorf, I., Krispina, S., et al. (2019). Irrigation-induced salinity affects olive oil quality and health-promoting properties. *J. Sci. Food Agric.* 99, 1180–1189. doi: 10.1002/jsfa.9287

Tattini, M., Bertoni, P., and Caselli, S. (1992). Genotypic responses of olive plants to sodium chloride. *J. Plant Nutr.* 15, 1467–1485. doi: 10.1080/01904169209364412

Vivaldi, G. A., Stripolli, G., Pascuzzi, S., Stellacci, A. M., and Camposeo, S. (2015). Olive genotypes cultivated in an adult high-density orchard respond differently to canopy restraining by mechanical and manual pruning. *Sci. Hort.* 192, 391–399. doi: 10.1016/j.scienta.2015.06.004

Vivaldi, G. A., Camposeo, S., Lopriore, L., Romero-Trigueros, C., and Pedrero, F. (2019). Using saline reclaimed water on almond grown in Mediterranean conditions: deficit irrigation strategies and salinity effects. *Water Sci. Tech. Water Supply 19* (5), 1413–1421. doi: 10.2166/ws.2019.008

Conflict of Interest: The authors declare that the research was conducted in the absence of any commercial or financial relationships that could be construed as a potential conflict of interest.

frontiers in Plant Science

ORIGINAL RESEARCH
published: 14 November 2019
doi: 10.3389/fpls.2019.01471

Plant Regeneration *via* Somatic Embryogenesis in Mature Wild Olive Genotypes Resistant to the Defoliating Pathotype of *Verticillium dahliae*

*Isabel Narváez[1], Carmen Martín[2], Rafael M. Jiménez-Díaz[3], Jose A. Mercado[1] and Fernando Pliego-Alfaro[1]**

[1] Instituto de Hortofruticultura Subtropical y Mediterránea "La Mayora" (IHSM-UMA-CSIC), Departamento de Botánica y Fisiología Vegetal, Universidad de Málaga, Málaga, Spain, [2] Departamento de Biotecnología-Biología Vegetal, ETS Ingeniería Agronómica, Alimentaria y de Biosistemas, Universidad Politécnica de Madrid, Madrid, Spain, [3] Departamento de Agronomía, College of Agriculture and Forestry (ETSIAM), Universidad de Córdoba, Campus de Excelencia Internacional Agroalimentario ceiA3, Edificio C-4 Celestino Mutis, Campus Rabanales, Ctra. de Madrid, Córdoba, Spain

OPEN ACCESS

Edited by:
Antonio Diaz Espejo, Institute of Natural Resources and Agrobiology of Seville (CSIC), Spain

Reviewed by:
Pilar S. Testillano, Superior Council of Scientific Investigations, Madrid, Spain
Bruno Mezzetti, Marche Polytechnic University, Italy

***Correspondence:**
Fernando Pliego-Alfaro
ferpliego@uma.es

Specialty section:
This article was submitted to Crop and Product Physiology a section of the journal Frontiers in Plant Science

Received: *11 June 2019*
Accepted: *22 October 2019*
Published: *14 November 2019*

Citation:
Narváez I, Martín C, Jiménez-Díaz RM, Mercado JA and Pliego-Alfaro F (2019) Plant Regeneration via Somatic Embryogenesis in Mature Wild Olive Genotypes Resistant to the Defoliating Pathotype of Verticillium dahliae. Front. Plant Sci. 10:1471. doi: 10.3389/fpls.2019.01471

Regeneration capacity, *via* somatic embryogenesis, of four wild olive genotypes differing in their response to defoliating *Verticillium dahliae* (resistant genotypes StopVert, OutVert, Ac-18 and the susceptible one, Ac-15) has been evaluated. To induce somatic embryogenesis, methodologies previously used in wild or cultivated olive were used. Results revealed the importance of genotype, explant type, and hormonal balance in the induction process. Use of apical buds obtained from micropropagated shoots following a methodology used in cultivated olive (4 days induction in liquid 1/2 MS medium supplemented with 30 μM TDZ–0.54 μM NAA, followed by 8 weeks in basal 1/2 MS medium) was adequate to obtain somatic embryos in two genotypes, StopVert and Ac-18, with a 5.0 and 2.5% induction rates, respectively; however, no embryogenic response was observed in the other two genotypes. Embryogenic cultures were transferred to basal ECO medium supplemented with 0.5 μM 2iP, 0.44 μM BA, and 0.25 μM indole-3-butyric acid (IBA) for further proliferation. Somatic embryos from StopVert were maturated and germinated achieving a 35.4% conversion rate. An analysis of genetic stability on StopVert, using Simple Sequence Repeats (SSRs) and Random Amplified Polymorphic DNA (RAPDs) markers, was carried out in embryogenic callus, plants regenerated from this callus and two controls, micropropagated shoots used as explant source, and the original mother plant. Polymorphism was only observed in the banding pattern generated by RAPDs in 1 of the 10 callus samples evaluated, resulting in a variation rate of 0.07%. This is the first time in which plants have been regenerated *via* somatic embryogenesis in wild olive.

Keywords: somatic embryo, oleaster, adult explants, embryo conversion, Verticillium wilt

INTRODUCTION

The cultivated olive *Olea europaea* L. subsp. *europaea* var. *sativa*, Oleaceae family, is a long-lived, evergreen medium-size tree, adapted to dry and poor soils. Fruits have high nutritional value due to their high lipid content. Olive is one of the most important oil crops within the Mediterranean basin (Rugini, 1995). This region accounts for over 96% of the 11.4 million ha of olive trees cultivated worldwide (Rallo et al., 2018). In 2017, total olive oil production was ca. 2,881 thousand tons, with Spain, Italy, Greece, and Portugal as more relevant producing countries (IOC, International Olive Council, 2018).

Wild olive (*O. europaea* L. subsp. *europaea* var. *sylvestris*) is considered as the main progenitor of cultivated olive since both have the same ploidy level (2n = 2x = 46) and similar morphological traits and environmental requirements (Besnard and Rubio de Casas, 2016). Wild genotypes could be useful germplasm sources in olive breeding for introducing resistance to biotic (Colella et al., 2008) or abiotic stress (Murillo et al., 2005). Additionally, in recent years, there has been an increasing interest in the use of pathogen-resistant selections of wild olive as rootstocks to reduce the negative impact of some diseases, especially Verticillium wilt (Jiménez-Fernández et al., 2016). This disease, caused by the soil-borne pathogen *Verticillium dahliae* Kleb., is considered as the main threat to olive production worldwide (Jiménez-Díaz et al., 2012). Most economically important cultivated genotypes are susceptible or extremely susceptible to this disease (López-Escudero et al., 2004). Some wild olive selections highly resistant to defoliating *V. dahliae* pathotype have been identified and used to develop a grafted commercial product, Vertirés, currently available to growers (Jiménez-Díaz, 2018; Jiménez-Díaz and Requena, 2018).

Although olive is generally difficult to manipulate *in vitro*, it has been possible to micropropagate selected olive cultivars through nodal segmentation of elongated shoots (Rugini, 1984; Roussos and Pontikis, 2002; Lambardi et al., 2013). In few cases, buds (Bahrami et al., 2010) or plants (Mencuccini and Rugini, 1993) have been obtained through adventitious organogenesis from petiole and leaf sections derived from *in vitro* grown shoots of adult origin. However, the most widely used method for adventitious regeneration in both cultivated and wild olive is somatic embryogenesis, although, in this case, most investigations have been carried out with juvenile material, i.e., either immature zygotic embryos (Rugini, 1988) or radicle and cotyledon segments from mature embryos (Orinos and Mitrakos, 1991; Mitrakos et al., 1992; Cerezo et al., 2011). Regarding adult material, Rugini and Caricato (1995) developed a double regeneration system, using petioles derived from shoots of adventitious origin as explants, to obtain somatic embryos and plants from the Italian cvs. Canino and Moraiolo. Other authors used leaf and petioles isolated from *in vitro* shoots of cultivars Dahbia (Mazri et al., 2013) and Picual (Toufik et al., 2014). In wild olive, self-rooted plants in greenhouse were an adequate source of explants; however, plant regeneration was not reported (Capelo et al., 2010).

Alterations originating during *in vitro* culture, referred as somaclonal variation (SV) (Larkin and Scowcroft, 1981), are one of the main drawbacks of *in vitro* techniques for clonal propagation or plant regeneration of elite germplasms. These variations can occur due to several factors, i.e., *in vitro* propagation method, genotype, type of explant, growth regulator type and concentration, time in culture, as well as stress generated during the *in vitro* phase (Bairu et al., 2011). In general, micropropagation through axillary branching seems to be quite reliable in terms of genetic stability (George and Debergh, 2008), while indirect somatic embryogenesis is considered to be a genetically unstable process, especially when material has been kept for prolonged time in culture (Vázquez, 2001; Bradaï et al., 2016). The balance and type of growth regulators affect the frequency of occurrence of SV; in fact, high levels of auxins and cytokinins induce changes in DNA methylation patterns (LoSchiavo et al., 1989) or ploidy levels (Bouman and De Klerk, 2001). Hence, somatic embryogenesis protocols should be assessed for their effects in the obtainment of true-to-type plants. To examine genetic stability several molecular markers have been recommended, being microsatellites or Simple Sequence Repeats (SSRs) and Random Amplified Polymorphic DNA (RAPDs) the most commonly used (Bairu et al., 2011). RAPD markers are considered less reproducible than SSRs; however, both methods have been employed in olive to ascertain genetic stability of *in vitro* material (García-Férriz et al., 2002; Doveri et al., 2008; Leva and Petruccelli, 2012).

The main objective of this study was to evaluate the embryogenic capacity of different explants of adult origin, from *V. dahliae*-resistant and susceptible genotypes, of wild olive. Afterwards, genetic stability of embryogenic callus as well as plants regenerated from somatic embryos was evaluated by using SSRs and RAPD markers.

MATERIALS AND METHODS

Plant Material and Culture Establishment

In vitro shoots from adult plants of wild olive genotypes highly resistant (namely Ac-18, OutVert and StopVert) or susceptible (namely Ac-15) to D *V. dahliae* (Colella et al., 2008; Jiménez-Fernández et al., 2016) were used as explants source. Shoot cultures had been established from lateral buds of self-rooted mother plants, grown in the greenhouse (**Supplementary Figure 1**), and were maintained on RP proliferation medium [DKW macro and micronutrients as modified by Roussos and Pontikis (2002), vitamins of Roussos and Pontikis (2002)] with a 2 mg/L zeatin riboside supplement (Vidoy-Mercado et al., 2012). Subculturing was carried out at 6–8 week intervals.

Somatic Embryogenesis Induction

To induce somatic embryogenesis, different types of explant were used: shoot apex with emerging leaf primordia (1.5–2 mm), the first pair of developing leaves without petiole (3–4 mm), the basal part of the following pair of developing leaves (4–5 mm), and petioles from this pair of leaves (1 mm). Leaves were cultured on the medium with adaxial side up.

Initially, and following the protocol of Capelo et al. (2010) for mature wild olive, explants from Ac-18 and Ac-15 genotypes

were cultured on MS induction medium supplemented with 12.25 μM indole-3-butyric acid (IBA)–4.56 μM zeatin (Zea) for 3 months. Afterwards, calli were transferred to MS medium without growth regulators for 12 weeks. Subculturing was carried out at 4-week intervals.

In a different experiment, the protocol of Mazri et al. (2013) for cultivated olive was evaluated, i.e., explants of the four genotypes (Ac-18, OutVert, StopVert and Ac-15) were cultured on 5 ml liquid induction medium composed by 1/2 MS mineral elements, MS vitamins, 100 mg/L myo-inositol, 30 μM TDZ and 0.54 μM NAA, in septate Petri dishes for 4 days, over an orbital shaker (platform size 41 × 41 cm, New Brunswick Scientific, Edison, NJ), at 80 rpm. Afterwards, explants were cultured on solid 1/2 MS medium without growth regulators for two recultures of 4 weeks each. Callus formed after each reculture (4 and 8 weeks) was characterized according to color, texture, and proliferation rate, estimated as the percentage area of explant covered by callus using a rating scale from 0–3 (0: no callus; 1: 1–40% explant surface covered with callus; 2: 40–80%; 3: > 80%) (**Supplementary Figure 2**). Afterwards, isolated calli were transferred to olive cyclic embryogenesis medium, ECO medium (Pérez-Barranco et al., 2009), containing 1/4 OM macroelements (Rugini, 1984), 1/4 MS microelements (Murashige and Skoog, 1962), 1/2 OM vitamins, 550 mg/L glutamine, 0.25 μM IBA, 0.5 μM 2iP, 0.44 μM BA, and a 200 mg/L cefotaxime supplement, for further proliferation. Callus was recultured in this medium at 4-week intervals.

In callus induction experiments, 20–40 shoot apices, 40 petioles, and 40 leaf explants of each type were used. Cultures were incubated at 25 ± 2°C in darkness. All culture media were supplemented with 30 g/L sucrose and media solidified with 6 g/L agar. The pH of media was adjusted to 5.74.

To evaluate multiplication rate of embryogenic callus from StopVert and Ac-18 genotypes, 0.5 g of globular structures, < 3 mm diameter, were cultured on 25 ml solid ECO medium in darkness (Pérez-Barranco et al., 2009). Average weight increment from five Petri dishes was calculated at 4-week intervals during four subcultures.

Maturation and Germination of Somatic Embryos

Globular somatic embryos, <3 mm diameter, from embryogenic callus of StopVert genotype were maturated according to Cerezo et al. (2011), i.e., embryos were cultured in Petri dishes containing basal ECO medium, supplemented with 1 g/L activated charcoal, for 2 months under dark. During the second month, somatic embryos were cultured onto a semipermeable cellulose acetate membrane (MW cut-off 12,000, Sigma D9777).

For germination, mature embryos were cultured on modified MS medium with 1/3 MS macroelements, MS microelements, and 10 g/L sucrose (Clavero-Ramírez and Pliego-Alfaro, 1990) for 2 recultures of 6 weeks each. Afterwards, isolated shoots were cultured on modified RP proliferation medium according to Vidoy-Mercado et al. (2012). Shoots derived from different germinated embryos were micropropagated separately. Embryo germination and shoot micropropagation were carried out under 40 $\mu mol \cdot m^{-2} \cdot s^{-1}$ light irradiance.

Analysis of Genetic Stability

Plant Material

The genetic stability of the embryogenic callus derived from shoot apex of StopVert genotype, as well as plants regenerated from this callus, was evaluated by SSRs and RAPDs analyses. The embryogenic callus had been maintained for over 20 months on ECO medium with regular subcultures at 4–5 week intervals. For regenerated plants, leaf pieces from 10 independent shoots micropropagated in RP medium were examined. Two controls were used, a) leaves from micropropagated shoots, used as explant source, and b) leaves from the original donor plant maintained in the greenhouse. The micropropagated shoots had been initiated from lateral buds of the donor plant and maintained in RP proliferation medium for over 36 months. Different plant materials used, and the number of samples analyzed is indicated in **Table 1**.

DNA Extraction

For genomic DNA extraction, embryogenic callus or leaf material, 0.04–0.06 g, was powdered in liquid nitrogen using the TissueLyser II (Qiagen). In the case of the donor plant, young leaves were washed in 70% ethanol prior to powdering. DNA was extracted using the protocol of Gawel and Jarret (1991), resuspended in sterile milliQ water and treated with 1 μl of RNase (10 μg/ml) at 37°C for 2 h. DNA concentration and purity were visualized on a 0.8% agarose gel.

SSRs Analysis

Five SSR markers were selected to evaluate genetic stability: AJ279854, AJ279859 and AJ279867 (Sefc et al., 2000), and AJ416322 and AJ416323 (De la Rosa et al., 2002) (**Table 2**). The forward primer of each pair was labelled with a fluorescent dye

TABLE 1 | Plant material of StopVert genotype used for genetic stability analysis.

Plant material	Origin	Time in culture	N° of samples analyzed
Control donor plant	Rooted cutting	–	1
Control *in vitro* shoots used as explant source	Micropropagated shoots derived from axillary buds of donor plant	36 months	10
Embryogenic callus	Shoot apex isolated from *in vitro* shoots	20 months	10
Regenerated shoots	Plants regenerated from somatic embryos	20 months in callus phase + 3 months on RP proliferation medium after isolation from the embryo	10

TABLE 2 | Microsatellites markers used in the genetic stability analysis of StopVert genotype.

Locus	Marker	Repeat motif	Sequence (5′-3′)	Allele size (bp)	T° annealing (°C)
AJ279854	ssrOeUA-DCA03	$(GA)_{19}$	HEX™-CCCAAGCGGAGGTGTATATTGTTAC TGCTTTTGTCGTGTTTGAGATGTTG	228–250	50
AJ279859	ssrOeUA-DCA09	$(GA)_{23}$	6-FAM™-AATCAAAGTCTTCCTTCTCATTTCG GATCCTTCCAAAAGTATAACCTCTC	161–205	55
AJ279867	ssrOeUA-DCA18	$(CA)_4CT(CA)_3(GA)_{19}$	6-FAM™-AAGAAAGAAAAAGGCAGAATTAAGC GTTTTCGTCTCTCTACATAAGTGAC	168-184	50
AJ416322	EMO13	$(CT)_4(CA)_8$	6-FAM™-AGGGTGGGGATAAAGAAGAAGTCAC	118-139	60
AJ416323	EMO30	$(AC)_8$	TTTTACCCCATATACCCCGATTCATT HEX™-GTCTCTGCCCAACAATG CATACATGAGTGTGTGTG	183-196	50

(ABI dyes: 6-FAM™ or HEX™). All PCRs were carried out in a Mastercycler (Eppendorf) DNA thermal cycler. PCR was carried out following the protocol of MyTaq™ DNA polymerase (Bioline), being the final volume 20 µl. Samples contained approximately 10 ng of genomic DNA, 0.5 µM of each primer, and 1.25 U of MyTaq DNA polymerase in the buffer provided by the enzyme manufacturer with all needed PCR reagents (containing dNTPs and $MgCl_2$). Amplification conditions were: 1 min at 95°C, 35 cycles of 15 s at 95°C, 15 s at the Tm of each specific pair of primers (**Table 2**), and 10 s at 72°C, with a final extension step of 10 min at 72°C. PCR products were visualized on a 1.5% agarose gel under non-denaturing conditions with ethidium bromide. Amplification products were analyzed in an automated ABI3730 sequencer by the company SECUGEN S.L. (Madrid, Spain). Results were analyzed with GeneMarker (v1.90 software, SoftGenetics, LLC).

RAPD Analysis

Five RAPD markers from Operon Technologies Inc. (Alameda/CA, USA) collection were used (A1: 5′- CAGGCCCTTC-3′; B7: 5′- GGTGACGCAG-3′; B15: 5′- GGAGGGTGTT-3′; E19: 5′- ACGGCGTATG-3′; F10: 5′- GGAAGCTTGG-3′). PCR was carried out modifying the protocol of MyTaq™ DNA polymerase, being the final volume of 25 µl. Samples contained approximately 10 ng of genomic DNA, 0.8 µM of a single decanucleotide, and 1.5 U of MyTaq DNA polymerase in the reaction buffer. Amplification conditions were: 2 min at 94°C, 35 cycles of 45 s at 92°C, 1 min at 37°C, and 2 min at 72°C, with a final extension step of 10 min at 72°C. PCR products were visualized by loading 12 µl on a 1.5% agarose gel under non-denaturing conditions. The size of the amplified bands was related by reference to the molecular size marker (100 Base-Pair Ladder, GE Healthcare). All PCRs were carried out at least in duplicate, in a Mastercycler (Eppendorf) DNA thermal cycler.

RESULTS

Somatic Embryogenesis Induction

Use of the protocol described by Capelo et al. (2010) for wild olive did not yield embryogenic callus in any of the explants evaluated from Ac-18 or Ac-15 genotypes. After 4 weeks on induction medium (MS supplemented with 12.25 µM IBA–4.56 µM zeatin), explants of Ac-15 genotype showed higher callus proliferation rate than those from the Ac-18 genotype. The higher amount of callus was observed in shoot apex and first pair of leaves, while smaller calluses appeared in petiole explants. After two additional recultures in induction medium, calluses became compact, of white color, and showed a noticeable increase in size; however, some calluses of Ac-15 genotype were easily crumbled. Following transfer to basal MS medium, calluses started to get brown and roots appeared in some of those derived from shoot apex explants; however, no clear embryogenic structures could be identified.

In a subsequent experiment, the protocol of Mazri et al. (2013) was assayed using the four genotypes. No noticeable changes were observed after 4 days in liquid induction medium (1/2 MS 30 µM TDZ-0.54 µM NAA) (**Figure 1A**). Calli started to form at the edges of explants after 2 weeks on solid basal medium (1/2 MS) and were clearly visible in most explants 2 weeks later (**Figure 1B**). A general increase in callus formation was observed after four additional weeks in 1/2 MS basal medium. Best response in terms of percentage of explants forming callus and amount of callus after 8 weeks of culture was observed in shoot apex explants (**Table 3**). Generally, calli were white and with a certain grade of compactness; in some cases, translucent areas were observed. Although all tested explants from the four genotypes produced callus, embryogenic structures (**Figure 1C**) were only visible in shoot apex derived callus from StopVert and Ac-18, yielding percentages of embryogenic induction of 5.0% and 2.5%, respectively (**Table 3**).

Embryogenic calli were isolated and cultured on ECO medium to enhance proliferation; however, while calli of StopVert performed well showing globular structures and stable growth rate throughout four subcultures (0.85 ± 0.12 g of weight increase per subculture) (**Figure 1D**), embryogenic callus from Ac-18 genotype grew poorly under these conditions (**Figure 1E**).

Maturation and Germination of Somatic Embryos

Following the protocol of Cerezo et al. (2011), 81 globular somatic embryos from StopVert genotype were transferred to ECO maturation medium over cellulose acetate membranes and 48 of them (59.3%) changed to a white opaque appearance

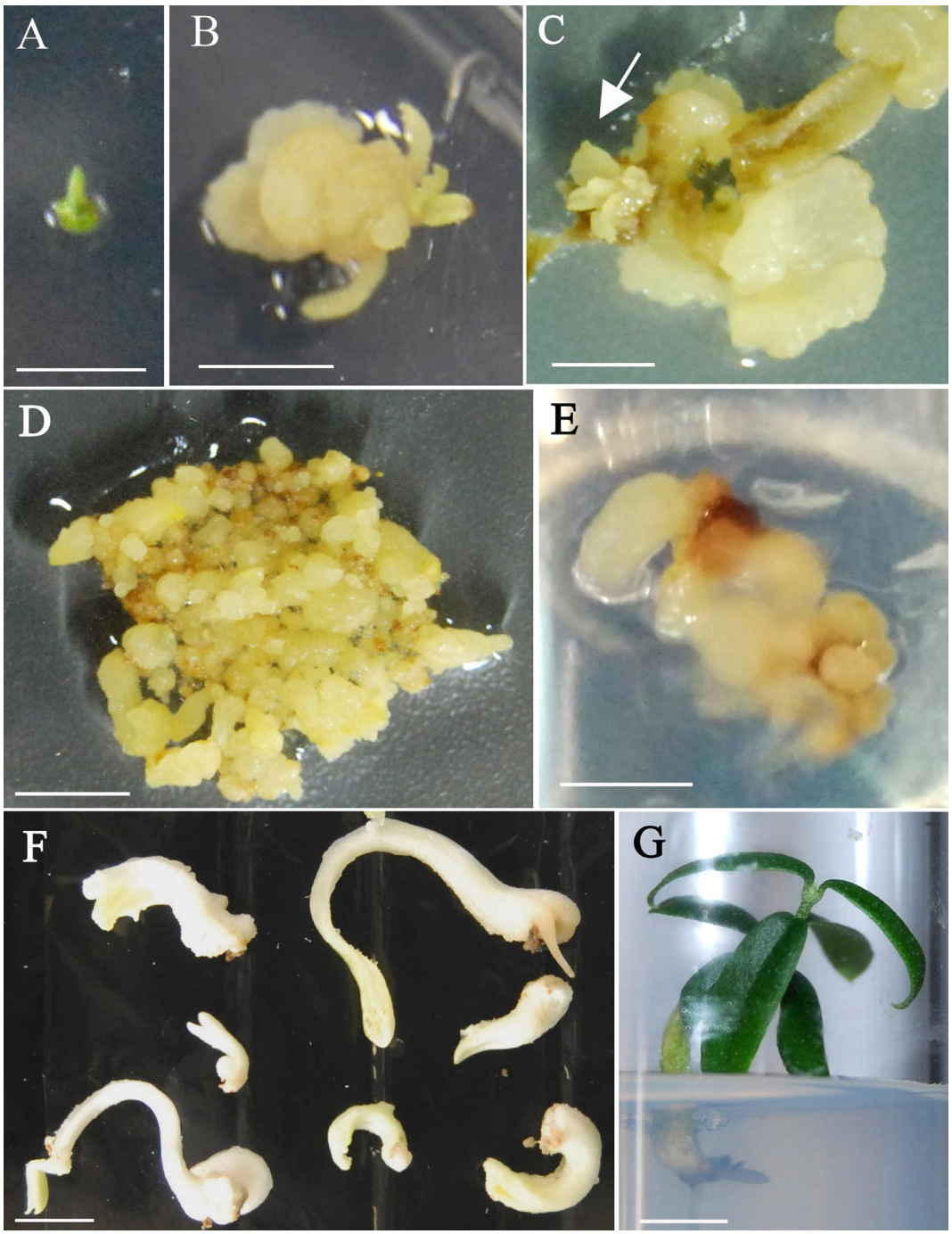

FIGURE 1 | Somatic embryogenesis induction and plant recovery from adult wild olive. **(A)** Shoot apex explants after 4 days on 1/2 MS liquid medium supplemented with 30 μM TDZ–0.54 μM NAA. **(B**) Callus after 4-week culture on 1/2 MS solid basal medium. **(C)** Callus after 8-weeks culture on 1/2 MS solid basal medium with emerging embryogenic structures (arrow). Calli from StopVert **(D)** and Ac-18 **(E)** genotypes proliferating in ECO medium supplemented with 0.25 μM IBA, 0.5 μM 2iP–0.44 μM BA and 200 mg/L cefotaxime. **(F)** Somatic embryos of StopVert selection with white opaque appearance following culture on semi-permeable cellulose acetate membrane on basal ECO medium with activated charcoal. **(G)** Plant of StopVert genotype regenerated from somatic embryo after 12 weeks on germination medium. Bars correspond to 0.5 cm **(A**–**D)** and 1 cm **(E**–**G)**.

(**Figure 1F**). Afterwards, these mature embryos were transferred to germination medium with 1/3 MS macroelements and a 10 g/L sucrose supplement. After 12 weeks, 17 independent shoots (35.4% shoot germination) were obtained, corresponding to embryos that had formed either a single shoot or a shoot and a root (**Figure 1G**). Shoots from different germinated embryos were cultured individually on RP medium to enhance development of axillary shoots.

TABLE 3 | *In vitro* response of different type of explants from four wild olive genotypes after 4 days induction in liquid 1/2 MS medium supplemented with 30 μM TDZ–0.54 μM NAA followed by 8 weeks culture on basal 1/2 MS medium.

Genotype	Explant	Explants with callus (%)	Amount of callus	Embryogenic callus (%)
StopVert	Shoot apex	100	2.6 ± 0.5	5.0
	Leaf (first pair)	100	1.7 ± 0.5	0
	Leaf (second pair)	64	0.7 ± 0.6	0
	Petiole	100	1.4 ± 0.8	0
OutVert	Shoot apex	100	2.0 ± 0.6	0
	Leaf (first pair)	90	1.1 ± 0.5	0
	Leaf (second pair)	87.5	1.1 ± 0.6	0
	Petiole	82	1.0 ± 0.6	0
Ac-18	Shoot apex	100	2.6 ± 0.5	2.5
	Leaf (first pair)	100	1.7 ± 0.5	0
	Leaf (second pair)	64	1.6 ± 0.5	0
	Petiole	100	2.8 ± 0.4	0
Ac-15	Shoot apex	100	3.0 ± 0	0
	Leaf (first pair)	100	1.7 ± 0.5	0
	Leaf (second pair)	100	1.5 ± 0.5	0
	Petiole	100	2.5 ± 0.7	0

The amount of callus was estimated by an arbitrary scale based on visual criteria (0: no callus; 1: < 40% explant surface covered by callus; 2: 40–80% explant surface covered by callus; 3: 80–100% explant surface covered by callus).

Microsatellites Assay

After amplification, fragments generated from all materials were compared to the mother plant. The five SSR markers produced six alleles or fragments. Band size ranged between 138 and 236 pb (**Table 4**), being similar to the values described by De la Rosa et al. (2002) and Sefc et al. (2000) for olive. Samples of embryogenic callus, shoots regenerated from this callus and control shoots used as explant source, were monomorphic when compared to the mother plant for each primer pair. All analyzed markers were homozygous, except for AJ279859, which was heterozygous (**Table 4**). Electropherograms for SSR ssrOeUA-DCA09 for each type of sample analyzed are shown in **Figure 2**. The genetic stability analysis using these molecular markers showed that the genetic fidelity was 100% with respect to the mother plant.

RAPDs Assay

In this analysis, all samples previously studied were included, except regenerated plant from embryo number 4, since with this sample attempts to get PCR amplification were unsuccessful. RAPD profiles were generated using primers A1, B7, B15, E19, and F10, which amplified a high number of bands. A total of 50 bands were obtained, ranging the number of bands obtained per amplification between 9 and 11, and their size between 200 and 1,800 bp (**Table 5**). The genetic stability analysis with these five RAPD markers showed that shoots regenerated from somatic embryos and control shoots used as explant source presented the same band pattern than that of the mother plant (**Figure 3**). However, an additional band of 650 bp was amplified in a callus sample with primer A1 (**Figure 3**), indicating a level of polymorphism of 0.2% in the samples of the callus analyzed. Considering all samples, the variation rate was 0.07%.

TABLE 4 | Allele size obtained with the amplification of five microsatellite markers in StopVert genotype.

Locus	Allele size (bp)			
	Donor plant	Axillary shoots *in vitro*	Embryogenic callus	Plants regenerated from somatic embryos
AJ279854	236	236	236	236
AJ279859	165/173	165/173	165/173	165/173
AJ279867	172	172	172	172
AJ416322	138	138	138	138
AJ416323	195	195	195	195

DISCUSSION

Somatic Embryogenesis Induction and Plant Regeneration From Adult Material in Wild Olive

Somatic embryogenesis has previously been observed in a few number of cultivated (Rugini and Caricato, 1995; Mazri et al., 2013; Toufik et al., 2014) and wild olive (Capelo et al., 2010) genotypes using adult explants. In general, embryogenic capacity is lower in mature explants than in those of juvenile origin. Cells of adult explants are less prone to dedifferentiation and reprogramming processes than their juvenile counterparts. Some authors pointed out that recalcitrance could have either a genetic (von Arnold, 2008) or epigenetic basis (Gahan, 2007). In this research, we have evaluated the embryogenic response of adult material from four wild olive genotypes, using two different induction protocols and different types of explants.

Genotype, type of explant, mineral formulation, and auxin/cytokinin ratio are key factors in embryogenic induction in adult material. In our case, embryogenic response was only observed in two out of the four selections evaluated. Along this line, Correia et al. (2011) pointed out the need to optimize culture conditions for a determined selection, since several genotypes could respond in a different manner. However, genotypes with a high embryogenic potential have less nutritional and hormonal requirements than those with low embryogenic capacity.

Type of explant plays a key role in embryogenic induction. Leaf sections (Corredoira et al., 2015) and shoot apex (San-José et al., 2010; Corredoira et al., 2015) of adult origin have been used in other woody species. In cultivated and wild olive, leaf and petiole explants had been recommended (Rugini and Caricato, 1995; Capelo et al., 2010; Mazri et al., 2013; Toufik et al., 2014); however, in this research, following comparison of three explant types, leaf, petiole, and shoot apex, embryogenic calli were only obtained when shoot apices were used, confirming previous observations of Corredoira et al. (2015) in eucalyptus. These authors indicated that shoot apex and leaves from the first node would be the most effective explants for somatic embryogenesis induction due to their high proliferation capacity and low differentiation stage.

Somatic embryogenesis induction generally requires addition of auxin and sometimes, cytokinin, to the culture medium. After hormonal treatment, some cells acquire embryogenic capacity being expressed in a medium without or with lower auxin concentration.

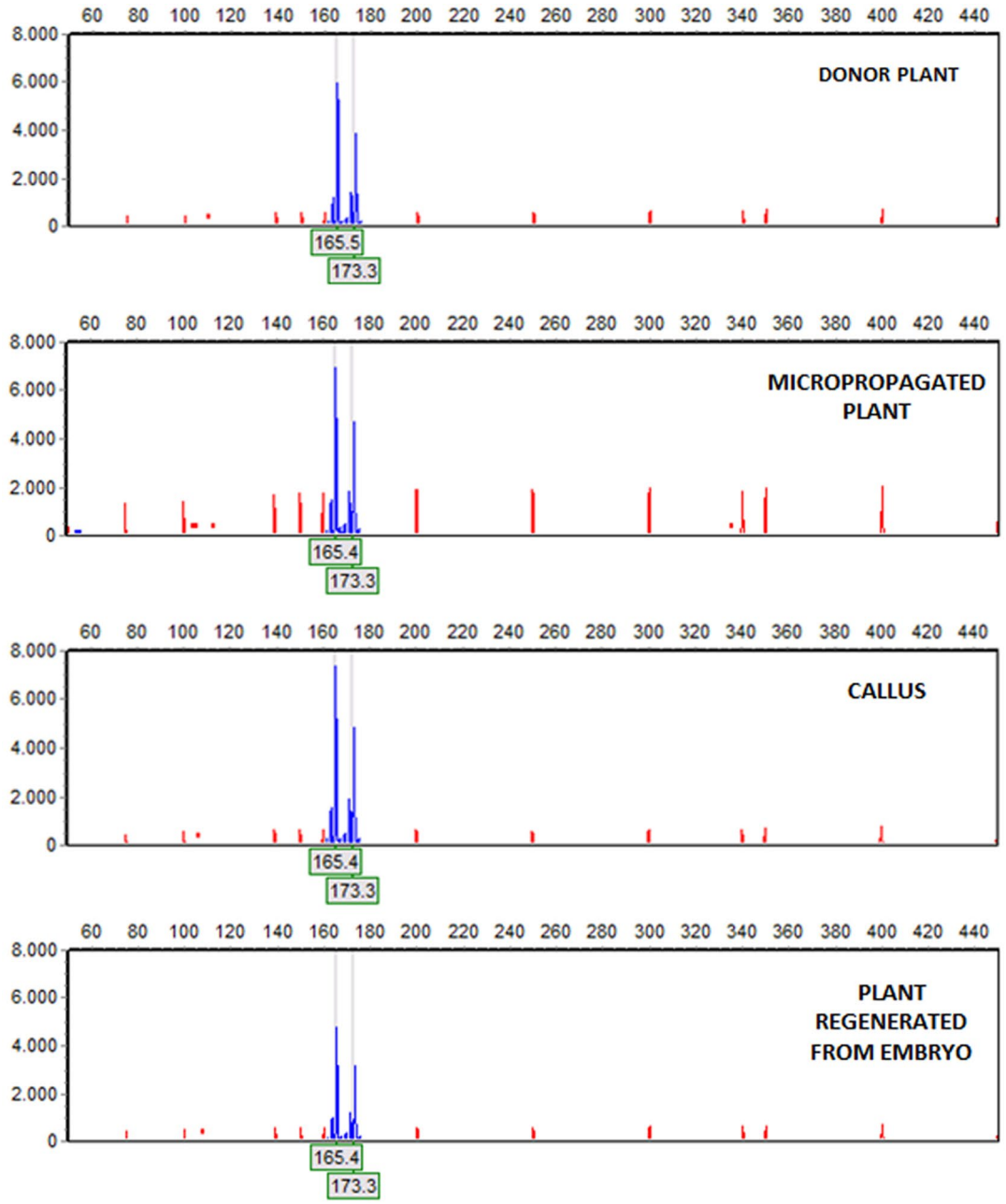

FIGURE 2 | Amplification of the (6-FAM™)ssrOeUA-DCA09 in material of StopVert genotype. Electropherograms, from top to bottom: donor plant, a micropropagated plant, a piece of embryogenic callus derived from shoot apex and a plant regenerated from a somatic embryo. Electropherograms showed heterozygous individuals with two alleles, being the fragments size 165 and 173 bp.

TABLE 5 | Number of scored bands and size band range (bp) with the amplification of five RAPDs markers in StopVert genotype.

Primers	N° of bands amplified	Size of band (bp)
A1	11	200-1600
B7	10	250-1600
B15	11	500-1800
E19	9	300-1300
F10	9	250-1400

In juvenile material from cultivated (Mitrakos et al., 1992) and wild olive (Orinos and Mitrakos, 1991), embryogenic induction process was achieved using a high auxin/cytokinin ratio (25 μM IBA–2.5 μM 2iP). In adult olive, positive results have been reported using either a low (Rugini and Caricato, 1995; Mazri et al., 2013) or a high (Capelo et al., 2010) auxin/cytokinin ratio. In our case, we only obtained embryogenic callus when using a high concentration of cytokinin (TDZ) and a low concentration of auxin (NAA),

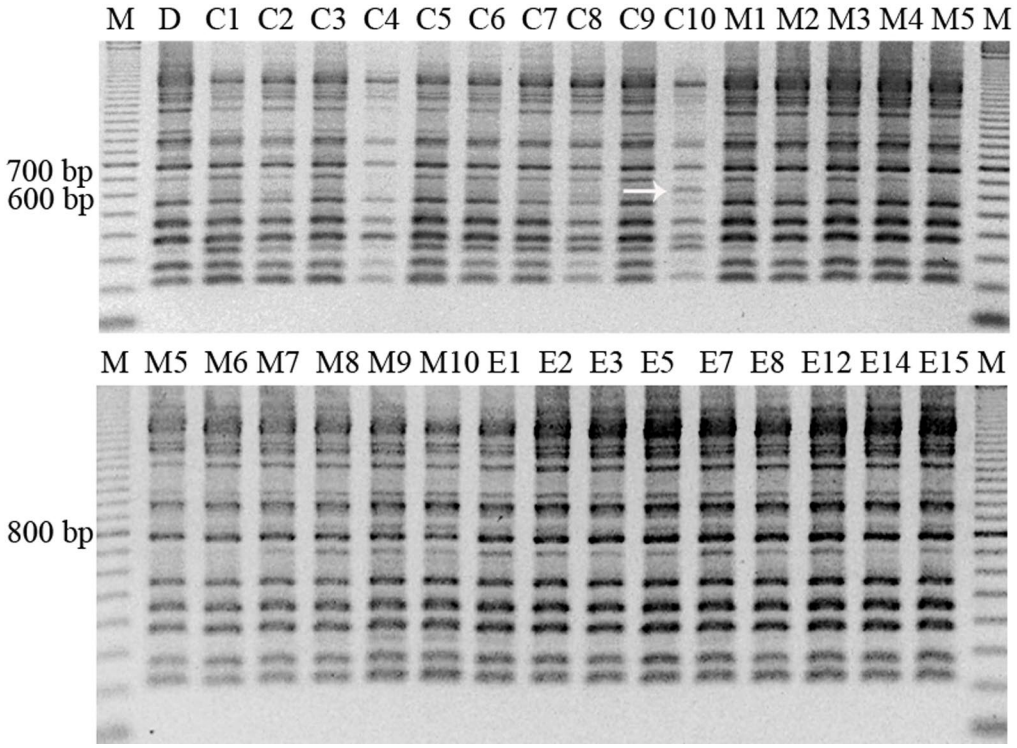

FIGURE 3 | RAPD pattern obtained with the primer A1 in different samples of material of StopVert genotype, corresponding to D (donor plant), C1–C10 (callus samples from embryogenic callus from shoot apex), M1–M10 (micropropagated shoots derived from axillary buds of donor plant), and E1–E15 (plants regenerated from somatic embryos). The arrow shows the sample with a different band pattern. M = marker (100–2000 bp).

as reported by Mazri et al. (2013). In species, such as *Arachis hypogaea,* TDZ was more effective than auxin to induce direct somatic embryogenesis (Murthy et al., 1995). This hormone has been related to the modification of endogenous auxin synthesis (Murthy et al., 1998); probably, in adult olive, an increase in endogenous auxin levels could have occurred; i.e., auxin increases have been shown to play a key role in embryogenic induction in other systems (Rodríguez-Sanz et al., 2014; Fehér, 2015; Corredoira et al., 2017). Interestingly, in *Pelargonium* × *hortorum,* presence of auxin biosynthesis inhibitors in a TDZ supplemented medium interfered with induction of the embryogenic process (Hutchinson et al., 1996). In any case, additional studies are needed to elucidate the mechanisms of action of TDZ (Guo et al., 2011). Percentages of embryogenic response in adult material are variable and, in general, lower than those observed for juvenile explants. Mazri et al. (2013) reported about 10% response in cv. Dahbia, whereas in wild olive, the obtained percentages were in the range 2.28–27.6% (Capelo et al., 2010). In this research, embryogenic induction rates of 2.5% and 5% were obtained for Ac-18 and StopVert genotypes, respectively. Moreover, the latter showed a much better proliferation capacity of the embryogenic callus, confirming the important effect of genotype.

Using the protocol developed by Cerezo et al. (2011), somatic embryos from StopVert genotype could be maturated and converted to plants. The percentage of shoot germination, 35.4%, was lower than that reported by Cerezo et al. (2011) for somatic embryos derived from radicle explants (55%). In adult olive, only Rugini and Caricato (1995) were able to regenerate plants from cvs. Canino and Moraiolo. To our knowledge, this is the first report where plant regeneration *via* somatic embryogenesis has been obtained in adult material from wild olive.

Regenerated Plants of the Wild Olive Genotype StopVert are Genetically Stable

The *in vitro* regeneration system plays a key role in the genetic stability of the material obtained. In olive plants, of juvenile origin, regenerated *via* somatic embryogenesis, contradictory results have been observed, i.e., Shibli et al. (2001) did not observe any changes in morphology, whereas Bradaï et al. (2016) reported a strong effect of genotype and time in culture in the appearance of variations such as fasciated shoots, three shoots per whorl, or double leaves. Leva (2009) obtained two variant phenotypes, BOS (shrubby) and COS (columnar), from somatic embryos derived of cotyledon explants. These results confirm previous observations of Karp (1994) and Wang and Wang (2012), about the important effect of genotype and time in culture in the occurrence of SV. In this investigation, morphological alterations were not observed in regenerated plants derived from somatic embryos of StopVert genotype.

Molecular markers have been widely used as a complementary tool to detect somaclonal variation in regenerated plants.

Lopes et al. (2009) did not find variations between embryogenic material and the mother plant in *O. europaea*, as well as in *O. maderensis*, using SSR markers. Similarly, in this investigation, no SSR variations were detected when comparing embryogenic callus and shoots regenerated from this callus with the controls. Contrary to these results, a low rate of variation in the embryogenic callus was obtained when using RAPD markers. All RAPD profiles generated were monomorphic, except for one callus sample, which amplified an additional 650 bp band with primer A1, absent in the rest of samples. Variations detected by RAPD markers in callus but not in the regenerated plants have also been found in other species such as *Picea glauca* (De Verno et al., 1999). In cork oak (Lopes et al., 2006), a high level of polymorphism was obtained using SSR markers in somatic embryos but not in regenerated plants. Some authors have proposed that this could occur due to *de novo* mutations during the differentiation–dedifferentiation process *in vitro* (Jain, 2001). Thus, embryogenic callus would be formed by a mix of stable and unstable cells, but only cells with an unaltered genome could regenerate plants (De Verno et al., 1999; Miñano et al., 2014). In this research, since regenerated plants showed uniformity with both molecular markers, it can be suggested that the protocol used to induce somatic embryogenesis from adult material in wild olive did not produce genetic alterations that could be detected by SSR and RAPD markers. Despite this fact, total genetic fidelity is not possible to assure since these techniques analyze only a piece of genome. Moreover, further molecular analysis as well as a study of true-to-type phenotype of regenerated plants would be recommended, especially if embryogenic callus were kept for a long time in culture. In any case, taking into account that commercial olive micropropagation shows a strong genotype effect (Zuccherelli and Zuccherelli, 2002), regeneration and genetic fidelity of adult plants derived from somatic embryos open new opportunities to propagate recalcitrant cultivars, i.e., obtained material could be used as revitalized mother plants and further multiplied either *in vitro,* through nodal segmentation of elongated shoots, or *in vivo,* by rooted minicuttings, as reported in other woody species (Martínez et al., 2012; Georget et al., 2017).

Conclusions

In this research, somatic embryogenesis has been induced from adult material of two wild olive genotypes, StopVert and Ac-18, highly resistant to D *V. dahliae* pathotype. The type of explant played a key role in the process, being the shoot apex the most responsive. Plants from somatic embryos of StopVert genotype have also been regenerated and molecular analysis using SSRs and RAPDs markers confirmed genetic fidelity of the recovered plants. As far as we know, this is the first time that plants have been regenerated *via* somatic embryogenesis using adult explants of wild olive. The protocol described in this research will open the door to propagate recalcitrant olive genotypes; in addition, it will allow the development of biotechnological tools, such as genetic transformation and gene editing, and their application to study the genetic mechanisms underlying resistance to D *V. dahliae* pathotype in these wild olive genotypes, with the final purpose of introducing this trait into cultivated olive.

DATA AVAILABILITY STATEMENT

The datasets generated for this study are available on request to the corresponding author.

AUTHOR CONTRIBUTIONS

IN was responsible for *in vitro* regeneration experiments. IN and CM carried out the molecular analysis. RJ-D developed the wild olive resistant genotypes used in this study and revised the manuscript. JM and FP-A planned this research, designed the experiments, and wrote the manuscript.

FUNDING

This investigation was funded by Junta de Andalucía (Grant No. P11-AGR-7992) and by the Ministerio de Ciencia e Innovación of Spain and Feder European Union Funds (Grant No. AGL2017-83368-C2-1-R).

ACKNOWLEDGMENTS

IN was awarded a Ph.D. Fellowship from Secretaría General de Investigación (Consejería de Innovación Ciencia y Empresa, Grant No. P11-AGR-7992), Ph.D. Program Advanced Biotechnology, University of Málaga.

SUPPLEMENTARY MATERIAL

The Supplementary Material for this article can be found online at: https://www.frontiersin.org/articles/10.3389/fpls.2019.01471/full#supplementary-material

REFERENCES

Bahrami, M. K., Azar, A. M., and Dadpour, M. R. (2010). Influence of thidiazuron in direct shoot regeneration from segments of *in vitro* leaves and axillary and apical buds of olive (*Olea europaea*). *Acta Hortic.* 884, 383–390. doi: 10.17660/ActaHortic.2010.884.46

Bairu, M. W., Aremu, A. O., and Van Staden, J. (2011). Somaclonal variation in plants: causes and detection methods. *Plant Growth Regul.* 63, 147–173. doi: 10.1007/s10725-010-9554-x

Besnard, G., and Rubio de Casas, R. (2016). Single vs multiple independent olive domestications: the jury is (still) out. *New Phytol.* 209, 466–470. doi: 10.1111/nph.13518

Bouman, H., and De Klerk, G. J. (2001). Measurement of the extent of somaclonal variation in begonia plants regenerated under various conditions. Comparison of three assays. *Theor. Appl. Genet.* 102, 111–117. doi: 10.1007/s001220051625

Bradaï, F., Pliego-Alfaro, F., and Sánchez-Romero, C. (2016). Somaclonal variation in olive (*Olea europaea* L.) plants regenerated *via* somatic embryogenesis: Influence of genotype and culture age on phenotypic stability. *Sci. Hortic.* 213, 208–215. doi: 10.1016/j.scienta.2016.10.031

Capelo, A. M., Silva, S., Brito, G., and Santos, C. (2010). Somatic embryogenesis induction in leaves and petioles of a mature wild olive. *Plant Cell Tissue Organ Cult.* 103, 237–242. doi: 10.1007/s11240-010-9773-x

Cerezo, S., Mercado, J. A., and Pliego-Alfaro, F. (2011). An efficient regeneration system *via* somatic embryogenesis in olive. *Plant Cell Tissue Organ Cult.* 106, 337–344. doi: 10.1007/s11240-011-9926-6

Clavero-Ramírez, I., and Pliego-Alfaro, F. (1990). Germinación *in vitro* de embriones maduros de olivo (*Olea europaea*). *Actas Hortic.* 1, 512–516.

Colella, C., Miacola, C., Amenduni, M., D'Amico, M., and Bubici, G. (2008). Sources of Verticillium wilt resistance in wild olive germplasm from the Mediterranean region. *Plant Pathol.* 57, 533–539. doi: 10.1111/j.1365-3059.2007.01785.x

Corredoira, E., Ballester, A., Ibarra, M., and Vieitez, A. M. (2015). Induction of somatic embryogenesis in explants of shoot cultures established from adult *Eucalyptus globulus* and *E. saligna* × *E. maidenii* trees. *Tree Physiol.* 35, 678–690. doi: 10.1093/treephys/tpv028

Corredoira, E., Cano, V., Bárányа, I., Solís, M. T., Rodríguez, H., Vieitez, A. M., et al. (2017). Initiation of leaf somatic embryogenesis involves high pectin esterification, auxin accumulation and DNA demethylation in *Quercus alba*. *J. Plant Physiol.* 213, 42–54. doi: 10.1016/j.jplph.2017.02.012

Correia, S., Lopes, M. L., and Canhoto, J. M. (2011). Somatic embryogenesis induction system for cloning an adult *Cyphomandra betacea* (Cav.) Sendt. (tamarillo). *Trees* 25, 1009–1020. doi: 10.1007/s00468-011-0575-5

De la Rosa, R., James, C. M., and Tobutt, K. R. (2002). Isolation and characterization of polymorphic microsatellites in olive (*Olea europaea* L.) and their transferability to other genera in the Oleaceae. *Mol. Ecol. Notes* 2, 265–267. doi: 10.1046/j.1471-8278

De Verno, L. L., Park, Y. S., Bonga, J. M., and Barret, J. D. (1999). Somaclonal variation in cryopreserved embryogenic clones of white spruce (*Picea glauca* (Moench) Voss). *Plant Cell Rep.* 18, 948–953. doi: 10.1007/s002990050689

Doveri, S., Sabino Gil, F., Díaz, A., Reale, S., Busconi, M., da Câmara Machado, A., et al. (2008). Standardization of a set of microsatellite markers for use in cultivar identification studies in olive (*Olea europaea* L.). *Sci. Hortic.* 116, 367–373. doi: 10.1016/j.scienta.2008.02.005

Fehér, A. (2015). Somatic embryogenesis — Stress-induced remodeling of plant cell fate. *Biochim. Biophys. Acta* 1849, 385–402. doi: 10.1016/j.bbagrm.2014.07.005

Gahan, P. B. (2007). Totipotency and cell cycle in *Protocols for Micropropagation of Woody Trees and Fruits*. Eds. Jain, S. M., and Häggman,H. (Dordrecht: Springer), 3–14.

García-Férriz, L., Ghorbel, R., Ybarra, M., Marí, A., Belaj, A., and Trujillo, I. (2002). Micropropagation from adult olive trees. *Acta Hortic.* 586, 879–882. doi: 10.17660/ActaHortic.2002.586.191

Gawel, N. J., and Jarret, R. L. (1991). A modified CTAB DNA extraction procedure of *Musa* and *Ipomoea*. *Plant Mol. Biol. Rep.* 9, 262–266. doi: 10.1007/BF02672076

George, E. F., and Debergh, P. C. (2008). Micropropagation: Uses and Methods in *Plant Propagation by Tissue Culture, 3rd Edition. Vol. 1. The Background*. Eds. George, E. F. , Hall, M. A. , and De Klerk,G. J. (Dordrecht: Springer), 29–65.

Georget, F., Courtel, P., Malo-Garcia, E., Hidalgo., M., Alpizar, E., Breitler, J. C., et al. (2017). Somatic embryogenesis-derived coffee plantlets can be efficiently propagated by horticultural rooted mini-cuttings: a boost for somatic embryogenesis. *Sci. Hortic.* 216, 177–185. doi: 10.1016/j.scienta.2016.12.017

Guo, B., Abbasi, B. H., Zeb, A., Xu, L. L., and Wei, Y. H. (2011). Thidiazuron: a multi-dimensional plant growth regulator. *Afr. J. Biotechnol.* 10, 8984–9000. doi: 10.5897/AJB11.636

Hutchinson, M. J., Murch, S. J., and Saxena, P. K. (1996). Morphoregulatory role of thidiazuron: Evidence of the involvement of endogenous auxin in thidiazuron induced somatic embryogenesis of geranium *(Pelargonium* x *hortorum* Bailey). *J. Plant Physiol.* 149, 573–579. doi: 10.1016/S0176-1617(96)80336-1

IOC, International Olive Council (2018) http://www.internationaloliveoil.org/estaticos/view/131-world-olive-oil-figures, (Accessed April 25 2019).

Jain, S. M. (2001). Tissue culture-derived variation in crop improvement. *Euphytica* 118, 153–166. doi: 10.1023/A:1004124519479

Jiménez-Díaz, R. M. (2018). Avances en el conocimiento y la gestión integrada de la Verticilosis del olivo. *Vida Rural* 453, 30–38.

Jiménez-Díaz, R. M., and Requena, E. (2018). El olivo Vertirés®: una solución innovadora para el control de la Verticilosis causada por los patotipos y razas de *Verticillium dahliae*. *Mercaei Magazine* 95, 132–144.

Jiménez-Díaz, R. M., Cirulli, M., Bubici, G., Jiménez-Gasco, M. M., Antoniou, P. P., and Tjamos, E. C. (2012). Verticillium wilt: A major threat to olive production. Current status and future prospects for its management. *Plant Dis.* 96, 304–329. doi: 10.1094/PDIS-06-11-0496

Jiménez-Fernández, D., Trapero-Casas, J. L., Landa, B. B., Navas-Cortés, J. A., Bubici, G., Cirulli, M., et al. (2016). Characterization of resistance against the olive-defoliating *Verticillium dahliae* pathotype in selected clones of wild olive. *Plant Pathol.* 65, 1279–1291. doi: 10.1111/ppa.12516

Karp, A. (1994). Origins, causes and uses of variation in plant tissue cultures in *Plant Cell and Tissue Culture*. Eds. Vasil, I. K., and Thorpe,T. A. (Dordrech: Kluwer Academic Publishers), 139–152.

Larkin, P. J., and Scowcroft, W. R. (1981). Somaclonal variation - a novel source of variability from cell cultures for plant improvement. *Theor. Appl. Genet.* 60, 197–214. doi: 10.1007/BF02342540

Lambardi, M., Ozudogru, E. A., and Roncasaglia, R. (2013). *In vitro* propagation of olive (*Olea europaea* L.) by nodal segmentation of elongated shoots in *Protocols for Micropropagation of Selected Economically-Important Horticultural Plants*. Eds. Lambardi, M., Ozudogru, E. A., and Jain, S. M. (New-York: Springer), 33–44.

Leva, A. R. (2009). Morphological evaluation of olive plants micropropagated *in vitro* culture through axillary buds and somatic embryogenesis methods. *Afr. J. Plant Sci.* 3, 37–43.

Leva, A. R., and Petruccelli, R. (2012). Monitoring of cultivar identity in micropropagated olive plants using RAPD and ISSR markers. *Biol. Plant* 56, 373–376. doi: 10.1007/s10535-012-0102-6

Lopes, T., Capelo, A., Brito, G., Loureiro, J., and Santos, C. (2009). Genetic variability analyses of the somatic embryogenesis induction process in *Olea* spp. using nuclear microsatellites. *Trees* 23, 29–36. doi: 10.1007/s00468-008-0251-6

Lopes, T., Pinto, G., Loureiro, J., Costa, A., and Santos, C. (2006). Determination of genetic stability in long-term somatic embryogenic cultures and derived plantlets of cork oak using microsatellite markers. *Tree Physiol.* 26, 1145–1152. doi: 10.1093/treephys/26.9.1145

López-Escudero, F. J., del Río, C., Caballero, J. M., and Blanco-López, M. A. (2004). Evaluation of olive cultivars for resistance to *Verticillium dahliae*. *Eur. J. Plant Pathol.* 110, 79–85. doi: 10.1023/B:EJPP.0000010150.08098.2d

LoSchiavo, F., Pitto, L., Giuliano, G., Torti, G., Nuti-Ronchi, V., Marazziti, D., et al. (1989). DNA methylation of embryogenic carrot cell cultures and its variations as caused by mutation, differentiation, hormones and hypomethylating drugs. *Theor. Appl. Genet.* 77, 325–331. doi: 10.1007/BF00305823

Martínez, T., Vidal, N., Ballester, A., and Vieitez, A. M. (2012). Improved organogenic capacity of shoot cultures from mature pedunculate oak trees through somatic embryogenesis as rejuvenation technique. *Trees* 26, 321–330. doi: 10.1007/s00468-011-0594-2

Mazri, M. A., Belkoura, I., Pliego-Alfaro, F., and Belkoura, M. (2013). Somatic embryogenesis from leaf and petiole explants of the Moroccan olive cultivar Dahbia. *Sci. Hortic.* 159, 88–95. doi: 10.1016/j.scienta.2013.05.002

Mencuccini, M., and Rugini, E. (1993). *In vitro* shoot regeneration from olive cultivar tissues. *Plant Cell Tissue Organ Cult.* 32, 283–288. doi: 10.1007/BF00042290

Mitrakos, K., Alexaki, A., and Papadimitriou, P. (1992). Dependence of olive morphogenesis on callus origin and age. *J. Plant Physiol.* 139, 269–273. doi: 10.1016/S0176-1617(11)80335-4

Miñano, H. S., Ibáñez, M. A., González-Benito, M. E., and Martín, C. (2014). Sequential study of the genetic stability of callus and regenerated shoots in Chrysanthemum. *Propag. Ornam. Plants* 14, 57–67. doi: 10.1111/j.1399-3054.1962.tb08052.x

Murashige, T., and Skoog, F. (1962). A revised medium for rapid growth and bioassays with tobacco tissue cultures. *Physiol. Plant* 15, 473–497.

Murillo, J. M., Madejon, E., Madejon, P., and Cabrera, F. (2005). The response of wild olive to the addition of a fulvic acid-rich amendment to soils polluted by trace elements (SW Spain). *J. Arid Environ.* 63, 284–303. doi: 10.1016/j.jaridenv.2005.03.022

Murthy, B. N. S., Murch, S. J., and Saxena, P. K. (1995). Thidiazuron-induced somatic embryogenesis in intact seedlings of peanut (*Arachis hypogaea*): Endogenous growth regulator levels and significance of cotyledons. *Physiol. Plant* 94, 268–276. doi: org/10.1111/j.1399-3054.1995.tb05311.x

Murthy, B. N. S., Murch, S. J., and Saxena, P. K. (1998). Thidiazuron: A potent regulator of *in vitro* plant morphogenesis. *In Vitro Cell. Dev. Biol. Plant* 34, 267. doi: org/10.1007/BF02822732

Orinos, T., and Mitrakos, K. (1991). Rhizogenesis and somatic embryogenesis in calli from wild olive (*Olea europaea* var. *sylvestris* (Miller) Lehr) mature zygotic embryos. *Plant Cell Tissue Organ Cult.* 27, 183–187. doi: 10.1007/BF00041288

Pérez-Barranco, G., Torreblanca, R., Padilla, I. M. G., Sánchez-Romero, C., Pliego-Alfaro, F., and Mercado, J. A. (2009). Studies on genetic transformation of olive (*Olea europaea* L.) somatic embryos: I. Evaluation of different aminoglycoside antibiotics for *nptII* selection; II. Transient transformation *via* particle bombardment. *Plant Cell Tissue Organ Cult.* 97, 243–251. doi: 10.1007/s11240-009-9520-3

Rallo, L., Barranco, D., Díez, C. M., Rallo, P., and Suárez, M. P. (2018). Strategies for olive (*Olea europaea* L.) breeding: Cultivated genetic resources and crossbreeding in *Advances in Plant Breeding Strategies: Fruits*. Eds. Al-Khayri, J., Jain, S. M., and Johnson,D. (Cham: Springer International Publishing AG), 535–600. doi: 10.1007/978-3-319-91944-7_14

Rodríguez-Sanz, H., Manzanera, J. A., Solís, M. T., Gómez-Garay, A., Pintos, B., Risueño, M. C., et al. (2014). Early markers are present in both embryogenesis pathways from microspores and immature zygotic embryos in cork oak, *Quercus suber* L. *BMC Plant Biol.* 14, 224. doi: 10.1186/S12870-014-0224-4

Roussos, P. A., and Pontikis, C. A. (2002). *In vitro* propagation of olive (*Olea europaea* L.) cv. Koroneiki. *Plant Growth Regul.* 37, 295–304. doi: 10.1023/A:1020824330589

Rugini, E. (1984). *In vitro* propagation of some olive (*Olea europaea sativa* L.) cultivars with different root-ability, and medium development using analytical data from developing shoots and embryos. *Sci. Hortic.* 24, 123–134. doi: 10.1016/0304-4238(84)90143-2

Rugini, E. (1988). Somatic embryogenesis and plant regeneration in olive (*Olea europaea* L.). *Plant Cell Tissue Organ Cult.* 14, 207–214. doi: 10.1007/BF00043411

Rugini, E. (1995). Somatic embryogenesis in olive (*Olea europaea* L.) in *Somatic Embryogenesis in Woody Plants*, vol. Vol. II . Eds. Jain, S. M. , Gupta, P. K., and Newton, R. J. (Dordrecht: Kluwer Academic Publishers), 171–189.

Rugini, E., and Caricato, G. (1995). Somatic embryogenesis and plant recovery from mature tissues of olive cultivars (*Olea europaea* L.) 'Canino' and 'Moraiolo'. *Plant Cell Rep.* 14, 257–260. doi: 10.1007/BF00233645

San-José, M. C., Corredoira, E., Martínez, M. T., Vidal, N., Valladares, S., Mallón, R., et al. (2010). Shoot apex explants for induction of somatic embryogenesis in mature *Quercus robur* L. trees. *Plant Cell Rep.* 29, 661–671. doi: 10.1007/s00299-010-0852-6

Sefc, K. M., Lopes, M. S., Mendoca, D., Rodrigues dos Santos, M., Laimer da Câmara Machado, M., and Da Câmara Machado, A. (2000). Identification of microsatellite loci in olive (*Olea europaea*) and their characterization in Italian and Iberian olive trees. *Mol. Ecol.* 9, 1171–1193. doi: 10.1046/j.1365-294x.2000.00954.x

Shibli, R. A., Shatnawi, M., Abu-Ein, and El-Juboory, K. H. (2001). Somatic embryogenesis and plant recovery from callus of 'Nabali' Olive (*Olea europaea* L.). *Sci. Hortic.* 88, 243–256. doi: 10.1016/S0304-4238(00)00241-7

Toufik, I., Guenoun, F., and Belkoura, I. (2014). Embryogenesis expression from somatic explants of olive (*Olea europaea* L.) cv Picual. *Moroccan J. Biol.* 11, 17–25.

Vázquez, A. M. (2001). Insight into somaclonal variation. *Plant Biosyst.* 135, 57–62. doi: 10.1080/11263500112331350650

Vidoy-Mercado, I., Imbroda-Solano, I., Barceló-Muñoz, A., and Pliego-Alfaro, F. (2012). Differential *in vitro* behavior of the spanish olive (*Olea europaea* L.) cultivars 'Arbequina' and 'Picual'. *Acta Hortic.* 949, 27–30. doi: 10.17660/ActaHortic.2012.949.1

von Arnold, S. (2008). Somatic embryogenesis in *Plant Propagation by Tissue Culture, 3rd Edition. Vol. 1. The Background*. Eds. George, E. F., Hall, M. A., and De Klerk, G. J. (Dordrecht: Springer), 335–354.

Wang, Q. M., and Wang, L. (2012). An evolutionary view of plant tissue culture: Somaclonal variation and selection. *Plant Cell Rep.* 31, 1535–1547. doi: 10.1007/s00299-012-1281-5

Zuccherelli, G., and Zuccherelli, S. (2002). *In vitro* propagation of fifty olive cultivars. *Acta Hortic.* 586, 931–934. doi: 10.17660/ActaHortic.2002.586.204

Conflict of Interest: The authors declare that the research was conducted in the absence of any commercial or financial relationships that could be construed as a potential conflict of interest.

frontiers in Plant Science

ORIGINAL RESEARCH
published: 18 November 2019
doi: 10.3389/fpls.2019.01472

High-Throughput System for the Early Quantification of Major Architectural Traits in Olive Breeding Trials Using UAV Images and OBIA Techniques

Ana I. de Castro[1], Pilar Rallo[2], María Paz Suárez[2], Jorge Torres-Sánchez[1], Laura Casanova[2], Francisco M. Jiménez-Brenes[1], Ana Morales-Sillero[2], María Rocío Jiménez[2] and Francisca López-Granados[1]*

[1] Department of Crop Protection, Institute for Sustainable Agriculture (IAS), Spanish National Research Council (CSIC), Córdoba, Spain, [2] Departamento de Ciencias Agroforestales, ETSIA, Universidad de Sevilla, Sevilla, Spain

OPEN ACCESS

Edited by:
Antonio Diaz Espejo, Institute of Natural Resources and Agrobiology of Seville (CSIC), Spain

Reviewed by:
Wei Guo, The University of Tokyo, Japan
Jorge Gago, University of the Balearic Islands, Spain

***Correspondence:**
Ana I. de Castro
anadecastro@ias.csic.es

Specialty section:
This article was submitted to Crop and Product Physiology, a section of the journal Frontiers in Plant Science

Received: *12 January 2019*
Accepted: *22 October 2019*
Published: *18 November 2019*

Citation:
de Castro AI, Rallo P, Suárez MP, Torres-Sánchez J, Casanova L, Jiménez-Brenes FM, Morales-Sillero A, Jiménez MR and López-Granados F (2019) High-Throughput System for the Early Quantification of Major Architectural Traits in Olive Breeding Trials Using UAV Images and OBIA Techniques. Front. Plant Sci. 10:1472. doi: 10.3389/fpls.2019.01472

The need for the olive farm modernization have encouraged the research of more efficient crop management strategies through cross-breeding programs to release new olive cultivars more suitable for mechanization and use in intensive orchards, with high quality production and resistance to biotic and abiotic stresses. The advancement of breeding programs are hampered by the lack of efficient phenotyping methods to quickly and accurately acquire crop traits such as morphological attributes (tree vigor and vegetative growth habits), which are key to identify desirable genotypes as early as possible. In this context, an UAV-based high-throughput system for olive breeding program applications was developed to extract tree traits in large-scale phenotyping studies under field conditions. The system consisted of UAV-flight configurations, in terms of flight altitude and image overlaps, and a novel, automatic, and accurate object-based image analysis (OBIA) algorithm based on point clouds, which was evaluated in two experimental trials in the framework of a table olive breeding program, with the aim to determine the earliest date for suitable quantifying of tree architectural traits. Two training systems (intensive and hedgerow) were evaluated at two very early stages of tree growth: 15 and 27 months after planting. Digital Terrain Models (DTMs) were automatically and accurately generated by the algorithm as well as every olive tree identified, independently of the training system and tree age. The architectural traits, specially tree height and crown area, were estimated with high accuracy in the second flight campaign, i.e. 27 months after planting. Differences in the quality of 3D crown reconstruction were found for the growth patterns derived from each training system. These key phenotyping traits could be used in several olive breeding programs, as well as to address some agronomical goals. In addition, this system is cost and time optimized, so that requested architectural traits could be provided in the same day as UAV flights. This high-throughput system may solve the

actual bottleneck of plant phenotyping of "linking genotype and phenotype," considered a major challenge for crop research in the 21st century, and bring forward the crucial time of decision making for breeders.

Keywords: remote sensing, unmanned aerial vehicle, table olive, breeding program, training system, tree crown area and volume, point cloud

INTRODUCTION

The olive tree (*Olea europaea* L.) area amounts to more than 10 million hectares world-wide, with over 97% of this being concentrated in the Mediterranean Basin (FAOSAT, 2017; IOC, 2017). The olive industry plays a key economic role in this area, since it accounts for 96% of the world's olive production, i.e. 18.5 million tons approximately. Spain leads the world ranking both in production and surface area, followed by Greece, Italy, and Turkey (FAOSAT, 2017). In addition, Mediterranean countries are the largest consumers of olive oil with a quota about two-thirds of world consumption (IOC, 2017). Besides being one of the most important agro-food chains in the Mediterranean Basin, olive growing constitutes a key element of rural society as a significant source of income and employment for rural populations (Stilliano et al., 2016). Furthermore, olives are expanding to many regions outside the Mediterranean Basin such as the United States, Australia, China, and South Africa as well as other sub-tropical and warm temperate areas, making the olive tree the most extensively cultivated fruit crop in the world (FAOSAT, 2017). Besides, olive products are very appreciated not only as healthy food, but also in medical and cosmetic use (Fabbri et al., 2009).

The need for the modernization of olive farms in producing countries and its diffusion outside traditional areas of growth have led to farm investments to improve the productive framework through more efficient crop management strategies, such as irrigation, pruning and harvesting mechanization, and new training systems (e.g. super-high-density hedgerow). These new growing techniques are encouraging the development of cross-breeding programs to release new olive cultivars more suitable for mechanization and use in intensive orchards, with high quality production and resistance to biotic and abiotic stresses (Fabbri et al., 2009; Stilliano et al., 2016; Rallo et al., 2018). Plant breeding programs have benefited from recent advances in genomics and biotechnology by improving genotyping efficiency (Rugini et al., 2016), whereas the lack of efficient phenotyping methods still represents an important bottleneck in these programs (White et al., 2012). Traditional methods to collect phenotypic data (i.e. observable morphological traits related to growth, development, and physiology) rely on manual or visual sampling, which is time-consuming and laborious (Madec et al., 2017; Yang et al., 2017). Improving the acquisition of crop traits such as morphological attributes, flowering time, and yield has therefore become the main challenge limiting designing and predicting outcomes in breeding programs (Zaman-Allah et al., 2015). This aspect is particularly crucial for olive breeding due to the large genetic variability commonly obtained in seedling progenies (Rallo et al., 2018), coupled with the great complexity of collecting data on common large olive plots, which requires major logistical considerations (Araus and Cairns, 2014).

To overcome the challenge of automated and fast collection of phenotypic crop data, high-throughput phenotyping platforms have become crucial due to their ability to rapidly phenotype large numbers of plots and field trials at a fraction of the cost, time, and labor of traditional techniques (White et al., 2012; Zaman-Allah et al., 2015; Yang et al., 2017). Among the high-throughput phenotyping platforms for non-destructive plant data collection under field conditions such as autonomous ground vehicles (Shafiekhani et al., 2017; Virlet et al., 2017), tractor-mounted (Montes et al., 2007), pushed platforms (Bai et al., 2016), or cable-driven (Newman et al., 2018); unmanned aerial vehicles (UAVs) have been highlighted due to their capacity to generate field scale information using a wide range of sensors and operating on demand at critical moments and at low flight altitude, thus meeting the critical requirements of the spatial, spectral, and temporal resolutions of breeding programs (Shi et al., 2016; Tattaris et al., 2016; Yang et al., 2017; Ostos et al., 2018; Torres-Sánchez et al., 2018a). Nevertheless, little information exists on the use of UAVs for olive breeding. In this regard, Díaz-Varela et al. (2015) used a camera on board a UAV platform to estimate tree height and crown diameter in both discontinuous and continuous canopy systems of olive orchards. However, early phenotyping of olive trees (i.e., phenotyping in the first few years after planting) using UAVs has not been addressed. The genotype evaluation in olive cross-breeding programs usually follows a multi-step protocol that includes the initial evaluation of seedlings and their successive clonally propagated selections in field trials (Rallo et al., 2018). Each of these field stages (seedlings, pre-selections, advance selections, comparative trials) involves a high cost of maintaining a large number of trees over the years required for the evaluation of the target traits according to the breeding goals. Tree vigor and other architectural traits are relevant parameters to be evaluated in any of these breeding stages, since early vigor is known to be related to the juvenile period length in seedlings (De la Rosa et al., 2006; Rallo et al., 2008), and vegetative growth habits are key to evaluate the suitability of selected genotypes to be cultivated under different planting systems, such as superhigh density hedges (Hammamia et al., 2012; Rosati et al., 2013). Therefore, the ability to quantify these traits through cost-efficient methods in young trees would allow the identification of desirable genotypes as early as possible, thus saving time, labor, and money (Rallo et al., 2018). In addition, the knowledge of tree geometry can be used as a valuable tool to design site-specific management strategies (De Castro et al., 2018a).

Geometric traits can be estimated from 3D point clouds or Digital Surface Models (DSMs) based on UAV-imagery due to the ability of UAVs to fly at low altitudes with high image overlap (Torres-Sánchez et al., 2015; Yang et al., 2017; De Castro et al., 2018b). In the context of woody crops, these 3D models offer the rapid and accurate assessment of growth traits in poplar (Peña et al., 2018), vineyard (Matese et al., 2017; De Castro et al., 2018a), almond (Torres-Sánchez et al., 2018b), lychee (Johansen et al., 2018), and olive (Díaz-Varela et al., 2015; Torres-Sánchez et al., 2015; Jiménez-Brenes et al., 2017). Among these approaches, 3D point clouds have been highlighted for improving 3D reconstruction as they provide more height information (Z-value) at each coordinate (X,Y), while DSMs are defined as 2.5D datasets as they have only one height value at each 2D coordinate (Monserrat and Crosetto, 2008; Torres-Sánchez et al., 2018b). However, the large amount of detailed crop data embedded in the UAV-based 3D point clouds information requires the development and implementation of robust image analyses. In this regard, object-based image analysis (OBIA) techniques have reached high levels of automation and adaptability to high-data images. Furthermore, OBIA overcomes the limitations of pixel-based methods by segmenting images into groups of adjacent pixels with homogenous spectral values, called "objects", which are used as basic elements of the classification analysis where spectral, topological, and contextual information are combined, thus providing successful automatic classifications in complicated agricultural scenarios (Blaschke et al., 2014; Peña et al., 2015; López-Granados et al., 2016; De Castro et al., 2018b).

As per the above discussion, a UAV-based high-throughput system was developed and tested in experimental trials within an olive breeding program with the aim to quantify plant architectural traits of very young olive trees. To achieve this goal, a full protocol to collect the UAV images and create 3D point clouds was described, and a novel and customizable 3D point cloud-based OBIA was developed to characterize the 3D structure of the young plants, measured by tree height, crown area, and volume, in the first two years after planting, without any user intervention. In addition, the potential applications of these estimated olive plant traits for olive breeding programs were discussed.

MATERIALS AND METHODS

Study Fields

The experiment was carried out in two field trials located in Morón de la Frontera, Sevilla (Southern Spain). Both fields were planted in October 2015 in the framework of the University of Sevilla table olive breeding program, which were drip-irrigated, with flat ground and an approximate surface area of 1.20 ha each. The two trials were selected to account for differences in training systems: the intensive discontinuous canopy (intensive trial) and the super high density continuous hedgerow (hedgerow trial). The first trial (intensive trial) consisted of trees planted at a 7 × 5-m spacing (286 trees/ha) in a north–south orientation as single trunk open vase forming a discontinuous canopy of scattered trees (**Figures 1B, D**). Twenty-six olive genotypes (10 trees per genotype) were included in the intensive trial in a randomized design with two trees per elementary plot and five repetitions. In the second trial (hedgerow orchard), olive trees were planted in a 1.75 × 5 m pattern (1143 trees/ha) and trained to a central leader system, designed to form a continuous canopy later in crop development (**Figures 1A, C**). The hedgerow trial comprised of 14 olive genotypes arranged in a randomized design with rows of 20 trees per elementary plot and three repetitions (60 trees per genotype). The experiment was carried out at two different early stages of tree development: 15 months after planting, i.e., when the plants completed their first growth cycle in the field; and 27 months after planting, after 2 years in the field, which corresponded with each flight date. No pruning was performed during the experimental period to allow the genotypes following their own growth habit.

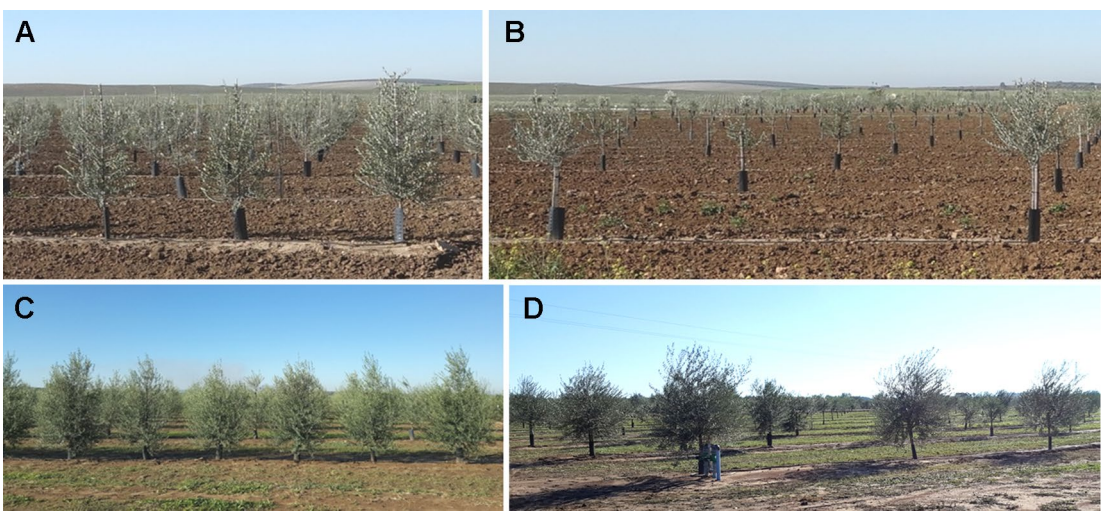

FIGURE 1 | General view of the olive field trial studied: **(A)** hedgerow trial and **(B)** intensive trial in 2017; and **(C)** hedgerow trial; and **(D)** intensive trial in 2018.

UAV-Based Phenotyping Platform

The remote images were acquired at midday on 16th January 2017 and 10th January 2018 with a low-cost commercial off-the-shelf camera, model Sony ILCE-6000 (Sony Corporation, Tokyo, Japan) mounted in a quadcopter model MD4-1000 (microdrones GmbH, Siegen, Germany), which was modified and calibrated to capture information in both NIR and visible light (green and red) by removing the internal NIR filter commonly present in the visible cameras and adding a 49-mm filter ring to the front nose of the lens, all done by the company Mosaicmill (Mosaicmill Oy, Vantaa, Finlandia) (**Figure 2**). This model has a 23.5 × 15.6 mm APS-C CMOS sensor, capable of acquiring 24 megapixel (6,000 × 4,000 pixels) spatial resolution images with 8-bit radiometric resolution (for each channel), and is equipped with a 20 mm fixed lens. The flights were carried out at the same time as the on-ground data were taken to ensure the same meteorological conditions, which consisted of sunny days with calm winds. Moreover, similar weather conditions were reported between flight campaigns.

The UAV can either be manually operated by radio control (1,000 m control range) or execute user-defined flight routes autonomously by using its Global Navigation Satellite System (GNSS) receiver and its waypoint navigation system. The UAV is battery powered and can load any sensor weighing up to 1.25 kg. The camera was mounted in the UAV facing downward for nadir capture, and the UAV routes were designed to take images at 50 m flight altitude, resulting in a spatial resolution of 1 cm pixel size, and with forward and side overlaps of 93% and 60%, respectively, which are large enough to achieve the 3D reconstruction of olive orchards, according to previous research (Torres-Sánchez et al., 2015; Torres-Sánchez et al., 2018a). Every yearly campaign consisted on a unique 15-min flight for both field trials that covered a surface of 5 ha. The flight operations fulfilled the list of requirements established by the Spanish National Agency of Aerial Security including the pilot license, safety regulations, and limited flight distance (AESA, 2017).

Point Cloud Generation

A 3D point cloud was generated by using the Agisoft PhotoScan Professional Edition software (Agisoft LLC, St. Petersburg, Russia) version 1.4.4 build 6848. The process was fully automatic, with the exception of the manual localization of six ground control points in the corners and in the center of each field trial with a Trimble R4 (Trimble, Sunnyvale, CA, USA) to georeference the 3D point cloud. The GPS worked in the Real Time Kinematic (RTK) model linked to a reference station of the GNSS RAP network at the Institute for Statistics and Cartography of Andalusia (IECA), Spain. This GNSS-RTK system provided real time-corrections that resulted in an accuracy of 0.02 m in planimetry and 0.03 m in altimetry. The whole automatic process involved two main stages: 1) aligning images, and 2) building field geometry. First, the camera position for each image and common points in the overlapping images were located and matched, which facilitated the fitting of camera calibration parameters. Next, the point cloud was built based on the estimated camera positions and the images themselves by applying the Structure from Motion (SfM) technique (**Figure 3**). Thus, every point consisted of x, y, and z coordinates, where z represents the altitude, i.e., the height above sea level. The point cloud files were saved in the ".las" format, a common public file format that allows the exchange of 3D point cloud data. More details about the software processing parameters are given in De Castro et al. (2018a).

OBIA Algorithm

The OBIA algorithm for the identification and characterization of the olive seedling was developed with Cognition Network programming language in the eCognition Developer 9.3 software

FIGURE 2 | The MD4-1000 UAV flying over the intensive trial in the second studied date (January 2018).

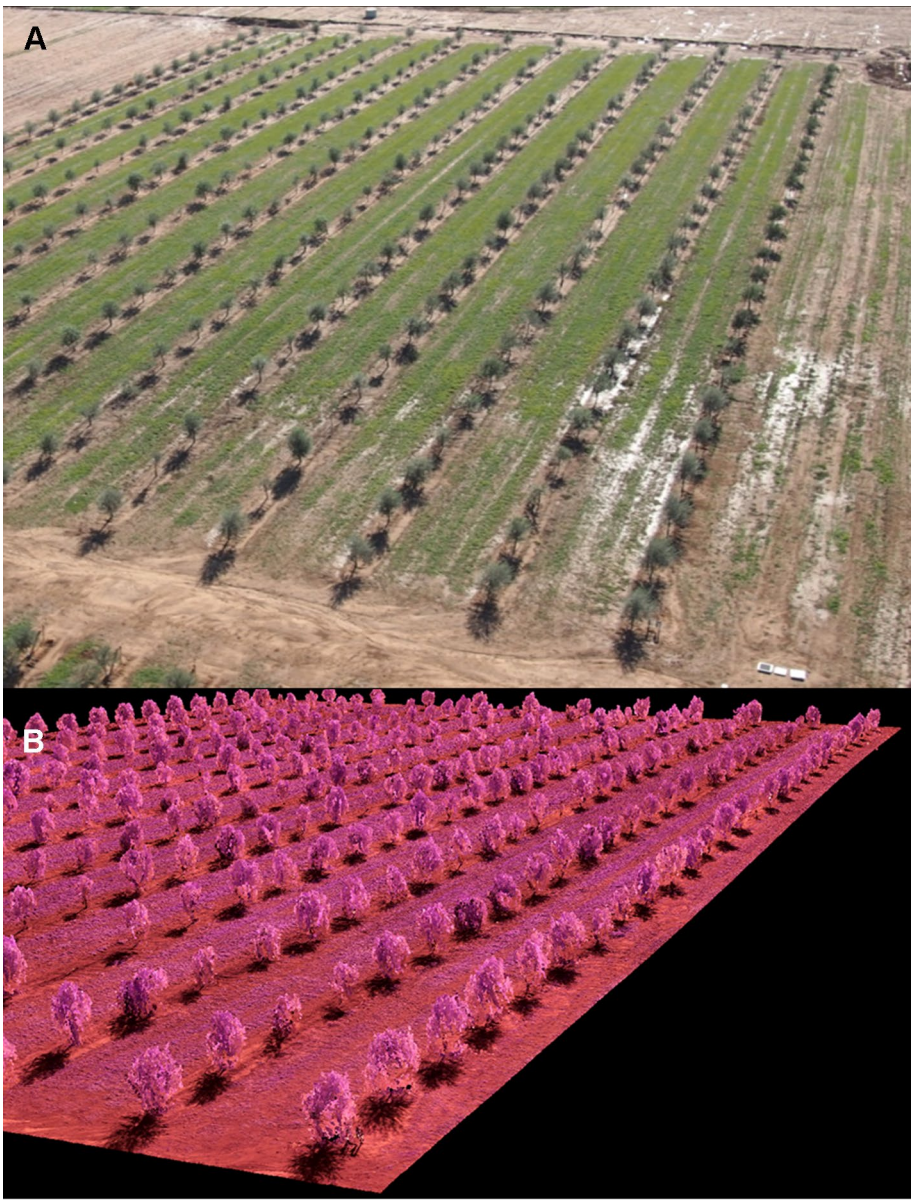

FIGURE 3 | (A) General View of the Intensive Field Trial-2018; and **(B)** Partial View of the Corresponding 3D Point Cloud Produced by the Photogrammetric Processing of the Remote Images Taken With the UAV Platform.

(Trimble GeoSpatial, Munich, Germany). The algorithm is fully automatic, it therefore requires no user intervention, and was composed of a sequence of phases (**Figure 4**), using only the 3D point cloud as input, as follows:

1. *Digital Terrain Model (DTM) generation*: A chessboard segmentation algorithm was used to segment the point cloud in squares of 2 m side size based on the studied olive tree dimension and the planting patterns (**Figure 4A**). Each square was then assigned a height value corresponding to the average of 15% of the lowest height points to create the DTM layer (**Figure 4A**), i.e., a graphical representation of the terrain height without any objects like plants and buildings, as based on previous studies (Torres-Sánchez et al., 2018b).
2. *Tree point cloud creation*: First, the height above the terrain of every point composing the cloud was obtained based on the DTM. Next, the 0.3 m value was used as the suitable threshold to accurately identify tree points and therefore create the tree point cloud (**Figure 4B**). This threshold was based on the tree size in the stage studied and the lack of cover crops. The height threshold is an easily implemented and accurate tool used for olive detection, either from the UAV photogrammetric point cloud (Fernández et al., 2016) or terrestrial laser scanner point cloud (Escolà et al., 2017).

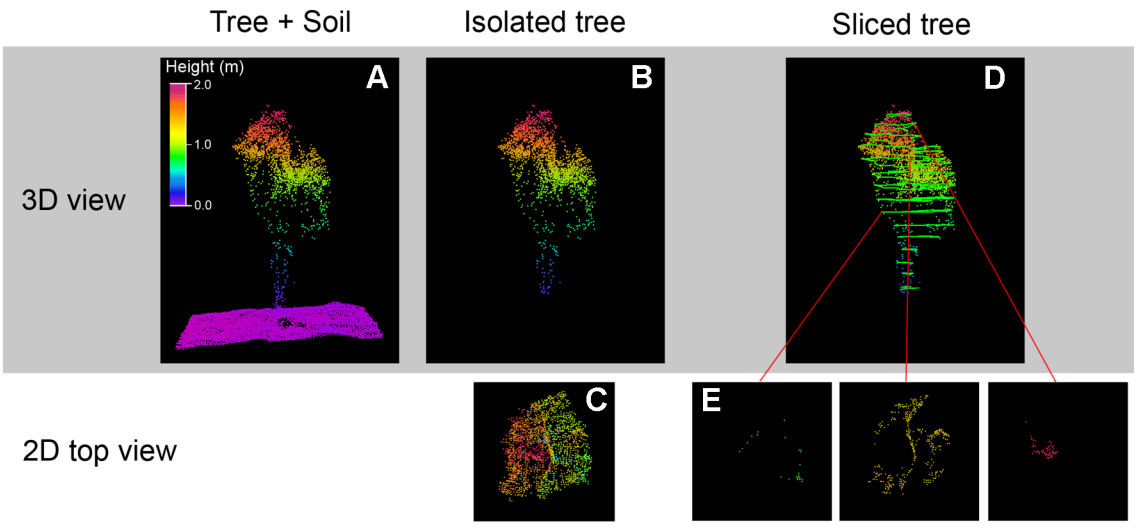

FIGURE 4 | Graphical examples of the Object Based Image Analysis (OBIA) procedure outputs for identification and characterization of the olive seedling: **(A)** 3D point cloud for a square of 2 m side size, DTM is represented in pink color; **(B)** tree point cloud; **(C)** 2D representation, following the x,y axes, of the tree point cloud; **(D)** sliced tree point cloud along Z axis; **(E)** points belonging to the point cloud included in the selected slice portion.

3. *Tree crown delineation*: After tree point identification, a grid of 0.1 m size was overlaid on the terrain and every projected square with the presence of a tree point was classified as tree, which were then merged to compound each individual tree crown. This parameter was fixed to 0.1 m to be well suited for tree reconstruction using UAV imagery (Torres-Sánchez et al., 2018b).
4. *Point cloud slicing*: Once the tree point cloud was divided into 2D-squares following the x,y axes, the tree point cloud was then segmented into slices from bottom to top along the Z axis according to intervals of 0.1 m (**Figure 4D**) resulting in 3D-grids (voxels) with 0.1 m side. Therefore, the point cloud was included into a tridimensional regular grid composed by small volumetric units (voxels) to be processed. Next, a new image layer called "Voxels" with a resolution of 0.1 m, similar to the voxel size, was created at the ground level, where each pixel stored the number of voxels above (i.e. voxels with the same x,y coordinates at different heights) containing points of the olive crown. The voxel size was set at 0.1 m according to Phattaralerphong and Sinoquet (2005), who reported that the optimal voxel sizes for crown volume estimates ranged from 10 to 40 cm. The size of the voxel has previously been related to the accuracy of the crown volume estimate (Park et al., 2010; Li et al., 2013; Zang et al., 2017), the larger the voxel size, the greater the estimation accuracy. However, oversized voxels lead to the creation of few voxels resulting in statistically insignificant descriptions of canopy features. Thus, taking into account the small size of the olive trees, 0.1 m was selected as the optimal voxel size.
   The voxel-based methodology is considered one of the more advanced techniques for accurately reproduced the tree (Hosoi and Omasa, 2006), where the voxel is the smallest information unit element of a three-dimensional matrix. This methodology allows process the coordinates of each voxel, analyze 3D-models as digital images and consider points measured from successive shots as a single voxel without oversampling (Fernández-Sarría et al., 2013), making voxel-based methodology one of the most useful methods in point cloud analysis. It has been successfully used in tree point cloud analysis generated by LiDAR (Hosoi and Omasa, 2006; Fernández-Sarría et al., 2013; Underwood et al., 2016) and photogrammetric techniques (Gatziolis et al., 2015; Dandois et al., 2017; Torres-Sánchez et al., 2018b).
   Due to the difficulty in obtaining information inside the tree crown of the UAV-photogrammetric approach, the squares surrounded by the crown limit were classified as tree crown, and those voxels taken into account in the process.
5. *Olive tree characterization*: For every olive tree, the volume occupied by the crown was automatically quantified in each pixel of the "Voxels layer" by multiplying the number stored, i.e. voxels containing olive crown points, and the voxel volume ($0.1 \times 0.1 \times 0.1$ m^3). Similarly, Underwood et al. (2016) calculated the crown volume in almond orchards using terrestrial LiDAR point clouds. Furthermore, the maximum height of each olive was calculated by subtracting the highest height value of the pixels that composed the olive crown to the DTM. Then, the rest of the geometric features (width, length, and projected area) were automatically calculated for every crown tree object delimited in a previous step (*Tree crown delineation*) of the process. Finally, the geometric features of each olive, as well the identification and location, were automatically exported as vector (e.g., shapefile format) and table (e.g., Excel or ASCII format) files.

The algorithm was fully automatic and common for both planting patterns and training systems, with only one exception in the *Tree crown delineation* phase for the super high density continuous hedgerow (hedgerow trial) on the second date. In this

training system, the tree exhibited adjacent canopies, starting the formation of a continuous canopy, i.e., a hedgerow trial, making it difficult to isolate the individual crown (**Figure 1C**). Thus, to solve this limitation, the location of every tree exported on the first date was used to identify each olive tree on the second date, so any square classified as "Tree" with its center at a distance of 1 m from the center of a tree was considered as part of that same tree. This 1 m-value was set taking into account the distance between trees. If no UAV image was available prior to the interception of the crowns, this issue could be solved by employing the planting pattern (distance between trees) or a grid with the position (x,y coordinates) of each tree.

Segmentation and slicing tasks are difficult, time consuming, and mostly performed by a human operator (Woo et al., 2002), thus the automation of these process in an OBIA algorithm enables objectivity and makes the olive characterization process time-efficient, reliable, and more accurate, removing errors from a subjective manual process.

Validation

DTM Generation

The point cloud-based DTM created for each training system and date was compared to the official DTMs extracted from the IECA (Andalusian Institute for Statistics and Cartography, Spain), a public body that guarantees the organization, coordination, rationality, and efficiency of cartographic production in Andalusia (IECA, 2018). This official information is generally updated every 10–15 years and does not have enough high resolution in all areas of the region.

The validation of the DTM was carried out on the basis of a 20 m grid over the studied fields by using ArcGIS 10.0 (ESRI, Redlands, CA, USA), resulting in 28 and 24 validation data points for the intensive and hedgerow training systems, respectively (**Figure 5A**). The distribution and quantity of the validation points made it possible to analyze the height variability in these field conditions. Then, the official IECA-DTM-based heights were compared to those estimated by the OBIA algorithm, and the coefficient of determination (R^2) derived from a linear regression model was calculated using JMP software (SAS, Cary, NC, USA).

Olive Tree Identification and Geometric Traits Validation

Individual olive trees were visually identified in the mosaicked and compared to the image classification process outputs, i.e. the individual tree point cloud, and the coincidence was measured by calculating the counting accuracy (Eq. 1)

$$Counting\ accuracy = \frac{OBIA\ identified\ olive\ trees}{Visual\ observed\ olive\ trees} \times 100 \quad (1)$$

For tree geometric features validation, manually ground-based measurements of trees were taken in each field trial and date coinciding with the image acquisition (**Figure 5B**). Three geometric traits, namely tree height, crown area, and volume, were evaluated by comparing the OBIA estimated value and the on-ground observed values (true data). In the case of intensive trials, all traits were measured in each individual tree (244 trees); in the case of hedgerow trials, the tree height was also surveyed in all individuals (806 trees), and due to time and labor limitations, the canopy features were measured at 4 individual trees per elementary plot (164 trees). The validation trees were identified in the field and located their position in the mosaicked images.

The height of the tree, as measured up to the apex of the top of the tree, was taken with a telescopic ruler. In addition, the height and crown diameters (maximum projected horizontal width and its perpendicular) were acquired using a tape, and the crown area and volume were estimated assuming a circle (Eq. 1) and a cone-shaped (Eq. 2) form, respectively, applying validated methods (Eq. 2 and Eq. 3) for olive tree geometric measurements (Pastor, 2005), as follows:

$$Field\ crown\ area = \pi\left(\frac{D_1 + D_2}{4}\right)^2 \quad (2)$$

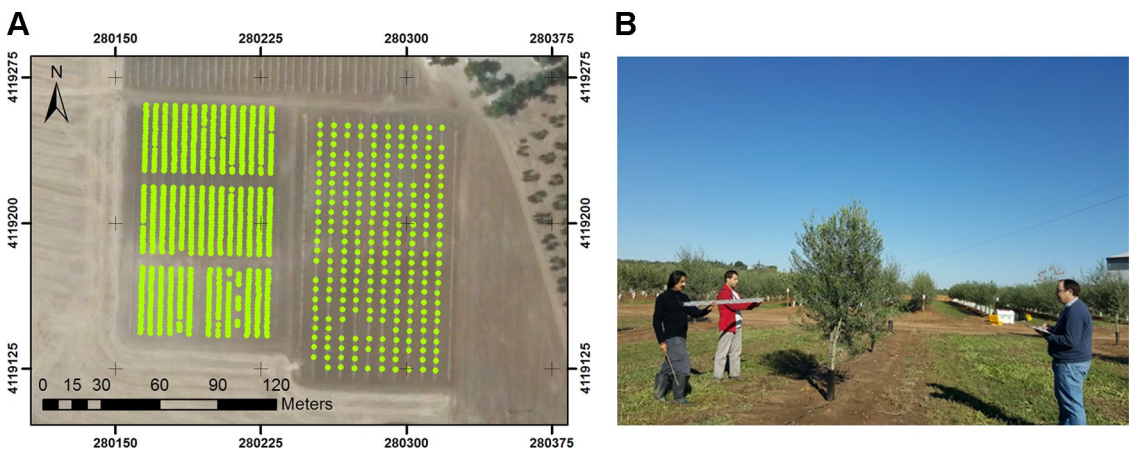

FIGURE 5 | Experimental set for validation: **(A)** point grid for DSM validation in both the hedgerow and the intensive trial; **(B)** manual measurements of olive crown width. The individuals in this manuscript have given written informed consent to publish these case details.

where D_1 is the is the widest length of the plant canopy through its center, and D_2 is the canopy width perpendicular to D_1.

$$Field\ crown\ volume = \frac{Field\ crown\ area \times Measured\ canopy\ height}{3} \quad (3)$$

Then, the on-ground measures were compared to the OBIA-estimated values in order to assess the efficacy of the OBIA algorithm to estimate the olive traits of the very young plants. The coefficient of determination (R^2) derived from a linear regression model was calculated using JMP software (SAS, Cary, NC, USA). The coefficient of determination (R^2) is the proportion of the variance in the dependent variable that is predictable from the independent variable (Mendenhall et al., 2009), whereas the root mean square error (RMSE) is the standard deviation of the residuals, i.e. prediction errors (Barnston 1992). Additionally, the bias statistic was also calculated for the height comparison (Eq. 4), which measures the difference between the expected value of the estimator and the actual value of the parameter being estimated and evaluates its tendency to overestimate or underestimate that parameter (Lehmann 1951).

$$Bias = \frac{y_m - x_m}{x_m} \times 100\% \quad (4)$$

where x_m is the mean height value of all field-measured trees, and y_m represents the mean detected OBIA height.

RESULTS

Point Cloud and DTM Generation

High density point clouds were generated due to the large image overlap, based on the flight configuration, and the high spatial resolution of the UAV-imagery (**Figure 6**). The number of points in the cloud ranged from 4,136 points/m^2 in the intensive trial in 2017 to 4,782 points/m^2 in the hedgerow orchard in 2018 (**Table 1**). No major differences in point density were found between the training systems. However, the number of points was greater on the second flight date due to the larger size of the trees at the second flight date, i.e., 27 months after planting, as the ground point density remained constant. This greater number of points suggests that a higher accuracy in geometric features estimation could be reached, as there is a strong underlying control of the 3D reconstruction quality based on point cloud density (Dandois et al., 2015).

As for the DTM, the algorithm generated it automatically and accurately from the point clouds achieving very high correlation with the official IECA-DTM for both intensive (R^2 = 0.90) and hedgerow trials (R^2 = 0.95), independently of the year and tree age. These results proved the suitability of the UAV-flight configuration to create appropriate point clouds as well as the performance of the OBIA algorithm for proper DTM generation. Some of the validation points for the hedgerow trial were dismissed in the comparison with the IECA-DTM as an anomalous area was found in this official DTM, making these validation points unusable.

Olive Tree Detection

The OBIA algorithm successfully identified the olive trees, obtaining accuracy values higher than 93% in all of the studied cases (**Table 2**), with independence of the training system and olive age, which demonstrated the OBIA-algorithm's robustness for tree detection at these early stages of growth. Furthermore, higher accuracy values were achieved in the later year of the

TABLE 1 | Point density for each flight date and training systems.

Flight dates	Training systems	Point density (points/m^2)
First year after planting	Intensive	4,136
January 2017	Hedgerow	4,152
Second year after planting	Intensive	4,441
January 2018	Hedgerow	4,782

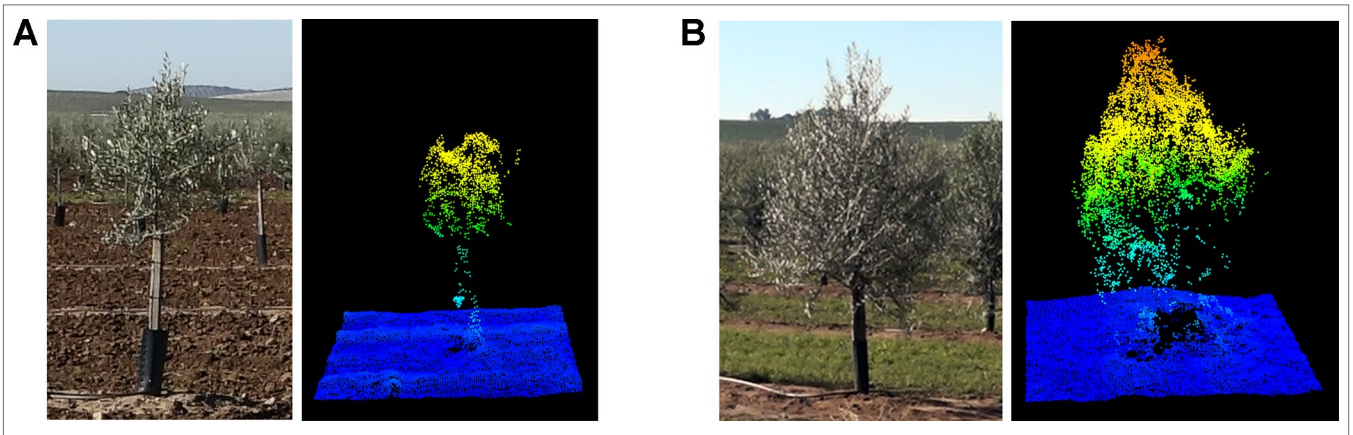

FIGURE 6 | Field photograph and tree point cloud for an olive tree composing the intensive trial in the consecutive years of data collection: **(A)** January 2017—15 months after planting; **(B)** January 2018—27 months after planting.

TABLE 2 | Accuracy attained by the OBIA algorithm in the olive tree detection.

Months after planting	Training systems	Field trees	OBIA detected trees	Accuracy (%)
15	Hedgerow	806	764	94.8
	Intensive	244	228	93.4
27	Hedgerow	804	794	98.8
	Intensive	243	243	100

study, i.e. 27 months after olive tree planting, reaching maximum precision or very close values, with results of 100% and 98.8% for intensive and hedgerow, respectively. This fact points out that, although it was possible to accurately create the tree point cloud and detect the olive trees at any of the studied olive ages, olive tree characterization could be affected by the plant age at these early stages.

Olive Tree Characterization

Height of Olive Tree

A summary of the field height measurements and those estimated by OBIA for the matched trees in both studied dates and trials at field level is shown in **Table 3**. Height data for both training systems were analyzed by performing an analysis of variance (ANOVA) at the 0.05 level of significance by a Tukey Honestly Significant Difference (HSD) range test using JMP software (JMP 12, SAS Institute Inc., Campus Drive, Cary, NC, USA 27513) (**Table 3**). Significant differences in height data between hedgerow and intensive systems were observed in all comparisons, with the exception of the OBIA estimated outputs at the first date. This fact suggests that manual measurements were able to detect differences in height growth caused by the training system on both dates, where the algorithm could only do so on the second date.

Analysis of variance of both measured and estimated height data between dates were also performed (data not shown) and significant differences were obtained in all of them, thus showing that both approaches (manual and estimated) detected the annual height growth. According to the field height measurements, height annual growth for intensive and hedgerow trials was 50.6% and 50.7%, respectively.

Based on the results shown in **Table 3**, the OBIA-estimated minimum values were lower than the field measurements, especially in 2017 due to the small size of some of the trees. The height estimates showed wider ranges of variation than the field measurements in all cases; although these differences were much smaller for the experiments in 2018. A similar trend was found for the average height, also obtaining greater agreement between the true and estimated measurements for the 2018 data. Thus, the height estimates were strongly influenced by the age of the olive plant at these growth stages, as stated above. It should be noted that the olive trees in the second year, i.e. 27 months after planting, were 3D reconstructed with a higher quality, as they showed values similar to those field measurements, suggesting that from this age, the estimation of this breeding trial at the individual tree level might be feasible.

Figure 7 shows the accuracy and graphical comparisons of the measured versus OBIA-estimated height at the individual tree level as affected by the pattern system and the olive tree age. As expected from the above results, correlations obtained for images taken in the first studied date (15 months after planting) were slightly lower than those reported for the second date (27 months after planting), i.e. after a growth cycle. At that first flight campaign, olive trees in an intensive pattern system achieved acceptable correlation values ($R^2 = 0.61$), higher values than those reported by Díaz-Varela et al. (2015) using UAV imagery reconstruction based on DSM ($R^2 = 0.53$) for height tree calculation of olive 5 years and 7 years after planting, i.e. with a larger size, which points out the feasibility of the our developed point-cloud based OBIA algorithm for the estimation of olive tree height in this growing system at the early age of 15 months after planting. No accurate results were obtained for hedgerow pattern at this first growth age.

Referring to the second flight campaign, low nRMSE (defined as the ratio of RMSE and the average value measured) values of 6.4 for intensive and 5.8 for hedgerow and R^2 values around 0.80 were reported for both training systems. Similarly, De Castro et al. (2018a) reached a very high correlation ($R^2 = 0.78$) in plant height estimation using UAV imagery and the OBIA approach in adult vineyards. Therefore, our results indicated that the OBIA algorithm accurately estimated the olive height at 27 months after planting, independent of the training system.

TABLE 3 | Summary of the field measured height and OBIA-estimated height for the matched trees at field scale.

	Months after planting	Training systems*	Minimum	Maximum	Range	Average	Standard deviation
Field data	15	Hedgerow	0.59	2.26	1.67	1.67a§	0.37
		Intensive	0.70	2.30	1.60	1.56b	0.28
	27	Hedgerow	1.15	3.25	2.10	2.51a	0.30
		Intensive	1.25	2.95	1.70	2.34b	0.31
OBIA data	15	Hedgerow	0.00	2.78	2.78	1.33a	0.55
		Intensive	0.34	2.28	1.95	1.30a	0.39
	27	Hedgerow	0.89	3.04	2.15	2.29a	0.32
		Intensive	1.25	3.09	1.84	2.22b	0.34

**764 and 228 trees for hedgerow and intensive trials, respectively in 2017; and 794 and 243 trees for hedgerow and intensive trials, respectively in 2018.*
§ For each column and months after planting mean values followed by different letter are statistically different at p = 0.05 (analysis of variance (ANOVA) by a Tukey Honestly Significant Difference (HSD) range test).

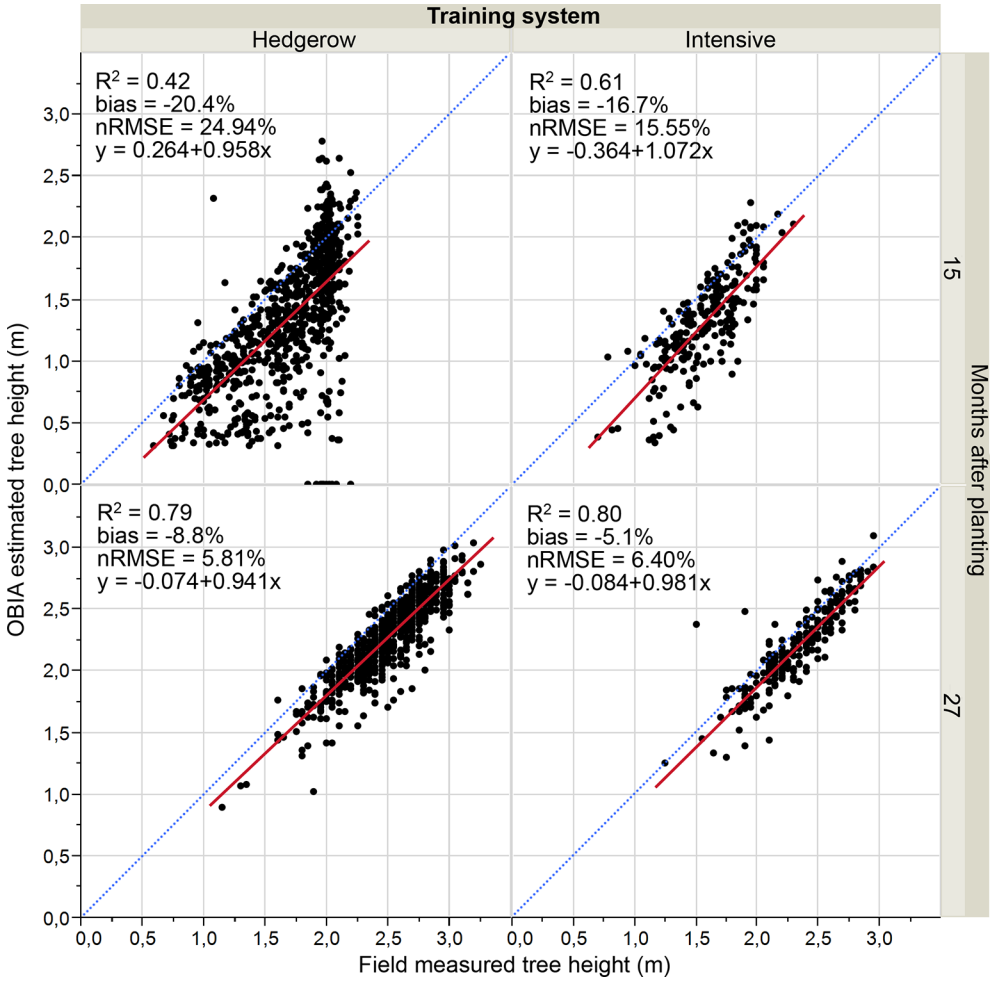

FIGURE 7 | Point cloud-OBIA estimated height vs. measured olive height divided by training system and tree age. The relative root mean square error (nRMSE) and coefficient of determination (R^2) derived from the regression fit are included for every scenario (p 0.0001). The red solid line is the fitted linear function and the blue dashed line represents the 1:1 line.

For both studied dates and growing systems, the comparison of the regression line with the 1:1 line and the negative bias indicated that the automatic OBIA algorithm underestimated the tree height parameter, especially on the first date that showed bias values higher than 16.7% for both patterns. The respective bias values for the second campaign images ranged from −5.1% to −8.8%, results comparable to those reached in the crown base height estimation of individual conifer trees in a forest scenario of 3.4% (Luo et al., 2018). Moreover, it should be pointed out that the underestimation was smaller for the intensive open vase orchard.

Olive Crown Parameters

Results of the validation work of the crown parameters, which consisted of comparing the OBIA estimated values to the calculated field data, are shown in **Figures 8** and **9** for areas and volumes, respectively. Much better correlations were achieved for both parameters in the 2018 data, i.e. the second flight campaign, thus following the same trend as the tree height. Similarly, the OBIA procedure also tended to a subtle underestimation of the crown parameters.

Analyzing the 2017 crown parameters results (**Figures 8A** and **9A**), both area and volume fits had low R^2 with slight variations between the two crop systems, for example, $R^2 = 0.48$ for the area parameter in both systems, and medium relative errors around 21%. In the case of the second campaign (**Figures 8B** and **9B**), the correlations were strengthened reaching higher determination coefficients, e.g. R^2 values of 0.63 and 0.79 for the area comparison in the hedgerow system and volume in the intensive orchard, respectively. Minor errors were also reported for crown area comparison that ranged from 12.7% and 14.8%. And further, the points got much closer to the 1:1 line distribution, although they indicated a tendency to underestimate the results, as most of the points were below the 1:1 line. The better findings could be due to the bigger size of the tree at that date. In the analysis by training system in that latter campaign, a better fit of the OBIA estimated

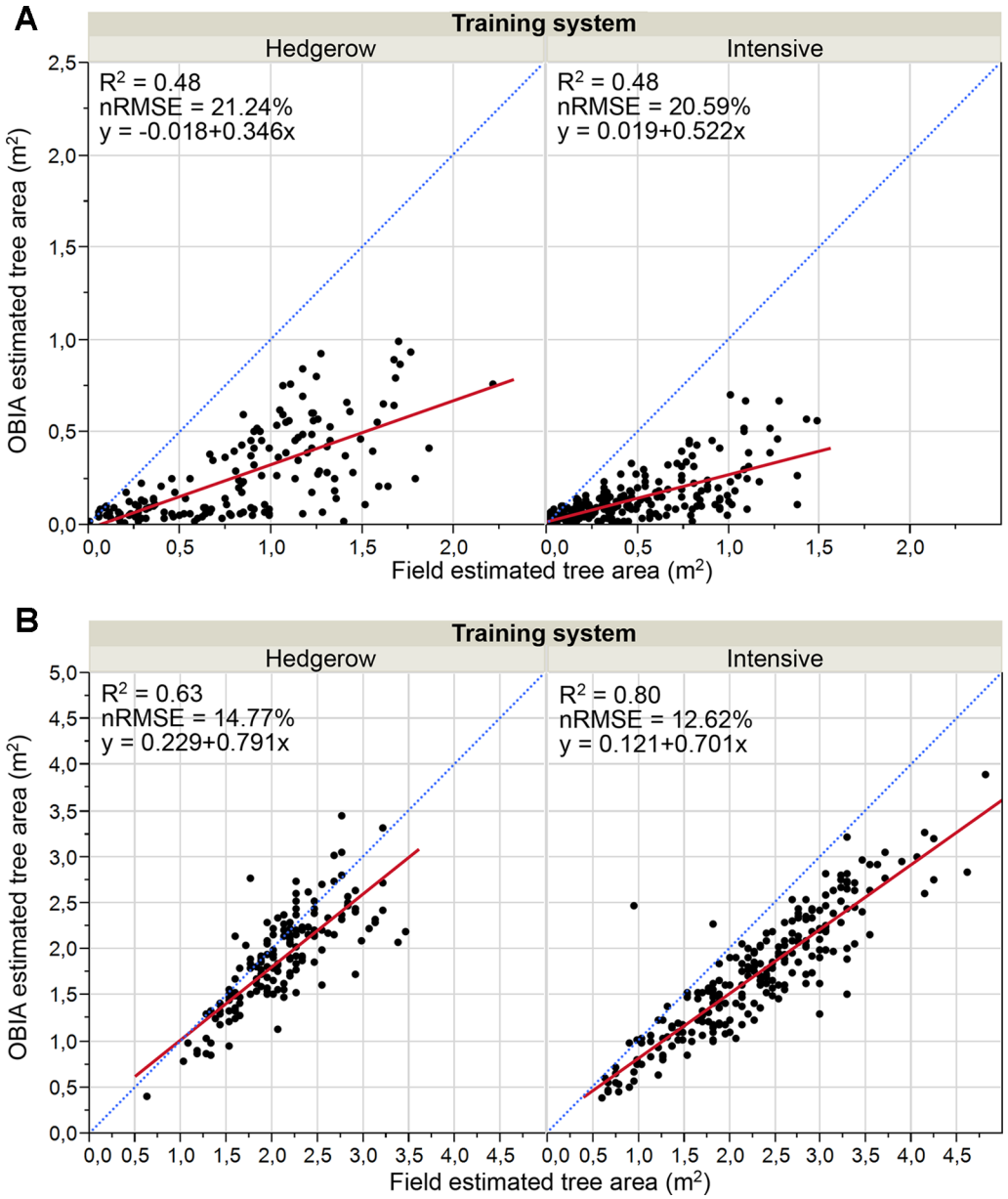

FIGURE 8 | Graphical comparisons of Point cloud-OBIA estimated and field estimated crown area by training system in: **(A)** January 2017, 15 months after olive plantation; **(B)** January 2018, 27 months after olive plantation. The normalized root mean square error (nRMSE) and coefficient of determination (R^2) derived from the regression fit are included for every scenario (p 0.0001). nRMSE was computed as the percentage of the average of measured values of tree variables. The red solid line is the fitted linear function and the blue dashed line represents the 1:1 line.

values to the manual truth data for canopy area and volume were achieved in the intensive orchard, which reported R^2 of 0.79 and 0.80, respectively.

However, the determination coefficients for both crown parameters in the hedgerow orchards were slightly lower than those reported for the intensive one, e.g., R^2 = 0.63 for area estimation (**Figure 8B**).

In summary, OBIA crown estimates of the olive trees in the first flight year were lower than those of the second year, i.e., 27 months after plantation, when the olive trees appear to reach a suitable size to be reconstructed using the point cloud-based OBIA algorithm developed. No clear differences in olive crown reconstruction were shown between both pattern systems using images at 15 months after olive plantation. Although the OBIA algorithm allowed the 3D reconstruction of the whole tree or hedgerow crown in the second year (**Figure 6**), better results were achieved in both the area and volume parameters for intensive orchards. In addition, the results showed a better fit for the canopy area than for the volume in all of the analyzed cases, reaching higher R^2 values.

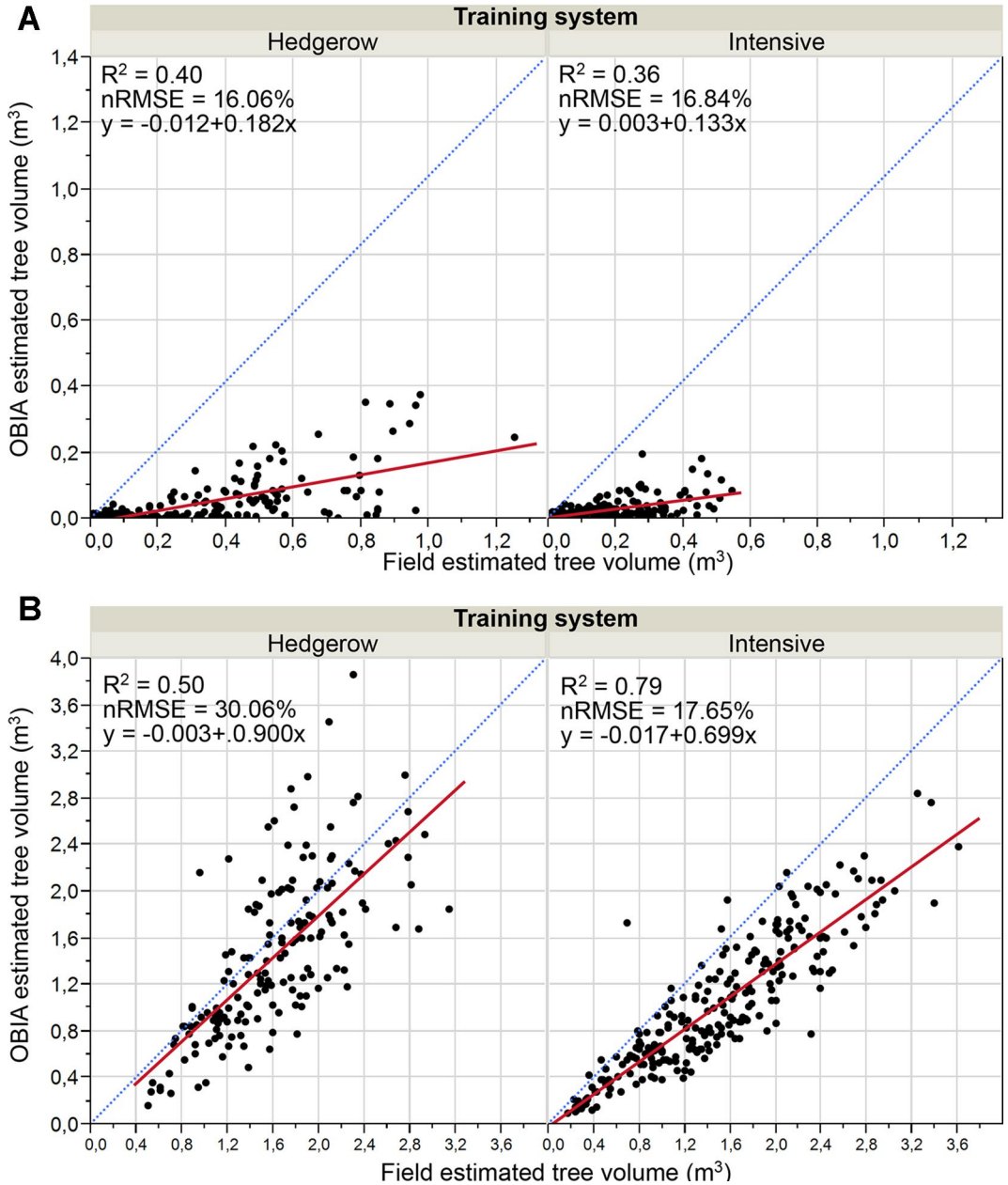

FIGURE 9 | Graphic comparisons of Point cloud-OBIA estimated and field estimated crown volume by pattern system in: **(A)** January 2017, 15 months after olive plantation; **(B)** January 2018, 27 months after olive plantation. The normalized root mean square error (nRMSE) and coefficient of determination (R^2) derived from the regression fit are included for every scenario (p 0.0001). nRMSE was computed as the percentage of the average of measured values of tree variables. The red solid line is the fitted linear function and the blue dashed line represents the 1:1 line.

DISCUSSION

The objective of this research was to develop an UAV-based high-throughput system for olive breeding program applications, which consisted of UAV-flight configurations, in terms of flight altitude and image overlaps, and a novel, automatic, and accurate OBIA algorithm development. The system was evaluated in two experimental trials in the framework of the University of Sevilla table olive breeding program, with the aim to determine the earliest date for the suitable and precocious quantifying of architectural traits in large numbers of individuals under field conditions. Thus, two training systems were evaluated at two very early tree growth stages: 15 and 27 months after planting.

The flight configuration led to the generation of high density point clouds with around 4,500 points/m^2 and the automatic and accurate DTM generation by means of the OBIA algorithm. In addition to the flight altitude and image overlap, which are defined in the flight configurations, the number of points are also

strongly affected by the sensor spatial resolution (Dandois et al., 2015). In that sense, Torres-Sánchez et al. (2018b) obtained point clouds with half the density using the same flight configuration as in our experiment, but with a camera sensor size of 4,032 × 3,024 pixels, i.e. half the spatial resolution that the camera used in our study, which was quantified sufficient for the accurate detection of almond trees and the estimation of geometric characteristics. Therefore, both the sensor and flight configuration used in our research were considered suitable for DTM generation.

The accuracy of the DTM, directly affected by point cloud densities, is a critical issue for 3D tree characterization, as reported by Dandois et al. (2015) and Torres-Sánchez et al. (2018a) in woody crops, and the basis for the calculation of height-related trials (Dandois and Ellis, 2010), so the higher the quality in the DTM generation, the more precise the tree height estimation. In addition, the olive trees were also successfully identified by the OBIA algorithm from the DTMs, independent of the pattern system and olive age. The fact that no differences in tree detection and DTM generation were found between both training systems suggests that the growth patterns derived from each system were not significantly different at those tree ages for these specific goals, proving the robustness of this algorithm in those scenarios. Moreover, the accurate and automatic DTM created by the OBIA algorithm could be used not only as the first step in the procedure of quantifying breeding olive traits at early stages, but also as a valuable tool for generating accurate DTMs in agricultural studies, since the official DTMs extracted from the IECA are not always up-to-date, do not have enough spatial resolution in some areas of the region or accounts with faulty points, as previously reported. In addition, the automatic tree detection process, especially of small plants, could be a useful tool for some agricultural demanding tasks, for example, to count individual plants in nurseries due to their large fields and logistical considerations (De Castro et al., 2018c).

The OBIA algorithm was developed to generate agronomical traits considered key targets in olive phenotyping studies such as tree height, area, and volume of the crown, so that breeders can use those architectural traits to select the best genotypes according to desired objectives. For the olive tree height, the estimates were affected by tree size, and directly related to tree age, achieving much better accuracies for bigger olives, i.e., 27 months after planting. At that tree age, the tree height trait acquisition is feasible regardless of the evaluated training systems. However, only trees growing in the intensive system could be moderately reconstructed in the case of olive plants 15 months after planting, which may be because this system encourages free growth without any dominance directed from the height of the last tie (**Figure 1A**), making the trees reach less height, but in a uniform way in all the points of the crown (Innovagri, 2018). On the other hand, the hedgerow pattern employs a central axis formation system that promotes the growth of the terminal bud that acts as a guide, as opposed to the lateral shoots (**Figure 1B**), thus prioritizing height growth (Innovagri, 2018). These differences in growth due to training system become more accentuated in the early years. In fact, the growth pattern had a significant influence on the underestimation of the height trial, which was especially marked for the hedgerow pattern in 2017 as the generated point cloud did not detect the narrow apexes in the top of the olive trees due to this structure of the olive trees, which in contrast, were considered in the on-ground validation measurements. These findings are in agreement with those of Díaz-Varela et al. (2015) in an olive orchard of individual olive trees 5 and 7 years after plantation, and Peña et al. (2018) in a 1-year-old poplar plantation, in which the undervalues were assigned to the rough reconstruction of the final apex. Similarly, Kattenborn et al. (2014) found a general underestimation in the height trait of palm trees using UAV-based photogrammetric point clouds and stated that extend height deviations are indispensable, making difficult the sub-decimeter accuracy, which might be attributed to uncertainties in the reference data acquisition.

Similar considerations about automatic estimations were found for olive crown parameters: underestimation of the OBIA values; and much better correlations in the second studied date due to the greater crown size by the growth of the trees during the 12 months after the first campaign (**Figure 1** and **Table 2**), and for intensive orchards because of the more favorable growth pattern for measurements, as stated above. The underestimation of tree area and volume is common in automatic process, since the tree canopies are manually estimated by applying a conventional geometric equation that considers tree crown projection as circle forms and the tree crowns as cone-shaped forms while the actual trees have a more complex internal structure, with branches and void space within, which is captured by the algorithms using point clouds (Underwood et al., 2016). Thus, the assumption of a geometric shape for the crown, the complexity of taking on-ground tree measurements and the operator expertise may compromise the validity of field data (Torres-Sánchez et al., 2015; Sola-Guirado et al., 2017). These assumptions produce inexact on-ground estimations, while 3-D architecture derived from the point cloud-based OBIA algorithm reconstructed the irregular shape of the tree crown, achieving better estimations of the olive trials than those estimated from the on-ground measurements (Torres-Sánchez et al., 2015). In any case, similar trends and magnitudes between OBIA-estimated and field data were found, for example, the trees identified as bigger on the ground were also quantified as a larger area by the OBIA algorithm in 2018 (**Figure 8B**), and *vice versa*. This fact points out the suitability of the OBIA-based measurements for phenotyping trials, as it improves the traditionally considered errors of field estimates.

In olives 15 months after planting, neither the area nor the volume could be accurately estimated, showing that the tree point cloud was not dense enough to reconstruct the crown architecture at that growth stage (**Figure 6**). This matter could be solved by modifying the flight configuration either by reducing the flight altitude or using a higher resolution sensor so that the number of points are increased. In addition, this solution could resolve the underestimation of the traits from the OBIA algorithm, since a higher point density might lead to a better detection of tree apexes and part of the lateral branching, which caused the underestimation of crown parameters. However, the flight altitude has also strong implications in the flight duration, area covered by each image, time-consumption, image processing, spectral resolution, and cost (De Castro et al., 2015a). In this sense, flights at low altitude would increase the

spatial resolution, i.e., more dense point cloud as well as the time and cost of the process (Gómez-Candón et al., 2014). Thus, an optimal combination of image overlap, sensor, and flight altitude is essential to optimize fieldwork for breeding applications in large-scale plant phenotyping studies. Therefore, a balance must be sought between the cost of refining the flight configuration and the earlier date to obtain the agronomic trait, i.e., the age of the plant, according to the desired target. Alternatively, the inclusion of oblique images in the analysis has shown potential to improve the DTM (James and Robson, 2014), although they have been mainly used for building damage assessment (Dong and Shan, 2013; Vetrivel et al., 2015) or quarry topography reconstruction (Rossi et al., 2017). Much less information exists on the use of oblique images for vegetation reconstruction that has been limited to forest trees after leaf fall (Fritz et al., 2013). Thus, a combination of nadir and oblique images could be tested in further research to check if this approach can improve the crown architecture reconstruction in agricultural vegetation. Apart from that, the underestimation issue could be solved applying an estimation corrector related to the tree characterization, age, and pattern system.

A higher level of agreement was reached in the second year, i.e. 27 months after planting, on the estimates of crown parameters, reaching a very high correlation and minor errors in both training system, and a slightly lower determination coefficient for volume in the hedgerow orchards, which could be attributed to inexact on-ground estimations, as stated above. Using a similar approach, i.e. UAV imagery and OBIA technology, Torres-Sánchez et al. (2015) estimated crown parameters with successful results both in single-tree and in hedgerow plantations, reporting R^2 values of 0.94 and 0.65 for area and volume estimations, respectively, which proved that this technological combination is very suitable to obtain automatic and accurate agronomic traits. However, those experiments were carried out in adult trees, where actual crown volume ranged from 16 to 40 m^3, making it a less complex scenario than that of olive trees shortly after planting. Comparatively, using that combination, weaker correlations (R^2 = 0.58 and nRMSE = 18.83% for individual trees and R^2 = 0.22 and nRMSE = 12.96% for hedgerow systems) were reached in crown diameter estimation when younger trees were analyzed (Díaz-Varela et al., 2015), which denotes an inverse relationship between both variables. Therefore, the accuracies obtained in this paper are considered highly satisfactory, since the experiments were carried out in the challenging initial growth stage of young olive trees.

In addition to its accuracy, this OBIA procedure was fully automatic, without any user intervention, making the quantification of the breeding trials time-efficient, reliable, and more accurate, removing errors from a manual intervention above explained (Jiménez-Brenes et al., 2017; De Castro et al., 2018b). In a previous research, Fernández et al. (2016) attempted to automatically detect olive using UAV-based point clouds, however, user intervention for manual point selection was required due to the difficulties they found in automatic identification, which led to a semi-automatic process that consumes time and resources, and could include a subjective element (De Castro et al., 2018b). Moreover, no field validation was performed by Fernández et al. (2016), so the use of a UAV-based point clouds methodology remained non-validated for olive trees. In this context, some authors have detected olive trees using UAV reporting classification accuracies over 90% (Torres-Sánchez et al., 2015; Jiménez-Brenes et al., 2017), although those studies were conducted under a DSM-based OBIA approach in adult olive trees. Therefore, our results are considered very successful as the automatic tree detection was carried out in very young olive orchards. Moreover, the time involved in the entire process took less than 5 h for the intensive orchard including 244 olive trees, which consisted of a 5 min flight; the point cloud generation, which took about 4 h; and running the algorithm, which was around 30 min. Thus, by using UAV-images in combination with the point-cloud based OBIA algorithm, an accurate DTM, number, and coordinates of each tree and their agronomic trials (height, area, volume) could be provided in the same day as UAV flights to breeders and farmers requesting plant architecture traits.

Rapid methods for identification and assessment of plant traits are considered a major challenge for crop research in the 21st century (White et al., 2012). The high-throughput system developed in this research can provide breeders demanded architectural traits as rapid as less than 5 h after flights. Moreover, this high-throughput system is able to 3D reconstruct olive trees around 1 year after plantation and calculates breeding traits as soon as 1 year or 2 years after plantation, depending on the trial and training system. Olive architectural traits are highly relevant in the evaluation of each breeding process stage: from the seedlings stage (De la Rosa et al., 2006; Rallo et al., 2008; Hammamia et al., 2012) to the advanced selections trials (Rallo et al., 2018), and are key to evaluate the adaptation of olive cultivars to new highly technified growing systems such as the super-high density hedgerows (Rosati et al., 2013; Rallo et al., 2014; Morales-Sillero et al., 2014). Furthermore, our UAV-based high-throughput system is cost and time optimized for large-scale plant phenotyping studies, so that the rapid, accurate, and timely outputs of this system could supply crucial information for the rapid selection of genotypes addressing, e.g., lower input demand, improved olive quality, the capacity to face threats such as *Xylella fastidiosa* or *Verticillium dahliae*, and climate change, among others (El Riachy et al., 2012; Fiorani and Schurr, 2013; Rallo et al., 2016).

Besides the breeding applications, this accurate and rapid obtainable information of plant traits and tree position in large fields could be useful to design precision agriculture strategies at orchard scale, such as fertilization, irrigation, designing of pruning tasks (Escolà et al., 2017; Peña et al., 2018; De Castro et al., 2018a), as well as site-specific canopy treatments at variable rate application adapted to the necessities and size of trees, which could result in savings herbicide of up to 70% (Solanelles et al., 2006). Nursery management could be also benefited from this technological system (De Castro et al., 2018c). Additionally, as the height tree and crown architecture estimation has been assessed in several training systems and growth stages, this technology could be used to evaluate the tree adaptation to different environmental conditions and/or growing systems (Díaz-Varela et al., 2015). In addition, the canopy monitoring throughout the growing cycle,

together with the spectral information also provided in this approach, could open new opportunities for early identification of biotic and abiotic stresses, as visible- and near infrared range have been proved useful to detect early changes in plant physiology (De Castro et al., 2015b). Finally, the mapping of agronomical traits would help to address the goal of developing prediction models that connect olive growth traits to yield (Sola-Guirado et al., 2017).

This UAV-based high-throughput system has been designed by using UAV, GPS, and Agisoft PhotoScan Professional Edition Photoscan and eCognition Developer software for taking images, georeferencing the ground control points, generation of 3D point cloud, and identifying and characterizing young olive trees, respectively. The developed OBIA algorithm is self-adaptive to different crop-field conditions, as row orientation, row and tree spacing, field slope, or olive tree dimensions. Moreover, as the voxel methodology is used to calculate the volume, LiDAR point cloud could also be as input, though these systems are slower than UAV technology (De Castro et al., 2018a). Although none of the software used in this research are open access, these were selected due to their versatility to develop the rule-set that could be transferred to some open source software available in the market.

Alternatively, terrestrial laser scanners have shown potential for 3D tree characterization (Underwood et al., 2016; Luo et al., 2018). In this context, Escolà et al. (2017) used a 2D light detection and ranging (LiDAR) on board an all-terrain vehicle estimating olive crown volume with R^2 values ranging from 0.56 to 0.82, depending on the algorithms used. The experiment was carried out in adult orchards, i.e., larger canopy sizes, and used a travel speed of 4 km/h, which requires more time. Moreover, LiDAR exhibits some weaknesses such as no spectral information is acquired, it is often difficult for it to hit the exact tops of trees (Luo et al., 2018), and problems of aligning LiDAR scans from both sides of the tree are reported (Rosell et al., 2009). Additionally, phenotyping platforms with ground vehicles are very difficult to use for cross-regional work due to the lack of maneuverability (Yang et al., 2017). On the other hand, higher point cloud densities were produced, which could imply a better 3D reconstruction, although none optimal densities have been proposed so far for agriculture (Escolà et al., 2017). Therefore, a comparison between tractor-mounted sensors and OBIA-UAV technology must be carried out in further research (Escolà et al., 2017; De Castro et al., 2018b).

In summary, the high-throughput system developed in this work consisted of UAV imagery and a robust point cloud based OBIA algorithm and allows the automatic, rapid, and accurate creation of Digital Terrain Models (DTMs) and identification of olive tree at any training system and age, as well as the extraction of olive architectural traits in large scale fields at a very young stage, that is, around 2 years after planting. In addition, tree height can be estimated with acceptable accuracy in an intensive trial at the first date, i.e. 15 months after planting. The early and accurate estimation of these traits through this cost-efficient methodology may drastically reduce the crucial time of decision making for tree breeders, therefore discarding the unwanted genotypes early and improving the performance of the breeding process (Fiorani and Schurr, 2013). Therefore, the time and cost saving of OBIA-based trait estimation as well as the higher accuracy, certainly justifies the utility of this technology rather than geometric assumptions based on manual measurement. Furthermore, the methodology may not only be applied in phenotyping tasks in olive breeding programs, but it will also support the modernization and intensification of the olive sector through a better management of these orchards, involving a beneficial effect on the market price of olive as well as the economic development especially in rural areas (White et al., 2012).

AUTHOR CONTRIBUTIONS

AIdC, PR, MPS, and FL-G conceived and designed the experiments. PR and MS designed the field trials and performed the olive field experiments. LC, AM-S, and MRJ collected and processed the ground-based data. AIdC, JT-S, FMJ-B, and FL-G performed the UAV flight experiments. AIdC, JT-S, and FMJ-B analyzed the data. FL-G, PR, and MPS contributed to the interpretation of the results, and with equipment and analysis tools. AIdC wrote the paper. FL-G and PR collaborated in the discussion of the results and revised the manuscript. All authors have read and approved the manuscript.

FUNDING

The breeding field trials in which the experiments were performed are funded by Interaceituna (Spanish Inter-professional Association for Table Olives) through the FIUS projects PR201402347 and PRJ201703174. This research was partly financed by the AGL2017-83325-C4-4-R (Spanish Ministry of Science, Innovation and Universities and AEI/EU-FEDER funds), and Intramural-CSIC 201940E074 Projects. Research of AC was supported by the Juan de la Cierva Program-Incorporación of the Spanish MINECO funds.

ACKNOWLEDGMENTS

We acknowledge support of the publication fee by the CSIC Open Access Publication Support Initiative through its Unit of Information Resources for Research (URICI). We thank Dr. José Manuel Peña his help in field work, and Aceitunas Guadalquivir S.L. and Javier del Barco for the maintenance of the field trials.

SUPPLEMENTARY MATERIAL

The Supplementary Material for this article can be found online at: https://www.frontiersin.org/articles/10.3389/fpls.2019.01472/full#supplementary-material

Animations of several figures of the paper are available as supplementary materials (**Supplementary Video File**) in the article electronic version, published online. These might be used by the interested reader in order to have a dynamic representation of the various processing phases.

REFERENCES

AESA. (2017) Aerial Work—Legal Framework. Available online: http://www.seguridadaerea.gob.es/LANG_EN/cias_empresas/trabajos/rpas/marco/default.aspx (accessed on 6 November 2017).

Araus, J. L., and Cairns, J. E. (2014). Field high-throughput phenotyping: the new crop breeding frontier. *Trends Plant Sci.* 19, 52–61. doi: 10.1016/j.tplants.2013.09.008

Bai, G., Ge, Y., Hussain, W., Baenziger, P. S., and Graef, G. (2016). A multi-sensor system for high throughput field phenotyping in soybean and wheat breeding. *Comput. Electron. Agric.* 128, 181–192. doi: 10.1016/j.compag.2016.08.021

Barnston, A. G. (1992). Correspondence among the Correlation, RMSE, and Heidke verification measures; refinement of the heidke score. *Weather Forecast* 7, 699–709. doi: 10.1175/1520-0434(1992)007<0699:CATCRA>2.0.CO;2

Blaschke, T., Hay, G. J., Kelly, M., Lang, S., Hofmann, P., Addink, E., et al. (2014). Geographic object-based image analysis – towards a new paradigm. *ISPRS J. Photogramm. Remote Sens.* 87, 180–191. doi: 10.1016/j.isprsjprs.2013.09.014

Díaz-Varela, R. A., de la Rosa, R., León, L., and Zarco-Tejada, P. J. (2015). High-resolution airborne UAV imagery to assess olive tree crown parameters using 3D photo reconstruction: application in breeding trials. *Remote Sens.* 7, 4213–4232. doi: 10.3390/rs70404213

Dandois, J. P., and Ellis, E. C. (2010). Remote sensing of vegetation structure using computer vision. *Remote Sens.* 2, 1157–1176. doi: 10.3390/rs2041157

Dandois, J. P., Olano, M., and Ellis, E. C. (2015). Optimal altitude, overlap, and weather conditions for computer vision UAV estimates of forest structure. *Remote Sens.* 7, 13895–13920. doi: 10.3390/rs71013895

Dandois, J. P., Baker, M., Olano, M., Parker, G. G., and Ellis, E. C. (2017). What is the point? Evaluating the structure, color, and semantic traits of computer vision point clouds of vegetation. *Remote Sens.* 9, 355. doi: 10.3390/rs9040355

De Castro, A. I., Ehsani, R., Ploetz, R., Crane, J. H., and Abdulridha, J. (2015a). Optimum spectral and geometric parameters for early detection of laurel wilt disease in avocado. *Remote Sens. Environ.* 171, 33–44. doi: 10.1016/j.rse.2015.09.011

De Castro, A. I., Ehsani, R., Ploetz, R. C., Crane, J. H., and Buchanon, S. (2015b). Detection of laurel wilt disease in avocado using low altitude aerial imaging. *PloS One* 10 (4), e0124642. doi: 10.1371/journal.pone.0124642

De Castro, A. I., Jiménez-Brenes, F. M., Torres-Sánchez, J., Peña, J. M., Borra-Serrano, I., and López-Granados, F. (2018a). 3-D characterization of vineyards using a novel UAV Imagery-Based OBIA Procedure for Precision Viticulture Applications. *Remote Sens.* 10, 584. doi: 10.3390/rs10040584

De Castro, A. I., Torres-Sánchez, J., Peña, J. M., Jiménez-Brenes, F. M., Csillik, O., and López-Granados, F. (2018b). An automatic random forest-OBIA algorithm for early weed mapping between and within crop rows using UAV imagery. *Remote Sens.* 10, 285. doi: 10.3390/rs10020285

De Castro, A. I., Maja, J. M., Owen, J., Robbins, J., and Peña, J. M. (2018c). "Experimental approach to detect water stress in ornamental plants using sUAS-imagery," in *Autonomous Air and Ground Sensing Systems for Agricultural Optimization and Phenotyping III. (*International Society for Optics and Photonics) *106640N*. doi: 10.1117/12.2304739

De la Rosa, R., Kiran, A. I., Barranco, D., and Leon, L. (2006). Seedling vigour as a preselection criterion for short juvenile period in olive breeding. *Aust. J. Agric. Res.* 57, 477–481. doi: 10.1071/ar05219

Dong, L., and Shan, J. (2013). A comprehensive review of earthquake-induced building damage detection with remote sensing techniques. *ISPRS J. Photogramm. Remote Sens.* 84, 85–99. doi: 10.1016/j.isprsjprs.2013.06.011

El Riachy, M., Priego-Capote, F., Rallo, L., Luque-de Castro, M. D., and León, L. (2012). Phenolic profile of virgin olive oil from advanced breeding selections. *Span. J. Agric. Res.* 10, 443–453. doi: 10.5424/sjar/2012102-264-11

Escolà, A., Martínez-Casasnovas, J. A., Rufat, J., Arnó, J., Arbonés, A., Sebé, F., et al. (2017). Mobile terrestrial laser scanner applications in precision fruticulture/horticulture and tools to extract information from canopy point clouds. *Precis. Agric.* 18, 111–132. doi: 10.1007/s11119-016-9474-5

Fabbri, A., Lambardi, M., and Ozden-Tokatli, Y. (2009). Olive Breeding, in: Breeding Plantation Tree Crops: Tropical Species, (New York, NY: Springer), 423–465. doi: 10.1007/978-0-387-1075 71201-7

FAOSTAT [WWW Document], 2017. Available at: URL http://www.fao.org/faostat/en/#data (Accessed March 19 2018)

Fernández, T., Pérez, J. L., Cardenal, J., Gómez, J. M., Colomo, C., and Delgado, J. (2016). Analysis of landslide evolution affecting olive groves using UAV and photogrammetric techniques. *Remote Sens.* 8, 837. doi: 10.3390/rs8100837

Fernández-Sarría, A., Martínez, L., Velázquez-Martí, B., Sajdak, M., Estornell, J., and Recio, J. A. (2013). Different methodologies for calculating crown volumes of Platanus hispanica trees using terrestrial laser scanner and a comparison with classical dendrometric measurements. *Comput. Electron. Agr.* 90, 176–185. doi: 10.1016/j.compag.2012.09.017

Fiorani, F., and Schurr, U. (2013). Future scenarios for plant phenotyping. *Annu. Rev. Plant Biol.* 64, 267–291. doi: 10.1146/annurev-arplant-050312-120137

Fritz, A., Kattenborn, T., and Koch, B. (2013). Uav-Based Photogrammetric Point Clouds - Tree STEM Mapping in Open Stands in Comparison to Terrestrial Laser Scanner Point Clouds. *ISPRS Arch.* 1, 141–146. doi: 10.5194/isprsarchives-XL-1-W2-141-2013

Gómez-Candón, D., De Castro, A. I., and López-Granados, F. (2014). Assessing the accuracy of mosaics from unmanned aerial vehicle (UAV) imagery for precision agriculture purposes in wheat. *Precis Agric.* 15, 44–56. doi: 10.1007/s11119-013-9335-4

Gatziolis, D., Lienard, J. F., Vogs, A., and Strigul, N. S. (2015). 3D Tree Dimensionality Assessment Using Photogrammetry and Small Unmanned Aerial Vehicles. *PloS One* 10, e0137765. doi: 10.1371/journal.pone.0137765

Hammamia, S. B. M., de la Rosa, R, Sghaier-Hammamic, B, León, L, Rapoport, H. F., (2012). Reliable and relevant qualitative descriptors for evaluating complex architectural traits in olive progenies. *Scientia Horticulturae* 143, 157–166

Hosoi, F., and Omasa, K. (2006). Voxel-based 3-D modeling of individual trees for estimating leaf area density using high-resolution portable scanning lidar. *IEEE Trans. Geosci. Rem. Sens.* 44, 3610–3618. https://ieeexplore.ieee.org/abstract/document/4014317. doi: 10.1109/TGRS.2006.881743

Innovagri. (2018). Available at: https://www.innovagri.es/investigacion-desarrollo-inovacion/principales-sistemas-de-formacion-en-el-olivar-en-seto.html.

Instituto de Estadística y Cartografía de Andalucía-Junta de Andalucía (IECA). (2018). Available at: https://www.juntadeandalucia.es/institutodeestadisticaycartografia/prodCartografia/bc/mdt.htm.

International Olive Council. (2017). Available online: http://www.internationaloliveoil.org (accessed on 1February 2018).

James, MR, and Robson, S. (2014). Mitigating systematic error in topographic models derived from UAV and ground-based image networks. Earth Surface Processes and Landforms, 39(10), 1413–1420. doi: 10.1002/esp.3609

Jiménez-Brenes, F. M., López-Granados, F., de Castro, A. I., Torres-Sánchez, J., Serrano, N., and Peña, J. M. (2017). Quantifying pruning impacts on olive tree architecture and annual canopy growth by using UAV-based 3D modelling. *Plant Methods* 13, 55. doi: 10.1186/s13007-017-0205-3

Johansen, K., Raharjo, T., and McCabe, M. F. (2018). Using multi-spectral UAV imagery to extract tree crop structural properties and assess pruning effects. *Remote Sens.* 10 (6), 854. doi: 10.3390/rs10060854

Kattenborn, T., Sperlich, M., Bataua, K., and Koch, B. (2014). Automatic Single Tree Detection in Plantations using UAV-based Photogrammetric Point clouds. *Int. Arch. Photogramm. Remote Sens. Spatial Inf. Sci.* XL-3, 139–144. doi: 10.5194/isprsarchives-XL-3-139-2014

López-Granados, F., Torres-Sánchez, J., de Castro, A. I., Serrano-Pérez, A., Mesas-Carrascosa, F. J., and Peña, J.-M. (2016). Object-based early monitoring of a grass weed in a grass crop using high resolution UAV imagery. *Agron. Sustain. Dev.* 36, 67. doi: 10.1007/s13593-016-0405-7

Lehmann, E. L. (1951). A General Concept of Unbiasedness. *Ann. Math Stat. Vol.* 22, 587–592. doi: 10.1214/aoms/1177729549

Li, J., Hu, B., and Noland, T. L. (2013). Classification of tree species based on structural features derived from high density LiDAR data. *Agr. For. Meteorol.*, 171–172, 104-114. doi: 10.1016/j.agrformet.2012.11.012

Luo, L., Zhai, Q., Su, Y., Ma, Q., Kelly, M., and Guo, Q. (2018). Simple method for direct crown base height estimation of individual conifer trees using airborne LiDAR data. *Optics Express* 26, A562–A578. doi: 10.1364/OE.26.00A562

Madec, S., Baret, F., de Solan, B., Thomas, S., Dutartre, D., Jezequel, S., et al. (2017). High-Throughput Phenotyping of Plant Height: Comparing Unmanned Aerial Vehicles and Ground LiDAR Estimates. *Front. Plant Sci.* 8, 2002. doi: 10.3389/fpls.2017.02002

Matese, A., Gennaro, S. F. D., and Berton, A. (2017). Assessment of a canopy height model (CHM) in a vineyard using UAV-based multispectral imaging. *Int. J. Remote Sens.* 38, 2150–2160. doi: 10.1080/01431161.2016.1226002

Mendenhall, W., Beaver, R. J., and Beaver, B. M. (2009). *Introduction to Probability and Statistics*. (Australia: Brooks/Cole, Cengage Learning).

Monserrat, O., and Crosetto, M. (2008). Deformation measurement using terrestrial laser scanning data and least squares 3D surface matching. *ISPRS J. Photogrammetry Remote Sens.* 63 (1), 142e154. doi: 10.1016/j.isprsjprs.2007.07.008

Montes, J. M., Melchinger, A. E., and Reif, J. C. (2007). Novel throughput phenotyping platforms in plant genetic studies. *Trends Plant Sci.* 12, 433–436. doi: 10.1016/j.tplants.2007.08.006

Morales-Sillero, A., Rallo, P., Jimenez, M. R., Casanova, L., and Suarez, M. P. (2014). Suitability of two table olive cultivars ('Manzanilla de Sevilla' and 'Manzanilla Cacerena') for mechanical harvesting in superhigh-density hedgerows. *Hortscience.* 49, 1028–1033.

Newman, M., Zygielbaum, A., and Terry, B. (2018). Static analysis and dimensional optimization of a cable-driven parallel robot. In *Cable-Driven Parallel Robots. Mechanisms and Machine Science*, vol. 53. Eds. Gosselin, P., Cardou, T., Bruckmann, A., and Pott, C. (Cham: Springer).

Ostos, F., de Castro, A. I., Torres-Sánchez, J., Pistón, F., and Peña, J. M. (2019). High-throughput phenotyping of bioethanol potential in cereals by using UAV-based multi-spectral imagery. *Front. Plant Sci.* 10, 948. doi: 10.3389/fpls.2019.00948

Park, H. J., Lim, S., Trinder, J. C., and Turner, R. (2010). Voxel-based volume modelling of individual trees using terrestrial laser scanners, in: Proceedings of 15th Australasian Remote Sensing & Photogrammetry Conf., Alice Springs, Australia. 1125–1133.

Pastor, M., editor. Cultivo del olivo con riego localizado: diseño y manejo del cultivo y las instalaciones, programación de riegos y fertirrigación (in Spanish) [Internet]. Mundi Prensa Libros S.A.; 2005. Available at: http://dialnet.unirioja.es/servlet/libro?codigo=8551.

Peña, J. M., Torres-Sánchez, J., Serrano-Pérez, A., de Castro, A. I., and López-Granados, F. (2015). Quantifying efficacy and limits of unmanned aerial vehicle (UAV) technology for weed seedling detection as affected by sensor resolution. *Sensors* 15, 5609–5626. doi: 10.3390/s150305609

Peña, J. M., Castro, A. I., Torres-Sánchez, J., Andújar, D., Martín, C. S., and Dorado, J. (2018). Estimating tree height and biomass of a poplar plantation with image-based UAV technology. *AIMS Agric. Food* 3, 313–326. doi: 10.3934/agrfood.2018.3.313

Phattaralerphong, J., and Sinoquet, H. (2005). A method for 3D reconstruction of tree crown volume from photographs: assessment with 3D-digitized plants. *Tree Physiol.* 25, 1229–1242. doi: 10.1093/treephys/25.10.1229

Rallo, P., Jimenez, R., Ordovas, J., and Suarez, M. P. (2008). Possible early selection of short juvenile period olive plants based on seedling traits. *Aust. J. Agr. Res.* 59, 933–940. doi: doi.10.1071/ar08013

Rallo, L., Barranco, D., Castro-Garcia, S., Connor, D. J., Gómez del Campo, M., and Rallo, P. (2014). High-Density Olive Plantations. *Hortic. Rev.* 41, 303–384. doi: 10.1007/s00122-003-1301-5

Rallo, L., Caruso, T., Díez, C. M., and Campisi, G. (2016). "Olive growing in a time of change: from empiricism to genomics," in *The Olive Tree Genome, Compendium of Plant Genomes* (Cham: Springer), 55–64. doi: 10.1007/978-3-319-48887-5_4

Rallo, L., Barranco, D., Díez, C. M., Rallo, P., Suárez, M. P., Trapero, C., et al. (2018). Strategies for olive (*Olea europaea* L.) breeding: cultivated genetic resources and crossbreeding; In *Advances in Plant Breeding Strategies: Fruits* (New York City, USA: Springer International Publishing).

Rosati, A., Paoletti, A., Caporali, S., and Perri, E. (2013). The role of tree architecture in super high density olive orchards. *Sci. Hortic.* 161, 24–29. doi: doi.10.1016/j.scienta.2013.06.044

Rosell, J. R., Llorens, J., Sanz, R., Arnó, J., Ribes-Dasi, M., Masip, J., et al. (2009). Obtaining the three-dimensional structure of tree orchards from remote 2d terrestrial lidar scanning. *Agric. For. Meteorol.* 149 (9), 1505–1515. doi: 10.1016/j.agrformet.2009.04.008

Rossi, P., Mancini, F., Dubbini, M., Mazzone, F., and Capra, A. (2017). Combining nadir and oblique UAV imagery to reconstruct quarry topography: methodology and feasibility analysis. *Eur. J. Remote Sens.* 50, 211–221. doi: 10.1080/22797254.2017.1313097

Rugini, E, Baldoni, L, Rosario, M, and Sebastiani, Leditors. (2016). *The Olive tree genome*. (New York: Springer International Publishing). 193. doi: 10.1007/978-3-319-48887-5

Shafiekhani, A., Kadam, S., Fritschi, F. B., and DeSouza, G. N. (2017). Vinobot and vinoculer: two robotic platforms for high-throughput field phenotyping. *Sensors* 17, 214. doi: 10.3390/s17010214

Shi, Y., Thomasson, J. A., Murray, S. C., Pugh, N. A., Rooney, W. L., Shafian, S., et al. (2016). Unmanned Aerial Vehicles for High-Throughput Phenotyping and Agronomic Research. *PloS One* 11, e0159781. doi: 10.1371/journal.pone.0159781

Sola-Guirado, R. R., Castillo-Ruiz, F. J., Jiménez-Jiménez, F., Blanco-Roldan, G. L., Castro-Garcia, S., and Gil-Ribes, J. A. (2017). Olive actual "on Year" yield forecast tool based on the tree canopy geometry using UAS imagery. *Sensors* 17 (8), 1743. doi: 10.3390/s17081743

Solanelles, F., Escolà, A., Planas, S., Rosell, J. R., Camp, F., and Gràcia, F. (2006). An electronic control system for pesticide application proportional to the canopy width of tree crops. *Biosyst. Eng.* 95, 473–481. doi: 10.1016/j.biosystemseng.2006.08.004

Stilliano, T., de Luca, A. I., Falcone, G., Spada, E., Gulisano, G., and Strano, A. (2016). Economic profitability assessment of mediterranean olive growing systems. *Bulg J. Agric. Sci.* 22 (No 4), 517–526.

Tattaris, M., Reynolds, M. P., and Chapman, S. C. (2016). A direct comparison of remote sensing approaches for high-throughput phenotyping in plant breeding. *Front. Plant Sci.* 7, 1131. doi: 10.3389/fpls.2016.01131

Torres-Sánchez, J., López-Granados, F., Serrano, N., Arquero, O., and Peña, J. M. (2015). High-throughput 3-D monitoring of agricultural-tree plantations with unmanned aerial vehicle (UAV) technology. *PloS One* 10, e0130479. doi: 10.1371/journal.pone.0130479

Torres-Sánchez, J., López-Granados, F., Borra-Serrano, I., and Peña, J. M. (2018a). Assessing UAV-collected image overlap influence on computation time and digital surface model accuracy in olive orchards. *Precis. Agric.* 19, 115–133. doi: 10.1007/s11119-017-9502-0

Torres-Sánchez, J., de Castro, A. I., Peña, J. M., Jimenez-Brenes, F. M., Arquero, O., Lovera, M., et al. (2018b). Mapping the 3D structure of almond trees using UAV acquired photogrammetric point clouds and object-based image analysis. *Biosyst. Eng.* 176, 172–184. doi: 10.1016/j.biosystemseng.2018.10.018

Underwood, J. P., Hung, C., Whelan, B., and Sukkarieh, S. (2016). Mapping almond orchard canopy volume, flowers, fruit and yield using lidar and vision sensors. *Comput. Electron. Agric.* 130, 83–96. doi: 10.1016/j.compag.2016.09.014

Vetrivel, A., Gerke, M., Kerle, N., and Vosselman, G. (2015). Identification of damage in buildings based on gaps in 3D point clouds from very high resolution oblique airborne images. *ISPRS J. Photogramm. Remote Sens.* 84, 85–89. doi: 10.1016/j.isprsjprs.2015.03.016

Virlet, N., Sabermanesh, K., Sadeghi-Tehran, P., and Hawkesford, M. J.Field scanalyzer. (2017). Field Scanalyzer: An automated robotic field phenotyping platform for detailed crop monitoring. *Funct. Plant Biol.* 44, 143–153. doi: 10.1071/FP16163

White, J. W., Andrade-Sanchez, P., Gore, M. A., Bronson, K. F., Coffelt, T. A., and Conley, M. M. (2012). Field-based phenomics for plant genetics research. *Field Crops Res.* 133, 101–112. doi: 10.1016/j.fcr.2012.04.003

Woo, H., Kang, E., Wang, S., and Lee, K. H. (2002). A new segmentation method for point cloud data. *Int. J. Mach Tool Manu* 42, 167–178. doi: 10.1016/S0890-6955(01)00120-1

Yang, G., Liu, J., Zhao, C., Li, Z., Huang, Y., Yu, H., et al. (2017). Unmanned aerial vehicle remote sensing for field-based crop phenotyping: current status and perspectives. *Front. Plant Sci.* 8, 1111. doi: 10.3389/fpls.2017.01111

Zang, Z., Cao, L., and Guanghui, S. (2017). Estimating forest structural parameters using canopy metrics derived from airborne lidar data in subtropical forests. *Remote Sens.* 9, 940. doi: 10.3390/rs9090940

Zaman-Allah, M., Vergara, O., Araus, J. L., Tarekegne, A., Magorokosho, C., Zarco-Tejada, P. J., et al. (2015). Unmanned aerial platform-based multi-spectral imaging for field phenotyping of maize. *Plant Methods* 11, 35. doi: 10.1186/s13007-015-0078-2

Conflict of Interest: The authors declare that the research was conducted in the absence of any commercial or financial relationships that could be construed as a potential conflict of interest.

frontiers in Plant Science

ORIGINAL RESEARCH
published: 19 November 2019
doi: 10.3389/fpls.2019.01484

Insights Into Olive Fruit Surface Functions: A Comparison of Cuticular Composition, Water Permeability, and Surface Topography in Nine Cultivars During Maturation

*Clara Diarte[1,2], Po-Han Lai[3], Hua Huang[4†], Agustí Romero[5], Tomás Casero[1], Ferran Gatius[1], Jordi Graell[1,2], Vicente Medina[1,6], Andrew East[3], Markus Riederer[4] and Isabel Lara[1,2]**

[1] Universitat de Lleida, Lleida, Spain, [2] Postharvest Unit-XaRTA, AGROTÈCNIO, Lleida, Spain, [3] Massey Agrifood Technology Partnership, Massey University, Palmerston North, New Zealand, [4] Julius-von-Sachs Institut für Biowissenschaften, Universität Würzburg, Würzburg, Germany, [5] Oliviculture, Oil Science and Nuts, IRTA-Mas de Bover, Constantí, Spain, [6] Applied Plant Biotechnology, AGROTÈCNIO, Lleida, Spain

OPEN ACCESS

Edited by:
José Manuel Martínez-Rivas, Instituto de la Grasa (IG), Spain

Reviewed by:
Georgios Liakopoulos, Agricultural University of Athens, Greece
Marilena Ceccarelli, University of Perugia, Italy

***Correspondence:**
Isabel Lara
lara@quimica.udl.cat

† Present address:
Hua Huang, Laboratory of Conservation and Sustainable Utilization of Plant Resources, South China Botanical Garden, Chinese Academy of Sciences, Guangzhou, China

Specialty section:
This article was submitted to Crop and Product Physiology, a section of the journal Frontiers in Plant Science

Received: 14 June 2019
Accepted: 25 October 2019
Published: 19 November 2019

Citation:
Diarte C, Lai P-H, Huang H, Romero A, Casero T, Gatius F, Graell J, Medina V, East A, Riederer M and Lara I (2019) Insights Into Olive Fruit Surface Functions: A Comparison of Cuticular Composition, Water Permeability, and Surface Topography in Nine Cultivars During Maturation. Front. Plant Sci. 10:1484. doi: 10.3389/fpls.2019.01484

Olive (*Olea europaea* L.) growing has outstanding economic relevance in Spain, the main olive oil producer and exporter in the world. Fruit skin properties are very relevant for fruit and oil quality, water loss, and susceptibility to mechanical damage, rots, and infestations, but limited research focus has been placed on the cuticle of intact olive fruit. In this work, fruit samples from nine olive cultivars ("Arbequina," "Argudell," "Empeltre," "Farga," "Manzanilla," "Marfil," "Morrut," "Picual," and "Sevillenca") were harvested from an experimental orchard at three different ripening stages (green, turning, and ripe), and cuticular membranes were enzymatically isolated from fruit skin. The total contents of cuticular wax and cutin significantly differed among cultivars both in absolute and in relative terms. The wax to cutin ratio generally decreased along fruit maturation, with the exception of "Marfil" and "Picual." In contrast, increased water permeance values in ripe fruit were observed uniquely for "Argudell," "Morrut," and "Marfil" fruit. The toluidine blue test revealed surface discontinuities on green samples of "Argudell," "Empeltre," "Manzanilla," "Marfil," and "Sevillenca" fruit, but not on "Arbequina," "Farga," "Morrut," or "Picual." No apparent relationship was found between water permeability and total wax coverage or the results of the toluidine blue test. The composition of cuticular waxes and cutin monomers was analyzed in detail, and sections of fruit pericarp were stained in Sudan IV for microscopy observations. Skin surface topography was also studied by means of fringe projection, showing large differences in surface roughness among the cultivars, "Farga" and "Morrut" fruits displaying the most irregular surfaces. Cultivar-related differences in cuticle and surface features of fruit are presented and discussed.

Keywords: *Olea europaea* L., cuticular wax, cutin, maturity stage, water permeance, skin surface topography

Except the vine, there is no plant which bears a fruit of as great importance as the olive.
Pliny the Elder (*attributed*)

INTRODUCTION

The olive (*Olea europaea* L.) tree is considered one of the oldest crops to have been domesticated by humans (Besnard et al., 2018). Around 90% of the world production of olives is used for the production of olive oil, and the rest is employed for the manufacture of table olives[1]. More than half of the total world olive production is grown in countries in the Mediterranean basin, Spain being the main olive oil producer and exporter in the world.

In Mediterranean areas, crops often develop under adverse environmental conditions, including restricted water availability, high temperatures, or elevated UV irradiation levels, which are expected to exacerbate in a scenario of global climate change. The performance of a given genotype under such conditions, as well as its resistance against pests and diseases, will be partly dependent upon the properties of fruit surface, which will act as the interface between the plant and the surrounding environment. Being the outer layer of the epidermis, the cuticle represents the first barrier against abiotic and biotic stress factors.

Plant cuticles are hydrophobic layers covering the epidermis of aerial, non-lignified plant organs, including the intact fruit. The cuticle scaffold is composed of the polyester cutin, an insoluble polymer matrix mostly containing hydroxy-, carboxy-, and epoxy-C_{16} and C_{18} fatty acids (Lequeu et al., 2003; Franke et al., 2005; Domínguez et al., 2011; Camacho-Vázquez et al., 2019). Different types of cuticular waxes, both in amorphous and crystalline form, and a variable amount of phenolics are integrated within or accumulate onto the surface of the cutin matrix (Samuels et al., 2008; Yeast and Rose, 2013; Lara et al., 2014). The cuticle is considered to limit transpirational water loss to prevent the desiccation of the fruit, but it also confers or modulates relevant properties such as the susceptibility to mechanical damage, infestations, and rots (Kunst and Samuels, 2002; Lara et al., 2014; Martin and Rose, 2014; Serrano et al., 2014; Riederer et al., 2015; Wang et al., 2016).

In spite of these considerations, very few published studies have addressed the composition of cuticles of intact olive fruit. Most of them have focused uniquely on cuticular waxes (Bianchi et al., 1992; Guinda et al., 2010; Vichi et al., 2016), whereas only one published study has also reported on cutin composition in fruit of this species (Huang et al., 2017). Compositional differences have been detected according to cultivar and maturation stage. These differences may relate to the water-proofing and mechanical properties of the cuticle, and thus be relevant for fruit resistance to abiotic and biotic stress-inducing factors.

In this study, olive fruit from nine oil- and table-cultivars differing in important quality traits were selected for the analysis of chemical composition and water permeability at three different maturity stages. With the purpose of widening the study on fruit surface differences across the considered genotypes, skin topography was non-destructively assessed by means of fringe projections (East et al., 2016). The bulk of results should help a better comprehension of the factors determining olive adaptations to the surrounding environment.

[1] International Olive Council (IOC). (2018). Statistics (http://www.internationaloliveoil.org/).

MATERIALS AND METHODS

Plant Material and Toluidine Blue Test

Fruit samples from nine olive (*Olea europaea* L.) autochthonous Spanish cultivars ("Arbequina," "Argudell," "Empeltre," "Farga," "Manzanilla," "Marfil," "Morrut," "Picual," and "Sevillenca") were hand-collected at an experimental orchard located at IRTA-Mas Bové (Constantí, Spain; 41°09' N, 1°12' E; altitude 100 m) from trees supplied with drip irrigation. Annual rainfall is 500 mm, and takes place mainly in April–May and September. Fertilization and cultural practices at the orchard are the usual in the producing area. Olives were picked at three different maturity stages (green, turning, and ripe) based on skin color during the usual harvest period (September to December) in 2016. Maturity index (0–7), fresh weight (g), flesh-to-stone ratio, and water content (% humidity) were determined on 50 fruits per cultivar and maturity stage. For the assessment of length and diameter (mm), 10 fruit were used (**Table 1**). Maturity index was scored on a 0–7 scale by subjectively categorizing each fruit within the sample according to skin and flesh color (Uceda and Frías, 1975); values indicate the weighted average of the 50 olives examined. Olive fly infestation was likewise assessed on 50 fruits per cultivar and maturity stage, by visually checking each fruit for egg deposition, and data shown as a percentage (**Table S1**). In order to visualize possible discontinuities on fruit surface, samples of fresh olives at the green stage (10 fruits per cultivar) were stained in a toluidine blue (TB) solution (0.05%, w/v) for 2 h (Tanaka et al., 2004), rinsed, and allowed to dry in air. Since ripe "Marfil" fruit turn white rather than black, the TB test was applied also to these samples.

Cuticle Isolation

Disks of fruit exocarp (two disks per fruit) were excised with a cork borer. Thirty to 75 olives, depending on fruit size, were processed so to obtain around 100 cm^2 of skin per cultivar and maturity stage as described elsewhere (Belge et al., 2014a). Because not enough skin sample can be obtained from one individual olive fruit to enable further analysis of cuticle composition, excised skin disks were pooled into one sample of biological material. Exocarp samples were distributed in two tubes (50 cm^2 per tube) for the enzymatic isolation of cuticular membranes (CM). Disks were incubated at 37°C in cellulase/pectinase solution (0.2% (w/v) cellulase, 100 U ml^{-1} pectinase, and 1 mM NaN_3 in 50 mM citrate buffer at pH 4.0 until no more material was released, and then washed in citrate buffer (50 mM, pH 4.0) until no material was left in suspension. After thoroughly rinsing in distilled water, CM disks were dried at 40°C, weighted, and then pooled and kept

TABLE 1 | Physical characteristics and toluidine blue test of olive fruits used in this study.

Cultivar	Maturity stage	Sampling date	Maturity Index	Weight (g)	F:S ratio*	Water content (%)	Length (mm)	Diameter (mm)	TB test*
"Arbequina"	Green	Sept 29	0.26	1.10	2.68	53.9	14.1 ab D	12.1 b CD	–
	Turning	Sept 29	2.14	1.27	3.18	55.2	13.4 b C	12.0 b B	ne
	Ripe	Nov 27	3.40	1.59	4.24	58.2	14.7 a D	13.0 a DE	ne
"Argudell"	Green	Sept 29	0.26	2.02	4.08	56.0	18.6 a C	13.9 b BC	+
	Turning	Nov 27	0.96	2.65	5.32	59.2	20.1 a B	15.3 ab A	ne
	Ripe	Nov 27	2.36	2.81	5.57	59.6	20.0 a BC	15.9 a B	ne
"Empeltre"	Green	Sept 29	0.48	3.18	4.05	56.1	23.7 a A	15.2 a B	+
	Turning	Sept 29	3.58	3.09	4.40	55.4	23.0 a A	15.0 a A	ne
	Ripe	Nov 27	5.00	3.13	4.00	49.3	24.1 a A	15.0 a BCD	ne
"Farga"	Green	Sept 29	0.36	1.28	2.47	54.8	16.9 b CD	10.8 b C	–
	Turning	Sept 29	2.04	1.74	3.18	58.7	19.0 a B	12.5 a B	ne
	Ripe	Nov 27	4.40	1.82	3.70	55.8	18.1 a C	12.0 a E	ne
"Manzanilla"	Green	Sept 29	0.12	4.57	8.31	70.1	24.0 a A	18.6 a A	+
	Ripe	Nov 27	5.88	4.65	7.68	66.6	23.9 a A	19.4 a A	ne
"Marfil"	Green	Sept 29	0.04	1.32	2.05	60.1	19.7 b BC	10.5 b C	+
	Ripe	Dec 12	0.96	1.98	3.95	53.6	21.6 a AB	13.3 a CDE	+
"Morrut"	Green	Sept 29	0.16	1.99	2.03	51.6	20.4 b BC	13.8 b BC	–
	Turning	Nov 27	1.04	2.34	2.52	51.1	20.4 b B	13.8 b A	ne
	Ripe	Jan 16	3.40	2.08	2.74	37.6	21.8 a AB	15.5 a BC	ne
"Picual"	Green	Sept 29	0.30	2.72	2.75	57.2	22.4 a AB	15.1 a B	–
	Turning	Nov 27	2.84	3.06	3.11	60.2	22.2 a AB	15.3 a A	ne
	Ripe	Nov 27	3.88	4.30	4.35	49.6	24.1 a A	17.3 a AB	ne
"Sevillenca"	Green	Sept 29	0.32	2.71	3.09	56.7	21.4 a ABC	14.1 a BC	+
	Ripe	Nov 27	3.16	3.32	4.97	52.0	22.1 a AB	15.5 a BC	ne

Values represent means of 50 fruits for maturity index, weight, F:S ratio, and water content, and of 10 fruits for length, diameter, and TB test. Different capital letters denote significant differences among the cultivars for a given maturation stage, and different lower-case letters stand for significant differences among maturation stages for a given cultivar, at $P \leq 0.05$ (Student's t-test). Fruit weight, F:S ratio, and water content were determined jointly for 50 fruits, and values reported represent the average of the 50 olives assessed. Maturity index values indicate the weighted average of the 50 olives within the sample (Uceda and Frías, 1975).
**F:S ratio, flesh to stone ratio; TB test, toluidine blue test (Tanaka et al., 2004): stained and non-stained fruits are denoted respectively as + and –; ne, not evaluated.*

in hermetically capped vials until analysis. Cuticle yields were expressed per unit of fruit surface area (μg cm^{-2}).

Extraction and Analysis of Cuticular Wax

CM samples (20 mg/replicate × 3 technical replicates) were dewaxed in chloroform (2 mg ml^{-1}) for 24 h at room temperature, with constant shaking. Chloroform extraction was done three times, and the chloroform extracts were pooled, incubated 15 min in an ultrasonic bath and filtered. Dewaxed CM (DCM) were dried and kept in hermetically capped vials for subsequent analysis of cutin monomers. The chloroform extracts were concentrated at 40°C using a rotatory evaporator, and waxes then transferred to a pre-weighed vial, dried in a vacuum concentrator at 40°C until complete dryness, and weighed to calculate total wax yields (μg cm^{-2}). Dotriacontane (C_{32}) was then added as an internal standard, and samples were derivatized during 15 min at 100°C in *N,O*-bis(trimethylsilyl)trifluoroacetamide (BSTFA) and pyridine (3:2, v/v), in order to obtain trimethylsilyl (TMSi) ethers and esters from free hydroxyl and carboxyl groups, respectively.

Wax samples (1 μl) were injected in on-column mode into a gas chromatography-mass spectrometry (GC-MS) system for compound identification and quantification. This GC equipment (Agilent 7890N) was coupled with a quadrupole mass selective detector (Agilent 5973N) and equipped with a capillary column (DB 5 MS UI, 30 m × 0.25 mm × 0.25 μm; SGE Europe Ltd., Milton Keynes, UK). Compounds were identified by comparison with their retention times with those of standards, and through their electron ionization-mass spectra using a mass spectral library (NIST 11 MS). Chromatographic conditions were as follows: oven was set at 100°C for 1 min, then raised by 15°C min^{-1} to 200°C, then by 5°C min^{-1} to 310°C, and finally held 10 min at 310°C. Helium was used as the carrier gas at 1.0 ml min^{-1}. A flame ionization detector (FID) was used for quantitative analysis of cuticular waxes, in the same chromatographic conditions as described above excepting that, at the last step, the oven was held at 310°C for 13 min and that a higher carrier gas flow (1.3 ml min^{-1}) was used. Data are expressed as a relative percentage (% over total waxes). Average chain length (ACL) of acyclic wax compounds was calculated as the weighted average number of carbon atoms, defined as

$$ACL = \frac{\Sigma C_n n}{\Sigma C_n}$$

where C_n is the percentage of each acyclic wax compound with n carbon atoms.

Extraction and Analysis of Cutin Monomers

DCM samples (roughly 10 mg/replicate × 3 technical replicates) were hydrolyzed for 2 h in 2 ml of 1 M HCl in 100% MeOH, esterified in the same solution during 2 h at 80°C, and added 2 ml saturated NaCl after cooling down. Cutin monomers were extracted three consecutive times in 2 ml hexane for 10 min using a mixer and centrifuged at 20°C. The collected supernatants were pooled and transferred into a pre-weighed vial, dried completely using a vacuum concentrator at 40°C, and then weighed to calculate total cutin yields (μg cm^{-2}). Heptadecanoate (C_{17}) and tricosanoate (C_{23}) were added as internal standards, and then samples were derivatized during 15 min at 100°C in BSTFA and pyridine (3:2, v/v). Derivatized samples (1 μl) were finally injected in on-column mode into a GC-MS and a GC-FID system for compound identification and quantification, respectively, under the same chromatographic conditions as described above for the analysis of cuticular waxes.

Determination of Cuticular Transpiration

Transpiration from the whole fruit was determined gravimetrically from measures of water loss over time as described elsewhere (Huang et al., 2017). Eight to twelve olives per sample were sealed with paraffin wax on the pedicel area (melting point 65°C; Roth, Karlsruhe, Germany). To reduce the relative humidity until approximately zero, fruit samples were placed in boxes over silica gel (AppliChem, Darmstadt, Germany) and kept at 25°C in an incubator (IPP 110, Memmert, Schwabach, Germany). Weight loss of the samples was monitored over time (five to six data points per individual sample) with an analytic electronic balance with ± 0.1 mg precision (MC-1 AC210S, Sartorius, Göttingen, Germany). Temperature inside the incubator was controlled continuously with a digital thermometer (Testoterm 6010, Lenzkirch, Germany) and the actual fruit temperature was measured using an infrared laser thermometer (Harbor Freight Tools, Calabasas, California). Transpiration rates (flux of water vapor; J in g m^{-2} s^{-1}) of the samples were calculated from changes in the fresh weight (ΔW in g) over time (Δt in s) and surface area (A in m^2) as indicated below:

$$J = \frac{\Delta W}{\Delta t \cdot A}$$

The permeance (P in m s^{-1}) was calculated from the transpiration rate (J) divided by the driving force:

$$P = \frac{J}{c^{*}_{ww}(a_{fruit} - a_{air})}$$

where c^{*}_{wv} was the water vapor content of air at saturation, obtained from tabulated values, a_{fruit} was the water activity in the fruit, which was assumed to be unity, and a_{air} was air water activity (that was close to zero).

Skin Surface Topography

Micro-topography of samples (25 olives per cultivar) was captured at two locations (180° apart) on the equatorial area of each individual fruit using fringe projection equipment (Primos™ Lite, Cranfield Image System, USA). Topography data were collected with an x-y resolution of 26.83 μm and z (vertical) resolution of 2 μm. Subsequent calculations to extract surface roughness descriptive parameters (Lai et al., 2018) were conducted with the accompanying proprietary software package (Primos™ v5.8, Cranfield Image Systems, USA).

Surface roughness parameters studied in this work were *Sa*, *Stm*, *Spm*, *Svm*, *Sk*, and *S* (Gadelmawla et al., 2002). *Sa* is the arithmetic average height parameter, defined as the mean of the absolute deviation of roughness irregularities from the mean line. *Stm* describes the mean distance between the lowest valley and the highest peak at the measured area. *Spm* is defined as the mean of the maximum height peaks, and *Svm* is the mean of the maximum depth valleys. *Sk* measures peak-to-valley surface roughness after excluding the predominant peaks and valleys, and hence illustrates the core roughness depth. *S* is the only horizontal parameter, defined as the average spacing between profile peaks at the mean line in the profile measured.

Microscopy Observations

Pericarp fruit samples were chopped to little cubes (roughly 2 mm per side) and fixed in a formaldehyde-acetic acid (FAA) solution [5% (v/v) formaldehyde and 5% (v/v) glacial acetic acid in 1:1 (v/v) ethanol-distilled water] for 12 h. Samples were dehydrated in aqueous solutions containing increasing ethanol concentrations up to 100% (v/v). Dehydrated samples were transferred to Eppendorf tubes for infiltration and polymerization in Technovit 7100® resin (Heraeus Kulzer GmbH, Wehrheim, Germany), and the resin was dried at 45°C for 24 h.

Resin-embedded samples were cut in 4-μm-thick sections using an ultramicrotome (Leica EM UC6, Leica Microsystems GmbH, Wetzlar, Germany), and subsequently stained on a slide for 15 min in a Sudan IV lysochrome solution [5% (w/v) in 85% (v/v) ethanol] in order to visualize the lipidic constituents of fruit cuticles. Excess staining was removed by rinsing in 50% (v/v) ethanol, and samples allowed to dry at room temperature. Olive pericarp sections were observed and photographed using a microscope (Leica DM4000 B) with a coupled camera (Leica DFC300 FX). Cuticle thickness was determined from five images obtained from five different fruit per cultivar and maturity stage with the Fiji image processing software (Schindelin et al., 2012).

Statistical Analysis

The statistical analyses were conducted with the JMP® Pro 13 software. Results were calculated as means ± standard deviations. Multifactorial analysis of variance (ANOVA) procedures were applied, with cultivar and maturation stage as the factors, and means were compared with the Student's t test ($p \leq 0.05$). PCA was used to help the interpretation of the data set obtained, using the Unscrambler software, version 9.1.2 (CAMO ASA, Oslo, Norway). Data were centered and weighed by the inverse of the

standard deviation of each variable, and full cross-validation was run as a validation procedure.

RESULTS

Olive cultivars assessed in this study included some preferentially used for oil production ("Argudell," "Picual," "Sevillenca"), for manufacturing of table olives ("Empeltre," "Manzanilla"), or for both purposes. The choice of genotypes comprised representatives of very early ("Empeltre," "Manzanilla"), early ("Sevillenca"), medium ("Arbequina," "Argudell," "Farga," "Picual"), and late ("Marfil," "Morrut") ripening patterns (Tous and Romero, 1993), as well as a range of fruit sizes (**Table 1**). Due to differing ripening patterns, data corresponding to the turning stage are lacking for three cultivars ("Manzanilla," "Marfil," and "Sevillenca"), as not enough fruit material was found at the sampling dates. The highest flesh to stone ratios, weight, and water contents were found for "Manzanilla," a very common table olive cultivar in Spain. The highest incidence of olive fly infestation was observed for "Empeltre" and "Manzanilla," which showed very high percentages of affected fruits, particularly in unripe olives (**Table S1**).

Surface Differences

Differences in surface characteristics were found among the nine olive cultivars assessed. Green fruits were stained with toluidine blue in order to visualize pores, cracks, or defects on the surface. Two groups of cultivars were revealed by the TB test: fruits of "Argudell," "Empeltre," "Manzanilla," "Marfil," and "Sevillenca" were stained, whereas those of "Arbequina," "Farga," "Morrut," and "Picual" were not, even after leaving the fruit samples in the staining solution for several hours.

Differences in skin topography of green fruit among the cultivars were also detected. "Farga" and "Morrut" fruits showed the most irregular surface as shown by higher values of vertical roughness parameters (*Sa*, *Stm*, *Spm*, *Svm*, and *Sk*). On the contrary, fruit of "Sevillenca," 'Empeltre," "Arbequina," and "Argudell" had smoother skin surface than other cultivars based on lower values of vertical parameters together with higher horizontal roughness as shown by *S*, representative of peak-to-peak spacing (**Table 2**). "Farga" samples displayed very different micro-topography and visual appearance as revealed by fringe projection data in comparison with other cultivars. In order to highlight the distinctive features of the surface of "Farga" olives, a boxplot of *Sa* as the most common roughness parameter is provided (**Figure S1**). Three-dimensional diagrams of raw data obtained from fringe projections, TB staining, and micrographs of Sudan IV-stained pericarp cross-sections for "Farga" and "Sevillenca" fruit are shown as an example to illustrate these differences (**Figure 1**), while results for the rest of cultivars assessed are presented as supplementary figures (**Figures S2, S3**, and **S4** respectively). The surface of "Sevillenca" green olives was not only smoother than that of "Farga" at the same maturity stage, but also displayed significantly thicker cuticles (**Table 3** and **Figure 1**).

Cuticle Characteristics and Changes Along Maturation

With the exception of "Arbequina," cuticle yields (mg cm^{-2} surface area) did not change significantly along fruit maturation (**Table 3**). Total cuticle amounts at the green and the ripe stages ranged from 1.9 to 3.1 mg cm^{-2} and from 2.0 to 3.8 mg cm^{-2}, respectively. At both maturity stages, the lowest yields were observed for "Manzanilla" fruit. Consistent with the lowest cuticle yields, "Manzanilla" olives also displayed the lowest values for cuticle thickness, irrespective of maturity stage. Cuticle thickness remained steady along on-tree maturation in five ("Argudell," "Farga," "Manzanilla," "Marfil," and "Picual") out of the nine cultivars studied, while a significant decrease was observed for the rest of the genotypes ("Arbequina," "Empeltre," "Morrut," and "Sevillenca") (**Table 3**).

Water permeance was determined in mature fruit of all nine cultivars studied. Two cultivar types could be defined according to permeability levels: a low-permeance group, including "Arbequina," "Empeltre," "Farga," "Manzanilla," "Picual," and "Sevillenca" and displaying water permeance values ranging from 7.21 ("Manzanilla") to 8.13 ("Picual") × 10^{-5} m s^{-1}, and a high-permeance cultivar set ("Argudell," "Marfil," and "Morrut") showing water permeance values above 11 × 10^{-5} m s^{-1} (**Table 3**). No changes in water permeance levels were observed along maturation for "Arbequina," "Argudell," or "Sevillenca," while

TABLE 2 | Surface roughness parameters (μm) measured in olive fruits at the green stage.

Cultivar	*Sa*	*Stm*	*Spm*	*Svm*	*Sk*	*S*
"Arbequina"	8.5 de	54.4 d	25.4 d	–29.0 a	27.0 de	839.4 a
"Argudell"	8.5 de	58.4 d	27.8 d	–30.6 a	27.0 de	772.6 bc
"Empeltre"	7.4 e	51.3 d	24.3 d	–27.1 a	23.5 e	818.2 ab
"Farga"	20.6 a	98.7 a	49.8 a	–48.9 c	60.2 a	678.6 e
"Manzanilla"	11.2 bc	76.5 bc	36.8 bc	–39.7 b	36.8 b	699.0 de
"Marfil"	9.8 cd	69.1 c	33.4 c	–35.7 b	30.5 cd	735.1 cd
"Morrut"	12.8 b	80.7 b	40.7 b	–40.0 b	39.3 b	654.8 e
"Picual"	10.0 cd	72.7 bc	34.8 c	–37.9 b	32.1 c	678.5 e
"Sevillenca"	7.4 e	51.4 d	24.7 d	–26.7 a	23.5 e	739.5 cd

Sa, Stm, Spm, and Svm are related to vertical roughness, Sk represents core roughness, and S stands for horizontal roughness. Values represent means of 25 olives per cultivar. Means followed by different letters within a column are significantly different at P ≤ 0.05 (Student's t test).

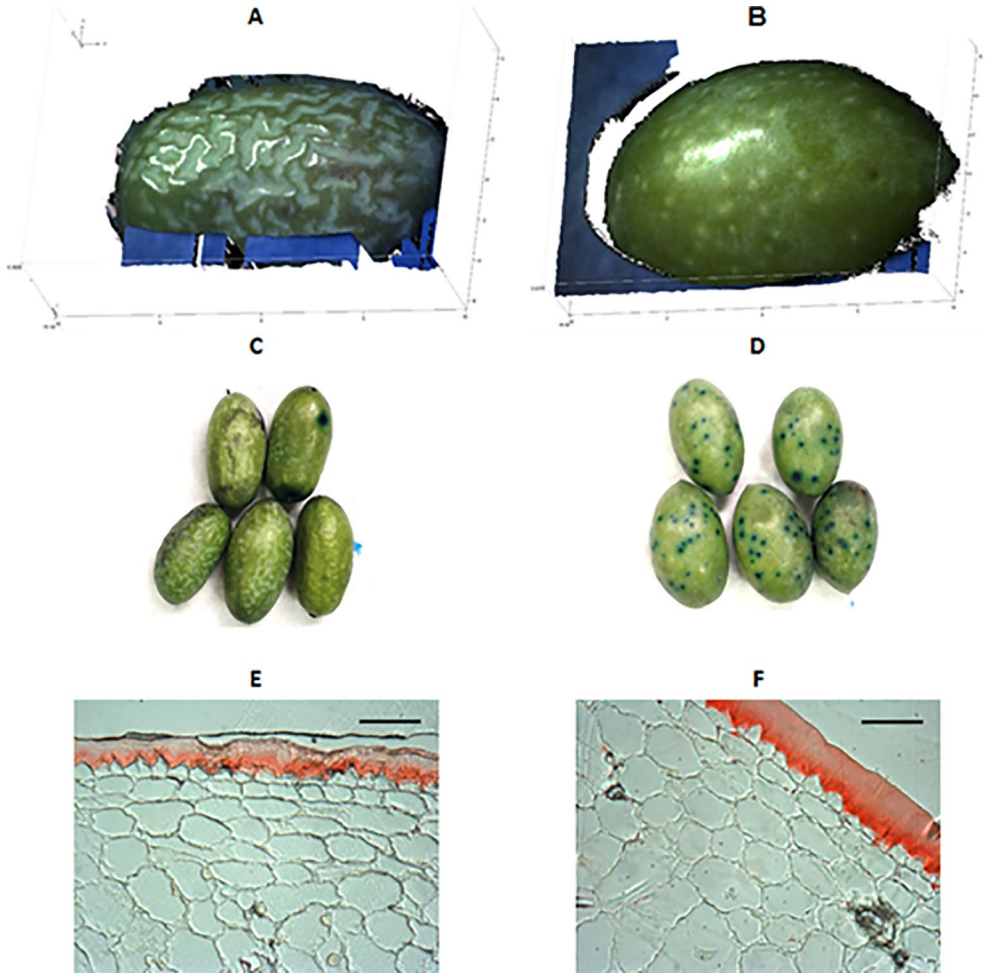

FIGURE 1 | An example of fruit surface differences between two olive cultivars (left, "Farga"; right, "Sevillenca") at the green stage. **(A**, **B)**: 3D-diagrams of raw data outputs from fringe projections. Blue and black areas represent background noise due to the shape and size of the olives, which did not cover the whole assessment window of the equipment. **(C**, **D)**: Toluidine blue (TB) staining. **(E**, **F)**: Sudan IV-stained cross-sections of fruit pericarp observed under a bright-field microscope (bar: 60 μm).

significant increases in mature as compared to green fruit were found for "Morrut" and "Picual" (38 and 19%, respectively).

Excepting "Marfil" and "Picual," wax yields decreased along maturation, both in absolute terms (μg cm^{-2}) and as a percentage over total cuticle (**Table 3**). Wax percentages ranged from 9.8% in "Farga" mature fruit to 39.1% in "Empeltre" green samples. When expressed as mass per surface area, yields ranged from roughly 230 μg cm^{-2} in "Farga" mature olives to over fivefold that much (1,284.5 μg cm^{-2}) in "Picual" mature fruit, consistent with thicker cuticles in these samples (**Table 3**). More cultivar-to-cultivar variation was observed for cutin, both regarding yields and time-course changes along on-tree maturation. Total cutin yields decreased over fruit maturation in "Arbequina" and "Farga" fruits (approximately 23 and 18%, respectively), whereas they increased in "Picual," "Argudell," and "Empeltre" fruits (by 38, 19, and 17%, in that order) and remained steady in the rest of the considered cultivars ("Manzanilla," "Marfil," "Morrut," and "Sevillenca"). Wax-to-cutin ratio declined with maturity stage in all cultivars with the exception of "Marfil," owing to increased wax contents.

Cuticular Wax Composition

Triterpenoids were the dominant fraction in cuticular waxes, relative percentages over total waxes ranging from 58 to roughly 81% (**Table 4**). For "Farga," "Marfil," and "Picual" olives, the total amount of triterpenoids decreased with maturity by 15, 18, and 23%, respectively, whereas no significant changes were observed for the rest of the cultivars considered. Maslinic (27 to 52%, contingent on cultivar and maturity stage) and oleanolic (19 to 43%) acids were detected in the wax fraction obtained from all the samples, with very minor contents of ursolic acid being identified additionally in "Farga," "Picual," and "Sevillenca" fruit (**Supplementary Table 2**). Relative contents of oleanolic acid decreased with maturity stage, while the amounts of maslinic acid generally showed limited changes, with the exception of

TABLE 3 | Total cuticle amounts, cuticular wax and cutin yields, wax to cutin ratios, cuticle thickness, and water permeance in olive fruits at the green, turning, and ripe stages.

Cultivar	Maturity stage	Cuticle yield (mg cm^{-2})		Wax yield (μg cm^{-2})		Wax (%)		Cutin yield (μg cm^{-2})		Cutin (%)		C16/C18	Wax/cutin ratio		Thickness (μm)		Permeance (× 10^{-5} m s^{-1})	
"Arbequina"	Green	3.1	a A	1163.6	a A	37.4	a AB	1205.4	a A	38.7	a A	0.41	0.97	a B	41.0	ab B	7.3	a B
	Turning	2.4	b DE	405.9	c D	16.7	c C	945.0	b BC	39.0	a A	0.33	0.43	c C	44.5	a A	7.9	a C
	Ripe	2.5	ab B	456.6	b D	18.5	b D	931.1	b BC	37.7	a AB	0.37	0.49	b EF	32.9	b BC	8.0	a B
"Argudell"	Green	2.9	a AB	649.4	a D	22.8	a E	846.9	b BC	29.8	b D	0.43	0.77	a C	35.0	a BC	11.2	a A
	Turning	3.6	a A	497.4	b C	13.7	c D	995.5	a B	27.4	b B	0.41	0.50	b C	34.2	a ABC	10.8	a A
	Ripe	2.7	a AB	453.5	b D	16.7	b DE	1021.4	a B	37.7	a AB	0.40	0.45	b F	36.3	a AB	11.9	a A
"Empeltre"	Green	2.3	a BCDE	903.6	a C	39.1	a A	722.7	b DE	31.3	a CD	0.35	1.26	a A	62.9	a A	na	
	Turning	2.8	a CD	882.6	a A	31.6	b A	826.0	ab CD	29.6	a B	0.44	1.08	a A	38.7	b ABC	na	
	Ripe	3.0	a AB	496.1	b CD	16.6	c DE	890.5	a BCD	29.9	a CD	0.38	0.56	b DE	32.9	b BC	7.4	B
"Farga"	Green	2.7	a ABCD	899.3	a C	34.0	a C	962.3	a B	36.4	a ABC	0.49	0.94	a BC	26.2	a C	na	
	Turning	2.3	a E	564.6	b BC	24.9	b B	807.8	b CD	35.7	a A	0.44	0.70	b B	33.6	a BC	na	
	Ripe	2.4	a B	229.7	c F	9.8	c F	789.1	b CD	33.5	a BC	0.37	0.29	c G	27.7	a BC	7.3	B
"Manzanilla"	Green	1.9	a E	566.3	a E	30.2	a D	620.1	a E	33.1	a BCD	0.44	0.92	a BC	25.5	a C	na	
	Turning	na		na		na		na		na		na	na		28.5	a C	na	
	Ripe	2.0	a B	364.7	b E	18.1	b D	527.5	a E	26.2	a D	0.43	0.69	b BC	25.7	a C	7.2	B
"Marfil"	Green	2.1	a CDE	320.2	b F	14.7	b F	810.0	a CD	37.3	a AB	0.29	0.40	b D	34.4	a BC	na	
	Turning	na		na		na		na		na		na	na		32.8	a C	na	
	Ripe	2.3	a B	581.0	a B	25.4	a B	756.1	a D	33.0	a BC	0.28	0.78	a AB	31.0	a BC	11.8	A
"Morrut"	Green	3.0	a A	994.8	a B	33.6	a C	933.9	a B	31.6	a CD	0.27	1.07	a B	44.4	a B	6.9	c B
	Turning	3.0	a BC	371.8	c D	12.2	c D	781.4	a D	25.7	b B	0.23	0.48	b C	32.2	b C	9.4	b B
	Ripe	2.8	a AB	437.5	b D	15.5	b E	886.1	a BCD	31.5	a CD	0.32	0.49	b EF	35.8	ab AB	11.1	a A
"Picual"	Green	2.7	a ABC	973.1	b BC	35.8	a BC	952.2	c B	35.1	a ABC	0.36	1.03	a B	37.0	a B	6.6	b B
	Turning	3.4	a AB	635.7	c B	19.0	b C	1230.9	b A	36.8	a A	0.32	0.52	c C	43.9	a AB	7.3	ab C
	Ripe	3.8	a A	1284.5	a A	33.5	a A	1543.9	a A	40.2	a A	0.33	0.83	b A	44.3	a A	8.1	a B
"Sevillenca"	Green	2.1	a DE	693.0	a D	33.2	a C	668.6	a E	31.9	a CD	0.41	1.05	a B	40.6	a B	7.3	a B
	Turning	na		na		na		na		na		na	na		31.6	b BC	7.6	a C
	Ripe	2.4	a B	535.8	b BC	21.9	b C	834.8	a CD	34.2	a BC	0.36	0.65	b CD	30.8	b BC	7.3	a B

Cuticular membranes were isolated from skin samples (around 100 cm^2) obtained from 30 to 75 olives, contingent upon fruit size. Wax and cutin data represent means of three technical replicates of this starting material. For cuticle thickness and water permeance, values represent means of five or 10 biological replicates, respectively (na, value not available). Different capital letters denote significant differences among the cultivars for a given maturity stage, and different lower-case letters stand for significant differences among maturity stages for a given cultivar, at $P \leq 0.05$ (Student's t test).

** Ratio of C_{16} to C_{18} cutin monomers.*

TABLE 4 | Relative amounts (% over total waxes) of wax compound types in cuticles isolated from olive fruits at the green, turning, and ripe stages.

Cultivar	Maturity stage	ACL *		Acyclic/cyclic ratio		Triterpenoids (%)		Fatty acids (%)		Fatty alcohols (%)		*n*-Alkanes (%)		Sterols (%)		Unidentified (%)	
"Arbequina"	Green	25.2	a AB	0.30	a BC	63.7	a CDE	7.4	a B	8.0	a BC	3.7	a A	1.1	a A	16.2	a AB
	Turning	25.0	a A	0.25	a ABC	68.3	a AB	9.0	a C	4.7	a AB	3.1	ab A	0.4	a B	14.5	a B
	Ripe	24.6	a BC	0.26	a CDE	67.6	a AB	9.6	a C	5.7	a C	2.3	b CD	0.8	a BCD	14.0	a BC
"Argudell"	Green	25.2	a AB	0.18	a D	70.0	a BCD	4.4	b CD	5.2	a D	3.2	a AB	0.9	a AB	16.4	a AB
	Turning	23.7	b B	0.21	a BC	64.7	a B	8.4	a CD	2.8	b B	2.6	a AB	1.1	a AB	20.5	a A
	Ripe	24.0	ab E	0.22	a DE	66.2	a AB	8.4	a C	3.4	b E	3.2	a BC	1.7	a A	17.1	a BC
"Empeltre"	Green	24.9	a AB	0.17	a D	71.3	a BC	5.2	b BCD	5.1	ab D	2.2	a BC	0.9	ab AB	15.4	a BC
	Turning	24.8	a A	0.19	a BC	73.3	a A	5.8	b E	7.0	a A	0.6	b D	0.4	b B	12.8	a B
	Ripe	24.2	b DE	0.22	a DE	70.2	a A	9.3	a C	3.6	b DE	2.7	a BCD	1.2	a ABC	13.0	a BC
"Farga"	Green	25.6	a A	0.20	b CD	73.5	a AB	6.9	b BC	6.0	a CD	2.0	ab CD	0.5	ab BC	11.1	b CD
	Turning	24.9	ab A	0.26	ab AB	70.6	a AB	11.0	a B	6.3	a A	1.3	b CD	0.4	b B	10.4	b B
	Ripe	24.4	b CD	0.33	a BC	62.9	b AB	12.7	a B	4.6	a CD	3.5	a B	0.8	a BCD	15.5	a BC
"Manzanilla"	Green	25.0	a AB	0.41	a AB	63.1	a DE	13.0	a A	11.5	a A	0.5	b E	0.38	a CD	11.6	a CD
	Ripe	24.9	b B	0.49	a A	58.4	a B	15. 8	a A	10.7	a A	2.0	a D	0.8	a BCD	12.4	a CD
"Marfil"	Green	25.5	a A	0.19	b D	74.8	a AB	7.3	b B	5.8	b CD	1.0	b DE	0.6	a BC	10.6	a D
	Ripe	25.4	a A	0.40	a AB	61.6	b AB	11.9	a B	8.1	a B	4.8	a A	0.6	a CD	13.1	a BC
"Morrut"	Green	23.9	b C	0.13	b D	70.7	a BCD	6.2	b BC	2.5	c E	0.5	b E	0.2	b CD	20.0	a A
	Turning	23.9	b B	0.31	a A	64.1	a B	15.2	a A	3.3	b B	2.0	a BC	1.5	a A	14.0	b B
	Ripe	24.7	a B	0.30	a CD	67.2	a AB	12.7	a B	5.0	a C	2.2	a CD	0.4	ab D	12.5	b C
"Picual"	Green	24.6	a BC	0.09	b D	80.8	a A	2.8	c D	4.5	a DE	0.2	b E	nd	b D	11.7	b CD
	Turning	23.9	b B	0.17	a C	72.1	ab AB	6.7	a DE	3.3	a BC	2.2	a B	1.5	a A	14.2	b B
	Ripe	24.2	b DE	0.16	a E	61.9	b AB	4.6	b D	3.6	a DE	1.8	a D	1.2	a ABC	26.9	a A
"Sevillenca"	Green	25.5	a A	0.44	a A	61.5	a E	15.7	a A	9.9	a AB	1.7	a CD	0.9	a AB	10.4	b D
	Ripe	24.4	b CD	0.34	a BC	58.1	a B	15.1	a A	3.0	b E	2.3	a CD	1.5	a AB	20.1	a AB

Cuticular membranes were isolated from skin samples (around 100 cm^2) obtained from 30 to 75 olives, contingent upon fruit size. Values represent means of three technical replicates of this starting material (nd, non-detectable). Different capital letters denote significant differences among the cultivars for a given maturity stage, and different lower-case letters stand for significant differences among maturity stages for a given cultivar, at $P \leq 0.05$ (Student's t test).

**ACL, average chain length of acyclic wax compounds.*

"Farga" and "Picual" olives which displayed a sustained decline over maturation, and "Sevillenca" samples for which, on the contrary, increased maslinic acid contents were found for the ripe as compared with the green stages.

Reduction of triterpenoid contents along maturation in "Farga," "Marfil," and "Picual" fruits, together with an increment in fatty acids, led to increased acyclic to cyclic compounds ratios (**Table 4**). Augmented percentages of fatty acids, alcohols, and *n*-alkanes over total waxes during maturation also caused increased acyclic to cyclic compounds ratios in "Morrut" samples, whereas the increase in fatty acids observed in "Argudell" and "Empeltre" was not important enough to significantly modify this ratio. Fatty acids and alcohols were the main types of acyclic compounds identified in cuticular waxes, with very minor percentages of *n*-alkanes, in contrast with reports for other fruit species, for which much higher *n*-alkane percentages in cuticular waxes have been reported (Belge et al., 2014a; Belge et al., 2014b). "Manzanilla" and "Sevillenca" samples displayed the highest relative percentages of fatty acids and alcohols (**Table 4**). Among fatty acids, the most abundant compounds detected lignoceric (24:0) and cerotic (26:0) acids, while tetracosanol (C_{24}) and hexacosanol (C_{26}) were the predominant alcohols (**Table S2**). The ACL of the acyclic compounds identified in the wax fraction decreased in the course of fruit maturation for most of the cultivars included in this work, with the exception of "Arbequina" and "Marfil," for which no significant differences were found, and "Morrut" which showed an increase from the turning to the ripe stages (**Table 4**).

Cutin Monomer Composition

C_{18}-type monomers stood out quantitatively in cutin composition of the cultivars considered, representing around two thirds (68.7 to 76.2%) over total cutin monomers identified (**Supplementary Table 3**). The predominant compound type detected in the cutin fraction was hydroxy-fatty acids, relative percentages ranging 40 to 59% (**Table 5**). Among these, *ω*-hydroxy fatty acids and *ω*-hydroxy fatty acids with midchain hydroxyl groups were particularly abundant, mainly 18-hydroxyoctadecenoic and 16-hydroxyhexadecanoic acids. The relative percentage of 18-hydroxyoctadecenoic showed in general a moderate decline along maturation, "Picual" samples displaying the highest contents of this cutin monomer (24.1, 21.5, and 22.5% at the green, turning, and black stage, respectively). A similar trend, with the exception of 'Morrut," was observed for 16-hydroxyhexadecanoic acid, "Manzanilla" and "Picual" fruits showing the highest amounts of this compound. The relative percentages of ω-hydroxy fatty acids with midchain hydroxyl groups remained steady throughout fruit maturation, "Farga" samples showing the highest values (29.4% at the green stage) (**Table 5**). The predominant cutin monomer of this type was 9/10,16-dihydroxyhexadecanoic acid, which did not show noticeable variations during fruit maturation (**Table S3**).

In terms of percentage over total cutin, α,ω-dicarboxylic (8.5 to 17.7%, depending on cultivar and maturity stage) and monocarboxylic (3.3 to 21.5%) fatty acids were also quantitatively important. With the exception of "Morrut" fruits, the content of dicarboxylic fatty acids decreased along maturation, while that of monocarboxylic fatty acids was significantly augmented in all the cultivars analyzed, excepting "Marfil" (**Table 5**). Within the dicarboxylic fatty acids family, 9-octadecenedioic acid was the most abundant compound identified, the highest amounts being found for "Picual" and "Morrut" olives (16.9 and 16.5%, respectively), roughly twice those determined in "Empeltre" fruit (**Supplementary Table 3**).

DISCUSSION

All olive samples used in this work were grown at the same orchard, under the same cultural practices. Therefore the chemical composition differences in isolated fruit cuticles among the studied cultivars are not likely to reflect different environmental conditions, and might underlie the observed features of surface topography as well as the resistance of each variety to biotic and abiotic stress factors. Water permeance of olive fruit may be modulated by different cuticle-related factors, including the presence of surface discontinuities, total wax coverage, wax-to-cutin ratio, acyclic-to-cyclic waxes ratio (which would potentially provide more efficient barriers against water loss), and ACL of acyclic wax compounds. However, no consistent relationships were found among all these variables. The toluidine test as well as cuticle yields or thickness were also apparently unrelated to water permeance values. No apparent connection was observed either between the presence of discontinuities on fruit surface as revealed by the toluidine test and the susceptibility to infestation by olive fly (*Bactrocera oleae*): among the cultivars used in this work, "Empeltre," "Farga," "Manzanilla," and "Sevillenca" are characterized by severe incidence of infestation, while "Arbequina," "Argudell," "Marfil," "Morrut," and "Picual" are less susceptible to this plague (Barrios et al., 2015), which do not agree with the groupings revealed by TB staining (**Table 1**).

However, our data suggest a relationship between TB staining results and descriptors of surface roughness. Vertical roughness parameters *Stm*, *Spm*, and *Svm* can be a good indicator for uneven surfaces and for surface cracks, which will normally have higher peaks and deeper valleys. An irregular surface can also display low horizontal roughness (*S*) values, because adjacent peaks would be close to each other. Among the olive cultivars considered herein, the lowest values for horizontal roughness were observed for "Farga," "Morrut," and "Picual" samples, together with deeper valleys as shown by *Svm* (**Table 2**). Interestingly, when roughness parameters and TB staining data were used to characterize the samples by means of a PCA model, a good correlation was found between *S*, *Svm*, and TB test results (**Figure S5**). Eighty six percent of total variability was explained by the two first principal components (PC) alone. The plot shows that stained fruits displayed higher values for *S* and *Svm*, and the lowest for *Sa*, *Stm*, *Spm*, and *Sk*. Albeit to a lesser extent, a correlation was also found between roughness parameters and the incidence of fruit infestation by the olive fly (*B. oleae*). Higher percentage of infested fruits (**Table S1**) was associated to high *Svm* values

TABLE 5 | Relative amounts (% over total cutin) of cutin monomer types in cuticles isolated from olive fruits at the green, turning, and ripe stages.

Cultivar	Maturity stage	FA* (%)		α,ω-diFA, mcOH (%)		α,ω-diFA, mcOH (%)		ω-OH FA (%)		ω-OH FA, mcOH (%)		α-OH FA (%)		Other OH FA (%)		Alcohols (%)		Unidentified (%)	
"Arbequina"	Green	5.0	b BC	11.5	a D	2.6	a B	30.4	a BCD	21.5	a B	1.9	a B	nd	C	2.0	ab D	25.2	a A
	Turning	18.0	a A	11.5	a B	2.1	ab B	28.3	ab B	16.0	b BC	0.9	b C	nd	C	1.7	b BC	21.5	c ABC
	Ripe	16.4	a BC	9. 6	a CD	2.0	b B	27.3	b B	18.3	ab BCD	1.2	ab C	nd	B	2.3	a BC	23.0	b A
"Argudell"	Green	5.3	b BC	14.6	a B	1.4	a D	32.1	a BC	21.1	a B	1.4	a B	nd	b C	3.0	a A	21.2	a CDE
	Turning	19.6	a A	10.9	b B	1.0	b CD	27.8	b B	18.1	a B	1.3	a BC	nd	b C	2.4	a AB	19.0	b C
	Ripe	20.2	a A	11.1	b C	1.4	a C	24.8	b C	19.6	a ABC	1.7	a C	0.3	a A	2.6	a BC	18.4	b E
"Empeltre"	Green	4.7	b BC	11.7	a CD	3.6	a A	28.9	a CD	21.8	a B	5.7	a A	0.1	a B	1.5	a E	22.1	a BC
	Turning	5.9	b C	9.5	b C	3.9	a A	26.2	a B	27.1	a A	5.6	a A	0.2	a BC	1.7	a C	20.0	a ABC
	Ripe	13.1	a CDE	8.5	c D	3.4	a A	23.1	b C	22.6	a A	5.6	a A	0.3	a AB	1.8	a DE	21.6	a ABC
"Farga"	Green	6.0	c B	11.2	a D	1.9	a C	26.8	a D	29.4	a A	1.6	a B	nd	b C	2.2	b CD	21.0	a CDE
	Turning	8.8	b C	11.2	a B	1.5	a BCD	28.4	a B	23.8	a A	2.0	a B	nd	b C	2.7	a A	21.7	a AB
	Ripe	19.7	a AB	9.7	a CD	1.5	a C	24.1	a C	20.8	a AB	1.2	a C	0.2	a AB	2.5	ab BC	20.3	a CD
"Manzanilla"	Green	5.6	b BC	17.0	a A	1.3	a D	33.9	a B	18.3	a BCD	1.3	a B	0.1	a B	2.8	a AB	19.8	a DE
	Ripe	13.3	a CD	13.9	a B	1.3	a C	28.4	b B	18.6	a ABCD	1.3	a C	0.4	a A	3.3	a A	19.5	a DE
"Marfil"	Green	10.2	a A	16.9	a A	2.6	a B	32.2	a BC	12.5	a D	1.8	a B	0.2	b AB	1.9	a D	21.7	a BCD
	Ripe	11.1	a DEF	14.4	b B	3.0	a A	29.5	a B	14.9	a CD	4.5	b B	0.3	a AB	1.7	a E	20.6	CD
"Morrut"	Green	4.3	c BC	17.7	a A	2.0	a C	32.9	a BC	13.7	a CD	1.9	a B	0.2	a A	1.9	a D	25.4	a A
	Turning	17.1	a AB	15.3	b A	1.7	a BC	28.4	a B	11.5	a C	1.6	a BC	0.4	a A	1.8	ab BC	22.2	b A
	Ripe	9.7	b EF	17.3	ab A	1.4	a C	29.7	a B	16.0	a BCD	1.8	a C	0.4	a A	1.6	b E	22.2	b AB
"Picual"	Green	3.3	c C	17.6	a A	0.9	b D	40.1	a A	14.7	a BCD	1.6	a B	0.1	a B	2.6	a BC	19.1	b E
	Turning	13.9	a B	15.7	b A	0.8	b D	34.5	b A	12.7	a CD	1.0	a C	0.3	a AB	2.0	b BC	19.2	b BC
	Ripe	9.6	b F	15.7	b AB	1.2	a C	34.9	b A	14.1	a D	1.4	a C	0.1	a AB	2.1	b CD	20.9	a BCD
"Sevillenca"	Green	5.4	b BC	13.6	a BC	2.3	a BC	31.1	a BCD	20.1	a BC	1.2	a B	0.1	a B	2.5	a BC	23.8	a AB
	Ripe	21.5	a A	11.3	b C	2.0	a B	24.3	b C	18.8	a ABCD	1.3	a C	0.3	a AB	1.8	b DE	18.7	b E

Cuticular membranes were isolated from skin samples (around 100 cm^2) obtained from 30 to 75 olives, contingent upon fruit size. Values represent means of three technical replicates of this starting material (nd, non-detectable). Different capital letters denote significant differences among the cultivars for a given maturity stage, and different lower-case letters stand for significant differences among maturation stages for a given cultivar, at $P \leq 0.05$ (Student's t test).

***** *Abbreviations: FA, monocarboxylic fatty acids; α,ω-diFA, α,ω-dicarboxylic fatty acids; α,ω-diFA, mcOH, α,ω-dicarboxylic fatty acids with mid-chain-hydroxy group; ω-OH FA, ω-hydroxy fatty acids; ω-OH FA, mcOH, ω-hydroxy fatty acids with mid-chain-hydroxy group; α-OH FA, α-hydroxy fatty acids; other OH FA, other hydroxy fatty acids.*

(**Figure S5**), which might suggest that deeper irregularities on the surface may favor egg deposition.

Cuticle thickness values were higher than those reported for fruit from other olive cultivars, including "Gentile di Chieti," "Carboncella," "Dritta," "Castiglionese," "Intosso," and "Kalamata" (Lanza and Di Serio, 2015). However, whereas that work found decreased cuticle thickness along maturation in all the cultivars assessed, a declining trend was observed in this study uniquely for "Arbequina," "Empeltre," "Morrut," and "Sevillenca," while cuticle thickness remained unchanged for the rest of cultivars considered. For tomato fruit (*S. lycopersicum* L.), cuticle thickness has been reported to increase during fruit development up to the mature green or breaker stage, and then to decrease thereafter until attaining full ripeness (Domínguez et al., 2008). Wide variation in thickness values has also been found among fruit species. Similar cuticle thickness has been reported for ripe tomato (*S. lycopersicum* L.), green and mature pepper (*Capsicum annuum* L.), and apple (*Malus pumila* L.) fruit in comparison with olive (Fernández et al., 1999), while that in mangoes (*Mangifera indica* L.) is reportedly thinner (Camacho-Vázquez et al., 2019).

A previous study on "Arbequina" (Huang et al., 2017) did not find significant differences in water permeance of fruit at different maturity stages, the observed values averaging 9.5×10^{-5} m s^{-1}. Similar results were found in the current study for "Arbequina," but not for all the rest of varieties: changes in water permeance throughout fruit maturation were determined for five out of the nine cultivars studied, data indicating significant increases for "Morrut" and "Picual" samples, which incidentally displayed the highest loss in water content from the green to the ripe stages (27.1 and 13.3% for "Morrut" and "Picual," respectively) (**Table 1**). Water permeances observed in this study ranged from 6.6 to 11.9×10^{-5} m s^{-1}, and were higher in comparison with those found for other fruit crops such as tomato (*S. lycopersicum* L.) and apple (*Malus domestica* Borkh), ranging respectively from 0.9 to 4.9×10^{-5} m s^{-1} (Leide et al., 2007; Leide et al., 2011) and from 4.6 to 5.3×10^{-5} m s^{-1} (Leide et al., 2018), but one order of magnitude lower than those observed for sweet cherry (*Prunus avium* L.) (1.4 to 3.7×10^{-4} m s^{-1}) (Athoo et al., 2015).

With the exception of "Arbequina," no significant changes in total cuticle yields were observed over maturation. Reports on changes in total cuticle yields (μg cm^{-2}) over fruit ripening of a model species such as tomato have been shown to be cultivar-dependent (Domínguez et al., 2008; España et al., 2014), while they were found to decrease over ripening of sweet cherry (Peschel et al., 2007). Contrarily to reports for tomato (Leide et al., 2007) or orange (*Citrus sinensis* Osbeck) (Wang et al., 2016) fruit, for which increased wax coverage was observed along maturation, the opposite was found in this work for olives, with the exception of "Marfil" samples. In contrast, the proportions of the different wax fractions in olive fruit have been recently reported to be generally unrelated to sampling date, and to be largely cultivar-dependent (Vichi et al., 2016). Cutin yields were between 25.7 and 40.2%, and showed minor variations over fruit maturation. These cutin percentages over total cuticle were similar to those reported for some berries such as sea buckthorn (*Hippophaë rhamnoides* L.), cranberry (*Vaccinium oxycoccos* L.), or lingonberry (*Vaccinium vitis-idaea* L.), but much higher than those in black currant (*Ribes nigrum* L.) or bilberry (*Vaccinium myrtillus* L.) (8 and 6%, respectively) (Kallio et al., 2006). Stable cutin yields together with decreased wax coverage led to a significant decline in wax to cutin ratios (**Table 3**), in contrast with an earlier work on "Arbequina," where no changes along fruit maturation were found (Huang et al., 2017). Both cutin yield and cutin percentage were inversely correlated to the observed olive fly egg deposition in the samples ($r = -0.59$ and $r = -0.57$ respectively), suggestive of a protective action of such compounds in the skin. This observation is in accordance with earlier suggestions that cultivar-related differences in olive fly egg deposition might be related to differential skin composition (Iannotta, 2007; Rizzo et al., 2007).

Triterpenes were the predominant cuticular wax compound type found in olive fruit as reported elsewhere (Lanza and Di Serio, 2015; Huang et al., 2017), and similarly to observations for other drupes such as sweet cherry (Peschel et al., 2007; Belge et al., 2014a) and peach (Belge et al., 2014b), as well as for blueberry (*Vaccinium* spp.) (Chu et al., 2016). Complete information on cuticle composition is available only for a handful of fruit species (reviewed in Lara et al., 2015). Whereas the triterpenoid fraction of cuticular waxes is dominated by triterpenoid alcohols in orange, Asian pear (*Pyrus sinkiangenesis* Yü and *Pyrus bretschneideri* Rehd) (Wu et al., 2017) as well as in fruit species within the *Solanaceae* family, triterpenoid acids predominate in grapes, olives, and *Rosaceae* fruit species. In fruit species in which triterpenoid acids are prevalent, the triterpenoid profile has been reported to consist uniquely of oleanolic acid (30% of total waxes) in mature grapes (*Vitis vinifera* L.) (Casado and Heredia, 1999), and of ursolic followed by oleanolic acid in peach and sweet cherry (Peschel et al., 2007; Belge et al., 2014a; Belge et al., 2014b). In olive fruit, the main triterpene compounds detected were maslinic and oleanolic acids, in agreement with previous works (Bianchi, 2003; Stiti et al., 2007; Guinda et al., 2010). An inverse relationship between triterpenoid acids and olive fly egg deposition has been reported elsewhere (Kombargi et al., 1998). Triterpenoids also have reportedly an important role in the mechanical strength of fruit cuticles (Tsubaki et al., 2013; Wu et al., 2018), and have been shown to be related to weight loss and softening rates in blueberry (Moggia et al., 2016). In this work, however, no such relationship was observed between the incidence of olive fly infestation and triterpene content (**Table 4**, **Table S1**). Contrarily, data show a positive correlation of triterpene acid levels to the percentage of affected fruit, with $r = 0.36$ and $r = 0.49$ for maslinic and oleanolic acids, respectively. Furthermore, when maturity stages were considered separately, high correlation coefficients were found for fruit at the turning stage (0.97 and 0.93 for maslinic and oleanolic acids, correspondingly). This may be relevant to understand resistance or tolerance to stress factors, as this physiological stage of the fruit coincides with environmental conditions which favor the development of pests and diseases (Vichi et al., 2016), and indeed olive fly infestation is particularly intense during the period of color change.

The profiles of fatty acids and fatty alcohols were in agreement with data reported by Huang et al. (2017), C_{24} and C_{26} being the most abundant compounds within both wax types. However, the percentage of *n*-alkanes over total waxes was very low in comparison with other fruit species: for example, *n*-alkanes accounted for 29.4% of total waxes in "Jesca" peaches at harvest (Belge et al., 2014b), whereas in the present study the highest amount detected was 4.8% in "Marfil" mature olives (**Table 4**). Accordingly, the ACL of acyclic wax compounds was lower than that found in other fruit species: ACL values were 28.8 to 29.9 in apple (Leide et al., 2018), sweet cherry (Athoo et al., 2015), and tomato (*S. lycopersicum* L.) (Leide et al., 2011).

C_{18}-type cutin monomers were 2 to 3.7 times more abundant than the C_{16}-type. Even so, 9/10,16-dihydroxyhexadecanoic was quantitatively the main ω-hydroxyacid with midchain hydroxyl groups identified in cutin samples, and an important compound in quantitative terms in cutin composition of all the olive cultivars considered herein. This compound has been reported to be prominent in cutin composition of mango (Camacho-Vázquez et al., 2019), a number of berries (Kallio et al., 2006; Järvinen et al., 2010), sweet cherry (Peschel et al., 2007), tomato (Leide et al., 2007), and pepper (*Capsicum* sp.) (Parsons et al., 2012). In contrast, cutin of mature persimmons (*Diospyros kaki* Thunb.) has been found to contain as much as 43.7% 9,10-epoxy-18-hydroxyoctadecanoic acid together with 17.4% 9/10,16-dihydroxyhexadecanoic acid (Tsubaki et al., 2013). In a great variety of plants, ω-hydroxy acids (either C_{16} or C_{18}) dominate cutin composition (Fich et al., 2016), with agrees with results shown herein for olive fruit (**Table 5**, **Table S3**).

CONCLUSIONS

This comparative study provided new insights in genotype-related differences in surface and cuticle features of olive fruit. Information on the chemical composition of both cuticular waxes and cutin in fruit of nine olive cultivars is reported for the first time, as well as water permeability at different maturity stages. Data on fruit micro-topography were also obtained by means of fringe projections, revealing genotype-related diversity of surface microstructure. Although water permeance of olive fruit might be controlled or fine-tuned by different cuticle-related traits, none of those considered herein appeared to suffice by itself to determine this trait, suggesting that additional properties of waxes and cutin, such as their physical structure or biomechanical properties, significantly influence the barrier functions of plant cuticles. Even so, the bulk of results reported herein should establish the basis for a better comprehension of olive crop adaptations to the surrounding environment. Further research will be paramount to elucidate the role of cuticle properties in olive resistance to plagues, rots, and adverse environmental conditions. The comprehension of these relationships would be thus very relevant for improving orchard management.

DATA AVAILABILITY STATEMENT

All datasets generated for this study are included in the article/supplementary material.

AUTHOR CONTRIBUTIONS

CD, JG, AR, and IL collected the samples. CD carried out the biochemical analyses. HH and MR determined cuticular transpiration. P-HL and AE were in charge of skin topography determinations. AR was responsible of the experimental orchards and the physicochemical characterization of fruit samples. TC and FG contributed to sample processing. CD and VM did the microscopy observations. CD and IL conceptualized and wrote the manuscript. All the Authors revised and approved the manuscript.

FUNDING

This work was funded by grant AGL2015-64235-R from the Plan Nacional de I+D, Ministry of Education and Science, Spain. CD is the recipient of a predoctoral scholarship granted by the Universitat de Lleida. PH-L was recipient of a PhD scholarship from Zespri™ International. HH was supported by an Oversea Study Program, Guangzhou Elite Project, China.

SUPPLEMENTARY MATERIAL

The Supplementary Material for this article can be found online at: https://www.frontiersin.org/articles/10.3389/fpls.2019.01484/full#supplementary-material

REFERENCES

Athoo, T. O., Winkler, A., and Knoche, M. (2015). Pedicel transpiration in sweet cherry fruit: mechanisms, pathways, and factors. *J. Am. Soc Hortic. Sci.* 140, 136–143. doi: 10.21273/jashs.140.2.136

Barrios, G., Mateu, J., Ninot, A., Romero, A., and Vichi, S. (2015). Sensibilidad varietal del olivo a *Bactrocera oleae* y su incidencia en la gestión integrada de plagas. *Phytoma* 268, 21–28.

Belge, B., Llovera, M., Comabella, E., Gatius, F., Guillén, P., and Graell, J. (2014a). Characterization of cuticle composition after cold storage of 'Celeste' and 'Somerset' sweet cherry fruit. *J. Agric. Food Chem.* 62, 8722–8729. doi: 10.1021/jf502650t

Belge, B., Llovera, M., Comabella, E., Graell, J., and Lara, I. (2014b). Fruit cuticle composition of a melting and a nonmelting peach cultivar. *J. Agric. Food Chem.* 62, 3488–3495. doi: 10.1021/jf5003528

Besnard, G., Terral, J. F., and Cornille, A. (2018). On the origins and domestication of the olive: a review and perspectives. *Ann. Bot.* 121, 385–403. doi: 10.1093/aob/mcx145

Bianchi, G., Murelli, C., and Vlahov, G. (1992). Surface waxes from olive fruits. *Phytochemistry* 31, 3503–3506.

Bianchi, G. (2003). Lipids and phenols in table olives. *Eur. J. Lipid Sci. Technol.* 105, 229–242. doi: 10.1002/ejlt.200390046

Camacho-Vázquez, C., Ruiz-May, E., Guerrero-Analco, J. A., Elizalde-Contreras, J. M., Enciso-Ortiz, E. J., and Rosas-Saito, G. (2019). Filling gaps in our knowledge on the cuticle of mangoes (*Mangifera indica*) by

analyzing six fruit cultivars: architecture/structure, postharvest physiology and possible resistance to fruit fly (Tephritidae) attack. *Postharvest Biol. Technol.* 148, 83–96. doi: 10.1016/j.postharvbio.2018.10.006

Casado, C. G., and Heredia, A. (1999). Structure and dynamics of reconstituted cuticular waxes of grape berry cuticle (*Vitis vinifera* L.). *J. Exp. Bot.* 50, 175–182. doi: 10.1093/jexbot/50.331.175

Chu, W., Gao, H., Cao, S., Fang, X., Chen, H., and Xiao, S. (2016). Composition and morphology of cuticular wax in blueberry (*Vaccinium* spp.) fruits. *Food Chem.* 219, 436–442. doi: 10.1016/j.foodchem.2016.09.186

Domínguez, E., López-Casado, G., Cuartero, J., and Heredia, A. (2008). Development of fruit cuticle in cherry tomato (*Solanum lycopersicum*). *Funct. Plant Biol.* 35, 403–411. doi: 10.1071/fp08018

Domínguez, E., Heredia-Guerrero, J. A., and Heredia, A. (2011). The biophysical design of plant cuticles: an overview. *New Phytol.* 189, 938–949. doi: 10.1111/j.1469-8137.2010.03553.x

East, A. R., Bloomfield, C., Trejo Araya, X., and Heyes, J. A. (2016). Evaluation of fringe projection as a method to provide information about horticultural product surfaces. *Acta Hortic.* 1119, 189–196. doi: 10.17660/ActaHortic.2016.1119.26

España, L., Heredia-Guerrero, J. A., Segado, P., Benítez, J. J., Heredia, A., and Domínguez, E. (2014). Biomechanical properties of the tomato (*Solanum lycopersicum*) fruit cuticle during development are modulated by changes in the relative amounts of its components. *New Phytol.* 202, 790–802. doi: 10.1111/nph.12727

Fernández, S., Osorio, S., and Heredia, A. (1999). Monitoring and visualising plant cuticles by confocal laser scanning microscopy. *Plant Physiol. Biochem.* 37, 789–794. doi: 10.1016/S0981-9428(00)86692-9

Fich, E. A., Segerson, N. A., and Rose, J. K. C. (2016). The plant polyester cutin: biosynthesis, structure, and biological roles. *Annu. Rev. Plant Biol.* 67, 207–233. doi: 10.1146/annurev-arplant-043015-111929

Franke, R., Briesen, I., Wojciechowski, T., Faust, A., Yephremov, A., and Nawrath, C. (2005). Apoplastic polyester in *Arabidopsis* surface tissues – A typical suberin and a particular cutin. *Phytochemistry* 66, 2643–2658. doi: 10.1016/j.phytochem.2005.09.027

Gadelmawla, E. S., Koura, M. M., Maksoud, T. M. A., Elewa, I. M., and Soliman, H. H. (2002). Roughness parameters. *J. Mater. Process. Technol.* 123, 133–145. doi: 10.1016/S0924-0136(02)00060-2

Guinda, A., Rada, M., Delgado, T., Gutiérrez-Adánez, P., and Castellano, J. M. (2010). Pentacylic triterpenoids from olive fruit and leaf. *J. Agric. Food Chem.* 58, 9685–9691. doi: 10.1021/jf102039t

Huang, H., Burghardt, M., Schuster, A. C., Leide, J., Lara, I., and Riederer, M. (2017). Chemical composition and water permeability of fruit and leaf cuticles of *Olea europaea* L. *J. Agric. Food Chem.* 65, 8790–8797. doi: 10.1021/acs.jafc.7b03049

Iannotta, N., Noce, M. E., Ripa, V., Scalercio, S., and Vizzarri, V. (2007). Assessment of susceptibility of olive cultivars to the *Bactrocera oleae* (Gmelin, 1790) and *Camarosporium dalmaticum* (Thüm.) Zachos & Tzav.-Klon. attacks in Calabria (Southern Italy). *J. Environ. Sci. Heal. B* 42, 789–793. doi: 10.1080/03601230701551426

Järvinen, R., Kaimainen, M., and Kallio, H. (2010). Cutin composition of selected northern berries and seeds. *Food Chem.* 122, 137–144. doi: 10.1016/j.foodchem.2010.02.030

Kallio, H., Nieminen, R., Tuomasjukka, S., and Hakala, M. (2006). Cutin composition of five Finnish berries. *J. Agric. Food Chem.* 54, 457–462. doi: 10.1021/jf0522659

Kombargi, W. S., Michelakis, S. E., and Petrakis, C. A. (1998). Effect of olive surface waxes on oviposition by *Bactrocera oleae* (Diptera: Tephritidae). *J. Econ. Entomol.* 91, 993–998. doi: 10.1093/jee/91.4.993

Kunst, L., and Samuels, A. L. (2002). Biosynthesis and secretion of plant cuticular wax. *Prog. Lipid Res.* 42, 51–80. doi: 10.1016/S0163-7827(02)00045-0

Lai, P. H., Gwanpua, S. G., Bailey, D.,. G., Heyes, J. A., and East, A. R. (2018). Skin topography changes during kiwifruit development. *Acta Hortic.* 1218, 427–433. doi: 10.17660/ActaHortic.2018.1218.59

Lanza, B., and Di Serio, M. G. (2015). SEM characterization of olive (*Olea europaea* L.) fruit epicuticular waxes and epicarp. *Sci. Hortic.* 191, 49–56. doi: 10.1016/j.scienta.2015.04.033

Lara, I., Belge, B., and Goulao, L. F. (2014). The cuticle as a modulator of postharvest quality. *Postharvest Biol. Technol.* 87, 103–112. doi: 10.1016/j.postharvbio.2013.08.012

Lara, I., Belge, B., and Goulao, L. F. (2015). A focus on the biosynthesis and composition of cuticle in fruits. *J. Agric. Food Chem.* 63, 4005–4019. doi: 10.1021/acs.jafc.5b00013

Leide, J., Hildebrandt, U., Reussing, K., Riederer, M., and Vogg, G. (2007). The developmental pattern of tomato fruit wax accumulation and its impact on cuticular transpiration barrier properties: effects of a deficiency in a β-ketoacyl-coenzyme A synthase (LeCER6). *Plant Physiol.* 144, 1667–1679. doi: 10.1104/pp.107.099481

Leide, J., Hildebrandt, U., Vogg, G., and Riederer, M. (2011). The positional sterile (*ps*) mutation affects cuticular transpiration and wax biosynthesis of tomato fruits. *J. Plant Physiol.* 168, 871–877. doi: 10.1016/j.jplph.2010.11.014

Leide, J., de Souza, A. X., Papp, I., and Riederer, M. (2018). Specific characteristics of the apple fruit cuticle: investigation of early and late season cultivars 'Prima' and 'Florina' (*Malus domestica* Borkh.). *Sci. Hortic.* 229, 137–147. doi: 10.1016/j.scienta.2017.10.042

Lequeu, J., Fauconnier, M., Chammai, A., Bronner, R., and Blée, E. (2003). Formation of plant cuticle: evidence of the peroxygenase pathway. *Plant J.* 36, 155–164. doi: 10.1046/j.1365-313X.2003.01865.x

Martin, L. B. B., and Rose, J. K. C. (2014). There's more than one way to skin a fruit: formation and functions of fruit cuticles. *J. Exp. Bot.* 16, 4639–4651. doi: 10.1093/jxb/eru301

Moggia, C., Graell, J., Lara, I., Schmeda-Hirschmann, G., Thomas-Valdés, S., and Lobos, G. A. (2016). Fruit characteristics and cuticle triterpenes as related to postharvestquality of highbush blueberries. *Sci. Hortic.* 211, 449–457. doi: 10.1016/j.scienta.2016.09.018

Parsons, E. P., Popopvsky, S., Lohrey, G. T., Lü, S., Alkalai-Tuvia, S., and Perzelan, Y. (2012). Fruit cuticle lipid composition and fruit post-harvest water loss in an advanced backcross generation of pepper (*Capsicum* sp.). *Physiol. Plant* 146, 15–25. doi: 10.1111/j.1399-3054.2012.01592.x

Peschel, S., Franke, R., Schreiber, L., and Knoche, M. (2007). Composition of the cuticle of developing sweet cherry fruit. *Phytochemistry* 68, 1017–1025. doi: 10.1016/j.phytochem.2007.01.008

Riederer, M., Arand, K., Burghardt, M., Huang, H., Riedel, M., and Schuster, A. (2015). Water loss from litchi (*Litchi chinensis*) and logan (*Dimocarpus logan*) fruits is biphasic and controlled by a complex pericarpal transpiration barrier. *Planta* 242, 1207–1219. doi: 10.1007/s00425-015-2360-y

Rizzo, R., and Lombardo, A. (2007). Factors affecting the infestation due to *Bactrocera oleae* (Rossi) in several Sicilian olive cultivars. *IOBC/WPRS Bull.* 30, 89–99.

Samuels, L. A., Kunst, L., and Jetter, R. (2008). Sealing plant surfaces: Cuticular wax formation by epidermal cells. *Plant Biol.* 59, 68–707. doi: 10.1146/annurev.arplant.59.103006.093219

Schindelin, J. L., Arganda-Carreras, I., Frise, E., Kaynig, V., Longair, M., and Pietzsch, T. (2012). Fiji: an open-source platform for biological-image analysis. *Nat. Methods* 9, 676–682. doi: 10.1038/nmeth.2019

Serrano, M., Coluccia, F., Torres, M., L'Haridon, F., and Métraux, J. P. (2014). The cuticle and plant defense to pathogens. *Front. Plant Sci.* 5, 274. doi: 10.3389/fpls.2014.00274

Stiti, N., Triki, S., and Hartmann, M. A. (2007). Formation of triterpenoids throughout *Olea europaea* fruit ontogeny. *Lipids* 42, 55–67. doi: 10.1007/s11745-006-3002-8

Tanaka, T., Tanaka, H., Machida, C., Watanabe, M., and Machida, Y. (2004). A new method for rapid visualization of defects in leaf cuticle reveals five intrinsic patterns of surface defects in Arabidopsis. *Plant J.* 37, 139–146. doi: 10.1046/j.1365-313X.2003.01946.x

Tous, J., and Romero, A. (1993). *Variedades del Olivo*. Barcelona, Spain: Fundación 'La Caixa' y AE2.

Tsubaki, S., Sugimura, K., Teramoto, Y., Yonemori, K., and Azuma, J. I. (2013). Cuticular membrane of *Fuyu* persimmon fruit is strengthened by triterpenoid nano-fillers. *PloS One* 8, 1–13. doi: 10.1371/journal.pone.0075275

Uceda, M., and Frías, L. (1975). Harvest dates. Evolution of the fruit of content, oil composition and oil quality in *Proceedings of II Seminario Oleícola International. Córboba, Spain: International Olive Oil Council (IOOC)*, 125–130.

Vichi, S., Cortés-Francisco, N., Caixach, J., Barrios, G., Mateu, J., and Ninot, A. (2016). Epicuticular wax in developing olives (*Olea europaea*) is highly dependent upon cultivar and fruit ripeness. *J. Agric. Food Chem.* 64, 5985–5994. doi: 10.1021/acs.jafc.6b02494

Wang, J., Sun, L., Xie, L., He, Y., Luo, T., and Sheng, L. (2016). Regulation of cuticle formation during fruit development and ripening in 'Newhall' navel orange

(*Citrus sinensis* Osbeck) revealed by transcriptomic and metabolic profiling. *Plant Sci.* 243, 131–144. doi: 10.1016/j.plantsci.2015.12.010

Wu, X., Yin, H., Chen, Y., Li, L., Wang, Y., and Hao, P. (2017). Chemical composition, crystal morphology and key gene expression of cuticular waxes of Asian pears at harvest and after storage. *Postharvest Biol. Technol.* 132, 71–80. doi: 10.1016/j.postharvbio.2017.05.007

Wu, X., Yin, H., Shi, Z., Chen, Y., Qi, K., and Qiao, X. (2018). Chemical composition and crystal morphology of epicuticular wax in mature fruits of 35 pear (*Pyrus* spp.) cultivars. *Front. Plant Sci.* 9, 1–14. doi: 10.3389/fpls.2018.00679

Yeast, T. H., and Rose, J. K. C. (2013). The formation of plant cuticle. *Plant Physiol.* 163, 5–20. doi: 10.1104/pp.113.222737

Conflict of Interest: The authors declare that the research was conducted in the absence of any commercial or financial relationships that could be construed as a potential conflict of interest.

frontiers in Plant Science

ORIGINAL RESEARCH
published: 27 November 2019
doi: 10.3389/fpls.2019.01544

It Is Feasible to Produce Olive Oil in Temperate Humid Climate Regions

Paula Conde-Innamorato[1]†, Mercedes Arias-Sibillotte[2]†, Juan José Villamil[1], Juliana Bruzzone[1], Yesica Bernaschina[1], Virginia Ferrari[1], Roberto Zoppolo[1], José Villamil[1] and Carolina Leoni[1]*

[1] Instituto Nacional de Investigación Agropecuaria (INIA), Programa Nacional de Investigación en Producción Frutícola, Estación Experimental INIA Las Brujas, Canelones, Uruguay, [2] Unidad de Ecofisiología de Frutales, Departamento de Producción Vegetal, Facultad de Agronomía, Universidad de la República, Montevideo, Uruguay

Worldwide olive industry has expanded into new climatic regions outside the Mediterranean basin due to an increase in extra virgin olive oil demand posing new challenges. This is the case of Uruguay, South America, where the olive crop area reached 10,000 hectares in the last 15 years and is intended to the production of EVOO. Uruguay has a temperate humid climate with mean precipitations above 1,100 mm per year but unequally distributed, mild winters, and warm summers, with mean annual temperatures of 17.7°C. Different agroecological conditions require local knowledge to achieve good productivity whereby the objective of this work was to show the feasibility and potential of olive oil production under our climatic conditions. For this the agronomic performance of Arbequina, Barnea, Frantoio, Leccino, Manzanilla de Sevilla, and Picual cultivars was evaluated along 10 years of full production. Phenology behavior, vegetative growth rate, productive efficiency, alternate bearing, and oil yield were determined. Sprouting and flowering processes occur in a wide window within the annual cycle between the months of August to November with great interannual variation. More than 8 t/ha fruit yield and 40% oil yields in dry weight basis were obtained in promising cultivars. However, alternate bearing arose as the main production limiting factor, with ABI values greater than 0.60 for most cultivars. We conclude that olive oil production in humid climate regions is feasible and the most promising cultivars based on productive efficiency are Arbequina and Picual.

Keywords: ***Olea europaea*** **L., olive cultivars, phenological behavior, oil yield, productive efficiency, alternate bearing**

OPEN ACCESS

Edited by:
José Manuel Martínez-Rivas, Instituto de la Grasa (IG), Spain

Reviewed by:
Carolina Sánchez-Romero, University of Málaga, Spain
Salvatore Camposeo, University of Bari Aldo Moro, Italy

***Correspondence:**
Paula Conde-Innamorato
pconde@inia.org.uy

†*These authors have contributed equally to this work*

Specialty section:
This article was submitted to Crop and Product Physiology, a section of the journal Frontiers in Plant Science

Received: *12 June 2019*
Accepted: *05 November 2019*
Published: *27 November 2019*

Citation:
Conde-Innamorato P, Arias-Sibillotte M, Villamil JJ, Bruzzone J, Bernaschina Y, Ferrari V, Zoppolo R, Villamil J and Leoni C (2019) It Is Feasible to Produce Olive Oil in Temperate Humid Climate Regions. Front. Plant Sci. 10:1544. doi: 10.3389/fpls.2019.01544

INTRODUCTION

In the last decades, the worldwide olive industry had expanded into new climatic regions outside the Mediterranean basin due to an increase in extra virgin olive oil (EVOO) demand associated to its beneficial effects on human health (International Olive Council. IOC, 2015). Among these new regions, some of them have Mediterranean like climate—San Diego, USA and México (Ayerza and Sibbett, 2001) and La Rioja, Argentina (Rondanini et al., 2014)—whereas others have quite different temperature regimes, particularly mild winters resulting in less chilling hours for flowering during winter dormancy—Argentina, Australia (Aybar et al., 2015; Torres et al., 2017). Also, different humid regions are under olive cultivation, from wet hot summers, and cold dry winters—Wudu, China (Wang et al., 2018) to tropical—Queensland, Australia (Mailer et al., 2010) or temperate humid regions with high humidity, precipitation above 1,100 mm/year and moderate temperatures—Southern Brazil and Uruguay (Torres et al., 2017). In all of these new regions, EVOO

is produced and particular olive profiles are obtained (Aguilera et al., 2005; Borges et al., 2017; Ellis and Gámbaro, 2018) showing the potential for EVOO expansion worldwide.

Oliviculture devoted to EVOO production is considered a new agricultural activity in Uruguay. However, olive introduction dates back to 1,780 along with the Spanish settlers (Pereira et al., 2018) and the first olive growing activity for virgin olive oil production started in the 1930s. Since 2002, modern orchards were planted for virgin olive oil production, increased from 500 to 9,000 hectares (Ackermann et al., 2018) with high technology olive oil mill. These new orchards were planted with certified material from Spain, Italy, Israel, and Argentina (Tous et al., 2005) being the main cultivar Arbequina (50%) followed by Picual, Coratina, Frantoio, Leccino, and Manzanilla de Sevilla (all adding up to around 40%). Uruguay is recognized by international olive oil sensory panels for its EVOO (Ellis and Gámbaro, 2018; ASOLUR, 2019). Currently, olive production accounts for 23% of the national area devoted to fruit crops, considering citrus, vineyards, and deciduous fruit trees, which evidences the importance of the olive in the fruit sector. Uruguay is the second smallest country in South America with 16.4 million hectares with agricultural aptitude and with little more than 3 million total inhabitants (Archivo General de la Nación, 2011; Instituto Nacional de Estadística. INE, 2011).

Modern olive plantations in Uruguay follow an intensive rainfed system within a range of 285–400 trees/ha, identified as system "S5" by IOC (International Olive Council. IOC, 2015). Less than 5% of the plantations are irrigated system "S6" (Rallo et al., 2013) although there are no official data. One of the reasons for not investing in irrigation in the productive systems is the annual pluviometry, generally greater than 1,100 mm per year, but highly variable among seasons and years. Due to the high frequency of periods of drought or pluviometric excesses in our conditions (Vaughan et al., 2017), the yield potentials of the productive systems are highly dependent on soil physical aptitude, topography, and associated soil management. The excess of rainfall at some given key stages of the vegetative—productive olive cycle (flowering—fruit set—ripening) generate different challenges for the development of olive trees in humid regions (Tous et al., 2005). According to the thermal requirements of the species proposed by Moriondo et al. (2008), Uruguay is an area suitable for the development of olive production. The average annual temperature is 17.7°C, varying from 19.8°C in the northwest zone to 16.6°C in the south coast. Isotherms have an incremental trend from the southeast to the northwest. The national averages of the annual extreme temperatures of the air present a maximum historical average of 22.6°C and a minimum average of 12.9°C (Castaño et al., 2011). The offer of winter cold varies between 500 and 1,000 chilling units, a factor that could be limiting for some deciduous fruit crops (Contarin and Curbelo, 1987; Severino et al., 2011). Average annual relative humidity between 70% and 78% associated to high annual rainfall, and moderate temperatures, favors the development of fungal diseases. The choice of cultivars with best behavior against pathogens is of utmost importance to achieve a sustainable orchard management (Leoni et al., 2018; Bernaschina et al., 2019).

There is extensive knowledge of the behavior of olive cultivars in traditional Mediterranean production areas, but not in regions with temperate-humid climate. Evaluation of a fruit species in a specific location requires the evaluation of its growth and development potential, precocity, and productive behavior (Klepo et al., 2013). Alternate bearing is a well-known condition in olive trees (Lavee, 2015), as well as its relationship with vigor and consequently with its productive efficiency. These conditions vary with cultivar but also with local agroecological conditions (Smith and Samach, 2013).

To identify limiting factors in olive production is necessary to start with cultivars phenological studies. After several years, the average and the overlap flowering period can be identified among cultivars in relation to climatic characteristics (Orlandi et al., 2005; Benlloch-González et al., 2018). Negative climatic events in non-traditional producing regions as Argentina and Chile, can result in null harvest, leading to regional alternate bearing processes (Cuevas et al., 1994; Goldschmidt, 2005; Beyá-Marshall and Fichet, 2017).

The objective of this work was to assess the feasibility and the potential of olive oil production in temperate-humid climate. For this, we evaluated the agronomic behavior of six cultivars characterizing their adaptability through phenology, growth rate, productive efficiency, alternate bearing index (ABI) and oil yield. This information is crucial for identifying promising cultivars in order to develop an integrated production strategy as well as to pursue technological development facing the expansion into new regions.

MATERIALS AND METHODS

Experimental Sites and Plant Materials

Two experiments were established, one at INIA "Las Brujas" Experimental Station in Southern Uruguay (34°40' S; 56°20' W; altitude 21 m) and the other at INIA "Salto Grande" Experimental Station in Northern Uruguay (31°16' S; 57°53' W; altitude 41 m).

At INIA "Las Brujas" Experimental Station (LB), olives trees of Arbequina, Barnea, Frantoio, Leccino, Manzanilla de Sevilla, and Picual cultivars were planted in 2002 at a density of 416 trees per hectare (4 m between trees and 6 m between rows). A randomized complete block design with four replicates and three trees per experimental unit was used. The soil at this site has a fine textured A horizon, with a maximum depth of 20 cm, with 2.5% of organic matter and pH 6.5 corresponding to a Typic-Vertic Argiudolls soil according to the USDA classification (Durán et al., 2006). The presence of argillic B-horizons close to soil surface requires raised beds to increase soil volume to be explored by roots and to facilitate drainage.

At INIA "Salto Grande" Experimental Station (SG) olive trees of Arbequina, Frantoio, Manzanilla de Sevilla, and Picual cultivars were planted in 2003 at a density of 333 trees per hectare (5 m × 6 m). A randomized complete block design with six replicates was used and three trees per experimental unit.

The soil at this site has a coarse textured A horizon, with a very good natural drainage and a maximum depth of 50 cm; therefore, there is no need for raised beds even though the strong textural differentiation between soil horizons. Soil natural fertility is poor, with less than 1.8% organic matter and a pH of 5.5. This type of soil corresponds to a Udifluvent soil according to the USDA classification (Durán et al., 2006).

Both experiments were managed with the same technological management for pruning, irrigation, and nutrition. Olive trees were trained as single-trunk vase, with three to four main branches. From 2002 to 2009, while the trees were filling its space within the row, pruning criteria was intended for training and thinning. From 2010 onwards, the control of tree height was included as a pruning criterion. Drip irrigation was installed at planting, arranged in simple rows with drippers spaced at 1 m and a flow of 4 l/h. After 5 years another identical line was added. Irrigation was applied to supply the water needed to replace 100% of the crop evapotranspiration (ETc) all throughout the irrigation season. Pest management was according to Integrate Pest Management guidelines (IOBC-WPRS, 2012) with control actions with horticultural oils and ant baits directed to *Saissetia oleae* and *Acromyrmex* and *Atta* ant species, respectively. For diseases, between four to six sprays per season with preventive cupric sprays complemented with other fungicides (QoIs, EBIs, dithiocarbamates) were applied for controlling Olive scab (*Venturia oleaginea*), Cercospora leaf spot (*Pseudocercospora cladosporioides*) and Anthracnose olive rot (*Colletotrichum* spp.) (**Supplementary Figure S1**).

Climate

Meteorological data was obtained with an automatic weather station from 2007 to 2017 (data available at http://www.inia.uy/gras/Clima/Banco-datos-agroclimatico). Daily average mean temperature differed in almost 3°C between the two sites, with an average of 16.3°C and 19.0°C at LB and 19.0°C and 21.8°C at SG, for October and November, respectively. Also, the average effective precipitation was 109 and 105 mm per month in October and November at LB, and 134 and 142 mm at SG (**Supplementary Table S1**).

The offer of winter cold was measured with positive chill unit method (UTAH+) (Linsley-Noakes et al., 1994) from May 1st to August 31st. The heat supply was measured with the GDH model in the period from July 1st to December 31st with a base temperature of 12.5°C (Galán et al., 2001).

Phenological Parameters

Phenological records were made through visual assessments in individual plants based on the BBCH scale (Sanz-Cortés et al., 2002) along 10 years in which trees were between 5 and 15 years old. For each sampling date a unique predominant phenological state was registered for the set of trees of each cultivar in each site. The beginning of sprouting corresponds to the state BBCH 53, the beginning of flowering to BBCH 61 (10% flowers open), full bloom to BBCH 65 (at least 50% of flowers open) and end of flowering to BBCH 68 (majority of petals fallen or faded).

Sprouting and flowering windows were defined based on the first and the last date registered for each stage per cultivar between 2007 and 2017, and the dates were registered as the day of the year (DOY), starting on January 1st. At INIA Salto Grande, only the flowering stages were recorded. Flowering length days number was calculated by date calendar subtraction between states 61 and 68 of the BBCH scale.

Productive Parameters

Fruit production (kg/tree) was measured per tree at both sites (n = 12 at LB, n = 18 at SG) and then fruit yield (t/ha) was calculated combining fruit production (kg/tree) and tree density (trees/ha) data. Canopy volume (CV, m^3/tree) was measured only in the central tree of the plot during the first years (2007 to 2011) and in all trees of each plot from 2012 onwards. CV was calculated according to the ellipsoid volume method defined by three semi-axes (equation 1) with E_b and E_c as the North and East semi-axis of the tree, and E_a as the difference between tree height minus height of the first leaf and divided by two (Miranda-Fuentes et al., 2015). CV was not estimated for Barnea because the shape of the canopy does not fit the volume of an ellipsoid.

$$CV = 4/3\pi \times E_a \times E_b \times E_c \quad (1)$$

For the period 2010–2017 and only for LB site, the productive efficiency (kg/m^3 canopy) was estimated considering the years with high production (years "on") and the ABI was calculated according to Monselise and Goldschmidt (1982) (equation 2).

$$ABI = (1/n\text{-}1) \times \Sigma (y_n - y_{n-1}) / (y_n + y_{n-1}) \quad (2)$$

where y = yields in year n, with n varying from 1 to 8.

Oil content (%) was measured on a sample of 200 g of olives per cultivar, with three replicates (Shahidi, 2001). Each sample was grounded with a hammer mill and humidity determined at 105°C for 48 h, then the dried sample was grounded with a mortar and oil content analyzed in duplicate following the Soxhlet method.

Olives were collected only at "on" years (2012, 2014, 2016, and 2017 at INIA Las Brujas; and 2012, 2014, 2015, and 2017 at INIA Salto Grande) at fruit ripening index (FRI) 3 based on a 0–7 scale (Uceda and Frias, 1975) with 0: intense green skin, 3: reddish or purple skin in more than half of the fruit, 4: black skin and white pulp and 7: black skin and totally purple pulp. FRI was calculated as (equation 3):

$$FRI = \Sigma (n_i * I) / N \quad (3)$$

where n_i = number of olives with i ripening level, I = ripening level going from 0 to 7, N = total number of olives evaluated (100 olives).

Statistical Analysis

Most data were subjected to analysis of variance (ANOVA) and the interaction "cultivar × site" was studied. To highlight the productive potential of the cultivars for each site, an independent analysis per site is presented. For canopy development data from 2007 to 2010 was analyzed by a non-lineal regression following an

exponential model (equation 4) and goodness of fit was estimated by Pearson correlation between measured and predicted values.

$$CV = a * e^{(b * \text{tree age})} \quad (4)$$

For the cumulative fruit yield a General Lineal Mixed Model was adjusted, considering cultivar and site and its interaction as fixed effect and site > block nested and block as a random factor. Tukey test at $p \leq 0.05$ were calculated to separate means. The statistical program used was InfoStat version 2017 (Di Rienzo et al., 2017).

RESULTS

Phenological Parameters

Flowering periods and sprouting (only for LB) were recorded along 10 years for six cultivars at LB and four at SG. Phenological data was analyzed following two different approaches: the lifespan in which the phenological phase occurred (**Figure 1**) and the length of the phenophases within each year (**Table 1**).

Sprouting windows started between the first week of August and the second week of September (**Figure 1**). The narrower variation in the beginning of sprouting at LB was registered for Barnea with a difference of 20 days among years, from 225 to 245 DOY. On the other hand, Leccino had the widest variation with a difference of 40 days, from 223 to 263 DOY.

Flowering windows from 10% flowers open (BBCH 61) to most petals fallen (BBCH 68) was highly variable among years. Considering all cultivars, the earliest date for BBCH 61 was 268 DOY in Manzanilla de Sevilla and the last date for BBCH 68 was 320 DOY in Arbequina. Therefore, the window for flowering in Southern Uruguay was 52 days, from the end of September to the end of November, for the 10 years evaluated.

The beginning of full bloom (BBCH 65) period at LB occurred between the second week of October and the second week of November, with a lifespan of 20 days in Barnea and 30 days in Manzanilla de Sevilla and Picual. At SG, the beginning of BBCH 65 occurred between the first and third week of October, with a lifespan of 5 days in Manzanilla de Sevilla and 17 days in Arbequina.

The average flowering length varied between 11.3 and 15.1 days at LB for Leccino and Arbequina, respectively, and between 11.3 and 12.0 days at SG for Arbequina and Frantoio, respectively. Despite cultivar nor site, the shortest flowering length was 7 days and the longest was 29 (**Table 1**).

The flowering behavior in two contrasting years regarding its thermal regimes was different (**Table 2**). In the warmest year (2017), the beginning of the flowering (BBCH 61) anticipated 15 and 18 days and the flowering length was 11 and 10 days longer respect to the coldest year (2016), for Arbequina and Frantoio, respectively.

Productive Parameters

The cultivars showed differences in canopy volume (CV), Frantoio presented the higher values and Arbequina the lower ones (**Table 3**, **Figure 2**). In 2011 with 9-year-old trees, because of pruning practices mainly to reduce tree height, no differences were found in CV. In 2016 with 14-year-old trees, despite pruning

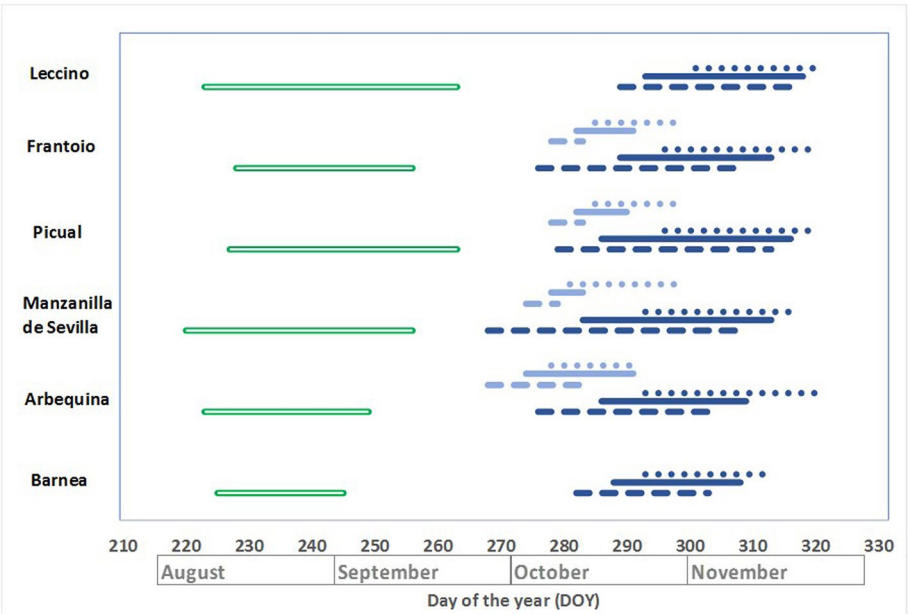

FIGURE 1 | Lifespan of key phenological stages at INIA Las Brujas (LB) and INIA Salto Grande (SG), based on 10 years data. Beginning of sprouting, green completed double line; beginning of flowering, blue dashed line; beginning of full bloom, blue complete line; end of flowering, blue dotted lines. Light lines and dark lines correspond to SG and LB sites, respectively.

TABLE 1 | Flowering length based on 10 years data (average with standard errors, minimum and maximum length) at INIA Las Brujas (LB) and INIA Salto Grande (SG).

Cultivar	LB			SG		
	Flowering length (days)	min. (days)	Max. (days)	Flowering length (days)	min. (days)	Max. (days)
Leccino	11.3 ± 1.2	7	14	–	–	–
Frantoio	14.2 ± 1.7	9	28	12.0 ± 3.2	7	18
Picual	13.5 ± 1.6	7	25	12.0 ± 3.2	7	18
Manzanilla de Sevilla	13.5 ± 1.9	7	29	11.8 ± 2.6	7	19
Arbequina	15.1 ± 1.8	7	28	11.3 ± 2.5	6	18
Barnea	12.1 ± 1.0	7	15	–	–	–

TABLE 2 | Chilling units (CHU) and heat supply (GDH) in the warmest and coldest years of the 10 years study at INIA Las Brujas and corresponding day of the year (DOY) for beginning and end of the flowering period, and flowering length for Arbequina and Frantoio cultivars.

Year	CHU[a]	GDH[b]	Cultivar	Beginning of flowering (DOY)	End of Flowering (DOY)	Flowering length (days)
2016	1353	691	Arbequina	291	308	17
			Frantoio	294	312	18
2017	926	756	Arbequina	276	304	28
			Frantoio	276	304	28
Historical mean[c]	1105	700				

[a]CHU (UTHA+) from May 1st to August 31st; [b] GDH temperature over 12.5°C from July 1st to December 31st; [c] Historical means of the period 1990 to 2017.

TABLE 3 | Average canopy volume per tree for five cultivars for 5-, 9- and 14-year-old trees at INIA Las Brujas.

Cultivar	Canopy volume (m^3/tree)					
	5-year-old trees		9-year-old trees		14-year-old trees	
Leccino	4.89	b	11.63	a	33.05	ab
Frantoio	10.95	a	15.25	a	39.07	a
Picual	6.84	ab	10.46	a	27.25	b
Manzanilla de Sevilla	5.28	b	11.98	a	28.46	b
Arbequina	5.11	b	8.74	a	25.88	b
Pr(>F)	0.004		0.124		< 0.0001	

Different letters in the column indicate significant differences (HSD Tukey $p \leq 0.05$).

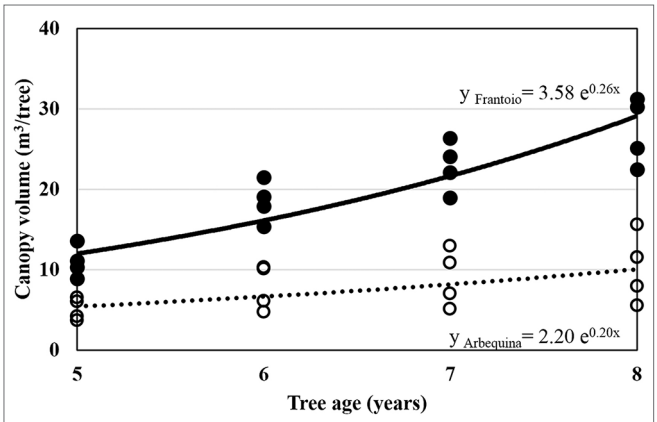

FIGURE 2 | Progress of canopy volume from 2007 to 2010 of olive trees growing at INIA Las Brujas. Full circles correspond to Frantoio and empty circles correspond to Arbequina. The line represents the fitted exponential model of canopy volume.

practices again Frantoio had the biggest tree size (CV: 39 m^3/tree) and Arbequina the smallest one (CV: 26 m^3/tree) (**Table 3**). In other words, in 2007 (5-year-old trees) Arbequina was 47% of Frantoio´s size, while at the end of the study period (14 year-old-trees) Arbequina was 66% of Frantoio´s size.

The progress of CV fitted an exponential model for the period 2007–2011. Arbequina had the lowest growth rate of change (0.20), estimated by parameter *b* of the exponential equation (equation 4) (**Table 4**, **Figure 2**).

Since no differences (p = 0.24) were found in CV/ha between LB and SG for each cultivar when the row space was filled, fruit yields were expressed in t/ha. Cumulative fruit yield presented significant differences among cultivars and regions ($p < 0.0001$) (**Figure 3**). Overall, cultivars produced more at LB than at SG. Arbequina (88 t/ha at LB, 58 t/ha at SG) and Picual (90 t/ha at LB, 63 t/ha at SG) presented the greatest cumulative yield in both sites. Frantoio was one of the most productive cultivars at LB with a cumulative fruit yield of 80 t/ha but at SG was the worst with18 t/ha. At LB site, Manzanilla de Sevilla and Leccino showed an intermediate fruit yield with 73 t/ha and 69 t/ha, respectively, whereas Barnea had a low fruit yield of 29 t/ha.

Alternate bearing behavior between the years "on" (high fruit production) followed by years "off" (low fruit production) was present in all cultivars (**Figure 3**). In 2013, the lowest fruit yield was recorded, being 0 t/ha for all cultivars except for Barnea which had a 1.6 t/ha fruit yield. The highest fruit yields where obtained in 2012 at LB and ranged between 10.4 t/ha to 21.3 t/ha for Barnea and Frantoio, respectively (Frantoio at SG was excluded in the range due to its extreme low fruit yield). At SG site, the alternate bearing behavior was typical along the years

TABLE 4 | Estimated parameters *a* (intercept) and *b* (growth rate of change) of the exponential model for the progress of canopy volume CV = *a* * *e*^(*b* * tree age) for five cultivars from 2007 to 2010, at INIA Las Brujas.

Cultivar	Intercept (*a*)		Growth rate of change (*b*)		Goodness of fit
	estimate	Std. error	estimate	Std. error	
Leccino	1.09^{+} [a]	0.60	0.33***	0.08	0.79
Frantoio	3.58**	1.01	0.26***	0.04	0.89
Picual	1.43 ns	1.03	0.30**	0.10	0.65
Manzanilla de Sevilla	1.60*	0.69	0.27***	0.06	0.80
Arbequina	2.20 ns	1.37	0.20*	0.09	0.53

[a]*** < 0.0001, ** < 0.001, * < 0.01, $^{+}$ < 0.05, ns: not significant.

except for 2014 and 2015 when the yield was high in both years. At LB site occurred the same but in 2016 and 2017.

Arbequina and Picual had the highest productive efficiency (kg/m^3 canopy) calculated for the "on" years, whereas Barnea had the lowest one (**Table 5**). All cultivars presented high ABI with values over 0.58. Barnea was the only cultivar that differed significantly for the ABI with the highest value (0.81).

For oil content, the interaction "cultivar × site" was not significant (p = 0.13 for dry weigh basis, and p = 0.43 for fresh weigh basis), whereas it was significant for average fruit yield (p < 0.001). Oil content in dry weight basis (DWB) and in fresh weight basis (FWB) were the highest in Frantoio and the lowest in Manzanilla de Sevilla in both sites. The average fruit yield (t/ha) per year was higher in Picual, Arbequina, and Frantoio in the LB site, followed by Manzanilla de Sevilla and Leccino and being the lowest in Barnea cultivar. In the SG site, Arbequina and Picual showed the higher yields, followed by Manzanilla de Sevilla and the lowest was for Frantoio cultivar (**Table 6**).

DISCUSSION

It Is Feasible to Produce Olive Oil in Humid Temperate Climate

Productive behavior of adult trees from six olive cultivars along 10 years, demonstrates that it is feasible to produce olive oil in humid temperate climate. In our experimental conditions with irrigation, annual average fruit yields including years "on" and "off", exceeded 8 t/ha with oil content above 36% DWB (**Table 6**). However, the interannual variability in thermal and rainfall regimes (Vaughan et al., 2017) affects regular production. Fruit and oil yields obtained were similar to those obtained in traditional Mediterranean basin regions (García et al., 2013; Gispert et al., 2013; Rallo et al., 2013; Díez et al., 2016; Marino et al., 2017) as well as in new olive growing regions (Tapia et al., 2009; Trentacoste et al., 2015; Beyá-Marshall and Fichet, 2017).

TABLE 5 | Productive efficiency calculated for the "on" years and alternate bearing index (ABI) for six cultivars at INIA Las Brujas.

Cultivar	Productive efficiency (kg/m^3)[a]	ABI[b]
Leccino	1.21 bc[c]	0.63 b
Frantoio	1.08 bc	0.60 b
Picual	1.99 a	0.60 b
Manzanilla de Sevilla	1.69 ab	0.67 b
Arbequina	2.10 a	0.59 b
Barnea	0.84 c	0.81 a

[a]*data only from "on" years,* [b] *data from the whole period,* [c] *different letters indicate significant differences within columns (HSD Tukey p ≤ 0.05).*

TABLE 6 | Oil content in dry weight (DWB) and in fresh weight basis (FWB) and annual fruit yield for the six cultivars evaluated at INIA Las Brujas (LB) and four cultivars evaluated at INIA Salto Grande (SG).

Cultivar	Oil content[a]		Fruit Yield[b]
	DWB (%)	FWB (%)	Average (t/ha/year)
LB[c]			
Leccino	41.5 ab[d]	17.1 ab	8.6 b
Frantoio	46.6 a	22.9 a	10.1 ab
Picual	45.0 ab	17.0 ab	11.3 a
Manzanilla de Sevilla	36.8 b	13.1 b	9.1 b
Arbequina	43.0 ab	17.7 ab	11.1 a
Barnea	44.2 ab	22.0 a	5.0 c
SG			
Frantoio	46.3 a	22.5 a	2.3 c
Picual	39.4 b	14.8 b	7.9 a
Manzanilla de Sevilla	36.7 b	12.6 c	5.1 b
Arbequina	40.0 b	16.0 b	7.9 a

[a]*data only from "on" years;* [b]*data from the whole period;* [c]*each region was analyzed separately;* [d]*different letters in the column indicate significant differences (HSD Tukey p ≤ 0.05).*

Alternate Bearing as the Main Production Limiting Factor

Alternate bearing was the main productive constraint identified in our conditions, evidenced by ABI values above 0.60 (**Table 5**), 60% higher than those already reported for the same cultivars

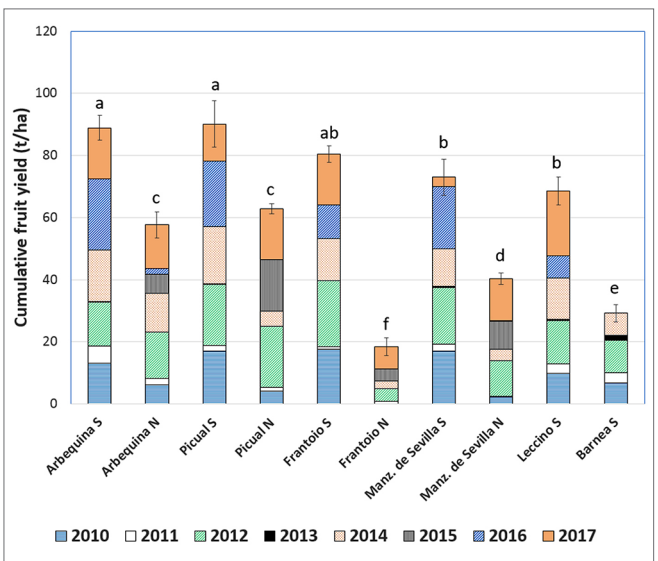

FIGURE 3 | Cumulative fruit yield of six cultivars at INIA Las Brujas and four at INIA Salto Grande between 2010 and 2017. Bars with a common letter are not significantly different (HSD Tukey $p \leq 0.05$).

(Tapia et al., 2009). These ABI values imply fruit yield variations between 0 and 25 t/ha per year, similar to those mentioned by Lavee (2007). Despite the methodological approach of the present work was not intended to identify the main causes of alternate bearing, the synchronization observed among the cultivars in their expression of years "on" and "off" (**Figure 3**) allowed us to infer some of them. Alternate bearing could not be explained only by endogenous effects, for example, the growth regulators involved in the previous harvest, called the "biochemical memory" of fruit load (Haberman et al., 2017). But adverse meteorological effects in annual olive cultivars production arise as the driving force for alternate bearing, similarly to others fruit trees (Guitton et al., 2012).

It is widely reported that temperatures during autumn and winter, measured as chilling units and subsequently as heat supply affect both the beginning and the length of the phenophases (Nieddu et al., 2002; Galán et al., 2005; Orlandi et al., 2005). In our conditions, the window for the occurrence of sprouting ourred between early August and early September whereas for flowering it took place from mid-October to mid-November (**Figure 1**). This phenological behavior is in accordance with those reported for other regions of the Southern Hemisphere (Torres et al., 2017).

In "warm" years, characterized by winters with reduced contribution of chilling units and springs with early heat supply, the flowering period both anticipated and expanded. Similar processes have been reported by Rallo and Martin (1991); however, the interaction between cold requirements and heat requirements, to release dormancy in the olive trees is still unknown and hasn´t been determined as it has been in deciduous fruit species that have endodormancy (Pope et al., 2014).

There is evidence that winter cold correlates positively with the intensity of flowering (Rallo and Martin, 1991; Haberman et al., 2017; Rallo and Cuevas, 2017). Nevertheless, regardless of whether cold is necessary to induce flowering and/or to release reproductive bud dormancy, the number of chilling units required for each cultivar could be a limitation for our conditions with high interannual variability. In fact, at SG site where the cold supply of chilling units is lower than at LB site, Frantoio cultivar is not recommended due to its high cold requirements (Aybar et al., 2015).

An adequate pollination is required to ensure fruit set and therefore a good harvest, which also depends on weather conditions (Fernández, 2014). In our springs during the "flowering window", although no extreme temperatures are present, average relative humidity above 70% in October and 60% in November as well as the probability of having 50% of the days with rain, affects negatively viable pollen-availability and therefore the fruit set. But also fruit set depends on pollen self-(in)compatibility of most olive cultivars (Marchese et al., 2016; Sánchez and Cuevas, 2018) where blooms synchronisms are crucial for our isolated plantation systems.

Productive Efficiency Supports the Selection of Agroecologically Adapted Cultivars

Perennial polycarpic plants often show an inverse correlation between vegetative growth and the fruit production (Obeso, 2002; Smith and Samach, 2013). Productive efficiency is a key indicator to select cultivars for different orchard designs, mainly focusing on plant density (Rosati et al., 2013). We found the best productive efficiency in Picual and Arbequina, due to their high fruit production associated to relative low canopy volume. As in other olive production regions, Arbequina, based on productive efficiency among other traits like compact tree shape and thin branches, could potentially be selected for high density orchards (Tous et al., 1998; García et al., 2013; Connor et al., 2014; Trentacoste et al., 2015; Gomez Del Campo et al., 2017; Marino et al., 2017). However high-density plantations under humid-temperate conditions should be carefully evaluated because the risk of air-borne disease epidemics, specially anthracnose olive rot caused by *Colletotrichum* spp. On the other hand, Frantoio presents low productive efficiency due to its high vigor, but high fruit production and oil yield at LB site. Vegetative growth rates and canopy volumes reached in the first 5 years showed the potential vegetative development under our agroecological conditions, compromising early bearing as it was described in super high-density systems (Camposeo et al., 2008; Gomez Del Campo et al., 2017). These vigorous growths require differential pruning and nutrition techniques among cultivars in order to improve productive efficiency.

There were significant differences among evaluated cultivars, Picual and Arbequina are the most productive cultivars in both evaluated sites, reaching annual average fruit yields of 11 and 8 t/ha, at LB and SG, respectively. Although Barnea in Israel presents high productive potential (Dag et al., 2011), it is not suitable for our agroecological conditions due to its low fruit yield and high ABI. Other works that compare cultivars have also highlighted Arbequina, Picual, and Frantoio in diverse locations as the most productive ones (Tapia et al., 2009; Marino et al., 2017).

Acceptable Oil Yields and Oil Contents

Oil contents were similar to those already reported in the Mediterranean basin, reinforcing the evidence that these are cultivar determined traits. The oil content in Frantoio was 46% DWB, as reported by Zeleke et al. (2012) while in Manzanilla de Sevilla only 37% DWB (**Table 6**), which associated with its great fruit weight makes it ideal for table olives (Rallo et al., 2018). Despite not measured in our study, virgin olive oils produced in Uruguay qualified as EVOO after evaluation of chemical and sensory properties (Ellis and Gámbaro, 2018) which reinforces the feasibility of EVOO production in temperate humid climates. Nevertheless, there is space for improving virgin oil yield, so studies aiming at understanding the reducing factors (weeds, diseases, soil pH) and limiting factors (water and nutrient supply) should be implemented.

Disease Management Challenges Safety Olive Oil Production

Sanitary management is an important issue arising in new olive producing regions, since new or not problematic pests could compromise olive oil production (Lavee, 2014). Particularly in temperate humid regions, weather conditions (frequent rain events, elevated air relative humidity, air temperature above 20°C) are conducive to severe epidemic outbreaks. In Uruguay, unlike in the Mediterranean basin, pests are of secondary importance but can likely cause harm in new plantations along the first

three-four years, as happens with the moth *Palpita forficifera*, with *Acromyrmex* and *Atta* ant species and with the scale *Saissetia oleae*. But undoubtedly diseases threaten olive production. Main fungal diseases are Olive scab (*Venturia oleaginea)*, Cercospora leaf spot (*Pseudocercospora cladosporioides*), and Anthracnose olive rot (*Colletotrichum* spp.), with anthracnose being the riskiest one due to its direct damage on fruits and oil quality (Leoni et al., 2018). The conducive weather conditions for these diseases occur almost all year round, challenging orchard disease management.

In summary, olive production for virgin olive oil in humid temperate climate regions with high interannual variability is feasible. Potential fruit yields are subjected to appropriate cultivar selection and the expression of these yields will strongly depend on the adverse climatic conditions that could deepen the intrinsic alternate bearing. Nevertheless, is possible to rise productive efficiency and reduce ABI, but more local research on cultivar × environment × orchard management interactions is needed. The challenge is to develop an integrated strategy to improve current status and to address emerging problems.

DATA AVAILABILITY STATEMENT

The datasets generated for this study are available on request to the corresponding author.

AUTHOR CONTRIBUTIONS

JV and PC-I contributed to experimental design PC-I, JV, JB, MA-S, and CL contributed to experimentation PC-I, MA-S, and CL conducted the data analysis and writing of the manuscript. All authors contributed to manuscript revision, read, and approved the submitted version.

FUNDING

The National Institute of Agricultural Research (Instituto Nacional de Investigación Agropecuaria – INIA, Uruguay) (Projects INIA HO08, INIA FR13) supported this work. We are grateful to David Bianchi, Richard Ashfield, and Jonathan Dávila for their collaboration in this project.

SUPPLEMENTARY MATERIAL

The Supplementary Material for this article can be found online at: https://www.frontiersin.org/articles/10.3389/fpls.2019.01544/full#supplementary-material

TABLE S1 | Average mean, maximum and minimum temperature, effective precipitation (Rain), precipitation days in the month, average relative humidity (RH) and evapotranspiration (Evap., Class A pan evaporation) from 2007 to 2017 and average historical data (1980–2009) at INIA Las Brujas and INIA Salto Grande, for October and November. Data was recorded from an automatic weather station (unless specified) and is available at http://www.inia.uy/gras/Clima/Banco-datos-agroclimatico.

FIGURE S1 | Disease management scheme implementes at the experimental sites. OS = Olive Scab (*Venturia oleagina*), CLS = Cercospora leaf spot (*Pseudocercospora cladosporioides*), AOR = Antracnose olive rot (*Colletotrichum* spp.). *Optional treatment: based on previous season disease level ** QoIs, EBI or ditiocarbamates.

REFERENCES

Ackermann, M. N., Gorga, L., and Arenare, L. (2018). Situación de la cadena del olivo. MGAP. Available: http://www.mgap.gub.uy/unidad-organizativa/oficina-de-programacion-y-politicas-agropecuarias/publicaciones/anuarios-opypa/2018 (Accessed May 2019).

Aguilera, M. P., Beltrán, G., Ortega, D., Fernández, A., Jiménez, A., and Uceda, M. (2005). Characterisation of virgin olive oil of Italian olive cultivars: 'Frantoio' and 'Leccino', grown in Andalusia. *Food Chem.* 89 (3), 387–391. doi: 10.1016/j.foodchem.2004.02.046

Archivo General de la Nación (2011). Censo-Guía de Archivos de Uruguay. Available: http://www.agn.gub.uy/pdf/censoguia.pdf. Accessed May 2019.

ASOLUR (2019). Asociación Olivícola del Uruguay. Available: http://www.asolur.org.uy/ (Accessed May 2019).

Aybar, V. E., De Melo-Abreu, J. P., Searles, P. S., Matias, A. C., Del Rio, C., Caballero, J. M., et al. (2015). Evaluation of olive flowering at low latitude sites in Argentina using a chilling requirement model. *Span. J. Agric. Res.* 13 (1), 1–10. doi: 10.5424/sjar/2015131-6375

Ayerza, R., and Sibbett, S. (2001). Thermal adaptability of olive (Olea europaea L.) to the Arid Chaco of Argentina. *Agr. Ecosyst. Environ.* 84 (3), 277–285. doi: 10.1016/S0167-8809(00)00260-7

Benlloch-González, M., Sánchez-Lucas, R., Benlloch, M., and Fernández-Escobar, R. (2018). An approach to global warming effects on flowering and fruit set of olive trees growing under fiveld conditions. *Sci. Hortic.* 240, 405–410. doi: 10.1016/j.scienta.2018.06.054

Bernaschina, Y., Alaniz, S., Conde-Innamorato, P., and Leoni, C. (2019). Comportamiento de cultivares de olivo (Olea europaea) frente a Venturia oleaginea, causante de repilo en Uruguay. *Agrociencia Uruguay* 23 (1), 1–9. doi: 10.31285/AGRO.23.1.1

Beyá-Marshall, V., and Fichet, T. (2017). Effect of crop load on the phenological, vegetative and reproductive behavior of the Frantoio olive tree (Olea europaea L.). *Cien. Investig. agrar.* 44, 43–53. doi: 10.7764/rcia.v44i1.1653

Borges, T. H., Pereira, J. A., Cabrera-Vique, C., Lara, L., Oliveira, A. F., and Seiquer, I. (2017). Characterization of Arbequina virgin olive oils produced in different regions of Brazil and Spain: Physicochemical properties, oxidative stability and fatty acid profile. *Food Chem.* 215, 454–462. doi: 10.1016/j.foodchem.2016.07.162

Camposeo, S., Ferrara, G., Palasciano, M., and Godini, A. (2008). Varietal behaviour according to the superintensive oliveculture training system. *Acta Hortic.* 791, 271–274. doi: 10.17660/ActaHortic.2008.791.38

Castaño, J. P., Giménez, A., Ceroni, M., Furest, J., and Aunchayna, R. (2011). Caracterización agroclimática del Uruguay 1980-2009. Serie Técnica INIA, 34.

Connor, D. J., Gómez-del-Campo, M., Rousseaux, M. C., and Searles, P. S. (2014). Structure, management and productivity of hedgerow olive orchards: A review. *Sci. Hortic.* 169, 71–93. doi: 10.1016/j.scienta.2014.02.010

Contarin, S. E., and Curbelo, L. A. (1987). Aporte para la regionalización del cultivo de frutales de hoja caduca en el país según la ocurrencia de frío invernal para el rompimiento del receso. Thesis Ing. Agr., UdelaR.

Cuevas, J., Rallo, L., and Rapoport, H. (1994). Crop load effects on floral quality in olive. *Sci. Hortic.* 59 (2), 123–130. doi: 10.1016/0304-4238(94)90079-5

Dag, A., Kerem, Z., Yogev, N., Zipori, I., Lavee, S., and Ben-David, E. (2011). Influence of time of harvest and maturity index on olive oil yield and quality. *Sci. Hortic.* 127 (3), 358–366. doi: 10.1016/j.scienta.2010.11.008

Díez, C. M., Moral, J., Cabello, D., Morello, P., Rallo, L., and Barranco, D. (2016). Cultivar and tree density as key factors in the long-term performance of super high-density olive orchards. *Front. Plant Sci.* 7 (1226), 1–13. doi: 10.3389/fpls.2016.01226

Di Rienzo, J. A., Casanoves, F., Balzarini, M. G., Gonzalez, L., Tablada, M., and Robledo, C. W. (2017). "InfoStat versión 2017". (http://www.infostat.com.ar: Grupo InfoStat, FCA, Universidad Nacional de Córdoba, Argentina).

Durán, A., Califra, A., Molfino, J. H., and Lynn, W. (2006). *Keys to soil taxonomy for Uruguay*. Washington (US): USDA, Natural Resources Conservation Service (NRCS).

Ellis, A. C., and Gámbaro, A. (2018). Characterisation of Arbequina Extra Virgin Olive Oil from Uruguay. *J. Food Res.* 7 (6), 79–90. doi: 10.5539/jfr.v7n6p79

Fernández, J. E. (2014). Understanding olive adaptation to abiotic stresses as a tool to increase crop performance. *Environ. Exp. Bot.* 103, 158–179. doi: 10.1016/j.envexpbot.2013.12.003

Galán, C., García-Mozo, H., Carinanos, P., Alcazar, P., and Dominguez-Vilches, E. (2001). The role of temperature in the onset of the Olea europaea L. pollen season in southwestern Spain. *Int. J. Biometeorol.* 45 (1), 8–12. doi: 10.1007/s004840000081

Galán, C., García-Mozo, H., Vázquez, L., Valenzuela, L., Díaz de la Guardia, C., and Trigo, M. M. (2005). Heat requirement for the onset of the Olea europaea L pollen season In several sites In Andalusia effect expected Future Climate change. *Int. J. Biometeorol.* 49, 184–188. doi: 10.1007/s00484-004-0223-5

García, J. M., Cuevas, M. V., and Fernández, J. E. (2013). Production and oil quality in 'Arbequina' olive (Olea europaea, L.) trees under two deficit irrigation strategies. *Irrig. Sci.* 31 (3), 359–370. doi: 10.1007/s00271-011-0315-z

Gispert, J. R., de Cartagena, F. R., Villar, J. M., and Girona, J. (2013). Wet soil volume and strategy effects on drip-irrigated olive trees (cv Arbequina). *Irrig. Sci.* 31 (3), 479–489. doi: 10.1007/s00271-012-0325-5

Goldschmidt, E. (2005). Regulatory aspects of alternate bearing in fruit trees. *Italus Hortus* 12 (1), 11–17.

Gomez Del Campo, M., Connor, D. J., and Trentacoste, E. R. (2017). Long-term Effect of Intra-Row Spacing on Growth and Productivity of Super-High Density Hedgerow Olive Orchards (cv Arbequina). *Front. Plant Sci.* 8, 1790–1790. doi: 10.3389/fpls.2017.01790

Guitton, B., Kelner, J. J., Velasco, R., Gardiner, S. E., Chagne, D., and Costes, E. (2012). Genetic control of biennial bearing in apple. *J. Exp. Bot.* 63 (1), 131–149. doi: 10.1093/jxb/err261

Haberman, A., Bakhshian, O., Cerezo, S., Paltiel, J., Adler, C., Ben-Ari, G., et al. (2017). A possible role for FT-encoding genes in interpreting environmental and internal cues affecting olive (Olea europaea L.) flower induction: olive flowering. *Plant Cell Environ.* 40, 1263–1280. doi: 10.1111/pce.12922

Instituto Nacional de Estadística. INE (2011). Estimaciones y proyecciones de población del Uruguay. Available: http://www.ine.gub.uy/resultados-de-busqueda?q=poblacion+total (Accessed May 2019).

International Olive Council. IOC. (2015). International olive oil production costs study Available: http://www.internationaloliveoil.org/documents/index/1815-international-olive-oil-production-costs-study (Accessed May 2019).

IOBC-WPRS (2012). "Commission IP - Guidelines and Endorsement, Guidelines for Integrated Production of Olives," in *IOBC Technical Guideline III*. IOBC-WPRS. International Organization for Biological and Integrated Control -West Palearctic Regional Section. ISBN: 978-92-9067-254-8.

Klepo, T., de la Rosa, R., Šatović, Z., León, L., and Belaj, A. (2013). Utility of wild germplasm in olive breeding. *Sci. Hortic.* 152, 92–101. doi: 10.1016/j.scienta.2012.12.010

Lavee, S. (2007). Biennial bearing in olive (Olea europaea). *Annales Ser. Hist. Nat.* 17, 101–112.

Lavee, S. (2014). Adaption of Commercial Olive Cultivation to New Production Zones and Environments Including in the Southern Hemisphere - Possibilities, Considerations and the Problems Involved. *Acta Hortic.* 1057, 27–40. doi: 10.17660/ActaHortic.2014.1057.1

Lavee, S. (2015). Alternate bearing in olive initiated by abiotic induction leading to biotic responses. *Adv. Hortic. Sci.* 29 (4), 213–219.

Leoni, C., Bruzzone, J., Villamil, J. J., Martínez, C., Montelongo, M. J., Bentancur, O., et al. (2018). Percentage of anthracnose (Colletotrichum acutatum s.s.) acceptable in olives for the production of extra virgin olive oil. *Crop Prot.* 108, 47–53. doi: 10.1016/j.cropro.2018.02.013

Linsley-Noakes, G., Allan, P., and Matthee, G. (1994). Modification of rest completion prediction models for improved accuracy in South African stone fruit orchards. *J. S. Afr. Soc Hortic. Sci.* 4 (1), 13–15.

Mailer, R. J., Ayton, J., and Graham, K. (2010). The Influence of Growing Region, Cultivar and Harvest Timing on the Diversity of Australian Olive Oil. *J. Am. Oil Chem. Soc* 87 (8), 877–884. doi: 10.1007/s11746-010-1608-8

Marchese, A., Marra, F. P., Costa, F., Quartararo, A., Fretto, S., and Caruso, T. (2016). An investigation of the self- and inter-incompatibility of the olive cultivars 'Arbequina' and 'Koroneiki' in the Mediterranean climate of Sicily. *Aust. J. Crop Sci.* 10 (1), 88–93.

Marino, G., Macaluso, L., Marra, F. P., Ferguson, L., Marchese, A., Campisi, G., et al. (2017). Horticultural performance of 23 Sicilian olive genotypes in hedgerow systems: vegetative growth, productive potential and oil quality. *Sci. Hortic.* 217, 217–225. doi: 10.1016/j.scienta.2017.01.046

Miranda-Fuentes, A., Llorens, J., Gamarra-Diezma, J. L., Gil-Ribes, J. A., and Gil, E. (2015). Towards an optimized method of olive tree crown volume measurement. *Sensors* 15 (2), 3671–3687. doi: 10.3390/s150203671

Monselise, S., and Goldschmidt, E. E. (1982). Alternate bearing in fruit trees. *Hortic. Rev.* 4, 128–173. doi: 10.1007/978-1-349-06519-6_5

Moriondo, M., Stefanini, F. M., and Bindi, M. (2008). Reproduction of olive tree habitat suitability for global change impact assessment. *Ecol. Modell.* 218, 95–109. doi: 10.1016/j.ecolmodel.2008.06.024

Nieddu, G., Sirca, C., and Chessa, I. (2002). Evaluation of the phenological behaviour of two olive tree varieties. *Adv. Hortic. Sci.* 16 (3/4), 138–143.

Obeso, J. R. (2002). The costs of reproduction in plants. *New Phytol.* 155 (3), 321–348. doi: 10.1046/j.1469-8137.2002.00477.x

Orlandi, F., Vazquez, L. M., Ruga, L., Bonofiglio, T., Fornaciari, M., Garcia-Mozo, H., et al. (2005). Bioclimatic requirements for olive flowering in two Mediterranean regions located at the same latitude (Andalucia, Spain and Sicily, Italy). *Ann. Agric. Environ. Med.* 12 (1), 47–52.

Pereira, J., Bernal, J., Martinelli, L., Villamil, J. J., and Conde, P. (2018). Original olive genotypes found in Uruguay identified by morphological and molecular markers. *Acta Hortic.* 1199, 7–14. doi: 10.17660ActaHortic.2018.1199.2

Pope, K., Da Silva, D., Brown, P., and Dejong, T. (2014). A biologically based approach to modeling spring phenology in temperate deciduous trees. *Agric. For. Meteorol.* 198-199, 15–23. doi: 10.1016/j.agrformet.2014.07.009

Rallo, L., and Cuevas, J. (2017). "Fructificación y producción," in *El cultivo del olivo,* Eds. D. Barranco, R. Fermnandez-Escobar and L. Rallo (Madrid: Mundi-Prensa), 145–186.

Rallo, L., and Martin, G. C. (1991). The Role of Chilling in Releasing Olive Floral Buds from Dormancy. *J. Am. Soc Hortic. Sci.* 116 (6), 1058. doi: 10.21273/jashs.116.6.1058

Rallo, L., Barranco, D., Castro-García, S., Connor, D. J., Gómez del Campo, M., and Rallo, P. (2013). "High-Density Olive Plantations," in *Horticultural Reviews*, vol. 41 . Ed. Janick, J. Hoboken (New Jersey, USA: John Wiley and Sons, Inc.) doi: 10.1002/9781118707418.ch07

Rallo, L., Díez, C., Morales-Sillero, A., Miho, H., Priego-Capote, F., and Rallo, P. (2018). Quality of olives: A focus on agricultural preharvest factors. *Sci. Hortic.* 233, 491–509. doi: 10.1016/j.scienta.2017.12.034

Rondanini, D., Castro, N., Searles, P., and Rousseaux, M. (2014). Contrasting patterns of fatty acid composition and oil accumulation during fruit growth in several olive varieties and locations in a non-Mediterranean region. *Eur. J. Agron.* 52, 237–246. doi: 10.1016/j.eja.2013.09.002

Rosati, A., Paoletti, A., Caporali, S., and Perri, E. (2013). The role of tree architecture in super high density olive orchards. *Sci. Hortic.* 161, 24–29. doi: 10.1016/j.scienta.2013.06.044

Sánchez, A., and Cuevas, J. (2018). 'Arbequina' olive is self-incompatible. *Sci. Hortic.* 230, 50–55. doi: 10.1016/j.scienta.2017.11.018

Sanz-Cortés, F., Martínez-Calvo, J., Badenes, M. L., Bleiholder, H., Hack, H., Llácer, G., et al. (2002). Phenological growth stages of olive trees (Olea europaea). *Ann. Appl. Biol.* 140 (2), 151–157. doi: 10.1111/j.1744-7348.2002.tb00167.x

Severino, V., Arbiza, H., Arias, M., Manzi, M., and Gravina, A. (2011). Modelos de cuantificación de frío efectivo invernal adaptados a la producción de manzana en Uruguay. *Agrociencia Uruguay* 15 (2), 19–28.

Shahidi, F. (2001). "Solvent Extraction of oilseeds, nutmeg, and other foods using the Soxhlet method," in *Current Protocols in Food Analytical Chemistry* (New York: John Wiley and Sons).

Smith, H. M., and Samach, A. (2013). Constraints to obtaining consistent annual yields in perennial tree crops. I: Heavy Fruit load dominates over vegetative growth. *Plant Sci.* 207, 158–167. doi: 10.1016/j.plantsci.2013.02.014

Tapia, F., Mora, F., and Santos, A. I. (2009). Preliminary Evaluation of 29 Olive (Olea europaea L.) Cultivars for Production and Alternate Bearing in the Huasco Valley, Northern Chile. *Chil. J. Agr. Res.* 69, 325–330. doi: 10.4067/S0718-58392009000300004

Torres, M., Pierantozzi, P., Searles, P., Rousseaux, M. C., García-Inza, G., Miserere, A., et al. (2017). Olive Cultivation in the Southern Hemisphere:

Flowering, Water Requirements and Oil Quality Responses to New Crop Environments. *Front. Plant Sci.* 8, 1830–1830. doi: 10.3389/fpls.2017.01830

Tous, J., Romero, A., and Plana, J. (1998). Comportamiento agronómico y comercial de cinco variedades de olivo en Tarragona. *Invest. Agr. Prod. Prot. Veg.* 13 (1–2), 97–109.

Tous, J., Villamil, J., Hermoso, J., and Albín, A. (2005). El olivo en Uruguay. *Olivae* 103, 56–61.

Trentacoste, E. R., Connor, D. J., and Gómez-del-Campo, M. (2015). Effect of olive hedgerow orientation on vegetative growth, fruit characteristics and productivity. *Sci. Hortic.* 192, 60–69. doi: 10.1016/j.scienta.2015.05.021

Uceda, M., and Frias, L. (1975). "Harvest Dates. Evolution of the Fruit Oil Content, Oil Composition and Oil Quality", II Seminario Oleícola Internacional: International Olive Oil Council, 125-130.

Vaughan, C., Dessai, S., Hewitt, C., Baethgen, W., Terra, R., and Berterretche, M. (2017). Creating an enabling environment for investment in climate services: The case of Uruguay's National Agricultural Information System. *Clim. Serv.* 8, 62–71. doi: 10.1016/j.cliser.2017.11.001

Wang, J., Ma, L., Gómez del Campo, M., Zhang, D., Deng, Y., and Jia, Z. (2018). Youth tree behavior of olive (Olea europaea L.) cultivars in Wudu, China: Cold and drought resistance, growth, fruit production, and oil quality. *Sci. Hortic.* 236, 106–122. doi: 10.1016/j.scienta.2018.03.033

Zeleke, K., Mailer, R., Eberbach, P., and Wünsche, J. (2012). Oil content and fruit quality of nine olive (Olea europaea L.) varieties affected by irrigation and harvest times. *N. Z. J. Crop Hortic. Sci.* 40 (4), 241–252. doi: 10.1080/01140671.2012.662159

Conflict of Interest: The authors declare that the research was conducted in the absence of any commercial or financial relationships that could be construed as a potential conflict of interest.

frontiers in Plant Science

ORIGINAL RESEARCH
published: 24 December 2019
doi: 10.3389/fpls.2019.01593

Cultivated Olive Diversification at Local and Regional Scales: Evidence From the Genetic Characterization of French Genetic Resources

Bouchaib Khadari[1,2], Ahmed El Bakkali[3], Laila Essalouh[1,4], Christine Tollon[1], Christian Pinatel[5] and Guillaume Besnard[6]*

[1] AGAP, University Montpellier, CIRAD, INRA, Montpellier SupAgro, Montpellier, France, [2] Conservatoire Botanique National Méditerranéen de Porquerolles (CBNMed), UMR AGAP, Montpellier, France, [3] INRA, UR Amélioration des Plantes et Conservation des Ressources Phytogénétiques, Meknès, Morocco, [4] Établissement Public Local d'Enseignement et de Formation Professionnelle Agricoles Nîmes-Rodilhan-CFPPA du Gard, Rodilhan, France, [5] Centre Technique de l'Olivier, Maison des Agriculteurs, Aix-en-Provence, France, [6] CNRS-IRD-UPS EDB, UMR 5174, Université Paul Sabatier, Toulouse, France

Molecular characterization of crop genetic resources is a powerful approach to elucidate the origin of varieties and facilitate local cultivar management. Here we aimed to decipher the origin and diversification of French local olive germplasm. The 113 olive accessions of the *ex situ* collection of Porquerolles were characterized with 20 nuclear microsatellites plus their plastid haplotype. We then compared this collection to Mediterranean olive varieties from the Worldwide Olive Germplasm Bank of Marrakech, Morocco. High genetic diversity was observed within local French varieties, indicating a high admixture level, with an almost equal contribution from the three main Mediterranean gene pools. Nearly identical and closely related genotypes were observed among French and Italian/Spanish varieties. A high number of parent–offspring relationships were also detected among French varieties and between French and two Italian varieties ('Frantoio' and 'Moraiolo') and the Spanish variety ('Gordal Sevillana'). Our investigations indicated that French olive germplasm resulted from the diffusion of material from multiple origins followed by diversification based on parentage relationships between varieties. We strongly suggest that farmers have been actively selecting olives based on local French varieties. French olive agroecosystems more affected by unexpected frosts than southernmost regions could also be seen as incubators and as a bridge between Italy and Spain that has enhanced varietal olive diversification.

Keywords: *Olea europaea* L., parentage analysis, simple sequence repeat, genetic structure, *ex situ* collection of Porquerolles, genetic resource management, core collection

OPEN ACCESS

Edited by:
José Manuel Martínez-Rivas, Instituto de la Grasa (IG), Spain

Reviewed by:
Cristian Silvestri, Università degli Studi della Tuscia, Italy
Enzo Perri, Council for Agricultural and Economics Research, Italy

****Correspondence:***
Bouchaib Khadari
khadari@supagro.fr

Specialty section:
This article was submitted to Crop and Product Physiology, a section of the journal Frontiers in Plant Science

Received: *05 August 2019*
Accepted: *13 November 2019*
Published: *24 December 2019*

Citation:
Khadari B, El Bakkali A, Essalouh L, Tollon C, Pinatel C and Besnard G (2019) Cultivated Olive Diversification at Local and Regional Scales: Evidence From the Genetic Characterization of French Genetic Resources. Front. Plant Sci. 10:1593. doi: 10.3389/fpls.2019.01593

INTRODUCTION

Olive (*Olea europaea* L.) is the iconic fruit crop of the Mediterranean Basin. Archaeological, historical, and genetic studies support a primary olive domestication in the Near East, probably starting during the Chalcolithic period (Kaniewski et al., 2012; Zohary et al., 2012; Besnard et al., 2013b). Then long-distance translocation of varieties followed by admixture events led to secondary multi-local diversification in central and western Mediterranean regions (Terral, 1997; Besnard et al., 2001a; Belaj

et al., 2002; Owen et al., 2005; Baldoni et al., 2006; Breton et al., 2008; Diez et al., 2015). Locally adapted varieties have thus been carefully selected by farmers in several Mediterranean areas and the domestication process is still ongoing (Besnard et al., 2001a; Khadari et al., 2003; Khadari et al., 2008; El Bakkali et al., 2013a; Besnard et al., 2018). Selected trees are still both clonally and seed propagated in traditional agroecosystems from different parts of the Mediterranean Basin (Aumeeruddy-Thomas et al., 2017; Besnard et al., 2018), implying a continuing role of sexual reproduction in varietal diversification, with potential contributions from local domesticated, feral, and wild olives. Due to this diversification process, a high frequency of parentage relationships could be expected among varieties, as previously observed within the Spanish olive germplasm (Diez et al., 2015) and in grapevine (Bowers et al., 1999; Lacombe et al., 2013). Furthermore, farmer selection of newly adapted olive trees could be viewed as a key process in agroecosystems under changing climatic and ecological conditions, such as those on the fringe of olive growing areas. But it is still unknown how farmer selection and varietal diversity relate to these changing environmental conditions. Today, in a context of global changes associated with the emergence of pests that threaten olive cropping, especially in southern Europe (e.g. *Xylella fastidiosa*), there is call for the selection of varieties adapted to new environmental conditions (De Ollas et al., 2019). The characterization of olive varieties in any germplasm bank and the elucidation of their origins are thus high priority to ensure efficient use of genetic resources in the future.

In France, olive is traditionally cultivated in southern regions on the rim of the Mediterranean Sea. Major development of olive cultivation was initiated by Phoenicians in Massalia, i.e. present day Marseille, around 2600 BP, while wild olives were already present and some local varieties were also likely cultivated (Terral et al., 2004). More than 100 French olive varieties are currently described based on morphological descriptors (Moutier et al., 2004; Moutier et al., 2011) and molecular markers (Khadari et al., 2003; Khadari et al., 2004). A few of them are considered as main varieties since they are cultivated over relatively large geographical areas, while more than 80 have a restricted distribution range, generally spanning a few townships. This particularly high diversity at the northern limit of the cultivated olive range may partly be the result of recurrent farmer selection of adapted varieties due to relatively frequent frosts that affect local olive germplasm. A significant portion of present varieties (14%) show a maternal origin from the western Mediterranean region, suggesting a local origin (Besnard et al., 2001a; Khadari et al., 2003). Previous studies based on nuclear genetic markers further supported an admixed origin for most French varieties with a prevalent genetic contribution from the eastern Mediterranean (Besnard et al., 2001a; Haouane et al., 2011), as similarly shown in Italian and Tunisian germplasm, respectively on the northern and southern shores of the Mediterranean Sea (Haouane et al., 2011; Belaj et al., 2012; Khadari and El Bakkali, 2018). Such an admixed origin could be seen as a genetic signature of local olive diversification in the central Mediterranean area. However, the local crop diversification process remains unclear, and may involve major progenitors, as shown, for instance, in Andalusian olives (Diez et al., 2015). In addition, it was also shown that cultivars growing in the eastern and western sides of the Rhone valley were differentiated (Khadari et al., 2003), possibly reflecting two pathways of olive cultivar introduction from the Italian and Iberian Peninsulas, respectively.

In the present study, we investigated the cultivated olive diversification process in southern France, with the aim of determining ways to efficiently manage local olive genetic resources. Both nuclear and chloroplast loci were used to characterize the genetic diversity of a set of varieties from the French Olive Germplasm Bank (FOGB) in comparison to the Worldwide Olive Germplasm Bank (WOGB) of Marrakech, Morocco (Haouane et al., 2011; El Bakkali et al., 2013b). We specifically aimed to: (1) assess genetic diversity within the FOGB collection and propose a nested set of French reference varieties representative of total genetic diversity; (2) compare the genetic diversity at two different geographical scales, i.e. local (France) and regional (Mediterranean area); and (3) clarify the origin of French olive germplasm by parentage analyses within and among French and Mediterranean varieties. Our results were examined in light of the diversification process founded on farmer selection within traditional agroecosystems probably hampered by frequent climatic accidents such as frost.

MATERIAL AND METHODS

Plant Material

The FOGB includes a total of 113 olive accessions, and is maintained on the island of Porquerolles, near Toulon in southern France (**Table 1**). These accessions are identified with a variety name and/or with tree coordinates in the collection (**Table 1**). Among the 63 accessions identified with a variety name, 14 are considered as being the main French varieties since they are cropped over broad areas compared to minor varieties (22), which have a limited distribution range, generally over a few townships, and to local varieties (27), which are only present in one or two orchards (**Table 1**; Moutier et al., 2004; Moutier et al., 2011).

Genotypes of French accessions were compared to those of other varieties collected throughout the Mediterranean Basin. Four hundred and sixteen accessions from 13 Mediterranean countries that are maintained in the World Olive Germplasm Bank of Marrakech (WOGB; **Supplementary Table S1**) were analyzed. Mediterranean varieties conserved in the WOGB collection are classified in three gene pools based on both the country origin and genetic structure, i.e. East (mostly from Cyprus, Egypt, Lebanon, and Syria), West (mostly from Morocco, Spain, and Portugal), and Central (mostly from Algeria, Italy, Slovenia, Croatia, Tunisia, and Greece; Haouane et al., 2011; El Bakkali et al., 2013b).

Datasets

Twenty microsatellite nuclear loci (SSR) were used for genotyping accessions of both FOGB and WOGB (**Table 2**), as described by El Bakkali et al. (2013b). These markers were selected based on their clear amplification, high polymorphism, and reproducibility, as reported by Trujillo et al. (2014). Alleles were carefully scored twice independently by two researchers.

TABLE 1 | List of the 113 French accessions analyzed in the present study classified according to tree coordinates, accession name, code SSR. Accessions showing molecular variants (one or two dissimilar alleles).

Tree coordinates	Accession name	SSR code	Variant code	Reference genotype	Reference variety	Importance of the variety	genetic structure	Chlorotype	French parentage	Mediterranean parentage	CC level
3_03	Aglandau	413	51	3_03	Aglandau	Main	Mosaic	E 1-1	3	1	CC_{43}
34_17	Aglandau	414									
33_25	Aglandau	414	51								
32_21	Amellau	459		32_21	Amellau	Secondary	Eastern	E 1-1	1	0	CC_{43}
32_03	Araban 06	460		32_03	Araban 06	Local	Mosaic	E 1-1	0	0	CC_{22}
31_05	Araban du Var	405									
35_07	Araban du Var	405		35_07	Araban du Var	Secondary	Mosaic	E 1-1	4	2	CC_{75}
27_13	Baguet	461		27_13	Baguet	Local	Mosaic	E 1-1	0	0	CC_{75}
26_05	Béchude	411		26_05	Béchude	Secondary	Mosaic	E 2-1	2	0	CC_{75}
36_02	Béchude	411									
36_22	Béchude	411									
34_04	Bé-dé-Cézé	462		34_04	Bé-dé-Cézé	Secondary	Mosaic	E 1-1	0	0	CC_{22}
37_23	Belgentiéroise	463		37_23	Belgentiéroise	Secondary	Mosaic	E 1-1	0	0	CC_{43}
1_13	Blanc de Paysac	412		1_13	Blanc de Paysac	Secondary	Eastern	E 1-1	0	0	CC_{75}
24_02	Blanc de Paysac	412									
37_11	Blanquetier	464		37_11	Blanquetier	Local	Mosaic	E 3-1	0	3	CC_{75}
36_11	Boube	416	47	36_11	Boube	Local	Western	E 1-2	6	30	CC_{75}
35_13	Boube	417	47								
15_05	Boube	416									
34_19	Bouteillan	465		34_19	Bouteillan	Main	Mosaic	E 1-1	1	0	CC_{22}
35_25	Broutignan	409	50	35_25	Broutignan	Secondary	Mosaic	E 1-1	1	0	CC_{22}
35_28	Broutignan	410									
35_22	Broutignan	410	50								
37_21	Brun	466		37_21	Brun	Secondary	Eastern	E 1-1	0	0	CC_{75}
32_33	Cailletier	429	3	32_33	Cailletier	Main	Central	E 1-1	6	18	CC_{75}
34_31	Cailletier	430	3								
33_31	Cailleton	467		33_31	Cailleton	Local	Mosaic	E 1-1	0	0	CC_{22}
33_13	Capelen	468		33_13	Capelen	Local	Mosaic	E 1-1	0	0	CC_{43}
15_02	Cayet Rouge	469		15_02	Cayet Rouge	Local	Mosaic	E 1-1	0	2	CC_{75}
33_10	Cayet Roux	421	54	33_10	Cayet Roux	Main	Mosaic	E 1-1	2	0	CC_{22}
6_11	Cayet Roux	422	54								
37_26	Cayet Roux	423	54								
3_12	Cayon	402		3_12	Cayon	Main	Mosaic	E 2-1	0	0	CC_{22}
33_04	Clermontaise	470		33_04	Clermontaise	Secondary	Mosaic	E 1-1	1	0	CC_{43}
20_15	Colombale	471		20_15	Colombale	Secondary	Mosaic	E 1-1	2	0	CC_{75}
7_14	Corniale	472		7_14	Corniale	Secondary	Mosaic	E 1-1	0	0	CC_{43}
8_04	Courbeil	473		8_04	Courbeil	Secondary	Mosaic	E 3-1	1	0	CC_{22}
33_07	Cul Blanc	474		33_07	Cul Blanc	Secondary	Mosaic	E 2-1	1	0	CC_{75}
7_03	Curnet	475		7_03	Curnet	Secondary	Eastern	E 3-1	0	0	CC_{43}
25_03	Darame	476		25_03	Darame	Local	Eastern	E 1-1	3	0	CC_{75}
32_20	Dent de Verrat	477		32_20	Dent de Verrat	Local	Central	E 3-1	0	0	CC_{22}
19_04	Filayre rouge	478		19_04	Filayre rouge	Local	Eastern	E 1-1	0	0	CC_{75}
26_10	Gardisson	479		26_10	Gardisson	Local	Mosaic	E 2-1	0	1	CC_{75}
15_07	Grapié	480		15_07	Grapié	Local	Mosaic	E 1-1	0	1	CC_{75}
32_09	Grassois	481		32_09	Grassois	Local	Central	E 1-1	2	2	CC_{43}
8_16	Gros vert	482		8_16	Gros vert	Local	Central	E 1-1	1	0	CC_{22}
17_13	Grossane	415		17_13	Grossane	Main	Mosaic	E 1-1	0	0	CC_{75}
37_05	Grossane	415									
35_01	Grosse Noire	483		35_01	Grosse Noire	Local	Eastern	E 1-1	1	0	CC_{43}
36_01	Grosse Violette	407	49								
35_04	Grosse Violette	408	49	35_04	Grosse Violette	Secondary	Eastern	E 1-1	0	1	CC_{75}
32_15	Linat	484		32_15	Linat	Local	Eastern	E 1-1	1	2	CC_{75}
16_08	Lucques	485		16_08	Lucques	Main	Mosaic	E 1-1	0	0	CC_{22}
1_17	Malausséna	486		1_17	Malausséna	Local	Mosaic	E 1-1	1	3	CC_{22}
35_16	Menudel	487		35_16	Menudel	Secondary	Mosaic	E 1-1	1	0	CC_{75}
13_16	Montaurounenque	424	18								
23_10	Montaurounenque	425	18	23_10	Montaurounenque	Secondary	Mosaic	E 2-1	0	0	CC_{43}
23_11	Montaurounenque	426	18								
31_15	Moufla	488		31_15	Moufla	Local	Eastern	E 1-1	1	3	CC_{75}
34_01	Négrette	427	52								

(Continued)

TABLE 1 | Continued

Tree coordinates	Accession name	SSR code	Variant code	Reference genotype	Reference variety	Importance of the variety	genetic structure	Chlorotype	French parentage	Mediterranean parentage	CC level
5_02	Négrette	428	52	5_02	Négrette	Main	Mosaic	E 1-1	5	0	CC_{75}
6_12	Olivière	403		6_12	Olivière	Main	Mosaic	E 3-1	3	0	CC_{75}
10_03	Petit Ribier	418	27	10_03	Petit Ribier	Main	Central	E 1-1	3	4	CC_{75}
16_14	Petit Ribier	419	27								
11_07	Petit Ribier	420	27								
22_02	Petite Noire	489		22_02	Petite Noire	Secondary	Mosaic	E 1-1	1	0	CC_{75}
36_07	Petite Violette	490		36_07	Petite Violette	Local	Mosaic	E 1-1	1	0	CC_{22}
17_07	Picholine	404		17_07	Picholine	Main	Mosaic	E 2-1	3	0	CC_{43}
30_15	Pigale	491		30_15	Pigale	Local	Mosaic	E 2-1	1	0	CC_{75}
6_06	Rascasset	492		6_06	Rascasset	Local	Mosaic	E 1-1	0	0	CC_{75}
6_01	Reymet	493	53	6_01	Reymet	Secondary	Central	E 1-1	1	1	CC_{22}
35_10	Ronde de VDB	494		35_10	Ronde de VDB	Local	Mosaic	E 1-1	2	1	CC_{75}
4_14	Rougette de l'Ardèche	495		4_14	Rougette de l'Ardèche	Main	Mosaic	E 2-1	1	0	CC_{43}
36_31	Rougette de Pignan	496		36_31	Rougette de Pignan	Secondary	Mosaic	E 1-1	0	0	CC_{22}
36_16	Rougette du Gard	497		36_16	Rougette du Gard	Secondary	Mosaic	E1.4	1	0	CC_{43}
33_16	Salonenque	498		33_16	Salonenque	Main	Eastern	E 1-1	0	2	CC_{43}
36_19	Sauzin Vert	499		36_19	Sauzin Vert	Local	Mosaic	E1.4	1	1	CC_{75}
2_05	Tanche	500		2_05	Tanche	Main	Eastern	E 1-1	0	1	CC_{75}
22_08	Taulelle	501		22_08	Taulelle	Local	Mosaic	E 1-1	0	0	CC_{22}
31_09	Tripue	502		31_09	Tripue	Local	Mosaic	E 1-1	0	0	CC_{22}
34_13	Verdale 13	503		34_13	Verdale 13	Secondary	Eastern	E 1-1	0	0	CC_{75}
10_10	Verdanel	504		10_10	Verdanel	Local	Mosaic	E 1-1	1	0	CC_{75}
22_14	Vilette	505		22_14	Vilette	Local	Mosaic	E 1-1	2	0	CC_{75}
10_04	10_04	431		10_04			Mosaic	E 1-1	2	0	
10_09	10_09	432		10_09			Mosaic	E 1-1	0	0	
13_12	13_02	433		13_12			Mosaic	E 1-1	0	0	
14_17	14_17	434		14_17			Mosaic	E 1-1	1	0	
16_04	16_04	406		16_04			Mosaic	E 1-1	0	0	
18_16	18_16	435		18_16			Mosaic	E 1-1	0	0	CC_{22}
19_02	19_02	436		19_02			Mosaic	E 1-1	1	0	CC_{43}
20_11	20_11	437		20_11			Mosaic	E 1-1	2	1	CC_{43}
23_04	23_04	438		23_04			Mosaic	E 1-1	1	0	
24_09	24_09	439		24_09			Eastern	E 1-1	0	0	
32_25	32_25	440		32_25			Mosaic	E 1-1	0	0	CC_{43}
33_00	33_00	441		33_00			Mosaic	E 3-1	0	0	CC_{22}
33_02	33_02	442		33_02			Mosaic	E 3-1	0	0	
33_19	33_19	443	33	33_19			Mosaic	E 1-1	1	0	CC_{43}
33_22	33_22	444		33_22			Mosaic	E 1-1	0	0	CC_{43}
33_32	33_32	445		33_32			Mosaic	E 1-1	3	0	
34_07	34_07	406									
34_10	34_10	446		34_10			Mosaic	E 1-1	4	0	
34_22	34_22	447		34_22			Central	E 1-1	1	1	CC_{43}
34_25	34_25	448		34_25			Mosaic	E 1-1	1	0	CC_{22}
34_28	34_28	449		34_28			Mosaic	E 1-1	2	2	
35_19	35_19	450		35_19			Mosaic	E 1-1	3	0	CC_{43}
35_31	35_31	451		35_31			Mosaic	E 1-1	0	0	CC_{22}
36_04	36_04	452		36_04			Eastern	E 1-1	2	2	
36_25	36_25	453		36_25			Mosaic	E 1-1	5	2	
36_28	36_28	454		36_28			Mosaic	E 3-3	1	0	
37_02	37_02	455		37_02			Mosaic	E 1-1	2	2	
37_25	37_25	456		37_25			Central	E 1-1	1	0	CC_{22}
9_01	9_01	457		9_01			Mosaic	E 1-1	2	0	
9_07	9_07	458		9_07			Mosaic	E 1-1	1	0	

Main varieties: planted in large areas.
Secondary varieties: present in a restricted distribution range, generally over a few townships.
Local varieties: only present in one or two orchards.

TABLE 2 | Genetic parameters of the 20 SSR loci in both FOGB (92 genotypes) and WOGB (311) collections.

N	Loci	FOGB						WOGB			
		Size	Na	Npa	He	Ho	PIC	Size	Na	He	Ho
1	DCA01[a]	203–268	7 (1)[1]	2	0.568	0.620	0.520	203–274	19	0.641	0.736
2	DCA03[a]	229–250	7		0.841	0.935	0.814	227–263	14	0.854	0.891
3	DCA04[a]	128–192	20 (1)	6	0.875	0.674	0.856	116–198	34	0.856	0.666
4	DCA05[a]	189–209	11		0.614	0.685	0.587	189–211	12	0.513	0.511
5	DCA08[a]	123–154	15	6	0.795	0.891	0.765	123–164	21	0.837	0.945
6	DCA09[a]	160–207	18 (1)	6	0.873	0.913	0.855	160–217	24	0.889	0.952
7	DCA11[a]	125–179	11	5	0.788	0.913	0.752	125–199	24	0.830	0.868
8	DCA14[a]	168–186	9	1	0.636	0.641	0.604	166–190	15	0.712	0.740
9	DCA15[a]	242–265	4		0.519	0.489	0.443	242–265	7	0.656	0.695
10	DCA16[a]	121–175	10	2	0.815	0.615	0.786	121–230	35	0.879	0.952
11	DCA18[a]	162–182	10	1	0.815	0.870	0.788	154–188	17	0.846	0.916
12	GAPU59[b]	206–226	7	2	0.585	0.565	0.546	206–238	11	0.623	0.592
13	GAPU71A[b]	207–239	5	1	0.325	0.337	0.296	205–255	16	0.476	0.555
14	GAPU71B[b]	116–141	6	1	0.801	0.924	0.765	116–144	8	0.807	0.900
15	GAPU101[b]	181–215	8		0.851	0.967	0.828	181–217	13	0.858	0.945
16	GAPU103A[b]	133–188	14	3	0.827	0.867	0.802	133–194	26	0.862	0.781
17	EMO03[c]	201–215	11 (1)	4	0.767	0.707	0.727	201–215	13	0.806	0.807
18	EMO90[c]	180–193	5		0.710	0.837	0.666	180–208	9	0.658	0.672
19	UDO-017[d]	152–168	6		0.784	0.804	0.745	144–172	9	0.777	0.820
20	UDO-036[d]	140–164	7	2	0.683	0.739	0.625	138–166	12	0.731	0.706
	Mean		**9.55**		**0.723**	**0.749**	**0.688**		**16.95**	**0.755**	**0.782**
	Total		**191 (4)**	**42**					**339**		

[1]*between brackets: number of specific alleles compared to the WOGB collection.*

[a]*Sefc et al., 2000,* [b]*Carriero et al., 2002,* [c]*De la Rosa et al., 2002,* [d]*Cipriani et al., 2002.*

Number of alleles (Na), number of private alleles (Npa), expected (He) and observed heterozygosity (Ho), polymorphism information content (PIC).

Genotyping of accessions with a specific allele (i.e. observed only once) was systematically repeated to ensure its occurrence. Plastid DNA (*cpDNA*) variations were also characterized using 39 markers, including 32 cpSSR loci, five indels (insertions/deletions), and two single nucleotide polymorphisms (SNPs), as described by Besnard et al. (2011).

DATA ANALYSIS

Genetic Diversity and Structure

The number of alleles per locus (*Na*), expected (*He*; Nei, 1987) and observed heterozygosity (*Ho*), and polymorphism information content (PIC) were estimated using the Excel Microsatellite Toolkit v.3.1 (Park, 2001).

A binary matrix containing only distinct French genotypes was built, using alleles scored as present (1) or absent (0) to assess genetic relationships within the FOGB collection. This matrix was used to construct a dendrogram based on Dice's similarity index (Dice, 1945) and the UPGMA algorithm with the NTSYS v2.02 software package (Rohlf, 1998).

The French (FOGB) and Mediterranean (WOGB) collections were compared based on different criteria: (1) genetic parameters such as the allele number (*Na*), expected and observed heterozygosity (*He* and *Ho*); (2) the distribution of pairwise genetic distances between cultivars using the index of Smouse and Peakall (1999) in GENALEX 6 program (Peakall and Smouse, 2006); (3) the allelic richness (*Ar*) using the ADZE program (Szpiech et al., 2008); (4) a principal coordinate analysis (PCoA) implemented in DARWIN 5.0.137 (Perrier et al., 2003) using the simple matching coefficient to describe relationships between genotypes based on the spatial distribution of the two first coordinate axes; and (5) the genetic structure within both collections using the model-based Bayesian clustering approach implemented in STRUCTURE v.2.2 (Pritchard et al., 2000) according to the parameters described in Haouane et al. (2011). Regarding the genetic structure, the reliability of the number of clusters (*K*) was checked using the *ad hoc* ΔK measure (Evanno et al., 2005) with the R program, whereas the similarity index between different replicates for the same *K* clusters (*H'*) was calculated using the CLUMPP v1.12 program (Jakobsson and Rosenberg, 2007).

Parentage Analysis

Parentage analyses were based on nuclear SSR data and aimed at detecting putative parent–offspring relationships among French varieties, as well as between these latter and varieties from the whole Mediterranean Basin. A putative parent–offspring pair is defined as any pair of individuals that share alleles across all loci and contain all true and false parent–offspring pairs (Jones et al., 2010). Indeed, the probability of two unrelated genotypes sharing alleles by chance at all loci is not trivial, especially for a large set of pairwise comparisons with a limited number of molecular markers. A key challenge addressed in our analyses was to correctly identify the true parent–offspring pairs within a dataset, while simultaneously excluding pairs that could potentially have shared alleles by chance. Considering the large panel of examined varieties without any available information on parentage relationships, pedigree reconstruction based on parental pair assignment may be not robust, as in cases when one parent is already known (Jones et al., 2010), and the probability of detecting

false parent–offspring pairs would thus need to be assessed. Here, in a first step, we conducted parentage analyses through a "single-parent search" (Jones et al., 2010) in order to identify putative parent–offspring pairs. Second, based on these results, we used parental pair assignment to construct pedigree among varieties.

For single-parent searches, we used a complete exclusion approach and two parentage assignment approaches where by the single most likely parent was chosen from a group of non-excluded candidate parents based on a likelihood method or on Bayesian posterior probability of a: (*i*) First, we used the exclusion-based method with the PARFEX v.1.0 macro (Sekino and Kakehi, 2012). This simple method examines genotype incompatibilities between offspring and parents based on Mendelian inheritance rules. A parentage relationship is established if a single parent of offspring remains non-excluded from a parental pool considering 0 or 1 mismatching allele at a single locus; (*ii*) we then used the likelihood-based method (Gerber et al., 2000) available in the PARFEX v.1.0 macro. This parentage inference relies on the difference in the log-likelihood ratio (LOD) between related and unrelated relationships. To define a threshold (LODc) to accept/reject possible parentage relationships (single parent), offspring were simulated using the allelic frequencies (L_{obs}) observed in our datasets and a random sampling of alleles (L_{rand}), while taking into account the genotypic error rate for random replacement of simulated genotypes at each marker (e_{sim}) and for LOD calculations (e_{calc}). Simulations were conducted using 1% error rates for e_{calc} and e_{sim}, 200 parents, and 10,000 offspring. The LODc was defined by the intersection of the distribution of L_{obs} and L_{rand}; (*iii*) Lastly, based on the exclusion-Bayes' theorem method (Christie, 2010) using SOLOMON package in the R program (Christie et al., 2013), the posterior probability of false parent–offspring pairs (among all pairs that share at least one allele across all loci) was assessed in a dataset to determine whether all putative parent–offspring pairs could be accepted with strict exclusion. The probability of observing shared alleles between unrelated individuals was calculated using 1,000 simulated datasets and 50,000,000 simulated genotypes. Finally, parentage inferences of each French genotype were considered as reliable when validated by the three approaches. By detecting single parent–offspring relationships, the identity of parents and offspring of each putative pair could not be determined. Networks of parent–offspring relationships were plotted with the "i*graph*" package in R environment (Csardi and Nepusz, 2006).

For parental pair assignments, putative parent–offspring relationships detected with the three previous approaches were re-used. We used the likelihood-based method (Gerber et al., 2000) to assess this panel of relationships because it appears to be the most conservative approach compared to the exclusion-Bayes' theorem method (see *Results*).

Core Collection Sampling

For agronomic experiments and breeding programs, it may be necessary to define sets of cultivars representative of French cultivated olive germplasm. French core collections were thus constructed from the FOGB collection according to the two-step method described by El Bakkali et al. (2013b). Nested core collections were constructed by combining two approaches implemented in the CoreHunter (Thachuk et al., 2009) and Mstrat (Gouesnard et al., 2001) programs. First, an initial core collection capturing total allelic diversity was constructed with Mstrat to estimate the sample size necessary to capture all observed alleles. Then CoreHunter with the "*Sh strategy*" was run with half of the initial constructed core collection in order to select a primary local core collection with the lowest number of accessions. This primary core collection was used as a kernel in Mstrat to capture the remaining alleles and 50 independent core collections were proposed.

RESULTS

Characterization of French Olive Germplasm and Definition of Reference Genotypes per Variety

One hundred and four distinct genetic profiles were obtained among the 113 accessions of the FOGB based on 20 SSR nuclear loci (**Table 1**). Among the 6328 pairwise comparisons, 10 were identical (0.16%), 13 (0.19%) were closely related and differing by one or two dissimilar alleles, whereas the remaining pairs were distinguished by three to 37 dissimilar alleles (**Figure 1A**). Closely related SSR profiles with one or two dissimilar alleles were considered as putative molecular variants resulting from somatic mutations and were thus classified as a single genotype. This was the case for ancient varieties such as 'Boube' or 'Négrette' and also for major varieties, such as 'Aglandau' or 'Cailletier', which are cultivated over broad geographic areas (**Supplementary Table S2**). The SSR profile considered as the reference genotype of the variety was chosen based on the high frequency of trees under the same molecular profile (**Table 1** and **Supplementary Table S2**). Hence, a total of 92 genotypes was defined among the 113 accessions analyzed and the most closely related pairs were ultimately distinguished by five dissimilar alleles; e.g. 'Petit Ribier' and '34-22' (**Figures 1B** and **2**; **Table 1**).

According to the methodology proposed by Khadari et al. (2003), a total of 63 varieties were validated as reference varieties by checking the morphological traits of olive stones and SSR profiles of several trees originating from different nurseries and orchards (**Table 1**). For instance, six trees of the 'Cailletier' variety from distinct origins were analyzed to define the reference genotype (Moutier et al., 2004). Similarly, a total of 15 and 18 trees from different nurseries and orchards were analyzed to validate the reference genotypes of the 'Petit Ribier' and 'Négrette' varieties, respectively (Moutier et al., 2004; Moutier et al., 2011). The remaining 30 accessions, classified by tree coordinates in the germplasm collection, are currently being validated to determine the reference genotype of each variety according to the methodology described here (**Table 1**).

Nuclear and Plastid DNA Polymorphism

Considering the 92 genotypes of the FOGB, a total of 191 alleles were revealed with an average of 9.55 alleles/locus (**Table 2**). Among the 191 alleles detected, 42 (22%) were observed

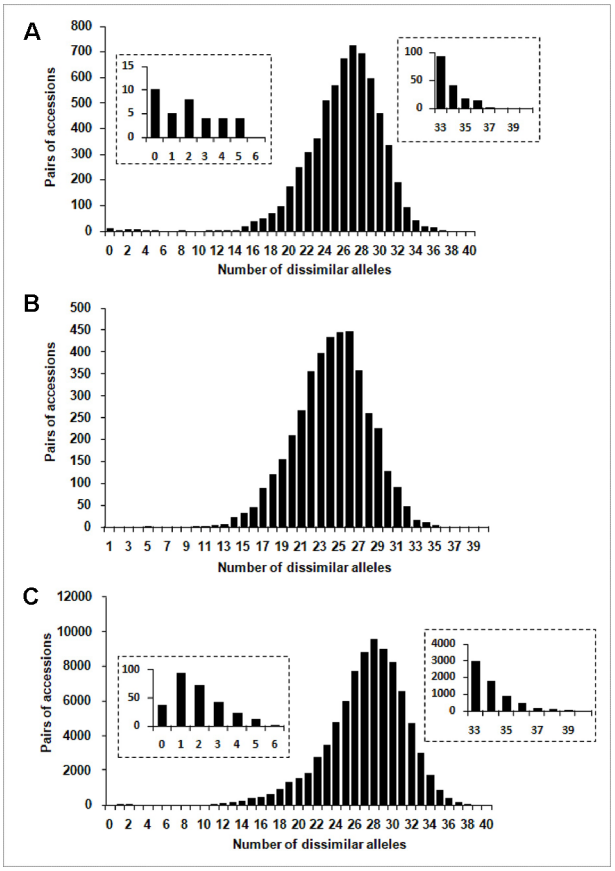

FIGURE 1 | Distribution of the number of dissimilar alleles for all pairwise comparisons for: **(A)** the 113 accessions in the FOGB collection, **(B)** the 92 French genotypes, and **(C)** the 416 accessions in the WOGB collection.

once. For each SSR locus, PIC values ranged from 0.296 at the GAPU71A locus to 0.856 at the DCA04 locus (mean 0.688). Only three out of the 20 loci used were able to discriminate between the 92 genotypes revealed among the 113 accessions analyzed, i.e. DCA04, DCA09, and GAPU101 (**Supplementary Table S3**).

The use of 39 chloroplastic loci revealed the presence of six chlorotypes in the French olive germplasm. As expected (see Besnard et al., 2013b), the most frequent chlorotype was E1.1 (79.4%). One of the five other haplotypes was detected once, i.e. E3.3 in the accession referred to as '36-28' (**Table 1**; **Figure 2**).

Comparison Between French and Mediterranean Olive Germplasm

Characterization and Pairwise Comparison Between the Two Germplasm Collections

Based on pairwise analysis of the WOGB with 20 nuclear loci, 404 single SSR profiles (min. 1 dissimilar allele) were identified among the 416 Mediterranean olive accessions. Among the 86320 pairwise comparisons, 36 were identical (0.04%), 166 (0.19%) were closely related (differing by one or two dissimilar alleles), whereas the remaining were distinguished by 3 to 40 dissimilar alleles (**Figure 1C**). Similar to the FOGB collection (see above), accessions showing identical profiles and those with one or two dissimilar alleles (molecular variants) were considered as belonging to the same genotype, leading to a total of 311 distinct genotypes among the 416 accessions analyzed (**Supplementary Table S1**).

Pairwise comparisons between the two collections revealed that eight French accessions were identical or closely related to 28 Mediterranean varieties (**Table 3**). Eighteen out of the 28 varieties originated from Italy, four from Lebanon, whereas the six remaining varieties were from Algeria (2), Spain (1), Cyprus (1), Greece (1), and Morocco (1).

SSR Polymorphism and Genetic Diversity

The 92 genotypes identified in the FOGB collection were used for comparison with the distinct WOGB genotypes. Among the 191 alleles revealed in the FOGB collection, 187 were present in the WOGB genotypes (339 alleles; **Table 2**). Only four alleles were detected in the French germplasm (**Table 2**); DCA04-172 in 'Amellau', DCA01-223 in 'Clermontaise', 'Lucques', 'Tripue', '35-31', and 'Rougette de Pignan', DCA09-175 in 'Clermontaise', and EMO03-204 in 'Rougette de Pignan'. Their presence was checked following a second genotyping.

A significant difference in allelic richness computed at a standardized G value of 92 individuals (Kruskal–Wallis test; P-value = 0.032; **Supplementary Table S4**) was observed between the FOGB and WOGB collections. However, the expected heterozygosity (*He*) between the two collections was not significantly different (Kruskal–Wallis test, P-value = 0.317). A similar pairwise genetic distance pattern [index of Smouse and Peakall (1999)] was observed in both FOGB and WOGB (**Figure 3**): ranging from 3 to 55 (with a mean of 29.01) in WGOB, and from 3 to 49 (mean of 27.36) in FOGB.

Genetic Structure

Admixture model-based Bayesian clustering was performed on both datasets, with a total of 395 distinct genotypes from both collections. According to ΔK and H', $K = 3$ was the most probable genetic structure model (ΔK = 554.11 and H' = 0.998; **Figure 4** and **Supplementary Figure S1**). Among the 92 French genotypes, 15, 8, and 1 were assigned, with a membership probability of $Q \geq 0.80$, to East, Central, and West gene pools, respectively; whereas, 68 (73.9%) genotypes were assigned to more than one group, with $Q < 0.80$ (**Table 1** and **Supplementary Table S6**).

A principal coordinate analysis (PCoA) was conducted and the findings were plotted according to genetic groups, as identified by the program. The first two principal axes explained 10.46% of the total genetic variance (**Figure 5**). French cultivars were classified within the main total diversity range observed in WOGB. The majority of French genotypes were classified in the Mosaic Mediterranean group ($Q < 0.80$; **Supplementary Table S6**).

Parentage Relationships Between French and Mediterranean Olive Cultivars

Relationship analyses were conducted using genotypes from the FOGB and WOGB collections with more than two dissimilar alleles. The eight genotypes of the WOGB detected

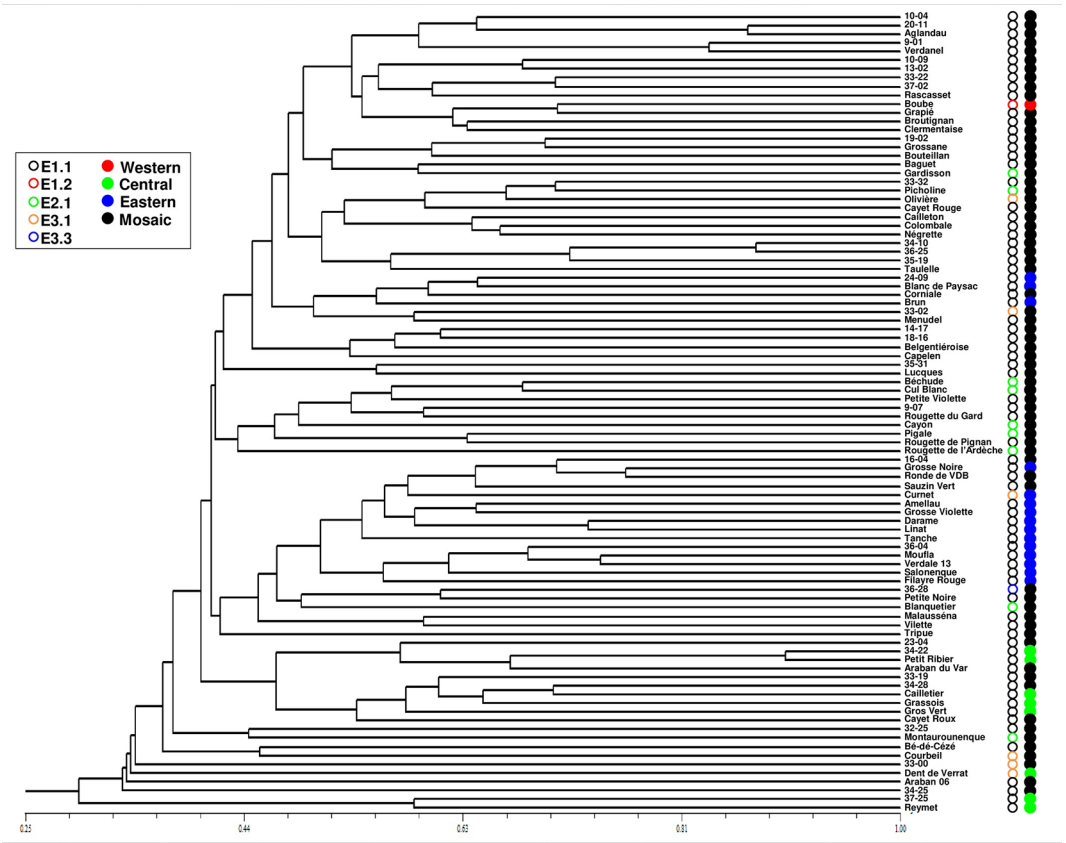

FIGURE 2 | Classification of the 92 genotypes identified among the 113 accessions in the FOGB collection using 20 SSR loci. Maternal lineage and assignment to each gene pool are indicated by circles. The closest genotypes are distinguished by five dissimilar alleles and most genotypes in the FOGB collection were shown as admixed and carrying the E1.1 plastid haplotype.

to be identical or genetically close to those of FOGB were also excluded (**Table 3**). Finally, 92 and 303 genotypes from FOGB and WOGB, respectively, were included in the analyses (**Table 1** and **Supplementary Table S1**).

Using the log-likelihood ratio (LOD) method, the LODc was estimated as the intersection between L_{rand} and L_{obs}. A threshold LOD at 4.22 allowed us to define the success rate in detecting true parent–offspring relationships at 97.7% (**Figure 6A**). We thus applied this value in parentage testing for the observed data. Otherwise, the exclusion-Bayes' theorem method indicated a posterior probability that any pair of genotypes shared at least one allele across all loci (no mismatching across all loci) by chance is Pr(Phi) = 0.00319, while it was 0.03547 for a false parent–offspring pair with a mismatch at one locus (**Figure 7**). Since we could not exclude the possibility that there might have been a few errors in our dataset (including somatic mutations and null alleles), we used the threshold <0.03547 as a cutoff for identifying putative parents.

The putative parent–offspring relationships with the highest probability were observed with the exclusion method (431 parent–offspring pairs), while the Bayesian and the LOD methods gave rise to the lowest number (368 and 239, respectively; **Supplementary Table S5**). The number of French genotypes with a putative parent–offspring relationship differed between methods: 81 genotypes for the Bayesian-based method, 75 for the exclusion method, and 68 for the LOD method.

For the French varieties, a total of 193 putative parent–offspring pairs were identified when validated by the three approaches. Among these, 101 were detected within the French germplasm since 51 French genotypes (55.4%) were found to have reliable parentage relationships with French varieties only (**Table 1** and **Supplementary Table S5**). Two French varieties showed a particularly high number of putative parent–offspring relationships, i.e. 'Boube' and 'Cailletier', with 36 and 24, respectively (**Figure 8**), but most of their parentage relationships were established with non-French varieties (30 and 18 putative parent–offspring pairs for 'Boube' and 'Cailletier', respectively). For other French varieties, the number of putative parent–offspring relationships varied from one to six within the French germplasm, and from one to four between French and other Mediterranean varieties (**Table 1** and **Supplementary Table S5**).

Most parent–offspring relationships identified belonged to the same genetic group (**Figure 9** and **Supplementary Figure S2**; **Table 4**). Varieties from 11 countries, except Cyprus, Egypt, and Lebanon, showed at least one putative parent–offspring relationship with a French variety. When comparing the origins of these cultivars, we found that varieties from France, Italy, and

TABLE 3 | Cases of genetically similar or close varieties found in the identification process between the FOGB and the WOGB based on 20 SSR loci.

	French variety (FOGB)	Mediterranean variety (WOGB)	Number of dissimilar alleles	Origin
1	#Boube	Gordal Sevillana$	2	Spain
		Santa Caterina	2	Italy
		Aguenaou	2	Algeria
2	#Cailletier	Arancino*	1	Italy
		Augellina*	1	Italy
		Correggiolo di pallesse*	1	Italy
		Frantoio*$	1	Italy
		Larcianese*	1	Italy
		Razzo*	1	Italy
		Puntino*	1	Italy
		San Lazzaro	2	Italy
		Baladi Ain	1	Lebanon
		Jlot	2	Lebanon
		BaladiTawil*	1	Lebanon
		Fakhfoukha	2	Morocco
3	#Petit Ribier	Filare	2	Italy
		Moraiolo$	1	Italy
		Tondello	2	Italy
		Alethriko	2	Cyprus
4	Cayon	Rougette de Mitidja	0	Algeria
5	Olivière	Kalokerida	0	Creece
6	Picholine	AbouChawkeh	0	Lebanon
7	Reymet	Ciliegino*	1	Italy
		Rosino*	1	Italy
		Rossellino*	1	Italy
		Pesciatino*	1	Italy
8	#33-19	Leccino*$	2	Italy
		Gremignolo*	2	Italy

Accessions showed similar in WOGB collection.

#French variety similar to foreign one and the reference variety.

$The reference variety for the case of similarity between French and Foreign varieties.

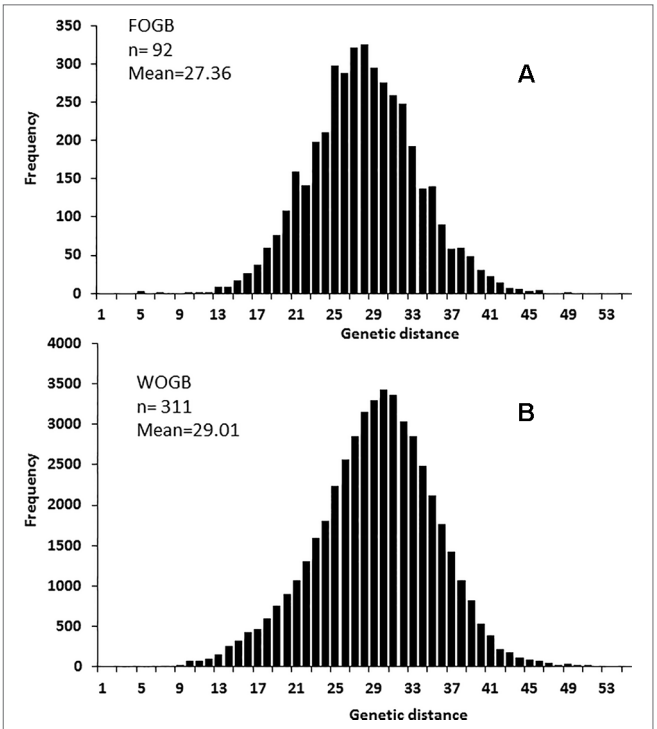

FIGURE 3 | Pairwise distribution of genetic distances using 20 SSR in: **(A)** the FOGB collection, and **(B)** the WOGB collection.

Spain had the highest proportion of parentage relationships (**Table 4**). Out of 115 Mediterranean cultivars, 51 (44.3%), 28 (24.3%), and 18 (15.6%) varieties, respectively, came from France, Italy, and Spain (**Table 4**). These results underline the importance of parentage relationships within the French germplasm and between French, Spanish, and Italian varieties.

Based on the 193 putative parent–offspring pairs, parentage relationships were examined by searching parental pairs with the likelihood approach. All varieties having at least one putative parent–offspring, as validated by at least one approach among the three used for a single parent search, were analyzed, including 86 French genotypes and 155 other Mediterranean varieties (**Supplementary Table S5**). A threshold LOD at 13.7 allowed us to define the success rate at 99.7% in detecting the most likely parental pair of the offspring based on the highest LOD score (**Figure 6B**). The French 'Boube' variety and the Spanish 'Lechin de Granada' variety were identified as the most likely parental pair for six Spanish varieties (**Table 5**; **Figure 10**): 'Negrillo de Iznalloz' was assigned with the highest LOD_{pp} value (23.6) and no allele mismatch, while the remaining most likely offspring were assigned at a LODpp ranging from 13.81 to 15.76, with an allele mismatch at one locus (**Table 5**). Moreover, the 'Boube' variety was identified as one of the most likely parents of the French '36_25' genotype, with a LODpp at 15.69 and one mismatch at locus DCA16 (**Table 5**), while the 'Lechin de Granada' variety was identified as the most likely parent of the 'Sevillano de Jumilla' variety, with no allele mismatch. The 'Boube' variety harbors the E1-2 maternal haplotype, and thus could not be the mother of the seven identified offspring that shared the E1-1 maternal haplotype. Surprisingly, we detected only one pair of parents involving the 'Cailletier' variety (**Table 5**), despite the high number of putative parent–offspring pairs detected using the single-parent search (24; **Supplementary Table S4**).

Sampling Varieties to Represent French Olive Genetic Diversity

A core collection was defined according to the two-step method proposed by El Bakkali et al. (2013b) (**Supplementary Figure S3**). Forty-three genotypes (46.7%) were necessary to capture the 191 alleles in the FOGB collection. Based on half of the initial sample size of 43 (23.9%), a primary core collection of 22 genotypes was constructed (CC_{22}; **Supplementary Table S7**). The 22 entries thus allowed the capture of 169 alleles (88.5%), three maternal haplotypes (18 E1-1, 1 E2-1, and 3 E3-1; 50%), and 17 reference varieties (**Supplementary Table S8**). This primary core collection (CC_{22}) was used as a kernel with MSTRAT to capture the remaining alleles. Hence, 43 entries (CC_{43}; 46.7%) were sufficient to capture the total diversity. 50 sets of 43 French varieties were generated using MSTRAT as the CC_{43} (**Supplementary Table S7**).

No differences were observed in the expected heterozygosity (*He*; Nei, 1987) in 50 independent runs. In addition to the 22 varieties used as a kernel, 18 varieties were found to be common in all of the 50 independent runs, while a combination of three

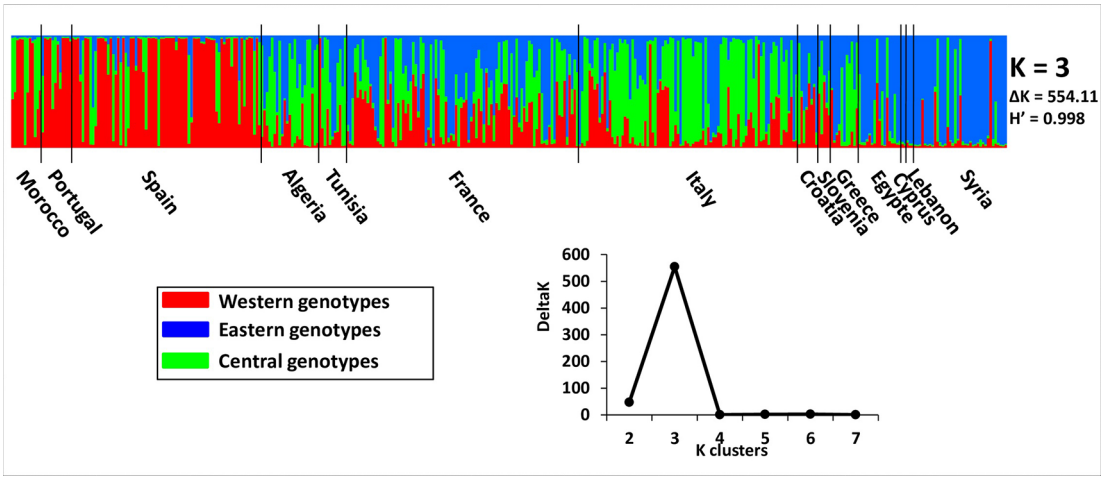

FIGURE 4 | The most probable genetic structure model using the program at $K = 3$ for 395 distinct genotypes from both collections. H' represents the similarity coefficient between runs for each K, and ΔK represents the *ad hoc* measure of Evanno et al. (2005).

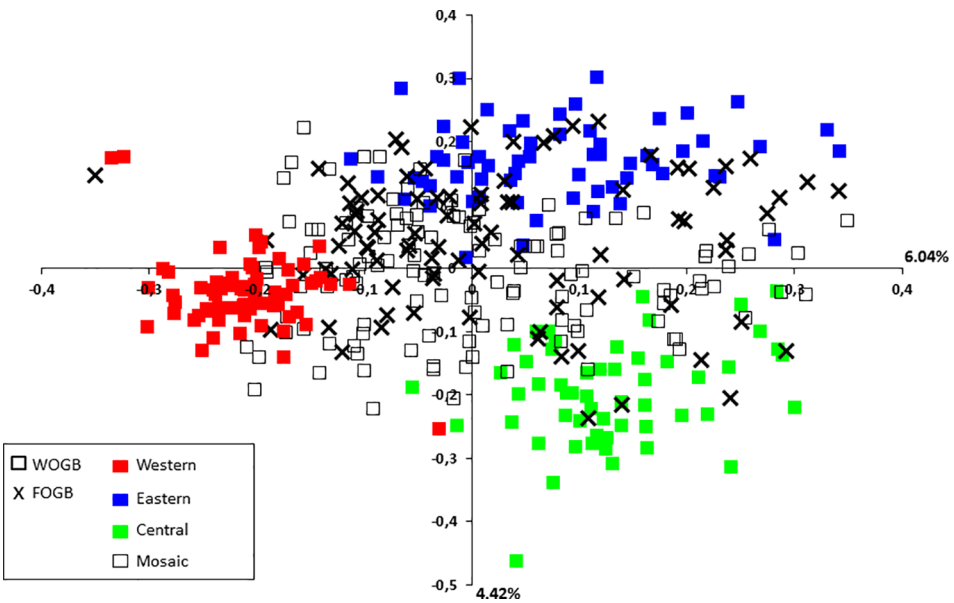

FIGURE 5 | Two-dimensional distribution of the principal coordinates analysis (PCoA) for the 395 distinct genotypes from both collections. Gene pools as identified by for genotypes of the WOGB collection are shown by different colors.

complement genotypes could be selected among a panel of seven genotypes to capture the total number of alleles (**Supplementary Table S7**). Among the 25 genotypes captured, 15 were validated as reference French varieties.

The French core collection CC_{43} was arbitrarily selected (**Supplementary Table S8**). Among the 43 entries sampled, only four *cpDNA* haplotypes were captured: E1.1 (34 individuals), E1.2 (1), E2.1 (4), and E3.1 (4; **Supplementary Table S8**). Moreover, 31 reference French varieties were selected among the 43 entries of CC_{43}. To select all reference varieties, the size was increased to 75 cultivars, which represented the third level of the French core collection (CC_{75}; **Supplementary Table S8**). Most of the varieties sampled in CC_{43} showed high admixture since 33 varieties (76.7%) belonged to more than one gene pool, while only six and four genotypes were assigned (with membership probabilities of $Q \geq 0.80$) to central and eastern gene pools, respectively (**Supplementary Table S8**). Genotypes selected for the primary core collection (CC_{22}) and for the core collection capturing all alleles (CC_{43}) had the lowest frequency of parentage relationships (8% and 22%, respectively; **Supplementary Table S8**). This pattern is in line with the findings obtained with the approach used to construct the core collection favoring genotypes without genetic relatedness.

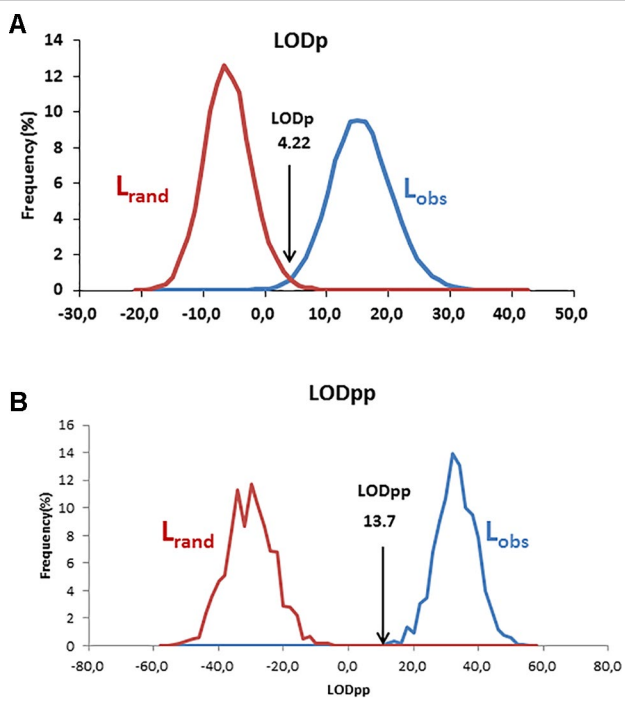

FIGURE 6 | Distribution and intersection between L_{obs} and L_{rand} using v1.0 macro software with the log-likelihood ratio (LOD) method using a single parent search **(A)** and paired parental search **(B)**.

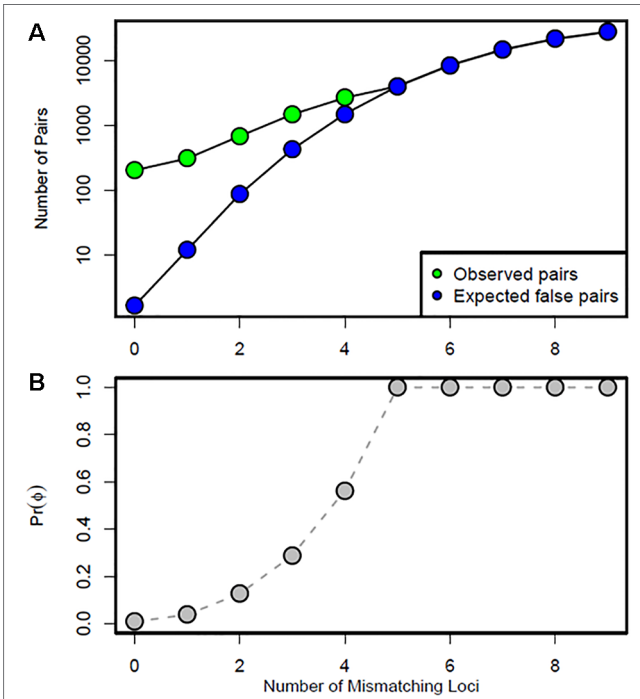

FIGURE 7 | Data simulation results: **(A)** number of observed putative (green points) and expected false (blue points) parent–offspring pairs in the test datasets, and **(B)** Bayesian prior probability Pr(Phi) according to the number of mismatching loci. Any pair that mismatched at one locus would have a 0.03547 probability of occurring by chance.

DISCUSSION

Our study first allowed us to generate a database for efficient identification of French varieties. We took advantage of this genetic characterization to investigate French olive genetic diversity and assess the importance of local genetic resources and their associated agroecosystems in the cultivated olive tree diversification process.

Diversification of French Olive Germplasm by Admixture

Primary selection and secondary diversification are two key processes in the history of olive domestication (Khadari and El Bakkali, 2018). Diversification can be viewed as a process that is driven mainly by farmer selection of trees harboring interesting traits. As this selection occurs within the agroecosystem, selected trees are most likely derived from crosses between varieties or previously selected clones, sometimes with pollen coming from feral or wild olive trees (for review, see Gaut et al., 2015; Besnard et al., 2018). Sociohistorical and ethnobiological investigations of traditional olive agroecosystems in northern Morocco have highlighted strong links between selected trees from clonally and seed propagated trees, indicating the continuing roles of cultivated, feral, and wild olive trees in the diversification process (Aumeeruddy-Thomas et al., 2017). Here we also showed an admixed origin of French varieties, suggesting a diversification process involving local and introduced genetic resources. Among the 92 French genotypes, 68 (73.9%) were admixed as they were assigned to more than one group with $Q < 0.80$. Most of them (82.6%) harbored the eastern maternal lineage [i.e. haplotypes E1-1 (73) and E1-2 (3)] originating from the eastern Mediterranean Basin, and it was introduced in the westernmost regions *via* the diffusion of oleiculture (Besnard et al., 2013b).

As previously suggested by several authors (Besnard et al., 2001a; Baldoni et al., 2006; Belaj et al., 2007; Breton et al., 2008; Besnard et al., 2013a; Diez et al., 2015), in our following arguments we assumed that the French olive germplasm was mainly derived from a diversification process involving local genetic resources, in addition to the introduction of cultivated olives belonging mainly to the Q2 genepool (central Mediterranean), as well as the Q1 genepool (western Mediterranean). First, we observed a clear genetic pattern derived from admixture germplasm from the central Mediterranean area, including French local genetic resources, as previously reported by Haouane et al. (2011); Diez et al. (2012), and El Bakkali et al. (2013a). Second, these local genetic resources harbored a maternal lineage from the eastern primary domestication center (Besnard et al., 2013b). Third, despite the reduction in allelic diversity (22.4%) as compared to Mediterranean cultivated olive, the French germplasm showed a similar expected heterozygosity and pairwise genetic distance pattern compared to Mediterranean olive germplasm, indicating that admixture was likely a consequence of this pattern. Fourth, we highlighted that approximately half of the *ex situ* collection of Porquerolles (46.7%) was necessary to capture all of the French diversity, which was mainly classified in the mosaic Mediterranean group. Finally, we observed substantial parentage relationships (parent–offspring) at a local scale within

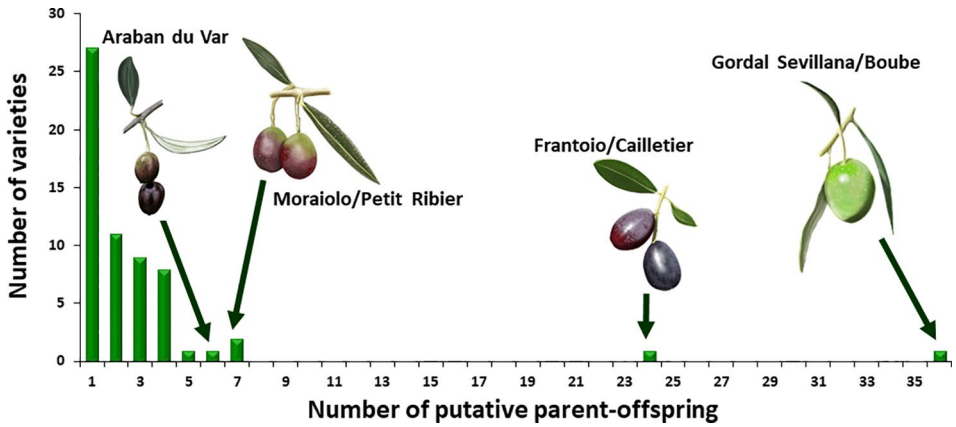

FIGURE 8 | Histogram of the number of putative parents-offsprings observed for French varieties.

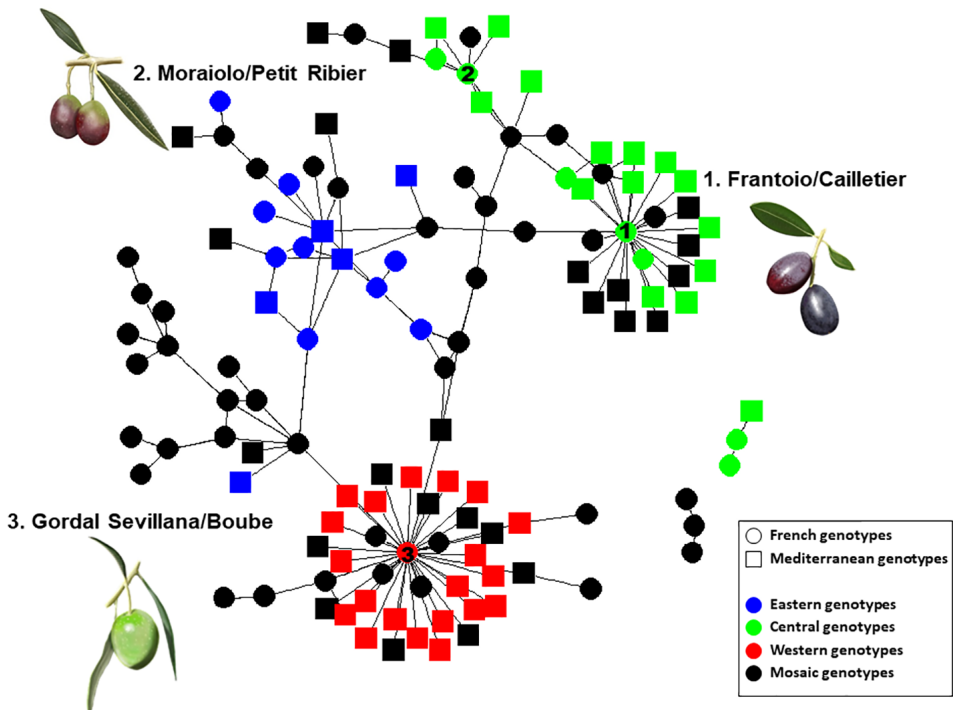

FIGURE 9 | Network of French and Mediterranean varieties showing parentage relationships according to different gene pools as identified by the program.

French varieties and at a regional scale between French, Italian, or Spanish varieties, indicating that selection from crossing between varieties was likely a key varietal diversification process within French agroecosystems and neighboring regions.

French Agroecosystems as a Bridge Between Italy and Spain for Olive Diversification

Identical and nearly identical genotypes were identified among French and other Mediterranean germplasm. This is evidence in favor of the translocation of varieties between distant regions (e.g. Besnard et al., 2001b; Haouane et al., 2011; Trujillo et al., 2014). Interestingly, we report for the first time the high genetic similarity between 'Cailletier', a major French variety, and the Italian 'Frantoio' variety. These two genotypes were here distinguished by only one allele on the reference genotype of each variety and may have represented distinct clones propagated from a single genotype (e.g. due to clonal selection; Bellini et al., 2008). A similar pattern was noted for the French 'Petit Ribier' variety and the Italian 'Moraiolo', variety as previously observed by Pinatel (2015) in a study using morphological descriptors.

TABLE 4 | Numbers and proportion of varieties per countries showing parent–offspring relationships, and their assignment to different gene pools.

Country	Number of genotypes	Number of varieties with relationships (%)	Number of relatives (%)	Number of genotypes assigned to each gene pool (%)			
				West	Center	East	Mosaic
France[1]	92	61 (66.3)	193	1 (1.6)	7 (11.5)	9 (14.8)	44 (72.1)
Morocco[2]	12	1 (8.3)	1 (0.5)	1 (100.0)			
Portugal[2]	12	2 (16.7)	2 (1.0)	2 (100.0)			
Spain[2]	75	18 (24.0)	21 (10.9)	15 (83.3)			3 (16.7)
Algeria[2]	24	3 (12.5)	3 (1.6)				3 (100.0)
France[2]	92	51 (55.4)	101 (52.3)	1 (2.0)	7 (13.7)	4 (7.8)	39 (76.5)
Tunisia[2]	11	1 (9.1)	1 (0.5)	1 (100.0)			
Italy[2]	92	28 (30.4)	42 (21.8)		12 (42.9)	3 (10.7)	13 (46.4)
Croatia[2]	8	3 (37.5)	5 (2.6)		1 (33.3)		2 (66.7)
Slovenia[2]	5	2 (40.0)	2 (1.0)		1 (50.0)		1 (50.0)
Greece[2]	12	1 (8.3)	1 (0.5)				1 (100.0)
Egypte[2]	17						
Cyprus[2]	2						
Lebanon[2]	4						
Syria[2]	37	5 (13.5)	14 (7.3)	1 (20.0)	1 (20.0)	2 (40.0)	1 (20.0)
Total[2]	**395[3]**	**115 (29.1)**	**193 (100.0)**	**21 (18.3)**	**22 (19.1)**	**9 (7.8)**	**63 (54.8)**

[1]Varieties identified as putative offspring.

[2]Varieties identified as putative parents.

[3]Eight genotypes were similar or genetically close between FOGB and WOGBM collections.

TABLE 5 | The most likely parental pairs of 10 varieties including Cailletier and two French genotypes based on the highest LODpp.

Cultivar name	N° Accession	Country	Assignation Q>0.8	Maternal lineage	LODpp	Incompatible markers	Putative pair parents	N° Accession	Country	Assignation Q > 0.8	Maternal lineage
Negrillo de Iznalloz	352	Spain	Western	E 1-1	23.6		Lechin de Granada	340	Spain	Western	E 1-1
							Boube	36_11	France	Western	E 1-2
Morisca	245	Spain	Western	E 1-1	15.756	DCA18	Lechin de Granada	340	Spain	Western	E 1-1
							Boube	36_11	France	Western	E 1-2
Machorron	247	Spain	Western	E 1-1	15.43	DCA9	Lechin de Granada	340	Spain	Western	E 1-1
							Boube	36_11	France	Western	E 1-2
Carrasqueño de Alcaudete	225	Spain	Western	E 1-1	14.495	DCA16	Lechin de Granada	340	Spain	Western	E 1-1
							Boube	36_11	France	Western	E 1-2
Mollar de cieza	348	Spain	Western	E 1-1	14.222	DCA18	Lechin de Granada	340	Spain	Western	E 1-1
							Boube	36_11	France	Western	E 1-2
Cañivano Negro	224	Spain	Western	E 1-1	13.812	DCA18	Lechin de Granada	340	Spain	Western	E 1-1
							Boube	36_11	France	Western	E 1-2
36_25	36_25	France	Mosaic	E 1-1	15.695	DCA16	34_10	34_10	France	Mosaic	E 1-1
							Boube	36_11	France	Western	E 1-2
Sevillano de Jumilla	272	Spain	Western	E 1-1	17.316		Lechin de Granada	340	Spain	Western	E 1-1
							Amargoso	219	Spain	Mosaic	E 1-1
9_01	9_01	France	Mosaic	E 1-1	20.634	GAPU103	Verdanel	10_1	France	Mosaic	E 1-1
							37_02	37_02	France	Mosaic	E 1-1
Cailletier	32_33	France	Central	E 1-1	28.831	DCA9	Cima di Melfi	92	Italy	Central	E 1-1
							Karme	640	Syria	Central	E 1-1

Maternal lineage, inferred ancestry (Q) among clusters at K = 3 for each genotype and LODpp values are indicated.

Both 'Cailletier' and 'Petit Ribier' varieties are mainly cultivated in southeastern France (Var, Alpes de Haute Provence and Alpes Maritimes), while 'Frantoio' and 'Moraiolo' are notably cultivated in Tuscany (Italy). These two varieties are also known to have been introduced in Corsica from Italy under the polyclonal denomination 'Ghermana' (Besnard et al., 2001b; Bronzini de Caraffa et al., 2002). Otherwise, the local French 'Boube' variety was found to be genetically similar to that of the oldest Spanish variety, i.e. 'Gordal Sevillana', and it was the only French variety clearly assigned to the western genepool (Q1). Pinatel (2015)

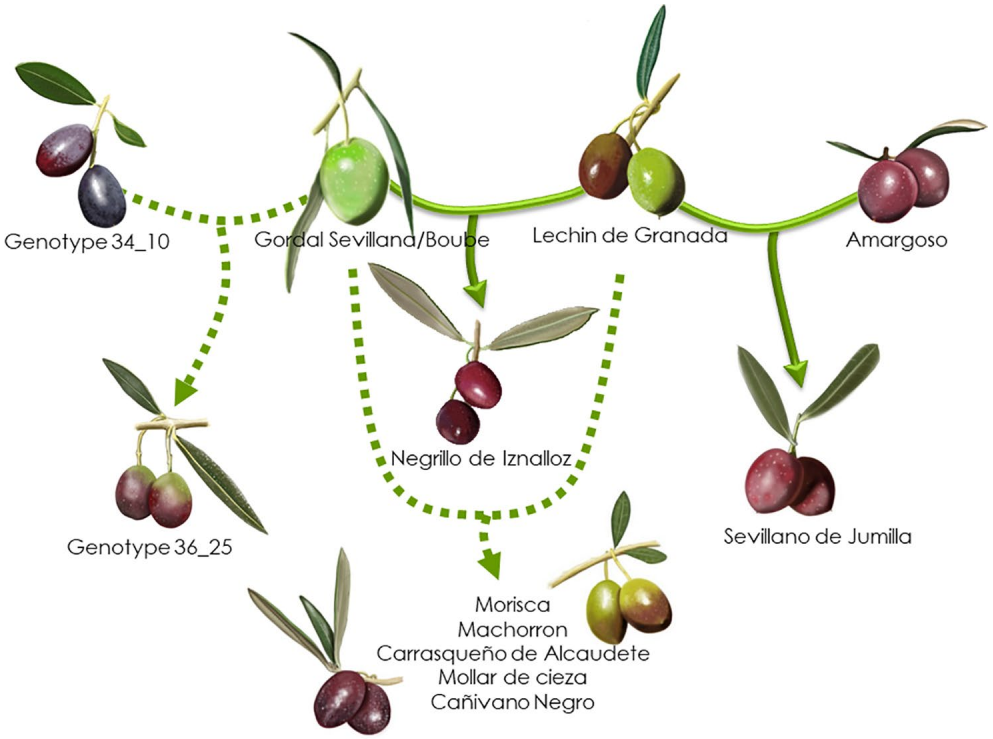

FIGURE 10 | Parentage relationships of French varieties based on the likelihood approach. The parentage relationships are illustrated with the highest LOD_{pp} value and no allele mismatch (full line) or with an allele mismatch at one locus (dashed line).

considered 'Boube' as a local variety (only present in three distant orchards in Alpes de Haute Provence, with a single centennial tree per orchard) that was probably cultivated in southern France in ancient times. Here our results suggest that the variety was probably introduced from the Iberian Peninsula due to the large olive fruit size. Its past importance in the western Mediterranean Basin needs to be reviewed as it was spread over broad areas (at least from Andalusia to southeastern France) and then was involved in varietal diversification, particularly in Spain, but also elsewhere (Diez et al., 2015).

Beyond the substantial parentage relationships within the French germplasm (53.89%), we clearly identified relationships (parent–offspring) between French and Italian varieties, as well as French and Spanish varieties, mainly based on 'Cailletier'/'Frantoio' and 'Boube'/'Gordal Sevillana' varieties, since they harbored the highest number of putative parent–offspring pairs (24 and 36, respectively). Interestingly, the 'Cailletier'/'Frantoio' variety assigned to the central cluster had robust relationships (parent–offspring) with varieties from Italy which belonged to the same cluster, as well as the 'Petit Ribier'/'Morailo' variety, while the 'Boube' variety displayed parentage relationships from Spanish germplasm. We observed that 'Cailletier'/'Frantoio' and 'Petit Ribier'/'Morailo' were the main progenitors of Italian/French varieties, while 'Boube'/'Gordal Sevillana' was the main progenitor of Spanish/French varieties. As previously reported by Diez et al. (2015), we confirmed that 'Gordal Sevillana' was one of the main progenitors of Spanish germplasm, but strikingly we found that it was likely the male parent of six French varieties, i.e. 'Clermontaise' and 'Courbeil', which are cultivated in southwestern area (Hérault and Pyrénées Orientales; Moutier et al., 2004) bordering northeastern Spain (Catalonia). This Spanish variety was considered by Diez et al. (2015) as being one of the main founders of the western genepool (Q1), and based on our results we hypothesize that it was also the founder of part of the French germplasm assigned to the Mosaic genetic group. In addition, we noted for the first time that 'Frantoio' and 'Morailo' were putative progenitors of numerous Italian and French varieties. This result also suggests that these two varieties have been major progenitors within the Central Mediterranean group (Q2).

French Olive Agroecosystems as Varietal Diversification Incubators

Surprisingly, despite the limited French olive growing area (southern continental France and Corsica), we identified a high number of varieties in the *ex situ* collection of Porquerolles, including a panel of at least 30 currently cultivated varieties (Moutier et al., 2004; Moutier et al., 2011). French olive growing is still mainly founded on a traditional system involving a diverse range of crops and varieties (Pinatel, 2015). This could be viewed as a key factor favoring varietal diversity, as previously noted by several authors (Gemas et al., 2004; Khadari et al., 2008; Kaya et al., 2013; Marra et al., 2013; Las Casas et al., 2014; Xanthopoulou et al., 2014).

Here, we assumed that the French varietal diversity could mainly be explained by active farmer selection, probably due to the impact of relatively frequent climatic accidents on local germplasm. Indeed, French olives are cultivated along the northern rim of the olive growing area where frost events are frequent—the last major one, in 1956, caused substantial damage in olive orchards, thus negatively impacting the socioeconomic sector (Pinatel, 2015). Moreover, we report for the first time that French genetic resources displayed substantial parentage relationships involving both local and foreign varieties (55 and 60, respectively), with more than half of the parent–offspring pairs occurring in local French germplasm (53.89%; **Table 1**). A similar pattern was observed in the western group (Q1 cluster), where the average number of first-degree relationships (full siblings or parent–offspring) was 16.25, while it was 2.0 in the Q2 (central Mediterranean) and Q3 (eastern Mediterranean) genetic clusters (Diez et al., 2015). Similarly, in grapevine, selection *via* crossing was previously identified by investigating the parentage relationships of 'Chardonnay', 'Gamay', and other wine grapes grown in northeastern France (Bowers et al., 1999). In their extended parentage analysis of the INRA grape germplasm repository (France; 2,344 unique genotypes), Lacombe et al. (2013) identified the full parentage of 828 cultivars including 447 traditional cultivars, which are likely derived from farmer selection in traditional agroecosystems. These processes have been reported in other perennial fruit cropping systems such as apricot, which is seed-propagated in oasis agroecosystems in the southern Maghreb region (Bourguiba et al., 2012; Bourguiba et al., 2013). Since the second half of 20th century, so-called "modern" perennial fruit cropping systems were managed with a single variety using agronomic practices that fostered yield improvement. They gradually replaced traditional agroecosystems which were based on higher diversity of crops and varieties than modern systems. Such diversified agroecosystems may still be found in mountainous areas around the Mediterranean Basin, as described, for instance, by Aumeeruddy-Thomas et al. (2017) in North Morocco. In southern France where olive and grapevine are often cultivated in the same locations, the olive varieties identified in the present study were mainly derived from crosses between local and foreign genetic resources, as we revealed by the parentage analysis.

CONCLUSION

Our results provide a clear picture regarding the importance of farmer selection in the olive varietal diversification process in traditional French agroecosystems. Indeed, we observed substantial parentage relationships within French olive germplasm and the proportion of parent–offspring pairs was still high (45.08% out the 193 putative parent–offspring pairs), even when not considering the Italian 'Frantoio' variety or the Spanish 'Gordal Sevillana' variety. Otherwise, we observed a pattern of parentage relationships from crossing: (*i*) between French and Spanish varieties within agroecosystems in southwestern France, especially in the Pyrénées Orientales area, and (*ii*) between French and Italian varieties in the southeastern France, particularly in the Alpes Maritimes area. We thus argue in favor of active farmer selection founded mainly on local French varieties, probably due to frequent climatic accidents such as frost. When examining diversification processes at the regional scale in all southern European countries, we consider that French agroecosystems are incubators for olive diversification and serve as a bridge between Italy and Spain (Khadari et al., 2003), thus highlighting the importance of diversification as one of the two key processes in the history of olive domestication (Khadari and El Bakkali, 2018).

DATA AVAILABILITY STATEMENT

All datasets for this study are included in the article/ **Supplementary Material**.

AUTHOR CONTRIBUTIONS

BK designed the research and wrote the manuscript with AEB and GB. AEB, LE, and CT performed microsatellite genotyping. BK and CP checked the reference list of French varieties. BK and AEB performed the data analysis. BK, AEB, and GB interpreted the data analysis. All co-authors participated in approving the final manuscript.

FUNDING

This work was conducted at the AGAP research unit and supported by the OliveMed/Agropolis Fondation N° 1202-066 project through the Investissements d'avenir/Labex Agro ANR-10-Labex-0001-01 managed by the French National Research Agency (ANR). GB was also supported by the LABEX TULIP (ANR-10-LABX-0041) and CEBA (ANR-10-LABX-25-01).

ACKNOWLEDGMENTS

We thank Sylvia Lochon-Menseau, Bruno Bernazeau, Daniel Bielmann (CBNMed collection Porquerolles), Hayat Zaher, Lhassane Sikaoui, and Abdelmajid Moukhli (WOGB of Marrakech) for their management of *ex situ* collections; Ronan Rivalon, Pierre Mournet, and Sylvain Santoni for laboratory assistance; Franck Curk for the olive fruit illustration in the figures and for his comments on the final draft of the manuscript.

SUPPLEMENTARY MATERIAL

The Supplementary Material for this article can be found online at: https://www.frontiersin.org/articles/10.3389/fpls.2019.01593/full#supplementary-material

TABLE S1 | List of accessions from the WOGB and FOGB collections (529 accessions); 416 and 113, respectively. Accessions are classified according to origin, maternal lineage, inferred ancestry (Q) among clusters at $K = 3$, and SSR code (code for our genotyping analyses). French cultivars showing relationships with other cultivars are indicated.

TABLE S2 | List of French varieties with genetically close SSR profiles which are distinct by one or two dissimilar alleles and considered as somatic mutations.

TABLE S3 | Optimal loci combination to discriminate the 92 French genotypes identified among the 113 accessions.

TABLE S4 | Comparison of allelic richness between the FOGB and WOGB collections. *Na* = Number of alleles; *Ar* = allelic richness.

TABLE S5 | List of French genotypes showing putative parent relationships with other genotypes using three approaches; the exclusion (mismatch marker), the log-likelihood ratio (LODp) and the exclusion-Bayes' theorem. Maternal lineage and inferred ancestry (Q) among clusters at $K = 3$ are indicated for each genotype, as well as results for each parentage approach.

TABLE S6 | Number and proportion of genotypes from different countries assigned to each of the three gene pools identified by under the assignation probability of $Q \geq 0.8$.

TABLE S7 | List of different nested French core collections with different sample sizes (CC_{22}, CC_{43}, and CC_{75}). (x) Corresponds to the presence of the accession in each core collection. Twenty-two varieties (CC_{22}) were sampled by the CoreHunter program when optimizing the Shannon and Weaver index "*Sh strategy*". CC_{22} was then used as a kernel in the Mstrat program to reconstruct the extended core collections: 43 varieties (CC_{43}) allowed us to capture all of the observed alleles, and 75 varieties (CC_{75}) included the remaining reference varieties not sampled in CC_{43}.

TABLE S8 | Description of different nested core collections constructed from the FOGB collection.

FIGURE S1 | Optimal number of clusters using the program and inferred population structure from $K = 2$ to $K = 4$ for 395 distinct genotypes from both collections. H' represents the similarity coefficient between runs for each K, and ΔK represents the *ad hoc* measure of Evanno et al. (2005).

FIGURE S2 | A network of French and Mediterranean varieties showing parentage relationships according to the genetic structure of varieties. Names of varieties and their assignment to different gene pools are indicated.

FIGURE S3 | Sampling efficiency based on the ability to capture the genetic diversity *via* the M-strategy (M-method) compared to a random strategy.

REFERENCES

Aumeeruddy-Thomas, Y., Moukhli, A., Haouane, H., and Khadari, B. (2017). Ongoing domestication and diversification in grafted olive–oleaster agroecosystems in Northern Morocco. *Reg. Environ. Change* 17, 1315–1328. doi: 10.1007/s10113-017-1143-3

Baldoni, L., Tosti, N., Ricciolini, C., Belaj, A., Arcioni, S., Pannelli, G., et al. (2006). Genetic structure of wild and cultivated olives in the central Mediterranean basin. *Ann. Bot.* 98, 935–942. doi: 10.1093/aob/mc1178

Belaj, A., Satovic, Z., Rallo, L., and Trujillo, I. (2002). Genetic diversity and relationships in olive (*Olea europaea* L.) germplasm collections as determined by randomly amplified polymorphic DNA. *Theor. Appl. Genet.* 105, 638–644. doi: 10.1007/s00122-002-0981-6

Belaj, A., Muñoz-Diez, C., Baldoni, L., Porceddu, A., Barranco, D., and Satovic, Z. (2007). Genetic diversity and population structure of wild olives from the north-western Mediterranean assessed by SSR markers. *Ann. Bot.* 100, 449–458. doi: 10.1093/aob/mcm132

Belaj, A., del Carmen Dominguez-García, M., Atienza, S. G., Urdiroz, N. M., de la Rosa, R., Satovic, Z., et al. (2012). Developing a core collection of olive (*Olea europaea* L.) based on molecular markers (DArTs, SSRs, SNPs), and agronomic traits. *Tree Genet. Genomes* 8, 365–378. doi: 10.1007/s11295-011-0447-6

Bellini, E., Giordani, E., and Rosati, A. (2008). Genetic improvement of olive from clonal selection to cross-breeding programs. *Adv. Hort. Sci.* 22, 73–86. doi: 10.1400/94380

Besnard, G., Baradat, P., Breton, C., Khadari, B., and Bervillé, A. (2001a). Olive domestication from structure of oleasters and cultivars using nuclear RAPDs and mitochondrial RFLPs. *Genet. Sel. Evol.* 33, S251–S268. doi: 10.1186/BF03500883

Besnard, G., Breton, C., Baradat, P., Khadari, B., and Bervillé, A. (2001b). Cultivar identification in olive based on RAPD markers. *J. Am. Soc. Hort. Sci.* 126, 668–675. doi: 10.21273/JASHS.126.6.668

Besnard, G., Hernandez, P., Khadari, B., Dorado, G., and Savolainen, V. (2011). Genomic profiling of plastid DNA variation in the Mediterranean olive tree. *BMC Plant Biol.* 11, 80. doi: 10.1186/1471-2229-11-80

Besnard, G., El Bakkali, A., Haouane, H., Baali-Cherif, D., Moukhli, A., and Khadari, B. (2013a). Population genetics of Mediterranean and Saharan olives: geographic patterns of differentiation and evidence for early generations of admixture. *Ann. Bot.* 112, 1293–1302. doi: 10.1093/aob/mct196

Besnard, G., Khadari, B., Navascués, M., Fernandez-Mazuecos, M., El Bakkali, A., Arrigo, N., et al. (2013b). The complex history of the olive tree: from Late Quaternary diversification of Mediterranean lineages to primary domestication in the northern Levant. *Proc. Biol. Sci.* 280, 20122833. doi: 10.1098/rspb.2012.2833

Besnard, G., Terral, J.-F., and Cornille, A. (2018). On the origins and domestication of the olive: a review and perspectives. *Ann. Bot.* 121, 385–403. doi: 10.1093/aob/mcx145

Bourguiba, H., Audergon, J. M., Krichen, L., Trifi-Farah, N., Mamouni, A., Trabelsi, S., et al. (2012). Loss of genetic diversity as a signature of apricot domestication and diffusion into the Mediterranean Basin. *BMC Plant Biol.* 12, 49. doi: 10.1186/1471-2229-12-49

Bourguiba, H., Khadari, B., Krichen, L., Trifi-Farah, N., Mamouni, A., Trabelsi, S., et al. (2013). Genetic relationships between local North African apricot (*Prunus armeniaca* L.) germplasm and recently introduced varieties. *Sci. Hort.* 152, 61–69. doi: 10.1016/j.scienta.2013.01.012

Bowers, J. E., Boursiquot, J. M., This, P., Chu, K., Johansson, H., and Meredith, C. (1999). Historical genetics: the parentage of Chardonnay, Gamay, and other wine grapes of Northeastern France. *Science* 285, 1562–1565. doi: 10.1126/science.285.5433.1562

Breton, C., Pinatel, C., Médail, F., Bonhomme, F., and Bervillé, A. (2008). Comparison between classical and Bayesian methods to investigate the history of olive cultivars using SSR-polymorphisms. *Plant Sci.* 173, 524–532. doi: 10.1016/j.plantsci.2008.05.025

Bronzini de Caraffa, V., Maury, J., de Rocca Serra, D., and Giannettini, J. (2002). Genetic characterization of olive tree (*Olea europaea* L.) intended for oil production in Corsica. *Acta Hort.* 586, 163–166. doi: 10.17660/ActaHortic.2002.586.27

Carriero, F., Fontanazza, G., Cellini, F. and Giorio, G. (2002). Identification of simple sequence repeats (SSRs) in olive (Olea europaea L.). *Theor. Appl. Genet.* 104 (2–3), 301–307. doi: 10.1007/s001220100691

Christie, M. R., Tennessen, J. A., and Blouin, M. S. (2013). Bayesian parentage analysis with systematic accountability of genotyping error, missing data and false matching. *Bioinformatics* 29, 725–732. doi: 10.1093/bioinformatics/btt039

Christie, M. R. (2010). Parentage in natural populations: novel methods to detect parent–offspring pairs in large data sets. *Mol. Ecol. Resour.* 10, 115–128. doi: 10.1111/j.1755-0998.2009.02687.x

Cipriani, G., Marrazzo, M. T., Marconi, R. and Cimato, A., Testolin, R. (2002). Microsatellite markers isolated in olive (*Olea europaea L.*) are suitable for individual fingerprinting and reveal polymorphism within ancient cultivars. *Theor. Appl. Genet.* 104 (2-3), 223–228. doi: 10.1007/s001220100685

Csardi, G., and Nepusz, T. (2006). The igraph software package for complex network research. *Inter. J. Complex Syst.*, 1695 (5), 1–9.

De La Rosa, R., James, C. M. and Tobutt, K. R. (2002). Isolation and characterization of polymorphic microsatellites in olive (Olea europaea L.) and their

transferability to other genera in the Oleaceae. *Mol. Ecol. Notes* 2 (3), 265–267. doi: 10.1046/j.1471-8286.2002.00217.x

De Ollas, C., Morillón, R., Fotopoulos, V., Puértolas, J., Ollitrault, P., Gómez-Cadenas, A., et al. (2019). Facing climate change: biotechnology of iconic Mediterranean woody crops. *Front. Plant Sci.* 10, 427. doi: 10.3389/fpls.2019.00427

Dice, L. R. (1945). Measures of the amount of ecologic association between species. *Ecology* 26, 297–302. doi: 10.2307/1932409

Diez, C. M., Imperato, A., Rallo, L., Baranco, D., and Trujillo, I. (2012). Worldwide core collection of olive cultivars based on simple sequence repeat and morphological markers. *Crop Sci.* 52, 211–221. doi: 10.2135/cropsci2011.02.0110

Diez, C. M., Trujillo, I., Martinez-Urdiroz, N., Barranco, D., Rallo, L., Marfil, P., et al. (2015). Olive domestication and diversification in the Mediterranean Basin. *New Phytol.* 206, 436–447. doi: 10.1111/nph.13181

El Bakkali, A., Haouane, H., Hadidou, A., Oukabli, A., Santoni, S., Udupa, S. M., et al. (2013a). Genetic diversity of on-farm selected olive trees in Moroccan traditional olive orchards. *Plant Genet. Resour.* 11, 87–105. doi: 10.1017/S1479262112000445

El Bakkali, A., Haouane, H., Moukhli, A., Van Damme, P., Costes, E., and Khadari, B. (2013b). Construction of core collections suitable for association mapping to optimize use of Mediterranean olive (*Olea europaea* L.) genetic resources. *PLoS One* 8, e61263. doi: 10.1371/journal.pone.0061263

Evanno, G., Regnaut, S., and Goudet, J. (2005). Detecting the number of clusters of individuals using the software , a simulation study. *Mol. Ecol.* 14, 2611–2620. doi: 10.1111/j.1365-294X.2005.02553.x

Gaut, B. S., Diez, C. M., and Morrell, P. L. (2015). Genomics and the contrasting dynamics of annuals and perennial domestication. *Trends Genet.* 31, 709–719. doi: 10.1016/j.tig.2015.10.002

Gemas, V. J. V., Almadanim, M. C., Tenreiro, R., Martins., A., and Fevereiro, P. (2004). Genetic diversity in the Olive tree (*Olea europaea* L. subsp. *europaea*) cultivated in Portugal revealed by RAPD and ISSR markers. *Genet. Resourc. Crop Evol.* 51, 501–511. doi: 10.1023/B:GRES.0000024152.16021.40

Gerber, S., Mariette, S., Streiff, R., Bodénès, R., and Kremer, A. (2000). Comparison of microsatellites and AFLP markers for parentage analysis. *Mol. Ecol.* 9, 1037–1048. doi: 10.1046/j.1365-294x.2000.00961.x

Gouesnard, B., Bataillon, T. M., Decoux, G., Rozale, C., Schoen, D. J., and David, J. L. (2001). *MSTRAT* An algorithm for building germplasm core collections by maximizing allelic or phenotypic richness. *J. Hered.* 92, 93–94. doi: 10.1093/jhered/92.1.93

Haouane, H., El Bakkali, A., Moukhli, A., Tollon, C., Santoni, S., Oukabli, A., et al. (2011). Genetic structure and core collection of the World Olive Germplasm Bank of Marrakech: towards the optimised management and use of Mediterranean olive genetic resources. *Genetica* 139, 1083–1094. doi: 10.1007/s10709-011-9608-7

Jakobsson, M., and Rosenberg, N. A. (2007). CLUMPP: a cluster matching and permutation program for dealing with label switching and multimodality in analysis of population structure. *Bioinformatics* 23, 1801–1806. doi: 10.1093/bioinformatics/btm233

Jones, A. G., Small, C. M., Paczolt, K. A., and Ratterman, N. L. (2010). A practical guide to methods of parentage analysis. *Mol. Ecol.* 10, 6–30. doi: 10.1111/j.1755-0998.2009.02778.x

Kaniewski, D., Van Campo, E., Boiy, T., Terral, J.-F., Khadari, B., and Besnard, G. (2012). Primary domestication and early uses of the emblematic olive tree: palaeobotanical, historical and molecular evidence from the Middle East. *Biol. Rev.* 87, 885–899. doi: 10.1111/j.1469-185X.2012.00229.x

Kaya, H. B., Cetin, O., Kaya, H., Sahin, M., Sefer, F., Kahraman, A., et al. (2013). SNP discovery by Illumina-based transcriptome sequencing of the olive and the genetic characterization of Turkish olive genotypes revealed by AFLP, SSR and SNP markers. *PLoS One* 8, e73674. doi: 10.1371/journal.pone.0073674

Khadari, B., and El Bakkali, A. (2018). Primary selection and secondary diversification: two key processes in the history of olive domestication. *Int. J. Agron.* 18, 560793. doi: 10.1155/2018/560793

Khadari, B., Breton, C., Moutier, N., Roger, J. P., Besnard, G., Bervillé, A., et al. (2003). The use of molecular markers for germplasm management in French olive collection. *Theor. Appl. Genet.* 106, 521–529. doi: 10.1007/s00122-002-1079-x

Khadari, B., Moutier, N., Pinczon Du Sel, S., and Dosba, F. (2004). Molecular characterisation of French olive cultivars using microsatellites: towards the establishment of a reference genotype database. *Oléag Corps Gras Lipides* 11, 225–229. doi: 10.1051/ocl.2004.0225

Khadari, B., Charafi, J., Moukhli, A., and Ater, M. (2008). Substantial genetic diversity in cultivated Moroccan olive despite a single major variety: a paradoxical situation evidenced by the use of SSR loci. *Tree Genet. Genomes* 4, 213–221. doi: 10.1007/s11295-007-0102-4

Lacombe, T., Boursiquot, J. M., Laucou, V., Di Vecchi-Staraz, M., Péros, J. P., and This, P. (2013). Large-scale parentage analysis in an extended set of grapevine cultivars (*Vitis vinifera* L.). *Theor. Appl. Genet.* 126, 401–414. doi: 10.1007/s00122-012-1988-2

Las Casas, G., Scollo, F., Distefano, G., Continella, A., Gentile, A., and La Malfa, S. (2014). Molecular characterization of olive (*Olea europaea* L.) Sicilian cultivars using SSR markers. *Biochem. Syst. Ecol.* 57, 15–19. doi: 10.1016/j.bse.2014.07.010

Marra, F. P., Caruso, T., Costa, F., Di Vaio, C., Mafrica, R., and Marchese, A. (2013). Genetic relationships, structure and parentage simulation among the olive tree (*Olea europaea* L. subsp. *europaea*) cultivated in Southern Italy revealed by SSR markers. *Tree Genet. Genomes* 9, 961–973. doi: 10.1007/s11295-013-0609-9

Moutier, N., Artaud, J., Burgevin, J.-F., Khadari, B., Martre, A., Pinatel, C., et al. (2004). *Identification et Caractérisation des Variétés d'Olivier Cultivées en France. Tome 1*. Turriers: Naturalia publications.

Moutier, N., Artaud, J., Burgevin, J.-F., Khadari, B., Martre, A., Pinatel, C., et al. (2011). *Identification et Caractérisation des Variétés d'Olivier Cultivées en France. Tome 2*. Turriers: Naturalia publications.

Nei, M. (1987). *Molecular evolutionary genetics* (New York: Columbia University Press).

Owen, C. A., Bita, E. C., Banilas, G., Hajjar, S. E., Sellianakis, V., Aksoy, U., et al. (2005). AFLP reveals structural details of genetic diversity within cultivated olive germplasm from the Eastern Mediterranean. *Theor. Appl. Genet.* 110, 1169–1176. doi: 10.1007/s00122-004-1861-z

Park, S. D. E. (2001). *Trypanotolerance in West African cattle and the population genetic effects of selection*. PhD Thesis, University of Dublin.

Peakall, R., and Smouse, P. E. (2006). Genalex 6: genetic analysis in Excel. Population genetic software for teaching and research. *Mol. Ecol. Notes* 6 (1), 288–295. doi: 10.1111/j.1471-8286.2005.01155.x

Perrier, X., Flori, A., and Bonnot, F. (2003). "Data analysis methods," in *Genetic diversity of cultivated tropical plants*. Eds. P. Hamon, M. Seguin, X. Perrier, and J.-C. Glaszmann (Montpellier: Enfield, Science Publishers), 43–76.

Pinatel, C. (2015). *L'Olivier: Histoire Ancienne et Contemporaine. Oliviers de Haute Provence* (Turriers, France: Naturalia Publications).

Pritchard, J. K., Stephens, M., and Donnelly, P. (2000). Inference of population structure from multilocus genotype data. *Genetics* 155, 945–959.

Rohlf, F. J. (1998). *NTSYSpc numerical taxonomy and multivariate analysis system version 2.0 user guide* (New York: Exeter Software).

Sefc, K. M., Lopes, M. S., Mendonça, D., Rodrigues Dos Santos, M., Laimer Da Câmara Machado, M., and Da Cámara Machado, L. (2000). Identification of microsatellites loci in Olive (*Olea europaea L.*) and their characterization in Italian and Iberian trees. *Mol. Ecol.* 9(8):1171–1173. doi: 10.1046/j.1365-294x.2000.00954.x

Sekino, M., and Kakehi, S. (2012). PARFEX v1.0: an EXCEL™-based software package for parentage allocation. *Conserv. Genet. Resour.* 4, 275–278. doi: 10.1007/s12686-011-9523-3

Smouse, P. E., and Peakall, R. (1999). Spatial autocorrelation analysis of individual multiallele and multilocus genetic structure. *Heredity* 82, 561–573. doi: 10.1038/sj.hdy.6885180

Szpiech, Z. A., Jakobsson, M., and Rosenberg, N. A. (2008). ADZE: a rarefaction approach for counting alleles private to combinations of populations. *Bioinformatics* 24, 2498–2504. doi: 10.1093/bioinformatics/btn478

Terral, J.-F., Alonso, N., Capdevila, R. B., Chatti, N., Fabre, L., Fiorentino, G., et al. (2004). Historical biogeography of olive domestication (*Olea europaea* L.) as revealed by geometrical morphometry applied to biological and archaeological material. *J. Biogeog.* 31, 63–77. doi: 10.1046/j.0305-0270.2003.01019.x

Terral, J.-F. (1997). *La domestication de l'olivier (Olea europaea L.) en Méditerranée nord-occidentale: Approche morphométrique et implications paléoclimatiques* (France: PhD, Université Montpellier II).

Thachuk, C., Crossa, J., Franco, J., Dreisigacker, S., Warburton, M., and Davenport, G. F. (2009). Core Hunter: an algorithm for sampling genetic resources based on multiple genetic measures. *BMC Bioinf.* 10, 243. doi: 10.1186/1471-2105-10-243

Trujillo, I., Ojeda, M. A., Urdiroz, N. M., Potter, D., Barranco, D., Rallo, L., et al. (2014). Identification of the Worldwide Olive Germplasm Bank of Córdoba (Spain) using SSR and morphological markers. *Tree Genet. Genomes* 10, 141–155. doi: 10.1007/s11295-013-0671-3

Xanthopoulou, A., Ganopoulos, I., Koubouris, G., Tsaftaris, A., Sergendani, C., Kalivas, A., et al. (2014). Microsatellite high-resolution melting (SSR-HRM) analysis for genotyping and molecular characterization of an *Olea europaea* germplasm collection. *Plant Genet. Resour.* 12, 273–277. doi: 10.1017/S147926211400001X

Zohary, D., Hopf, M., and Weiss, E. (2012). *Domestication of plants in the Old World: the origin and spread of cultivated plants in Southwest Asia, Europe, and the Mediterranean Basin* (New York: Oxford University Press).

Conflict of Interest: The authors declare that the research was conducted in the absence of any commercial or financial relationships that could be construed as a potential conflict of interest.

frontiers in Plant Science

ORIGINAL RESEARCH
published: 15 January 2020
doi: 10.3389/fpls.2019.01631

Evaluation of Olive Pruning Effect on the Performance of the Row-Side Continuous Canopy Shaking Harvester in a High Density Olive Orchard

António Bento Dias[1]*, *José M. Falcão*[2], *Anacleto Pinheiro*[1] and *José O. Peça*[1]

[1] Departmento de Engenharia Rural, Instituto de Ciências Agrárias e Ambientais Mediterrânicas (ICAAM), University of Évora, Évora, Portugal, [2] Torre das Figueiras Sociedade Agrícola Lda, Monforte, Portugal

OPEN ACCESS

Edited by:
José Enrique Fernández, Institute of Natural Resources and Agrobiology of Seville (CSIC), Spain

Reviewed by:
Louise Ferguson, University of California, Davis, United States
Sergio Castro-Garcia, Universidad de Córdoba, Spain

***Correspondence:**
António Bento Dias
adias@uevora.pt

Specialty section:
This article was submitted to Crop and Product Physiology, a section of the journal Frontiers in Plant Science

Received: *13 June 2019*
Accepted: *19 November 2019*
Published: *15 January 2020*

Citation:
Dias AB, Falcão JM, Pinheiro A and Peça JO (2020) Evaluation of Olive Pruning Effect on the Performance of the Row-Side Continuous Canopy Shaking Harvester in a High Density Olive Orchard. Front. Plant Sci. 10:1631. doi: 10.3389/fpls.2019.01631

In 2009, the Side-Row Continuous Canopy Shaking Harvester project was set to develop such technology. The prototype comprises two symmetrical harvesters trailed by a farm tractor. Each harvester has a vibratory rotor with flexible rods, a catching platform with conveyors belts delivering fruits to a temporary storage bag. The removal efficiency of canopy shakers are influenced by factors like shaking frequency, ground speed as well as the dimension and shape of olive canopy. In 2014 authors started a trial to evaluate the influence of pruning in olive yield and in the performance of the Side-Row Continuous Canopy Shaking Harvester. The trial was established in an irrigated olive orchard of Picual cultivar planted in 1996 with the array 7 m x 3.5 m. In a randomised complete block design with three replications, four treatments are being compared leading to 12 plots with 30 trees/plot. The treatments under study are: T1—manual pruning using chain saws, in 2014 and 2017; T2—mechanical pruning: topping and hedging the two sides of the canopy, followed by manual pruning complement to remove wood suckers inside the canopy, in 2014 and 2017; T3—mechanical pruning: topping the canopy parallel to the ground and hedging southeast side of the canopy in 2014 and 2017; topping the canopy in July 2015 (summer pruning); hedging northwest side in winter 2016; T4—mechanical pruning: topping and hedging the two sides of the canopy in 2014 and 2017; topping the canopy in July 2015 (summer pruning). Regarding to olive yield per tree, significant differences were found among treatments on different years. However, no significant differences were found regarding the average olive yield per tree, over the period of 2014–2017. Regarding to the olive removal efficiency, only in 2016, significant differences were found among treatments on different years. No significant differences were found regarding the average of the olive removal efficiency, over the period of 2014–2017.

Keywords: canopy, shaker, olive, pruning, performance

INTRODUCTION

In Portugal there are currently 40,000 ha of high density olive groves (200 to 500 trees per hectare), mostly irrigated. Despite the recent diffusion of the super high density olive grove, still there will be more than 1.5 million ha of high density olive groves worldwide.

Olive harvest in high density olive orchards is usually performed by a tractor mounted trunk shaker and a canvas manually placed on the ground under the tree. Less labor demanding solutions based on inverted umbrellas linked to the trunk shaker have limited use since trees are very closely spaced to allow the umbrella to open.

Only changing from a discrete trunk shaking to a continuous canopy shaking principle will improve working capacity and will reduce the dependency over scarce and expensive labor. Grape and coffee over-the-row canopy harvesters could be used with good results in young intensive olive orchards not higher than 2.5 to 3.5 m or wider than 2 m (Ravetti and Robb, 2010). The same authors reported harvest efficiencies of 86 to 96% with a Colossus straddle harvester in an 8 years old olive grove, in Australia. This over-the-row machine is too heavy and expensive, hardly suitable to the difficult wet soil conditions encountered in the Mediterranean countries. A row-side, instead of over-the-row, concept imposing fewer limitations on tree growth is a technique bound for intensive orchards and may even be adequate for the large trees of the traditional non-irrigated orchards (Castro-García et al., 2011). Peterson (1998) designed and tested a prototype for continuous harvesting of oranges based on the side-by-side canopy shaker principle. Ferguson et al. (2002) used a side-by-side canopy prototype to harvest table olives with 90% harvest efficiency in the center of the canopy, but with significant efficiency losses in the leading and trailing edges of the canopy. The use of a canopy shaker prototype in traditional olive groves with large canopy trees showed lower efficiency than the obtained with trunk shakers (Sola-Guirado et al., 2014). In the prototype used by Sola-Guirado et al. (2016) it was found that an increase in vibration frequency or vibration amplitude enhances harvest efficiency. In 2009 the authors started a research project to develop the Side-Row Continuous Canopy Shaking Harvester—SRCCSH (Peça et al., 2014), which has been intensively tested ever since.

Cultivar, tree shape, canopy density, and pruning affect mechanical harvesting efficiency with canopy shakers (Ferguson et al., 2010).

It has been reported (Ferguson and Castro-García, 2014) that with adequate mechanical pruning, a canopy shaker harvester in table olives has provided greater harvest efficiency than manual harvesting of manually pruned trees, although this year there was a significant decrease in olive production in trees subjected to mechanical pruning. The same authors also reported that in a hedgerow olive grove, the application of mechanical pruning did not lead to significant differences in olive production compared to manual pruning. Harvesting efficiency with side-by-side canopy shaker in the mechanically pruned trees did not differ significantly from that of manual harvesting in manually pruned trees (Ferguson and Castro-García, 2014).

This paper presents and discusses the results of research conducted on a 20-year-old intensive olive grove to evaluate the influence of mechanical pruning on olive production and the performance of the SRCCSH.

MATERIALS AND METHODS

Olive Orchard

The high density olive orchard (HD) used in the trial was established in 1996 in Herdade da Torre das Figueiras in the Alentejo region of southern Portugal (lat. 39°03'34.04" N; 07° 28'22.00"W). This drip irrigated HD olive orchard of Picual cultivar was installed in an array of 7 m x 3.5 m.

The orchard was planted on Chromic Luvisol soil (FAO). This region is semi-arid with strong continental influence and an annual rain mean of 500 mm concentrated in the winter.

The orchard is drip irrigated twice a week, from May till October, receiving annually an estimated volume of 1,500–2,000 m^3/ha.

The HD olive orchard was sprayed to control olive leaf spot [*Flusicladium oleaginum (Castagne) Ritschel & U. Braun*], olive moth (*Prays oleae* Bernard), olive fly (*Bactrocera oleae* Gmelin.) and olive anthracnose (*Colletotrichum acutatum* Simmons *or Colletotrichum gloeosporioides* Penz.). Weed control was done spraying glyphosate in the rows and with a shredder between rows. About 80 units of nitrogen, 30 units of phosphorus, and 50 units of potassium were applied to the soil and by drip irrigation in average by year.

Equipment

Mechanical pruning was performed using an R&O (Reynolds & Oliveira Ltd.) disk-saw pruning machine (**Figure 1**), with a 3.0 m cutting bar (Peça et al., 2002), mounted on a front loader of a 97 *kW* (DIN) 4WD agricultural tractor.

The manual pruning complement to the mechanical pruning was executed by telescopic chain saws.

The SRCCSH is a prototype (**Figure 2**) developed to remove fruits from the tree brunches, collect, and transport the fruits to temporary storage (Peça et al., 2014).

FIGURE 1 | Pruning machine mounted in a tractor.

The SRCCSH is based on two symmetrical machines, each one trailed by a farm tractor, moving alongside a same tree row, harvesting both sides of the trees. Fruit removal is made by a vibratory rotor with flexible rods for engaging and shaking the olive bearing branches. Vibration frequency of the vibratory rotor can be altered adjusting the tractor power-take-off speed. Removed olives are collected on a platform and conveyed to a temporary storage bag.

Operational parameters of SRCCSH were adjusted at the beginning of the harvesting season (**Table 1**).

Treatments

Four treatments (T1, T2, T3, T4), shown in **Table 2**, are being compared in a randomized complete block design with three replications leading to 12 plots, of one line each, with 30 trees per plot.

Treatment 1 (T1)—manual pruning performed in 2014 and 2017. One man per tree performed selective cuts with a chainsaw to control canopy dimension, removing branches with excessive growth, either overhanging the canopy toward the space between rows or taller than the vibratory mast of the SRCCSH.

Treatment 2 (T2)—mechanical pruning followed by a manual pruning complement was made in 2014 and 2017. Mechanical pruning consisted on a horizontal cut (topping) at the uppermost part of the canopy and a vertical cut on each side of the tree (hedging). Topping was done at approximately 3.6 m (2014) and 3.3 m (2017) in height, from the ground; hedging was done at approximately 1.8 m from the tree trunk. Manual pruning complement was performed to remove wood suckers inside the canopy and also wood stumps on each side of canopy.

FIGURE 2 | Row side continuous canopy shaker.

TABLE 1 | Operation parameters of Side-Row Continuous Canopy Shaking Harvester.

Harvesting season	2014	2015	2016	2017
Ground speed (*km/h*)	0.6	0.6	0.6	0.75
PTO of left unit (*rpm*)	430	430	540	610
PTO of right unit (*rpm*)	430	500	540	540

Treatment 3 (T3)—mechanical pruning performed each year. In 2014, trees were topped (as in T2) followed by a vertical cut (hedging) of the southeastern side of the canopy. In July 2015 a summer topping at 3.6 m height (from the ground) was done to control growth suckers developed in uppermost part of the canopy after 2014 topping. In March 2016 the northwestern side of the canopy was hedged at a distance of 2.0 m from the tree trunk. In March 2017, trees were topped at 3.3 m height (from the ground) and hedged on the southeastern side of the canopy at a distance of 1.8 m from the tree trunk.

Treatment 4 (T4)—mechanical pruning performed in 2014, 2015, and 2017. In 2014, trees were topped (as in T2) and hedging each side of the canopy. In July 2015, a summer topping at 3.6 m height was done to control growth suckers developed at the uppermost part of the canopy, after 2014 topping. In March 2017 a horizontal cut was made at 3.3 m height followed by hedging both sides of the canopy at a distance of 1.8 m from the tree trunk.

Assessments

Pruning operations were timed to calculate the work rates. Tree measurements of the height of the tree from the ground, width of the canopy and the distance from the base of the canopy to the ground were recorded in five trees randomly selected in each plot. Measurements were done in the same trees in the entire period of tests (2014 to 2017) and taken before and after pruning interventions or in early spring for the non-pruning years.

The mass of olives caught by the SRCCSH was measured weighing the bags from each plot.

The evaluation of the mass of olive removed but not caught by the harvester was done weighing the fruits collected on canvas placed under a group of three olive trees at three locations randomly selected in each plot.

To quantify the mass of olives not removed by the harvester, all trees in each plot were vibrated by a trunk shaker complemented by manual harvest with poles.

Total yield per tree was obtained adding the mass of olives caught by the harvester (in the bags) to the mass of olives dropped to the ground (on the canvas) plus the mass left on the tree

Harvest efficiency was calculated as follows:

$$Harvest\ efficiency\ (\%) = \frac{\text{Mass of olives caught per tree}}{\text{Total yield per tree}}$$

One-way analysis of variance were performed to annual data and general linear model univariate analysis for average data, using IBM SPSS version 24 software. Mean separation was performed by Multiple Range Duncan test at 5 and 10% significance level.

RESULTS

Pruning Work Rate

Figure 3 shows the manual pruning work rates obtained in 2014 and 2017. More severe pruning interventions justify a reduction in the work rate in 2017.

TABLE 2 | Treatments: pruning interventions sequence.

Treatment	2014	2015	2016	2017
T1	Manual			Manual
T2	+ Manual Compl.			+ Manual Compl.
T3		Summer		
T4		Summer		

Manual, manual pruning; Manual Compl., manual pruning complement; Summer, summer pruning.

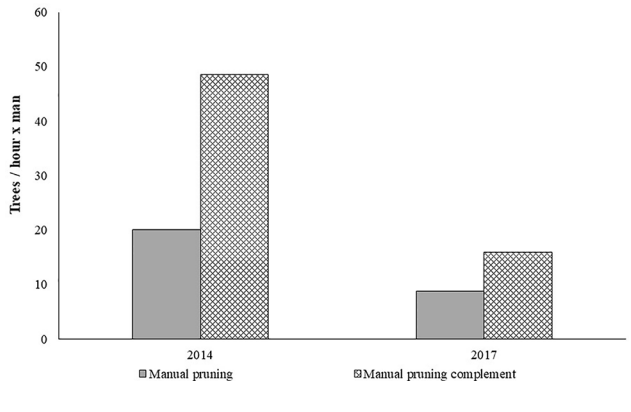

FIGURE 3 | Average work rates of manual pruning.

To avoid low work rates of manual pruning complement reported in previous research work (Peça et al, 2002) a clarification of what should consist the manual pruning complement and continuously monitoring the pruning workers led to higher work rates compared with strictly manual pruning intervention.

In **Figure 4** an estimation of the speed of advance of the tractor with the disk pruning machine is shown as a function of the type of cut.

Lateral cuts of the canopy allow the tractor to move faster since the volume of leaf mass that is eliminated is smaller than in the horizontal cuts of the upper part of the canopy. In the horizontal cut the tractor has to move slower to reduce the risk of leaf and branches mass accumulating in front of the cutter bar, locking the cutter disks.

Summer cuts tend to require the tractor to move even slower, since the branches to be cut are highly flexible and tend to bend in front of the disk saw, aggravated when disks are not conveniently sharped.

Figure 5 shows the working rate of the disk pruning machine in each treatment.

Topping and hedging on both faces corresponds to a working capacity of 155 to 180 trees per hour.

Topping and hedging of only one side did not show a higher work rate (186 to 192 trees per hour) because of the non-productive return path required to restart the work in the same direction.

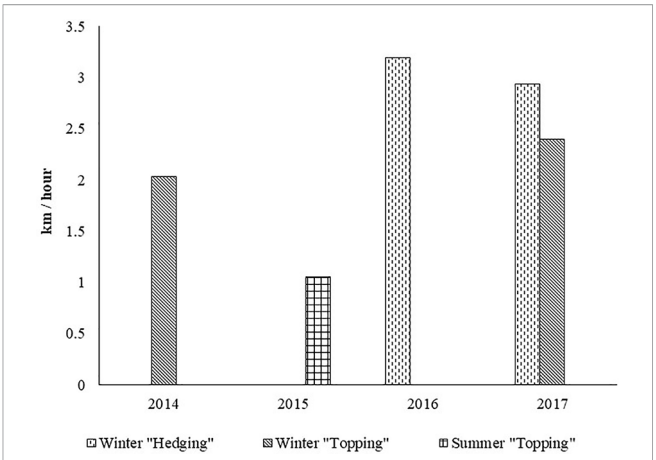

FIGURE 4 | Estimated speed of advance of the tractor with the disk pruning machine is shown as a function of the type of cut.

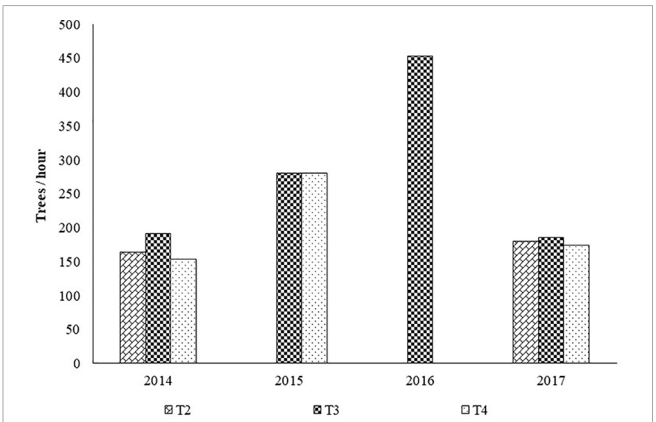

FIGURE 5 | Average work rates (trees/hour x man) by treatment with the disk saw pruning machine. Legend: T1, treatment 1; T2, treatment 2; T3, treatment 3; T4, treatment 4.

Summer topping despite being carried out at a lower working speed than the winter topping, registered a greater working capacity, since only one machine pass was necessary for each row of trees, whereas two passes were required in winter topping due to wider canopies and limited cutter bar width.

Pruning Costs

Based on the working capacities presented in **Figures 3** and **5**, the pruning costs were determined. The following assumptions were considered: 70 €/h for contractor work charges for mechanical pruning; 70 €/man-day for contractor work charges for manual pruning; 7.5 h of effective work per day.

Figure 6 shows the cost of pruning in each year and by treatment, showing also the total value per treatment over the period 2014 to 2017.

In 2014, the interventions with the disk pruning machine, comprising topping and hedging of both sides (T4) had a cost similar to that of strictly manual pruning (T1).

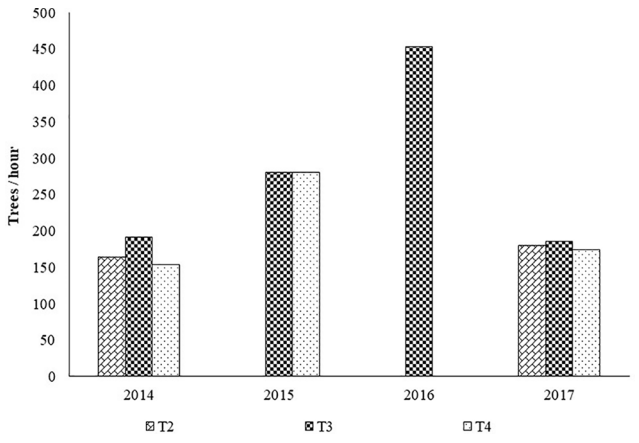

FIGURE 6 | Pruning costs per treatment. Legend: T1, treatment 1; T2, treatment 2; T3, treatment 3; T4, treatment 4.

When, in addition to topping and hedging, a manual complement (T2) is added, pruning became more expensive than strictly manual pruning (T1).

In 2017, as a result of a more severe pruning intervention, the work rate was lower compared to what had occurred in 2014. As a consequence, the cost weight of manual pruning gave rise to higher pruning costs in T1 and T2 treatments than in T3 and T4 treatments.

Concerning total values, the cost of strictly mechanical pruning was lower than pruning with manual interventions.

Canopy Dimensions

Tree Height

Figure 7 shows the height of the trees, per year and treatment, before and after winter pruning. It shows the extent of the reduction in height as well as the recovery observed from one pruning intervention to the next. In treatment 3 and treatment 4 the recovery in tree height over the entire period of 2014 up to 2017 are influenced by the pruning interventions made in the summer of 2015.

The height of the trees is a relevant dimension in that the highest rods of the vibratory mast of the SRCCSH are at approximately 3.6 m above the ground.

Canopy Width

This dimension is relevant in that, once the interface of the SRCCSH has been positioned in relation to the trunk of the olive tree, the rods of the vibratory mast must penetrate the canopy, leaving the steel guiding tubes of the rods outside the canopy. Since the SRCCSH allows lateral placement of the vibratory mast, **Figure 8**, adequate canopy width limits should be between 1.5 and 3.6 m.

Figure 9 shows the average canopy width of the trees, per year and treatment, before and after winter pruning. It shows the extent of the reduction in canopy width as well as the recovery observed from one pruning intervention to the next.

Olive Yield

Figure 10 shows the average yield of olives per tree in each year. There were significant differences ($P < 0.05$) between the years, with the highest production achieved in 2015, which was significantly higher ($P \leq 0.05$) than in the other years, which differed from each other. These results confirm the alternate bearing typical of this species, which can be changed with pruning interventions. After the decrease in production verified from 2015 to 2016, it would be expected that in 2017 there would be an increase in production. However, pruning interventions executed in 2017, with a reduction in the canopy volume and the elimination of potentially productive branches, resulted in a decrease in production compared to 2016. **Figure 11** shows olive yield by treatment in each year and the average yield of the trial. In 2014, significant differences ($P < 0.05$) were registered in olive yield per tree between treatments. Treatment 3 has revealed significantly ($P \leq 0.05$) higher yield than the other treatments, as consequence of the smaller pruning intensity applied. The disk-saw pruning machine performs non-selective trimming of the canopy. In treatment T3, the significantly higher production may have been originated in productive branches issued in the previous year on the northwestern side of the canopy which was left uncut 2014. In treatments T2 and T4, the lateral cuts on both sides eliminated a considerable part of the productive branches issued in the previous year, diminishing productive potential in comparison with treatment T3. In the case of treatment T1, despite having been subjected to manual pruning, which has greater selectivity, the elimination of a considerable part of the canopy reduced the productive potential.

In 2015 significant differences in olive yield were registered between treatments ($P < 0.05$). Treatment 3 obtained a significantly lower yield ($P \leq 0.05$) than the other treatments as a consequence of the higher yield obtained in the previous year. Given that the olive tree is characterized by an alternate bearing, a year with low production allows more vegetative growth. The greater leaf mass developed this year will boost higher yield the following year. This characteristic explains the considerable increase in production that occurred in treatments T1, T2, and T3 from 2014 to 2015. In the case of treatment T3 this increase was not so pronounced, since in 2014 the vegetative growth was conditioned by the existing tree production.

In 2016 significant differences ($P < 0.05$) were found in olive yield between treatments. Treatment 3 and treatment 4 show significantly ($P \leq 0.05$) lower yield than treatments 1 and 2. The fall in production of treatment 3 compared to treatments 1 and 2 is associated with a reduction in canopy volume due to topping in summer 2015 and cutting in the northwest side in winter 2016, which left these trees with lower leaf mass and consequently with lower fruiting potential. High production in a smaller tree canopy (T4 in 2015) will tend to penalize the release of productive branches and consequently the production of 2016. In 2017 production shows the opposite trend to 2016, although without significant differences between treatments ($P > 0.1$). On average, no significant differences between treatments were found ($P > 0.1$)

These results show the potential of mechanical pruning as a method for reducing labor dependence, without significant

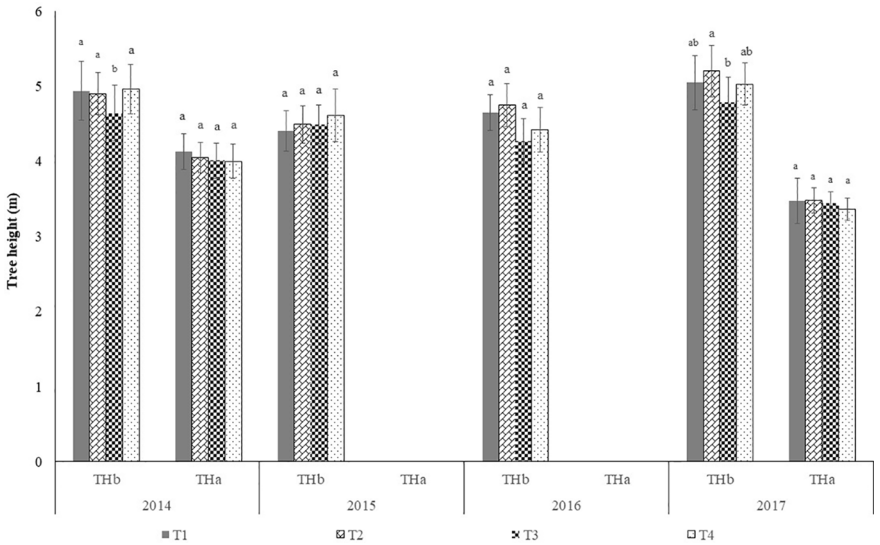

FIGURE 7 | Tree height before and after winter pruning in each year (mean±sd). Legend: THb, tree height before winter pruning; THa, tree height after winter pruning; T1, treatment 1; T2, treatment 2; T3, treatment 3; T4, treatment 4. In each year, before and after pruning, columns followed by the same letter are not significantly different by Duncan multiple range test at the 5% level.

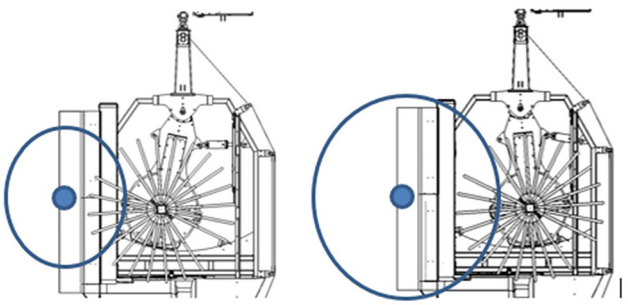

FIGURE 8 | Top view of the Side-Row Continuous Canopy Shaking Harvester showing lateral position of the vibratory mast.

negative influence in olive production, in line with the results obtained in traditional olive orchards by Pastor and Humanes (1998) Dias (2006); Dias et al. (2012), and Dias et al. (2014). The results obtained in this trial differ from those obtained by Ferguson et al. (2002) in an olive grove for table olives, who found that topping and hedging every 2 years causes a decrease in olive yield, particularly in the pruning year. This decrease in production did not affect the gross net return because the fruits being of a larger caliber benefited of a better market price.

The present work also seems to reveal that frequent mechanical pruning interventions tend to penalize olive yield. It appears desirable to perform a more intense mechanical pruning spaced in time, as recommended by Pastor and Humanes (1998) for high density olive groves.

Manual pruning complement to mechanical pruning did not increase olive yield in comparison to the obtained in trees with the absence of manual pruning complement.

Manual pruning complement to the mechanical pruning (T2), particularly in following years to the mechanical pruning, should be regarded as a potentially important technique, since it may contributed to higher yields as verified by Dias et al. (2014) on a traditional olive orchard after more than 10 years submitted to mechanical pruning.

Harvester Efficiency

Figure 12 shows the removal efficiency of olives by the SRCCSH in each year. Significant differences ($P < 0.05$) were observed between the years, with the highest efficiency being achieved in 2014, which was significantly higher ($P < 0.05$) than those observed in the other years which didn't differ from each other. It should be noted that the result obtained in 2014 had several constraints:

- low level of production;
- olives with anthracnose disease;
- olives at an advanced maturity stage (practically all black).

Figure 13 shows harvester efficiency per treatment in each year and the average efficiency over the period 2015 to 2017.

In 2017, **Figures 7** and **9** show that, before pruning, treatments T1, T2, and T4 had canopies of similar size, leading to admit the same at 2016 harvest. However, harvest efficiency was significantly higher in T4 than in the other treatments. Possibly the significantly lower yield of T4 relative to T1 and T2, may be a justification, since the same detaching vibrating energy is available for fewer fruits. This could also justify the significantly higher value of efficiency of treatment T3 relative to treatments T1 and T2. Ferguson and Castro-García, (2014) also obtained significantly higher harvesting efficiency on trees with lower yields compared to those submitted to manual pruning that were harvested by hand. However, these results

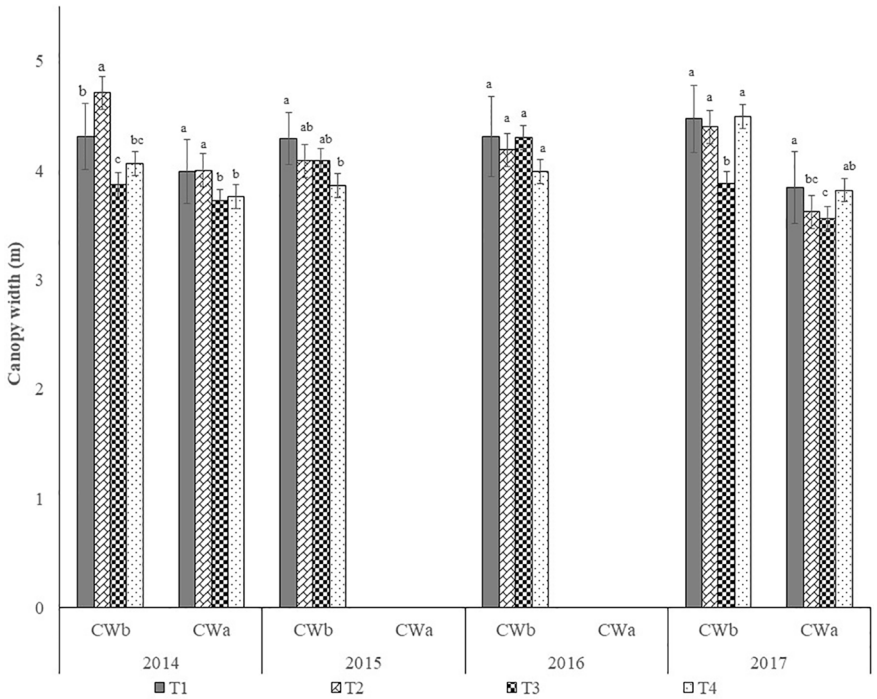

FIGURE 9 | Canopy width before and after pruning in each year (mean±sd). Legend: CWb, canopy width before winter pruning; CWa, canopy width after winter pruning; T1, treatment 1; T2, treatment 2; T3, treatment 3; T4, treatment 4. In each year, before and after pruning, columns followed by the same letter are not significantly different by Duncan multiple range test at the 5% level, with exception of CWa in 2014 and 2017, where p≤0.1.

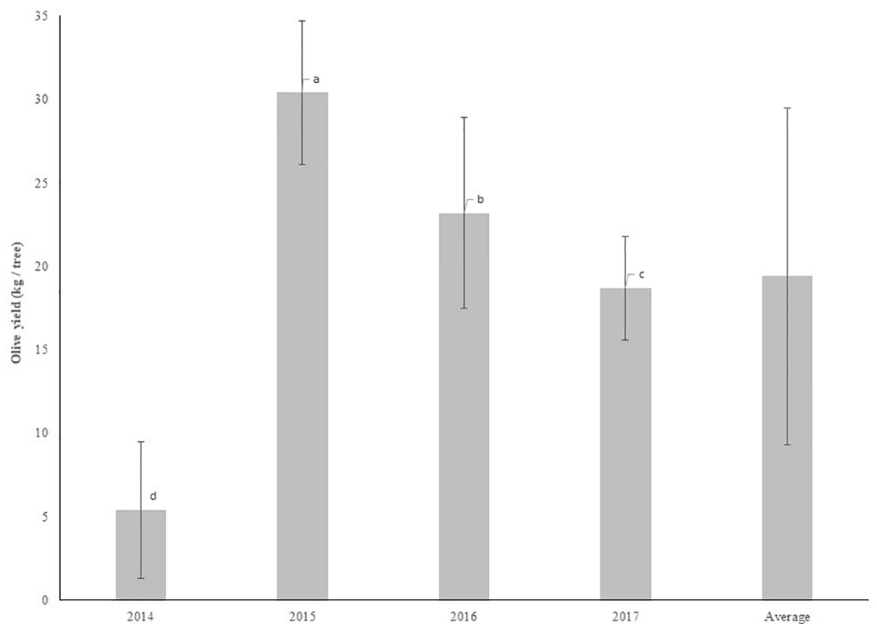

FIGURE 10 | Olive yield by year (mean±sd). Legend: T1, treatment 1; T2, treatment 2; T3, treatment 3; T4, treatment 4. Columns followed by the same letter are not significantly different by Duncan multiple range test at the 5% level.

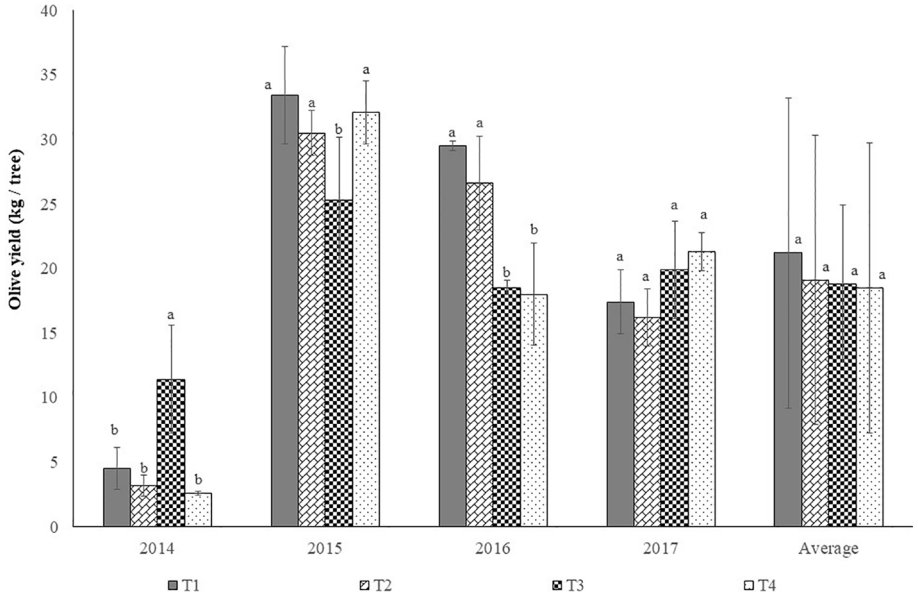

FIGURE 11 | Olive yield by treatment in each year and the average yield of the trial (mean±sd). Legend: T1, treatment 1; T2, treatment 2; T3, treatment 3; T4, treatment 4. In each year and in average, columns followed by the same letter are not significantly different by Duncan multiple range test at the 5% level, with the exception of 2015, where $p < 0.1$.

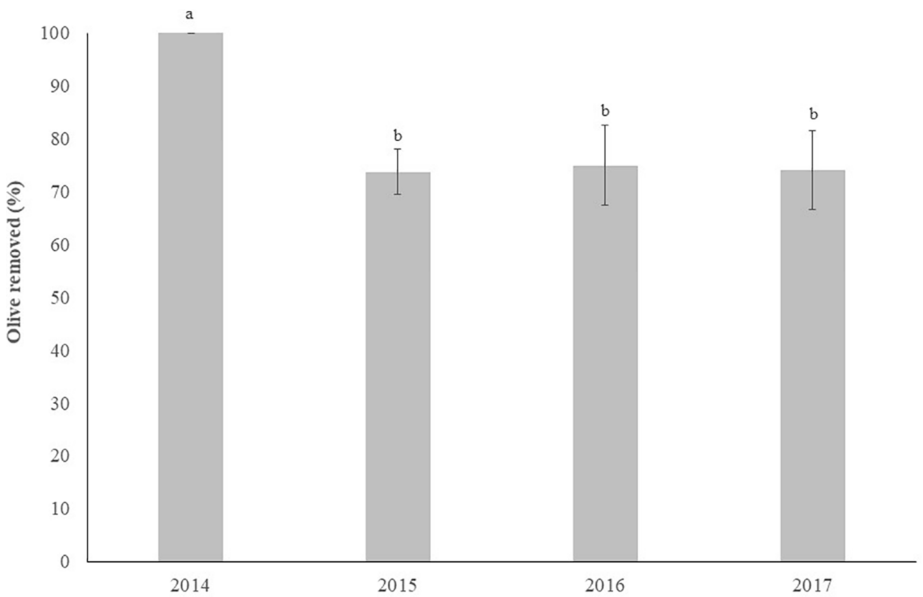

FIGURE 12 | Effect of year in the harvester efficiency (mean±sd). Columns followed by the same letter are not significantly different by Duncan multiple range test at the 5% level.

refer to only 1 year and were obtained from trees intended for the production of table olives. In 2017 no significant differences ($P > 0.1$) were found between treatments in harvest efficiency. Although no data is available concerning the regrowth after 2017 pruning, **Figures 7** and **9** reveal that canopy size was left with similar volume in all treatments. Taking in account that no significant differences were found in olive yield among treatments (**Figure 11**), this may justify that no significantly differences were also found in harvest efficiency.

In 2015 significant differences ($P < 0.05$) were found between treatments in harvest efficiency. At the 2015 harvest, and assuming that the size of the trees is revealed by their dimensions in 2016 (**Figure 7**), it can be appreciated that trees of T3 and T4 are lower than the trees of T1 and T2.

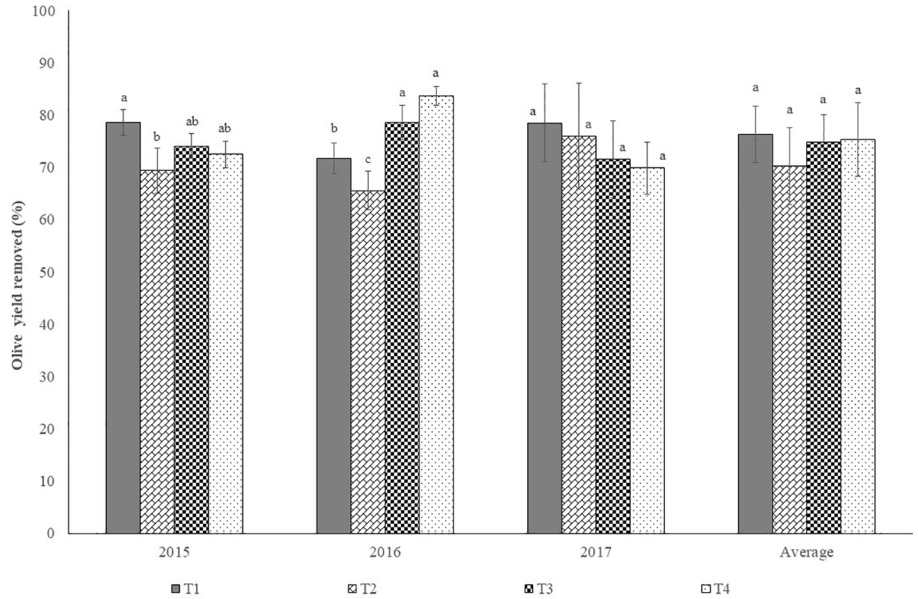

FIGURE 13 | Harvester efficiency (%) by treatment, in each year and the average of the trial (mean±sd). Legend: T1, treatment 1; T2, treatment 2; T3, treatment 3; T4, treatment 4. Columns followed by the same letter are not significantly different by Duncan multiple range test at the 5% level.

At harvest olives were below the 4 m height, whereas in treatments T1 and T2 production was above the 4 m mark. However, the results of harvest efficiency in 2015 reveal that more factors not counted for at the present work have to be considered. Fruit detachment force and fruit weight presented a low correlation with harvest efficiency (Gil-Ribes et al., 2011). The spatial distribution of the olive in the canopy, associated with the trajectory described by the active organs of the vibrating mast, may assume an increasing importance when deciding pruning interventions to enhance harvest efficiency without jeopardizing yields and at contained costs. The influence of the manual intervention done in 2014 in T1 and T2, may be still influence the transmission of vibrating energy to the canopy in the following years, especially in 2015. Also, it is not understood why, similar canopies as in T3 and T4, bearing significantly different yield capacity, showed also similar harvest efficiency.

On average (period 2015 to 2017), no significant differences ($P > 0.05$) among treatments in harvest efficiency were found.

CONCLUSIONS

In the period of 4 years, on average, there were no significant differences ($P \leq 0.05$) between treatments in olive production.

In view of this fact:

- the cost with only mechanical pruning is lower than pruning with manual interventions.
- manual complement pruning was not relevant since it did not lead to increased production and led to an increase in pruning costs, as had already occurred in the traditional olive grove trial. Complementary manual pruning interventions only make sense to eliminate excess wood accumulated over a relatively long period of time and should be carried out sporadically. Two supplementary annual pruning interventions over a 4-year period are not advisable.
- the option for pruning with a disk machine on the side faces in alternate years has also not been interesting since it does not reduce the pruning costs, it does not enhance production of olives. Carrying out the cuts on the sides of the canopy more frequently, while allowing the canopy volume to be controlled, does not allow for the full production potential of the regrowth that appear after the cuts on the side faces.

In terms of the influence of pruning on the performance of the SRCCSH, there were no significant differences between treatments.

DATA AVAILABILITY STATEMENT

All datasets generated for this study are included in the article/supplementary material.

AUTHOR CONTRIBUTIONS

AD conceived and designed the experiment. AD, JF, AP, and JP performed the evaluation. AD and JP analyzed the data and wrote the paper.

FUNDING

This work is funded by National Funds through FCT—Foundation for Science and Technology under the Project UID/AGR/00115/2013 and by Portuguese Agriculture Ministry research program PRODER under the project 55344.

ACKNOWLEDGMENTS

We gratefully acknowledge "Torre das Figueiras Sociedade Agrícola Lda" for access to olive orchards where this research was conducted. We also thank Luis Caeiro, Manuel Machadinha, and Tiago Silva for assistance in olive collection data.

REFERENCES

Castro-García, S., Blanco-Roldán, G. L., Muñoz-Tejada, R., and Gil-Ribes, J. A. (2011). Estudio de los parámetros de vibración de un sacudidor de copa en la recolección mecanizada del olivar tradicional. Proc. VI Congreso Ibérico de AgroIngenieria, Evora, Portugal, 4-7, setembro.

Dias, A. B., Peça, J. O., and Pinheiro, A. (2012). Long term evaluation of the influence of mechanical pruning on olive growing. *Agron. J.* 1041, 23–25. doi: 10.2134/agronj20110137

Dias, A. B., Pinheiro, A., and Peça, J. O. (2014). Fifteen years evaluation of the influence of mechanical pruning on olive yield. *Acta Hort.* 7, 391–397. doi: 10.17660/ActaHortic.2014.1057.39

Dias, A. B. (2006). A mecanização da poda da oliveira. Contribuição da máquina de podar de discos. [phd dissertation thesis],Universidade de Évora.

Ferguson, L., and Castro-García, S. (2014). Transformation of an Ancient Crop: Preparing California 'Manzanillo' Table Olives for Mechanical Harvesting, Hortechnology 24, (3), 274–280. doi: 10.21273/HORTTECH.24.3.274

Ferguson, L., Krueger, W. H., Reyes, H., and Metheney, P. (2002). Effect of Mechanical Pruning on California Black Ripe (Olea europea L.) cv. 'Manzanillo' Table Olive Yield. *Acta Hortic.* 586, 281–284. doi: 10.17660/ActaHortic.2002.586.54

Ferguson, L., Rosa, U. A., Castro-Garcia, S., Lee, S. M., Guinard, J. X., Burns, J., et al. (2010). Mechanical harvesting of California table and oil olives. *Adv. Hortic. Sci.* 24(1), 53–63.

Gil-Ribes, J. A., Blanco-Roldán, G. L., Castro-García, S., Aguera Vera, J., Munoz Tejada, R., Jiménez-Jiménez, F., et al. (2011). Introduccion de un Sistema Sacudidor de Copa Para La Recolección Mecanizada del Olivar Tradicional de Almazara Proceedings XV Scientific-technical Symposium of olive oil, Expoliva, Oli-37;.

Pastor, M., and Humanes, J. (1998). A poda del olivo – moderna olivicultura, 3ª edición (corregida y actualizada), Madrid, Editorial agrícola Española S.A.

Peça, J. O., Dias, A. B., Pinheiro, A. C., Santos, L., Morais, N., Pereira, A. G., et al. (2002). Mechanical pruning of olive trees as an alternative to manual pruning. *Acta Hortic.* 586, 295–299. doi: 10.17660/ActaHortic.2014.1057.48

Peça, J. O., Dias, A. B., Pinheiro, A., Cardoso, V., Reynolds de Souza, D., and Falcão, J. M. (2014). Side-Row Continuous Canopy Shaking Harvester for Intensive Olive Orchards. *Acta Hortic.*, 391–397. doi: 10.13031/2013.19409

Peterson, D. L. (1998). Mechanical Harvester for Processed Oranges, Applied Engineering in Agriculture, 14, (5), 455–458. doi: 10.13031/2013.19409

Ravetti, L., and Robb, S. (2010). Continuous mechanical harvesting in modern Australian olive growing systems. *Adv. Hortic. Sci.* 24 (1), 71–77. doi: 10.1016/j.biosystemseng.2013.12.007

Sola-Guirado, R. R., Castro-García, S., Blanco-Roldán, G. L., Jiménez-Jiménez, F., Castillo-Ruiz, F. J., and Gil-Ribes, J. A. (2014). Traditional olive tree response to oil olive harvesting technologies. *Biosyst. Eng.* 118, 186–193. doi: 10.5424/sjar/2016142-7909

Sola-Guirado, R. R., Jiménez-Jiménez, F., Blanco-Roldán, G. L., Castro-García, S., Castillo-Ruiz, F. J., and Gil-Ribes, J. A. (2016). Vibration parameters assessment to develop a continuous lateral canopy shaker for mechanical harvesting of traditional olive trees. *Spanish J. Agric. Res.* 14 (2), e0204. doi: 10.5424/sjar/2016142-7909

Conflict of Interest: The authors declare that the research was conducted in the absence of any commercial or financial relationships that could be construed as a potential conflict of interest.

frontiers in Plant Science

ORIGINAL RESEARCH
published: 13 February 2020
doi: 10.3389/fpls.2020.00066

Association Study of the 5′UTR Intron of the *FAD2-2* Gene With Oleic and Linoleic Acid Content in *Olea europaea* L.

*Amelia Salimonti[1], Fabrizio Carbone[1], Elvira Romano[1], Massimiliano Pellegrino[1], Cinzia Benincasa[1], Sabrina Micali[2], Alessandro Tondelli[3], Francesca L. Conforti[4], Enzo Perri[1], Annamaria Ienco[5] and Samanta Zelasco[1]**

[1] Research Centre for Olive, Citrus and Tree Fruit, CREA, Rende, Italy, [2] Research Centre for Olive, Citrus and Tree Fruit, CREA Roma, Italy, [3] Research Centre for Genomics and Bioinformatics, CREA, Fiorenzuola D'Arda, Italy, [4] Department of Pharmacy, Health and Nutritional Sciences, University of Calabria, Rende, Italy, [5] Research Centre for Forestry and Wood, CREA, Arezzo, Italy

Cultivated olive (*Olea europaea* L. subsp. *europaea* var. *europaea*) is the most ancient and spread tree crop in the Mediterranean basin. An important quality trait for the extra virgin olive oil is the fatty acid composition. In particular, a high content of oleic acid and low of linoleic, linolenic, and palmitic acid is considered very relevant in the health properties of the olive oil. The oleate desaturase enzyme encoding-gene (*FAD2-2*) is the main responsible for the linoleic acid content in the olive fruit mesocarp and, therefore, in the olive oil revealing to be the most important candidate gene for the linoleic acid biosynthesis. In this study, an *in silico* and structural analysis of the 5′UTR intron of the *FAD2-2* gene was conducted with the aim to explore the natural sequence variability and its role in the gene expression regulation. In order to identify functional allele variants, the 5′ UTR intron was isolated and partially sequenced in 97 olive cultivars. The sequence analysis allowed to find a 117-bp insertion including two long duplications never found before in *FAD2-2* genes in olive and the existence of many intron-mediated enhancement (IME) elements. The sequence polymorphism analysis led to detect 39 SNPs. The candidate gene association study conducted for oleic and linoleic acids content revealed seven SNPs and one indel significantly associated able to explain a phenotypic variation ranging from 7% to 16% among the years. Our study highlighted new structural variants within the *FAD2-2* gene in olive, putatively involved in the regulation mechanisms of gene expression associated with the variation of the content of oleic and linoleic acid.

Keywords: *FAD2-2* gene, SNP, association study, 5′UTR intron, *Olea europaea*

OPEN ACCESS

Edited by:
José Manuel Martínez-Rivas, Instituto de la Grasa (IG), Spain

Reviewed by:
Juan De Dios Alché, Experimental Station of Zaidín (EEZ), Spain
Maria Cecilia Rousseaux, Centro Regional de Investigaciones Científicas y Transferencia Tecnológica de La Rioja (CRILAR CONICET), Argentina
Qing Liu, Commonwealth Scientific and Industrial Research Organisation (CSIRO), Australia

***Correspondence:**
Samanta Zelasco
samanta.zelasco@crea.gov.it

Specialty section:
This article was submitted to Crop and Product Physiology, a section of the journal Frontiers in Plant Science

Received: *03 July 2019*
Accepted: *16 January 2020*
Published: *13 February 2020*

Citation:
Salimonti A, Carbone F, Romano E, Pellegrino M, Benincasa C, Micali S, Tondelli A, Conforti FL, Perri E, Ienco A and Zelasco S (2020) Association Study of the 5′UTR Intron of the FAD2-2 Gene With Oleic and Linoleic Acid Content in Olea europaea L.. Front. Plant Sci. 11:66. doi: 10.3389/fpls.2020.00066

INTRODUCTION

Cultivated olive (*Olea europaea* L. subsp. *europaea* var. *europaea*) is the most ancient and spread tree crop in the Mediterranean basin. Despite the economic, cultural, and ecological importance of olive groves in the Mediterranean area, now extending to other regions, olive has been a poorly characterized species at genetic and genomic level compared to other fruit tree crops. The species is characterized by a very big genome size (1C = 1,400–1,500 Mbp) (Loureiro et al., 2007; Unver et al., 2017), a cross-pollinating reproductive biology leading to a high heterozygosity (Dìez et al., 2011; Besnard et al., 2014; Kaya et al., 2016) and a long generation time. All these aspects, together with the scarce knowledge about the inheritance of most genes controlling agronomical performance and quality traits, have severely restricted breeding strategies to clonal or varietal selection (Rugini et al., 2011). Understanding the basis of quantitative traits may help plant breeders to improve crop yields, resistance to abiotic and biotic stress conditions, end-use quality, and other important characteristics that are controlled by multiple genes exhibiting a quantitative distribution of phenotypes (Kaya et al., 2016). Loci controlling quantitative traits can be identified either by QTL mapping in a biparental segregating population or by association mapping (Belò et al., 2008) in natural populations (Flint-Garcia et al., 2003). Until now, in olive several genetic maps have been built (De la Rosa et al., 2003; Wu et al., 2004; El Aabidine et al., 2010; Dominguez-Garcia et al., 2011; Atienza et al., 2014; Ipek et al., 2016; Marchese et al., 2016) aimed to detect QTL-associated markers for traits, such as fruiting (Ben Sadok et al., 2013; Atienza et al., 2014), flowering (Ben Sadok et al., 2013), trunk diameter (Atienza et al., 2014), and fatty acid composition (Hernández et al., 2017) using different molecular markers and approaches. However, biparental QTL mapping has many limitations in tree species due to their long generation times and juvenile period, high levels of heterozygosity, time-consuming trait evaluation, slow physiological maturation, and high levels of genetic variation between parents (Tian et al., 2014; Kaya et al., 2016).

In recent years, association mapping (AM) methods have been developed to detect the correlations between genotypes and phenotypes on the basis of linkage disequilibrium (LD) (Rafalski, 2010). AM has been a part of research on complex traits in various fruit trees, including peach (Aranzana et al., 2010; Cao et al., 2012), apricot (Olukolu, 2010), sweet cherry (Ganopoulos et al., 2011; Khadivi-Khub, 2014), almond (Kadkhodaei et al., 2011; Font i Forcada et al., 2015), grapevine (Barnaud et al., 2010) and apple (Kumar et al., 2013).

Olive core collection construction has been reported (Belaj et al., 2012; El Bakkali et al., 2013) and very recently new wide SNP polymorphisms in the whole genome and candidate genes were discovered (D'Agostino et al., 2018; Belaj et al., 2018; Cultrera et al., 2019). However, genome data are still incomplete and referred to a few genotypes (Cultrera et al., 2019) while several transcriptomic experiments have been already conducted leading to new candidate genes (García-López et al., 2014; Leyva-Pérez et al., 2014; Carmona et al., 2015; Guerra et al., 2015; Koudounas et al., 2015; Gómez-Lama Cabanás et al., 2015; González-Plaza et al., 2016; Iaria et al., 2015; Alagna et al., 2016; Grasso et al., 2017; Leyva-Pérez et al., 2018). Attempts of genome wide association studies were conducted using molecular markers such as SSR, AFLP, RFLP, and SNP (Ipek et al., 2015; Kaya et al., 2016; Ben-Ayed et al., 2017). However, until high level of genome sequencing information will be available and a whole oriented genome obtained, a candidate gene association mapping seems the most promising approach.

An important quality trait for the extra virgin olive oil is the fatty acid composition. In particular, a high content of oleic acid and low on linoleic, linolenic, and palmitic acid is considered very relevant in the health properties of the olive oil (Quintero-Florez et al., 2015). Recently, it has been shown that dietary supplementation with oleic acid reduces intestinal inflammation and tumor development in mice (Ducheix et al., 2018). In olive, oleic acid content ranges from 57% to 78%, while linoleic acid varies between 7% and 19% (Salas et al., 2000). A significant negative correlation exists between oleic and linoleic acid content (Sabetta et al., 2013; Hernández et al., 2017) since linoleic acid is directly formed by desaturation of oleic acid, which is catalyzed by the oleate desaturase activity (Shanklin and Cahoon, 1998). To date, oleate desaturase encoding gene (*FAD2*) has been isolated and characterized from many plant species, such as rapeseed (Yang et al., 2012), soybean (Heppard et al., 1996; Li et al., 2007), sunflower (Hongtrakul et al., 1998; Martínez-Rivas et al., 2001), peanut (Jung et al., 2000; Chi et al., 2011), flax (Krasowska et al., 2007), safflower (Guan et al., 2012a; Guan et al., 2012b; Cao et al., 2013), sesame (Jin et al., 2001), and cotton (Liu et al., 1999; Zhang et al., 2009). Arabidopsis has only a single *FAD2* gene (Okuley et al., 1994), while most of other plant species possess small or large gene families in which each member is specifically or constitutively expressed in different organs. For example, in grape, *FAD2* is encoded by a small *FAD2* gene family with two members (Lee et al., 2012), while in safflower the *FAD2* gene family is unusually large with 11 functionally diverse members (Cao et al., 2013).

In olive, two genes encoding microsomal oleate desaturases (*OepFAD2-1* and *OepFAD2-2*) have been described and well characterized (Hernández et al., 2005; Hernández et al., 2009; Hernández et al., 2011), whereas only one gene corresponding to the chloroplast oleate desaturase (*OeFAD6*) has been reported (Banilas et al., 2005; Hernández et al., 2011). The *FAD2-2* gene has been considered the main responsible for the linoleic acid content in the olive fruit mesocarp until now (Hernández et al., 2009) but recently in wild olive (*Olea europaea* L. subsp. *europaea* var. *sylvestris*), usually named oleaster, five *FAD2* genes were found (Unver et al., 2017). These authors named *FAD2-3* to the previously characterized *FAD2-2* gene (Hernández et al., 2005; Hernández et al., 2009).

The *FAD2* gene is the most important candidate gene for the linoleic acid biosynthesis in other species as well (Okuley et al., 1994; Belò et al., 2008; Singh et al., 2009; Guan et al., 2012a; Guan et al., 2012b; Font i Forcada et al., 2012);. Several studies focused on this key gene in order to modify the enzyme activity for enhancing the oleic acid content through natural or induced

mutations in different species (Tanhuanpää et al., 1998; Hu et al., 2006; Mroczka et al., 2010; Yang et al., 2012; Wells et al., 2014).

However, in the cultivated olive studies aiming to evaluate natural allele variation in modulating the fatty acid composition are still scarce (Ipek et al., 2015; Ben-Ayed et al., 2017; Cultrera et al., 2019). Hernández et al. (2017) found the co-localized QTLs for oleic and linoleic acids, as well as for monounsaturated and polyunsaturated fatty acids, and for the oleic/linoleic ratio in linkage group 20 of Arbequina cultivar. However, the authors did not individuate a single segregating locus controlling the biosynthesis of oleic and linoleic acids. Fine-mapping of this QTL region and the analysis of sequence data are needed in order to highlight the genetic-molecular mechanism underlying the intra-specific natural variation of fatty acid composition in olive oil.

Most of *FAD2* genes isolated in several plant species carry out in their 5′-UTR a large intron, which plays a role in the enhancement of *FAD2* gene expression (Kim et al., 2006; Mroczka et al., 2010; Xiao et al., 2014; Zeng et al., 2017). In sesame, *cis*-elements having a role for the intron-mediated enhancement of *FAD2* gene expression and the promoter-like activity of the intron sequence were identified. The sesame and Arabidopsis *FAD2* introns conferred up to 100-fold enhancement of GUS expression in transgenic tissues of *Arabidopsis* as compared with intron-less controls (Kim et al., 2006).

To clarify the molecular mechanism underlying the natural variation of oleic and linoleic acid content in olive tree species, the *FAD2* 5′UTR intron was analyzed in this work through a bioinformatic, structural, and association study conducted in 97 olive varieties.

MATERIALS AND METHODS

Plant Materials

The research was carried out at the CREA Research Centre for Olive, Citrus, and Tree Fruit official olive tree collection located in Mirto Crosia, Cosenza, Italy on the Ionian coast (39° 37′ 00′′ North latitude, 16° 45′ 53′′ East longitude) at 6 m a.s.l. Olive trees were planted since 1997 with four to five replicates for each variety spaced with a regular planting pattern of 4 × 6 m. The collection maintains more than 500 olive cultivars and accessions collecting from other official collections and commercial nurseries. The olive trees are grown using a vase training system, pruned with a turn of 3 years and usually irrigated during the summer with 1200 mc/ha on average using a localized drip irrigation system. Soil management is mainly characterized by permanent grass. All the cultivars here studied come from Italy with different regional origin (**Table S1**).

Phenotyping

A set of 97 olive varieties was chosen in order to cover the largest range of the phenotypic variability of fatty acid composition into the olive germplasm available into the collection (**Table S1**). Samplings of 10 to 15 kg drupes at the initial stage of veraison, were carried out from 1 or 2 replicate for each cultivar from 2003 to 2007 and olive oil was extracted within 6/12 hours from harvest using a hammer mill "Oliomio 50" (Toscana Enologica Mori). Olive oil samples were packed in 250-ml dark bottles and stored in a fresh place until analysis. The determination of fatty acid composition was evaluated according to the European Commission Regulation. The fatty acid methyl esters (FAMEs) were prepared following the method described by Christie et al. (1998). FAMEs were obtained by treating 0.15 g of oil with 100 µl of a methanolic solution of 2N potassium hydroxide and n-hexane to make up a final volume of 1.5 ml. The resulting solution was shacked vigorously for 5 min at room temperature. Afterwards, an aliquot of the supernatant (0.2 µl) was dissolved in n-hexane to make up a final volume of 2 ml from which 20 µl were injected into a gas chromatographer (GC). The analyses were conducted by means of an Agilent GC (6890N) equipped with a capillary column SP-2340 (60 m × 0.25 mm i.d., 0.2 µm f.t., Supelco) and a flame ionization detector (FID). Nitrogen was used as carrier gas. The temperature of the column, injector, and detector were set at 180°C, 230°C, and 260°C, respectively. The separation of the analytes was carried out by programming the temperature as follows: 110°C held for 5 min, increase of 3°C/min to 150°C and held for 16 min, increase of 4°C/min to 230°C and held for 27 min. Peaks were identified by comparing their retention times with those of authentic reference compounds. The results were expressed as relative area percent of total FAMEs. Because of the high degree of correlation between oleic and linoleic fatty acids (Sabetta et al, 2013; Hernández et al., 2017), both fatty acids were taken in account.

Climate parameters (average temperature and rainfall) were registered under the same period, from April to November, kindly provided by ARSAC, Agrometereology Service. Pearson and Spearman correlation coefficients of the both climate and phenotypic traits among years were calculated using the PAST software (Hammer et al., 2001).

Population Structure Analysis

SSR analysis was conducted according to Ben Mohamed et al. (2017) using a set of 21 microsatellite markers. A combination of three SSR loci was used in multiplex PCR amplification strategy. DCA3-6Fam, DCA18-6Fam, DCA8-VIC, DCA5-VIC, DCA11-PET, DCA16-6Fam, DCA9-NED (Sefc et al., 2000), GAPU82-NED, GAPU71B-6Fam, (Carriero et al., 2002), UDO4-VIC, UDO12-NED, UDO15-NED (Cipriani et al., 2002) and EMO090-NED (De la Rosa et al., 2002), OLEST1-6Fam, OLEST7-PET, OLEST9-6Fam, OLEST12-6Fam, OLEST14-VIC, OLEST15-VIC, OLEST20-NED, OLEST23-PET (Mariotti et al., 2016) loci were used in this work. PCR products were separated on an ABI PRISM Genetic Analyzer 3130xl (Applied Biosystems Inc., Foster City, CA, USA). Frantoio and Leccino authenticated cultivars were included into the analysis as internal reference to verify the correctness of molecular data. SSR fragments were analyzed by Gene Mapper 3.7 software (Applied Biosystems, USA).

The data obtained by scoring of SSR profiles were used to evaluate the genetic structure of population using STRUCTURE v.2.3.4 (Pritchard et al., 2000) software with K ranging from 1 to 12. The admixture model with correlated allele frequency, a

burn-in length of 100.000 followed by 100.000 runs at each K, with three iterations for very K, were used. The true value of K was determined by the Evanno method (Evanno et al., 2005) implemented in Structure Harvester web version 0.6.93 (Earl and Von Holdt, 2012). The Wright's inbreeding coefficient Fst was calculated using PopGene 1.32.

Cloning and Sequence Analysis of *FAD2-2* Genomic Clone Including 5′UTR Intron

Genomic DNA from young and healthy leaves collected from the same 97 olive cultivars was prepared using the GenElute™ Plant Genomic DNA Miniprep Kit (Sigma-Aldrich), according to the manufacturer's protocol. DNA quantification and quality evaluation were carried out by the NanoDrop 2000 spectrophotometer (Thermo Scientific) and samples were then diluted to 10 ng/μl. *Oep*FAD2-2 cDNA sequence isolated from olive by Hernández et al. (2005) was used as template for drawing primer pairs for targeted PCR gene-walking approach to isolate the complete *FAD2-2* gene in the olive cv. Nocellara Messinese. At first, two gene-specific primers (F: 5′-TGAAGGGCGAGCAGTGTGT-3′; R: 5′-CAACTCATTTGATCTTCAACAACCA-3′) were drawn on the 5′ and 3′ terminals of the full-length cDNA sequence, available at the NCBI database (accession n. AY733077.1). These primers amplified the whole genomic region of the gene, which turned out to be much longer than the cDNA sequence; different rounds of nested PCRs followed by direct amplicon sequencing were then performed until the entire genomic sequence was covered. Amplification reactions were performed in a final volume of 20 μl in the presence of 20 ng template DNA, 1× PCR buffer, 1.5 mM of $MgCl_2$, 0.5 μM of forward and reverse primers, 0.2 mM of each deoxynucleotide, and 1U Taq DNA polymerase (Invitrogen by Life technologies). Polymerase chain reactions were performed, using a Verity™ Thermal Cycler (Applied Biosystems), as follows: 94°C for 3 min followed by 35 cycles at 94°C for 45 s, 56°C for 30 s, 72°C for 1 min and 30 s, then 72°C for 10 min. PCR products were analyzed on 1.2% agarose gel in 1X TAE. Subsequently, the olive *FAD2-2* gene was sub-cloned into six fragments of approximately 600 bp in PCR-XL-TOPO® vector (Invitrogen by Life technologies) and the recombinant vectors were transformed into competent *E. coli* cells, following the manufacturer's protocol. The primer list is reported in **Table S2**.

Direct sequencing in both directions of the PCR products was performed on an ABI3130 Genetic Analyzer (Applied Biosystems-Hitachi, United States) using the ABI Prism BigDye Terminator v.3.1. Ready Reaction Cycle Sequencing Kit (Applied Biosystems). An overlapping region on both ends of at least 100 bp from each gene fragment allowed the reconstruction of the entire genomic sequence. The obtained sequences were aligned to the reference cDNA sequence (Hernández et al., 2005) and assembled by SeqMan v.7.0.0 (DNASTAR Lasergene) leading to the two alleles of the gene. In order to confirm the data about homozygous/heterozygous samples for the 117 bp insertion/deletion obtained from the sequence alignment, a gene-specific primer pair (F:5′-CAAGGGATGTTAGGTTGCAG-3′; R:5′-GAGAAATATCAACATCTGTAGGC-3′) was drawn on the sequence fragment containing the insertion/deletion, the DNA of the remaining 96 cultivars was amplified and the corresponding PCR products were analyzed on 1.2% agarose gel in 1X TAE.

In order to evaluate the polymorphisms in the 5′UTR intron, four fragments of about 550 nucleotides length in the intron region of the *FAD2-2* gene were amplified with a set of specific primers (**Table S3**) and sequenced by Sanger method in the 96 olive cultivars selected. Sequence alignment was conducted using the same software above described and SNPs, indels mutations were identified excluding rare SNPs and Indel with a frequency <5%.

The two allelic forms of *FAD2-2* gene of the cv. Nocellara messinese were aligned between them by Clustal Omega Mega-Multiple Sequence Alignment with the Neighbor-joining method (https://www.ebi.ac.uk/Tools/msa/clustalo/10122018), then they were aligned to cv. Farga (Cruz et al., 2016) (https://blast.ncbi.nlm.nih.gov/Blast.cgi/10122018) and var. *sylvestris* (Unver et al., 2017) whole genomes. A publicly available web database, PlantCARE (http://bioinformatics.psb.ugent.be/webtools/plantcare/html/10112018), was used to locate *Cis*-Acting Regulatory Elements in the intron sequence. The intron region of the two allelic forms of *FAD2-2* isolated in *Olea europaea* and in some other plant species (*Sesamum indicum*, *Glycine max*, *Arabidopsis thaliana*, *Brassica napus*, *Perilla frutescens*, *Camelina sativa*, *Carthamus oxyacanthus*, *Carthamus persicus*, *Carthamus tinctorius*, *Salvia hispanica, Sinapis alba*) was analyzed by IMEter v2.0 software, its algorithm is a good predictor of how well the intron sequence will enhance gene expression (Parra et al., 2011).

Polymorphism, Linkage Disequilibrium Estimation and Single SNP-Based Association Analysis

DnaSp v6. software was used for DNA polymorphism analysis, haplotype reconstruction from unphased data, intragenic recombination (IR) and linkage disequilibrium (LD) degree. For haplotype reconstruction, the algorithm provided by PHASE (Stephens et al., 2001; Stephens and Donnelly, 2003) was used with 1,000 iterations, thinning intervals equal to 10 and 1,000 burn-in iterations. LD between polymorphic sites was estimated by the correlation coefficient (r) calculated from inferred haplotypes. Both the Fischer's exact test and Chi-square test were used for evaluating significant pairwise associations and Bonferroni correction was also applied. Linkage disequilibrium decay was calculated with the software R 3.4.1 (R Core Team, 2017) by using r^2 parameters.

Single SNP association analysis was conducted using oleic and linoleic acid content data from 2003 to 2007 years. The mixed linear model (MLM) in Tassel 5.2.51v was implemented with the kinship matrix (K matrix) and the Q matrix, in order to take into account the effects of relatedness among varieties and population structure. The K matrix was calculated using Past software from the 21 SSR markers used for the population structure analysis. Correction for multiple testing was carried out using the estimated false discovery rate (FDR) values (Storey and Tibshirani, 2003) in the R package using function *p.adjust*. Markers with FDR ≤ 0.05 were considered significant.

Manhattan plots were visualized using TASSEL 5.2.51v for the single SNP association study. The indels found in the 5′UTR intron were treated as a single polymorphism and computed in association analysis. The TASSEL 5.2.51v software calculates genotypic effect and not allele effect as deviations from the estimated value of the genotypic class with lowest frequency. The class with lowest frequency is set as zero effect, then the other genotype effects are given as deviations between their estimated values and the lowest frequency class.

RESULTS

Phenotyping: Fatty Acid Composition Variation

Average rainfall and temperature registered were in a range between 240 (2004) and 658 mm (2005) and 20°C (2005) to 23°C (2003) (**Figure S1**) under the period 2003 to 2007. Highly significant correlations were obtained for temperature among the years with a Pearson's correlation index ranging from 0.95 to 0.99 while no significant correlations were observed for rainfall among the year except for 2003, 2004 versus 2007 year (**Table 1**), indicating a large rainfall fluctuation over the years. A wide range of variation was observed for the acidic composition (oleic acid: 53–78%; linoleic acid: 3.4–22.5%) covering a large part of the natural variation described for olive (**Table S1**).

Since the frequency of phenotypic data showed an asymmetric distribution (**Figure 1**), correlation indexes were calculated using a nonparametric statistical test (Spearman's correlation index). High significant correlations were observed for both oleic and linoleic acid content among the years at high significance level (P = 0.01). The Spearman's correlation index ranged from 0.65 to 0.9 and from 0.61 to 0.9 for oleic and linoleic acid, respectively (**Table 1**).

Population Structure Analysis

The population structure analysis conducted on the 97 olive varieties using a set of 21 SSR markers leaded to 2 main groups, here named 'Red' and 'Green' (**Figure S2**). A differentiation related to geographic origin was discovered for Sicily and Sardinia cultivars belonging mainly to the red group, while almost all the Abruzzo and Molise cultivars were clustered in the green group. Worthy to note, that almost all the cultivars from Abruzzo clustering in the green group showed a reduced oleic acid content on average (63.64%) in respect of cultivars from Sicilia and Sardinia belonging to the red group showing on average oleic acid content of 68.7% and 68.9% respectively. However, the red and green groups showed a weak difference each other for the oleic acid content, on average 69.3% and 67.5% respectively.

Not a clear differentiation related to geographic origin was highlighted for the other varieties and a lot of admixed genotypes were found. Membership >0.9 was found for the following group of varieties: "Ghiannara," "Procanica," "Reale," "Corsicana da olio," "Nostrale di Fiano Romano," "Ottobrina," "Gaggiolo," and "Mignolo." This group of cultivars was considered of clonal origin and excluded from association analysis except one of them ("Mignolo") considered as reference cultivar.

The Wright's inbreeding coefficient Fst (Fst = 0.033) confirmed a low degree of population differentiation.

Genomic Organization, Polymorphisms and Cis-Regulatory Elements of the Olive *FAD2-2* Gene 5′UTR Intron

The molecular cloning of *FAD2-2* gene in cv. Nocellara messinese, led to isolate two heterozygous allelic forms, here named *OeFAD2-2a* and *OeFAD2-2b* of 3535 bp and 3624 bp length characterized by 2143- and 2242-bp single introns in the 5′UTR, respectively (**Figure 2A**). Their sequences were deposited in GenBank database (Accession numbers MN586855 and MN586856 respectively). The alignments of *OeFAD2-2a* and *OeFAD2-2b* to both wild and cultivated olive whole genomes allowed to locate *OeFAD2-2* on chromosome 17 (Unver et al., 2017) and scaffold Oe6_s00121 (Cruz et al., 2016).

The alignment of the intron regions between the two allele forms revealed three indels: 117, 13, and 5 bp length (**Figure 2A**). The insertion of 117 bp showed two long duplications of 49 and 53 bp (**Figure 2B**) and allowed to distinguish 10, 31, and 45

TABLE 1 | Pearson correlation indexes (A, B) for climate parameters and Spearman correlation indexes (C, D) for fatty acid composition among years. The asterisks indicate the significance of statistical test.

A

Temperature	2003	2004	2005	2006
2004	0.95***			
2005	0.95***	0.95***		
2006	0.97***	0.98***	0.98***	
2007	0.97***	0.98***	0.98***	0,99***

B

Temperature	2003	2004	2005	2006
2004	−0.04			
2005	−0.05	0.04		
2006	−0.05	0.33***	−0.05	
2007	0.15*	0.07	−0.04	0.07

C

Oleic acid	2003	2004	2005	2006
2004	0.83***			
2005	0.9***	0.88***		
2006	0.69***	0.65***	0.71***	
2007	0.83***	0.88***	0.9***	0.67***

D

Oleic acid	2003	2004	2005	2006
2004	0.8***			
2005	0.8***	0.9***		
2006	0.6***	0.61***	0.6***	
2007	0.7***	0.6***	0.86***	0.61***

**significant (P = 0.05); ***high significant (P = 0.01).*

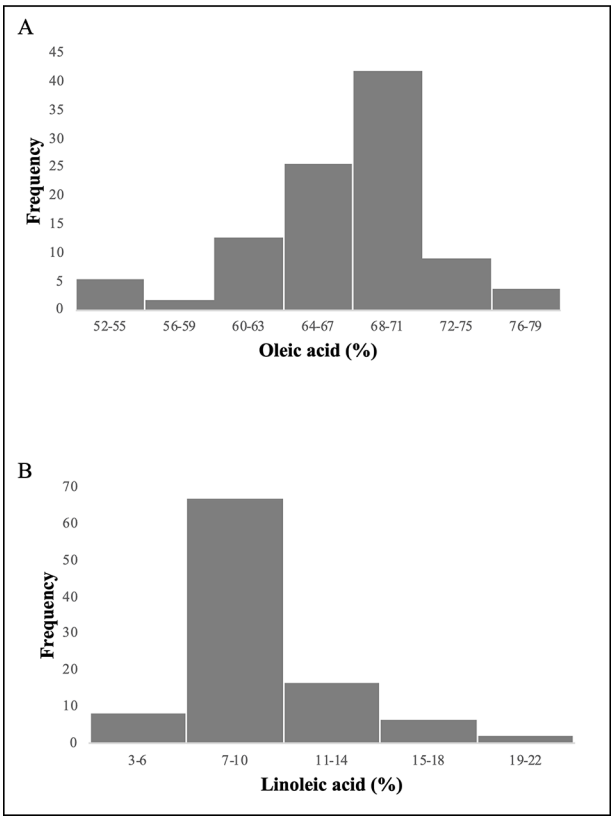

FIGURE 1 | Frequency distribution of the 97 olive varieties for oleic acid **(A)** and linoleic acid **(B)** content.

cultivars in homozygous deletion, homozygous insertion, and heterozygous status, respectively.

Intron sequences showed standard splicing borders GT … AG and were located 11bp from the ATG translation initiation codon. The GC content was 31% indicating a rich component of A+T typically found in other 5′UTR introns (Lozinsky et al., 2014).

The *OeFAD2-2b* intron sequence was analyzed for known *cis*-acting elements through a web search of publicly available database (PlantCARE). Several *cis*-acting regulatory elements were found (**Figure 3**, **Table S4**), most of them similar to those found in the *SeFAD2* promoter, leading us to speculate a promoter-like role for intron sequence in olive too. The analysis of the intron region of the two allelic forms *OeFAD2-2a* and *OeFAD2-2b* by IMEter v2.0 software revealed a score of 18.11 and 18.24 respectively, higher than *Sesamum indicum* (11.65) and *Brassica napus* (11.76) scores as reported in (**Table S5**). The higher the IMEter score, the more likely the intron is expected to enhance gene expression; in particular, introns that moderately enhance expression tend to have IMEter v2.0 scores above 10 and introns that strongly enhance expression tend to have scores above 20. The pentamer CGATT appears to be an important part of the Intron-Mediated Enhancement (IME) signal, in fact is one of many pentamers used by the IMEter to score introns, and it is the pentamer which shows the biggest difference in frequency between a set of promoter-proximal and promoter-distal introns (Parra et al., 2011). This sequence was detected twice in the 5′ UTR intron sequence of *OeFAD2-2*, within TATA box and TGACG-motif/TATAbox, respectively (**Figure 3**).

The SNPs and indel analysis conducted on the 5′UTR intron of the 97 olive cultivars detected 39 SNPs (**Figure 3**). Considering a whole length of the longest of the 5′UTR intron (2242 bp) and excluding indels, a SNP frequency of 1/53 bp was observed. All the selected SNPs were considered common (minor allele frequency > 5%). Among the 39 SNPs individuated, 7 were located within or in close vicinity of *cis*-regulatory elements (**Figure 3**).

Polymorphism Diversity and Linkage Disequilibrium Estimation

Nucleotide diversity (π) was estimated at 0.0038 indicating a high genetic diversity within the population sample further encouraging the association study. The number of the reconstructed haplotypes by using the DnaSP software was 115. The level of LD between pairs of loci using the inferred haplotypes data of the association population, provided high significant correlations among 16 SNP polymorphisms (**Table 2**) with a range of R from −0.17 to 1. Negative signals indicated a negative correlation between SNPs frequency. The highest positive correlations were found among the following polymorphisms: SNP9, SNP13, SNP14, SNP15, SNP20 with a range of R varying from 0.81 to 1 and between SNP23 and SNP26 with a 0.87 correlation index (**Table 2**). LD decay calculated using inferred haplotypes showed a very quickly decay with a R^2 dropping to < 0.1 at least 200bp distance within the 5′UTR intron of *FAD2-2* gene (**Figure 4**). The intragenic recombination test confirmed this pattern indicating 174 different recombination events in the 115 calculated haplotypes with 19 minimum number of recombination events. Tajima neutrality test was not statistically significant (D = 0.84) indicating no selection pressure for the 5′UTR intron.

Trait-Marker Association Analysis

The association analysis, carried out between 39 SNPs and oleic and linoleic acid content for 4 years, using the mixed linear model (MLM) with Q matrix and kinship included, allowed to individuate 20 significant associations (P< 0.05) after correction for multiple testing, for 7 SNPs (**Figure 5**). The SNP3, SNP23, SNP26 and SNP29 resulted significantly associated in three years, the SNP16 in two years, while the SNP2 and the SNP19 were significant only for one year (**Figure 5**). Among the indels analyzed, only the 13bp indel was significantly associated to both oleic and linoleic acid but only in 2006 year (data not shown). Marked differences in oleic acid content were observed between homozygous and heterozygous genotypes for SNP3, SNP23, and SNP26 (**Figure 5**) for all three years where they resulted significantly associated. This pattern of gene action suggested an over- or under dominance effects. Homozygous genotypes decreased oleic acid content with the same pattern for all three years with a negative effect of −3 and −10 for TT and CC

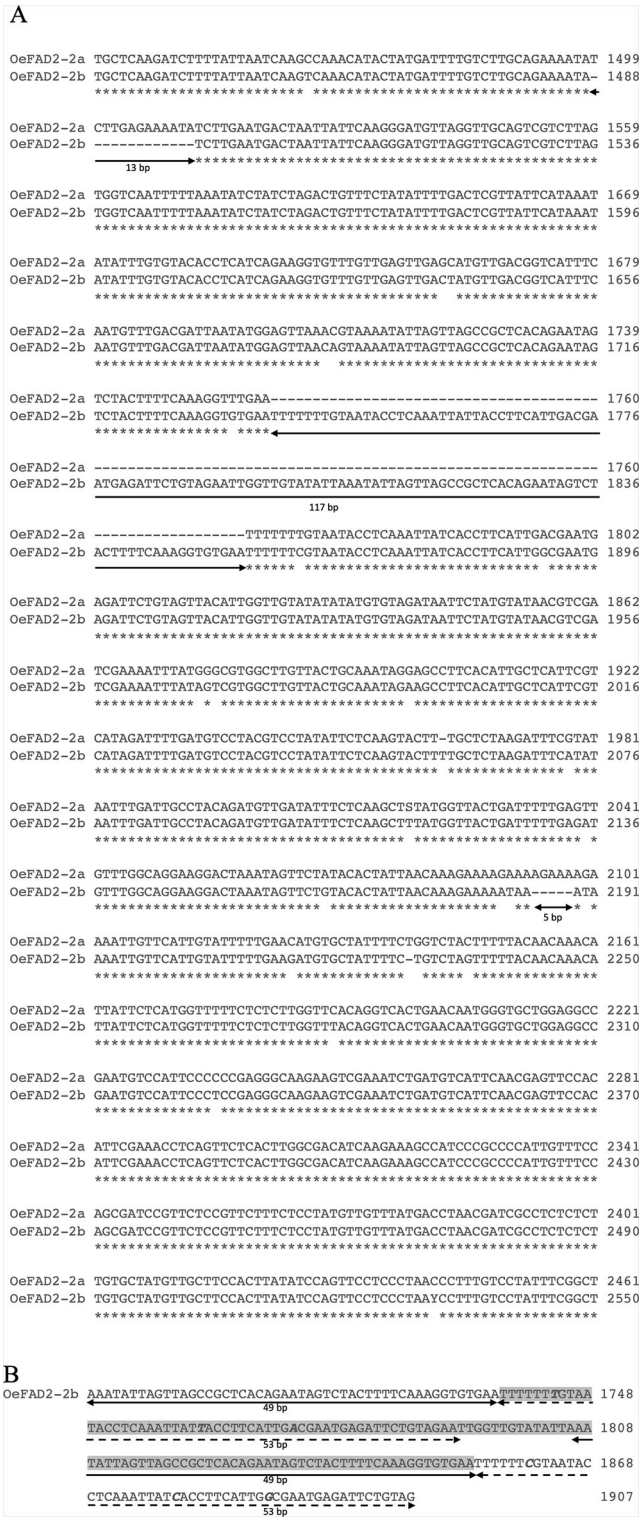

FIGURE 2 | (A) Alignment of a fragment of the intron region of *OeFAD2-2a* and *OeFAD2-2b* from cultivar Nocellara messinese. Three long indels of 13 bp, 117 bp and 5 bp, respectively, are underlined. **(B)** Partial view of *OeFAD2-2b* intron region spanning the 117 nucleotide-long insertion (highlighted in grey). Two stretches of 49 nucleotides (underlined with a solid black line) and 53 nucleotides (dashed black line) are duplicated. Polymorphic bases within duplications are marked in bold italic. * Similar nucleotide.

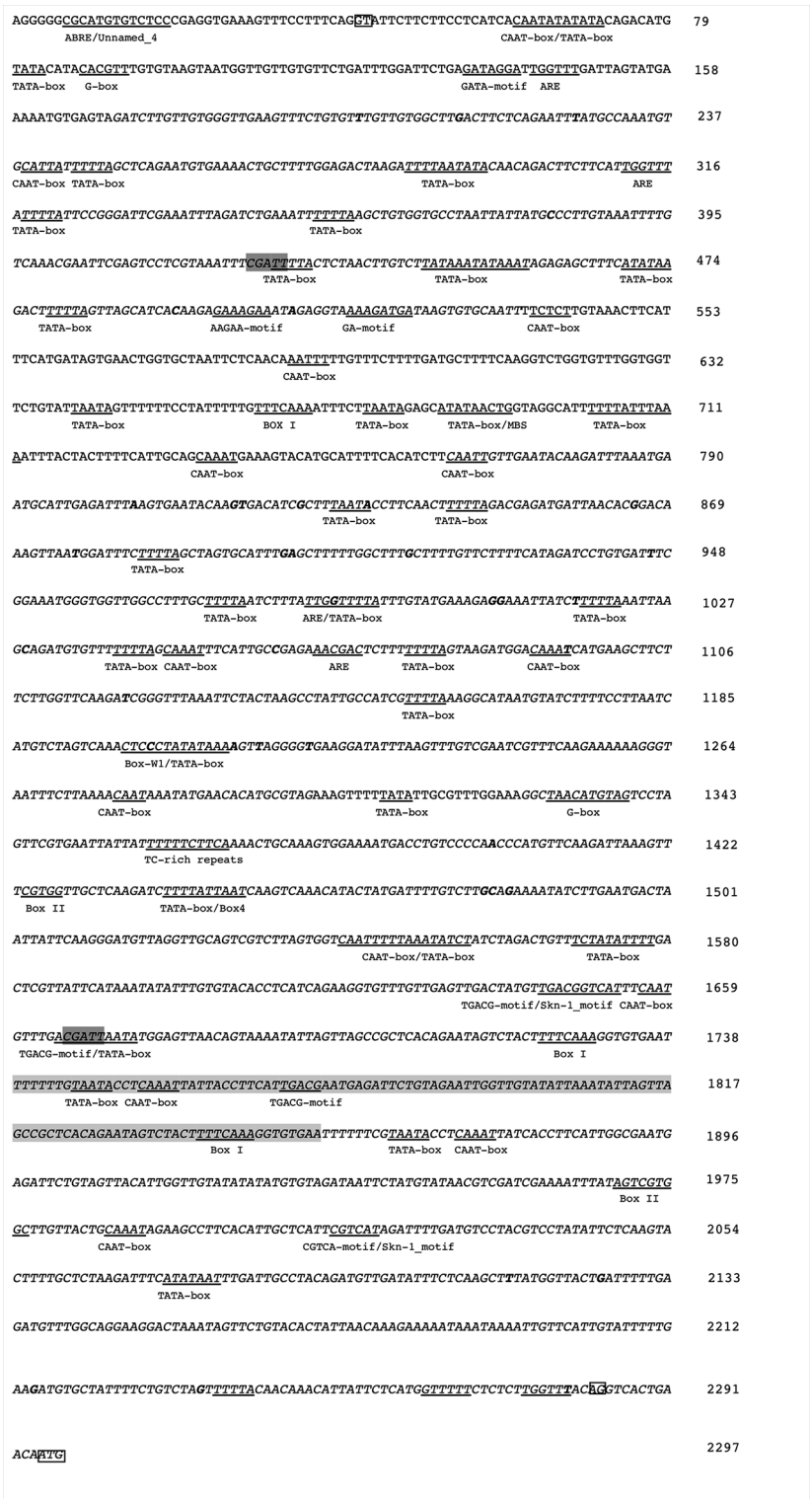

FIGURE 3 | Partial nucleotide sequence of the *OeFAD2-2b* 5′UTR from olive cultivar Nocellara messinese. In italics the sequence regions analyzed in other 96 cultivars and in bold single-nucleotide polymorphisms (SNPs). In the boxes, the GT and AG dinucleotides at both ends of the intronic region and ATG as translational initiation are shown. The insertion of 117bp, not present in the sequence of the *OeFAD2-2a* allele, is shaded grey. In dark grey the pentamer CGATT belonging to IME signals. Moreover, several potential *cis*-regulatory elements are underlined and designated with the names of each of the motifs.

genotypes, respectively, versus the heterozygous genotype in the SNP3. Similar values of genotype effects were observed for both the SNP23 and SNP26, with −5 and −6 values for the CC and TT homozygous genotypes. Less marked differences were observed for linoleic acid content (**Figure 5**), probably due to the minor range of variation. Interestingly, genetic population structure analysis clustered almost all the Abruzzo cultivars in a single group showing the CC/TT homozygous genotype for both the SNP23 and SNP26 except the cultivar Dritta showing heterozygous genotype for the latter SNP.

The SNP26 was located within the joint elements box-W1/TATA box (**Figure 3**). The SNP2 resulted significantly associated only to the linoleic acid in 2004 with a gene action pattern consistent with an additive effect. The SNP16 seemed to show a similar pattern too. The SNP19 had a pattern probably consistent with an over dominance effect considering the great increment of linoleic acid by heterozygous genotype in respect of that of two homozygous one. The indel of 13bp resulted significantly associated after multiple testing correction (data not shown) for 10 individual polymorphisms contributing to explain 13% and 9% phenotypic variance for the oleic and linoleic acid content, respectively. The proportion of phenotypic variation explained by the associated SNPs and indel varied among the years ranging from 7% to 16% (**Figure 5**). On average SNP3, SNP23, SNP26 explained the major phenotypic variance with 9.7%, 9.6% and 11% for oleic acid content.

DISCUSSION

In this work, starting from the cDNA of the *FAD2-2* gene isolated from Hernández et al. (2005), a complete genomic clone was isolated by a gene-walking approach and four fragments of the 5′UTR intron were characterized through an *in silico* and structural analysis with the aim to explore the natural allelic variability of *FAD2-2* in 97 olive varieties and its role in the gene expression regulation. The molecular cloning of *FAD2-2* gene allowed to distinguish two allelic forms, *OeFAD2-2a* and *OeFAD2-2b*. A single intron in the 5′UTR was isolated, and three indels were individuated. In particular, the insertion of 117 bp showed very interestingly two long duplications of 49 and 53 bp. No duplications have been previously individuated in the 5′UTR intron of *FAD2-2* genes in olive. Similarly, Cultrera et al. (2019) analyzing polymorphisms of different gene fragments belonging to crucial metabolic pathways, found a tandem duplication made up of a 166 bp motif within *OeSUT1* exon in olive. Zeng et al. (2017) found a transposable element insertion at position −26 bp in the 5′ upstream region from the translation start codon in *FAD2* gene in *Sinapis alba*. Martínez-Rivas et al. (2001) and Cao et al. (2013) asserted the *FAD2* genes family evolved by duplication from constitutive expressed *FAD2* genes, and recently, it was confirmed in wild olive (Unver et al., 2017).

In this work, the hypothetical mechanisms concerning the origin and evolution of introns have not been explored, but the presence of two duplications within the 5′UTR intron led us to speculate other mechanisms could be occurred in the differentiation of *FAD2* genes, such as the multiplication of a preexisting intron by tandem duplication or creation of a new intron by internal gene duplication (Gao and Lynch, 2009; Ma et al., 2016).

It is known that the presence of a 5′UTR intron can enhance gene expression depending on different characteristics of the intron: i) different size of the intron; ii) distribution of the motifs dispersed throughout the 5′ intron region iii) position of intron with respect to the 5′UTR and the translation start site (Chung et al., 2006). The 5′UTR lengths vary dramatically among individual genes in higher eukaryotes and can range from a few to thousands of base pairs. This large range of 5′UTR lengths suggests that there may be greater regulation of specific mRNA subsets (Leppek et al., 2018). Without any doubt, the duplication event here found, increased the size of the intron in the 5′UTR of the *FAD2-2* gene in olive.

The IMEter score here found for *OeFAD2-2a* and *OeFAD2-2b* introns indicated a medium-high induction of the gene expression. Genes with the most powerful IME signals appear to be highly and widely expressed housekeeping genes (Parra et al., 2011). A phylogenetic analysis of FAD2 and FAD6 enzymes conducted by Hernández et al. (2005) led to classify *OeFAD2-2* gene as housekeeping-type. Expression analysis of olive *FAD2-2* gene showed that it is highly expressed in mesocarp and seed during the ripening period of olive fruit (Hernández et al., 2009). Different authors reported a constitutively expression of *FAD2-2* genes but with a differentiated spatial and temporal expression level regulation as well (Jin et al., 2001; Zhang et al., 2009; Dar et al., 2017). *FAD2* genes seem to play a key role for some crucial processes for the plant survival such as fatty acid synthesis, plant development, cold and salt tolerance (Dar et al., 2017). In olive, *FAD2-2* gene was shown to be the main gene responsible for the oleic acid desaturation with a differentiated gene expression during the ripening stages well correlated with linoleic acid biosynthesis pattern (Hernández et al., 2009). Furthermore it seems involved in cold tolerance (Matteucci et al., 2011). It was also shown in olive a different expression level between two olive cultivars, Picual and Arbequina, induced by low and high temperature, darkness, and wounding, without changing the oleic and linoleic acid contents in the mesocarp (Hernández et al., 2011). In addition, in Arbequina cultivar, *FAD2-2* is involved in the response to draught (Hernández et al., 2009). Expression levels of olive *FAD2* genes have also been studied in relation to regulated deficit irrigation and salt stress (Hernández et al., 2018; Moretti et al., 2019)."

The *in silico* analysis of the 5′UTR intron in the *FAD2-2* gene showed *cis*-acting elements putatively involved in above described responses. Additional *cis*-acting elements found in the duplications such as TATA box and CAAT box; TGACG-motif and the Box 1 involved to abscisic acid (ABA) and light response, respectively were found and seem to indicate an evolutionary pathway toward an enhancing of the expression level rather than new functionalization. In fact, it could also have to do with the evolutionary option aiming to maintain high the energetic and time costs to transcribe and splice introns, option

TABLE 2 | Results of the LD analysis where the distance between pair of SNPs and their significant pairwise associations were calculated using both the statistical D′ and R.

SNP1	SNP2	Dist	D′*	R*
SNP5	SNP9	324	–1	–0.175
SNP5	SNP13	383	–1	–0.183
SNP4	SNP9	437	–0.833	–0.186
SNP13	SNP167	1338	–0.835	–0.186
SNP14	SNP167	1313	–1	–0.193
SNP15	SNP167	1312	–1	–0.193
SNP5	SNP20	513	–1	–0.195
SNP12	SNP23	194	–1	–0.196
SNP12	SNP26	337	–1	–0.199
SNP4	SNP14	521	–1	–0.201
SNP4	SNP15	522	–1	–0.202
SNP2	SNP12	653	0.696	0.203
SNP2	SNP25	908	0.228	0.227
SNP4	SNP13	496	–1	–0.233
SNP2	SNP4	169	–0.458	–0.236
SNP6	SNP14	394	0.35	0.239
SNP6	SNP15	395	0.35	0.239
SNP12	SNP25	255	–1	–0.241
SNP2	SNP168	2023	0.636	0.245
SNP14	SNP23	157	–1	–0.263
SNP15	SNP23	156	–1	–0.264
SNP14	SNP26	300	–1	–0.266
SNP15	SNP26	299	–1	–0.267
SNP5	SNP23	565	–0.816	–0.27
SNP4	SNP5	113	0.349	0.273
SNP13	SNP23	182	–0.894	–0.273
SNP5	SNP26	708	–0.819	–0.274
SNP11	SNP12	32	1	0.277
SNP6	SNP20	499	0.333	0.281
SNP2	SNP11	621	–0.329	–0.284
SNP9	SNP23	241	–1	–0.291
SNP20	SNP23	52	–0.905	–0.294
SNP9	SNP26	384	–1	–0.295
SNP11	SNP168	1402	–0.895	–0.298
SNP20	SNP26	195	–0.906	–0.298
SNP6	SNP9	310	0.404	0.306
SNP13	SNP26	325	–1	–0.309
SNP25	SNP168	1115	0.817	0.313
SNP6	SNP13	369	0.401	0.318
SNP4	SNP26	821	–0.754	–0.323
SNP14	SNP25	218	–1	–0.323
SNP15	SNP25	217	–1	–0.324
SNP25	SNP167	1095	0.564	0.337
SNP20	SNP25	113	–0.851	–0.339
SNP11	SNP20	174	0.741	0.34
SNP13	SNP25	243	–0.917	–0.343
SNP4	SNP11	452	0.576	0.344
SNP167	SNP168	20	0.546	0.351
SNP9	SNP25	302	–1	–0.357
SNP11	SNP167	1382	–0.7	–0.362
SNP5	SNP11	339	0.781	0.366
SNP11	SNP13	44	0.856	0.369
SNP4	SNP23	678	–0.875	–0.37
SNP11	SNP15	70	1	0.371
SNP11	SNP14	69	1	0.372
SNP2	SNP6	296	0.673	0.385
SNP2	SNP26	990	0.466	0.387
SNP5	SNP25	626	–0.964	–0.392
SNP23	SNP168	1176	0.845	0.397
SNP6	SNP12	357	0.789	0.402
SNP9	SNP11	15	1	0.412
SNP4	SNP25	739	–0.804	–0.417

(Continued)

TABLE 2 | Continued

SNP1	SNP2	Dist	D'*	R*
SNP2	SNP23	847	0.513	0.421
SNP26	SNP167	1013	0.59	0.426
SNP26	SNP168	1033	0.922	0.428
SNP23	SNP167	1156	0.667	0.488
SNP12	SNP20	142	1	0.604
SNP12	SNP13	12	1	0.644
SNP11	SNP26	369	−0.905	−0.648
SNP9	SNP12	47	1	0.674
SNP23	SNP25	61	0.832	0.679
SNP11	SNP23	226	−0.968	−0.685
SNP12	SNP14	37	1	0.746
SNP12	SNP15	38	1	0.746
SNP25	SNP26	82	0.917	0.757
SNP11	SNP25	287	−0.874	−0.759
SNP9	SNP20	189	0.903	0.81
SNP14	SNP20	105	1	0.81
SNP15	SNP20	104	1	0.81
SNP13	SNP20	130	0.91	0.854
SNP13	SNP14	25	1	0.863
SNP13	SNP15	26	1	0.863
SNP23	SNP26	143	0.88	0.87
SNP9	SNP14	84	1	0.903
SNP9	SNP15	85	1	0.903
SNP9	SNP13	59	0.952	0.91
SNP14	SNP15	1	1	1

**Significant pairwise associations using both the Fischer's exact test and Chi-square test and Bonferroni correction.*

that could be significant enough to influence the organism's phenotype. For instance, some highly expressed genes are found under strong selection to remain intron-poor for transcriptional efficiency, whereas other genes are found to have longer and numerous introns to enhance expression (Lozada-Chávez et al., 2018). No relationships were found when the 117 bp insertion was analyzed for significant associations with the acidic content variation, but other biological processes, here not studied, could be involved.

A double presence of the pentamer CGATT as part of IME signals, the very near location of the intron (11bp) to the translational starting site and the duplications within the sequence probably could contribute overall to enhance the gene expression level (Chung et al., 2006; Lozinsky et al., 2014).

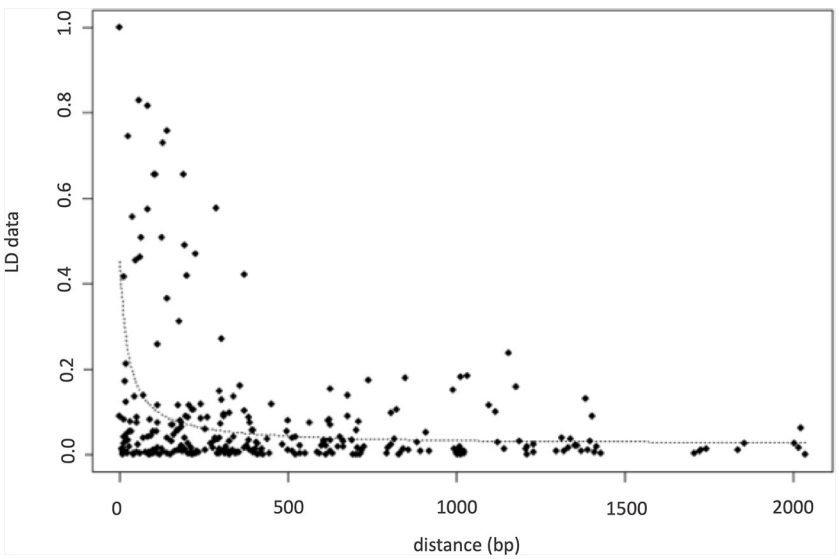

FIGURE 4 | LD decay calculated on inferred haplotypes using r^2 parameters.

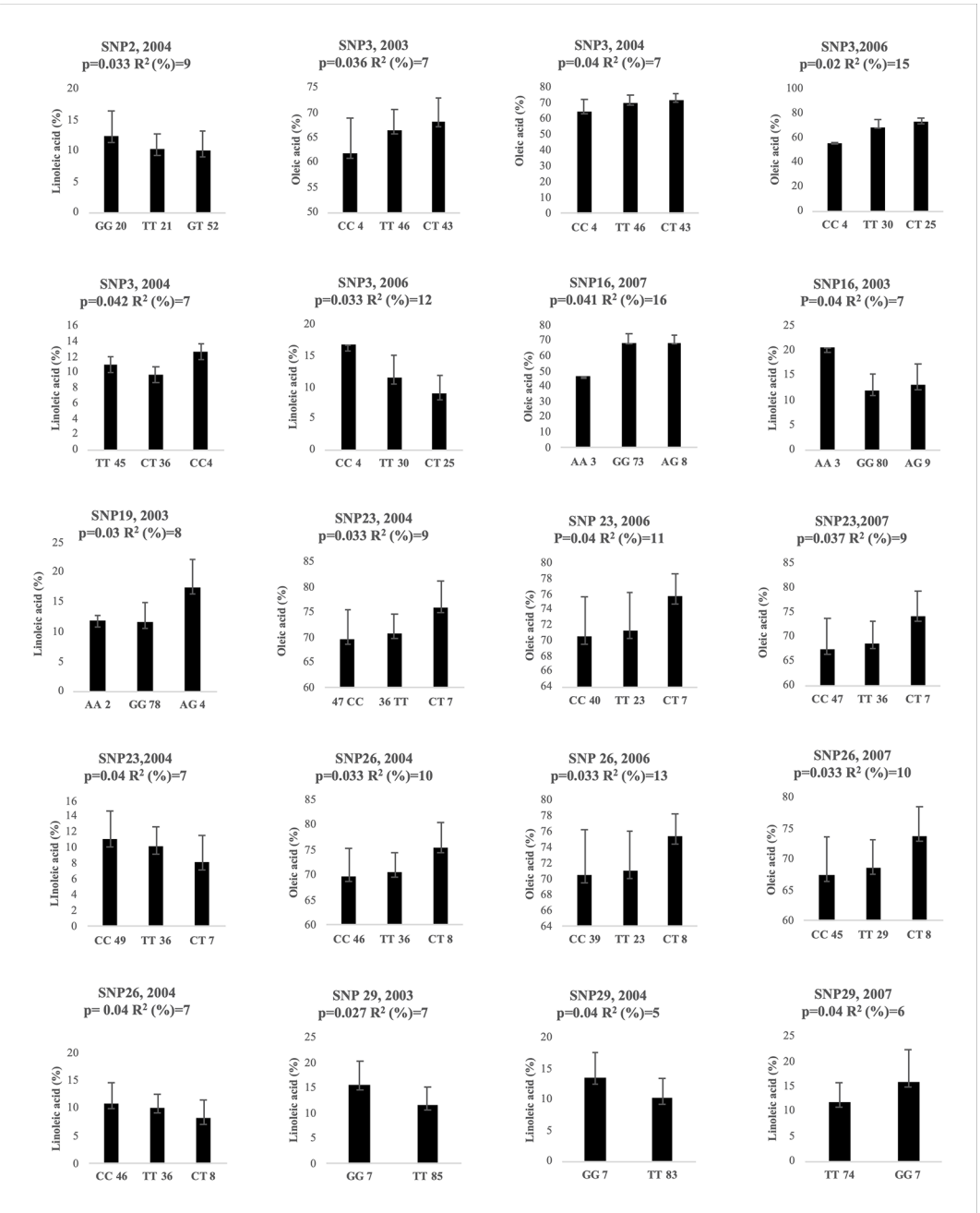

FIGURE 5 | Genotypic effects of the significantly associated SNPs on oleic and linoleic acid content in different years. The X-axis indicates the genotype status of cultivars (letters) and the absolute frequency of genotypes (number). $R^{2:}$ is the statistical used for association analysis and p is the Benjamini-Hochberg Adjusted p value.

The SNP frequency detected in the 5′UTR intron was lower than those found in intron region of genes belonging to the same primary biosynthetic pathway such as acyl carrier protein (ACP) genes (Cultrera et al., 2019), even if this author found on average a higher SNP frequency than other species. Although in this study the neutrality test was not significant, it is worthy to note that 5′UTR introns may be subject to different selective forces from the introns in CDSs and 3′UTRs, possibly due to a specific regulatory role in gene expression (Chung et al., 2006). For instance, differences in the rate of evolution of *FAD2* 5′UTR were found in *Gossypium* species (Liu et al., 2001) suggesting that the selection pressure on these regions could be really different.

Although the Wright's inbreeding coefficient indicated a low degree of population differentiation in general confirmed also by

a weak difference in oleic acid content between red and green group, interesting correlations were observed among almost all the Abruzzo cultivars, (clustering in the green group), their allelic homozygous status for the both SNP23 and SNP26 and oleic acid content. Moreover, the same average oleic acid content found in Sicilian and Sardinian cultivars clustering in the same group, suggested a strong genetic relationship as found also by other authors (Baldoni et al., 2006). Similarly, other authors found a correlation between phenotypic traits and genetic population structure in olive (D'Agostino et al., 2018; Zhu et al., 2019) confirming a high heritability of the analyzed traits (D'Agostino et al., 2018).

The correlation between alleles in a population is stated by LD (Myles et al., 2009). The pattern and extent of LD determines the resolution of association mapping studies (Flint-Garcia et al., 2003). For outcrossing species like most trees, rapid LD decay was reported (Krutovsky and Neale, 2005; Ingvarsson, 2005; Wegrzyn et al., 2010) and for these species, a large number of markers are required to detect significant marker-trait associations (Flint-Garcia et al., 2003; Myles et al., 2009). In fact, a high number of recombination events have been here found and very quick LD decay has been observed, but if the physical position of mutations was known, probably a slower LD decay would had expected as observed by Cultrera et al. (2019).

The association study allowed to individuate 7 SNPs significantly associated to the oleic and linoleic content variation. Some of these associations were confirmed along the years although rainfall fluctuations were observed. These results confirmed the high heritability of fatty acid composition (Ripa et al., 2008; Dabbou et al., 2010; De la Rosa et al., 2016). However, a low number of genotypes associated with a few SNPs (SNP3, SNP16 and SNP19) for the trait "low oleic/high linoleic content" were observed due to a sampling bias of the population that explains in fact the asymmetric distribution of the frequency classes for oleic and linoleic acid traits. This pattern of distribution of phenotypic variation will need to be enlarged in the future studies.

All the SNPs significantly associated, were located near or outside of the *cis*-acting elements putatively involved in fatty acid biosynthesis regulation. The 5′ and 3′ untranslated regions (UTRs) are non-coding and do not directly contribute to the protein sequence. Free from the constraints of encoding proteins, UTRs can form considerable Watson–Crick and non-canonical base pairing that can potentially impact every step of translation (Leppek et al., 2018). Despite the evolutive conservation of the 5′ UTR intron, the high structural variability found among and within the species makes difficult to speculate about a specific regulation mechanism (Lozinsky et al., 2014).

All the associations identified in this study explained a small proportion of the phenotypic variance. These small effects attributed to individual SNPs were consistent with earlier studies in accordance with polygenic quantitative models of plant traits (Eckert et al., 2009; Tian et al., 2014).

Although a higher number of genotypes probably are needed in olive, two SNPs in high LD seem to give a contribute to the oleic acid increasing/linoleic acid reduction in a genotypic way referring to a under/over-dominance effect of the heterozygous CT genotypes. These results are consistent with the high heterozygous status of the olive genome (Muleo et al., 2016) and led us to speculate that acidic composition variation within *Olea europaea* L. species might be regulated by mutations within the *FAD2-2* 5′UTR intron.

In conclusion, our work confirmed the presence of a large intron within the 5′UTR of the *FAD2-2* gene also in the olive tree, highlighting the presence of a double duplication. The *in silico* analysis addressed us toward a putative role of the 5′UTR intron in the regulation of gene expression showing several *cis*-regulatory elements. Furthermore, the LD and association analysis showed that the SNP23 and SNP26 resulted strictly associated each other and seemed to contribute to the increase of oleic acid/reduction of linoleic acid. These results will be validated by an analysis of gene expression in order to confirm the putative regulation mechanisms here raised.

DATA AVAILABILITY STATEMENT

The sequencing data has been deposited in GenBank and can be found using the following accession numbers: Oe-FAD2-2a (BankIt2272927 Seq1 MN586855) and Oe-FAD2-2b (BankIt2272927 Seq2 MN586856).

AUTHOR CONTRIBUTIONS

SZ designed, wrote the manuscript, statistical analysis about phenotyping, genetic population structure, LD and association mapping study. AS and SM isolated FAD2-2 full gene, 5′UTR intron. AS conducted SSR genotyping and all the bioinformatic analysis. FC and AT helped for bioinformatic and statistical analysis. FL conducted running of SSR fragments to the genetic sequencer. CB, ER, MP, and EP conducted phenotyping for chemical composition of olive oil. AI conducted statistical analysis using R software package.

ACKNOWLEDGMENTS

The authors are really grateful to Mr. Caterisano and Mr. Cirone from ARSAC, Agrometeorology Service for agrometeorological data providing.

SUPPLEMENTARY MATERIAL

The Supplementary Material for this article can be found online at: https://www.frontiersin.org/articles/10.3389/fpls.2020.00066/full#supplementary-material

REFERENCES

Alagna, F., Cirilli, M., Galla, G., Carbone, F., Daddiego, L., Facella, P., et al. (2016). Transcript analysis and regulative events during flower development in olive (*Olea europaea* L.). *PloS One* 11 (4), e0152943. doi: 10.1371/journal.pone.0152943

Aranzana, M. J., Abbassi, E. K., Howad, W., and Arús, P. (2010). Genetic variation, population structure and linkage disequilibrium in peach commercial varieties. *BMC Genet.* 11, 69. doi: 10.1186/1471-2156-11-69

Atienza, S. G., De la Rosa, R., Leon, L., Martin, A., and Belaj, A. (2014). Identification of QTL for agronomic traits of importance for olive breeding. *Mol. Breeding.* 34, 725–737. doi: 10.1007/s11032-014-0070-y

Baldoni, L., Tosti, N., Ricciolini, C., Belaj, A., Arcioni, S., Pannelli, G., et al. (2006). Genetic Structure of Wild and Cultivated Olives in the Central Mediterranean Basin. *Ann. Bot.* 98, 935–942. doi: 10.1093/aob/mcl178

Banilas, G., Moressis, A., Nikoloudakis, N., and Hatzopoulos, P. (2005). Spatial and temporal expressions of two distinct oleate desaturases from olive (*Olea europaea* L.). *Plant Sci.* 168, 547–555. doi: 10.1016/j.plantsci.2004.09.026

Barnaud, A., Laucou, V., This, P., Lacombe, T., and Doligez, A. (2010). Linkage disequilibrium in wild French grapevine, *Vitis vinifera* L. subsp. silvestris. *Heredity.* 104, 431–437. doi: 10.1038/hdy.2009.143

Belò, A., Zheng, P., Luck, S., Shen, B., Meyer, D. J., Li, B., et al. (2008). Whole genome scan detects an allelic variant of fad2 associated with increased oleic acid levels in maize. *Mol. Genet. Genomics* 279, 1–10. doi: 10.1007/s00438-007-0289-y

Belaj, A., Del Carmen Dominguez-García, M., Atienza, S. G., Martín Urdíroz, N., De la Rosa, R., Satovic, S., et al. (2012). Developing a core collection of olive (*Olea europaea* L.) based on molecular markers (DArTs, SSRs, SNPs) and agronomic traits. *Tree Genet. Genomes.* 8, 365–378. doi: 10.1007/s11295-011-0447-6

Belaj, A., De la Rosa, R., Lorite, I. J., Mariotti, R., Cultrera, N. G. M., Beuzón, C. R., et al. (2018). Usefulness of a new large set of high throughput EST-SNP Markers as a tool for olive germplasm collection management. *Front. Plant Sci.* 9, 1320. doi: 10.3389/fpls.2018.01320

Ben Mohamed, B., Zelasco, S., Ben Ali, S., Guasmi, F., Triki, T., Conforti, F. L., et al. (2017). Exploring olive trees genetic variability in the South East of Tunisia. *Genet. Mol. Res.* 16, 4. doi: 10.4238/gmr16039850

Ben Sadok, I. B., Celton, J. M., Essalouh, L., Aabidine, A. Z. E., Garcia, G., Martínez, S., et al. (2013). QTL mapping of flowering and fruiting traits in olive. *PloS One* 8, e62831. doi: 10.1371/journal.pone.0062831

Ben-Ayed, R., Ennouri, K., Ben Hlima, H., Smaoui, S., Hanana, M., Mzid, R., et al. (2017). Identification and characterization of single nucleotide polymorphism markers in *FADS2* gene associated with olive oil fatty acids composition. *Lipids Health Dis.* 16, 138. doi: 10.1186/s12944-017-0530-6

Besnard, G., El Bakkali, A., and Francki, M. (2014). Sequence analysis of single-copy genes in two wild olive subspecies: nucleotide diversity and potential use for testing admixture. *Genome.* 57, 145–153. doi: 10.1139/gen-2014-0001

Cao, K., Wang, L., Zhu, G., Fang, W., Chen, C., and Luo, J. (2012). Genetic diversity, linkage disequilibrium, and association mapping analyses of peach (*Prunus persica*) landraces in China. *Tree Genet. Genomes.* 8, 975–990. doi: 10.1007/s11295-012-0477-8

Cao, S., Zhou, X. R., Wood, C. C., Green, A. G., Singh, S. P., Liu, L., et al. (2013). A large and functionally diverse family of *Fad2* genes in safflower (*Carthamus tinctorius* L.). *BMC Plant Biol.* 13, 5. doi: 10.1186/1471-2229-13-5

Carmona, R. M., Zafra, A., Seoane, P., Castro, A. J., Guerrero-Fernández, D., Castillo-Castillo, T., et al. (2015). ReprOlive: a database with linked data for the olive tree (Olea europaea L.) reproductive transcriptome. *Front. Plant Sci.* 6, 625. doi: 10.3389/fpls.2015.00625

Carriero, F., Fontanazza, G., Cellini, F., and Giorio, G. (2002). Identification of simple sequence repeats (SSRs) in olive (*Olea europaea* L.). *Theor. Appl. Genet.* 104, 301–307. doi: 10.1007/s001220100691

Chi, X., Yang, Q., Pan, L., Chen, M., He, Y., Yang, Z., et al. (2011). Isolation and characterization of fatty acid desaturase genes from peanut (*Arachis hypogaea* L.). *Plant Cell. Rep.* 30, 1393–1404. doi: 10.1007/s00299-011-1048-4

Christie, W. W. (1998). "The preparation of derivatives of fatty acids," in *Gas Chromatography Lip* (Ayr, Scotland: The Oily Press).

Chung, B. Y. W., Simon, C., Firth, A. E., Brown, C. M., and Hellens, R. P. (2006). Effect of 5′UTR introns on gene expression in *Arabidopsis thaliana*. *BMC Genomics* 7, 120. doi: 10.1186/1471-2164-7-120

Cipriani, G., Marrazzo, M. T., Marconi, R., and Cimato, A. (2002). Microsatellite markers isolated in olive (*Olea europaea* L.) are suitable for individual fingerprinting and reveal polymorphism within ancient cultivars. *Theor. Appl. Gen.* 104, 223–228. doi: 10.1007/s001220100685

Core Team, R. (2017). R: A language and environment for statistical computing (version 3.4. 1). R Foundation for Statistical Computing, Vienna, Austria.

Cruz, F., Julca, I., Gómez-Garrido, J., Loska, D., Marcet-Houben, M., Cano, E., et al. (2016). Genome sequence of the olive tree, *Olea europaea*. *GigaSci.* 5, 29. doi: 10.1186/s13742-016-0134-5

Cultrera, N. G. M., Sarri, V., Lucentini, L., Ceccarelli, M., Alagna, F., Mariotti, R., et al. (2019). High levels of variation within gene sequences of *Olea europaea* L. *Front. Plant Sci.* 9, 1932. doi: 10.3389/fpls.2018.01932

Dìez, C. M., Trujillo, I., Barrio, E., Belaj, A., Barranco, D., and Rallo, L. (2011). Centennial olive trees as a reservoir of genetic diversity. *Ann. Bot.* 108, 797–807. doi: 10.1093/aob/mcr194

D'Agostino, N., Taranto, F., Camposeo, S., Mangini, G., Fanelli, V., Gadaleta, S., et al. (2018). GBS-derived SNP catalogue unveiled wide genetic variability and geographical relationships of Italian olive cultivars. *Sci. Rep.* 8, 15877. doi: 10.1038/s41598-018-34207-y

Dabbou, S., Rjiba, I., Echbili, A., Gazzah, N., Mechri, B., and Hammami, M. (2010). Effect of controlled crossing on the triglyceride and fatty acid composition of virgin olive oils. *Chem. Biodivers.* 7, 1801–1813. doi: 10.1002/cbdv.200900385

Dar, A. A., Choudhury, A. R., Kancharla, P. K., and Arumugam, N. (2017). The FAD2 Gene in plants: occurrence, regulation, and role. *Front. Plant Sci.* 8, 1789. doi: 10.3389/fpls.2017.01789

De la Rosa, R., James, C. M., and Tobutt, K. R. (2002). Isolation and characterization of polymorphic microsatellites in olive (*Olea europaea* L.) and their transferability to other genera in the Oleaceae. *Mol. Ecol. Notes.* 2, 265–267. doi: 10.1046/j.1471-8286.2002.00217.x

De la Rosa, R., Angiolillo, A., Guerrero, C., Pellegrini, M., Rallo, L., Besnard, G., et al. (2003). A first linkage map of olive (*Olea europaea* L.) cultivars using RAPD, AFLP, RFLP and SSR markers. *Theor. Appl. Genet.* 106, 1273–1282. doi: 10.1007/s00122-002-1189-5

De la Rosa, R., Arias-Calderón, R., Velasco, L., and León, L. (2016). Early selection for oil quality components in olive breeding progenies. *Eur. J. Lipid Sci. Tech.* 118, 1160–1167. doi: 10.1002/ejlt.201500425

Dominguez-Garcia, M. C., Belaj, A., De la Rosa, R., Satovic, Z., Heller-Uszynska, K., Kilian, A., et al. (2011). Development of DArT markers in olive (*Olea europaea* L.) and usefulness in variability studies and genome mapping. *Sci. Hortic-Amsterdam.* 136, 50–60. doi: 10.1016/j.scienta.2011.12.017

Ducheix, S., Peres, C., Härdfeldt, J., Frau, C., Mocciaro, G., Piccinin, E., et al. (2018). Deletion of Stearoyl-CoA Desaturase-1 from the intestinal epithelium promotes inflammation and tumorigenesis, reversed by dietary oleate. *Gastroenterology.* 155, 1524–1538. doi: 10.1053/j.gastro.2018.07.032

Earl, D. A., and Von Holdt, B. M. (2012). Structure Harvester: a website and program for visualizing STRUCTURE output and implementing the Evanno method. *Cons. Genet. Res.* 4, 359–361. doi: 10.1007/s12686-011-9548-7

Eckert, A. J., Bower, A. D., Wegrzyn, J. L., Pande, B., Jermstad, K. D., Krutovsky, K. V., et al. (2009). Association genetics of coastal douglas fir (*Pseudotsuga menziesii* var. *menziesii*, Pinaceae). I. cold-hardiness related traits. *Genetics* 182, 1289–1302. doi: 10.1534/genetics.109.102350

El Aabidine, A. Z. E., Charafi, J., Grout, C., Doligez, A., Santoni, S., Moukhli, A., et al. (2010). Construction of a genetic linkage map for the olive based on AFLP and SSR markers. *Crop Sci.* 50, 2291–2302. doi: 10.2135/cropsci2009.10.0632

El Bakkali, E., Haouane, H., Moukhli, A., Costes, E., Van Damme, P., and Khadari, B. (2013). Construction of core collections suitable for association mapping to optimize use of mediterranean olive (*Olea europaea* L.) genetic resources. *PloS One* 8, e61265. doi: 10.1371/journal.pone.0061265

Evanno, G., Regnaut, S., and Goudet, J. (2005). Detecting the number of clusters of individuals using the software structure: a simulation study. *Mol. Ecol.* 14, 2611–2620. doi: 10.1111/j.1365-294X.2005.02553.x

Flint-Garcia, S. H., Thornsberry, J. M., and Buckler, E. S. (2003). Structure of linkage disequlibrium in plants. *Ann. Rev. Plant Biol.* 54, 357–374. doi: 10.1146/annurev.arplant.54.031902.134907

Font i Forcada, C., Fernández i Martí, A.Socias i Company R. (2012). Mapping quantitative trait loci for kernel composition in almond. *BMC Genet.* 13, 47. doi: 10.1186/1471-2156-13-47

Font i Forcada, C. F., Oraguzie, N., Reyes-Chin-Wo, S., Espiau, M. T., and i Martí, A. F. (2015). Identification of genetic loci associated with quality traits in

almond *via* association mapping. *PloS One* 10, e0127656. doi: 10.1371/journal.pone.0127656

Gómez-Lama Cabanás, C., Schilirò, E., Valverde-Corredor, A., and Mercado-Blanco, J. (2015). Systemic responses in a tolerant olive (*Olea europaea* L.) cultivar upon root colonization by the vascular pathogen *Verticillium dahliae*. Front. *Microbiol.* 6, 928. doi: 10.3389/fmicb.2015.00928

Ganopoulos, I. V., Kazantzis, K., Chatzicharisis, I., Karayiannis, I., and Tsaftaris, A. S. (2011). Genetic diversity, structure and fruit trait associations in Greek sweet cherry cultivars using microsatellite based (SSR/ISSR) and morpho-physiological markers. *Euphytica.* 181, 237–251. doi: 10.1007/s10681-011-0416-z

Gao, X., and Lynch, M. (2009). Ubiquitous internal gene duplication and intron creation in eukaryotes. *Proc. Natl. Acad. Sci. U.S.A.* 49, 20818–20823. doi: 10.1073/pnas.0911093106

García-López, M. C., Vidoy, I., Jiménez-Ruiz, J., Muñoz-Mérida, A., Fernández-Ocaña, A., De la Rosa, R., et al. (2014). Genetic changes involved in the juvenile-to-adult transition in the shoot apex of *Olea europaea* L. occur years before the first flowering. *Tree Genet. Genomes.* 10, 585–603. doi: 10.1007/s11295-014-0706-4

González-Plaza, J. J., Ortiz-Martín, I., Muñoz-Mérida, A., García-López, C., Sánchez-Sevilla, J. F., Luque, F., et al. (2016). Transcriptomic analysis using olive varieties and breeding progenies identifies candidate genes involved in plant architecture. *Front. Plant Sci.* 7, 240. doi: 10.3389/fpls.2016.00240

Grasso, F., Coppola, M., Carbone, F., Baldoni, L., Alagna, F., Perrotta, G., et al. (2017). The transcriptional response to the olive fruit fly (*Bactrocera oleae*) reveals extended differences between tolerant and susceptible olive (*Olea europaea* L.) varieties. *PloS One* 12 (8), e0183050. doi: 10.1371/journal.pone.0183050

Guan, L. L., Wang, Y. B., Shen, H., Hou, K., Xu, Y. W., and Wu, W. (2012a). Molecular cloning and expression analysis of genes encoding two microsomal oleate desaturases (FAD2) from safflower (*Carthamus tinctorius* L.). *Plant Mol. Biol. Rep.* 30, 139–148. doi: 10.1007/s11105-011-0322-5

Guan, L. L., Xu, Y. W., Wang, Y. B., Chen, L., Shao, J. F., and Wu, W. (2012b). Isolation and characterization of a temperature-regulated microsomal oleate desaturase gene (CtFAD2-1) from safflower (*Carthamus tinctorius* L.). *Plant Mol. Biol. Rep.* 30, 391–402. doi: 10.1007/s11105-011-0349-7

Guerra, D., Lamontanara, A., Bagnaresi, P., Orrù, L., Rizza, F., Zelasco, S., et al. (2015). Transcriptome changes associated with cold acclimation in leaves of olive tree (*Olea europaea* L.). *Tree Genet. Genomes.* 11, 113. doi: 10.1007/s11295-015-0939-x

Hammer, Ø., Harper, D. A. T., and Ryan, P. D. (2001). PAST: paleontological statistics software package for education and data analysis. *Palaeontol. Electron.* 4, 9.

Heppard, E. P., Kinney, A. J., Stecca, K. L., and Miao, G. H. (1996). Developmental and growth temperature regulation of two different microsomal ω-6 desaturase genes in soybeans. *Plant Physiol.* 110, 311–319. doi: 10.1104/pp.110.1.311

Hernández, M. L., Mancha, M., and Martínez-Rivas, J. M. (2005). Molecular cloning and characterization of genes encoding two microsomal oleate desaturases (*FAD2*) from olive. *Phytochemistry* 66, 1417–1426. doi: 10.1016/j.phytochem.2005.04.004

Hernández, M. L., Padilla, M. N., Mancha, M., and Martínez-Rivas, J. M. (2009). Expression analysis identifies *FAD2-2* as the olive oleate desaturase gene mainly responsible for the linoleic acid content in virgin olive oil. *J. Agric. Food Chem.* 57, 6199–6206. doi: 10.1021/jf900678z

Hernández, M. L., Padilla, M. N., Sicardo, M. D., Mancha, M., and Martínez-Rivas, J. M. (2011). Effect of different environmental stresses on the expression of oleate desaturase genes and fatty acid composition in olive fruit. *Phytochemistry.* 72, 178–187. doi: 10.1016/j.phytochem.2010.11.026

Hernández, M. L., Belaj, A., Sicardo, M. D., Leon, L., De la Rosa, R., Martin, A., et al. (2017). Mapping quantitative trait loci controlling fatty acid composition in olive. *Euphytica* 213, 1. doi: 10.1007/s10681-016-1802-3

Hernández, M. L., Velázquez-Palmero, D., Sicardo, M. D., Fernández, J. E., and Diaz-Espejo, A. J. M. (2018). Effect of a regulated deficit irrigation strategy in a hedgerow 'Arbequina' olive orchard on the mesocarp fatty acid composition and desaturase gene expression with respect to olive oil quality. *Agric. Water Manage.* 204, 100–106. doi: 10.1016/j.agwat.2018.04.002

Hongtrakul, V., Slabaugh, M. B., and Knapp, S. J. (1998). A seed specific D-12 oleate desaturase gene is duplicated, rearranged, and weakly expressed in high oleic acid sunflower lines. *Crop Sci.* 38, 1245–1249. doi: 10.2135/cropsci1998.0011183X003800050022x

Hu, X., Sullivan-Gilbert, M., Gupta, M., and Thompson, S. A. (2006). Mapping of the loci controlling oleic and linolenic acid contents and development of *fad2* and *fad3* allele-specific markers in canola (*Brassica napus* L.). *Theor. Appl. Genet.* 113, 497–507. doi: 10.1007/s00122-006-0315-1

Iaria, D. L., Chiappetta, A., and Muzzalupo, I. (2015). A *de novo* transcriptomic approach to identify flavonoids and anthocyanins "switch-off" in olive (*Olea europaea* L.) drupes at different stages of maturation. *Front. Plant Sci.* 6. doi: 10.3389/fpls.2015.01246

Ingvarsson, P. K. (2005). Nucleotide polymorphism and linkage disequilibrium within and among natural populations of European aspen (*Populus tremula* L., Salicaceae). *Genetics.* 169, 945–953. doi: 10.1534/genetics.104.034959

Ipek, M., Ipek, A., Seker, M., and Gul, M. K. (2015). Association of SSR markers with contents of fatty acids in olive oil and genetic diversity analysis of an olive core collection. *Gen. Mol. Res.* 14, 2241–2252. doi: 10.4238/2015.March.27.10

Ipek, A., Yilmaz, K., Sikici, P., Tangu, A. N., Oz, A. T., Bayraktar, M., et al. (2016). SNP discovery by GBS in olive and the construction of a high-density genetic linkage map. *Biochem. Genet.* 54, 313–325. doi: 10.1007/s10528-016-9721-5

Jin, U. H., Lee, J. W., Chung, Y. S., Lee, J. H., Yi, Y. B., Kim, Y. K., et al. (2001). Characterization and temporal expression of a x-6 fatty acid desaturase cDNA from sesame (*Sesamum indicum* L.) seeds. *Plant Sci.* 161, 935–941. doi: 10.1016/S0168-9452(01)00489-7

Jung, S., Swift, D., Sengoku, E., Patel, M., Teule, F., Powell, G., et al. (2000). The high oleate trait in the cultivated peanut [*Arachis hypogaea* L.]. I. Isolation and characterization of two genes encoding microsomal oleoyl-PC desaturases. *Mol. Gen. Genet.* 263, 796–805. doi: 10.1007/s004380000244

Kadkhodaei, S., Khayyam Nekouei, M., Shahnazari, M., Etminani, H., Imani, A., Ghaderi-Zefrehei, M., et al. (2011). Molecular tagging of agronomic traits using simple sequence repeats: Informative markers for almond ('Prunus dulcis') molecular breeding. *Aust. J. Crop Sci.* 5, 1199.

Kaya, H. B., Cetin, O., Kaya, H. S., Sahin, M., Sefer, F., and Tanyolac, B. (2016). Association mapping in Turkish olive cultivars revealed significant markers related to some important agronomic traits. *Biochem. Genet.* 54, 506–533. doi: 10.1007/s10528-016-9738-9

Khadivi-Khub, A. (2014). Regression association analysis of fruit traits with molecular markers in cherries. *Plant Syst. Evol.* 300, 1163–1173. doi: 10.1007/s00606-013-0953-0

Kim, M. J., Kim, H., Shin, J. S., Chung, C. H., Ohlrogge, J. B., and Suh, M. C. (2006). Seed-specific expression of sesame microsomal oleic acid desaturase is controlled by combinatorial properties between negative cis-regulatory elements in the *SeFAD2* promoter and enhancers in the 5′-UTR intron. *Mol. Genet. Genom.* 276, 351–368. doi: 10.1007/s00438-006-0148-2

Koudounas, K., Manioudaki, M. E., Kourti, A., Banilas, G., and Hatzopoulos, P. (2015). Transcriptional profiling unravels potential metabolic activities of the olive leaf non-glandular trichome. *Front. Plant Sci.* 6, 633. doi: 10.3389/fpls.2015.00633

Krasowska, A., Dziadkowiec, D., Polinceusz, A., Plonka, A., and Łukaszewicz, M. (2007). Cloning of flax oleic fatty acid desaturase and its expression in yeast. *J. Am. Oil. Chem. Soc* 84, 809–816. doi: 10.1007/s11746-007-1106-9

Krutovsky, K. V., and Neale, D. B. (2005). Nucleotide diversity and linkage disequilibrium in cold-hardiness and wood quality-related candidate genes in Douglas-fir. *Genetics* 171, 2029–2041. doi: 10.1534/genetics.105.044420

Kumar, S., Garrick, D. J., Bink, M. C., Whitworth, C., Chagné, D., and Volz, R. K. (2013). Novel genomic approaches unravel genetic architecture of complex traits in apple. *BMC Genomics* 14, 393. doi: 10.1186/1471-2164-14-393

Lee, K. R., Kim, S. H., Go, Y. S., Jung, S. M., Roh, K. H., Kim, J. B., et al. (2012). Molecular cloning and functional analysis of two *FAD2* genes from American grape (*Vitis labrusca L.*). *Gene.* 509, 189–194. doi: 10.1016/j.gene.2012.08.032

Leppek, K., Das, R., and Barna, M. (2018). Functional 5′ UTR mRNA structures in eukaryotic translation regulation and how to find them. *Nat. Rev. Mol. Cell. Biol.* 19, 158–174. doi: 10.1038/nrm.2017.103

Leyva-Pérez, M. O., Valverde-Corredor, A., Valderrama, R., Jiménez-Ruiz, J., Munoz-Merida, A., Trelles, O., et al. (2014). Early and delayed long-term transcriptional changes and short-term transient responses during cold acclimation in olive leaves. *DNA Res.* 22, 1–11. doi: 10.1093/dnares/dsu033

Leyva-Pérez, M. O., Jiménez-Ruiz, J., Gomez-Lama Cabanas, C., Valverde-Corredor, A., Barroso, J. B., Luque, F., et al. (2018). Tolerance of olive (*Olea*

europaea) cv Frantoio to *Verticillium dahliae* relies on both basal and pathogen-induced differential transcriptomic responses. *New Phytol.* 7, 671–686. doi: 10.1111/nph.14833

Li, L., Wang, X., Gai, J., and Yu, D. (2007). Molecular cloning and characterization of a novel microsomal oleate desaturase gene from soybean. *J. Plant Physiol.* 164, 1516–1526. doi: 10.1016/j.jplph.2006.08.007

Liu, Q., Singh, S. P., Brubaker, C. L., Sharp, P. J., Green, A. G., and Marshall, D. (1999). Molecular cloning and expression of a cDNA encoding a microsomal x-6 fatty acid desaturase from cotton (*Gossypium hirsutum*). *Funct. Plant Biol.* 26, 101–106. doi: 10.1071/PP98118

Liu, Q., Brubaker, C. L., Green, A. G., Marshall, D. R., Sharpe, P. J., and Singh, S. P. (2001). Evolution of the FAD2-1 fatty acid desaturase 5′UTR intron and the molecular systematic of *Gossypium* (Malvaceae). *Am. J. Bot.* 88, 92e102. doi: 10.2307/2657130

Loureiro, J., Rodriguez, E., Costa, A., and Santos, C. (2007). Nuclear DNA content estimations in wild olive (*Olea europaea* L. ssp. *europaea* var. *sylvestris* Brot.) and Portuguese cultivars of O. *europaea* using flow cytometry. *Gen. Res. Crop Evol.* 54, 21–25. doi: 10.1007/s10722-006-9115-3

Lozada-Chávez, I., Stadler, P. F., and Prohaska, S. J. (2018). Genome-wide features of introns are evolutionary decoupled among themselves and from genome size throughout Eukarya. *bioRxiv*. doi: 10.1101/283549

Lozinsky, S., Yang, H., Forseille, L., Cook, G. R., Ramirez-Erosa, I., and Smith, M. A. (2014). Characterization of an oleate 12-desaturase from *Physaria fendleri* and identification of 5′UTR introns in divergent FAD2 family genes. *Plant Phy. Bioch.* 75, 114–122. doi: 10.1016/j.plaphy.2013.12.016

Ma, M. Y., Lan, X. R., and Niuet, D. K. (2016). Intron gain by tandem genomic duplication: a novel case in a potato gene encoding RNA-dependent RNA polymerase. *PeerJ.* 4, e2272. doi: 10.7717/peerj.2272

Marchese, A., Marra, F. P., Caruso, T., Mhelembe, K., Costa, F., Fretto, S., et al. (2016). The first high-density sequence characterized SNP-based linkage map of olive (*Olea europaea* L. subsp. *europaea*) developed using genotyping by sequencing. *Aust. J. Crop Sci.* 10, 857–863. p. 7520 doi: 10.21475/ajcs.2016.10.06

Mariotti, R., Cultrera, N. G. M., Mousavi, S., Baglivo, F., Rossi, M., Albertini, E., et al. (2016). Development, evaluation, and validation of new EST-SSR markers in olive (*Olea europaea* L.). *Tree Genet. Genomes* 12, 120. doi: 10.1007/s11295-016-1077-9

Martínez-Rivas, J. M., Sperling, P., Luhs, W., and Heinx, E. (2001). Spatial and temporal regulation of three different microsomal oleate desaturase genes (FAD2) from normal-type and high-oleic varieties of sunflower (*Helianthus annuus* L.) Mol. *Breeding.* 8, 159–168. doi: 10.1023/A:1013324329322

Matteucci, M., D'Angeli, S., Errico, S., Lamanna, R., Perrotta, G., and Altamura, M. M. (2011). Cold affects the transcription of fatty acid desaturases and oil quality in the fruit of *Olea europaea* L. genotypes with different cold hardiness. *J. Exp. Bot.* 62, 3403–3420. doi: 10.1093/jxb/err013

Moretti, S., Francini, A., Hernández, M. L., Martínez-Rivas, J. M., and Sebastiani, L. (2019). Effect of saline irrigation on physiological traits, fatty acid composition and desaturase genes expression in olive fruit mesocarp. *Plant Physiol. Biochem*. (in press). 141, 423–430. doi: 10.1016/j.plaphy.2019.06.015

Mroczka, A., Roberts, P. D., Fillatti, J. J., Wiggins, B. E., Ulmasov, T., and Voelker, T. (2010). An intron sense suppression construct targeting soybean *FAD2-1* requires a double-stranded RNA-producing inverted repeat T-DNA insert. *Plant Physiol.* 153, 882–891. doi: 10.1104/pp.110.154351

Muleo, R., Morgante, M., Cattonaro, F., Scalabrin, S., Cavallini, A., Natali, L., et al. (2016). "Genome sequencing, transcriptomics, and proteomics," in *The Olive Tree Genome*. Eds. E. Rugini, L. Baldoni, R. Muleo and L. Sebastiani (Cham: Springer International Publishing), 141–161. doi: 10.1007/978-3-319-48887-5_9

Myles, S., Peiffer, J., Brown, P. J., Ersoz, E. S., Zhang, Z., Costich, D. E., et al. (2009). Association mapping: critical considerations shift from genotyping to experimental design. *Plant Cell* 21, 2194–2202. doi: 10.1105/tpc.109.068437

Okuley, J., Lightner, J., Feldmann, K., Yadav, N., Lark, E., and Browse, J. (1994). *Arabidopsis FAD2* gene encodes the enzyme that is essential for polyunsaturated lipid synthesis. *Plant Cell.* 6, 147–158. doi: 10.2307/3869682

Olukolu, B. (2010). The genetics of chilling requirements in apricot (*Prunus armeniaca* L.). [Dissertation] Clemson University.

Parra, G., Bradnam, K., Rose, A. B., and Korf, I. (2011). Comparative and functional analysis of intron-mediated enhancement signals reveals conserved features among plants. *Nucleic. Acids Res.* 39, 13. doi: 10.1093/nar/gkr043

Pritchard, J. K., Stephens, M., and Donnelly, P. J. (2000). Inference of population Structure using multilocus genotype data. *Genetics* 155, 945–959.

Quintero-Florez, A., Sinausia Nieva, L., Sanchez-Ortiz, A., Beltran, G., and Perona, J. S. (2015). The fatty acid composition of virgin olive oil from different cultivars is determinant for foam cell formation by macrophages. *J. Agric. Food. Chem.* 63, 6731–6738. doi: 10.1021/acs.jafc.5b01626

Rafalski, J. A. (2010). Association genetics in crop improvement. *Curr. Opin. Plant Biol.* 13, 174–180. doi: 10.1016/j.pbi.2009.12.004

Ripa, V., De Rose, F., Caravita, M. A., Parise, M. R., Perri, E., Rosati, A., et al. (2008). Qualitative evaluation of olive oils from new olive selections and effects of genotype and environment on oil quality. *Adv. Hortic. Sci.* 22, 95–103.

Rugini, E., De Pace, C., Gutiérrez-Pesce, P., and Muleo, R. (2011). "Olea," in *Wild Crop Relatives: Genomic and Breeding Resources, Temperate Fruits*. Ed. K. Chittaranjan (Berlin-Heidelberg: Springer-Verlag), 79–114. doi: 10.1007/978-3-642-16057-8_5

Sabetta, W., Blanco, A., Zelasco, S., Lombardo, L., Perri, E., Mangini, G., et al. (2013). Fad7 gene identification and fatty acids phenotypic variation in an olive collection by EcoTILLING and sequencing approaches. *Plant Physiol. Biochem.* 69, 1–8. doi: 10.1016/j.plaphy.2013.04.007

Salas, J. J., Sànchez, J., Ramli, U. S., Arif, M. M., Williams, M., and Harwood, J. L. (2000). Biochemistry of lipid metabolism in olive and other oil fruits. *Progr. Lip. Res.* 39, 151–180. doi: 10.1016/S0163-7827(00)00003-5

Sefc, K. M., Lopes, S., Mendonca, D., Dos Santos, M. R., Laimer Da Câmara Machado, M., and Da Câmara Machado, A. (2000). Identification of microsatellite loci in olive (*Olea europaea*) and their characterization in Italian and Iberian olive trees. *Mol. Ecol.* 9, 1171–1173. doi: 10.1046/j.1365-294x.2000.00954.x

Shanklin, J., and Cahoon, E. B. (1998). Desaturation and related modifications of fatty acids. *Ann. Rev. Plant Physiol. Plant Mol. Biol.* 49, 611–641. doi: 10.1146/annurev.arplant.49.1.611

Singh, R., Tan, S. G., Panandam, J. M., Rahman, R. A., Ooi, L. C. L., Low, E. T. L., et al. (2009). Mapping quantitative trait loci (QTLs) for fatty acid composition in an interspecific cross of oil palm. *BMC Plant Biol.* 9, 114. doi: 10.1186/1471-2229-9-114

Stephens, M., and Donnelly, P. (2003). A comparison of bayesian methods for haplotype reconstruction from population genotype data. *Am. J. Hum. Genet.* 73, 1162–1169. doi: 10.1086/379378

Stephens, M., Smith, N., and Donnelly, P. (2001). A new statistical method for haplotype reconstruction from population data. *Am. J. Hum. Genet.* 68, 978–989. doi: 10.1086/319501

Storey, J. D., and Tibshirani, R. (2003). Statistical significance for genome wide studies. *Proc. Natl. Acad. Sci. U.S.A.* 100, 9440–9445. doi: 10.1073/pnas.1530509100

Tanhuanpää, P., Vilkki, J., and Vihinen, M. (1998). Mapping and cloning of *FAD2* gene to develop allele-specific PCR for oleic acid in spring turnip rape (*Brassica rapa* ssp. oleifera). *Mol. Breeding.* 4, 543–550. doi: 10.1023/A:1009642317634

Tian, J., Chang, M., Du, Q., Xu, B., and Zhang, D. (2014). Single-nucleotide polymorphisms in *PtoCesA7* and their association with growth and wood properties in *Populus tomentosa*. *Mol. Genet. Genomics* 289 (3), 439–455. doi: 10.1007/s00438-014-0824-6

Unver, T., Wu, Z., Sterck, L., Turktas, M., Lohaus, R., Li, Z., et al. (2017). Genome of wild olive and the evolution of oil biosynthesis. *Proc. Natl. Acad. Sci. U.S.A.* 114, E9413–E9422. doi: 10.1073/pnas.1708621114

Wegrzyn, J. L., Eckert, A. J., Choi, M., Lee, J. M., Stanton, B. J., Sykes, R., et al. (2010). Association genetics of traits controlling lignin and cellulose biosynthesis in black cottonwood (*Populus trichocarpa*, Salicaceae) secondary xylem. *New Phytol.* 188, 515–532. doi: 10.1111/j.1469-8137.2010.03415.x

Wells, R., Trick, M., Soumpourou, E., Clissold, L., Morgan, C., Werner, P., et al. (2014). The control of seed oil polyunsaturate content in the polyploid crop species *Brassica napus.* Mol. *Breeding.* 33, 349–362. doi: 10.1007/s11032-013-9954-5

Wu, S. B., Collins, G., and Sedgley, M. (2004). A molecular linkage map of olive (*Olea europaea* L.) based on RAPD, microsatellite, and SCAR markers. *Genome.* 47, 26–35. doi: 10.1139/g03-091

Xiao, G., Zhang, Z. Q., Yin, C. F., Liu, R. Y., Wu, X. M., Tan, T. L., et al. (2014). Characterization of the promoter and 5′-UTR intron of *oleic acid desaturase*

(*FAD2*) gene in *Brassica napus*. *Gene* 545, 45–55. doi: 10.1016/j.gene.2014.05.008

Yang, Q., Fan, C., Guo, Z., Qin, J., Wu, J., et al. (2012). Identification of *FAD2* and *FAD3* genes in *Brassica napus* genome and development of allele-specific markers for high oleic and low linolenic acid contents. *Theor. Appl. Genet.* 125, 715–729. doi: 10.1007/s00122-012-1863-1

Zeng, F., Roslinsky, V., and Cheng, B. (2017). Mutations in the promoter, intron and CDS of two *FAD2* generate multiple alleles modulating linoleic acid level in yellow mustard. *Sci. Rep.* 7, 8284. doi: 10.1038/s41598-017-08317-y

Zhang, D., Pirtle, I. L., Park, S. J., Nampaisansuk, M., Neogi, P., Wanjie, S. W., et al. (2009). Identification and expression of a new delta-12 fatty acid desaturase (*FAD2-4*) gene in upland cotton and its functional expression in yeast and *Arabidopsis thaliana* plants. *Plant Physiol. Biochem.* 47, 462–471. doi: 10.1016/j.plaphy.2008.12.024

Zhu, S., Niu, E., Shi, A., and Mou, B. (2019). Genetic diversity analysis of olive germplasm (*Olea europaea* L.) with genotyping-by-sequencing technology. *Front. Genet.* 10, 755. doi: 10.3389/fgene.2019.00755

Conflict of Interest: The authors declare that the research was conducted in the absence of any commercial or financial relationships that could be construed as a potential conflict of interest.

frontiers in Plant Science

ORIGINAL RESEARCH
published: 20 February 2020
doi: 10.3389/fpls.2020.00073

Re.Ger.O.P.: An Integrated Project for the Recovery of Ancient and Rare Olive Germplasm

Monica Marilena Miazzi[1†], Valentina di Rienzo[2†], Isabella Mascio[1,2], Cinzia Montemurro[1,2*], Sara Sion[1], Wilma Sabetta[2,3], Gaetano Alessandro Vivaldi[4], Salvatore Camposeo[4], Francesco Caponio[1], Giacomo Squeo[1], Graziana Difonzo[1], Guiliana Loconsole[1,2], Giovanna Bottalico[1,2], Pasquale Venerito[5], Vito Montilon[1], Antonella Saponari[5], Giuseppe Altamura[5], Giovanni Mita[6], Alessandro Petrontino[2], Vincenzo Fucilli[2,4] and Francesco Bozzo[2,4]*

[1] Department of Soil, Plant and Food Sciences, University of Bari Aldo Moro, Bari, Italy, [2] SINAGRI S.r.l.—Spin Off of the University of Bari Aldo Moro, Bari, Italy, [3] Unit of Bari CNR Institute of Biosciences and Bioresources, Bari, Italy, [4] Department of Agricultural and Environmental Sciences, University of Bari Aldo Moro, Bari, Italy, [5] CRSFA-Centro Ricerca, Sperimentazione e Formazione in Agricoltura, "Basile Caramia" Locorotondo, Bari, Italy, [6] Unit of Lecce, CNR Institute of Sciences of Food Production, Lecce, Italy

The olive tree is one of the most important economic, cultural, and environmental resources for Italy, in particular for the Apulian region, where it shows a wide diversity. The increasing attention to the continuous loss of plant genetic diversity due to social, economic and climatic changes, has favored a renewed interest in strategies aimed at the recovery and conservation of these genetic resources. In the frame of a project for the valorization of the olive Apulian biodiversity (Re.Ger.O.P. project), 177 minor genotypes were recovered in different territories of the region. They were submitted to morphological, molecular, technological and phytosanitary status analysis in comparison with reference cultivars, then they were propagated and transferred in an *ex situ* field. All the available information was stored in an internal regional database including photographic documentation and geographic position. The work allowed obtaining information about the genetic diversity of Apulian germplasm, to clarify cases of homonymy and synonymy, to check the sanitary status, and to identify candidate genotypes useful both to set up breeding programs and to enrich the panel of olive cultivars available to farmers for commercial exploitation.

Keywords: olive, rare germplasm, homonymy and synonymy, characterization, diversity, resources for breeding

OPEN ACCESS

Edited by:
Antonio Diaz Espejo, Institute of Natural Resources and Agrobiology of Seville (CSIC), Spain

Reviewed by:
Innocenzo Muzzalupo, Council for Agricultural and Economics Research, Italy
Cristian Silvestri, Università degli Studi della Tuscia, Italy
Maria Manuela Rigano, University of Naples Federico II, Italy

***Correspondence:**
Isabella Mascio
mascioisa@gmail.com
Cinzia Montemurro
cinzia.montemurro@uniba.it

†These authors have contributed equally to this work

Specialty section:
This article was submitted to Crop and Product Physiology, a section of the journal Frontiers in Plant Science

Received: *14 June 2019*
Accepted: *17 January 2020*
Published: *20 February 2020*

Citation:
Miazzi MM, di Rienzo V, Mascio I, Montemurro C, Sion S, Sabetta W, Vivaldi GA, Camposeo S, Caponio F, Squeo G, Difonzo G, Loconsole G, Bottalico G, Venerito P, Montilon V, Saponari A, Altamura G, Mita G, Petrontino A, Fucilli V and Bozzo F (2020) Re.Ger.O.P.: An Integrated Project for the Recovery of Ancient and Rare Olive Germplasm. Front. Plant Sci. 11:73. doi: 10.3389/fpls.2020.00073

INTRODUCTION

The cultivated olive (*Olea europaea* subsp. europaea var. europaea) is a typical fruit tree crop of the Mediterranean Basin where it is spread on over eight million of hectares. In Italy, the olive culture represents one of the most important economic, cultural and environmental resource (Clodoveo et al., 2014; Famiani et al., 2014). The Italian olive germplasm is estimated to include about 800 cultivars, most of them landraces vegetatively propagated at a farm level since ancient times

(Muzzalupo, 2012), and new local genotypes are continuously described. This wealth is due to the high environmental variability of Italian growing area, and it represents an opportunity for the Italian olive oil sector. The increasing attention to the continuous loss of plant genetic diversity, known as genetic erosion, due to social, economic and climatic changes, determined targeted international policies to preserve plant species subjected to extinction risk. The International Treaty on Plant Genetic Resources for Food and Agriculture (FAO, 2001) created a mechanism for an equitable use of these resources and envisaged the creation of a global information system to facilitate the recovery and sharing of plant genetic resources (Sardaro et al., 2018). Plant biodiversity is a resource of genes useful to adaptation to environmental changes. The characterization of ancient and rare plant genetic resources is prominent as source of agronomical traits important for cropping system evolution (Caruso et al., 2014; Vivaldi et al., 2015; Rosati et al., 2018a; Rosati et al., 2018b), reduction of water consumption (Pellegrini et al., 2016), facing emergent diseases resistance (Saponari et al., 2019) and resilience to climate changes (Taranto et al., 2018).

Apulia region (Italy) hosts one third of the Italian olive cultivated area, with about 50 million of olive trees showing a wide diversity. The particular conformation of the Regional territory, stretched on more than 400 Km, offers a great variability of pedoclimatic conditions (Sardaro et al., 2015). Due to its geographical position, Apulia was a cross point for commercial routes since ancient times, allowing a remarkable complexity and richness in autochthonous varieties as documented in several researches (D'Agostino et al., 2018).

In 2013, the integrated project Re.Ger.O.P. (Apulian Olive Germplasm Recovery) focused the attention on the Apulian olive biodiversity through a structured program of activities including historical investigation, cataloguing, genetic and technological characterization, sanitary status investigation and conservation of the collected local germplasm.

Morphological descriptors are an important tool to study the genetic diversity within a cultivated plant species; indeed, they represent the phenological traits normally used in taxonomic classification (Blazakis et al., 2017). The International Union for the Protection of New Varieties of Plants (UPOV) established both parameters and methodology for olive germplasm characterization (UPOV, 2011).

Nonetheless, in the last two decades, the morphological descriptors have been integrated with molecular markers, such as SSR markers that have demonstrated a very good efficiency in olive genotyping (Muzzalupo et al., 2008; Muzzalupo et al., 2014; Boucheffa et al., 2017; Chiappetta et al., 2017; Boucheffa et al., 2019; Sion et al., 2019), population genetics (Albertini et al., 2011; Mousavi et al., 2017; di Rienzo et al., 2018a), and traceability of products (Pasqualone et al., 2015; Montemurro et al., 2015; Binetti et al., 2017; Sabetta et al., 2017).

An essential prerequisite in the genetic resources' conservation is also the assessment of the phytosanitary status (Fontana et al., 2019). As for other vegetative propagated crops, olive is affected by several pathogens (viruses, fungi, bacteria and phytoplasmas) that persist in the budwood and can be transmitted and disseminated with it, with severe economic effects on yield and production quality (Martelli et al., 2002; Loconsole et al., 2010). The use of 'healthy' plants for new plantations is crucial for the quality of crop production, restraining the spread of pathogens and diseases, and potentially reducing chemical applications and the environmental impacts of agricultural practices (García-Mier et al., 2013). Moreover, the use of local varieties, recovered from autochthonous germplasm, could support programs of resistance evaluation to emergent pests (Giampetruzzi et al., 2016; Saponari et al., 2019).

Despite the economic importance of olive (ISMEA, 2019), few major cultivars are generally used for virgin olive oil (VOO) production, neglecting the heritage of minor cultivars that could be an important resource to broaden the product offer to the consumers. Indeed, the genotype component, coupled with the extraction technology, strongly affect the VOO characteristics in terms of quality, oxidative stability and organoleptic features (Rotondi et al., 2010; Caponio et al., 2018a; Caponio et al., 2018b; Tamborrino et al., 2019).

The aim of this work was to obtain information about genetic variability among Apulian germplasm, to clarify cases of homonymy and synonymy, to check the sanitary status, and to identify candidate genotypes useful both to set up breeding programs and to enrich the existent panel of olive cultivars. The integrated approach here proposed allowed to reach a deep knowledge on several aspects connected to the olive germplasm for a faster and efficient recognition of the best candidates suitable for commercial and economic valorization.

MATERIALS AND METHODS

Collection of Olive Germplasm

To identify the minor genotypes spread in Apulia region (Southern Italy), bibliographic researches about the varieties cultivated in the past centuries were conducted in cooperation with local farmers and by means of meetings organized along the regional territory. Plants were recovered in the marginal areas of the Apulian provinces of Foggia, Bari, Brindisi, Taranto, BAT (Barletta–Andria–Trani) and Lecce (**Figure 1**). Genotypes were geo-referenced trough cartography and GPS data of the fields. In addition, a photographic documentation with a geotag system and 3D photographs for remote recognition of tree canopy, rural landscape and soil characteristics were obtained. A total of 177 genotypes were collected and they were submitted to the different characterizations, depending on the availability of the plant material (**Supplementary Table 1**).

Morphological Characterization

The morphological characterization was performed on 97 genotypes using 24 descriptors indicated by UPOV, including three descriptors for the leaf, 11 for the fruit, and 10 for the stone (**Supplementary Table 2**). Each genotype was represented by one to three trees, depending on genotype; in few cases the tree

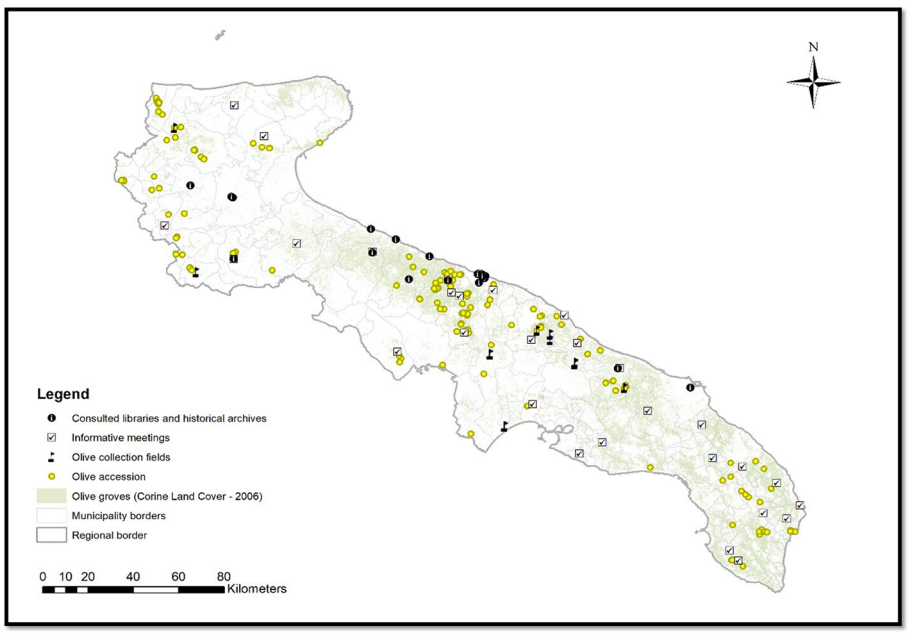

FIGURE 1 | Geographic map of 'Apulia' with collection sites of samples.

consisted in a primary branch only. Observations were made on 50 leaves, 50 fruits and 50 stones per genotype. Leaves were collected in late spring, on 1-year shoots; fruits were harvested in middle autumn, with a pigmentation index between 3 and 5 (Camposeo et al., 2013). The morphological data were converted in a discrete data matrix (**Supplementary Table 3**) and used to obtain a Neighbour–Joining dendrogram performed with Darwin software version 6.0.010 (http://darwin.cirad.fr) (Felsenstein, 1985), using 10,000 bootstrap replications. The data were compared with the reference cultivars present in the OLEA database (OLEADB, http://www.oleadb.it) which includes 1,626 cultivars preserved in 102 field collections of different countries (Bartolini et al., 2014).

Genetic Characterization

The molecular characterization was performed on 177 Apulian genotypes using 11 preselected microsatellite markers suitable for olive cultivar discrimination (Sefc et al., 2000; Carriero et al., 2002; Cipriani et al., 2002; Dela Rosa et al., 2002; Baldoni et al., 2009) (**Supplementary Table 4**). The obtained genetic profiles were compared with that of 59 olive cultivars diffused in all the Italian territory and maintained at the conservation field of Palagiano (TA, Italy), used as references (**Supplementary Table 1**). For genomic DNA extraction, three young leaves of each sample were lyophilized and finely grinded, and 50 mg of tissue were used, following the protocol of Spadoni et al. (2019). DNA quality and concentration were assessed using a NanoDropTM ND2000C (Thermo Fisher Scientific, Waltham, MA, USA), and normalized at 50 ng/µl into a 96-well plate (Nunc 96-Well Multiwell Plates). DNA amplification and analysis were conducted according to di Rienzo et al. (2018a). Detection, sizing and data collection were carried out using the GeneMapper 5.0 software (Applied Biosystems, Foster City, CA, USA).

Genetic diversity was investigated through different genetic indices, such as Number of alleles (Na), effective alleles (Ne), Shannon's information index (I), observed (Ho) and expected (He) heterozygosity and fixation index (F) (Wright, 1949) implemented in GENALEX software v.6.5 (http://anu.edu.au./BoZo/GenAIEx). This software was also used to calculate the allelic similarity for codominant data based on the pairwise relatedness, following the Lynch and Ritland estimator (LRM) (Lynch and Ritland, 1999). To determine the most informative primers, the polymorphic information content (PIC) (Botstein et al., 1980) was calculated by using Cervus v 3.0 (Kalinowski et al., 2007).

To study the relationships among genotypes, an Unweighted Neighbor–Joining dendrogram was generated in DARWIN software v. 6.0.010 (http://darwin.cirad.fr), using bootstrapping with 1,000 replicates to determine support for each node.

To infer the structure of olive germplasm, a Bayesian clustering algorithm implemented in STRUCTURE software version 2.3.4 (https://web.stanford.edu/group/pritchardlab/structure.html) (Pritchard et al., 2000) was used. To evaluate the optimal number of sub-populations (K), ten independent runs for each K (from 1 to 10) were performed, using 100,000 MCMC repetitions and 100,000 burn-in periods. The optimal K value was determined depending on ΔK test (Evanno et al., 2005) using the STRUCTURE HARVESTER software (Earl and Von Holdt, 2012). Genotypes were assigned to defined populations if

the value of the corresponding membership coefficient (qi) was higher than 0.6, otherwise they were considered to be of admixed ancestry.

Technological Characterization of Virgin Olive Oils

The technological characterization was performed on 34 genotypes (**Supplementary Table 1**) using 1 kg of olives from a homogeneous batch collected by hand during the harvest season 2014–2015 from at least two different trees, when the pigmentation index was about 2 (Squeo et al., 2016). The extraction of the corresponding monovarietal virgin olive oils (VOO) was obtained within 12 h after harvesting, using a semi-industrial scale hammer crusher (RETSCH GmbH 5657, Haan, Germania) provided with three hammers positioned at 120° on a single plane. Thirty counter beaters (height = 5 mm) were embedded in the side of the chamber with an angle of 42° while the lower part of the chamber was covered by a grid with 65 holes (φ = 5 mm). The angular velocity was set at 2,850 rpm (Caponio and Catalano, 2001). The recovered olive paste was indirectly heated at 30 ± 1°C using a hot water treatment and mixed for 15 min. Thereafter, the oily phase was collected by a basket centrifuge (Marelli Motori S.p.A., Arzignano, VI, Italia) with a bowl of 19 cm, at rotational speed of 2,700 rpm. Once extracted, the oils were stored in 100 ml dark glass bottles until the analyses.

For the technological characterization, fatty acids (FA) and sterols composition was determined as described respectively in Difonzo et al. (2018) and the Commission Regulation (EEC) No 2568/91. Briefly, for FA analysis, about 20 mg of oil was added with 1 ml of hexane and vortexed. Then, 1 ml of KOH solution in methanol (2 N) was added and the sample sonicated by an ultrasound bath (CEIA, Viciomaggio, Italy) for 6 min at 25°C. Two microliters of the recovered upper layer, containing the fatty acids methyl esters (FAME), were withdrawn and injected into the GC system (Regulation (ECC) No 2568/91). The GC-FID system was composed by an Agilent 7890A gas chromatograph (Agilent Technologies, Santa Clara, CA, USA) equipped with a FID detector (set at 220°C) and a SP2340 capillary column, 60 m × 0.25 mm (i.d.) × 0.2 μm film thickness (Supelco Park, Bellefonte, PA, USA). The identification of each fatty acid was carried out by comparing the retention time with that of the corresponding standard methyl ester (Sigma-Aldrich, St. Louis, MO, USA) and the results were expressed as area percentage respect to the total FAs area.

For sterols composition, about 5 g of oil were added with α-colestanol as internal standard, and sample was subjected to saponification with a solution of KOH in ethanol (2 N) under heating. Sample was transferred in a separating funnel and washed three times with ethyl ether in order to collect the unsaponifiable fraction. The etheric phase was neutralized and filtered by sodium sulphate anhydrous and dried. The sterol fraction, resuspended in chloroform (5%), was separated from the unsaponifiable matter by tin layer chromatography and then recovered, filtered and silanised. Finally, about 1 μl of the solution was injected in the GC system (Agilent 7890A) using a capillary column HP-5 30 m × 0.32 mm (i.d.) × 0.25 μm film thickness (Agilent Technologies, Santa Clara, CA, USA). The injector temperature was 290°C with a split ratio of 1:25. The identification was carried out by comparing the retention time with those reported in the official method (Commission Regulation (EEC) No 2568/91). Single sterols content was reported as area percentage respect to the total sterol area, while the total content was calculated using the internal standard method and expressed as mg kg. All the chemical analyses on VOOs were made in triplicate, in all cases, with a coefficient of variation <5%. Descriptive statistics of the VOOs characteristics were calculated using Microsoft Excel 2010 (Microsoft Inc., Redmond, WA, USA). The principal component analysis (PCA) was also performed and the CAT (Chemometric Agile Tool) R-based chemometric software (R version 3.1.0 (2014-04-10) on the autoscaled matrix, was used.

Phytosanitary Evaluation of Olive Germplasm

The phytosanitary characterization was performed on 129 accessions, assessing either the presence of viruses listed in the phytosanitary requirements (D.M 20/11/2006) (**Supplementary Table 1**; **Supplementary Table 5**) and the bacterium *Xylella fastidiosa*. For the viruses, a previously validated one tube RT-PCR protocol was used (Loconsole et al., 2010), while for *X. fastidiosa*, the standard procedure based on CTAB-protocol for the extraction of total DNA and qPCR was applied (Harper et al., 2010; EPPO - PM 7/24 (3), 2018). Olive accessions resulted infected by CLRV and OLYaV, were submitted to sanitation treatments by *in vivo* or *in vitro* thermotherapy (Bottalico et al., 2004; Acquadro et al., 2009; Chiumenti et al., 2013; Abou Kubaa et al., 2018; Spanò et al., 2018). In *in vivo* thermotherapy, 2-year old infected plants were exposed to 35–38°C for 3–4 months; successively their vegetative tips were excised and micro-grafted on 1-year old "virus-free" seedlings (Onay et al., 2004; Wu et al., 2007; Farahani et al., 2011) (**Supplementary Figure 1**). In *in vitro* thermotherapy, young shoots were excised from 2-year old infected plants; nodal cutting explants were surface sterilized washing in running water and dipping in a NaClO (7–9% Cl active) solution for 20 min, then washed in steril water for three times for 1'–2' for each one. The explants were cultivated in Petri dishes with 25 ml of Olive media (Rugini, 1984) modified with zeatin 1.0 mg l^{-1} and mannitol 36 g l^{-1}. Petri dishes were maintained in growth chamber at 24°C with a 16 h light/8 h dark period and 3,000 lx light intensity. The *in vitro* sprout shoots were subcultivated on the same media composition every 20 days for 4 months. When shoots became about 2 cm long they were submitted to *in vitro* thermotherapy. The shoots transferred in glass vessels with 100 ml of the same media were exposed to 35–38°C, 16 h light/8 h dark period and 3,000 lx light intensity for 1 month, then their vegetative tips (0.5–0.8 cm) were directly micro-grafted on "virus-free" seedlings. The micrografted plants were protected by a plastic bag and maintained in a chamber room for 1 month at the same condition described before. Plastic bags were gradually removed, and the plants were transferred in greenhouse. Micrografted plants resulted negative to OLYaV and CLRV at a first testing, were maintained in greenhouse and checked two times in 18–24 months after the first assay. Finally,

'healthy plants' were transferred in screen house and maintained isolated to avoid any type of contamination, and routinely tested for the pathogens reported before.

RESULTS

Plant Material

Historical investigations about the varieties locally cultivated in the past centuries in Apulia, and the prospections on the territory allowed to identify a total of 177 minor genotypes survived in marginal olive orchards (**Supplementary Table 1**; **Figure 1**). All the genotypes were geo-referenced through cartography and GPS, and all data were merged in a database specifically created as repository of molecular, morphological, phytosanitary and technological information (data available on request to Apulia Region Misura 10.2.1: www.psr.regione.puglia.it).

Morphological Characterization

Fruit and stone separated the 97 Apulian olive genotypes in clusters and allowed to recognize 32 varieties already described in OLEADB, as well-known cultivated varieties. Among the remaining 64 genotypes, 49 genotypes were not described in OLEADB but they were called with a local name, and 15 genotypes were nameless and they were tagged as "unknown". The dendrogram grouped the olive genotypes in three main clusters (**Figure 2**). Cluster I consists of 20 genotypes including the white-fruit phenotype such as 'Oliva bianca' (I A) and 'Leucocarpa 1' (I B), and all the genotypes characterized by pointed apex and asymmetric stone, such as 'Cornale', 'Cornulara' and 'Pizzutella 1'. This cluster also includes four unknown genotypes (Unknown-7, Unknown_13, Pendolino-type 1, Koroneiki-type) and eight not described genotypes: 'Cornetto', 'Leucocarpa 2', 'Passa dolce' 'Pizzutella bianca', 'Primamezzana 4', 'San Giovanni', 'Signora Francesca', and 'Trigno'. Cluster II included 48 genotypes, 25 not present in OLEADB ('Canua 1', 'Fragile', 'Fragolina', 'Grappa', 'Mennella', 'Orniella', 'Primamezzana 3', 'Rumanella', 'Sanguinella', 'Silletta 2', 'Silletta Nisi', 'Torremaggiorese', 'Torremaggiore', 'Uaccdain', four 'Ogliarola', seven 'Cellina'), and one oleaster. Cluster III comprises 29 genotypes characterized by medium-high fruit size and stone weight and size: three genotypes not described in OLEADB ('Ogliarola di Biccari', 'Oliva maggiorata' and 'Rosciolone' etc.), five accessions of 'Ogliarola' and 'Cellina 7'

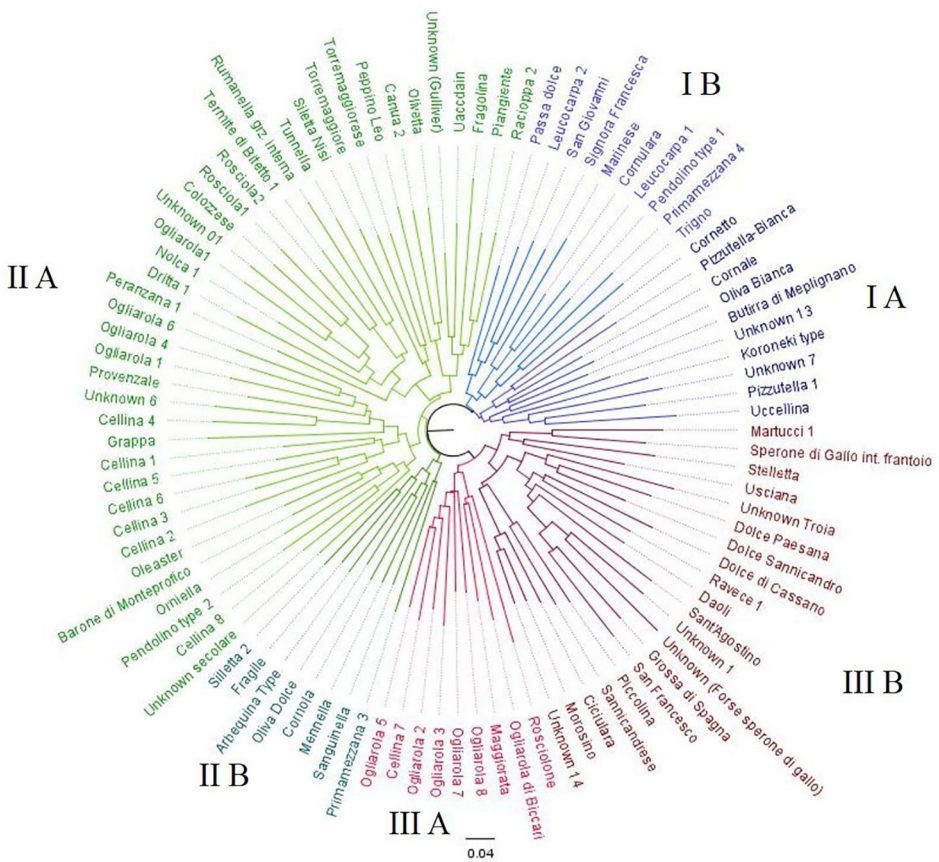

FIGURE 2 | Dendrogram generated by Neighbor-Joining clustering method, illustrating the relationships among 97 olive Apulian genotypes, using the morphological markers.

(subcluster IIIA), three table olives cultivars ('Grossa di Spagna', 'Sant'Agostino' and 'San Francesco'), and five other genotypes (Unknown-1, Unknown-14, 'Troia', 'Sperone di Gallo' and 'Martucci 1') (sub-cluster III B). This sub-cluster also includes two of the most typical 'sweet olives', 'Dolce di Cassano', and 'Dolce di Sannicandro', and seven local genotypes ('Ciciulara', 'Daoli', 'Dolce paesana', 'Morosino', 'Piccolina', 'Sannicandrese', and 'Stelletta'). Most of "unknown" genotypes showed high similarity with cultivars 'Ogliarola' and 'Cellina'; only 'Unknown 3' and 'Unknown 5' did not revealed similarity with any other variety, showing a unique profile (**Table 1**).

Genetic Characterization

The eleven selected SSR markers successfully amplified the 177 olive studied samples, confirming to be highly informative as indicated by PIC values that was higher than 0.5 at all loci (mean 0.72), except for EMOL (**Table 2**). Total number of alleles (Na) of 113 alleles was obtained, with a mean of 10 alleles per locus, ranging from four alleles for EMOL to 17 alleles for DCA09. The average number of effective alleles (Ne) was 4.86, ranging from 1.57 (EMOL) to 11.02 (DCA09). The observed Heterozygosity (Ho) varied between 0.10 for EMOL and 0.89 for DCA09 (mean Ho = 0.64), whereas the expected Heterozygosity (He) ranged between 0.36 (EMOL) and 0.91 (DCA09) (mean He = 0.74). The Fixation Index (F) was positive for all markers except for DCA05, GAPU71b and GAPU101. The Na in the reference cultivars was higher (143), and Ho (mean 0.71) was lower than He (mean 0.79). On the whole collection (local genotypes and reference cultivars), the total Number of alleles was 172 (**Table 2**), with a mean of 16 alleles per locus, ranging from 10 alleles for EMOL to 27 alleles for DCA18. The average number of effective alleles (Ne) was 6.43, ranging from 1.79 (EMOL) to 13.61 (DCA09). Shannon's information index (I) ranged from 0.93 (EMOL) to 2.73 (DCA09). The observed Heterozygosity (Ho) varied between 0.19 for EMOL and 0.85 for GAPU101 (mean Ho = 0.66), whereas the expected Heterozygosity (He) ranged between 0.44 (EMOL) and 0.93 (DCA09) (mean He = 0.80). The Fixation Index (F) was positive for all markers except for GAPU71b. The genetic analysis was also carried out on the three clusters resulting by the Neighbor Joining Analysis (**Supplementary Table 6**). The Na for the cluster I (11 genotypes), the cluster II (87 genotypes) and the cluster III (137 genotypes) was 70, 162 and 106, respectively, while Ne was 4.23, 7.53 and 4.68, respectively.

Estimation of pairwise relatedness (LRM) revealed gave a coefficient ranging from −0.147 to of 0.5, that corresponds to identical genetic profiles. Full identity was revealed between the samples 'Ogliarola 2, 5, and 6', between 'Peranzana 2' and 'Peranzana 3', and between the samples 'Donna Francesca' and

TABLE 1 | Results of the clustering of the 97 Apulian genotypes based on morphological traits. Known genotypes indicate genotypes present in the databank OLEADB.

Cluster	Sub-cluster	Profile	Genotypes described in OLEADB	Genotypes undescribed in OLEADB	Unknown genotypes	Other new genotypes
I	I A	1	Pizzutella, Uccellina	–	Unknown 7, Koroneiki-type	–
		2	Butirra di Melpignano	–	Unknown 13	–
		3	Cornale, Marinese, Oliva bianca	Cornetto, Pizzutella bianca	–	–
	I B	4	Leucocarpa 1, Cornulara	Trigno, Primamezzana 4	Pendolino-type 1	–
		5	–	Leucocarpa 2, Passa dolce, San Giovanni, Signora Francesca	–	–
II	II A	6	Piangente, Racioppa	Fragolina, Uaccdain	Unknown (Gulliver)	–
		7	Peppino Leo, Olivetta	Canua 1,	–	–
		8	–	Silletta Nisi, Torremaggiore Sacco, Torremaggiorese	–	–
		9	Colozzese, Dritta, Nolca, Rosciola (1, 2), Termite di Bitetto, Tunnella	Rumanella, Ogliarola 1	Unknown 01	–
		10	Peranzana	–	–	–
		11	Provenzale	Grappa, Cellina 3, Ogliarola 2,5,7,	Unknown 6	–
		12	–	Cellina 2,4,5,8,9		–
		13	Barone di Monteprofico	Orniella, Cellina 6	Pendolino-type 2	Oleaster
		14	–	–	Unknown secolare	–
	II B	15	Corniola, Oliva dolce	Fragile, Mennella, Silletta	Arbequina-type	–
		16	–	Primamezzana 1, Sanguinella		–
III	III A	17	–	Ogliarola 3,4,6,8,9, Cellina 7		–
		18	–	Ogliarola di Biccari, Oliva maggiorata, Rosciolone	–	–
	III B	19	–	Ciciulara, Morosino, Piccolina, Sannicandrese,	Unknown 14	–
		20	Grossa di Spagna, Sant'Agostino, San Francesco	Daoli	Unknown 1, Unknown (SG)	–
		21	Dolce di Cassano, Ravece	–	–	–
		22	Dolce di Sannicandro	Dolce paesana	Unknown Troia	–
		23	Sperone di gallo, Usciana	Stelletta	Martucci 1	–

TABLE 2 | Genetic indices obtained by SSR analysis on 177 minor Apulian accessions.

Minor Apulian genotypes (177)	Locus	Na	Ne	I	Ho	He	F	PIC
	DCA03	11	6.48	2.04	0.82	0.85	0.03	0.829
	DCA05	11	3.82	1.74	0.76	0.74	–0.02	0.716
	DCA09	17	11.02	2.51	0.89	0.91	0.03	0.902
	DCA13	8	3.24	1.55	0.44	0.69	0.37	0.664
	DCA15	9	3.37	1.49	0.35	0.70	0.50	0.662
	DCA17	15	4.99	1.94	0.65	0.80	0.19	0.777
	DCA18	14	6.52	2.13	0.77	0.85	0.09	0.83
	GAPU71b	8	3.99	1.54	0.83	0.75	–0.11	0.713
	GAPU101	8	5.04	1.76	0.85	0.80	–0.07	0.773
	EMO90	8	3.44	1.47	0.56	0.71	0.20	0.67
	EMOL	4	1.57	0.68	0.10	0.36	0.72	0.332
	TOTAL	113						
	Mean	10	4.86	1.71	0.64	0.74	0.18	0.72
Reference cultivars (59)								
	DCA03	11	5.22	1.92	0.88	0.81	–0.09	0.79
	DCA05	11	3.91	1.74	0.73	0.74	0.02	0.72
	DCA09	16	10.45	2.50	0.69	0.90	0.24	0.90
	DCA13	14	3.22	1.69	0.51	0.69	0.26	0.67
	DCA15	7	3,61	1.53	0.73	0.72	–0.01	0.69
	DCA17	17	6.88	2.25	0.62	0.85	0.27	0.84
	DCA18	22	9.02	2.56	0.76	0.89	0.14	0.88
	GAPU71b	10	4.97	1.89	0.84	0.80	–0.06	0.78
	GAPU101	14	8.17	2.33	0.83	0.88	0.05	0.87
	EMO90	12	4.41	1.84	0.75	0.77	0.04	0.75
	EMOL	9	2.64	1.32	0.46	0.62	0.26	0.58
	TOTAL	143						
	Mean	13	5.68	1.96	0.71	0.79	0.10	0.77
Whole collection (236)	**DCA03**	12	6.27	2.05	0.83	0.84	0.01	0.824
	DCA05	12	5.12	1.93	0.75	0.8	0.07	0.785
	DCA09	21	13.61	2.73	0.84	0.93	0.1	0.922
	DCA13	15	4.19	1.83	0.45	0.76	0.4	0.738
	DCA15	13	4.8	1,9	0.45	0.79	0.43	0.769
	DCA17	22	7	2.33	0.64	0.86	0.25	0.844
	DCA18	27	9.67	2.63	0.77	0.9	0.14	0.889
	GAPU71b	11	5.84	1.99	0.83	0.83	–0.01	0.81
	GAPU101	15	7.33	2.25	0.85	0.86	0.02	0.85
	EMO90	15	5.08	1.95	0.61	0.8	0.24	0.782
	EMOL	10	1.79	0.93	0.19	0.44	0.57	0.411
	TOTAL	172						
	Mean	16	6.43	2.05	0.66	0.8	0.2	0.78

Size range (bp); Na, number of observed alleles; Ne, number of effective alleles; I, Shannon's information index; Ho, observed heterozygosity; He, expected heterozygosity; F, fixation index; PIC, polymorphic information content.

'San Francesco'. These genotypes showed high similarity also with 'Colmona' and 'Lecllin' (0.4 < LRM < 0.5), while 'Dolce di Cassano' was very similar to 'Dolce di Sannicandro' (**Table 3**). Several cases of homonymies were observed regarding, in particular, cultivars 'Ogliarola', 'Cellina', 'Racioppa', and 'Nolca' (**Table 4**).

The dendrogram obtained by the Neighbor Joining Analysis disclosed the inter-individual relationship between genotypes, revealing three main clusters (**Figure 3**). Cluster I includes 11 Apulian cultivars and two Calabrian reference cultivars 'Ciciariello' and 'Tonda di Filogaso'. Cluster II includes few table olive varieties (sub-cluster IIA), a group of reference cultivars (sub-cluster II B.1), most of the samples collected in Lecce province, in particular 'Ogliarola' and 'Cellina' (sub-cluster IIB2.1), and the genotypes characterized by pointed apex and asymmetric stone ('Crnlecchie', 'Cornale' and 'Cornola') (sub-cluster II B2.2). Cluster III includes genotypes coming from all over Apulia except from Lecce province (**Figure 3**).

TABLE 3 | List of pairwise relatedness based on LRM estimator (Lynch and Ritland, 1999).

Genotypes with LRM = 0.5	
OGLIAROLA2	OGLIAROLA5
OGLIAROLA2	OGLIAROLA6
OGLIAROLA5	OGLIAROLA6
PERANZANA2	PERANZANA3
SAN FRANCESCO	DONNA FRANCESCA
Genotypes with an 0.5 > LRM > 0.4	
COLMONA	LCELLIN
COLMONA	SAN FRANCESCO
LCELLIN	SAN FRANCESCO
COLMONA	DONNA FRANCESCA
LCELLIN	DONNA FRANCESCA
DOLCE DI CASSANO	DOLCE DI SANNICANDRO
UACCIDIN 2	MELE
RUMANELLA GRAZIANO INTERNA	ROTONDELLA O ROSCIOLA
CAZZALORA	GROSSA DI SPAGNA

TABLE 4 | Cases of homonymies based on LRM estimator (Lynch and Ritland, 1999).

Homonyms LRM < 0.2	
CELLINA 7	CELLINA 1, 2, 3, 4, 6, 5, 8
DRITTA 2	DRITTA 1
MELILL 1	MELILL 2
NOLCA 1	NOLCA 2
OGLIAROLA 01	OGLIAROLA 1, 2, 3, 4, 5, 6, 7,8
OGLIAROLA	OGLIAROLA 2, 3, 4, 5, 6, 7, 8
OGLIAROLA 2	OGLIAROLA 3, 8
OGLIAROLA 3	OGLIAROLA 4, 5, 6, 7
OGLIAROLA 4	OGLIAROLA 8
OGLIAROLA 5	OGLIAROLA 8
PENDOLINO TYPE1	PENDOLINO TYPE2
PEPPERINELLA CHIEUTI 1	PEPPERINELLA CHIEUTI 2
PRIMEMEZZANA 3	PRIMEMEZZANA 4
PROVENZALE	PROVENZALE CHIEUTI
PROVENZALE	PRUVENZALE
PROVENZALE CHIEUTI	PRUVENZALE
PASOLINA	PASOLA OSTUNI
PIZZUTA SEPPUNISI	PIZZUTA
PIZZUTA SEPPUNISI	PIZZUTA ESTERNA GRAZIANO
PIZZUTA	PIZZUTA ESTERNA GRAZIANO
RACIOPPA 1	RACIOPPA 2
RACIOPPA 2	RACIUEPP
RUMANELLA 1	RUMANELLA 2
RUMANELLA 2	RUMANELLA GRAZIANO INT.
ROSCIOLA 1	ROSCIOLA 2
ROSCIOLA SERRA	ROSCIOLA 1
ROSCIOLONE	ROSCIOLA 1
SILETTA NISI	SILLETTA 1, 2
TRIGNA	TRIGNO

The population structure indicated a maximum for ΔK at K = 2 (**Supplementary Figure 2**), separating the national Italian germplasm from the local varieties under investigation (**Supplementary Figure 2A**).

Technological Characterization of Mono-Varietal Oils

FA and sterol composition of the samples under study resulted within the limit set by the European regulations (Commission Regulation (EEC) No 2568/91, Official Journal of the European Communities, 1991) (**Table 5**). Five main fatty acids were detected, with oleic acid being the most abundant, followed by palmitic, linoleic, stearic and palmitoleic. Oleic acid accounted for about 97% of the total Mono Unsaturated Fatty Acids (MUFA) content, ranging from less than 59% ('Cornale') to around 80% ('Bianca') (mean value of 71.23%). Palmitoleic acid was the second most abundant monounsaturated fatty acid (mean value of 1.52%) ranging from 0.1 ('Signora Francesca') to 3.05% ('Dolce di Cassano'). Among Saturated Fatty Acids (SFA), palmitic acid was the most abundant (85%), ranging from 9.67% ('Limongella') to 19.99 ('Mennella') (mean value of 14.46%). It was followed by stearic acid (11%) and arachidic acid (0.50%) (**Table 5**). Poly Unsaturated Fatty Acids (PUFA) were the less abundant fatty acids (mean 9.67%), and were represented for more than 96% by linoleic acid (mean value of 9.36%). Linolenic acid showed a mean value of 0.31%, with a minimum of 0.14% ('Sannicandrese') and a max. 0.80% ('Pizzuta Graziano'). Palmitic, oleic and linoleic acids showed the highest variability among the dataset according to the IQR, followed by palmitoleic fatty acid. Oleic/linoleic and MUFA/PUFA ratios were very similar because, as previously reported, oleic and linoleic acids accounted for the great majority of MUFA and PUFA, respectively. Cultivar 'Bianca' had the highest value of oleic/linoleic (19.35), while 'Cornale' showed the lowest value (3.63), having the lowest and the highest content of oleic and linoleic, respectively. The same genotype showed the highest and lowest values of MUFA/PUFA ratio. About the sterol composition, apparent β-sitosterol was the most abundant form, ranging from 93% ('Marinese', 'Mennella', 'Rumanella' and 'Silletta') to 95.3% ('Torremaggiorese'), highlighting also a small variability among the oils. Campesterol and stigmasterol were the next abundant sterols with mean values of 2.7 and 1.1%, respectively. 'Racioppa' featured the lowest amount of campesterol (1.9%) and 'Sepponisi' the highest (3.7%) whilst 'Torremaggiorese' and 'Leucocarpa', and 'Pizzuta' cultivars had the minimum and maximum stigmasterol content (0.3 and 2.7%, respectively). Total sterol content was always higher than 1,000 mg kg^{-1} and reached a maximum of 2,791 mg kg in 'Racioppa' oil. Fatty acids and sterols of the VOOs were also explored by means of PCA and used to study the similarity among the oils (**Supplementary Figure 3**). The first two principal components (PCs) explained around 35% of the total dataset variability. In particular PC1, which explained 26% of the data variability, was mostly affected by oleic and linoleic acids together with the sum of MUFA, PUFA and the respective ratios, while PC2, which explained about 9.5% of the data variability, was strongly influenced by single saturated fatty acids ($C_{17:0}$, $C_{20:0}$) and by sterols. No clear samples clusters were observed in the score plot and the majority of them stand around the origin.

Evaluation of Phytosanitary Status and Sanitation

Out of 129 analyzed genotypes, only 16 satisfied the sanitary status "virus free". While no infection associated to the viruses ArMV, SLRV, OLV-1, OLV-2, CMV, TNV and to the bacterium *X. fastidiosa* was found on all the samples, 106 genotypes resulted infected by OLYaV, two genotypes by CLRV and five genotypes by both OLYaV and CLRV (**Supplementary Table 7**). Forty-four genotypes infected by OLYaV and CLRV were submitted to sanitation treatments, and 30 and 14 genotypes were treated respectively, with *in vivo* and *in vitro* thermotherapy, followed by micrografting (**Supplementary Table 7**). Thirty-eight out of 44 genotypes were assessed free from OLYaV and CLRV, 25 by *in vivo* thermotherapy and 13 by *in vitro* thermotherapy. Overall, 81 "healthy plants" were produced, including the 76 coming from sanitation treatments. Moreover 42 out of them, belonging to 20 presumed different varieties, also genetically and pomologically characterized, were maintained in screen house as Primary Sources to be shortly registered in the national certification system (DDG 06/12/2016).

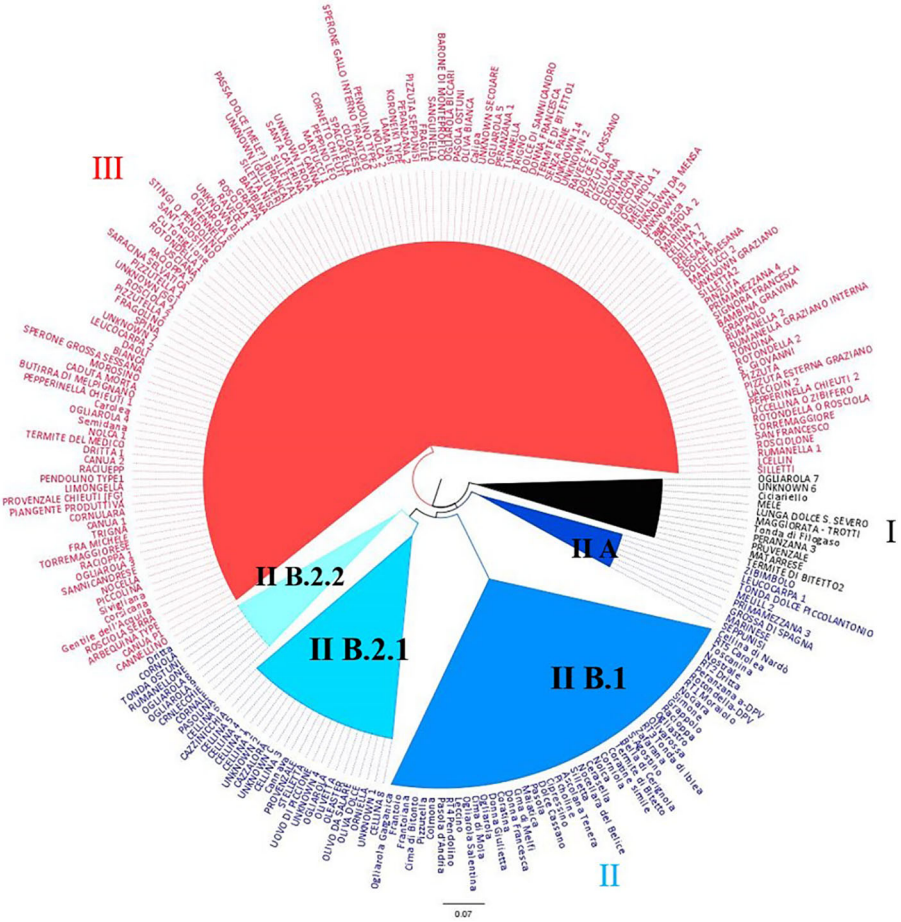

FIGURE 3 | Dendrogram generated by Neighbor-Joining clustering method, illustrating the phylogenetic relationships among 236 olive genotypes, using the SSR markers.

Database Release and Olive Germplasm Management

All data obtained from the molecular, morphological, phytosanitary and technological characterization were collected in a database integrated with the regional GIS portal (**Supplementary Figure 4**), accessible on request to Apulia region website (misura 10.2.1: www.psr.regione.puglia.it). The database contains additional information about the GPS position of field collections, reports of public meetings, consulted documents related to olive cultivation history, and geotagged photographs related to the recovered genotypes, the pictures of the countryside and rural landscape where the genotypes were found and further detailed pictures about leaves, flowers, fruits and stem.

DISCUSSION

Olive tree is a primary economic source for Apulia region, where it has a wide and ancient varietal richness, still largely uncharacterized and not exploited. In order to enhance the production of oil and table olives, it is essential to proceed to an accurate varietal identification and characterization of this germplasm. The regional Re.Ger.O.P. project allowed to identify, collect and characterize this marginalized germplasm investigating morphological, molecular, technological and phytosanitary aspects, and supported *in situ* and *ex situ* conservation. Based on the bibliographic sources, notary studies, meetings, archives and libraries, numerous varieties locally cultivated in the past centuries, were identified, mainly in the minor olive groves, or as single specimens' relicts of old orchards. A total of 177 olive genotypes were collected from all the Apulian provinces and compared with a set of 59 Italian cultivars already characterized and used as reference. Although several authors have already described the genetic diversity of ancient and local Italian cultivars and evaluated the phenological, physiological and molecular characteristics (Erre et al., 2012; Lombardo et al., 2019), this work represents the first investigation conducted with a multidisciplinary approach.

The morphological characterization of 97 minor genotypes based on descriptors of leaf, fruit, and stone, revealed an extremely variability within the Apulian olive germplasm.

TABLE 5 | Descriptive statistics of the purity characteristics of the monovarietal oils obtained from 34 minor olive Apulian accessions.

	Min	Max	Mean	Q1	Q3	IQR
Fatty acids composition (area %)						
Myristic acid $C_{14:0}$	0.00	0.03	0.01	0.00	0.02	0.02
Palmitic acid $C_{16:0}$	9.67	19.99	14.46	12.52	16.08	3.56
Palmitoleic acid $C_{16:1}$	0.10	3.05	1.52	0.83	2.08	1.25
Margaric acid $C_{17:0}$	0.00	0.31	0.09	0.04	0.13	0.09
Heptadecenoic acid $C_{17:1}$	0.02	0.33	0.12	0.08	0.14	0.06
Stearic acid $C_{18:0}$	0.97	2.82	1.91	1.65	2.16	0.51
Oleic acid $C_{18:1}$	58.73	79.73	71.23	69.16	74.36	5.20
Linoleic acid $C_{18:2}$	4.12	16.18	9.36	7.61	10.70	3.09
Linolenic acid $C_{18:3}$	0.14	0.80	0.31	0.23	0.36	0.13
Arachidic acid $C_{20:0}$	0.22	0.60	0.50	0.46	0.56	0.10
Gadoleic acid $C_{20:1}$	0.15	0.49	0.34	0.30	0.39	0.10
Behenic acid $C_{22:0}$	0.00	0.18	0.08	0.05	0.11	0.06
Lignoceric acid $C_{24:0}$	0.00	0.20	0.03	0.00	0.05	0.05
SFA	12.63	22.39	17.07	15.59	18.33	2.74
MUFA	62.29	81.27	73.21	71.67	75.98	4.31
PUFA	4.51	16.41	9.67	7.92	11.09	3.18
Oleic/Linoleic	3.63	19.35	8.47	6.53	9.64	3.10
MUFA/PUFA	3.80	18.02	8.33	6.47	9.48	3.01
Sterols composition (area %)						
Cholesterol	0.00	0.40	0.20	0.00	0.20	0.20
Brassicasterol	0.00	0.10	0.00	0.00	0.00	0.00
Campesterol	1.90	3.70	2.70	2.40	3.00	0.60
Campestanol	0.10	1.00	0.40	0.30	0.50	0.30
Stigmasterol	0.30	2.70	1.10	0.80	1.40	0.60
Δ-7-Campesterol	0.00	0.90	0.20	0.00	0.30	0.30
Apparent β-Sitosterol	93.00	95.30	93.50	93.10	93.70	0.60
Δ-7-Stigmastenol	0.00	0.50	0.30	0.20	0.30	0.10
Δ-7-Avenasterol	0.10	0.80	0.40	0.30	0.60	0.30
Total sterols (mg kg)	1017	2791	1846	1390	2222	832

Q1, first quartile; Q3, third quartile; IQR, inter-quartile range; SFA, total saturated fatty acids; MUFA, total mono-unsaturated fatty acids; PUFA, total poly-unsaturated fatty acids.

Forty-nine genotypes were recognized as already described varieties, while 64 were found to be known only with local name or nameless. These genotypes could be both the result of the processes of hybridization or between cultivars or between cultivars and wild oleaster naturally present in Apulian countryside. The dendrogram obtained using the morphological markers separated the germplasm in three main clusters. One group included the white-fruit genotypes, such as 'Oliva bianca' and Leucocarpa, and genotypes characterized by the pointed apex and asymmetric stone, such as 'Cornale', 'Cornulara' etc. A second group included various phenotypes, while the third group included 29 genotypes characterized by medium-high weight and size of fruit and stone, including several important table olives such as 'Grossa di Spagna', 'Sant'Agostino', 'Rosciolone', 'Grappolo' and 'San Francesco', and the most typical Apulian 'sweet olives', such as 'Dolce di Cassano', and 'Dolce di Sannicandro'. This clusterisation was not supported by the SSRs analysis since the microsatellites did not separate the cultivars according to the fruit size and weight. In contrast, this clustering was obtained by Montemurro et al. (2005) using AFLPs and by D'Agostino et al. (2018) using GBS analysis, probably due to the multilocus strategy of these two approaches.

Both the Neighbor Joining dendrogram and Structure analysis revealed a clear differentiation between the national Italian germplasm from the local one, indicating that it could have a different origin. The richness in alleles of the Apulian germplasm is also confirmed by the high total number of alleles in Cluster II that includes the large part of the Apulian genotypes. It is interesting to observe that in the Cluster II, that grouped both Apulian genotypes and national cultivars, the total number of alleles is higher than Cluster III. This could be explained by the fact that the national cultivars originated by different ancestors coming from different parts of Mediterranean basin (D'Agostino et al., 2018); thus, they are characterized by a more heterogeneous gene pool reflecting their multiple origin.

The genetic analysis confirmed a large genetic diversity on the whole sample of the olive trees analyzed, indicating an observed heterozygosity lower than the expected heterozygosity. This is in contrast with the fact that olive is a predominantly allogamous species (Diaz et al., 2006; Farinelli et al., 2008), but similar results were obtained by other researches on Apulian olive germplasm (Muzzalupo et al., 2009; Boucheffa et al., 2017; di Rienzo et al., 2018b). This could be explained with the fact that reproduction in olive is strongly influenced by the rating of self-incompatibility, which is, in turn, under the effects of the genetic control but also environmental and climatic conditions (Lavee, 2013; Montemurro et al., 2019).

The Lynch and Ritland analysis highlighted only a single true case of synonymy between the genotype 'Donna Francesca' and 'San Francesco', probably as the result of a misnaming. On the contrary, several homonymies were observed, mostly regarding the varieties 'Ogliarola' and 'Cellina', that are the two most common cultivars in southern Apulia area. It is probable that, under the generic denomination 'Ogliarola' (meaning 'producer of oil'), different genotypes derived by clonal variation or spontaneous crossing between cultivars and/or feral forms, are included (Muzzalupo et al., 2014; D'Agostino et al., 2018). 'Ogliarola' and 'Cellina' are both susceptible to *X. fastidiosa* (Giampetruzzi et al., 2016) but the showed great variability among samples of these two cultivars could represent an interesting aspect in order to recognize a different behaviour of the plants to the disease.

Morphological and molecular analyses clustered together the genotypes 'Peranzana', 'Provenzale', 'Dritta' 'Torremaggiorese' and 'Torremaggiore'. These varieties all originate from the Sub-Appennino Dauno area, which is a geographical area characterized by mountains that create the conditions for the genetic isolation of olive genotypes. It is possible that these varieties have a common genetic background to those introduced in Apulia from the south France (Provenza) at the end of 1700 (Fiore, 2018).

Oil macro and micro components defines the product's nutritional, qualitative and sensorial features (Boskou, 2006; D'Imperio et al., 2007; Rotondi et al., 2010). Fatty acids and sterols profiles and content greatly affect the nutritional and stability characteristics of the product and they are strongly linked to the genotype.

Overall, the VOOs obtained from the 34 studied Apulian accessions were generally rich in MUFA content, which was always higher than 60% of total fatty acids, and oleic acid appears to be the most significant variable affecting the samples distribution. Oleic acid influences oil stability to oxidation

(Choe and Min, 2009) and plays an important nutritional role (Huang and Sumpio, 2008). The samples 'Cornale', 'Mennella', 'Oleaster', 'Racioppa' and 'Sannicandrese' showed the lowest amount of oleic acid (below 70%) and were well separated from the cloud in the PCA score plot. About linoleic acid content, in 28 out of 34 samples it ranged from 7.33 to 16.18%, values quite higher than those reported for others Apulian typical virgin oils such as Coratina (Aparacio and Luna, 2002; Rotondi et al., 2010). In particular, 'Nolca', 'Cornale', 'Fragolina', 'Mennella', 'Oleaster', 'Pasola', 'Pizzutella', 'Racioppa', 'Sig. Francesca', 'Sannicandrese', 'Silletta Nisia', 'Silletta', 'Torre Maggiorese' and 'Pasolina' were characterized by a linoleic content higher than 10%.

Although several variables could affect the oxidative stability of the oils, in particular the antioxidants content (Velasco and Dobarganes, 2002), it is well known that oleic/linoleic and MUFA/PUFA ratios are useful indices for forecasting VOO stability. Modification in the contents of oleic and linoleic acids are related to different factors, including the latitude and altitude of olive cultivation (Inglese et al., 2011). A minimum ratio oleic/linoleic of 7 was established as an indicator of oil oxidative stability (Kiritsakis et al., 1998). In our samples, this ratio was highly variable, with 23 oils showing the minimum ratio oleic/linoleic >7, thus forecasting a good stability and shelf-life of VOOs. In particular, oil of cultivar Bianca stands out for a very high ratio oleic/linoleic, thus it is expected to be very stable to oxidation.

About the sterols total content, it is well known that sterols contribute to the oil antioxidant activity (Choe and Min, 2009) and have positive effect on human health (Kritchevsky and Chen, 2005; Regulation (EU) No 432/2012). A wide variability among the VOOs was observed, ranging between 1,017 mg kg^{-1}, close to the minimum EU limit (Commission Regulation (EEC) No 2568/91), and 2,791 mg kg^{-1}, which is quite higher than values generally reported for VOOs (Manai-Djebali et al., 2012; Lukić et al., 2013). 'Racioppa' oil, in particular, showed the highest total sterols content and could be interesting as a source for breeding programs and commercial valorization.

The high linolenic content is typically present in naturally sweet olives, and it might be an indicator for increased desaturase activity for the conversion of oleic acid to linoleic acid (Aktas et al., 2014). The virgin olive oil from 'Dolce di Cassano' which is a "naturally debittered olive" used for both oil extraction and for cooked consumption, presents the highest levels of palmitoleic, margaric and linolenic acids. The sweetness of this cultivar is an interesting character that could be exploited in order set up a pilot trial for the production of frozen olives ready to be cooked in fry pan.

In conclusion, this research has shown the presence of genotypes with interesting technological features that deserve to be deeper explored. The conservation of these genetic resources should be implemented by measures that minimize the risk of spreading diseases such as *Xylella*. The phytosanitary analyses showed that Apulian olive germplasm is in overall good phytosanitary status. OLYaV was the predominant viral agent, in accordance with the past evidences in Southern Italy (Fontana et al., 2019), while only seven genotypes were infected by CLRV. The sanitation treatments adopted resulted very effective in eliminating both viruses with 83% and 92% efficiency for *in vivo* and *in vitro* thermotherapy, respectively. Thus, the protocols here described, resulted to be very efficient and could be suggested to simultaneously and quickly remove these two viruses. The 42 primary sources produced by Re.Ger.O.P project have been officially declared compliant to the phytosanitary requirements for the commercialization of certified materials in EU (Annex I of DDG 6/12/2016).

Several works have been made on the phenotypic and genetic variability of local olive germplasm at regional level (Erre et al., 2010; Hmmam et al., 2018; Mousavi et al., 2019; Rotondi et al., 2018) including Apulia region (Salimonti et al., 2013; di Rienzo et al., 2018a). Nevertheless, this study represents the first investigation conducted with a multidisciplinary approach, taking into consideration several aspects about the biodiversity of the Apulian germplasm. The Re.Ger.O.P. project has allowed, through the integration of different activities and competences, to bring out, in the Apulian olive germplasm, a richness, certainly not unexpected, but now completely ascertained. The cultural history of this region, thanks to the geographical location that has make it a transit point for centuries, explains the complexity of relationships existing among the hundreds of cultivars of the wide Apulian olive-growing panorama. At the same time, we can observe how, in Apulia, a heritage of unique genetic diversity has been preserved, which certainly deserve to be deepened and valued. The information obtained are encouraging, and they will help to valorize this germplasm with economic advantages and it will prevent genetic erosion.

DATA AVAILABILITY STATEMENT

This article contains previously unpublished data. The name of the repository and accession number(s) are not available.

AUTHOR CONTRIBUTIONS

VF, FB, SC, CM, FC, and GB designed the experiment. PV, GV, AP, and GA collected the plant material. GB, VM, AS, and GL performed the sanitary state characterization. FC, GS, and GD performed the technological characterization and analyses. SC and GV performed the morphological characterization and analyses. VR, MM, CM, SS, IM, WS, and GM performed the molecular characterization and analyses. IM, CM, FC, MM, and SC were involved in data interpretation. IM, VR, MM, FC, SC, CM, and GL wrote the manuscript. MM, IM, and CM implemented the manuscript. All authors read and approved the final manuscript.

FUNDING

This research was supported by Apulia region within the: PROGRAMMA SVILUPPO RURALE FEASR 2014–2020 Asse II "Miglioramento dell'Ambiente e dello Spazio Rurale" Misura

10.2.1 "Progetti per la conservazione e valorizzazione delle risorse genetiche in agricoltura"-trascinamento della Misura 214 Az. 4 sub azione a) del PSR 2007–2013 Progetti integrati per la biodiversità—Progetto Re.Ger.O.P. "Recupero del Germoplasma Olivicolo Pugliese" Progetto di continuità.

SUPPLEMENTARY MATERIAL

The Supplementary Material for this article can be found online at: https://www.frontiersin.org/articles/10.3389/fpls.2020.00073/full#supplementary-material

REFERENCES

Abou Kubaa, R., Morelli, M., Campanale, A., Morano, M., Susca, L., La Notte, P. F., et al. (2018). Improvement of a protocol for sanitation and early diagnostic validation of autochthonous grapevine germplasm, in: *Proceedings of the 19th Congress of ICVG*, Santiago Chile. pp. April 9-12, 128–129.

Acquadro, A., Papanice, M. A., Lanteri, S., Bottalico, G., Portis, E., Campanale, A., et al. (2009). Production and fingerprinting of virus-free clones in a reflowering globe artichoke. *Plant Cell Tiss Organ Cult*. 100 (3), 329–337. doi: 10.1007/s11240-009-9654-3

Aktas, A. B., Ozen, B., Tokatli, F., and Sen, I. (2014). Comparison of some chemical parameters of a naturally debittered olive (Olea europaea L.) type with regular olive varieties. *Food Chem.* 161, 104–111. doi: 10.1016/j.foodchem.2014.03.116

Albertini, E., Torricelli, R., Bitocchi, E., Raggi, L., Marconi, G., Pollastri, L., et al. (2011). Structure of genetic diversity in *Olea europaea* L. *cultivars Cent. Italy. Mol. Breed.* 27, 533–547. doi: 10.1007/s11032-010-9452-y

Aparacio, R., and Luna, G. (2002). Characterisation of monovarietal virgin olive oils. *Eur. J. Lipid Sci. Technol.* 4, 614–627. doi: 10.1002/1438-9312(200210)104:9/10<614::AID-EJLT614>3.0.CO;2-L

Baldoni, L., Cultrera, N. G., Mariotti, R., Ricciolini, C., Arcioni, S., Vendramin, G. G., et al. (2009). A consensus list of microsatellite markers for olive genotyping. *Mol. Breed* 24, 213–231. doi: 10.1007/s11032-009-9285-8

Bartolini, G., Cerreti, S., Briccoli Bati, C., Stefani, F., Zelasco, S., Perri, E., et al. (2014). *Oleadb: worldwide database for the management of genetic resources of olive (Olea europaea L.)* (Rome: X National Congress on Biodiversity), 18–23.

Binetti, G., Del Coco, L., Ragone, R., Zelasco, S., Perri, E., Montemurro, C., et al. (2017). Cultivar classification of apulian olive oils: use of artificial neural networks for comparing NMR, NIR and merceological data. *Food Chem.* 219, 131–138. doi: 10.1016/j.foodchem.2016.09.041

Blazakis, K. N., Kosma, M., Kostelenos, G., Baldoni, L., Bufacchi, M., and Kalaitzis, P. (2017). Description of olive morphological parameters by using open access software. *Plant Meth.* 13 (1), 11. doi: 10.1186/s13007-017-0261-8

Boskou, D. (2006). *Olive oil- Chemistry and technology. 2nd Edition*. Ed. D. Boskou (Champaign: Academic Press and AOCS Press). doi: 10.1201/9781439832028

Botstein, D., White, R. L., Skolnick, M., and Davis, R. W. (1980). Construction of a genetic linkage map in man using restriction fragment length polymorphisms. *Am. J. Hum. Gen.* 32, 314–331.

Bottalico, G., Saponari, M., Campanale, A., Mondelli, G., Gallucci, C., Serino, E., et al. (2004). Sanitation of virus-infected olive trees. *J. Plant Path* 86, 311.

Boucheffa, S., Miazzi, M. M., di Rienzo, V., Mangini, G., Fanelli, V., Tamendjari, A., et al. (2017). The coexistence of oleaster and traditional varieties affects genetic diversity and population structure in Algerian olive (*Olea europaea*) germplasm. *Gen. Res. Crop Evol.* 64 (2), 379–390. doi: 10.1007/s10722-016-0365-4

Boucheffa, S., Tamendjari, A., Sanchez-Gimeno, A. C., Rovellini, P., Venturini, S., di Rienzo, V., et al. (2019). Diversity assessment of Algerian wild and cultivated olives (*Olea europaea* L.) by molecular, morphological, and chemical traits. *Eur. J. Lipid Sci. Technol.* 121, 1800302, 1–14. doi: 10.1002/ejlt.201800302

Camposeo, S., Vivaldi, G. A., and Gattullo, C. E. (2013). Ripening indices and harvesting times of different olive cultivars for continuous harvest. *Sci. Hortic.* 151, 1–10. doi: 10.1016/j.scienta.2012.12.019

Caponio, F., and Catalano, P. (2001). Hammer crushers vs disk crushers: the influence of working temperature on the quality and preservation of virgin olive oil. *Euro. Food Res. Tech.* 213 (3), 219–224. doi: 10.1007/s002170100364

Caponio, F., Squeo, G., Brunetti, L., Pasqualone, A., Summo, C., Paradiso, V. M., et al. (2018a). Influence of the feed pipe position of an industrial scale two-phase decanter on extraction efficiency and chemical-sensory characteristics of virgin olive oil. *J. Sci. Food Agric.* 98, 4279–4286. doi: 10.1002/jsfa.8950

Caponio, F., Squeo, G., Curci, M., Silletti, R., Paradiso, V. M., Summo, C., et al. (2018b). Calcium carbonate effect on alkyl esters and enzymatic activities during olive processing. *Ital. J. Food Sci.* 30, 381–392.

Carriero, F., Fontanazza, G., Cellini, F., and Giorio, G. (2002). Identification of simple sequence repeats (SSRs) in olive (*Olea europaea* L.). *Theor. App. Gen.* 104, 301–307. doi: 10.1007/s001220100691

Caruso, T., Campisi, G., Marra, F. P., Camposeo, S., Vivaldi, G. A., Proietti, P., et al. (2014). Growth and yields of the cultivar Arbequina in high density planting systems in three different olive growing areas in Italy. *Acta Hortic.* 1057, 341–348. doi: 10.17660/ActaHortic.2014.1057.40

Chiappetta, A., Muto, A., Muzzalupo, R., and Muzzalupo, I. (2017). New rapid procedure for genetic characterization of Italian wild olive (*Olea europaea*) and traceability of virgin oils by means of SSR markers. *Sci. Hortic.* 226, 42–49. doi: 10.1016/j.scienta.2017.08.022

Chiumenti, M., Campanale, A., Bottalico, G., Minafra, A., De Stradis, A., Savino, V. N., et al. (2013). Sanitation trials for the production of virus-free fig stocks. *J. Plant Path.* 95, 655–658.

Choe, E., and Min, D. B. (2009). Mechanisms of antioxidants in the oxidation of foods. *Compr. Rev. In Food Sci. Food Saf.* 8 (4), 345–358. doi: 10.1111/j.1541-4337.2009.00085.x

Cipriani, G., Marrazzo, M. T., Marconi, R., Cimato, A., and Testolin, R. (2002). Microsatellite markers isolated in olive (*Olea europaea* L.) are suitable for individual fingerprinting and reveal polymorphism within ancient cultivars. *Theor. Appl. Genet.* 104, 223–228. doi: 10.1007/s001220100685

Clodoveo, M. L., Camposeo, S., De Gennaro, B., Pascuzzi, S., and Roselli, L. (2014). In the ancient world, virgin olive oil was called "liquid gold" by Homer and "the great healer" by Hippocrates. Why has this mythic image been forgotten? *Food Res. Int.* 62, 1062–1068. doi: 10.1016/j.foodres.2014.05.034

D'Agostino, N., Taranto, F., Camposeo, S., Mangini, G., Fanelli, V., Gadaleta, S., et al. (2018). GBS-derived SNP catalogue unveiled wide genetic variability and geographical relationships of Italian olive cultivars. *Sci. Rep.* 8, 15877 1–13. doi: 10.1038/s41598-018-34207-y

D'Imperio, M., Dugo, G., Alfa, M., Mannina, L., and Segre, A. L. (2007). Statistical analysis on Sicilian olive oils. *Food Chem.* 102, 956–965. doi: 10.1016/j.foodchem.2006.03.003

De La Rosa, R., James, C. M., and Tobutt, K. R. (2002). Isolation and characterization of polymorphic microsatellites in olive (*Olea europaea* L.) and their transferability to other genera in the Oleaceae. *Mol. Ecol. Notes* 2, 265–267. doi: 10.1046/j.1471-8286.2002.00217.x

di Rienzo, V., Sion, S., Taranto, F., D'Agostino, N., Montemurro, C., Fanelli, V., et al. (2018a). Genetic flow among olive populations within the Mediterranean basin. *PeerJ* 6, e5260. doi: 10.7717/peerj.5260

di Rienzo, V., Miazzi, M. M., Fanelli, V., Sabetta, W., and Montemurro, C. (2018b). The preservation and characterization of Apulian olive germplasm biodiversity. *Acta Hortic.* 1199, 1–6. doi: 10.17660/ActaHortic.2018.1199.1

Diaz, A., Martin, A., Rallo, P., Barranco, D., and Rosa, R. D. L. (2006). Self-incompatibility of 'Arbequina' and 'Picual' olive assessed by SSR markers. *J. Am. Soc Hortic. Sci.* 131, 250–255. doi: 10.21273/JASHS.131.2.250

Difonzo, G., Pasqualone, A., Silletti, R., Cosmai, L., Summo, C., Paradiso, V. M., et al. (2018). Use of olive leaf extract to reduce lipid oxidation of baked snacks. *Food Res. Int.* 108, 48–56. doi: 10.1016/j.foodres.2018.03.034

Earl, D. A., and Von Holdt, B. M. (2012). Structure Harvester: a website and program for visualizing structure output and implementing the Evanno method. *Cons. Gen. Res.* 4 (2), 359–361. doi: 10.1007/s12686-011-9548-7

EPPO - PM 7/24 (3) (2018). Xylella fastidiosa. *EPPO Bull.* 48, 175–218. doi: 10.1111/epp.12469

Erre, P., Chessa, I., Munoz-Diez, C., Belaj, A., Rallo, L., and Trujillo, I. (2010). Genetic diversity and relationships between wild and cultivated olives (*Olea europaea* L.) in Sardinia as assessed by SSR markers. *Gen. Res. Crop Evol.* 57, 41–54. doi: 10.1007/s10722-009-9449-8

Erre, P., Chessa, I., Munoz, C., Rallo, L., and Trujillo, I. (2012). Genetic diversity of olive germplasm in Sardinia by SSR markers: wild olives, ancient trees and local cultivars. *Acta Hortic.* 949, 39–45. doi: 10.17660/ActaHortic.2012.949.4

Evanno, G., Regnaut, S., and Goudet, J. (2005). Detecting the number of clusters of individuals using the software structure: a simulation study. *Mol. Ecol.* 14, 2611–2620. doi: 10.1111/j.1365-294X.2005.02553.x

Famiani, F., Farinelli, D., Rollo, S., Camposeo, S., Di Vaio, C., and Inglese, P. (2014). Evaluation of different mechanical fruit harvesting systems and oil quality in very large size olive trees. *Spanish J. Agric. Res.* 12 (4), 960–972. doi: 10.5424/sjar/2014124-5794

FAO. (2001). http://www.fao.org/faostat/en/#home

Farahani, F., Razeghi, S., Peyvandi, M., Attaii, S., and Mazinani, M. H. (2011). Micrografting and micropropagation of olive (*Olea europea* L.) Iranian cultivar Zard. *Afr. J. Plant Sci.* 5, 671–675.

Farinelli, D., Hassani, D., and Tombesi, A. (2008). Self–sterility and cross–pollination responses of nine olive cultivars in Central Italy. *Acta Hortic.* 791, 127–136. doi: 10.17660/ActaHortic.2008.791.16

Felsenstein, J. (1985). Confidence limits on phylogenies: an approach using the bootstrap. *Evolution* 39 (4), 783–791. doi: 10.1111/j.1558-5646.1985.tb00420.x

Fiore, M. A. (2018). *Ulivi ed olio in alta Daunia nel periodo Normanno-Svevo*. Ed. M. Fiore, 1–83.

Fontana, A., Piscopo, A., De Bruno, A., Tiberini, A., Muzzalupo, I., and Albanese, G. (2019). Impact of Olive Leaf Yellowing Associated Virus on Olive (*Olea europaea* L.). *Eur. J. Lipid Sci. Technol.* 121, 1800472. doi: 10.1002/ejlt.201800472

García-Mier, L., Guevara-González, R. G., Mondragón-Olguín, V. M., Del Rocío Verduzco-Cuellar, B., and Torres-Pacheco, I. (2013). Agriculture and bioactives: achieving both crop yield and phytochemicals. *Int. J. Mol. Sci.* 14 (2), 4203–4222. doi: 10.3390/ijms14024203

Giampetruzzi, A., Morelli, M., Saponari, M., Loconsole, G., Chiumenti, M., Boscia, D., et al. (2016). Transcriptome profiling of two olive cultivars in response to infection by the CoDiRO strain of *Xylella fastidiosa* subsp. pauca. *BMC Genomics* 27: 17, 475. doi: 10.1186/s12864-016-2833-9

Harper, S., Ward, L., and Clover, G. (2010). Development of LAMP and real-time PCR methods for the rapid detection of *Xylella fastidiosa* for quarantine and field applications. *Phytopathol.* 100, 1282–1288. doi: 10.1094/PHYTO-06-10-0168

Hmmam, I., Mariotti, R., Ruperti, B., Cultrera, N., Baldoni, L., and Barcaccia, G. (2018). Venetian olive (*Olea europaea*) germplasm: disclosing the genetic identity of locally grown cultivars suited for typical extra virgin oil productions. *Gen. Res. Crop Evol.* 65 (6), 1733–1750. doi: 10.1007/s10722-018-0650-5

Huang, C. L., and Sumpio, B. E. (2008). Olive oil, the mediterranean diet, and cardiovascular health. *J. Am. Coll. Surg.* 207 (3), 407–416. doi: 10.1016/j.jamcollsurg.2008.02.018

Inglese, P., Famiani, F., Galvano, F., Servili, M., Esposto, S., and Urbani, S. (2011). 3 factors affecting extra-virgin olive oil composition. *Hortic. Rev.* 38, 83. doi: 10.1002/9780470872376

Istituto di Servizi per il Mercato Agricolo Alimentare (ISMEA), Scheda di settore olio di oliva. Maggio (2019). http://www.ismea.it/istituto-di-servizi-per-il-mercato-agricolo-alimentare.

Kalinowski, S. T., Taper, M. L., and Marshall, T. C. (2007). Revising how the computer program CERVUS accommodates genotyping error increases success in paternity assignment. *Mol. Ecol.* 16, 1099–1106. doi: 10.1111/j.1365-294X.2007.03089.x

Kiritsakis, A. K., Nanos, G. D., Polymenoupoulos, Z., Thomai, T., and Sfakiotakis, E. Y. (1998). Effect of fruit storage conditions on olive oil quality. *J. Am. Oil Chem. Soc* 75, 721–724. doi: 10.1007/s11746-998-0212-7

Kritchevsky, D., and Chen, S. C. (2005). Phytosterols health benefits and potential concerns: a review. *Nutr. Res.* 25 (5), 413–428. doi: 10.1016/j.nutres.2005.02.003

Lavee, S. (2013). Evaluation of the need and present potential of olive breeding indicating the nature of the available genetic resources involved. *Sci. Hortic.* 161, 333–339. doi: 10.1016/j.scienta.2013.07.002

Loconsole, G., Saponari, M., Faggioli, F., Albanese, G., Bouyahia, H., Elbeaino, T., et al. (2010). Inter-laboratory validation of PCR-based protocol for detection of olive viruses. *Bull. OEPP/EPPO Bull.* 40, 423–428. doi: 10.1111/j.1365-2338.2010.02416.x

Lombardo, L., Fila, G., Lombardo, N., Epifani, C., Duffy, D. H., Godino, G., et al. (2019). Uncovering olive biodiversity through analysis of floral and fruiting biology and assessment of genetic diversity of 120 Italian cultivars with minor or marginal diffusion. *Biology* 8, 62. doi: 10.3390/biology8030062

Lukić, M., Lukić, I., Krapac, M., Sladonja, B., and Piližota, V. (2013). Sterols and triterpene diols in olive oil as indicators of variety and degree of ripening. *Food Chem.* 136 (1), 251–258. doi: 10.1016/j.foodchem.2012.08.005

Lynch, M., and Ritland, K. (1999). Estimation of pairwise relatedness with molecular markers. *Genetics* 152, 1753–1766.

Manai-Djebali, H., Krichène, D., Ouni, Y., Gallardo, L., Sánchez, J., Osorio, E., et al. (2012). Chemical profiles of five minor olive oil varieties grown in central Tunisia. *J. Food Comp. Anal.* 27 (2), 109–119. doi: 10.1016/j.jfca.2012.04.010

Martelli, G. P., Salerno, M., Savino, V., and Prota, U. (2002). An appraisal of diseases and pathogens of olive, in: ISHS IV International Symposium on Olive Growing. *Acta Hortic.* 586, 701–708. doi: 10.17660/ActaHortic.2002.586.150

Montemurro, C., Simeone, R., Pasqualone, A., Ferrara, E., and Blanco, A. (2005). Genetic relationships and cultivar identification among 112 olive genotypes using AFLP and SSR markers. *J. Hortic. Sci. Biotech.* 80 (1), 105–110. doi: 10.1080/14620316.2005.11511899

Montemurro, C., Miazzi, M. M., Pasqualone, A., Fanelli, V., Sabetta, W., and Di Rienzo, V. (2015). Traceability of PDO olive oil "Terra di Bari" using high resolution melting. *J. Chem.* 2015, 1–7. doi: 10.1155/2015/496986

Montemurro, C., Dambruoso, G., Bottalico, G., and Sabetta, W. (2019). Self-incompatibility assessment of some Italian olive genotypes (*Olea europaea* L.) and cross-derived seedling selection by SSR markers on seed endosperms. *Front. Plant Sci.* 10: 22, 1–13. doi: 10.3389/fpls.2019.00451

Mousavi, S., Mariotti, R., Bagnoli, F., Costantini, L., Cultrera, N. G. M., Arzani, K., et al. (2017). The eastern part of the fertile crescent concealed an unexpected route of olive (*Olea europaea* L.) differentiation. *Ann. Bot.* 119 (8), 1305–1318. doi: 10.1093/aob/mcx027

Mousavi, S., Stanzione, V., Mencuccini, M., Baldoni, L., Bufacchi, M., and Mariotti, R. (2019). Biochemical and molecular profiling of unknown olive genotypes from central Italy: determination of major and minor components. *Euro. Food Res. Tech.* 245 (1), 83–94. doi: 10.1007/s00217-018-3142-0

Muzzalupo, I., Lombardo, N., Salimonti, A., and Perri, E. (2008). Molecular characterization of Italian olive cultivars by microsatellite markers. *Adv. Hortic. Sci.* 22 (2), 142–151.

Muzzalupo, I., Stefanizzi, F., and Perri, E. (2009). Evaluation of olives cultivated in southern italy by simple sequence repeat markers. *Hortic. Sci.* 44 (3), 582–588. doi: 10.21273/HORTSCI.44.3.582

Muzzalupo, I., Giovanni Vendramin, G., and Chiappeta, A. (2014). Genetic biodiversity of Italian olives (*Olea europaea*) germoplasm analyzed by SSR markers. *Sci. World J.* 2014, 12. doi: 10.1155/2014/296590

Muzzalupo, I. (2012). *Olive Germplasm– Italian Catalogue of Olive Varieties* (Rijeka, Croatia: InTech), 430. doi: 10.5772/54437

Official Journal of the European Communities. (1991). European Community Regulation No 2568/1991, N. L. 248 of 5 September 1991.

Onay, A., Pirinç, V., Yıldırım, H., and Basaran, D. (2004). *In vitro* micrografting of mature pistachio (*Pistacia vera* var. Siirt). *Plant Cell Tissue Organ Cult.* 77, 215–219. doi: 10.1023/B:TICU.0000016822.71264.68

Pasqualone, A., di Rienzo, V. D., Miazzi, M. M., Fanelli, V., Caponio, F., and Montemurro, C. (2015). High resolution melting analysis of DNA microsatellites in olive pastes and virgin olive oils obtained by talc addition. *Euro. J. Lipid Sci. Tech.* 117 (12), 2044–2048. doi: 10.1002/ejlt.201400654

Pellegrini, G., Ingrao, C., Camposeo, S., Tricase, C., Contò, F., and Huisingh, D. (2016). Application of water footprint to olive growing systems in the Apulia region: a comparative assessment. *J. Cleaner Prod.* 112, 2407–2418. doi: 10.1016/j.jclepro.2015.10.088

Pritchard, J. K., Stephens, M., and Donnelly, P. (2000). Inference of population structure using multilocus genotype data. *Genetics* 155 (2), 945–959.

Rosati, A., Paoletti, A., Al Hariri, R., Morelli, A., and Famiani, F. (2018a). Resource investments in reproductive growth proportionately limit investments in whole-tree vegetative growth in young olive trees with varying crop loads. *Tree Phys.* 38, 1267–1277. doi: 10.1093/treephys/tpy011

Rosati, A., Paoletti, A., Al Hariri, R., and Famiani, F. (2018b). Fruit production and branching density affect shoot and whole-tree wood to leaf biomass ratio in olive. *Tree Phys.* 38, 1278–1285. doi: 10.1093/treephys/tpy009

Rotondi, A., Alfei, B., Magli, M., and Pannelli, G. (2010). Influence of genetic matrix and of crop year on chemical and sensory profiles of Italian monovarietal extra virgin olive oils. *J. Sci. Food Agric.* 90, 2641–2646. doi: 10.1002/jsfa.4133

Rotondi, A., Ganino, T., Beghè, D., Di Virgilio, N., Morrone, L., Fabbri, A., et al. (2018). Genetic and landscape characterization of ancient autochthonous olive trees in northern Italy. *Plant Biosyst.* 152 (5), 1067–1074. doi: 10.1080/11263504.2017.1415993

Rugini, E. (1984). In vitro propagation of some olive cultivars with different rootability and medium development using analitycal data from developing shoots and embryos. *Sci. Hortic.* 24, 123–134. doi: 10.1016/0304-4238(84)90143-2

Sabetta, W., Miazzi, M. M., di Rienzo, V., Fanelli, V., Pasqualone, A., and Montemurro, C. (2017). Development and application of protocols to certify the authenticity and the traceability of Apulian typical products in olive sector. *Riv. Ital. Sost. Grasse* 94, 37–43.

Salimonti, A., Simeon, V., Cesaric, G., Lamaj, F., Cattivelli, L., Perri, E., et al. (2013). A first molecular investigation of monumental olive trees in Apulia region. *Sci. Hortic.* 162, 204–212. doi: 10.1016/j.scienta.2013.08.005

Saponari, M., Giampetruzzi, A., Loconsole, G., Boscia, D., and Saldarelli, P. (2019). *Xylella fastidiosa* in olive in Apulia: where we stand. *Phytopathology* 109 (2), 175–186. doi: 10.1094/PHYTO-08-18-0319-FI

Sardaro, R., Fucilli, V., and Acciani, C. (2015). Measuring the value of rural landscape in support of preservation policies. *Sci. Regionali* 14 (2), 125–138. doi: 10.3280/SCRE2015-002005

Sardaro, R., Bozzo, F., Petrontino, A., and Fucilli, V. (2018). Community preferences in support of a conservation programme for olive landraces in the Mediterranean area. *Acta Hortic.* 1199, 183–188. doi: 10.17660/ActaHortic.2018.1199.30

Sefc, K. M., Lopes, M. S., Mendonça, D., Rodrigues Dos Santos, M., Laimer Da Câmara Machado, M., and Da Câmara Machado, A. (2000). Identification of microsatellite loci in olive (*Olea europaea* L.) and their characterization in Italian and Iberian olive trees. *Mol. Ecol.* 9, 1171–1193. doi: 10.1046/j.1365-294x.2000.00954.x

Sion, S., Taranto, F., Montemurro, C., Mangini, G., Camposeo, S., Falco, V., et al. (2019). Genetic characterization of Apulian olive germplasm as potential source in new breeding programs. *Plants* 8, 268. doi: 10.3390/plants8080268

Spadoni, A., Sion, S., Gadaleta, S., Savoia, M. A., Piarulli, L., Fanelli, V., et al. (2019). A simple and rapid method for genomic DNA extraction and microsatellite analysis in tree plants. *J. Agr. Sci. Technol.* 21, 1215–1226.

Spanò, I. R., Bottalico, G., Corrado, A., Campanale, A., Di Franco, A., and Mascia, T. (2018). A protocol for producing virus-free artichoke genetic resources for conservation, breeding and production. *Agriculture* 8, 36. doi: 10.3390/agriculture8030036

Squeo, G., Silletti, R., Summo, C., Paradiso, V. M., Pasqualone, A., and Caponio, F. (2016). Influence of calcium carbonate on extraction yield and quality of extra virgin oil from olive (Olea europaea L. cv. Coratina). *Food Chem.* 209, 65–71. doi: 10.1016/j.foodchem.2016.04.028

Tamborrino, A., Romaniello, R., Caponio, F., Squeo, G., and Leone, A. (2019). Combined industrial olive oil extraction plant using ultrasounds, microwave, and heat exchange: Impact on olive oil quality and yield. *J. Food Eng.* 245, 124–130. doi: 10.1016/j.jfoodeng.2018.10.019

Taranto, F., Nicolia, A., Pavan, S., De Vita, P., and D'Agostino, N. (2018). Biotechnological and digital revolution for climate-smart plant breeding. *Agronomy* 8, 277. doi: 10.3390/agronomy8120277

UPOV (2011). Guidelines for the conduct of tests for distinctness, homogeneity and stability. *Olive*. TG/99/3 (www.upov.int). 1–55.

Velasco, J., and Dobarganes, C. (2002). Oxidative stability of virgin olive oil. *Euro. J. Lipid Sci. Tech.* 104 (9-10), 661–676. doi: 10.1002/1438-9312(200210)104:9/10<661::AID-EJLT661>3.0.CO;2-D

Vivaldi, G. A., Strippoli, G., Pascuzzi, S., Stellacci, A. M., and Camposeo, S. (2015). Olive genotypes cultivated in an adult high-density orchard respond differently to canopy restraining by mechanical and manual pruning. *Sci. Hortic.* 192, 391–399. doi: 10.1016/j.scienta.2015.06.004

Wright,S. (1949). The genetic structure of populations. *Ann. Eugen.* 15, 323–354. doi: 10.1111/j.1469-1809.1949.tb02451.x

Wu, H. C., Du Toit, E. S., and Reinhardt, C. F. (2007). Micrografting of *Protea cynaroides*. *Plant Cell Tissue Organ Cult.* 89, 23–28. doi: 10.1007/s11240-007-9208-5

Conflict of Interest: Authors MC, LG, BG, FV and FB are participants to SINAGRI s.r.l. without any kind of salary; VR, IM, WS, and AP were consultants of SINAGRI s.r.l.

The remaining authors declare that the research was conducted in the absence of any commercial or financial relationships that could be construed as a potential conflict of interest.

frontiers in Bioengineering and Biotechnology

ORIGINAL RESEARCH
published: 03 March 2020
doi: 10.3389/fbioe.2020.00151

In vitro Antifungal Activity of Olive (*Olea europaea*) Leaf Extracts Loaded in Chitosan Nanoparticles

Innocenzo Muzzalupo[1,2], Giuliana Badolati[1], Adriana Chiappetta[3]*, Nevio Picci[1] and Rita Muzzalupo[1]*

[1] Dipartimento di Farmacia, Scienze della Salute e della Nutrizione – Universitá della Calabria (DFSSN-UNICAL), Ed. Polifunzionale, Arcavacata di Rende (CS), Rende, Italy, [2] Centro di Ricerca Olivicoltura, Frutticoltura, Agrumicoltura, Consiglio per la Ricerca in Agricoltura e L'analisi dell'Economia Agraria (CREA-OFA), Rende, Italy, [3] Dipartimento di Biologia, Ecologia e Scienza della Terra, Università della Calabria, Arcavacata di Rende, Italy

OPEN ACCESS

Edited by:
Haifeng Zhao, South China University of Technology, China

Reviewed by:
Selin Şahin Sevgili, Istanbul University, Turkey
Lukasz Stepien, Institute of Plant Genetics (PAN), Poland

***Correspondence:**
Innocenzo Muzzalupo
innocenzo.muzzalupo@crea.gov.it; muzzalupoi@hotmail.com
Adriana Chiappetta
adriana.chiappetta@unical.it

Specialty section:
This article was submitted to Industrial Biotechnology, a section of the journal Frontiers in Bioengineering and Biotechnology

Received: *13 September 2019*
Accepted: *13 February 2020*
Published: *03 March 2020*

Citation:
Muzzalupo I, Badolati G, Chiappetta A, Picci N and Muzzalupo R (2020) In vitro Antifungal Activity of Olive (Olea europaea) Leaf Extracts Loaded in Chitosan Nanoparticles. Front. Bioeng. Biotechnol. 8:151. doi: 10.3389/fbioe.2020.00151

Olive leaf extract is characterized by a high content of phenols and flavonoids (oleuropein, luteolin, and their derivatives). These compounds are defined as secondary metabolites and exert such as anti-inflammatory, antioxidant, and antimicrobial activities. We investigated the *in vitro* antifungal activity of two olive leaf extracts (named *EF1* and *EF2*) against a *Fusarium proliferatum* (AACC0215) strain that causes diseases to many economically important plants and synthesizing diverse mycotoxins. In this work, we aimed to identify the most appropriate concentration between the tested two olive leaf extracts to develop a safe, stable and efficient drug delivery system. Qualitative and quantitative analyses of the two olive leaf extracts by (HPLC) were performed. Furthermore, we also evaluated the antifungal effects of the two leaf extracts when encapsulated in chitosan-tripolyphosphate nanoparticles. The major compound in both *EF1* and *EF2* was oleuropein, with 336 and 603 mg/g, respectively, however, high concentrations of flavonoid were also present. *EF1* and *EF2* showed a concentration depended effect on *F. proliferatum* (AACC0215) viability. Our results showed a great efficacy of *EF1*/nanoparticles at the higher concentration tested (12X) against the target species. In this case, we observed an inhibition rate to both germination and growth of 87.96 and 58.13%, respectively. We suggest that *EF1* olive leaf extracts, as free or encapsulated in chitosan-tripolyphosphate nanoparticles, could be used as fungicides to control plant diseases. Finally, future application of these findings may allow to reduce the dosage of fungicides potentially harmful to human health.

Keywords: antifungal activity, olive leaf extracts, oleuropein, biofungicides, nanoformulates

Abbreviations: CS, chitosan; CSNPs, chitosan nanoparticles; DLS, dinamic light scattering; EE, encapsulation efficiency; EF1, leaf extract 1; EF2, leaf extract 2; HPLC, high performance liquid chromatography; NPs, nanoparticles; Ole, oleuropein; PBS, phosphate-buffered saline; PDA, potato dextrose agar; PDI, polydispersityindex.

INTRODUCTION

Nanoparticle formulation is beneficial in different fields including electronics, textiles, mobile phones, food, paper, robotics, fertilizers, pesticides, and agrochemical industries. In recent years, an increased interest has been developed for natural polymers which have a versatility due to their chemical, physical and functional properties. The wide range of potential applications has led to their use in various fields of research, mainly in the biomedical, cosmetics, food and pharmaceuticals (Agnihotri et al., 2004; Manna and Patil, 2009).

Chitosan (CS) has emerged as one of the most promising polymers for the formation of nanoparticles (NPs) (Kashyap et al., 2015), mainly due to its biodegradable and biocompatible properties, its moderate or lack of toxicity to animals and humans, and for its antimicrobial and antifungal activity (López-León et al., 2005; Zhou and Chen, 2008; Akamatsu et al., 2010). Chitosan nanoparticles have gained considerable popularity as a carrier for the active ingredient delivery for various applications owing to their biocompatibility, biodegradability, high permeability, cost-effectiveness, and non-toxicity (Shukla et al., 2013). Various procedures can be employed to synthesize CSNPs, such as emulsion formation, coacervation, spray drying, ionotropic gelation. The method selected is mainly dependent on the substances encapsulated, and the route of administration. So, by varying the concentration and the molecular weight of the polymer and by using copolymers and crosslinking agents, efficient delivery systems for the pharmaceutical, biomedical and agricultural industry could be obtained (Höhne et al., 2007; Nasti et al., 2009).

In agriculture, NPs could be used as vectors to control release of agrochemicals, such as fertilizers, pesticides, herbicides and plant growth regulators (Cota-Arriola et al., 2013). Plants are continuously exposed to a series of pathogenic microorganisms such as fungi, oomycetes and bacteria, which can attack the plant both above and below ground (Buhtz et al., 2015) and cause the evolution of devastating epidemics and significant yield losses of annual crops, seriously affecting the economy. Several fungal species belonging to the genus *Fusarium* are known for their ability to colonize a wide variety of host plants, such as tomatoes, potatoes, cereal and tobacco (Desjardins, 2003; Schweigkofler et al., 2004; Alves-Santos et al., 2007; Nguyen et al., 2016). The most common symptoms of the disease are wilting, yellow leaves, dry collar, chlorosis, premature leaf drop, browning of the vascular system and growth arrest. When the disease spreads to the whole plant, necrosis and death occurs (Trapero-Casas and Jiménes-Dìaz, 1985). *Fusarium* produces mycotoxins which can have an important role in pathogen virulence during infection of the plant (Nguyen et al., 2016). The control of these fungi, responsible for pre- and post-harvested diseases of agricultural products, is an issue that remains unresolved, along with the excessive environmental impacts of chemicals to tackle this problem. Current efforts are focused to search new strategies and effective alternatives for microbial control and to reduce the excessive use of synthetic fungicides which negatively impact the environment and human and animal health (Cota-Arriola et al., 2013; Rodriguez-Maturino et al., 2015).

Plants have been a rich source of bioactive compounds for millennia, while the use of plant derivatives to produce nanobiotechnological formulations has gained scientific and technological importance in recent years (Joanitti and Silva, 2014). *Olea europaea* belongs to the Oleaceae family and it is native of the Mediterranean region. Olive oil, fruit and leaves have been recognized as important components of medicine and of a healthy diet. The extract from olive leaves were reported to have anticancer, antioxidative and anti-inflammatory properties (Le Toutour and Guedon, 1992; Anter et al., 2011). In addition to the health benefits described above, it is claimed that extracts from olive leaves may aid in the treatment of a broad range of infectious diseases. They have important pharmacological properties attributable primarily to the phenolic content (Omar, 2010). The main phenolic compound present in the leaves and fruits of olive tree is oleuropein (*Ole*) (Bianco et al., 1999; Goldsmith et al., 2015) and the detectable amount ranges from 17% to 23%, depending on the harvesting period (Le Toutour and Guedon, 1992). Olive leaves extract is characterized by a high content of phenolic compounds and flavonoids such as *Ole*, hydroxytyrosol and their derivatives (Zorić et al., 2016) and luteolin 7-glucoside and their derivatives (Sudjana et al., 2009). The antimicrobial activity of *Ole* and leaf extracts has been examined previously (Markin et al., 2003; Sudjana et al., 2009).

In this work, we aimed to identify the most appropriate concentration between the tested two olive leaf extracts to develop a safe, stable and efficient drug delivery system. These CSNPs were synthesized by a chemical route and displayed certain characteristics defined by preparation conditions. The physical and chemical characterization of the nanoformulation such as mean particle size, zeta potential values, polydispersity index (PDI), and EE were evaluated. In this study, the CSNPs antifungal effect was evaluated against *F. proliferatum* (AACC0215) strain through an *in vitro* assay, looking at different concentrations and preparations of the olive leaf extracts.

EXPERIMENTAL

Sample Preparation

The plant material used for the extraction is represented by fresh leaves of Carolea cultivar collected in November 2015 from plants grown in the Botanical Gardens of the University of Calabria, Arcavacata di Rende (CS) (GPS coordinates: latitude 39.357548; longitude 16.228990). The plants were identified by Dr. Nicodemo Passalacqua curator of the Botanical Gardens of University of Calabria.

Extraction and Characterization of the Olive Leaf Extracts

The method used for the extraction of olive leaf extracts is that described in Muzzalupo et al. (2011) with some modifications. Olive leaves (20 grams corresponding to about 100 leaves) were homogenized in 100 mL of a mixture of acetone and methanol in a ratio of 1:1 (v/v). The homogenization was carried out using an Ultra-TURRAX® (IKA, Seneco Science, Milan, Italy) for 5 min at room temperature. The homogenized mixture was vacuum

filtered, and the liquid portion was recovered. The pellet was re-homogenized with the previous mixture and the process was repeated a further two times. The filtrate obtained was evaporated to dryness with a rotavapor (Strike 202 Rotary Evaporator, Steroglass, Perugia, Italy) and resuspended with 80 mL of distilled water. The filtrate was washed, in the separating funnel, with different solvents with increasing polarity: *n*-hexane, ethyl ether, chloroform and ethyl acetate. All solvents used are pure (ACS grade solvents, Sigma-Aldrich, Milano, Italy). The washings with *n*-hexane and ethyl ether were discarded, instead those from the chloroform and ethyl acetate phases were recovered and kept separate.

The extract obtained from the chloroform was referred to as "*leaf extract 1" (EF1)*, while that derived from ethyl acetate as "*leaf extract 2" (EF2)*. The two extracts were made anhydrous with sodium sulfate, filtered and evaporated to dryness and stored at −20°C in the dark.

Determination of Total Phenolic Compounds

The total phenolic content of each extract was determined spectrophotometrically at 750 nm using Folin-Ciocalteu reagent (Fuentes et al., 2012). To 1 mL of the sample to be tested were added 0.5 mL of Folin-Ciocolteu (Sigma-Aldrich) and left in the dark for 5 min. Subsequently 3 mL of Na_2CO_3 (Sigma-Aldrich) at 20% and 5.5 mL of distilled water were added. After 20 min, spent in the dark and at room temperature, samples were centrifuged at 3,500 rpm for 10 min. A calibration curve was calculated using pure *Ole* (Extrasynthèse, ZI Lyon-Nord, Genay, France). The total phenolic compounds are expressed as *Ole* milligrams per grams of extract.

Identification of Phenolic Compounds Contained in Each Extract by HPLC

Both extracts (*EF1* and *EF2*), solubilized in methanol, were characterized performing HPLC analysis. The procedure used is that reported by Montedoro et al. (1992): HPLC JASCO LC-2000 plus equipped with a pump PU-2080 and UV-2075 detector (JASCO), with a RP-18 column Spherisorb ODS-2 (160 mm x 4.6 mm, Waters, Vimodrone, Italy) and injection volume of 20 μL; the flow rate was 1 mL/min at room temperature; the mobile phase used was 2% acetic acid in water (A) and methanol (B) for a total running time of 45 min, and the gradient conditions were as follows: 95% A-5% B for 2 min, 75% A-25% B for 8 min, 60% A-40% B for 10 min, 60% A-50% B for 10 min and 0% A-100% B for 10 min, until it stops; the eluents were detected at 280 nm. As phenolic standards were used: *Ole*, verbascoside, luteolin-4′-O-glucoside, luteoloside, luteolin, apigenin-7-O-glucoside and apigenin, all purchased from Extrasynthése.

Preparation and Characterization of the CSNPs

The CSNPs were prepared by ionotropic gelation method, reported by Rampino et al. (2013), with some modifications. Dispersions of chitosan were prepared, at a concentration of 1 mg/mL, by dissolving the medium molecular weight chitosan (50,000–190,000 Da, 75–85% deacetylated, Sigma Aldrich) in a solution of hydrochloric acid to 0.04% (v/v) and then stirring for 1 h. The pH of the CS solution was adjusted to 5.5 by NaOH. 1 mL of *Ole* or *EF1* or *EF2* water solution was added to 5 mL of the chitosan solution leaving it under stirring for a few minutes and adjusting the pH to 5.5. Tripolyphosphate (Sigma Aldrich) was dissolved in distilled water to a final concentration of 2 mg/mL and was added dropwise to the chitosan solution in a volumetric ratio of 1:5. The resulting solution was stirred for 30 min at room temperature. Moreover, CSNPs without the leaf extract were prepared. All formulations assayed (1X, solutions and carried CSNPs) were prepared at a final concentration of 100 mg/L of *Ole* (**Table 1**).

All nanoformulations were characterized in terms of particle size, size distribution, PDI and zeta potential using a Zetasizer ZS (Malvern Instrument Ltd., Malvern), based on the DLS technique. DLS measurements of the samples were performed at 25°C with a detection angle of 90°.

Evaluation of Drug Loaded Efficiency

The extracts UV spectrum had a single maximum of absorption at 280 nm and this aspect allowed us to treat the extracts as a single component. The EE was calculated using the following formula (Shi et al., 2014):

$$EE\% = \frac{total\ amount\ of\ drug - free\ drug}{total\ amount\ of\ drug} \times 100$$

Where drug means the phenolic compounds under study (*EF1*, *EF2* and *Ole*). Each preparation was filtered using the syringe filters with a porosity equal to 0.2 μm (Millipore, Italy). 100 μL of filtrate are taken and brought to a final volume of 5 mL with distilled water. The amount of free and total drug was calculated by using the V-530 spectrophotometer (JASCO) at 280 nm (Mazzotta et al., 2020).

TABLE 1 | Phenolic compounds (Oleuropein – *Ole*; leaf extract 1 – *EF1*; leaf extract 2 – *EF2*) used as free or encapsulated in CSNPs, for *in vitro* assays against *Fusarium proliferatum* (AACC0215).

Code samples	Composition	Concentration tested (1X) [mg/L]
Ole	Oleuropein (standard)	100
EF1	Oleuropein	$100.0^{a} \pm 1.0$
	Luteolin-4-*O*-glucoside	$18.0^{a} \pm 0.1$
	Luteolin-7-glucoside	$43.0^{a} \pm 0.2$
	Verbascoside	$5.0^{a} \pm 0.1$
	Phenols unidentified	$137.0^{a} \pm 1.2$
	Totals phenols	**$303.0^{a} \pm 2.6$**
EF2	Oleuropein	$100.0^{a} \pm 1.0$
	Luteolin-4-*O*-glucoside	$14.0^{a} \pm 0.1$
	Luteolin-7-glucoside	$25.0^{b} \pm 0.2$
	Verbascoside	$8.0^{a} \pm 0.1$
	Phenols unidentified	$35.0^{b} \pm 0.2$
	Totals phenols	**$182.0^{b} \pm 1.6$**

Means with different letters for the same quality parameter differ significantly by Tukey's test ($p < 0.05$). Data are average ±SEM ($n = 3$).

In vitro Olive Leaf Extracts Release

The release of *Ole* and leaf extracts from CSNPs was estimated using the method reported in Varuna Kumara and Basavaraj (2015), with some modifications. 2 mL of CSNPs/*Ole* or CSNPs/*EF2* were taking and placing in pre-treated dialysis tubes Spectra/Por 4 (MWCO: 12–14 kD, Spectrum Laboratories, Inc., Canada). These were dipped into 50 mL of PBS solution (pH = 5.9) and left to stir at room temperature. At predetermining time points, 2 mL of the medium were taken and replaced with the same volumetric amount of fresh PBS. The solution was analyzed by UV-VIS spectrophotometry to evaluate the drug content.

Assessment of Antifungal Activity

Used Strains

In order to evaluate the antifungal activity of prepared extracts, the *F. proliferatum* (AACC0215) strain were used. Isolation and identification of the strain was described in a previous study (Muto et al., 2014). In brief, *F. proliferatum* (AACC0215) was isolated from colonized cloves of garlic (*Allium sativum*) collected at Altomonte, Cosenza, Italy in the year 2013, and taxonomically characterized as described in Muto et al. (2014). This strain was sub-cultured on potato dextrose broth (PDB) and incubated in darkness at 24°C. The suspension was diluted to a concentration of 1×10^5 spores/mL. Afterward it was divided into 1.5 mL aliquots and stored at −80°C in 25% glycerol (Steinkellner and Mammerler, 2007).

In vitro Test for the Evaluation of Germination

To verify the ability and success of *F. proliferatum* (AACC0215) to germinate in the presence of *EF1*, *EF2,* and *Ole*, different tests were performed using multiwell plates for cell cultures (Sigma-Aldrich). Inside of each well 200 μL of test preparation and 10 μL of conidial suspension at a concentration of 1×10^5 conidia/mL were added. **Table 1** shows the composition of the analyzed individual preparations, respectively, containing *Ole*, *EF1* and *EF2* in solution or carrier to the CSNPs. The concentration used for each treatment was 3, 6, 9, and 12 times the initial one. As a control, the fungus was inoculated into the wells containing sterile water. The *F. proliferatum* (AACC0215) was incubated at 25–27°C in the dark and under aerobic conditions. After 24 h, 20 μL of each solution were taken to prepare slides by using a Malassez cell. The samples were observed under an optical microscope (DMRB Leica Microsystems, Milan, Italy) at × 400 magnification, equipped with a digital camera (DFC490 Leica Microsystems). The evaluation of germinated conidia and index of germination were performed according to Benslim et al., 2016. The conidia were considered as germinated when the germ tube length exceeded the diameter of the conidium (**Figure 1**; Boch et al., 1999; Rosengaus et al., 2000).

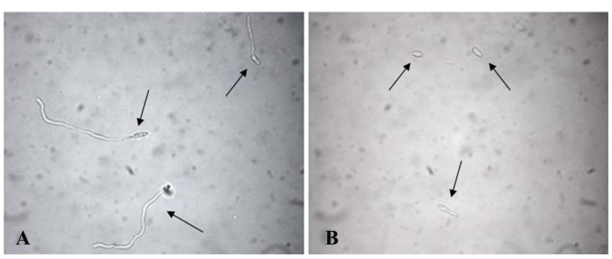

FIGURE 1 | Conidia of *Fusarium proliferatum* (AACC0215) germinated in distilled water **(A)** and in presence of *Ole* **(B)** after 24 h. The samples were observed under an optical microscope at X400 magnification. The "arrow heads" indicate the germinated **(A)** and the non-germinated conidia **(B)**.

For each slide, a total of 500 conidia were counted, by determining the percentage of inhibition rate (*% IRg*) by using the following formula:

$$\% \, IRg = \frac{N^\circ \, germinated \, conidia \, in \, control - N^\circ \, germinated \, conidia \, in \, treatments}{N^\circ germinated \, conidia \, in \, control} \times 100$$

In vitro Inhibition to Growth

The essays were conducted as described in Taskeen-Un-Nisa et al. (2011) with small modifications. Assays were performed in Petri plates containing 25 mL of PDA supplemented with streptomycin and ampicillin, at a final concentration of 6 mg/L each. At the center of the plates, a sterile polycarbonate filter with 0.8 μM porosity (Isopore Membrane Filters, Millipore) was placed on the PDA and 50 μL of the solutions to be tested were added on it.

In order to test the *in vitro* activity of the individual preparations at increasing concentrations, volumes of 3, 6, 9, and 12 times more than the starting solution described in **Table 1** were loaded on the polycarbonate filter in the Petri capsule. In this way a thin and uniform film was formed on the surface.

PDA plates, to which a filter of 50 μL of ethanol had been added, were used as controls. Subsequently, the dry filters were inoculated at the center with 4 μL of conidial suspension at a concentration of 1×10^5 spores/mL and they were incubated in the dark at 24°C under aerobic conditions for 6 days. At the end of incubation, the capsule was photographed, and the image was analyzed by using the ImageJ software (vers. 1.49v National Institutes of Health, United States) to calculate the area, expressed in square millimeters, occupied by the mycelium.

The percentage of growth inhibition *(I%)* was calculated using the following formula (Chin Ming et al., 2015):

$$I\% = \frac{A_C - A_T}{A_C} \times 100$$

Where A_C represents the average value of the area of mycelium used as a control and A_T the average area value of the mycelium inoculated on plates treated with the individual preparations (*Ole*, *EF1* and *EF2* free and carrier to the CSNPs) (Kaiser et al., 2005; Taskeen-Un-Nisa et al., 2011).

Statistical Analysis

Statistical analysis was performed with XLSTAT v.2016. All data obtained from *in vitro* tests were compared by using One-way ANOVA, with Tukey's multiple comparison test. All results are the mean of at least three individual experiments. All the values obtained from chemical analysis and biological

tests are calculated from triplicate data were expressed as means ±standard error.

RESULTS AND DISCUSSION

Analysis of Olive Leaf Extracts

The identification of the phenolic compounds was carried out by comparing the retention times obtained from the HPLC analysis of the olive leaf extracts and those of the available standards. The results of the HLPC analysis of *EF1* and *EF2* showed a different content of phenols, in relation to the extraction procedure followed and their hydrophilicity (**Table 2**). In chloroform (*EF1*) and ethyl acetate (*EF2*) olive leaf extracts four phenol compounds were identified and quantified: *Ole*, verbascoside, luteolin-4′-O-glucoside, and luteolin-7-glucoside (**Figure 2**). Phenol compounds apigenin, luteolin, and apigenin-7-O-glucoside were not detected.

The most abundant compound of chloroform and ethyl acetate olive leaf extracts is *Ole*, with 336 mg/g and 603 mg/g of extract, respectively. Furthermore, in both olive leaf extracts, there are numerous (over 30) unidentified phenolic compounds, which represented 460 and 118 mg/g of extract, respectively (**Table 2**).

The *EF2* extract had a lower level of total phenols when compared to *EF1* extract, 0.75 g and 1.04 g of extract, respectively. This suggests that most of the compounds present in the olive leaves were less hydrophilic phenols (Tan et al., 2014). Consistent with this, chloroform is less polar than ethyl acetate. The obtained results are in line with previously published data for *O. europaea* leaves, where *Ole* was identified as the major phenol compound extract (Yateem et al., 2014).

TABLE 2 | Quantitative and qualitative analysis of *EF1* and *EF2* phenolic compounds analyzed by HPLC.

Compound	N° peak	T_R (min)	Yield in *EF1* (mg/g)	Yield in *EF2* (mg/g)
Verbascoside	**4**	23.3	$18.5^a \pm 3.3$	$47.9^b \pm 4.7$
Luteolin-7-glucoside	**2**	26.6	$143.5^a \pm 12.3$	$147.8^a \pm 13.4$
Oleuropein	**1**	28.3	$335.7^a \pm 22.3$	$603.2^b \pm 42.3$
Luteolin-4-*O*-glucoside	**3**	30.9	$61.4^a \pm 5.3$	$82.7^a \pm 7.5$
Unidentified*	–	–	$460.3^a \pm 32.3$	$118.4^b \pm 10.2$

*Means with different letters for the same quality parameter differ significantly by Tukey's test ($p < 0.05$). Data are average ±SEM ($n = 3$). *Sum of (over 30) unidentified substances.*

Nanoparticles Preparation and Characterization

Chitosan nanoparticles were prepared by ionotropic gelation with the dropwise addition of tripolyphosphate to a chitosan solution. Formation of NPs occurs quickly upon mixing tripolyphosphate and chitosan solutions and this is due to the electrostatic interactions between the positively charged primary amino groups of chitosan and the negatively charged groups of tripolyphosphate (Servat-Medina et al., 2015). The different formulations of CSNPs,

TABLE 3 | The particle size, polydispersity index (PDI), zeta potential (Z-P), and encapsulation efficiency (EE%).

Formulation	Particle size (nm)	PDI	Z-P (mV)	EE (%)
CSNPs	$260.3^a \pm 29.4$	$0.257^a \pm 0.031$	$25.0^a \pm 1.72$	–
CSNPs/Ole	$254.6^a \pm 20.7$	$0.250^a \pm 0.025$	$16.9^b \pm 0.71$	$62.2^a \pm 3.4$
CSNPs/EF1	$258.7^a \pm 17.2$	$0.207^a \pm 0.042$	$15.7^b \pm 1.31$	$94.5^b \pm 5.2$
CSNPs/EF2	$269.4^a \pm 36.3$	$0.229^a \pm 0.032$	$11.5^b \pm 2.08$	$73.1^c \pm 4.7$

Means with different letters for the same quality parameter differ significantly by Tukey's test ($p < 0.05$). Data are average ±SEM ($n = 3$).

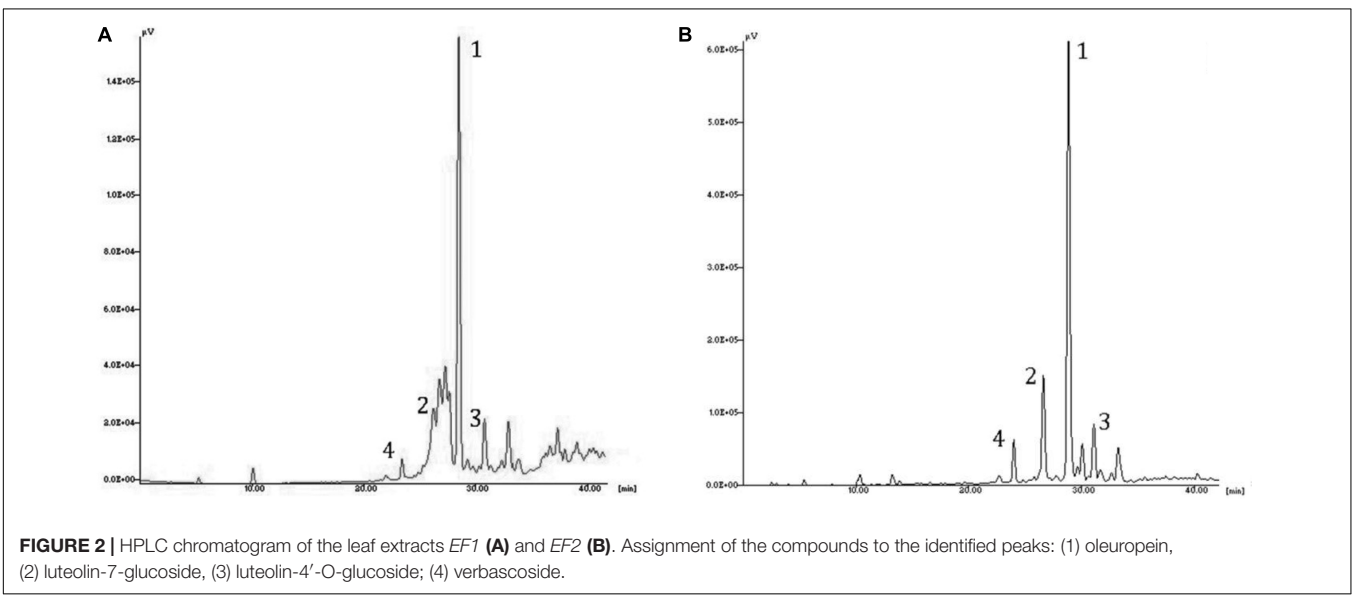

FIGURE 2 | HPLC chromatogram of the leaf extracts *EF1* **(A)** and *EF2* **(B)**. Assignment of the compounds to the identified peaks: (1) oleuropein, (2) luteolin-7-glucoside, (3) luteolin-4′-O-glucoside; (4) verbascoside.

containing different concentrations of *Ole*, showed good stability over time. They were stored in the dark at 4°C. When monitored after 30–40 days, they did not show sedimentation, creaming or flocculation. The particle size, PDI, zeta potential and EE are displayed in **Table 3** for all nanoformulations.

The NPs have always shown dimensions between 250 to 270 nm. As for the PDI values, these are always lower than 0.3 and this indicates a clear homogeneity of the system. No significant differences were seen in the Z-potential except for CSNPs/*EF2* whose values are lower than those of CSNPs, indicating a greater presence of negative charge density. This result could possibly be related to the chemical nature of the unidentified compounds present in different percentages in the two leaf extracts.

During the formation of NPs, bioactive molecules are trapped both inside and on the surface of such particles. However, there is an initial burst release probably due to the drug on the surface, followed by a prolonged release (Bahreini et al., 2014).

Commercial *Ole* is completely released after 2 h of dialysis, while *Ole* in CSNPs is released more slowly, reaching the maximum value of 77% after 6 h (**Figure 3A**). *EF1* after 45 h of dialysis against water has a negligible release, probably due to a lower hydrophilia. *EF2* extract, both in solution and in NPs, is released in a lower percentage and more slowly than *Ole* (**Figure 3B**). Specifically, the free solution *EF2* reaches a release value equal to 62% after 5 h, instead the release values of *EF2* encapsulated in the NPs, reach the maximum value, equal to 38%, only after 30 h. This behavior may, probably, depend on the presence of lipophilic compounds

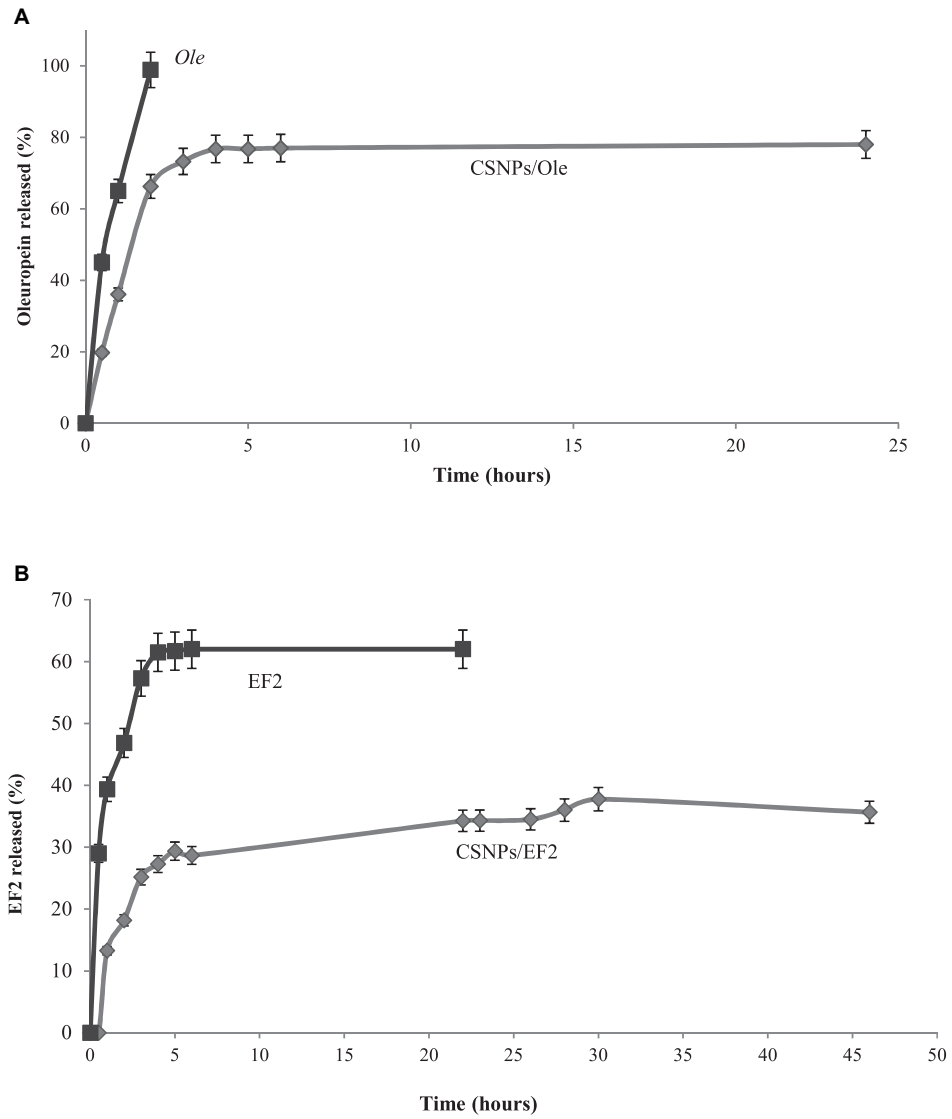

FIGURE 3 | (A) *In vitro* release profile of the commercial oleuropein in solution (*Ole*) (■) and in chitosan nanoparticles (CSNPs/*Ole*) (●). Data are average ±S.E.M. (*n* = 3). **(B)** *In vitro* release profile of EF2 leaf extract in solution (■) and in chitosan nanoparticles (CSNPs/EF2) (●). Data are average ± SEM (*n* = 3).

in leaves, including lipophilic phenols, that are not allowed to pass into PBS.

Assessment of Antifungal Activity

In vitro Test for the Evaluation of Germination

The antifungal activity of *Ole*, *EF1*, and *EF2* in solution or carrier on the CSNPs on conidial germination of *F. proliferatum* (AACC0215) is shown in **Table 4**. The obtained results were compared with distilled water. All formulations show an inhibition percentage of conidial germination versus control.

The maximum inhibition percentage of conidial germination was obtained at the 12X concentration (87.96%), in CSNPs/*EF1* formulation, while the lowest one was obtained at the 1X concentration (10.19%) of *Ole* solutions. The empty CSNPs markedly reduced conidial germination of *Fusarium* compared to the control, equal to 48.71%. The mechanism of action could be based on the electrostatic interaction between the amine group of chitosan and the negatively charged compounds (phospholipids, proteins, amino acids) of the cell membrane of fungi (Rabea et al., 2003; Liu et al., 2004).

The results obtained have shown a reduction in the germination capacity of the conidia, depending on the concentrations employed, except for the solution prepared with *EF2* (**Table 4**). A reduction in the germination capacity of conidia was recorded as the concentration increased. In fact, in the presence of *Ole* the highest percentage of inhibition of germination was obtained at the highest concentration used 12 mg/L (12X) with a percentage of 58.50%, while with the CSNPs/*Ole* complex the maximum (67.41%) was obtained at the concentration of 900 mg/L (9X).

Regarding the leaf extract *EF1*, the germination capacity of the conidia is very limited compared to *Ole*, reaching a maximum value of 68.72% at the lowest concentration (1X). However, in the CSNPs/*EF1* system, the inhibition of germination increases to between 52.45% (1X) and 61.17% (9X) (**Table 4**). The formulation that records the greatest reduction in germination capacity of *F. proliferatum* (AACC0215) conidia, reaching 87.96% (12X), is CSNPs/*EF1* at the highest concentration assayed. Considering the solution containing only CSNPs, it produced an *IRg%* equal to 48.71. This result is the same in all treatments because there is no drug inside the CSNPs, so the concentration of each component of the NPs is the same in all the concentrations tested.

The CSNPs/*Ole* and CSNPs/*EF1* complex results suggest that these systems act with an enhanced effect at the highest concentrations. It is the behavior of the CSNP/*Ole* formulations obtained with a low *Ole* content (1X and 3X) that have not shown the expected performance with respected to IRg%. The IRg% decreases significantly compared to the control, this result can be

TABLE 4 | *In vitro Fusarium proliferatum* (AACC0215) percentage of inhibition rate (% IRg) in the presence of pure chitosan nanoparticles (CSNPs), oleuropein (*Ole*), leaf extract 1 (*EF1*) and leaf extract 2 (*EF2*) free in solution or encapsulated into NPs.

	IRg (%)				
Formulation	***1X***	***3X***	***6X***	***9X***	***12X***
CSNPs	$48.71^{a}\pm0.49$	$48.71^{a}\pm0.49$	$48.71^{a}\pm0.49$	$48.71^{a}\pm0.49$	$48.71^{a}\pm0.49$
Ole	$10.19^{a,b}\pm4.01$	$12.96^{b,c}\pm1.26$	$22.11^{a,b}\pm4.26$	$47.19^{c,d}\pm2.62$	$58.50^{d,e}\pm1.58$
CSNPs/*Ole*	$13.23^{a,b}\pm1.34$	$28.00^{b,c}\pm1.01$	$66.28^{c,d}\pm2.04$	$67.41^{c,d}\pm2.28$	$62.75^{c,d}\pm4.07$
EF1	$68.72^{a,b}\pm1.72$	$68.48^{a,b}\pm2.40$	$84.87^{b,c}\pm2.03$	$86.18^{b,c}\pm1.38$	$84.66^{b,c}\pm2.80$
CSNPs/*EF1*	$52.45^{a,a}\pm3.16$	$55.01^{a,b}\pm2.74$	$57.42^{a,b}\pm2.90$	$61.17^{b,b}\pm4.19$	$87.96^{c,c}\pm2.50$
EF2	$44.10^{a,a}\pm4.56$	$50.37^{b,b}\pm1.03$	$58.90^{c,c}\pm4.33$	$26.55^{d,d}\pm2.66$	$36.27^{e,e}\pm3.51$
CSNPs/*EF2*	$37.00^{a,b}\pm4.19$	$54.45^{b,c}\pm3.11$	$62.39^{c,d}\pm1.68$	$57.37^{d,e}\pm2.07$	$67.81^{e,d}\pm1.11$

The germination tests were conducted in sterile water. The first letter refers to the significance of the same preparation for the different concentrations, the second is related to the significance of all the preparations for the same concentration. Means with different letters for the same quality parameter differ significantly by Tukey's test ($p < 0.05$). Data are average ±SEM ($n = 3$).

TABLE 5 | *In vitro Fusarium proliferatum* (AACC0215) percentage of growth inhibition (% I) in the presence of pure chitosan nanoparticles (CSNPs), oleuropein (*Ole*), leaf extract 1 (*EF1*) and leaf extract 2 (*EF2*) free in solution or encapsulated into NPs.

	I (%)				
Formulation	***1X***	***3X***	***6X***	***9X***	***12X***
CSNPs	$-22.41^{a,a}\pm5.43$	$17.62^{b,a}\pm0.48$	$21.57^{b,a}\pm7.31$	$40.85^{c,a}\pm1.34$	$41.93^{c,a}\pm3.17$
Ole	$-27.40^{a,a}\pm10.15$	$-13.41^{a,b}\pm16.43$	$58.02^{b,b}\pm1.91$	$52.43^{b,b}\pm4.78$	$33.45^{c,a}\pm5.88$
CSNPs/*Ole*	$-27.96^{a,a}\pm2.42$	$22.06^{b,c}\pm7.91$	$66.31^{c,b}\pm10.47$	$64.99^{c,c}\pm1.87$	$51.62^{c,b}\pm7.30$
EF1	$49.38^{a,b}\pm11.41$	$31.48^{b,b}\pm1.67$	$46.56^{a,b}\pm0.29$	$53.34^{a,b}\pm4.99$	$48.52^{a,b}\pm2.88$
CSNPs/*EF1*	$-7.38^{a,a}\pm5.66$	$10.38^{b,c}\pm1.73$	$28.45^{c,a}\pm3.79$	$44.37^{d,b}\pm2.57$	$58.13^{e,c}\pm3.05$
EF2	$4.64^{a,b}\pm0.93$	6.99 ± 5.08 *a,b*	$23.53^{b,a}\pm4.98$	$-16.41^{c,b}\pm5.77$	$3.55^{a,b}\pm0.67$
CSNPs/*EF2*	$9.85^{a,c}\pm3.13$	$15.02^{a,c}\pm1.31$	$32.60^{b,b}\pm1.73$	$19.98^{c,c}\pm5.13$	$32.20^{b,c}\pm1.96$

The first letter refers to the significance of the same preparation for the different concentrations, the second is related to the significance of all the preparations for the same concentration. Means with different letters for the same quality parameter differ significantly by Tukey's test ($p < 0.05$). Data are average ± SEM ($n = 3$).

attributed to a decrease of the CSNPs chelated positive charges by the hydroxyl groups of the *Ole*. With respect to *EF2*, the obtained results showed a decrease in the inhibition of germination at the highest concentrations tested with a value of 26.55% at the concentration 9X. The increased germination capacity may depend on the presence of impurity within the extract that is likely to be used as a source of energy from the fungus and which could stimulate germination of spores.

In vitro Inhibition to Growth

The results obtained have shown an antifungal activity for almost all the analyzed samples, with the exception of six formulations (*CSNPs, Ole* 1X, and 3X; CSNPs/*OLE* 1x; CSNPs/*EF1* 1x; *EF2* 9x, **Table 5**) that induce a stimulation in growth.

In almost all the concentrations tested, the empty CSNPs inhibited *F. proliferatum* (AACC0215) growth by 17.62, 21.57, 40.85, and 41.93%, respectively. Pure *Ole* and *EF1* at higher concentrations, both in solution and in CSNPs, exhibit a higher inhibition rate of growth than *EF2* (**Table 5**). *Ole* showed good antifungal activity at concentrations of 600 mg/L and 900 mg/L (6X and 9X) with a *I%* equal, respectively, at 58.02% and 52.43% when administered directly and at 66.31 and 64.99% if encapsulated in CSNPs. *EF1* fungicidal effect was quite similar to all concentrations used. *EF1* solution has shown inhibitory activity already at the lowest concentration (1X) with a *I%* equal to 49.38%. When *EF1* was combined with CSNPs, *F. proliferatum* (AACC0215) growth inhibition was found to be directly proportional to the concentration used, reaching a value of 58.13% at the highest concentration (12X). *EF2* pure exhibited lower antifungal activity with a maximum inhibition value of 23.53% at concentration 6X. However, the maximum of growth inhibition percentage was obtained at 6X and 12x concentration by using the complex CSNPs/*EF2* (32.60 and 32.20%, respectively).

All formulations containing CSNPs have an activity of *I%* greater or not significant compared to the control. Only in the case of CSNPs/*EF2* the higher concentrations appear to have significantly lower values than the control. These results, as mentioned above, is probably due to the presence of impurities of the extract *EF2* that the mushroom uses as a source of energy and which stimulate its growth.

In this study, it was observed that the tested phenolic compounds exert a cytotoxic activity *in vitro* against *F. proliferatum* (AACC0215) and this activity increase when they are complexed with CSNPs. These results are in line with other studies in which phenols extract from olive leaves show an antifungal activity (Markin et al., 2003; Steinkellner and Mammerler, 2007; Goldsmith et al., 2015; Rodriguez-Maturino et al., 2015; Zorić et al., 2016). As reported by Ansari et al. (2013) the phenols antimicrobial activity could be due to a synergistic action of the antioxidant and chelating power of the hydroxyl groups of the phenolic ring that form hydrogen bonds with cell wall proteins of microorganisms. Chitosan also exhibits antimicrobial activity based on the electrostatic interaction between the amine group of chitosan and the negatively charged compounds (phospholipids, proteins, amino acids) of the cell membrane of fungi (Rabea et al., 2003; Liu et al., 2004). Therefore, the interaction between phenolic compounds complexed with CSNPs cause an alteration of the integrity and permeability of the microbial cell.

CONCLUSION

Olive leaf extract-encapsulated CSNPs were obtained by ionotropic gelation method. The characterization of synthesized NPs showed that the size of leaf extract/CSNPs was 254.6–269.4 nm, the EE ranged from 62.2 at 94.5% and Zeta potential varied from 11.5 at 25.0 mV. As for the polydispersity index values, the lower was 0.207 and this indicates a clear homogeneity of the system. The nanoformulation thus achieved may be explored for the target delivery of phenols for disease control.

Considering the highest concentration (12X) tested, leaf extract/CSNPs showed greater efficacy than pure extracts (*EF1* and *EF2*) and the commercial formulation (*Ole*) against *F. proliferatum* (AACC0215). We suggest that the *EF1* olive leaf extracts, as free or encapsulated in chitosan-tripolyphosphate nanoparticles, could be used as fungicides to control plant diseases. Finally, future application of these findings may allow to reduce the dosage of fungicides potentially harmful to human health.

DATA AVAILABILITY STATEMENT

All datasets generated for this study are included in the article/supplementary material.

AUTHOR CONTRIBUTIONS

IM, AC, NP, and RM designed the research, analyzed the data, and discussed the results. GB performed the research and discussed the results. All authors contributed to improving the manuscript and approved the final manuscript.

FUNDING

The projects "Olio extra vergine d'oliva digital ID management – ODIN," POR Calabria 2014–2020; "L'aglio Testa Rossa Cardinale della valle dell'Esaro e del Fullone (nuova selezione varietale)", PSR Calabria 2007–2013; Salvaguardia e valorizzazione del patrimonio olivicolo italiano con azioni di ricerca nel settore della difesa fitosanitaria – SALVAOLIVI" MIPAAF D.M. 33437/2017; "Characterization and enhancement of table and dual-purpose olives – ALIVE" MIPAAF D.M. 93880/2017 financially supported this study.

ACKNOWLEDGMENTS

Dr. Lorena Tavano is kindly thanked for her assistance in nanoparticle preparations. The authors would like to thank Dr. Tiziana Belfiore and Dr. Veronica Vizzarri for their counseling on phytopathogenic fungi.

REFERENCES

Agnihotri, S. A., Mallikarjuna, N. N., and Aminabhavi, T. M. (2004). Recent advances on chitosan-based micro and nanoparticles in drug delivery. *J. Control Release* 100, 5–28. doi: 10.1016/j.jconrel.2004.08.010

Akamatsu, K., Kaneko, D., Sugawara, T., Kikuchi, R., and Nakoo, S. I. (2010). Three preparation methods for monodispersed chitosan microspheres using the SPG membrane emulsification technique and mechanisms of microsphere formation. *Ind. Eng. Chem. Res.* 49, 3236–3241. doi: 10.1021/ie901821s

Alves-Santos, F. M., Martínez-Bermejo, D., Rodríguez-Molina, M. C., and Diez, J. J. (2007). Cultural characteristics, pathogenicity and genetic diversity of *Fusarium oxysporum* isolates from tobacco fields in Spain. *Physiol. Mol. Plant. Pathol.* 71, 26–32. doi: 10.1016/j.pmpp.2007.09.007

Ansari, M., Anurag, A., Fatima, Z., and Hameed, S. (2013). Natural phenolic compounds: a potential antifungal agent. *Microb. Pathog. Strateg. Combat. them Sci. Technol. Educ.* 1, 1189–1195.

Anter, J., Fernandez-Bedmar, Z., Villatoro-Pulido, M., Demyda-Peyras, S., Moreno-Millán, M., Alonso-Moraga, A., et al. (2011). A pilot study on the DNA-protective, cytotoxic, and apoptosis-inducing properties of olive-leaf-extracts. *Mutat. Res.* 723, 165–170. doi: 10.1016/j.mrgentox.2011.05.005

Bahreini, E., Aghaiypour, K., Abbasalipourkabir, R., Mokarram, A. R., Goodarzi, M. T., and Saidijam, M. (2014). Preparation and nanoencapsulation of L-asparaginase II in chitosan-tripolyphosphate nanoparticles and *in vitro* release study. *Nanoscale Res. Let.* 9, 340–353. doi: 10.1186/1556-276X-9-340

Benslim, A., Mezaache-Aichour, S., Haichour, N., Chebel, S., and Mihoub Zerroug, M. (2016). Evaluation of inhibition of fungal spore germination by rhizospheric bacterial extracts. *ARRB* 11, 1–7. doi: 10.9734/arrb/2016/31228

Bianco, A. D., Muzzalupo, I., Piperno, A., Romeo, G., and Uccella, N. (1999). Bioactive derivatives of oleuropein from olive fruits. *J. Agric. Food Chem.* 47, 3531–3534. doi: 10.1021/jf981240p

Boch, C. H., Jeger, M. J., Mughogho, L. K., Cardwell, K. F., and Mtisi, E. (1999). Effect of dew point temperature and conidium age on germination, germ tube growth and infection of maize and sorghum by *Peronosclerospora sorghi*. *Mycol. Res.* 103, 859–864. doi: 10.1017/S0953756298007886

Buhtz, A., Witzel, K., Strehmel, N., Ziegler, J., Abel, S., and Grosch, R. (2015). Perturbations in the primary metabolism of Tomato and *Arabidopsis thaliana*plants infected with the soil-borne fungus *Verticillium dahliae*. *PLoS One* 10:e0138242. doi: 10.1371/journal.pone.0138242

Chin Ming, E., Sunar, N. M., Leman, A. M., and Othman, N. (2015). Direct growth inhibition assay of total airborne fungi with application of biocide-treated malt extract agar. *MethodsX* 2, 340–344. doi: 10.1016/j.mex.2015.07.002

Cota-Arriola, O., Cortez-Rocha, M., Burgos-Hernandez, A., Ezquerra-Brauer, J., and Plascencia-Jatomea, M. (2013). Controlled release matrices and micro/nanoparticles of chitosan with antimicrobial potential: development of new strategies for microbial control in agriculture. *J. Sci. Food Agric.* 93, 1525–1536. doi: 10.1002/jsfa.6060

Desjardins, A. E. (2003). Gibberella from A (venaceae) to Z (eae). *Annu. Rev. Phytopathol.* 41, 177–198. doi: 10.1146/annurev.phyto.41.011703.115501

Fuentes, E., Báez, M. E., Bravo, M., Cid, C., and Labra, F. (2012). Determination of total phenolic content in olive oil Samples by UV–visible spectrometry and multivariate calibration. *Food Anal. Methods* 5, 1311–1319. doi: 10.1007/s12161-012-9379-5

Goldsmith, C. D., Vuong, Q. V., Sadeqzadeh, E., Stathopoulos, C. E., Roach, P. D., and Scarlett, C. J. (2015). Phytochemical properties and anti-proliferative activity of *Olea europaea* L. leaf extracts against pancreatic cancer cells. *Molecules* 20, 12992–13004. doi: 10.3390/molecules200712992

Höhne, S., Frenzel, R., Heppe, A., and Simon, F. (2007). Hydrophobic chitosan microparticles: heterogeneous phase-reaction of chitosan with hydrophobic carbonyl reagents. *Biomacromolecules* 8, 2051–2058. doi: 10.1021/bm0702354

Joanitti, G. A., and Silva, L. P. (2014). The emerging potential of by-products as platforms for drug delivery systems. *Curr. Drug Targets* 15, 478–485. doi: 10.2174/1389450111314990171

Kaiser, C., van der Merwe, R., Bekker, T. F., and Labuschagne, N. (2005). *In-vitro* inhibition of mycelial growth of several phytopathogenic fungi, including *Phytophthora cinnamomic* by soluble silicon. South African Avocado Growers'. *Assoc. Yearb.* 28:74.

Kashyap, P. L., Xiang, X., and Heiden, P. (2015). Chitosan nanoparticle based delivery systems for sustainable agriculture. *Int. J. Biol. Macromol.* 77, 36–51. doi: 10.1016/j.ijbiomac.2015.02.039

Le Toutour, B., and Guedon, D. (1992). Antioxidative activities of *Olea europaea* leaves and related phenolic compounds. *Phytochemistry* 31, 1173–1178. doi: 10.1016/0031-9422(92)80255-D

Liu, H., Du, Y., Wang, X., and Sun, L. (2004). Chitosan kills bacteria through cell membrane damage. *Int. J. Food Microbiol.* 95, 147–155. doi: 10.1016/j.ijfoodmicro.2004.01.022

López-León, T., Carvalho, E. L. S., Seijo, B., Ortega-Vinuesa, J. L., and Bastos-González, D. (2005). Physicochemical characterization of chitosan nanoparticles: electrokinetic and stability behavior. *J. Colloid Interface Sci.* 283, 344–351. doi: 10.1016/j.jcis.2004.08.186

Manna, V., and Patil, S. (2009). Borax mediated layer-by-layer self-assembly of neutral poly(vinyl-alcohol) and chitosan. *J. Phys. Chem. B.* 113, 9137–9142. doi: 10.1021/jp9025333

Markin, D., Duek, L., and Berdicevsky, I. (2003). *In vitro* antimicrobial activity of olive leaves. *Mycoses* 46, 132–136. doi: 10.1046/j.1439-0507.2003.00859.x

Mazzotta, E., De Benedittis, S., Qualtieri, A., and Muzzalupo, R. (2020). Actively targeted and redox responsive delivery of anticancer drug by chitosan nanoparticles. *Pharmaceutics* 12:26. doi: 10.3390/pharmaceutics12010026

Montedoro, G., Servili, M., Baldioli, M., and Miniati, E. (1992). Simple and hydrolyzable phenolic compounds in virgin olive oil. I: their extraction, separation, and quantitative and semiquantitative evaluation by HPLC. *J. Agric. Food Chem.* 40, 1571–1576. doi: 10.1021/jf00021a019

Muto, A., Pisani, F., Pacenza, M., Greco, F., Tavano, L., Gagliardi, O., et al. (2014). Isolation and characterization of Fusarium species associated with cloves of garlic (Allium sativa). Final report of project "L'aglio Testa Rossa Cardinale della valle dell'Esaro e del Fullone (nuova selezione varietale)", PSR Calabria 2007-2013 Misura 124 "Cooperazione per lo sviluppo di nuovi prodotti, processi e tecnologie nei settori agricolo e alimentare, e in quello forestale. Calabria region, Italy, 15–55.

Muzzalupo, I., Stefanizzi, F., Perri, E., and Chiappetta, A. A. (2011). Transcript levels of CHL P gene, antioxidants and chlorophylls contents in olive (*Olea europaea* L.) pericarps: a comparative study on eleven olive cultivars harvested in two ripening stages. *Plant Foods Hum. Nutr.* 66, 1–10. doi: 10.1007/s11130-011-0208-6

Nasti, A., Zaki, N. M., de Leonardis, P., Ungphaiboon, S., Sansongsak, P., Rimoli, M. G., et al. (2009). Chitosan/TPP and chitosan/TPP-hyaluronic acid nanoparticles: systematic optimization of the preparative process and preliminary biological evaluation. *Pharm. Res.* 26, 1918–1930. doi: 10.1007/s11095-009-9908-0

Nguyen, T. T. X., Dehne, H.-W., and Steiner, U. (2016). Histopathological assessment of the infection of maize leaves by *Fusarium graminearum*. *F. proliferatum*, and *F. verticillioides*. *Fungal Biol.* 120, 1094–1104. doi: 10.1016/j.funbio.2016.05.013

Omar, S. H. (2010). Oleuropein in olive and its pharmacological effects. *Sci. Pharm* 78, 133–154. doi: 10.3797/scipharm.0912-18

Rabea, E. I., Mohamed, E. T., Steven, C. V., Smagghe, G., and Steurbaut, W. (2003). Chitosan as antimicrobial agent: applications and mode of action. *Biomacromolecules* 4, 1457–1465. doi: 10.1021/bm034130m

Rampino, A., Borgogna, M., and Blasi, P. (2013). Chitosan nanoparticles: preparation, size evolution and stability. *Int. J. Pharm.* 455, 219–228. doi: 10.1016/j.ijpharm.2013.07.034

Rodriguez-Maturino, A., Troncoso-Rojas, R., Sánchez-Estrada, A., González-Mendoza, D., Ruiz-Sanchez, E., Zamora-Bustillos, R., et al. (2015). Antifungal effect of phenolic and carotenoids extracts from chiltepin (*Capsicum annum var. glabriusculum*) on Alternaria alternata and Fusarium oxysporum. *Rev. Argent. Microbiol.* 47, 72–77. doi: 10.1016/j.ram.2014.12.005

Rosengaus, R. B., Lefebvre, M. L., and Traniello, J. F. A. (2000). Inhibition of fungal spore germination by nasutitermes: evidence for a possible antiseptic role of soldier defensive secretions. *J. Chem. Ecol.* 26, 21–39. doi: 10.1023/A:1005481209579

Schweigkofler, W., O'Donnell, K., and Garbelotto, M. (2004). Detection and quantification of airborne conidia of *Fusarium circinatum*, the causal agent of pine pitch canker, from two California sites by using a real-time PCR approach combined with a simple spore trapping method. *Appl. Environ. Microbiol.* 70, 3512–3520. doi: 10.1128/AEM.70.6.3512-3520.2004

Servat-Medina, L., González-Gómez, A., Reyes-Ortega, F., Sousa, I. M. O., Queiroz, N. D. C. A., Zago, P. M. W., et al. (2015). Chitosan–tripolyphosphate nanoparticles as *Arrabidaeachica* standardized extract carrier: synthesis, characterization, biocompatibility, and antiulcerogenic activity. *Int. J. Nanomed.* 10, 3897–3907. doi: 10.2147/IJN.S83705

Shi, Y., Wan, A., Shi, Y., Zhang, Y., and Chen, Y. (2014). Experimental and mathematical studies on the drug release properties of aspirin loaded chitosan nanoparticles. *BioMed Res. Int.* 2014, 1–8. doi: 10.1155/2014/613619

Shukla, S. K., Mishra, A. K., Arotiba, O. A., and Mamba, B. B. (2013). Chitosan-based nanomaterials: a state-of-the-art review. *Int. J. Biol. Macromol.* 59, 6–58. doi: 10.1016/j.ijbiomac.2013.04.043

Steinkellner, S., and Mammerler, R. (2007). Effect of flavonoids on the development of *Fusarium oxysporum* f. sp. Lycopersici. *J. Plant. Interact* 2, 17–23. doi: 10.1080/17429140701409352

Sudjana, A. N., D'Orazio, C., Ryan, V., Rasool, N., Ng, J., Islam, N., et al. (2009). Antimicrobial activity of commercial *Olea europaea* (olive) leaf extract. *Int. J. Antimicrob. Agents* 33, 461–463. doi: 10.1016/j.ijantimicag.2008.10.026

Tan, S. P., Parks, S. E., Stathopoulos, C. E., and Roach, P. D. (2014). Extraction of flavanoids form bitter melon. *Food Nutr. Sci.* 5, 458–465.

Taskeen-Un-Nisa, A. H., Yaqub Bhat, M., Pala, S. A., and Mir, R. A. (2011). *In vitro* inhibitory effect of fungicides and botanicals on mycelial growth and spore germination of *Fusarium oxysporum*. *J. Biopest* 4, 53–56.

Trapero-Casas, A., and Jiménes-Dìaz, R. M. (1985). Fungal wilt and root rot diseases of chickpea in southern Spain. *Phytopathology* 75, 1146–1551.

Varuna Kumara, J. B., and Basavaraj, M. (2015). Synthesis, characterization and hemocompatibility evaluation of curcumin encapsulated chitosan nanoparticles for oral delivery. *IJAR* 3, 604–611.

Yateem, H., Afaneh, I., and Al-Rimawi, F. (2014). Optimum conditions for oleuropein extraction from olive leaves. *IJAST* 4, 153–157.

Zhou, H. Y., and Chen, X. G. (2008). Biocompatibility and characteristics of chitosan/cellulose acetate microspheres for drug delivery. *Front. Mater. Sci. China* 5:367–378. doi: 10.1007/s11706-011-0146-0

Zorić, N., Kopjar, N., Kraljić, K., Oršolić, N., Tomić, S., and Kosalec, I. (2016). Olive leaf extract activity against *Candida albicans* and *C. dubliniensis* – the in vitro viability study. *Acta Pharm.* 66, 411–421. doi: 10.1515/acph-2016-0033

Conflict of Interest: The authors declare that the research was conducted in the absence of any commercial or financial relationships that could be construed as a potential conflict of interest.

frontiers in Plant Science

ORIGINAL RESEARCH
published: 20 March 2020
doi: 10.3389/fpls.2020.00308

Heterologous Expression of the *AtNPR1* Gene in Olive and Its Effects on Fungal Tolerance

*Isabel Narváez[1], Clara Pliego Prieto[2], Elena Palomo-Ríos[1], Louis Fresta[1], Rafael M. Jiménez-Díaz[3,4], Jose L. Trapero-Casas[4], Carlos Lopez-Herrera[4], Juan M. Arjona-Lopez[4], Jose A. Mercado[1] and Fernando Pliego-Alfaro[1]**

[1] Instituto de Hortofruticultura Subtropical y Mediterránea "La Mayora", Departamento de Botánica y Fisiología Vegetal, Universidad de Málaga, Málaga, Spain, [2] Departamento de Genómica y Biotecnología, Fruticultura Subtropical y Mediterránea (IFAPA), Unidad Asociada de I+D+i al CSIC, Málaga, Spain, [3] Departamento de Agronomía, College of Agriculture and Forestry (ETSIAM), Universidad de Córdoba, Campus de Excelencia Internacional Agroalimentario ceiA3, Córdoba, Spain, [4] Instituto de Agricultura Sostenible, Consejo Superior de Investigaciones Científicas, Avenida Menéndez Pidal s/n, Campus de Excelencia Internacional Agroalimentario ceiA3, Córdoba, Spain

OPEN ACCESS

Edited by:
Antonio Diaz Espejo, Institute of Natural Resources and Agrobiology of Seville (CSIC), Spain

Reviewed by:
Irene García, Institute of Plant Biochemistry and Photosynthesis (IBVF), Spain
Scott Merkle, University of Georgia, United States

***Correspondence:**
Fernando Pliego-Alfaro
ferpliego@uma.es

Specialty section:
This article was submitted to Crop and Product Physiology, a section of the journal Frontiers in Plant Science

Received: *20 June 2019*
Accepted: *03 March 2020*
Published: *20 March 2020*

Citation:
Narváez I, Pliego Prieto C, Palomo-Ríos E, Fresta L, Jiménez-Díaz RM, Trapero-Casas JL, Lopez-Herrera C, Arjona-Lopez JM, Mercado JA and Pliego-Alfaro F (2020) Heterologous Expression of the AtNPR1 Gene in Olive and Its Effects on Fungal Tolerance. Front. Plant Sci. 11:308. doi: 10.3389/fpls.2020.00308

The *NPR1* gene encodes a key component of systemic acquired resistance (SAR) signaling mediated by salicylic acid (SA). Overexpression of *NPR1* confers resistance to biotrophic and hemibiotrophic fungi in several plant species. The *NPR1* gene has also been shown to be involved in the crosstalk between SAR signaling and the jasmonic acid-ethylene (JA/Et) pathway, which is involved in the response to necrotrophic fungi. The aim of this research was to generate transgenic olive plants expressing the *NPR1* gene from *Arabidopsis thaliana* to evaluate their differential response to the hemibiotrophic fungus *Verticillium dahliae* and the necrotroph *Rosellinia necatrix*. Three transgenic lines expressing the *AtNPR1* gene under the control of the constitutive promoter CaMV35S were obtained using an embryogenic line derived from a seed of cv. Picual. After maturation and germination of the transgenic somatic embryos, the plants were micropropagated and acclimated to *ex vitro* conditions. The level of *AtNPR1* expression in the transgenic materials varied greatly among the different lines and was higher in the *NPR1*-780 line. The expression of *AtNPR1* did not alter the growth of transgenic plants either *in vitro* or in the greenhouse. Different levels of transgene expression also did not affect basal endochitinase activity in the leaves, which was similar to that of control plants. Response to the hemibiotrophic pathogen *V. dahliae* varied with pathotype. All plants died by 50 days after inoculation with defoliating (D) pathotype V-138, but the response to non-defoliating (ND) strains differed by race: following inoculation with the V-1242 strain (ND, race 2), symptoms appeared after 44–55 days, with line *NPR1*-780 showing the lowest disease severity index. This line also showed good performance when inoculated with the V-1558 strain (ND, race 1), although the differences from the control were not statistically significant. In response to the necrotroph *R. necatrix*, all the transgenic lines showed a slight delay in disease development, with mean area under the disease progress curve (AUDPC) values 7–15% lower than that of the control.

Keywords: genetic transformation, SAR response, *Olea europaea*, soil-borne pathogens, white root rot, Verticillium wilt

INTRODUCTION

Olive (*Olea europaea*) is a fruit crop widely cultivated in the countries of the Mediterranean Basin. The species, which is relatively sensitive to cold but highly resistant to heat and drought, was probably domesticated in the Middle East and Central Mediterranean 5500 years B.P. (Rallo et al., 2018). Since then, it has played key roles in the history, economy, culture and environment of this region. Over the last 30 years, the high quality, nutritional properties and health benefits of olive oil (Pérez-Jiménez et al., 2007) have given rise to an increasing interest in this crop linked to changes in its mode of cultivation, such as increasing orchard densities and using selected varieties under irrigation regimes. In addition, olive cultivation has been extended worldwide (Rugini et al., 2011).

Olive culture is threatened by the hemibiotrophic soil-borne fungus *Verticillium dahliae* (Jiménez-Díaz et al., 2012). In a recent estimation with cv. Arbequina in Córdoba, Spain, yield decreases of 84 and 56% were recorded for 3- and 4-year-old affected orchards, respectively (R. M. Jiménez-Díaz and J. L. Trapero-Casas, unpublished data, IAS-CSIC, Córdoba, 2018). Genetic and virulence variation occurring in populations of *V. dahliae* are the main hindrances to the effective management of this disease. Populations of *V. dahliae* comprise two types of pathogenic variation, namely, defoliating (D) and non-defoliating (ND) pathotypes (i.e., symptom types) and pathogenic races 1 and 2 (Jiménez-Díaz et al., 2017). Isolates of the D pathotype cause defoliation of cotton, olive, and okra, whereas isolates of the ND pathotype do not defoliate these species (Jiménez-Díaz et al., 2017). Isolates of race 1, which is avirulent on tomato plants with the resistance gene *Ve1* (de Jonge et al., 2012), belong to the ND pathotype, whereas the Ve1-resistance breaking isolates of race 2 can be found with both D and ND pathotypes (Jiménez-Díaz et al., 2017). According to investigations carried out in tomato (de Jonge et al., 2012), race 1 is characterized by possessing the *Ave1* gene, which encodes a virulence factor that, when it is recognized by the leucine-rich repeat-receptor like protein (LRR-RLP) encoded by the *Ve1* gene, induces the expression of defense mechanisms underlying resistance in the host plant. Race 2 lacks *Ave1* and is pathogenic to cultivars with the *Ve1* gene because a lack of recognition between the factors prevents the induction of defense mechanisms.

The necrotrophic pathogen *R. necatrix*, the causal agent of white root rot, is widely distributed and causes economically important losses in different fruit trees (Sztejnberg, 1980; ten Hoopen and Krauss, 2006); it is also known to affect olive (Sztejnberg, 1980; Guillaumin et al., 1982; García Figueras and Celada Brouard, 2001; Roca et al., 2016). The entire life cycle of *R. necatrix* occurs in the soil, where it can survive for many years. Its mycelia colonize the roots of healthy plants adjacent to infected roots. This fungus invades the plant through the root system, causing generalized rotting of tissues. The symptoms in the aerial parts can develop either quickly or slowly, leading to wilting of leaves, death of branches, and eventually, the death of the tree (Pliego et al., 2012).

Host resistance is the single most practical and efficient method for the management of Verticillium wilt (VW) in olive, but its effectiveness is curtailed by the widespread occurrence of the highly virulent D pathotype in Spain and elsewhere (Jiménez-Díaz et al., 2012). Most widely grown olive cultivars, such as Arbequina and Picual, are highly susceptible to D *V. dahliae*; moreover, the valuable resistance against ND pathotypes found in cultivars such as Frantoio and Changlot Real is overcome by the D pathotype (López-Escudero et al., 2004; Trapero et al., 2015). To the best of our knowledge, no olive selections have been found showing tolerance to *R. necatrix*; for example, García et al. (2009) evaluated 12 different cultivars growing in 2 L containers, and all of them showed a high level of susceptibility to the pathogen.

Plants have different systems of defense against pathogens; among them, SAR (systemic acquired resistance), generated by an increase in SA (salicylic acid) in the site of infection and distal tissues, and ISR (induced systemic resistance), which provides local induced resistance. SAR is established against infections by biotrophic and hemibiotrophic pathogens, with the *NPR1* gene as a key regulator in this pathway (Cao et al., 1997); in Arabidopsis, the NPR1 protein is located in an inactive oligomeric form in the cytoplasm in the absence of pathogens. Following SA-induced changes in the redox state of cells, monomers are released, migrating to the nucleus and inducing SAR signaling, which results in the accumulation of the PR1 (antifungal), PR2 (β-1,3-glucanases), and PR5 (thaumatin-like) proteins (Ali et al., 2018). In contrast, in ISR signaling, jasmonic acid (JA) and ethylene (Et) play key roles. ISR signaling is a defense response against necrotrophic pathogens (Glazebrook, 2005) involving local accumulation of PR3 (Class I, II, IV, V, VI, VII chitinases), PR4 (Class I, II chitinases), and PR12 (defensin) proteins (Ali et al., 2018). However, although SAR and ISR signaling involve different pathways, there exists an overlap between them resulting in either antagonistic or synergistic actions. El Oirdi et al. (2011) found that the necrotrophic fungus *Botrytis cinerea* produces a polysaccharide that, through elicitation of SA signaling and increased *NPR1* expression, inhibits the JA pathway, favoring fungal attack. The suppressive effects of *NPR1* on the JA pathway are well known (Spoel et al., 2003). Alternatively, some toxins imitate JA in silencing the SA pathway, hence increasing the virulence of the pathogen (Zheng et al., 2012). Finally, a synergistic action between the SA and JA signaling pathways has also been demonstrated (van Wees et al., 2000).

The *AtNPR1* gene has been overexpressed in different mono- and dicotyledonous species, inducing resistance to several biotrophic (Cao et al., 1998; Wally et al., 2009), hemibiotrophic (Lin et al., 2004; Makandar et al., 2006; Kumar et al., 2013), and necrotrophic plant pathosystems (Wally et al., 2009; Parkhi et al., 2010b). Taking into account the specificity in the interaction between a species and a given transgene (Islam, 2006), the goal of this investigation was to evaluate the behavior of *AtNPR1* transgenic olive plants following inoculation with either of these two fungi, i.e., the hemibiotrophic *V. dahliae* or the necrotrophic *R. necatrix*.

MATERIALS AND METHODS

Plant Material

Olive embryogenic cultures were established from the radicle of a mature zygotic embryo, cv. Picual, line P1, as indicated by Orinos and Mitrakos (1991). For maintenance, the medium and culture conditions established by Pérez-Barranco et al. (2009) were used, i.e., olive cyclic embryogenesis medium [ECO basal medium containing 1/4 OM (Rugini, 1984) macroelements, 1/4 MS (Murashige and Skoog, 1962) microelements, 1/2 OM vitamins and 550 mg/L glutamine, supplemented with 0.25 μM IBA, 0.5 μM 2iP, 0.44 μM BA and 200 mg/L cefotaxime] in darkness at 25 ± 2°C. Subculturing was carried out at 4-week intervals. The embryogenic culture consisted of small pro-embryogenic masses and globular embryos.

Binary Vector and Olive Transformation

A DNA fragment containing the *AtNPR1* gene was cloned into the binary plasmid pK7WG2.0, which includes the neomycin phosphotransferase (*nptII)* gene for selection of transformed material. The expression of the *AtNPR1* and *nptII* genes was controlled by the constitutive promoters CaMV35S and NOS (nopaline synthase), respectively. This binary vector was introduced into the disarmed *Agrobacterium tumefaciens* strain AGL1 (Lazo et al., 1991) by the freeze-thaw method (Höfgen and Willmitzer, 1988).

For transformation experiments, *Agrobacterium* cultures were incubated at 28°C in LB medium supplemented with 10 mg/L rifampicin and 100 mg/L spectinomycin at 250 rpm. Prior to somatic embryo inoculation, the bacterial suspension was centrifuged at 4000 × *g* for 10 min, and the pellet was washed with 10 mM $MgSO_4$ and finally resuspended in ECO medium at 0.5–0.6 OD_{600}.

Genetic transformation experiments were carried out following the protocol described by Torreblanca et al. (2010). A total of 1064 globular somatic embryos (SE) obtained from the embryogenic culture were inoculated with a diluted *Agrobacterium* culture for 20 min under mild agitation. After that, the explants were blotted, dried on sterile filter paper and cultured in ECO solid medium without antibiotics at 25°C in darkness for 48 h. After coculturing, the SEs were washed with ECO liquid medium supplemented with 250 mg/L cefotaxime and timentin at 25°C for 2 h, dried on sterile filter paper and transferred to selection medium, i.e., solid ECO medium supplemented with three antibiotics (250 mg/L cefotaxime, 250 mg/L timentin, and 50 mg/L paromomycin). To select transformed cells, during the first month, embryogenic structures were re-cultured individually onto fresh medium once a week, during the next 2 months at 2-week intervals and monthly afterward. Transformed material was recovered using a progressive selection strategy, i.e., at the beginning, a concentration of 50 mg/L paromomycin was used with progressive increases up to 150 mg/L. Embryogenic lines proliferating in ECO medium supplemented with 150 mg/L paromomycin were grown individually in 25 mL ECO liquid medium supplemented with 250 mg/L cefotaxime and 12.5–25 mg/L paromomycin in an orbital shaker at 120 rpm for 3 weeks. After that, the embryogenic suspensions were filtered through a 2-mm mesh, and the obtained SEs were used for further proliferation in ECO medium. Afterward, 120–150 SE of 1–3 mm in diameter from the selected lines were cultured in maturation ECO medium (basal ECO medium without growth regulators and cefotaxime, supplemented with 1 g/L activated charcoal) over cellulose acetate membranes for 8 weeks as indicated by Cerezo et al. (2011). Then, the mature embryos were transferred to germination medium (Clavero-Ramírez and Pliego-Alfaro, 1990), i.e., modified MS with 1/3 MS macroelements, MS microelements, and 10 g/L sucrose for 12 weeks under 40 $\mu mol \cdot m^{-2} \cdot s^{-1}$ irradiance level. The obtained shoots were isolated and multiplied in RP medium [DKW macro- and micronutrients as modified by Roussos and Pontikis (2002) and vitamins of Roussos and Pontikis (2002)] supplemented with 2 mg/L zeatin riboside, as indicated by Vidoy-Mercado et al. (2012). Shoots were rooted after a 3-day pulse in basal RP liquid medium supplemented with 10 mg/L IBA and subsequently transferred to basal solid RP medium supplemented with 1 g/L activated charcoal. Acclimatization to *ex vitro* conditions was carried out in jiffy trays with peat moss:perlite (1:1) under a plastic tunnel with gradual lowering of relative humidity for 6–8 weeks. Subsequently, plants were grown in a confined greenhouse with a cooling system, 30°C maximum temperature, and daylight conditions. Plants recovered from non-transformed embryogenic calli were used as controls.

Phenotypic Analysis of Transgenic Plants

The *in vitro* behavior of the transgenic *AtNPR1* lines was evaluated. For this purpose, 20 shoot segments, 1.5–2 cm in length, with two nodes and deprived of the shoot apex, were isolated from each transgenic line and cultured in RP medium supplemented with 2 mg/L zeatin riboside (Vidoy-Mercado et al., 2012). After 8 weeks, the number of axillary shoots and their lengths were quantified over three subcultures. To evaluate rooting capacity, 2-cm-long apical shoots with at least one node were used. Rooting conditions were as previously described (see section "Binary Vector and Olive Transformation"). After 9 weeks, the number of roots and the length of the main root were measured. The non-transgenic line P1 was used as a control, and the experiment was carried out in triplicate.

Rooted plants were acclimatized to *ex vitro* conditions as previously indicated (see section "Binary Vector and Olive Transformation"). After 9 months of growth in the confined greenhouse under natural daylight conditions, the plant height and the diameter of the main stem were measured. Fourteen plants per transgenic and control line were evaluated.

Molecular Analysis of Transgenic Plants

The transgenic nature of *AtNPR1* embryogenic lines was confirmed by PCR amplification of a 732-bp fragment from the *AtNPR1* gene and a 700-bp fragment from *nptII*. Genomic DNA was extracted from calli using the protocol of Healey et al. (2014). To amplify the *AtNPR1* gene, the primers

used were F: 5′-AATTGAAGATGACGCTGCTCG-3′ and R: 5′-CGACGATGAGAGAGTTTACGG-3′; for *nptII*, the following primers were employed: F: 5′-GAGGCTATTCGGCTATGACTG-3′ and R: 5′-ATCGGGAGCGGCGATACCGTA-3′. All PCRs were prepared in a final volume of 20 μl containing 0.5–1 μl of genomic DNA and 0.5 μM of each primer. Amplification conditions consisted of 4 min at 95°C, followed by 30 cycles of 1 min at 95°C, 45 s at 59°C, and 1 min at 72°C, with a final extension step of 10 min at 72°C.

Approximately 100 mg of *in vitro* leaves from *AtNPR1* transgenic and non-transgenic control lines were collected, powdered in liquid nitrogen and kept at −80°C until used. RNA was extracted using a Spectrum™ Plant Total RNA kit (Sigma-Aldrich) following the manufacturer's instructions. The concentration and purity of the extracted RNA was assessed using a NanoDrop ND-1000 spectrophotometer (NanoDrop Technologies, Inc., Montchanin, DE, United States). The integrity of RNA samples was visualized on a 1.5% agarose gel under non-denaturing conditions. RNA was treated with DNase I Recombinant, RNase Free (Roche), and cDNA was synthesized by using an iScript™ cDNA Synthesis Kit (Bio-Rad) according to the manufacturer's instructions.

Quantitative real-time PCR (qRT-PCR) was performed using iTaq™ Universal SYBR Green Supermix (Bio-Rad) in a final reaction volume of 20 μl containing 0.5 μM of each primer and 1 μl of diluted cDNA in a CFX96™ thermocycler (Bio-Rad). For *AtNPR1* amplification, the primers used were designed by Silva et al. (2015) (F: 5′-ATCAGAAGCAACTTTGGAAGGTAGA-3′ and R: 5′-ACCGCCATAGTGGCTTGTTT-3′). The olive ubiquitin gene (F: 5′-ATGCAGATCTTTGTGAAGAC-3′ and R: 5′-ACCACCACGAAGACGGAG-3′) was used as a housekeeping gene for normalization (Gómez-Jiménez et al., 2010). PCR conditions were 30 s at 95°C, 40 cycles of 5 s at 95°C and 30 s at 60°C, followed by a melting curve from 65 to 95°C with 0.5°C increments at 5 s intervals. Relative *AtNPR1* expression levels in *in vitro* leaves were calculated using the $2^{-\Delta\Delta CT}$ method (Livak and Schmittgen, 2001). An arbitrary value of 1 was given to the line with the lowest gene expression. The experiment was carried out in triplicate, i.e., three independent RNA extractions with three technical replicates for each extraction.

Western Blot Detection of *AtNpr1*

The *At*NPR1 protein was detected by western blotting in olive leaf extracts from the control and transgenic plants before and after treatment with SA. Twelve-month-old plants growing in a greenhouse were transferred to a growth chamber with a 16 h photoperiod of 150 $\mu mol \cdot m^{-2} \cdot s^{-1}$ at 25°C 1 week before treatment. Four plants per genotype were sprayed until runoff with a solution of 0.5 mM SA, and leaf samples were taken after 0 and 24 h of treatment. Samples (0.2 g) were extracted in 2 mL extraction buffer (50 mM Tris–HCl, pH 7.5, 150 mM NaCl, 0.5 mM EDTA, 0.1% Triton-X-100, 0.2% Nonidet P-40, 50 μM MG-132 and 50 mM DTT). Homogenates were centrifuged at 23,000 rpm at 4°C for 20 min, and the supernatant was used as the protein extract.

Proteins (60 μg) were separated by SDS-PAGE on 12.5% polyacrylamide gels (Laemmli, 1970), transferred to nitrocellulose membranes (Amersham Protran) using a Trans-blot SD semi-dry transfer cell (Bio-Rad) and blocked with 1% non-fat milk powder at RT. The blots were incubated with a polyclonal antibody against *At*NPR1 (AS12 1854, Agrisera) diluted 1:2500 overnight at 4°C. The membranes were washed three times with blocking solution and incubated with donkey anti-rabbit IgG secondary antibody conjugated with horseradish peroxidase at a dilution of 1:5000. SuperSignal West Femto Maximum Sensitivity Substrate (Thermo Fisher Scientific) was used for chemiluminescence detection. Three independent protein extractions and western blots were performed for the control and each transgenic line.

Quantification of Endochitinase Activity

Endochitinase activity was measured in young leaves from control and transgenic plants grown in the greenhouse for 10 months. Leaves were powdered in liquid nitrogen and kept at −80°C until use. Samples (0.2 g) were homogenized in 2 mL 50 mM sodium acetate buffer, pH 5.5, with an Ultra-Turrax. Then, the extracts were centrifuged for 20 min at 13,000 rpm and 4°C, and the supernatant was collected. Endochitinase activity was quantified following the protocol of Emani et al. (2003). Protein extracts (100 μL) were incubated with 25 μL of 250 μM fluorescent substrate 4-methylumbelliferyl-β-D-N,N′,N″-triacetylchitotrioside (MUC), dissolved in 0.1 M citrate buffer, pH 3, at 37°C for 1 h in darkness. After incubation, the reaction was stopped with 1 mL of 0.2 M sodium carbonate. Fluorescence was measured in a Clariostar Monochromator Microplate Reader (BMG LABTECH) at 350 nm (excitation) and 450 nm (emission). To quantify endochitinase activity, a standard curve (0.1–10 μM) of the fluorescent compound 4-methylumbelliferone (MU), a product of the hydrolysis of MUC by endochitinases, was carried out. The total protein of each extract was quantified using the Bradford method (Bradford, 1976) with a Bio-Rad Protein Assay following the manufacturer's instructions. Endochitinase activity was expressed as pmol of 4-MU per hour produced by μg of total protein (pmol 4-MU·h^{-1}·μg of total $protein^{-1}$). Three independent protein extractions per line and three determinations per protein extract were carried out.

Expression of PR1 Genes in Transgenic Plants

Contigs predicted to encode a basic form of pathogenesis-related protein 1-like in *O. europaea* var. *sylvestris* were searched in the NCBI databases. Those showing homology with regions of PR1-encoding genes from other species were selected for gene expression analysis in leaf tissue from control and transgenic plants by qRT-PCR (**Supplementary Table 1**).

Primer sequences for the endogenous control genes and the predicted *O. europaea* var. *sylvestris* PR1 genes are shown in **Supplementary Table 2**. Primer pairs were chosen to generate fragments between 70 and 140 bp and designed using Primer 3 software[1]. Primer specificity was tested by performing

[1]http://bioinfo.ut.ee/primer3-0.4.0/

conventional PCR and confirmed by the presence of a single melting curve during qRT-PCR. Serial dilutions (1:10, 1:20, 1:50, and 1:200) were made from a pool of cDNA from each treatment and time point, and calibration curves were performed for each gene. For qRT-PCR, the reaction mixture consisted of the first-strand cDNA template, primers (500 nmol final concentration) and SYBR Green Master Mix (SsoAdvanced Universal SYBR Green Supermix, Bio-Rad) in a total volume of 20 μl. The PCR conditions were as follows: 30 s at 95°C, followed by 40 cycles of 15 s at 95°C and 30 s at 60°C, 3 min at 72°C, and 1 min at 95°C. The reactions were performed using an iQ5 real-time PCR detection system (Bio-Rad). The ubiquitin gene was used as an endogenous control for normalization. Relative quantification of the expression levels for the target was analyzed using comparative Ct methods. An arbitrary value of 1 was given to the control, non-transformed line. All reactions were carried out in triplicate.

Verticillium dahliae Infection Assay

Disease reactions to the D and ND *V. dahliae* pathotypes of three *AtNPR1* transgenic lines as well as the non-transgenic control P1, which is highly susceptible to this pathogen (Narvaez et al., 2018), were assessed as previously described (Jiménez-Fernández et al., 2016). Monosporic *V. dahliae* isolates from cotton (V-138: D pathotype, race 2) and olive (V-1242: ND pathotype, race 2; and V-1558: ND pathotype, race 1) (Jiménez-Díaz et al., 2017) were used.

Plants had been grown in 12-cm diameter plastic pots containing a peat moss:perlite substrate (1:1 ratio) and 2 g of Osmocote fertilizer in a confined greenhouse under the natural temperature and photoperiod for over 9 months prior to inoculation with the pathogen. The inoculum consisted of *V. dahliae* mycelia and microsclerotia formed in a cornmeal-sand mixture (CMS; sand:cornmeal:deionized water, 9:1:2, w/w) (Jiménez-Díaz et al., 2017). Inocula were produced in Erlenmeyer flasks containing 400 g of autoclaved (twice at 121°C for 2.5 h) CMS mixture infested with twelve 5-mm-diameter discs from the growing edge of 7-day-old cultures on potato dextrose agar (PDA, Difco Laboratories Inc.) and incubated at 24 ± 1°C in the dark for 1 month. The infested CMS was shaken at 7-day intervals to facilitate the homogeneous colonization of the substrate by the fungus. Then, the infested CMS substrate was thoroughly mixed with a pasteurized soil mixture (clay loam:peat, 2:1, v/v; pH 8.4, 27.5% water holding capacity) at a rate of 10% (v/v) (hereafter referred to as the infested soil mixture). The inoculum density of *V. dahliae* in the infested soil mixture was estimated by serial dilutions on agar plates supplemented with 30 mg/L aureomycin (AAAu) incubated at 24 ± 1°C in the dark for 7 days.

For inoculation, 10-month-old plants were uprooted, and their root systems were washed to remove all the soil. Then, the bare-root plants were transplanted to 13 cm× 13 cm× 12 cm disinfested plastic pots containing the infested soil mixture. Non-inoculated control plants were transferred to a soil mixture containing sterile CMS. After inoculation, the plants were incubated in a growth chamber for variable periods of time, depending on the experiment, at 22 ± 2°C, 60–80% relative humidity and a 14 h photoperiod of fluorescent light of 360 $\mu mol \cdot m^{-2} \cdot s^{-1}$. The plants were watered every 1–2 days, as needed, and fertilized every 3 weeks with 100 mL Hoagland's nutrient solution.

Disease reaction in the plants was assessed by the incidence (percentage of plants showing disease symptoms) and severity of foliar symptoms. Symptoms were assessed on individual plants on a 0 to 4 rating scale according to the percentage of affected leaves and twigs (0 = no symptoms, 1 = 1–33%, 2 = 34–66%, 3 = 67–100%, and 4 = dead plant) at 2- to 3-day intervals throughout the duration of the experiments. Disease progress curves and the area under the disease progress curve (AUDPC) were also calculated as described by Campbell and Madden (1990). At the end of experiments, isolations on AAAu were carried out with shoot segments from the inoculated plants to confirm infection of the plant by the pathogen.

Two experiments (I and II) were conducted. Experiment I comprised three *AtNPR1* transgenic lines, the non-transgenic P1 line, and 10-month-old plants of the wild olive clones Ac-15 and Ac-18, previously shown to be highly susceptible and resistant to D *V. dahliae*, respectively. These wild olive lines were used as additional controls to assure adequate experimental conditions for VW development (Jiménez-Fernández et al., 2016). These plants were obtained through micropropagation using the protocol of Vidoy-Mercado et al. (2012). The inoculum consisted of *V. dahliae* isolate 138 (D, race 2), with a mean density in the potting soil mixture of 6.5×10^7 cfu·g $soil^{-1}$. The experiment lasted 18 weeks.

A second experiment (Experiment II) was carried out to determine whether the race of the isolate would have an influence on the reaction of transgenic lines to the ND pathotype. Thus, isolates V-1558 (ND, race 1) and V-1242 (ND, race 2) were included for inoculation of the same three *AtNPR1* transgenic lines, together with P1 as a non-transgenic control. The mean inoculum density in the potting soil mixture was 3.1×10^7 cfu·g $soil^{-1}$ for isolate V-1558 and 6.0×10^7 cfu·g $soil^{-1}$ for isolate V-1242. The experiment lasted 19 weeks.

For each plant genotype, there were 10 and 8 replicated pots (one plant per pot) for inoculated plants in Experiments I and II, respectively, and four non-inoculated plants in each of the experiments, distributed in a completely randomized design.

Rosellinia necatrix Infection Assay

Assays were carried out as described by Ruano Rosa and López Herrera (2009); wheat grains were submerged in distilled water for 24 h and then autoclaved at 121°C and 0.1 MPa for 40 min. Afterward, wheat grains were inoculated with discs from colonies of *Rn* 400 isolate, previously grown on PDA medium, and incubated for 15 days at 24°C in darkness. Over 10-month-old plants growing in a peat moss:perlite (1:1) substrate were inoculated with colonized wheat seeds (1.05 g/L) and grown under greenhouse conditions at 25°C for 2 months. To evaluate the disease reaction, visual symptoms were scored twice a week using a 1–5 scale: (1) healthy plant; (2) leaf chlorosis; (3) first symptoms of wilting and rolling/curling in the leaves; (4) wilted plant with first symptoms of leaf desiccation; and (5) dead plant. The AUDPC values were calculated as described

by Campbell and Madden (1990). Ten inoculated plants and 4 non-inoculated plants from each transgenic and control P1 line were used.

Statistical Analysis

The data were subjected to analysis of variance (ANOVA) using SPSS software version 23. The Levene test for homogeneity of variances was performed prior to ANOVA, and multiple mean comparisons were performed by Tukey's test. The Kruskal–Wallis test was used for mean comparison in the case of non-homogeneous variances. Pairwise mean comparisons were performed with the Mann–Whitney *U* test. All tests used a significance threshold of $P = 0.05$.

RESULTS

Generation of Transgenic *AtNPR1* Olive Plants

A total of 1064 globular SEs from the P1 line were inoculated with the *A. tumefaciens* AGL1 disarmed strain carrying the pK7WG2.0 binary vector with the *AtNPR1* gene (**Figure 1A**). After 24 weeks of culture in solid ECO medium supplemented with 150 mg/L paromomycin, all non-*Agrobacterium*-inoculated embryos were necrotic, while 10 inoculated explants showed proliferation (**Figure 1B**). These calli were cultured individually in liquid ECO medium supplemented with 12.5–25 mg/L paromomycin for 3 weeks. Then, the calli were filtered, and SEs were transferred to solid ECO medium supplemented with 150 mg/L paromomycin (**Figure 1C**). Three independent lines proliferated after this additional selection phase, yielding a transformation rate of 0.28%.

After several subcultures, SEs from selected transgenic lines were transferred to ECO basal maturation medium over cellulose acetate membranes (**Figure 1D**) and germinated in modified MS medium with 1/3 macroelements. The percentages of SE maturation were similar in the control and transgenic lines, approximately 30%, whereas the rates of shoot germination were slightly higher in the transgenic *NPR1* lines, 42–53% vs. 23% in the control. Shoots from all lines could be recovered and micropropagated (**Figure 1E**) in modified RP medium following the protocol of Vidoy-Mercado et al. (2012). Axillary shoots were rooted (**Figure 1F**) and acclimatized to greenhouse conditions (**Figures 1G,H**).

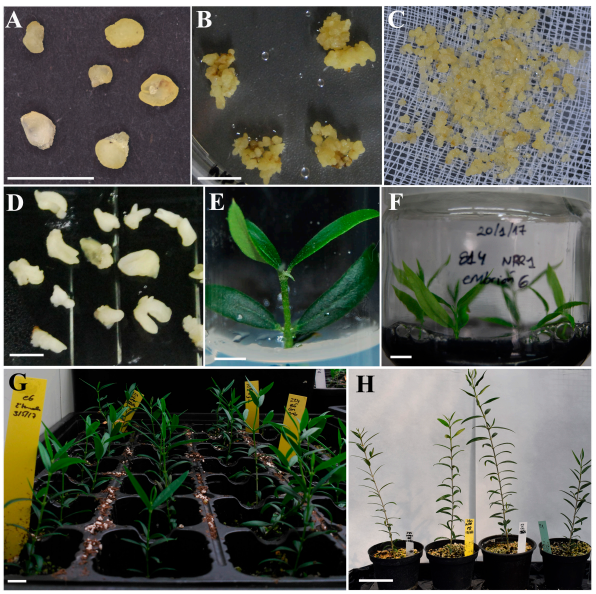

FIGURE 1 | Obtainment of olive lines transformed with the *NPR1* gene from *Arabidopsis thaliana*. **(A)** Globular somatic embryos used for inoculation with *A. tumefaciens*. **(B)** Transgenic callus from the *NPR1*-814 line growing in ECO selection medium supplemented with 150 mg/L paromomycin. **(C)** Transgenic callus from the *NPR1*-814 line after 3 weeks of selection in liquid ECO medium supplemented with 25 mg/L paromomycin. **(D)** Transgenic somatic embryos cultured on maturation medium over a semi-permeable cellulose acetate membrane. **(E)** Micropropagated shoots from the *NPR1*-814 line cultured on RP medium. **(F)** Transgenic *NPR1*-814 shoots cultured on RP medium supplemented with activated charcoal after 3 days in liquid medium with 10 mg/L IBA for rooting. **(G)** Acclimated plants from the *NPR1*-224 line after 6 weeks in the growth chamber. **(H)** From left to right, acclimated plants derived from the transgenic *NPR1*-224, *NPR1*-780, and *NPR1*-814 lines and the non-transformed P1 line after 9 months of growth in the greenhouse. Bars correspond to 0.5 cm **(A,B,D,E)**, 1 cm **(F,G)**, and 5 cm **(H)**.

Molecular Characterization of *AtNPR1* Plants

Genomic DNA was isolated from embryogenic calli, and PCR amplification of the *nptII* and *AtNPR1* genes was used to confirm their transgenic nature (**Figure 2**). All transgenic lines amplified a 700-bp fragment from the *nptII* gene (**Figure 2A**), as well as a 732-bp DNA band corresponding to the amplification of the *AtNPR1* gene (**Figure 2B**). DNA from the non-transformed control callus did not show any PCR amplification.

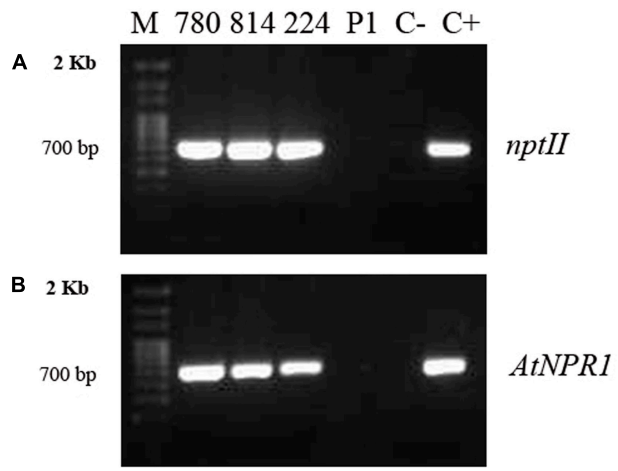

FIGURE 2 | PCR amplifications of the *nptII* **(A)** and *AtNPR1* **(B)** gene fragments from genomic DNA extracted from embryogenic callus from the different transgenic *AtNPR1* lines and non-transformed line P1. 780, 814, and 224: transgenic *AtNPR1* lines; P1, non-transgenic control; C–, negative control (without DNA); C+, 35S, *AtNPR1* binary plasmid; M, molecular marker.

Expression analysis of *AtNPR1* was carried out with qRT-PCR in RNA extracted from the leaves of the micropropagated transgenic plants (**Figure 3**). The highest level of *AtNPR1* expression was detected in the *NPR1*-780 line, whereas *NPR1*-224, and *NPR1*-814 showed lower values. As expected, *AtNPR1* expression was not detected in the non-transgenic control.

*At*NPR1 was detected in protein extracts from the control and transgenic leaves by western blotting using a commercial *At*NPR1 polyclonal antibody (**Figure 4**). This antibody recognizes a protein of approximately 66 kDa in *A. thaliana*. A band of this size was detected in the *NPR1*-780 line and, at lower intensity, in *NPR1*-224. Two additional bands of approximately 40 and 28 kDa were also detected in all lines, although their intensity was higher in *NPR1*-780. The NPR1 protein was induced after treatment of the olive plants with 0.5 mM SA for 24 h. The NPR1 band was detected in all the extracts, including the control line (**Figure 4**).

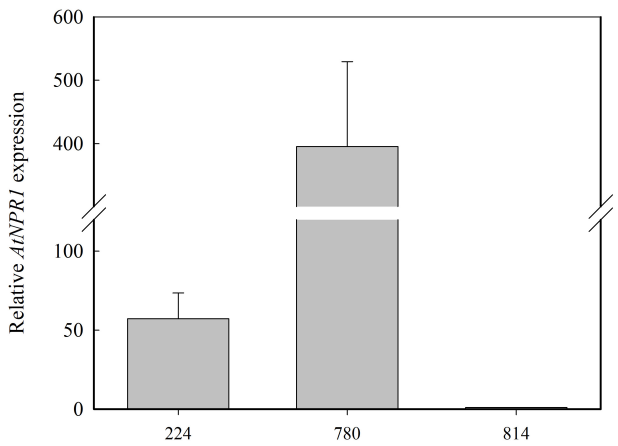

FIGURE 3 | Relative *AtNRP1* expression in leaves from transgenic olive plants. The mRNA values are shown relative to the lowest value obtained in line *NPR1*-814, which was assigned a value of 1. Data correspond to the mean ± SD of three independent RNA extractions.

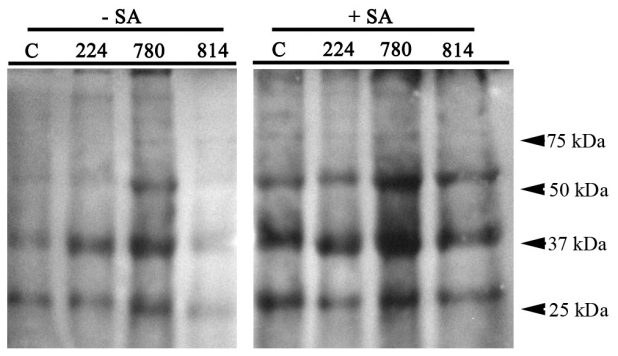

FIGURE 4 | Western blot detection of *At*NPR1 protein in leaf extracts of control (C) and transgenic olive plants. Plants were sprayed with 0.5 mM salicylic acid until runoff, and leaf samples were obtained before (–SA) and 24 h after SA treatment (+SA).

PR1 Expression and Endochitinase Activity in Transgenic *AtNPR1* Plants

Among the 11 contigs predicted to encode a basic form of pathogenesis-related protein 1-like in *O. europaea* var. *sylvestris* found in the NCBI database, four of them showed homology to PR1 genes from *Vitis vinifera*, *Prunus mume*, *Medicago truncatula*, and *Jatropha curcas* (**Supplementary Table 1**). The expression of these genes in leaves was measured by qRT-PCR. Only the gene XM_022999257.1 showed differential expression in control and transgenic plants (**Figure 5**). This PR1 gene was overexpressed in *NPR1*-780 and *NPR1*-814 lines.

Endochitinase activity was measured in leaves of control and transgenic plants growing in the greenhouse to determine whether the expression of *AtNPR1* was associated with a constitutive ISR response. No significant differences were found in chitinase activity between the control and transgenic lines (**Figure 6**).

Phenotypic Characterization of Transgenic *AtNPR1* Plants

To determine the effect of constitutive expression of the *AtNPR1* gene on olive growth, the *in vitro* and *ex vitro* behaviors were examined. For the *in vitro* characterization, axillary shoots were cultured in RP proliferation medium, and several micropropagation parameters were evaluated after 8 weeks of culture (**Table 1**). Line *NPR1*-814 showed the highest micropropagation rate, as shown by the highest number of shoots per explant and mean shoot length. In contrast, the *NPR1*-780 line showed lower values than the non-transgenic control (**Table 1**). Rooting was not affected in any transgenic line (**Table 1**).

The length and diameter of the main shoot were evaluated in 9-month-old plants growing in the greenhouse. Line *NPR1*-814 showed the highest values for both parameters evaluated,

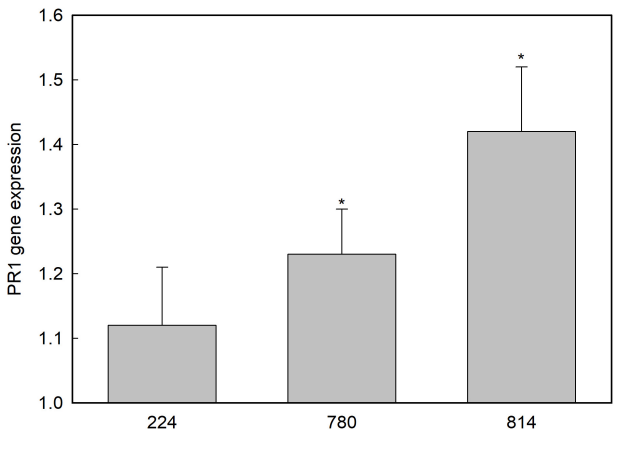

FIGURE 5 | Expression of the PR1-like gene XM_022999257.1 in the leaves of transgenic olive plants. Gene expression is shown as relative to the control non-transgenic plant value, which was given an arbitrary value of 1. Asterisks indicate significant differences from the control by *t*-test at $P = 0.05$.

TABLE 1 | *In vitro* characterization of transgenic *AtNPR1* olive plants.

Genotype	Shoots per explant	Length of shoot (cm)	Rooted explants (%)	Roots per explant	Length of main root (cm)
Control	1.9 ± 0.5a	4.2 ± 1.6b	92.1	2.5 ± 1.1a	1.9 ± 1.4
NPR1-224	1.9 ± 0.6a	4.2 ± 1.4b	86.2	3.2 ± 1.1a	1.2 ± 0.7
NPR1-780	1.6 ± 0.7b	3.9 ± 1.7b	89.5	2.3 ± 1.3a	1.2 ± 0.5
NPR1-814	2.1 ± 0.5a	5.1 ± 1.1a	85.4	3.1 ± 1.7a	1.9 ± 1.7

The data correspond to the mean ± SD. Within each column, means with different letters are significantly different by the Kruskal–Wallis (shoots per explant) or Tukey test (length of shoot) at P = 0.05.

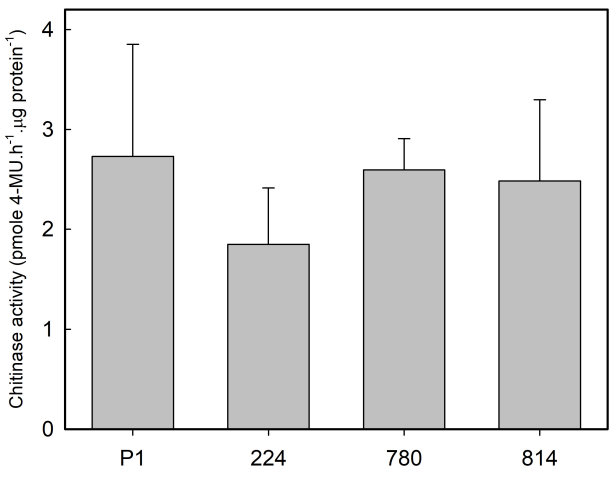

FIGURE 6 | Chitinase activity in the leaves of control (P1) and transgenic olive plants expressing the *AtNPR1* gene. The data correspond to the mean ± SD of three independent protein extractions.

and these values were significantly higher than those of the non-transgenic control (**Table 2**).

Verticillium dahliae Infection Assay

No symptoms developed in non-inoculated plants in either experiment. In Experiment I, symptoms of VW in the susceptible wild olive Ac-15 started to develop by 3 weeks after inoculation with D *V. dahliae* V-138, and all plants had died 3 weeks later. Similarly, severe disease symptoms developed in control P1 and all *AtNPR1* transgenic lines; these plants started to develop symptoms by 25 days after inoculation, and all plants died 25 days later (results not shown). As expected, the resistant genotype Ac-18 did not develop any disease symptoms.

Subsequently, Experiment II was carried out to determine whether the reaction of the transgenic *AtNPR1* and control P1 lines to the ND pathotypes would be influenced by the race of the isolate. The race 2 ND isolate V-1242 induced the development of first symptoms by 44 and 55 days after inoculation in the *NPR1*-224 and P1 lines, respectively. By 19 weeks after inoculation, the incidence of VW ranged from 50 to 75% in the transgenic lines, while 100% of control plants were affected (**Table 3**). Interestingly, the severity of symptoms was much lower in *NPR1*-780, the line with the highest relative expression of the transgene, than in the other transgenic lines and the non-transgenic control (**Table 3**). In addition, the AUDPC mean value in line *NPR1*-780 was lower than those of the other lines (**Figure 7**). Conversely, the incidence of symptoms induced by race 1 ND isolate V1558 ranged from 50 to 75% in all lines by 19 weeks after inoculation. Following inoculation with this isolate, no significant differences were found among the control P1 and transgenic lines, either in the severity of symptoms (**Table 3**) or AUDPC values (**Figure 7**). For both isolates, V-1242 and V-1558, the pathogen could be recovered from virtually all inoculated plants (**Table 3**).

Rosellinia necatrix Infection Assay

No symptoms developed in non-inoculated plants. Disease symptoms in plants of non-transgenic control P1 appeared 7 days after inoculation with the *Rn* 400 isolate, and all plants died by 25 days post-inoculation. All transgenic lines showed AUDPC values 7–15% lower than the control, with the best response being observed in the *NPR1*-814 line (**Figure 8**), although these differences were not significant.

DISCUSSION

Transformation with genes involved in the regulation of defense pathways against a wide spectrum of pathogens is a useful tool in biotechnological breeding (Lin et al., 2004). In this investigation, olive embryogenic cells were transformed with the *AtNPR1* gene, which is known to play a key role in the SAR response, to evaluate its effect in inducing tolerance to the hemibiotrophic pathogen *V. dahliae* and the necrotrophic fungus *R. necatrix*.

TABLE 2 | *Ex vitro* characterization of transgenic *AtNPR1* olive plants.

Genotype	Shoot length (cm)	Stem diameter (cm)
Control	18.7 ± 2.6b	0.19 ± 0.02b
NPR1-224	18.6 ± 3.6b	0.23 ± 0.02a
NPR1-780	19.5 ± 4.2b	0.20 ± 0.02b
NPR1-814	23.7 ± 4.3a	0.23 ± 0.01a

The data correspond to the mean ± SD. Within each column, means with different letters are significantly different by the Tukey test at P = 0.05.

TABLE 3 | Response of transgenic *AtNPR1* olive plants to inoculation with *Verticillium dahliae*, non-defoliating strains V1242 and V1558.

V. dahliae isolate	Genotype	Plants with symptoms (%)	Symptom severity	Infected plants (%)
V-1242	P1	100a	0.67	100
	NPR1-224	75ab	0.90	100
	NPR1-780	50b	0.27*	85.7
	NPR1-814	62.5ab	0.77	87.5
V-1558	P1	50	0.87	100
	NPR1-224	75	1.12	100
	NPR1-780	62.5	0.73	87.5
	NPR1-814	50	0.43	100

Asterisks indicate significant differences from the control P1 line by the Mann–Whitney U test at P = 0.05. The percentages of plants with symptoms were analyzed with the Chi-square test at P = 0.05.

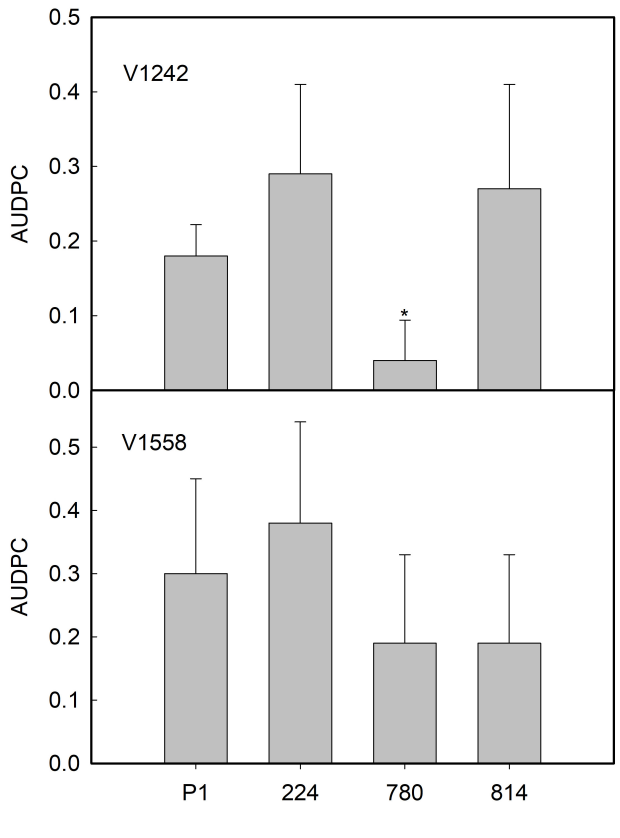

FIGURE 7 | Average values of area under the disease progress curve (AUDPC) in control (P1) and transgenic *AtNPR1* olive plants inoculated with *Verticillium dahliae*, non-defoliating strains V-1242 and V-1558. Data represent the mean ± SE. Asterisks indicate significant differences from control P1 by the Mann–Whitney *U* test at $P = 0.05$.

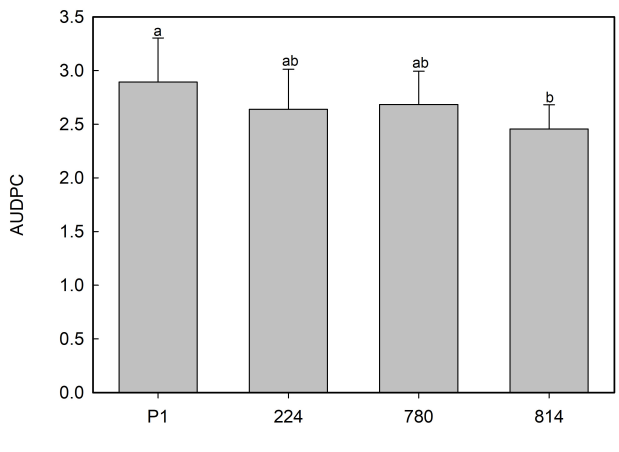

FIGURE 8 | Average values of area under the disease progress curve (AUDPC) in control (P1) and transgenic *AtNPR1* olive plants inoculated with *Rosellinia necatrix*. Data represent the mean ± SE. Different letters indicate significant differences by LSD test at $P = 0.05$.

The genetic transformation protocol, including successive exposures to increasing concentrations of paromomycin, was successful in selecting transgenic embryogenic cells. This strategy could be an advantage for selection, avoiding the excessive stress caused in olive cells by *A. tumefaciens* inoculation; this approach favors cell proliferation and results in a better appearance of the callus. The transformation efficiency was 0.28%, whereas in other studies carried out in olive using the same type of explant and the hypervirulent *A. tumefaciens* strain AGL1, transformation rates were higher; for example, Narvaez et al. (2018) obtained a 1.5% transformation rate with the antifungal protein afp of *Aspergillus giganteus*, while with the *FTa1* gene from *M. truncatula* (*MtFTa1*), it was 2.56% (Haberman et al., 2017). These differences in transformation rates could be explained by the size of the transgene. Whereas the sequences of cDNA of *afp* and *MtFTa1* are less than 1 kb, the size of the *AtNPR1* gene, which contains non-coding regions, is approximately 2 kb. Additionally, in the plasmid used, pK7WG2.0, the *nptII* gene is located close to the left border of the T-DNA; therefore, the large size of *AtNPR1* and its location in the right border could hinder the insertion of the *nptII* gene, making selection of transgenic cells more difficult.

The correct expression of the *AtNPR1* gene in transgenic plants was confirmed after detecting *At*NPR1 protein by western blotting, and the protein content in the extracts correlated with gene expression. The amount of *At*NPR1 protein in the transgenic leaves increased after treatment with SA, but unexpectedly, a band of similar size was also detected in the control. This result suggests that *At*NPR1 polyclonal antibody cross-reacts with endogenous olive NPR1; in fact, a search

in the *O. europaea* var. *sylvestris* genome yielded two genes (XP_022864634.1 and XP_022864635.1) putatively encoding a BTB/POZ domain and ankyrin repeat-containing NPR1 proteins sharing 53% identity with *At*NPR1. Lin et al. (2004) also used a polyclonal antibody to detect *At*NPR1 in transgenic tomato. In addition to the protein with the expected size, they found in wild-type and transgenic plants that the antibody reacted with other proteins of smaller size, in the range 45 to 35 kDa, which could be derived from endogenous NPR1 homologs.

Overexpression of either *AtNPR1* or its homologs has caused negative effects on the growth or development of plants, i.e., in strawberry, Silva et al. (2015) obtained shorter plants, with reduced canopy size, following transformation with this gene; moreover, the level of transgene expression was negatively correlated with plant size. In olive, the *NPR1*-780 line, with the highest transgene expression and amount of NPR1 protein, showed a lower number of shoots of shorter length under *in vitro* proliferation; however, these differences were not observed in 9 months old plants growing in the greenhouse. Differential behavior under growth chamber or greenhouse conditions was also observed in rice plants overexpressing the *AtNPR1* gene; these plants showed the LMS phenotype (*lesion mimic spot*) when growing in a chamber under low light, while only a growth reduction was noticed following transfer to the greenhouse; moreover, these transgenic rice plants were more sensitive to abiotic stress, such as salinity and drought, as well as to viral infections (Quilis et al., 2008). Molla et al. (2016) reported that some negative effects of *AtNPR1* expression could be avoided by using a specific green tissue promoter instead of a constitutive promoter.

Silva et al. (2015) hypothesized that the reduction in growth and development observed in *AtNPR1*-transformed strawberries could be due to constitutive activation of defense pathways. These transgenic plants constitutively expressed a *PR5* gene (thaumatin); however, their SA content was similar to that of the control plants. Other *PR* genes have also been shown to be constitutively expressed following transformation with this gene or its homologs, i.e., *PR1b* and *PBZ1/PR10* in rice (Chern et al., 2005), *PR1* and genes coding for glucanases (*PR2*) and chitinases (*PR3*) in tomato (Lin et al., 2004). In contrast, constitutive overexpression of *AtNPR1* in Arabidopsis (Cao et al., 1998), wheat (Makandar et al., 2006), or cotton (Kumar et al., 2013) did not induce the expression of *PR* genes in the absence of pathogens or elicitors. In this research, four genes putatively encoding PR1 were identified; only one of them was slightly upregulated in transgenic plants, although the level of expression did not correlate with *AtNPR1* gene expression or protein content. On the other hand, Parkhi et al. (2010a) only found increases in chitinase activity in *AtNPR1* cotton plants following inoculation with *Fusarium oxysporum* or after elicitation with SA. Basal endochitinase activity in leaves was similar in control and transgenic olive plants; hence, *AtNPR1* expression apparently did not induce constitutive expression of *PR* genes coding for these enzymes, at least in the absence of fungal stimulus. According to Niggeweg et al. (2000), variations in the interaction between *NPR1* and bZIP transcription factors (*TGA*) could explain differences in *PR* gene expression.

Regarding the response to *V. dahliae*, a hemibiotrophic fungal pathogen, olive plants expressing the *AtNPR1* gene did not show any resistance to the D isolate (V138), confirming previous observations by Parkhi et al. (2010a) in cotton; however, behavior against ND pathotypes varied with the race of the isolate, i.e., the *NPR1*-780 line with the highest transgene expression showed the lowest AUDPC and severity symptom values following inoculation with ND isolate V-1242 (race 2, absence of the *Ave1* gene). The performance of transgenic plants following inoculation with ND V-1558 (race 1, presence of the *Ave1* gene) was somewhat different, and no significant differences among the control and transgenic lines could be observed. In any case, it appears that the *Ve1* gene is not present in the P1 line, since control plants lack resistance to this pathotype. Moreover, the observed differences between pathotypes could confirm that an alternative infection mechanism depending on the fungal race is operating, as shown by Fradin et al. (2009) in *V. dahliae*-susceptible tomato. Our results in olive are in accordance with the previous observations of Parkhi et al. (2010a) in cotton, where a positive response to ND *V. dahliae* was observed in *AtNPR1* transgenic plants. Resistance to this pathogen seems to involve JA signaling (Fradin et al., 2011; Gao et al., 2013), and overexpression of GhFMO1 (a defense protein in SA signaling) in tobacco increased susceptibility to this fungus (Xu et al., 2014). However, other investigations have shown the importance of SAR signaling in response to *Verticillium*. In potato, overexpression of a polymorphic sequence of cDNA-AFLP, *StoNPR1*, isolated from a *Verticillium*-resistant genotype of *Solanum torvum* (Wang et al., 2010), conferred resistance through induction of genes involved in the SA biosynthetic pathway, including *ICS1* (*isochorismate synthase 1*) (Deng-Wei et al., 2014). Similarly, in cotton, Gong et al. (2017) reported that decreased resistance was observed following silencing of SA-upregulated ribosomal protein gene *L18* (*Ga*RPL18), while Tang et al. (2019) found that silencing of three *Wall Are Thin* genes resulted in increased SA levels and lignin synthesis and, subsequently, enhanced resistance to *V. dahliae*. Our results indicate a beneficial effect of SAR response in one of the olive-ND *V. dahliae* isolates used.

Transformation with *AtNPR1* has successfully been used to induce tolerance to necrotrophic fungi such as *B. cinerea*, *Alternaria radicina*, and *Sclerotinia sclerotiorum* in carrot (Wally et al., 2009) and *Alternaria alternata*, *Rhizoctonia solani*, and *F. oxysporum* in cotton (Parkhi et al., 2010b; Joshi et al., 2017). Defense against necrotrophic pathogens would be dependent on the JA/Et pathways; however, Berrocal-Lobo and Molina (2004) demonstrated that resistance to *F. oxysporum* was mediated by Et, JA, and SA in Arabidopsis and that the *NPR1* gene was involved. Along this line, Mur et al. (2006) indicated that SA-JA interactions in pathogen attack would depend on the relative concentration of the hormones, i.e., transient synergistic effects would be found at low hormonal concentrations, whereas higher concentrations and longer exposure times would result in antagonistic effects.

In Arabidopsis plants overexpressing the *NPR1* gene and inoculated with the necrotrophic pathogen *Fusarium graminearum*, Makandar et al. (2010) found that defense mediated by SA-*NPR1* would contribute to the control of disease,

while JA-mediated signaling would favor infection by restricting the activation of defense regulated by SA-*NPR1*. In any case, a positive role of JA in defense could not be rejected since double mutants (*npr1* and insensitive to JA, *jar1*) were more susceptible to the disease than single *npr1* mutants. The fact that this fungus has a short biotrophic phase in the early stages of infection (Goswami and Kistler, 2004) could partially explain the role of SA signaling in defense. In this investigation, one of the transgenic lines showed slower disease progression than the control following inoculation with the necrotrophic fungus *R. necatrix*, suggesting that, in this pathosystem, overexpression of *NPR1* slightly improves the response of plants to the fungus, although no correlation could be found between this positive effect and transgene expression or basal endochitinase activity.

CONCLUSION

Heterologous expression of the *NPR1* gene from *A. thaliana* in olive does not confer resistance to a D pathotype of the hemibiotroph fungus *V. dahliae*, although it improved the plant response to ND pathotypes. Similarly, a slight improvement in plant behavior was observed following inoculation with the necrotrophic fungus *R. necatrix*. However, the level of resistance attained in both cases does not make it a feasible approach to control these diseases.

DATA AVAILABILITY STATEMENT

The datasets generated for this study are available on request to the corresponding author.

AUTHOR CONTRIBUTIONS

IN and LF were responsible for obtaining, maintaining, and characterizing the transgenic plants. IN, CP, and EP-R carried out the molecular analysis. RJ-D and JT-C performed the *V. dahliae* assays. CL-H and JA-L carried out the *R. necatrix* assays. JM and FP-A planned this research, designed the experiments, and wrote the manuscript.

FUNDING

This investigation was funded by the Junta de Andalucía (Grant No. P11-AGR-7992) and by the Ministerio de Ciencia e Innovación of Spain and Feder European Union Funds (Grant No. AGL2017-83368-C2-1-R).

ACKNOWLEDGMENTS

IN was awarded a Ph.D. Fellowship from Secretaría General de Investigación (Consejería de Innovación Ciencia y Empresa, Junta de Andalucía, Spain, Grant No. P11-AGR-7992), Ph.D. Program Advanced Biotechnology, University of Málaga. LF was awarded a Master fellowship from IAMZ, Zaragoza, Spain.

SUPPLEMENTARY MATERIAL

The Supplementary Material for this article can be found online at: https://www.frontiersin.org/articles/10.3389/fpls.2020.00308/full#supplementary-material

REFERENCES

Ali, S., Ganai, B. A., Kamili, A. N., Bhat, A. A., Mir, Z. A., Bhat, J. A., et al. (2018). Pathogenesis-related proteins and peptides as promising tools for engineering plants with multiple stress tolerance. *Microbiol. Res* 212–213, 29–37. doi: 10.1016/j.micres.2018.04.008

Berrocal-Lobo, M., and Molina, A. (2004). Ethylene response factor 1 mediates *Arabidopsis* resistance to the soilborne fungus *Fusarium oxysporum*. *Mol. Plant Microbe Interact.* 17, 763–770. doi: 10.1094/MPMI.2004.17.7.763

Bradford, M. M. (1976). A rapid and sensitive method for the quantitation of microgram quantities of protein utilizing the principle of protein-dye binding. *Anal Biochem.* 7, 248–254. doi: 10.1016/0003-2697(76)90527-3

Campbell, C. L., and Madden, L. V. (1990). *Introduction to Plant Disease Epidemiology*. New York, NY: John Wiley and Sons Inc.

Cao, H., Glazebrook, J., Clarke, J. D., Volko, S., and Dong, X. (1997). The *Arabidopsis NPR1* gene that controls systemic acquired resistance encodes a novel protein containing ankyrin repeats. *Cell* 88, 57–63. doi: 10.1016/S0092-8674(00)81858-9

Cao, H., Li, X., and Dong, X. (1998). Generation of broad-spectrum disease resistance by overexpression of an essential regulatory gene in systemic acquired resistance. *Plant Biol.* 95, 6531–6536. doi: 10.1073/pnas.95.11.6531

Cerezo, S., Mercado, J. A., and Pliego-Alfaro, F. (2011). An efficient regeneration system via somatic embryogenesis in olive. *Plant Cell Tissue Organ Cult.* 106, 337–344. doi: 10.1007/s11240-011-9926-6

Chern, M., Fitzgerald, H. A., Canlas, P. E., Navarre, D. A., and Ronald, P. C. (2005). Overexpression of a rice *NPR1* homolog leads to constitutive activation of defense response and hypersensitivity to light. *Mol. Plant Microbe Interact.* 18, 511–520. doi: 10.1094/MPMI-18-0511

Clavero-Ramírez, I., and Pliego-Alfaro, F. (1990). Germinación *in vitro* de embriones maduros de olivo (*Olea europaea*). *Actas de Horticultura* 1, 512–516.

de Jonge, R., van Esse, H. P., Maruthachalam, K., Bolton, M. D., Santhanam, P., Saber, M. K., et al. (2012). Tomato immune receptor Ve1 recognizes effector of multiple fungal pathogens uncovered by genome and RNA sequencing. *Proc. Natl Acad. Sci. U.S.A.* 109, 5110–5115. doi: 10.1073/pnas.1119623109

Deng-Wei, J., Liu, Y., Ce, S., Min, C., and Qing, Y. (2014). Cloning and characterization of a *Solanum torvum NPR1* gene involved in regulating plant resistance to *Verticillium dahliae*. *Acta Physiol. Plant* 36, 2999–3011. doi: 10.1007/s11738-014-1671-0

El Oirdi, M., El Rahman, T. A., Rigano, L., El Hadrami, A., Daayf, F., Vojnov, A., et al. (2011). *Botrytis cinerea* manipulates the antagonistic effects between immune pathways to promote disease development in tomato. *Plant Cell* 23, 2405–2421. doi: 10.1105/tpc.111.083394

Emani, C., Garcia, J. M., Lopata-Finch, E., Pozo, M. J., Uribe, P., Kim, D. J., et al. (2003). Enhanced fungal resistance in transgenic cotton expressing an endochitinase gene from *Trichoderma virens*. *Plant Biotechnol. J* 1, 321–336. doi: 10.1046/j.1467-7652.2003.00029.x

Fradin, E. F., Abd-El-Haliem, A., Masini, L., Van Den Berg, G. C., Joosten, M. H., and Thomma, B. P. H. J. (2011). Interfamily transfer of tomato *Ve1* mediates *Verticillium* resistance in *Arabidopsis*. *Plant Physiol.* 156, 2255–2265. doi: 10.1104/pp.111.180067

Fradin, E. F., Zhang, Z., Juárez-Ayala, J. C., Castroverde, C. D. M., Nazar, R. N., Robb, J., et al. (2009). Genetic dissection of Verticillium wilt resistance mediated by tomato Ve1. *Plant Physiol.* 150, 320–332. doi: 10.1104/pp.109.136762

Gao, W., Long, L., Zhu, L.-F., Xu, L., Gao, W.-H., Sun, L.-Q., et al. (2013). Proteomic and virus-induced gene silencing (VIGS) analyses reveal that gossypol, brassinosteroids, and jasmonic acid contribute to the resistance of

cotton to *Verticillium dahliae*. *Mol. Cell Proteomics* 12, 3690–3703. doi: 10.1074/mcp.M113.031013

García, F., Calvet, C., Camprubí, A., Estaún, V., Ninot, A., and Tous, J. (2009). "Evaluación de la sensibilidad de diferentes variedades de olivo a *Rosellinia* (ana. *Dematophora necatrix)*," in *II Jornadas Nacionales de Olivicultura de la SECH*, Tarragona, 17.

García Figueras, F., and Celada Brouard, B. (2001). Incidencia de *Dematophora necatrix* en olivo. *Frutic. Prof.* 120, 51–54.

Glazebrook, J. (2005). Contrasting mechanisms of defense against biotrophic and necrotrophic pathogens. *Annu. Rev. Phytopathol.* 43, 205–227. doi: 10.1146/annurev.phyto.43.040204.135923

Gómez-Jiménez, M. C., Paredes, M. A., Gallardo, M., Fernández-García, N., Olmos, E., and Sánchez-Calle, I. M. (2010). Tissue-specific expression of olive *S-adenosyl methionine decarboxylase* and *spermidine synthase* genes and polyamine metabolism during flower opening and early fruit development. *Planta* 232, 629–647. doi: 10.1007/s00425-010-1198-6

Gong, Q., Yang, Z., Wang, X., Butt, H. I., Chen, E., He, S., et al. (2017). Salicylic acid-related cotton (*Gossypium arboreum*) ribosomal protein GaRPL18 contributes to resistance to *Verticillium dahliae*. *BMC Plant Biol.* 17:59. doi: 10.1186/s12870-017-1007-5

Goswami, R. S., and Kistler, H. C. (2004). Heading for disaster: *Fusarium graminearum* on cereal crops. *Mol. Plant Pathol.* 5, 515–525. doi: 10.1111/j.1364-3703.2004.00252

Guillaumin, J. J., Mercier, S., and Dubos, B. (1982). Les pourridiés à Armillariella et Rosellinia en France sur vigne, arbres fruitiers et cultures florales I. Etiologie et symptomatologie. *Agronomie* 2, 71–80. doi: 10.1051/agro:19820110

Haberman, A., Bakhshian, O., Cerezo-Medina, S., Paltiel, J., Adler, C., Ben-Ari, G., et al. (2017). A possible role for flowering locus T-encoding genes in interpreting environmental and internal cues affecting olive (*Olea europaea* L.) flower induction. *Plant Cell Environ.* 40, 1263–1280. doi: 10.1111/pce.12922

Healey, A., Furtado, A., Cooper, T., and Henry, R. J. (2014). Protocol: a simple method for extracting next-generation sequencing quality genomic DNA from recalcitrant plant species. *Plant Methods* 10, 21–28. doi: 10.1186/1746-4811-10-21

Höfgen, R., and Willmitzer, L. (1988). Storage of competent cells for *Agrobacterium* transformation. *Nucleic Acids Res.* 16:9877. doi: 10.1093/nar/16.20.9877

Islam, A. (2006). Fungus resistance transgenic plants: strategies, progress and lessons learnt. *Plant Tissue Cult Biotech.* 16, 117–138. doi: 10.3329/ptcb.v16i2.1113

Jiménez-Díaz, R. M., Cirulli, M., Bubici, G., Jiménez-Gasco, M. M., Antoniou, P., and Tjamos, E. (2012). Verticillium wilt, a major threat to olive production current status and future prospects for its management. *Plant Dis.* 96, 304–329. doi: 10.1094/PDIS-06-11-0496

Jiménez-Díaz, R. M., Olivares-García, C., Trapero-Casas, J. L., Jiménez-Gasco, M. M., Navas-Cortés, J. A., Landa, B. B., et al. (2017). Variation of pathotypes and races and their correlations with clonal lineages in *Verticillium dahliae*. *Plant Pathol.* 66, 651–666. doi: 10.1111/ppa.12611

Jiménez-Fernández, D., Trapero-Casas, J. L., Landa, B. B., Navas-Cortés, J. A., Bubici, G., Cirulli, M., et al. (2016). Characterization of resistance against the olive-defoliating *Verticillium dahliae* pathotype in selected clones of wild olive. *Plant Pathol.* 65, 1279–1291. doi: 10.1111/ppa.12516

Joshi, S. G., Kumar, V., Janga, M. R., Bell, A. A., and Rathore, K. S. (2017). Response of *AtNPR1*-expressing cotton plants to *Fusarium oxysporum* f. sp. vasinfectum isolates. *Physiol. Mol. Biol. Plants* 23, 135–142. doi: 10.1007/s12298-016-0411-x

Kumar, V., Joshi, S. G., Bell, A. A., and Rathore, K. S. (2013). Enhanced resistance against *Thielaviopsis basicola* in transgenic cotton plants expressing *Arabidopsis NPR1* gene. *Transgenic Res.* 22, 359–368. doi: 10.1007/s11248-012-9652-9

Laemmli, U. K. (1970). Cleavage of structural proteins during the assembly of the head of bacteriophage T4. *Nature* 227, 680–685. doi: 10.1038/227680a0

Lazo, G. R., Stein, P. A., and Ludwig, R. A. (1991). A DNA transformation-competent *Arabidopsis* genomic library in Agrobacterium. *Biotechnology* 9, 963–967. doi: 10.1038/nbt1091-963

Lin, W., Lu, C. F., Wu, J. W., Cheng, M. L., Lin, Y. M., Black, L., et al. (2004). Transgenic tomato plants expressing the *Arabidopsis NPR1* gene display enhanced resistance to a spectrum of fungal and bacterial diseases. *Transgenic Res.* 13, 567–581. doi: 10.1007/s11248-004-2375-9

Livak, K. J., and Schmittgen, T. D. (2001). Analysis of relative gene expression data using real-time quantitative PCR and the 2-ΔΔCt. *Methods* 25, 402–408. doi: 10.1006/meth.2001.1262

López-Escudero, F. J., del Río, C., Caballero, J. M., and Blanco-López, M. A. (2004). Evaluation of olive cultivars for resistance to *Verticillium dahliae*. *Eur. J. Plant Pathol.* 110, 79–85. doi: 10.1023/B:EJPP.0000010150.08098.2d

Makandar, R., Essig, J. S., Schapaugh, M. A., Trick, H. N., and Shah, J. (2006). Genetically engineered resistance to Fusarium head blight in wheat by expression of *Arabidopsis NPR1*. *Mol. Plant Microbe Interact.* 19, 123–129. doi: 10.1094/MPMI-19-0123

Makandar, R., Nalam, V., Chaturvedi, R., Jeannotte, R., Sparks, A. A., and Shah, J. (2010). Involvement of salicylate and jasmonate signaling pathways in *Arabidopsis* interaction with *Fusarium graminearum*. *Mol. Plant-Microbe Interact.* 23, 861–870. doi: 10.1094/MPMI-23-7-0861

Molla, K. A., Karmakar, S., Chanda, P. K., Sarkar, S. N., Datta, S. K., and Datta, K. (2016). Tissue-specific expression of *Arabidopsis NPR1* gene in rice for sheath blight resistance without compromising phenotypic cost. *Plant Sci.* 250, 105–114. doi: 10.1016/j.plantsci.2016.06.005

Mur, L. A. J., Kenton, P., Atzorn, R., Miersch, O., and Wasternack, C. (2006). The outcomes of concentration-specific interactions between salicylate and jasmonate signaling include synergy, antagonism, and oxidative stress leading to cell death. *Plant Physiol.* 140, 249–262. doi: 10.1104/pp.105.072348

Murashige, T., and Skoog, F. (1962). A revised medium for rapid growth and bio assays with tobacco tissue cultures. *Physiol. Plant.* 15, 473–497. doi: 10.1111/j.1399-3054.1962.tb08052.x

Narvaez, I., Khayreddine, T., Pliego, C., Cerezo, S., Jiménez-Díaz, R. M., Trapero Casas, J. L., et al. (2018). Usage of the heterologous expression of the antimicrobial gene *afp* from *Aspergillus giganteus* for increasing fungal resistance in olive. *Front. Plant Sci.* 9:680. doi: 10.3389/fpls.2018.00680

Niggeweg, R., Thurow, C., Weigel, R., Pfitzner, U., and Gatz, C. (2000). Tobacco TGA factors differ with respect to interaction with *NPR1*, activation potential and DNA binding properties. *Plant Mol. Biol.* 42, 775–788.

Orinos, T., and Mitrakos, K. (1991). Rhizogenesis and somatic embryogenesis in calli from wild olive (*Olea europaea* var. *sylvestris* (Miller) Lehr) mature zygotic embryos. *Plant Cell Tissue Organ Cult.* 27, 183–187. doi: 10.1007/BF00041288

Parkhi, V., Kumar, V., Campbell, L. M., Bell, A. A., and Rathore, K. S. (2010a). Expression of *Arabidopsis NPR1* in transgenic cotton confers resistance to nondefoliating isolates of *Verticillium dahliae* but not the defoliating isolates. *J. Phytopathol.* 158, 822–825. doi: 10.1111/j.1439-0434.2010.01714.x

Parkhi, V., Kumar, V., Campbell, L. M., Bell, A. A., Shah, J., and Rathore, K. S. (2010b). Resistance against various fungal pathogens and reniform nematode in transgenic cotton plants expressing *Arabidopsis NPR1*. *Transgenic Res.* 19, 959–975. doi: 10.1007/s11248-010-9374-9

Pérez-Barranco, G., Torreblanca, R., Padilla, I. M. G., Sánchez-Romero, C., Pliego-Alfaro, F., and Mercado, J. A. (2009). Studies on genetic transformation of olive (*Olea europaea* L.) somatic embryos: I. Evaluation of different aminoglycoside antibiotics for nptII selection; II. Transient transformation via particle bombardment. *Plant Cell Tissue Organ. Cult.* 97, 243–251. doi: 10.1007/s11240-009-9520-3

Pérez-Jiménez, F., Ruano, J., Perez-Martinez, P., Lopez-Segura, F., and Lopez-Miranda, J. (2007). The influence of olive oil on human health: not a question of fat alone. *Mol. Nutr. Food Res.* 51, 1199–1208. doi: 10.1002/mnfr.200600273

Pliego, C., López-Herrera, C., Ramos, C., and Cazorla, F. M. (2012). Developing tools to unravel the biological secrets of *Rosellinia necatrix*, an emergent threat to woody crops. *Mol. Plant Pathol.* 13, 226–239. doi: 10.1111/j.1364-3703.2011.00753.x

Quilis, J., Peñas, G., Messeguer, J., Brugidou, C., and San Segundo, B. (2008). The *Arabidopsis AtNPR1* inversely modulates defense responses against fungal, bacterial, or viral pathogens while conferring hypersensitivity to abiotic stresses in transgenic rice. *Mol. Plant Microbe Interact.* 21, 1215–1231. doi: 10.1094/MPMI-21-9-1215

Rallo, L., Barranco, D., Díez, C. M., Rallo, P., Suárez, M. P., et al. (2018). "Strategies for olive (*Olea europaea* L.) breeding: Cultivated genetic resources and crossbreeding," in *Advances in Plant Breeding Strategies: Fruits*, eds J. Al-Khayri, S. M. Jain, and D. Johnson (Cham: Springer International Publishing AG), 535–600. doi: 10.1007/978-3-319-91944-7_14

Roca, L. F., Romero, J., Raya, M. C., and Trapero, A. (2016). "Decaimiento y muerte de olivos por *Rosellinia necatrix* en el Alentejo portugués," in *XVIII Congreso de la Sociedad Española de Fitopatología*, Palencia, R–0133.

Roussos, P. A., and Pontikis, C. A. (2002). *In vitro* propagation of olive (*Olea europaea* L.) cv. *Koroneiki*. *Plant Growth Regul.* 37, 295–304. doi: 10.1023/A:1020824330589

Ruano Rosa, D., and López Herrera, C. J. (2009). Evaluation of *Trichoderma* spp. as biocontrol agents against avocado white root rot. *Biol. Control* 51, 66–71. doi: 10.1016/j.biocontrol.2009.05.005

Rugini, E. (1984). *In vitro* propagation of some olive (*Olea europaea sativa* L.) cultivars with different root-ability, and medium development using analytical data from developing shoots and embryos. *Sci. Hortic* 24, 123–134. doi: 10.1016/0304-4238(84)90143-2

Rugini, E., De Pace, C., Gutierrez-Pesce, P., and Muleo, R. (2011). "Olea," in *Wild Crop Relatives: Genomic and Breeding Resources, Temperate Fruits*, ed. C. Kole (Heidelberg: Springer-Verlag), 79–117.

Silva, K. J. P., Brunings, A., Peres, N. A., Zhonglin, M., and Folta, K. M. (2015). The *Arabidopsis NPR1* gene confers broad-spectrum disease resistance in strawberry. *Transgenic Res.* 24, 693–704. doi: 10.1007/s11248-015-9869-5

Spoel, S. H., Koornneef, A., Claessens, S. M. C., Korzelius, J. P., Van Pelt, J. A., Mueller, M. J., et al. (2003). NPR1 modulates cross-talk between salicylate- and jasmonate-dependent defense pathways through a novel function in the cytosol. *Plant Cell* 15, 760–770. doi: 10.1105/tpc.009159

Sztejnberg, A. (1980). Host range of *Dematophora necatrix*, the cause of white root rot disease in fruit trees. *Plant Dis.* 64, 662. doi: 10.1094/PD-64-662

Tang, Y., Zhang, Z., Lei, Y., Hu, G., Liu, J., Hao, M., et al. (2019). Cotton WATs modulate SA biosynthesis and local lignin deposition participating in plant resistance against *Verticillium dahliae*. *Front. Plant Sci.* 10:526. doi: 10.3389/fpls.2019.00526

ten Hoopen, G. M., and Krauss, U. (2006). Biology and control of *Rosellinia bunodes*, *Rosellinia necatrix* and *Rosellinia pepo*: a review. *Crop. Prot.* 25, 89–107. doi: 10.1016/j.cropro.2005.03.009

Torreblanca, R., Cerezo, S., Palomo-Ríos, E., Mercado, J. A., and Pliego-Alfaro, F. (2010). Development of a high throughput system for genetic transformation of olive (*Olea europaea* L.) plants. *Plant Cell Tissue Organ. Cult.* 103, 61–69. doi: 10.1007/s11240-010-9754-0

Trapero, C., Rallo, L., López-Escudero, F. J., Barranco, D., and Díez, C. M. (2015). Variability and selection of Verticillium wilt resistant genotypes in cultivated olive and in the *Olea* genus. *Plant Pathol.* 64, 890–900. doi: 10.1111/ppa.12330

van Wees, S. C. M., de Swart, E. A. M., van Pelt, J. A., van Loon, L. C., and Pieterse, C. M. J. (2000). Enhancement of induced disease resistance by simultaneous activation of salicylate- and jasmonate dependent defense pathways in *Arabidopsis thaliana*. *Proc. Natl. Acad. Sci. U.S.A.* 97, 8711–8716. doi: 10.1073/pnas.130425197

Vidoy-Mercado, I., Imbroda-Solano, I., Barceló-Muñoz, A., and Pliego-Alfaro, F. (2012). Differential *in vitro* behaviour of the Spanish olive (*Olea europaea* L.) cultivars *'Arbequina'* and *'Picual'*. *Acta Hortic.* 949, 27–30. doi: 10.17660/ActaHortic.2012.949.1

Wally, O., Jayaraj, J., and Punja, Z. K. (2009). Broad-spectrum disease resistance to necrotrophic and biotrophic pathogens in transgenic carrots (*Daucus carota* L.) expressing an *Arabidopsis NPR1* gene. *Planta* 231, 131–141. doi: 10.1007/s00425-009-1031-2

Wang, Z., Guo, J. L., Zhang, F., Huang, Q. S., Huang, L. P., and Yang, Q. (2010). Differential expression analysis by cDNA-AFLP of *Solanum torvum* upon *Verticillium dahliae* infection. *Russ. J. Plant Physiol.* 57, 676–684. doi: 10.1134/S1021443710050110

Xu, L., Zhang, W., He, X., Liu, M., Zhang, K., Shaban, M., et al. (2014). Functional characterization of cotton genes responsive to *Verticillium dahliae* through bioinformatics and reverse genetics strategies. *J. Exp. Bot.* 65, 6679–6692. doi: 10.1093/jxb/eru393

Zheng, X. Y., Spivey, N. W., Zeng, W., Liu, P. P., Fu, Z. Q., Klessig, D. F., et al. (2012). Coronatine promotes *Pseudomonas syringae* virulence in plants by activating a signaling cascade that inhibits salicylic acid accumulation. *Cell Host Microbe* 11, 587–596. doi: 10.1016/j.chom.2012.04.014

Conflict of Interest: The authors declare that the research was conducted in the absence of any commercial or financial relationships that could be construed as a potential conflict of interest.

Advantages of publishing in Frontiers

OPEN ACCESS
Articles are free to read for greatest visibility and readership

FAST PUBLICATION
Around 90 days from submission to decision

HIGH QUALITY PEER-REVIEW
Rigorous, collaborative, and constructive peer-review

TRANSPARENT PEER-REVIEW
Editors and reviewers acknowledged by name on published articles

Frontiers
Avenue du Tribunal-Fédéral 34
1005 Lausanne | Switzerland

Visit us: www.frontiersin.org
Contact us: info@frontiersin.org | +41 21 510 17 00

REPRODUCIBILITY OF RESEARCH
Support open data and methods to enhance research reproducibility

DIGITAL PUBLISHING
Articles designed for optimal readership across devices

FOLLOW US
@frontiersin

IMPACT METRICS
Advanced article metrics track visibility across digital media

EXTENSIVE PROMOTION
Marketing and promotion of impactful research

LOOP RESEARCH NETWORK
Our network increases your article's readership